EFFECTS OF ICE LOSS ON MARINE BIODIVERSITY

EDITED BY: Katrin Linse, Ilka Peeken and Anne Helene Solberg Tandberg
PUBLISHED IN: Frontiers in Marine Science

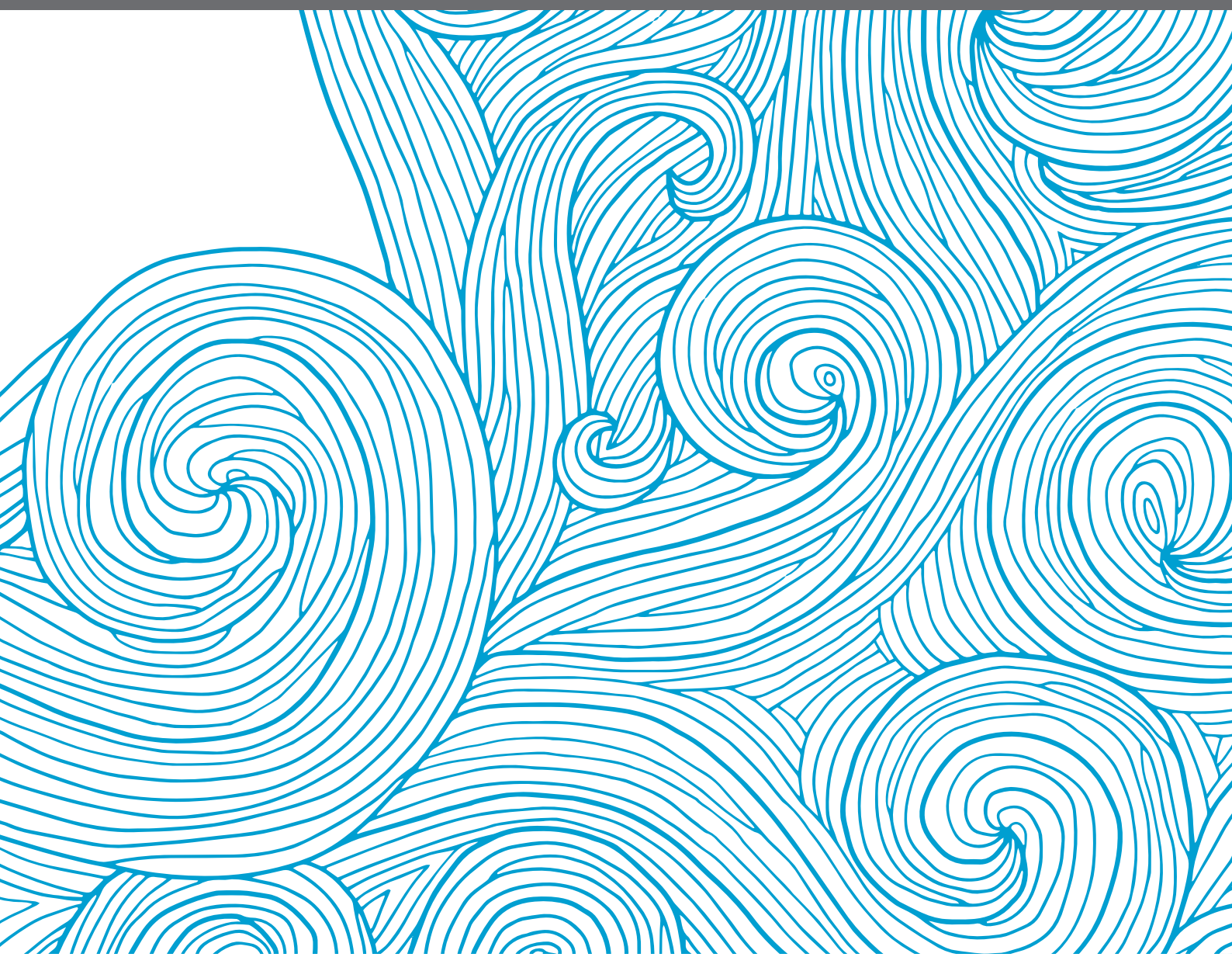

frontiers Research Topics

frontiers

ISSN 1664-8714
ISBN 978-2-88971-977-8
DOI 10.3389/978-2-88971-977-8

About Frontiers

Frontiers is more than just an open-access publisher of scholarly articles: it is a pioneering approach to the world of academia, radically improving the way scholarly research is managed. The grand vision of Frontiers is a world where all people have an equal opportunity to seek, share and generate knowledge. Frontiers provides immediate and permanent online open access to all its publications, but this alone is not enough to realize our grand goals.

Frontiers Journal Series

The Frontiers Journal Series is a multi-tier and interdisciplinary set of open-access, online journals, promising a paradigm shift from the current review, selection and dissemination processes in academic publishing. All Frontiers journals are driven by researchers for researchers; therefore, they constitute a service to the scholarly community. At the same time, the Frontiers Journal Series operates on a revolutionary invention, the tiered publishing system, initially addressing specific communities of scholars, and gradually climbing up to broader public understanding, thus serving the interests of the lay society, too.

Dedication to Quality

Each Frontiers article is a landmark of the highest quality, thanks to genuinely collaborative interactions between authors and review editors, who include some of the world's best academicians. Research must be certified by peers before entering a stream of knowledge that may eventually reach the public - and shape society; therefore, Frontiers only applies the most rigorous and unbiased reviews.
Frontiers revolutionizes research publishing by freely delivering the most outstanding research, evaluated with no bias from both the academic and social point of view. By applying the most advanced information technologies, Frontiers is catapulting scholarly publishing into a new generation.

What are Frontiers Research Topics?

Frontiers Research Topics are very popular trademarks of the Frontiers Journals Series: they are collections of at least ten articles, all centered on a particular subject. With their unique mix of varied contributions from Original Research to Review Articles, Frontiers Research Topics unify the most influential researchers, the latest key findings and historical advances in a hot research area! Find out more on how to host your own Frontiers Research Topic or contribute to one as an author by contacting the Frontiers Editorial Office: frontiersin.org/about/contact

EFFECTS OF ICE LOSS ON MARINE BIODIVERSITY

Topic Editors:
Katrin Linse, British Antarctic Survey (BAS), United Kingdom
Ilka Peeken, Alfred Wegener Institute Helmholtz Centre for Polar and Marine Research (AWI), Germany
Anne Helene Solberg Tandberg, University Museum of Bergen, Norway

Citation: Linse, K., Peeken, I., Tandberg, A. H. S., eds. (2021). Effects of Ice Loss on Marine Biodiversity. Lausanne: Frontiers Media SA. doi: 10.3389/978-2-88971-977-8

Table of Contents

frontiers in Marine Science

EDITORIAL
published: 11 November 2021
doi: 10.3389/fmars.2021.793020

Editorial: Effects of Ice Loss on Marine Biodiversity

Katrin Linse[1]*, *Ilka Peeken*[2] *and Anne Helene Solberg Tandberg*[3]

[1] *Biodiversity, Evolution & Adaptation Team, British Antarctic Survey, Cambridge, United Kingdom,* [2] *Polar Biological Oceanography, Helmholtz Centre for Polar and Marine Research, Alfred Wegener Institute, Bremerhaven, Germany,* [3] *Natural History Department, University Museum, University of Bergen, Bergen, Norway*

Keywords: zooplankton, phytoplankton, zoobenthos, meiofauna, *in-situ* habitat images

Editorial on the Research Topic

Effects of Ice Loss on Marine Biodiversity

The Arctic and Antarctic oceans are undergoing changes in the extent of their sea-ice and ice-shelves (IPCC, in press). These have important impacts on the biodiversity, structure, and function of sea ice biota, pelagic and benthic communities, and will change the composition, distribution, and productivity of all species in these ecosystems (Constable et al., 2014; Lannuzel et al., 2020). Decreasing Arctic sea ice has led to a northwards shift in phytoplankton distributions (Nöthig et al., 2015; Metfies et al., 2016) and phytoplankton blooms were discovered in autumn (Ardyna et al., 2014). Shifts were also observed in the vertical and horizontal distributions of zooplankton communities (Wassmann et al., 2015). In the Antarctic, gigantic icebergs have calved from ice shelves and in some cases, entire ice shelves have collapsed enabling sunlight and currents to reach the underlying benthic communities and providing new space for pelagic ecosystems (e.g., Vernet et al., 2019). The benthic habitats and their faunal inhabitants under floating Antarctic ice shelves are among the least known marine communities on Earth.

This Research Topic aimed to address all aspects of marine biodiversity science that introduce new knowledge to improve our understanding of the effects ice loss (sea ice and ice shelf) has on the pelagic and benthic communities in the polar oceans (**Figure 1**). Contributions were delivered by 61 participating authors providing up-to-date information on the species richness and biogeographic responses in marine biodiversity adapted to ice-covered environments, on their phylogeographic relationships and how they affect biogeochemical cycles, on the status of the effects of ice loss on marine biogeochemistry and biodiversity on regional and global scales, on how feedbacks and controls could change these systems and ultimately, on what new conditions might be present in these regions on decadal and longer time scales.

Reduction of sea-ice in the Arctic resulted in a massive loss of the previous typical multiyear ice, with a reduction of biodiversity of the sea-ice associated protists (Hop et al., 2021) and an increase of primary production (Arrigo and Van Dijken, 2015). North of Svalbard Ehrlich et al. show loss in biodiversity for the sympagic meiofauna, with nematodes totally absent and only a low number of flatworms. In addition, hardly any sympagic amphipods were present, suggesting the strong connectivity of these organisms with multiyear ice. A study of lipid biomarkers gives further insight in the transfer of sea-ice derived carbon for higher trophic levels. While Kohlbach et al. (2016) demonstrated a strong dependence of the sympagic and pelagic organisms on sea-ice derived carbon in the Central Arctic, Kohlbach et al. suggest that for Barents Sea amphipods this is only a surplus food source. Calanoid copepods already shifted their food demand entirely on pelagic resources and thus might have already adapted to the changing sea ice conditions in this region. By applying high-throughput amplicon sequencing, Kalenitchenko et al. show a distinct difference of protists diversity between the Arctic Ocean and the Central Arctic suggesting a low connectivity

OPEN ACCESS

Edited and reviewed by:
Thomas Wilke,
University of Giessen, Germany

***Correspondence:**
Katrin Linse
kl@bas.ac.uk

Specialty section:
This article was submitted to Marine Evolutionary Biology, Biogeography and Species Diversity, a section of the journal Frontiers in Marine Science

Received: *11 October 2021*
Accepted: *19 October 2021*
Published: *11 November 2021*

Citation:
Linse K, Peeken I and Tandberg AHS (2021) Editorial: Effects of Ice Loss on Marine Biodiversity. Front. Mar. Sci. 8:793020. doi: 10.3389/fmars.2021.793020

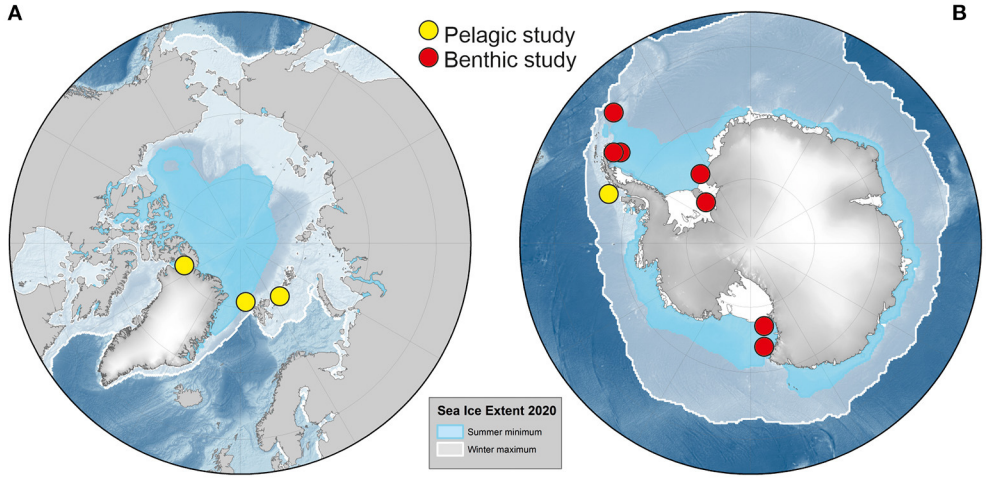

FIGURE 1 | Locations of pelagic and benthic biodiversity study sites in the Arctic and Antarctic and current seasonal sea ice extent. **(A)** Arctic, **(B)** Antarctic and Southern Ocean. The maps are drawn to 55° latitude. Sea ice extent data are from https://nsidc.org/cryosphere/sotc/sea_ice.html.

between these regions and imply that the ongoing changes in sea ice cover will not result in a high productive Nares Strait ecosystem.

Moving to the Antarctic, particularly the western Antarctic Peninsula is the key region, where rapid sea ice loss has been reported with major consequences for the ecosystem (Constable et al., 2014). By applying whole community metatranscriptomic together with lipidomics Bowman et al. analyzed how lipid production and utilization was influenced by changing light conditions. They show an intrinsic adaptation behind various pelagic species, implying future changes in the phytoplankton composition, and the production of lipid-rich food sources with the ongoing change of the sea ice cover along the western Antarctic Peninsula.

Effects of changes and status-quo of benthic communities and their biodiversity were studied in the Antarctic Peninsula, Weddell, and Ross seas. The Prince Gustav Channel area had been influenced by the break-up of the Prince Gustav ice shelf, retreating glaciers, and changes in sea-ice cover but its benthic biodiversity had been never assessed. The meiobenthic and nematode communities, analyzed by Pantó et al. using metabarcoding and environmental proxy characterization, revealed high densities at all depths based on availability of fresh organic sedimentary matter. As shown by Di Franco et al. also abundance and community structure of macrobenthic peracarids were affected by length of sea ice cover and associated blooms of the primary producers. Drennan et al. reported a diverse and spatially heterogenous annelid fauna, including wide-spread, circum-Antarctic species as well as yet unnamed species in an area with dynamic recent glacial history. The *in-situ* habitat heterogeneity in the Prince Gustav Channel was illustrated by Almond et al. showing that locations previously covered by the ice shelf held distinct and unique communities. In the Ross Sea, Cummings et al. investigating macro-infaunal and mega-epifaunal benthos showed that organic seabed fluxes and sea ice cover were important for the community structure.

Describing and understanding the marine communities and their biodiversity under the floating ice shelves is still a gap in our knowledge, as these communities are mostly accessible to study after the collapse. Multidisciplinary collaborations with geological and glaciological scientists using shelf ice core bore holes gave a first glimpse into these unknown ecosystems as reviewed by Griffiths et al. who also presented the first record of hard rock suspension feeder community hundreds of kilometers away from the open ocean. These unique, unstudied ecosystems, like under the Filchner-Ronne Ice shelf, are under future climate threads as Naughten et al. (2021) are predicting significant changes in the oceanographic settings.

This volume provides a brief indication of the current state of the art and indicates some of the pressing issues and questions related to ice and biodiversity loss in the Polar Regions. We, the editors, hope that this Research Topic will form the basis of further discussion and will foster future cross-polar region research in the effects of ice loss on marine biodiversity.

AUTHOR CONTRIBUTIONS

KL wrote the first draft of the manuscript KL, IP, and AT wrote sections of the manuscript. KL drafted the figure. All authors contributed to manuscript, read, and approved the submitted version.

ACKNOWLEDGMENTS

We thank our authors for submitting their research to our topic. We are especially grateful to the reviewers who returned their comments within the requested timeline. Special thanks to Huw J. Griffiths for providing the maps for the figure.

REFERENCES

Ardyna, M., Babin, M., Gosselin, M., Devred, E., Rainville, L., and Tremblay, J. E. (2014). Recent Arctic Ocean sea ice loss triggers novel fall phytoplankton blooms. *Geophys. Res. Lett.* 41, 6207–6212. doi: 10.1002/2014GL061047

Arrigo, K. R., and Van Dijken, G. L. (2015). Continued increases in Arctic Ocean primary production. *Prog. Oceanogr.* 136, 60–70. doi: 10.1016/j.pocean.2015.05.002

Constable, A. J., Melbourne-Thomas, J., Corney, S. P., Arrigo, K. R., Barbraud, C., Barnes, D. K. A., et al. (2014). Climate change and Southern Ocean ecosystems I: how changes in physical habitats directly affect marine biota. *Glob. Change Biol.* 20, 3004–3025. doi: 10.1111/gcb.12623

Hop, H., Wold, A., Meyer, A., Bailey, A., Hatlebakk, M., Kwasniewski, S., et al. (2021). Winter-spring development of the zooplankton community below sea ice in the Arctic Ocean. *Front. Mar. Sci.* 9, 1–21. doi: 10.3389/fmars.2021.609480

IPCC (in press). "Climate change 2021: the physical science basis," in *Contribution of Working Group I to the Sixth Assessment Report of the Intergovernmental Panel on Climate Change*, eds V. Masson-Delmotte, P. Zhai, A. Pirani, S. L. Connors, C. Péan, S. Berger, N. Caud, Y. Chen, L. Goldfarb, M. I. Gomis, M. Huang, K. Leitzell, E. Lonnoy, J. B. R. Matthews, T. K. Maycock, T. Waterfield, O. Yelekçi, R. Yu, and B. Zhou (Cambridge University Press).

Kohlbach, D., Graeve, M., Lange, B. A., David, C., Peeken, I., and Flores, H. (2016). The importance of ice algae-produced carbon in the central Arctic Ocean ecosystem: food web relationships revealed by lipid and stable isotope analyses. *Limnol. Oceanogr.* 61, 2027–2044. doi: 10.1002/lno.10351

Lannuzel, D., Tedesco, L., Van Leeuwe, M., Campbell, K., Flores, H., Delille, B., et al. (2020). The future of Arctic sea-ice biogeochemistry and ice-associated ecosystems. *Nat. Clim. Change* 10, 983–992. doi: 10.1038/s41558-020-00940-4

Metfies, K., Von Appen, W. J., Kilias, E., Nicolaus, A., and Nothig, E. M. (2016). Biogeography and photosynthetic biomass of arctic marine pico-eukaroytes during summer of the record sea ice minimum 2012. *PLoS ONE* 11:e0148512. doi: 10.1371/journal.pone.0148512

Naughten, K. A., De Rydt, J., Rosier, S. H. R., Jenkins, A., Holland, P. R., and Ridley, J. K. (2021). Two-timescale response of a large Antarctic ice shelf to climate change. *Nat. Commun.* 12:1991. doi: 10.1038/s41467-021-22259-0

Nöthig, E. M., Bracher, A., Engel, A., Metfies, K., Niehoff, B., Peeken, I., et al. (2015). Summertime plankton ecology in Fram Strait - a compilation of long- and short-term observations. *Polar Res.* 34:23349. doi: 10.3402/polar.v34.23349

Vernet, M., Geibert, W., Hoppema, M., Brown, P. J., Haas, C., Hellmer, H. H., et al. (2019). The Weddell Gyre, Southern Ocean: present knowledge and future challenges. *Rev. Geophys.* 57, 623–708. doi: 10.1029/2018RG000604

Wassmann, P., Kosobokova, K. N., Slagstad, D., Drinkvvater, K. F., Hoperoft, R. R., Moore, S. E., et al. (2015). The contiguous domains of Arctic Ocean advection: trails of life and death. *Prog. Oceanogr.* 139, 42–65. doi: 10.1016/j.pocean.2015.06.011

Conflict of Interest: The authors declare that the research was conducted in the absence of any commercial or financial relationships that could be construed as a potential conflict of interest.

frontiers in Marine Science

ORIGINAL RESEARCH
published: 14 August 2019
doi: 10.3389/fmars.2019.00479

Biodiversity and Species Change in the Arctic Ocean: A View Through the Lens of Nares Strait

Dimitri Kalenitchenko[1,2†], Nathalie Joli[1,2†], Marianne Potvin[1,2], Jean-Éric Tremblay[1] and Connie Lovejoy[1,2]*

[1] *Département de Biologie and Québec Océan, Université Laval and Takuvik Joint International Laboratory (UMI 3376), Université Laval (Canada) – CNRS (France), Québec, QC, Canada,* [2] *Institut de Biologie Intégrative et des Systèmes (IBIS), Université Laval, Québec, QC, Canada*

OPEN ACCESS

Edited by:
Anne Helene Solberg Tandberg, University Museum of Bergen, Norway

Reviewed by:
Zi-Min Hu, Institute of Oceanology (CAS), China
Anna Vader, The University Centre in Svalbard, Norway

***Correspondence:**
Connie Lovejoy
connie.lovejoy@bio.ulaval.ca

†Present address:
Dimitri Kalenitchenko, Centre for Arctic Gas Hydrate, Environment and Climate (CAGE), Department of Geosciences, UiT – The Arctic University of Norway in Tromsø, Tromsø, Norway
Nathalie Joli, CNRS UMR 8197, Institut de Biologie de l'École Normale Supérieure, Paris, France

Specialty section:
This article was submitted to Marine Evolutionary Biology, Biogeography and Species Diversity, a section of the journal Frontiers in Marine Science

Received: *06 May 2019*
Accepted: *16 July 2019*
Published: *14 August 2019*

Citation:
Kalenitchenko D, Joli N, Potvin M, Tremblay J-É and Lovejoy C (2019) Biodiversity and Species Change in the Arctic Ocean: A View Through the Lens of Nares Strait. Front. Mar. Sci. 6:479. doi: 10.3389/fmars.2019.00479

Nares Strait is the northern most outflow gateway of the Arctic Ocean, with a direct connection to the remaining multi-year ice covered central Arctic Ocean. Nares Strait itself flows into the historically highly productive North Water Polynya (Pikialasorsuaq). Satellite data show that Nares Strait ice is retreating earlier in the season. The early season surface chlorophyll signal, which was a characteristic of the North Water, has also moved north into Nares Strait. However, given the vast differences in the hydrography and physical oceanographic structure of the North Water and Nares Strait there is no *a priori* reason to assume that the species assemblages and overall productivity of this region between Greenland and Canada will be maintained in the face of ongoing sea ice decline. The North Water's high marine mammal and bird populations are dependent on seasonally persistent diatom dominated phytoplankton productivity, and although there have been several studies on North Water phytoplankton, virtually nothing is known about the communities in Nares Strait. Here we investigated the microbial eukaryotes, including phytoplankton in Nares Strait using high-throughput amplicon sequencing. Samples were collected from Kennedy Channel below the northern ice edge of Nares Strait through the Kane Basin and into the northern limit of the North Water. The physical oceanographic structure and initial community rapidly changed between the faster flowing Kennedy Channel and the comparatively wider shallower Kane Basin. The community changes were evident in both the upper euphotic zone and the deeper aphotic zone. Heterotrophic taxa were found in the deeper waters along with ice algae that would have originated further to the north following release from the ice. Although there was a high proportion of pan-Arctic species throughout, the Nares Strait system showed little in common with the Northern North Water station, suggesting a lack of connectivity. We surmise that a direct displacement of the rich North Water ecosystem is not likely to occur. Overall our study supported the notion that the microbial eukaryotic community, which supports ecosystem function and secondary productivity is shaped by a balance of historic and current processes, which differed by seascape.

Keywords: marine microbial eukaryotes, pan-Arctic biome, *Phaeocystis*, North Water Polynya, diatoms (Bacillariophyta), ice loss

INTRODUCTION

The Arctic Ocean is being impacted by climate warming and extensive summer ice-retreat in most sectors (Krishfield et al., 2014) including Nares Strait. Nares Strait between Greenland and Ellesmere Island (Canada) is the northernmost outflow gateway of the Arctic Ocean (Münchow and Melling, 2008). The strait connects the Lincoln Sea with Baffin Bay (**Figure 1**). The Lincoln Sea, at the edge of the Arctic Deep Basins, covers the Northern Ellesmere Shelf with source waters from the Beaufort Sea and Canada Basin, and the North Greenland Shelf with source waters from the Central Arctic. The flow out of Nares Strait with an average of 0.8 ± 0.3 Sv is a major source of Arctic and modified Pacific Water (PW) to the North Atlantic and is equivalent to the inflow from Bering Strait into the Arctic Ocean (Coachman and Aagaard, 1988; Münchow et al., 2006). The southward flow exits Nares Strait through a 25 km wide channel with a 220-m deep sill at Smith Sound (Cape York, **Figure 1**) where an ice arch typically forms in winter. This ice arch (or ice bridge) is crucial in maintaining the North Water Polynya, also known as *Pikialasorsuaq* (Jennings et al., 2011), which is a major ecological feature in Northern Baffin Bay. A second more northern ice arch usually forms at the boundary between Nares Strait and the Lincoln Sea, this ice arch regulates ice transport and the open water season within Nares Strait (Moore and McNeil, 2018). The two ice arches breach in summer and the sea ice transported through Nares Strait has a major influence on the surface salinity of the Labrador Sea. Over the last two decades, the date of formation and locations of the ice arches have become variable, which influences the opening date and extent of the North Water Polynya. Over this time period, the earliest open water has been moving north, away from the eastern side of the North Water and into Nares Strait (Preußer et al., 2015). Early season surface chlorophyll, detected via satellite, is also moving away from the North Water into Nares Strait (Marchese et al., 2017).

Generally, arctic photosynthetic planktonic productivity is thought to follow retreating ice edges, and as surface nutrients are drawn down chlorophyll concentrations and phytoplankton productivity become non-detectable (Renaut et al., 2018). In contrast, the North Water Polynya has a much longer productive season, supporting large populations of migrant and resident marine mammal and bird populations (Heide-Jørgensen et al., 2013). The massive annual production of the North Water is linked to regional hydrography, which is influenced by cyclonic circulation. Briefly, deep nutrient rich Atlantic Water (AW) flows north along the Greenland side of Baffin Bay. The deep water upwells along the Greenland coast, providing a source of nutrients to the phytoplankton community, with impacts on local stratification and microbial eukaryotic species distribution (Joli et al., 2018). Due to geography and the Coriolis force, the flow is eventually deflected west to join the south flowing Baffin and Labrador Current system along the coast of Canada. The northern limit of the north flowing deep AW in the North Water is variable. The narrowest most southerly point of Nares Strait at Cape York is still sufficiently wide for opposing baroclinic flows (Leblond, 1980; Münchow et al., 2015) and subsurface north flowing AW could penetrate into Kane Basin, but not to the same extent as in the North Water. In contrast to the North Water, Nares Strait is thought to be a flow through system, consisting of deep channels and more shallow basins (Jackson et al., 2014). This leads to the supposition that Nares Strait and the North Water have different water mass histories, which could lead to distinct marine microbial eukaryote communities.

The differences in hydrography between the North Water Polynya and the Nares Strait system are substantial and as surface productivity moves north there is no *a priori* reason to expect a simple northward displacement of microbial community structure between the two systems. Microbial eukaryotes track their water mass of origin but are subject to differing degrees of selective pressures within their local environment (Monier et al., 2015; Onda et al., 2017). However, little to nothing is known about the species composition of phytoplankton and other microbial eukaryotes within Nares Strait and whether they are similar to species previously reported from the North Water or elsewhere in the Arctic. Given the importance of species for microbial food web function, the biological carbon pump, and benthic pelagic coupling (Mitra et al., 2014; Stasko et al., 2018), there is an urgent need to better understand the species composition of phytoplankton and associated other protist species in this northernmost gateway. To address this, we carried out a survey of microbial eukaryotes in Nares Strait using high-throughput sequencing (HTS) targeting the V4 region of 18S rRNA and the 18S rRNA gene. We sampled the major water masses in the euphotic zone and deeper waters in Kennedy channel and Kane Basin (**Figure 1**). These communities were then compared with a station at the top of the North Water. We also identified likely characteristic or indicator species from the different water masses and regions.

MATERIALS AND METHODS

Study Site

Nares Strait (**Figure 1**) includes Robeson Channel, Hall Basin, Kennedy Channel, and Kane Basin (Vincent and Marsden, 2010). Briefly, the Kennedy Channel is delimited on the northern end by Cape Baird (81° 22.2′ N, 64° 25.8′ W) and Cape Morton (81° 12′ N, 62° 48′ W) and on the southern end by Cape Lawrence (80° 25.2′ N, 69° 13.2′ W) and Cape Jackson (80° 9.6′ N, 67° 0′ W). The seabed can be simplified as a smooth slope progressing north to south from 500 to 250 m depth (**Figure 1**). Kane Basin with an area of 3900 km^2 at the southern end of Nares Strait lies between Kennedy Channel in the north and Smith Sound (78° 15′ N, 74° 0′ W) in the south. Kane Basin is the shallowest region of Nares Strait with a depth 250 m over 72% of the basin. At the center of the northern reaches of the North Water, Stn 120 (77° 19.33′ N, 75° 19.37′ W; **Figure 1**) with a depth of 560 m is influenced by the Northern Baffin Bay currents described above. This study was carried out over 3 days in early August 2014 when the sea ice cover was >90% above Kennedy Channel, but with open waters to the

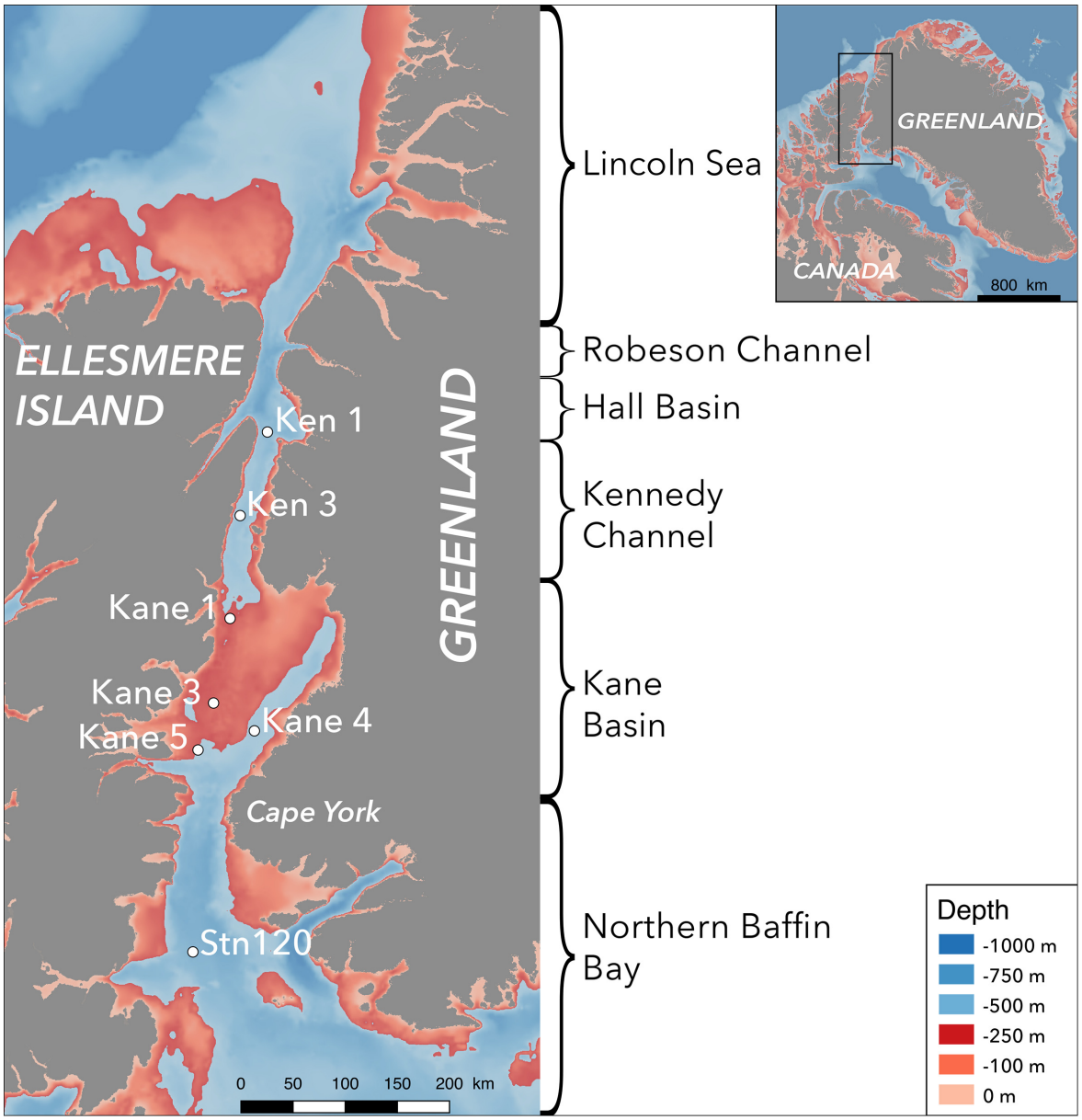

FIGURE 1 | Map of the Nares Strait and top of Baffin Bay, indicating the names of the geographical features and sampling sites. The color scale on the map indicates depth, with shallow depths from 0 and 250 m in reds and deeper waters in blues.

south where all samples were collected. (Canadian Ice Service archive data[1]).

Field Sampling

Sampling was carried out onboard the Canadian icebreaker CCGS Amundsen starting at the top of Kennedy Channel beginning at 18:00 UTC, 3 August and ending in the northern reaches of the North Water at 19:00 UTC on 6 August in 2014 (**Table 1** and **Figure 1**). Seawater was collected directly from 12-L Niskin-type bottles mounted on a Rosette system equipped with a conductivity, temperature, depth profiler (CTD, Sea-Bird SBE-911, Sea-Bird Electronics Inc.), and sensors for chlorophyll fluorescence (Seapoint Sensors Inc.), dissolved oxygen (Seabird SBE-43), fluorescent colored dissolved organic matter (*f*CDOM, Wetlabs ECO), and photosynthetically available radiation (PAR, 400–700 nm; QSP-2300 Biospherical Instruments). Salinity is reported using the TEOS-10 Practical Salinity scale (International Oceaographic Congress et al., 2010). The oxygen sensor was calibrated onboard against Winkler titrations (Ardyna et al., 2011). Chlorophyll concentrations from the fluorescence probe were calibrated from extracted Chl *a* (Ardyna et al., 2011). The *f*CDOM units are relative from factory calibrations. Nutrients

[1]https://iceweb1.cis.ec.gc.ca/Archive/

were sampled directly from the Niskin-type bottles, with samples pre-filtered through a glass fiber filter (GF/F, Whatman) into acid cleaned polyethylene tubes and stored in the dark at 4°C. Nitrite + nitrate (referred to as nitrate hereafter), phosphate, and silicate concentrations were measured colorimetrically (Grasshoff et al., 1999) with a Bran and Luebbe AutoAnalyzer III within a few hours of collection on board the ship.

Discreet sample depths were selected during the downward cast based on the temperature–salinity (TS) and Chl *a* profiles and samples were collected on the upcast. Specifically, for the upper water column (euphotic zone) we targeted: near surface (1 or 2 m), above the Chl *a* fluorescence maximum (Chl max), the Chl max, and below the Chl max (ca. 50 m). For the deeper waters (aphotic zone), the target depths were: the deep temperature minimum, which is characteristic of PW; and at the temperature maximum, which is characteristic of AWs. When sampling opportunities were limited by ship logistics, the temperature minimum was targeted first, followed by at least one sample below this PW mass from presumed AW with warmer temperatures and greater salinities (**Supplementary Table S1**).

Samples for phytoplankton and bacterial enumeration were collected for flow cytometric analysis (FCM) directly from the Niskin-type bottles and fixed by adding 90 μL of 25% glutaraldehyde to 1.8 mL of seawater for a final concentration of 1% (v/v). Preserved samples were left for 30 min at 4°C in the dark, flash frozen in liquid nitrogen, and stored at −80°C. For nucleic acids, water for each depth sampled was collected into cleaned (rinsed with 5% HCL, followed by three rinses each of Milli-Q® water and sample water) 7-L polycarbonate (PC) carboys. For each depth, 5–6 L of seawater was first pre-filtered through a 50-μm mesh, and then sequentially filtered through a 47-mm 3 μm pore size polycarbonate filter and a 0.2-μm pore-size Sterivex™ filter unit (Millipore). The PC filters were placed in microfuge tubes containing RNAlater™ (Thermo Fisher Scientific), which was also added to the Sterivex units. After 30 min at room temperature, filters were transferred to −80°C until analysis. All samples were filtered and preserved within 3 h of collection.

Contribution of Pacific Water to Nares Strait

Water masses evident from the TS diagrams (**Figure 2**) were further characterized by nitrate and phosphate concentrations (**Supplementary Table S1**). To estimate the PW contribution we assumed a linear relationship between total nitrate and phosphate for the AW and PW (Jones et al., 1998; Kawai et al., 2008).

$$NO_3^{AW} = 17.499 \times PO_4^{AW} - 3.072.$$

$$NO_3^{PW} = 13.957 \times PO_4^{AW} - 11.306.$$

The putative proportion of PW was then used as an additional factor for classifying water masses using the unweighted pair group method with arithmetic mean (UPGMA) based on the Euclidian distance similarity matrix calculated with the R package "vegan" v2.4 (Dixon, 2003). Although this method of estimating Pacific versus AW proportions is most often used for describing deeper water masses, where nutrient ratios are more conserved, we applied this to the upper water column samples as well. Given that water from Pacific influenced regions in the Arctic tends to be higher in *f*CDOM compared to AW (Granskog et al., 2012; Gonçalves-Araujo et al., 2018; Makarewicz et al., 2018), our estimated PW proportions were compared with *f*CDOM concentrations.

Laboratory Procedures

The FCM samples were analyzed using a BD Accuri™ C6 flow cytometer (BD Biosciences), equipped with a blue (640 nm) laser. The flow rate was set at 25 mL min^{-1}, and picophytoplankton (1–3 μm) and nanophytoplankton (3–15 μm) were separated based on side scatter and chlorophyll *a* fluorescence (SSC) at 670 nm. For Bacteria and Archaea enumeration, SYBR™ Green (Roche Diagnostic) was added and cells counted as in Marie et al. (2001). Bacteria and Archaea cannot be distinguished by FCM and are referred as Bacteria for convenience.

Nucleic acids from the large and small fractions were extracted from their respective filters, using the AllPrep Mini Kit (Qiagen), with DNA and RNA recovered from the same filters as described previously (Przytulska et al., 2016; Thaler et al., 2017). Following the added DNAase step, RNA purity was verified by PCR as suggested by the manufacturer. RNA was then converted to cDNA using the Applied Biosystems™ High Capacity cDNA Reverse Transcription Kit (Thermo Fisher Scientific). The V4 region of 18S rRNA and 18S rRNA gene was amplified using primers E572F (CYG CGG TAA TTC CAG CTC) and E1009R (CRA AGA YGA TYA GAT ACC RT) as in Comeau et al. (2011). Amplicons were tagged for multiplexing with MiSeq

TABLE 1 | Station location, day, and time of sampling in August 2014.

Region	Station	Depths sampled	Day	Time (UTC)	Latitude (N)	Longitude (W)	z_{Max} (m)
Kennedy Channel	Ken 1	8	03	17:59	81° 22.014	63° 57.427	497
	Ken 3	4	04	07:34	80° 48.022	67° 17.830	403
Kane Basin	Kane 1	4	04	18:34	79° 59.882	69° 45.413	245
	Kane 3	5	05	08:51	79° 21.005	71° 51.908	219
	Kane 4	5	05	13:16	79° 00.371	70° 29.284	208
	Kane 5	8	06	03:58	79° 0.056	73° 12.133	244
NBB	Stn 120	8	06	18:37	77° 19.369	75° 42.156	562

The solar time at these longitudes is approximately UTC – 4 h. Z_{Max} refers to the maximum depth of the station, the top of the North Water is referred to as Northern Baffin Bay (NBB) in the table.

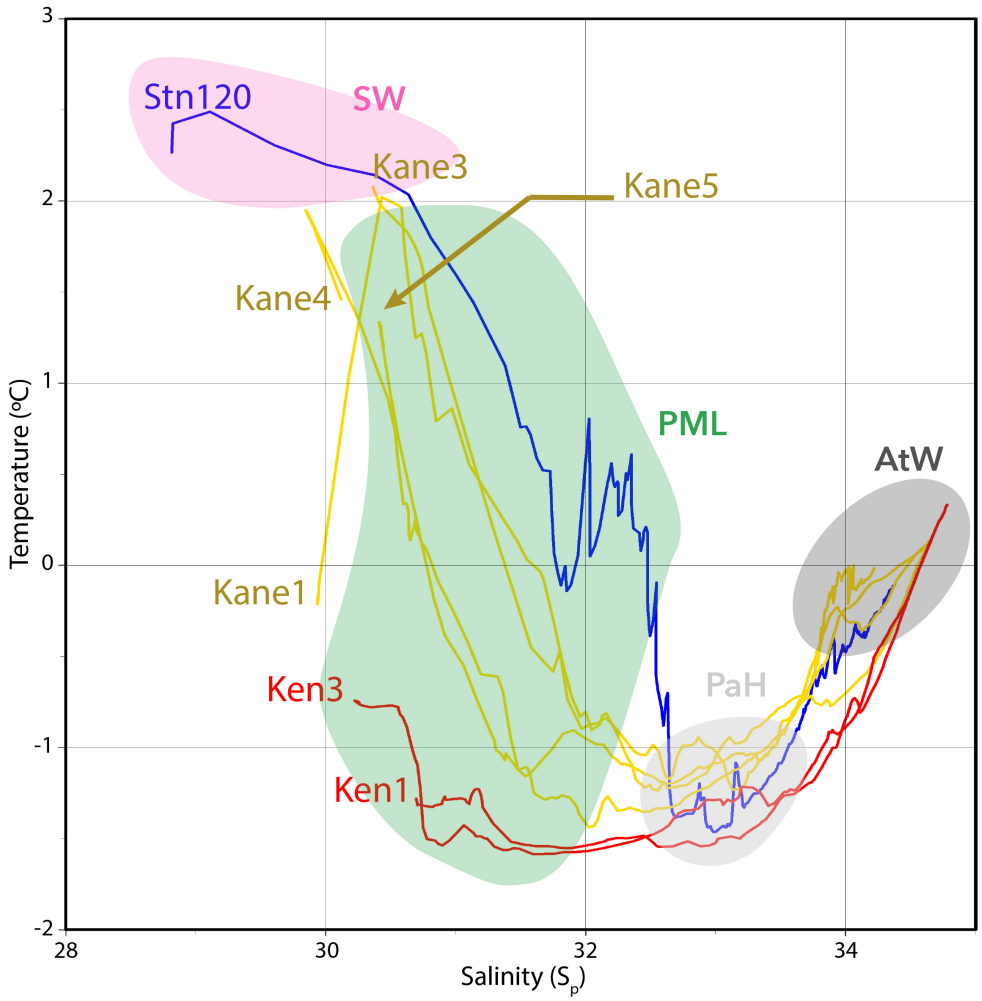

FIGURE 2 | Temperature versus salinity plots of the seven stations. Kennedy Channel stations (Ken) and Kane Basin (Kane) 1 in red; Kane Basin stations 3, 4, and 5 in yellow; and Station 120 in dark blue. The water masses identified in the text are indicated by shading with the polar mixed layer (PML) in green, Pacific Halocline (PaH) in light gray, and deep Atlantic water (AtW) in dark gray. The warmer surface waters (SW) are indicated in pink.

specific linking primers and sequenced on an Illumina MiSeq® by the "Plateforme d'Analyses Génomiques" (IBIS, Université Laval, Canada). Raw sequences are available under Bioproject PRJEB24314 in the European Nucleotide Archive (ENA). Reads originating from DNA template and RNA templates will be referred to as rDNA and rRNA, respectively.

Sequence Data Analysis

We first merged the forward and reverse read pairs using BBMerge (v 37.36, Bushnell et al., 2017) followed by quality filtering with a maxEE parameter of 1 in vsearch (Rognes et al., 2016). The sequence pool was reduced by selecting unique sequences to decrease the computational need for the chimera checking and operational taxonomic unit (OTU) clustering in USEARCH (Edgar, 2010). A similarity threshold of 98%, which was used to define OTUs, generated 1909 OTUs. We then selected the most abundant read of each OTU and found the closest known sequence in our arctic centric microbial eukaryote database (Lovejoy et al., 2016) using the Wang method in mothur (v1.39, Schloss et al., 2009). An OTU table was constructed using the number of copies of each unique sequence of different OTUs and samples. The final OTU table was trimmed to remove OTUs belonging to metazoa and resampled down to 1362 sequences, which was equal to the retained reads for sample *120-40m-L-RNA*. This particular sample had a high proportion of Ctenophora reads and since our goal was to compare beta diversity and the most common OTUs in the different regions, we felt this was preferable to discarding the sample.

Diversity

The two size fractions were independently used to determine beta diversity in the rDNA and rRNA communities. The Bray–Curtis dissimilarity matrices were calculated using the QIIME python package (Caporaso et al., 2010) and the resulting matrices converted into rooted dendrograms using UPGMA. We then matched samples and clustering patterns from the rRNA reads

with the rDNA reads using the R package "phytools" (v0.1.2, Revell, 2011).

For the remaining analyses the large and small fraction results were combined; reads from the same sample that belonged to the same OTU of one size fraction were added to the reads of the other size fraction. Because individual OTUs were mostly found in one or the other fraction, this mathematical operation should not mask or over represent a given OTU.

To explore the gains and losses of abundant OTUs from the northernmost site of Nares Strait through to Stn 120 in the North Water, we categorized OTUs based on their original occurrence at the Kennedy 1 (Ken 1) station. Ken 1 OTUs with occurrences >0.01% were classified based on presence in rRNA and rDNA and by depth (euphotic versus aphotic). Since the goal was not to identify a rare biosphere, for this analysis OTUs with <0.01% of total reads were categorized as "not detected."

We used the Multinomial Species Classification Method (CLAM) test (Chazdon et al., 2011) function in R to find characteristic or indicator OTUs in the two depth categories of the three regions (Kennedy Channel, Kane Basin, and Stn 120 as the North Water representative). Separation of the samples and OTUs was based on a super-majority specialization threshold of 0.75 and a *p*-value of 0.01 divided by the number of OTUs to adjust for multiple comparisons. The rarity threshold was set at 24 sequences. The pairwise CLAM test classified each of the OTUs into: generalists, environment 1 specialist, environment 2 specialist, and OTUs too rare to be assigned to the previous three categories. Three comparisons (Kane vs. Kennedy, Kennedy vs. St 120, and Kane vs. St 120) were applied separately to communities categorized as euphotic rDNA, euphotic rRNA, aphotic rDNA, and aphotic rRNA. This method identified taxa that occurred in single to multiple geographic regions. OTUs were considered characteristic of a particular region if found both the rDNA and the rRNA, since reads from only one of the templates have a greater chance of being either sequencing artifacts (rRNA only) or from dead cells (rDNA) (Blazewicz et al., 2013). The regional indicator OTUs accounting for >1% of the reads in either the euphotic or aphotic zones were further identified using BLASTn analysis (Camacho et al., 2009) against the large NCBI non-redundant nucleotide database (Release 223); all resulting *e*-values were 0.0. Phylogenies of named species were verified by aligning available related longer 18S rRNA genes and RAxML (Stamatakis, 2006).

RESULTS

Oceanographic Properties

Overall, we sampled the four major water masses that flow through Nares Strait (**Figure 2**), with the contribution of PW based on nutrient ratios generally consistent with the TS classifications (**Supplementary Figure S1**). The Deeper AW was defined by high salinity (33.95–34.78, median 34.29), a low putative contribution of PW (5–24%, median 13%) with temperatures around 0°C (−0.46 to +0.33°C, median −0.03°C). The Pacific Halocline was defined by salinities from 32.52 to 33.98 (median 33.13), temperatures from −1.38 to −0.54°C (median −1.21°C), and PW from 22 to 64% (median 42%). Above the Pacific Halocline was a broadly defined Polar Mixed Layer (PML; **Supplementary Figure S1**). Four of the surface samples clustered apart from the PML, with properties consistent ice melt and influenced by solar heating (**Supplementary Figure S1**). This Surface Water was fresher with salinities of 28.89–30.45 (median 30.13), relatively warm from +1.86 to +2.43°C (median +1.91°C) and estimated PW from 14 to 19%. This distinctive Surface Water was first detected in the lower Kane Basin, and had similar physical properties to Surface Water at Stn 120.

Photosynthetically available radiation was <1% of surface irradiance for all of the sampling depths collected from below the PML (**Supplementary Table S1**). Oxygen concentrations tended to be under-saturated in the Kennedy Channel photic zone ranging from 89 to 94% and more variable in the upper waters of the Kane Basin. Oxygen was always under-saturated in the deeper samples going as low as 66% in some of the Kane Basin waters (**Supplementary Table S1**). *f*CDOM was relatively high in all samples from the Nares Strait PML, with a maximum of 11.1 for Ken1–2 m and a minimum 8.66 at Kane3–2 m. The Surface Water *f*CDOM from Nares Strait ranged from 8.25 to 8.67, but was lower at Stn 120 with a value of 6.46. The *f*CDOM values tended to be lower in the Pacific Halocline and AW with median of 7.47 and 5.34, respectively (**Supplementary Table S2**). Within the two major depth categories (euphotic versus aphotic) in Nares Strait, the percent PW based on nutrient ratios was significantly correlated with *f*CDOM (**Figure 3**). The *f*CDOM values were generally lower in the deeper waters and higher in the upper waters. Stn 120 was exceptional with all depths, including the Surface Water and PML samples falling close to the Nares Strait deeper water regression line (**Figure 3**).

The Kennedy Channel sites (Ken 1 and Ken 3) had relatively low chlorophyll and high nutrient concentrations throughout the water column, including within the euphotic zone. A subsurface chlorophyll maximum (SCM) was not detected at either of these two stations (**Supplementary Figure S2**). In contrast, there was a pronounced SCM in Kane Basin, with nutrients depleted in the upper waters. SCM Chl *a* concentrations in Kane 1 and Kane 5 on the western side of Kane Basin were ca. 5 mg m^{-3} and concentrations from Kane 4 on the eastern side were ca. 1.75 mg m^{-3} (**Supplementary Figure S2**). Stn 120 nutrients and Chl *a* levels were both relatively low throughout the water column (**Supplementary Figure S2**).

Euphotic zone bacteria concentrations were lowest at the Ken 1 station and with little change through Nares Strait averaging $1.6 \pm 0.4 \times 10^5$ cells ml^{-1}. By way of comparison, the Stn 120 bacteria concentrations were significantly greater (Wilcoxon test: $W = 0$, p-value = 0.002) with $4.4 \pm 1.3 \times 10^5$ cells ml^{-1}. Bacteria concentrations in the deeper waters increased with decreasing latitude, with a significant correlation between the latitude of collection and log transformed bacteria concentration (ANOVA, $F = 21.89$, p-value = 0.0003). We did not detect any significant latitudinal trends in picophytoplankton or nanophytoplankton concentrations in either euphotic or aphotic water masses (**Supplementary Table S2**).

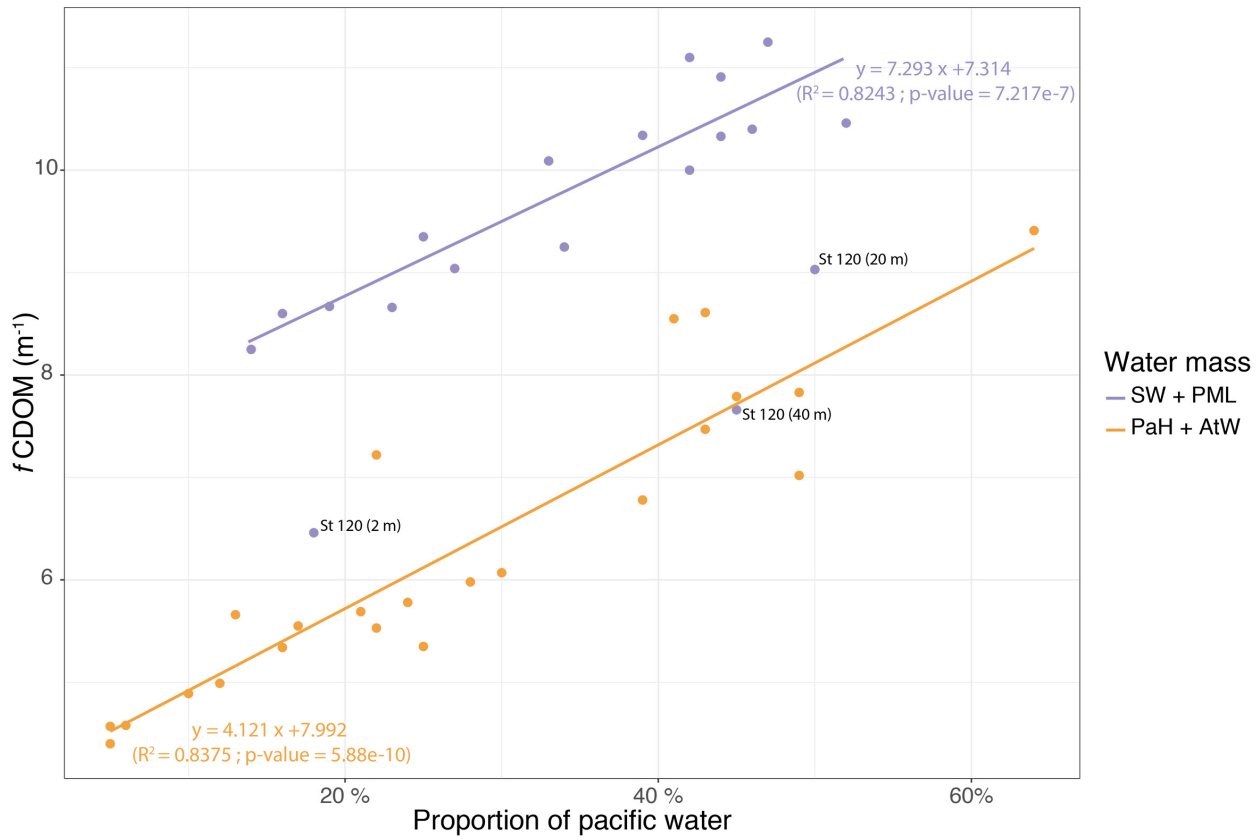

FIGURE 3 | Plot and linear regression of the *f*CDOM values against the calculated PW contribution in the surface (upper line) and deep layer (lower line) of the Nares Strait samples. The Stn. 120 values are indicated separately as gray dots.

Beta Diversity of the Microbial Community

Four libraries per sample were generated consisting of the large and small fractions from RNA and DNA with a total of 15,473,183 reads from the 42 samples (**Table 1**). Of these 2,249,442 sequences were retained after removing metazoa, chimeras, and poor quality reads. To facilitate the analyses for beta diversity and other metrics, the libraries were rarefied down to 1362 reads per library. The 228,816 remaining sequences were then clustered into 1426 OTUs at a similarity level of 98%. Within Nares Strait, the euphotic zone (upper water) samples and the aphotic zone (deeper) samples were separated using Bray–Curtis clustering (**Figure 4**). The Stn 120 communities from rRNA and rDNA were also segregated by depth; however, the 71 and 101 m small fraction communities varied by template. The rDNA communities clustered with the Stn 120 deeper samples, while the rRNA communities from the same depths clustered with euphotic zone samples (**Figure 4**).

Within the broad depth categories, both the rDNA and the rRNA communities predominantly clustered by region (**Figure 4**). One exception to this geographical pattern was the 1 m depth small size fraction community from of the most northern Kane Basin station (Kane 1–1 m S), which clustered with the upper water column Kennedy Channel communities. The Pacific Halocline and AWs clustered together by region with Kane Basin and Kennedy Channel communities forming separate clusters. The Stn 120 deeper communities tended to group within sub-clusters of the Kane Basin. Finally, the large and small fractions formed sub-clusters within their respective regions and depth categories.

Taxonomic Affiliations

At the level of major groups, diatom reads represented >50% of the rDNA and rRNA euphotic zone reads in Kennedy Channel and the Kane 3 and Kane 5 stations, with ca. 40% in Kane 4 (**Figure 5**). Phytoplankton, other than diatoms, were mostly chlorophytes and haptophytes. Among the more abundant heterotrophic flagellates were choanoflagellates, Picozoa, and uncultivated marine stramenopiles (MASTs). In contrast, the Stn 120 euphotic zone communities were <10% diatoms, with higher proportions of chrysophytes, which were rare to absent in the Nares Strait stations (**Figure 5**).

Diatom reads were also present in deeper waters especially in Ken 3 and Kane 1, but for the most part the deeper samples were dominated by heterotrophic groups. These included uncultivated presumably parasitic marine alveolates (MALVs), dinoflagellates, and Rhizaria, which together accounted for over 90% of the rDNA reads and ca. 80% of rRNA reads. The Stn 120, deeper

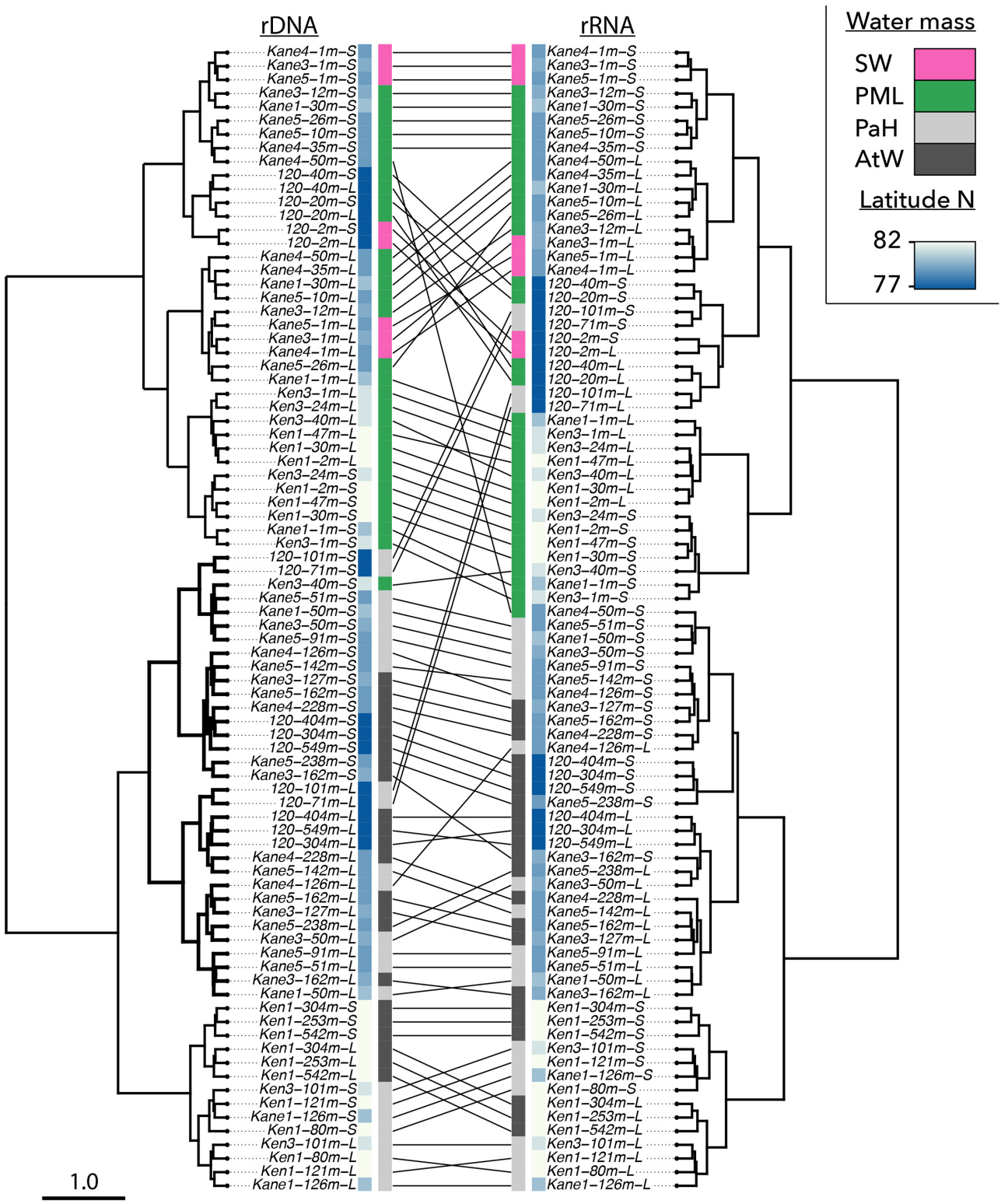

FIGURE 4 | Beta-diversity shown by Bray–Curtis Cluster analyses based on community dissimilarity from the rDNA (left) and rRNA (right) community matrices. In this figure large and small fraction are shown separately. Sample names consist of sampling station, the depth and the fraction (L for large and S for small). Lines between the left and right clusters connect rDNA samples to the corresponding rRNA samples. The inner colored bars indicate the latitude of the samples (in blues), and the water mass classification as given in **Figure 2**. Here, pink for surface water (SW), green for polar mixed layer (PML) waters, light gray for Pacific Halocline (PaH), and dark gray for deep Atlantic Water (AtW).

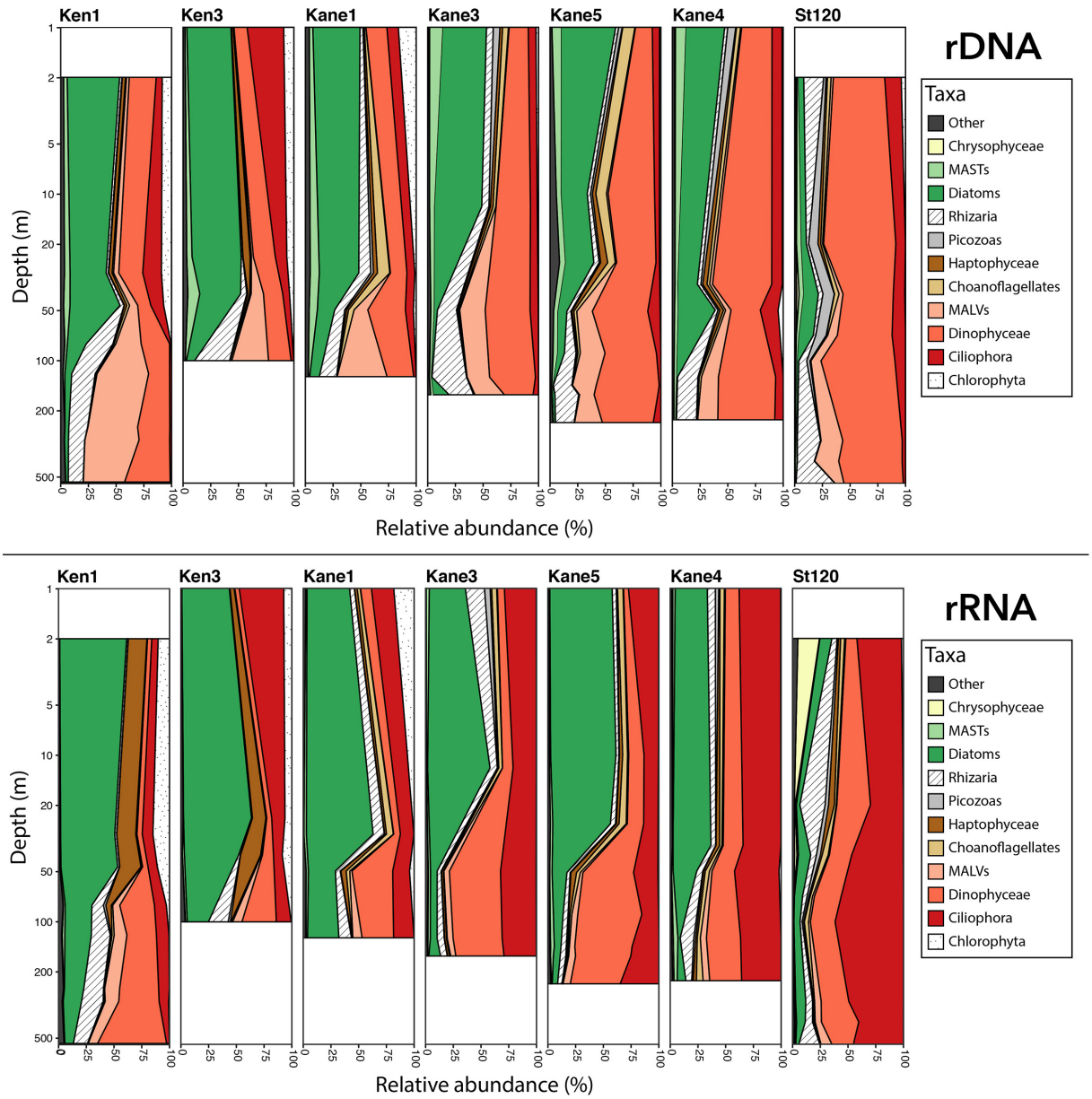

FIGURE 5 | Depth profiles showing the relative proportion of the dominant eukaryote major groups. **Upper panel** shows rDNA and **lower panel** shows rRNA. MASTs and MALVs are defined in the text.

communities resembled the deep water from the more northern stations in terms of major groups and were dominated by dinoflagellates in the rDNA and ciliates in the rRNA. In general, dinoflagellates tended to be overrepresented in the rDNA compared to rRNA and ciliates showed the opposite trend, with a higher proportion of reads in the rRNA compared to rDNA.

At the level of OTUs, the majority (60%) of microbial eukaryotes in Ken 1 were found in all of the "downstream" sites, including Stn 120 (**Supplementary Figures S3, S4**). The "Not detected in Ken1" OTUs at the entrance of Kane basin represented a higher proportion of the community in the rRNA than in the rDNA (W = 1121.5, p-value = 0.03). The only major taxonomic shift based on original abundance and location in Ken 1 was within the "photic rRNA and rDNA" category. The initial high proportion of chlorophyte OTUs in the Ken 1, Ken 3, and Kane 1 were replaced by ciliate OTUs in stations further south (**Supplementary Figure S5**).

Regional Descriptors

We then investigated the distribution and relative abundance of 52 dominant OTUs that were defined as having >1% of reads in the euphotic zone (**Figure 6**) or in the deeper aphotic waters (**Figure 7**). The CLAM test separated out indicator or characteristic OTUs associated with specific regions at the

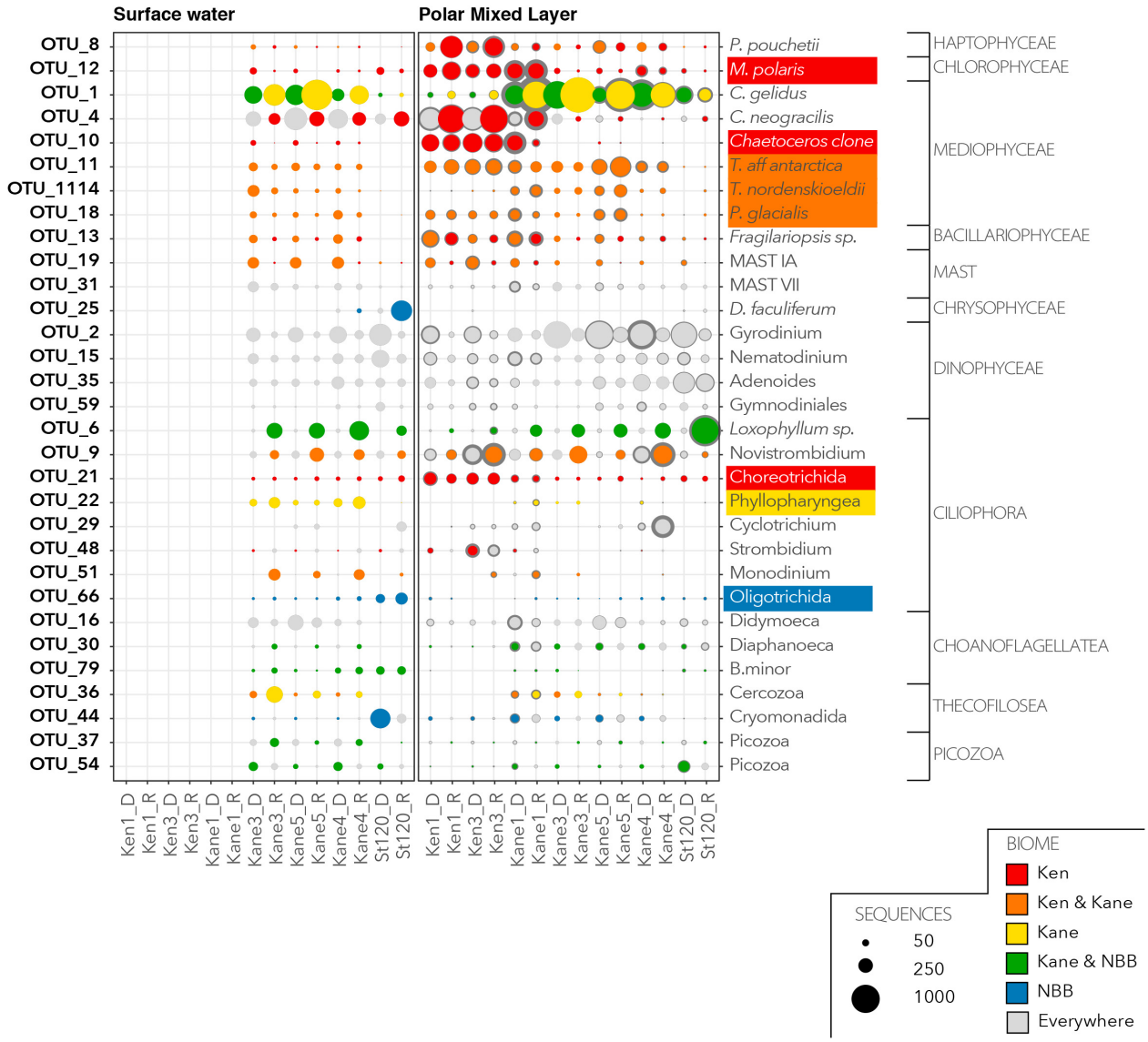

FIGURE 6 | Characteristic OTUs from the euphotic zone communities. Bubble plots of the mean relative abundance of the dominant OTUs in the euphotic zone, separated by water mass categories given in **Figure 2**. For each dominant OTU the bubble size is the mean (light gray or colored dot) and confidence interval (dark gray exterior circle) for the number of OTU reads from each of the rDNA and rRNA communities. Based on the results of the CLAM test, the bubbles with primary colors indicate specificity to a region (red for Kennedy Channel; yellow for Kane Basin; and blue for Northern Baffin Bay). The bubbles in a secondary color are a mix of the contributing primary colors and show OTUs that are considered characteristic of two regions. If an OTU was characteristic of a region in both rDNA and rRNA they were considered representative of the region and the taxonomic assignment is shaded by the color code for the region.

time of sampling. OTU10, OTU21, and OTU12 were the best indicators for the Kennedy Channel euphotic zone (**Figure 6**). OTU10 corresponded to *Chaetoceros* aff. *neogracilis*, OTU21 was a Choreotrich ciliate that matched a Beaufort Sea clone (**Supplementary Table S3**), and OTU12 was *Micromonas polaris*. A number of other OTUs were characteristic of rRNA in the Kennedy Channel but also abundant elsewhere in rDNA, these included *Phaeocystis pouchetti* (OTU8) and a second *C. neogracilis* (OTU4). The deeper waters of Kennedy Channel were characterized by two uncultivated MALVs; OTU26 and OTU82, both with closest matches to other Arctic MALVs (**Supplementary Table S3**). In addition we found the sea ice diatom *Nitzschia frigida* (OTU41 and OTU57) (**Figure 7**).

There was only one narrowly defined Kane Basin euphotic zone regional descriptor: OTU22, which could only be identified as an unclassified Phyllopharyngea ciliate with 99% similar to a sequence from a mesocosm experiment in near Bergen, Norway (**Supplementary Table S3**). *Chaetoceros gelidus* (OTU1) was also prominent in the rRNA communities. There were no deep water Kane Basin descriptors. Several OTUs could be considered descriptors of two contiguous regions (**Figure 6**). For example, OTU11, OTU1114, and OTU18 were associated with both the

FIGURE 7 | Characteristic OTUs from the aphotic zone communities as for **Figure 6** showing the deep water aphotic zone communities.

Kane Basin and the Kennedy Channel within the PML. OTU11 matched *Thalassiosira* aff. *antarctica*, OTU1114 was identified as the Arctic–Boreal species *Thalassiosira nordenskioedii*, and OTU18 was 99% similar to *Porosira glacialis* a psychrophilic diatom (Svenning et al., 2019) in the Thalassiosiraceae. Another MALV, OTU14 was characteristic of the deeper waters of the two regions with closest match to other deep water sequences (**Figure 7** and **Supplementary Table S3**).

For Stn 20, the otherwise rare OTU25 *Dinobryon faculiferum* had a high number of reads in the Surface Water rRNA and a Cryomonadida (OTU44) was abundant in the rDNA (**Figure 6**). The unidentified Oligotrichida OTU66 was found in both rRNA and rDNA in the Surface Water. Several OTUs were characteristic of rRNA in Kane Basin and Stn 120, and also found in the rDNA in all regions. In particular were OTU54, which is an uncultured Picozoa previously detected in the Central Arctic, and OTU79, which was identified as the choanoflagellate *Bicosta minor*. The ciliate *Loxophyllum* sp. (OTU6), which was predominantly in the rRNA of Stn20 and Kane Basin, matched an Arctic ciliate clone (**Supplementary Table S3**).

DISCUSSION

Despite a recent history of being in the dark under multiyear ice, even at Ken 1, the most northern station, there was clear separation between the euphotic and deeper communities. The euphotic zone was dominated by diverse pan-Arctic photosynthetic taxa. The communities in the deeper waters, with the exception of senescent ice algae, were mostly heterotrophic

flagellates, parasitic alveolates, and rhizarians. Within the two broad depth categories, Kennedy Channel and Kane Basin microbial eukaryotic communities clustered apart from each other, mostly driven by the presence of additional taxa in Kane Basin compared to the Kennedy Channel.

Pan-Arctic Phytoplankton Species

Recent culturing efforts have resulted in descriptions of a growing list of endemic species in Arctic Seas (Chamnansinp et al., 2013; Simon et al., 2017; Daugbjerg et al., 2018), many of which were recovered in this first 18S rRNA amplicon study in Nares Strait. Most of the other dominant environmental OTUs detected from the top of Kennedy Channel and through Kane Basin have been previously reported from the Arctic (Lovejoy, 2014) including the Central Arctic, consistent with a pan-Arctic circumpolar Arctic Biome. This reservoir of arctic species tended to remain within their original water masses. However, the changes in relative abundance of species and species associations from the rRNA data indicated that the communities were likely responsive to local environmental conditions. Regional indicator species included *M. polaris*, *Chaetoceros neogracilis*, *C. gelidus*, *Phaeocystis pouchettii*, and several *Thalassiosirales*.

Micromonas polaris (reported as CCMP2099) is practically ubiquitous across the Arctic (Lovejoy et al., 2007; Balzano et al., 2012), but here was characteristic of the Kennedy Channel. *M. polaris* maintains viable cells over prolonged periods of darkness and throughout the polar night (Vader et al., 2015; Joli et al., 2017) and has been reported from ice covered Central Arctic Ocean (Bachy et al., 2011), perhaps persisting by way of phagotrophy (McKie-Krisberg, 2014). The higher proportion of *M. polaris* in Kennedy Channel is consistent with a source population from under the sea-ice. *M. polaris* is well adapted to cold temperatures and low light levels (Lovejoy et al., 2006; Liefer et al., 2018) and able to begin growth before seasonal sea-ice melt in late winter (Joli et al., 2017). The species tends to persist across the Arctic over summer and can dominate photosynthetic biomass under low light conditions in the SCM (Lovejoy et al., 2007).

The two *Chaetoceros* species *C. neogracilis* and *C. gelidus* are both small celled hyalochaetes (lightly silicified and lacking chloroplasts in setae). Although *C. neogracilis* has been reported globally, it is thought that the majority of reports outside of Polar and other ice influenced waters are misidentifications (Balzano et al., 2017). *C. neogracilis* occurs mostly as single cells, sometimes as doublets and the lack of distinguishing features under light microscopy could lead to other small species being misidentified as *C. neogracilis*. The 18S rRNA sequences currently available point to this species being restricted to ice influenced regions including the Baltic and White Sea (Majaneva et al., 2012). In the Nares Strait system, two closely related *C. neogracilis* OTUs were common but had distinct distribution patterns (**Figure 6**). OTU10 was predominant in the Kennedy channel and the Kane 1 sites, whereas OTU4 persisted over the entire region. The ecological separation of the two OTUs highlights the diversity within the current species and a need for further taxonomic revision as suggested by Balzano et al. (2017).

Chaetoceros gelidus showed a very different distribution to *C. neogracilis* and was particularly common in the rRNA libraries from Kane Basin, but also detected in rDNA from Stn 120 (**Figure 6**). *C. gelidus* has recently been described as a separate species from *C. socialis*, which is widely reported throughout the Arctic (Chamnansinp et al., 2013), and many older records of *C. socialis* are probably the newer species. A number of 18S rRNA surveys have confirmed that *C. gelidus* is widely distributed in the Arctic; with reports from the Beaufort Sea (Balzano et al., 2017), the West Greenland Coast (Riisgaard et al., 2015), and the Northern Baffin Bay (Joli et al., 2018). The species thrives under a large range of conditions, for example during a 4 months study of the North Water in 1998, what was likely *C. gelidus* (reported as *C. socialis*) was found throughout the summer (Booth et al., 2002). The *C. socialis–gelidus* complex can form large colonies and, in our study, the same OTU (OTU1) was detected below the euphotic zone, consistent with sedimentation and potentially viable cells moving into the deeper waters of Baffin Bay that could resurface during upwelling events.

Phaeocystis pouchetii, which was found in Kane Basin and Kennedy Channel, has been associated with high biomass (bloom) events, which can have negative impacts other ecosystem properties (Pavlov et al., 2017). *P. pouchetii* also persists over the polar night (Vader et al., 2015) and is a main component of under ice and spring blooms across the Arctic (Riisgaard et al., 2015). Although *P. pouchetii* can occur as small single cells, colonies can become large under bloom conditions and contribute to carbon export and an enhanced biological carbon pump (Wollenburg et al., 2018).

Larger chain forming diatoms in the Thalassiosirales are also associated with blooms, including the North Atlantic spring bloom. In our study, *T.* aff. *antarctica* and *P. glacialis* were dominant in the PML in both Kennedy Channel and Kane Basin. *T. nordenskioeldii*, which has a more pronounced Arctic–Boreal distribution (Luddington et al., 2016), was relatively more common in the Kane Basin.

Arctic Deep Communities

The water that flows into Nares Strait is influenced by the circulation of the Beaufort Gyre and the position of the transpolar drift (Bauch and Cherniavskaia, 2018). In 2014, we were able to discriminate between two deep water masses, based on TS characteristics, which were consistent with Pacific and Atlantic origins. The distinct Pacific layer between the PML and deep AW echo TS profiles from the Canada Basin and Beaufort Gyre. These waters enter Nares Strait from the Western Lincoln Sea flowing over the Northern Ellesmere Shelf (Jackson et al., 2014). The similarity of the microbial eukaryotic communities in the deep Pacific and AW in Kennedy Channel was somewhat surprising, given the strong influence of water masses in the upper 200 m of the Beaufort Sea (Lovejoy and Potvin, 2011; Monier et al., 2015). The long residence time in the Beaufort Gyre and environmental selection for deep water species may have homogenized these communities. However, the species that were recovered suggested some local and more recent influences. Within Nares Strait, we found regional differences, with the Kennedy Channel deep communities differing from Kane Basin

deep communities. Notably, major indicator taxa for deep Kennedy Channel samples were two putative parasitic MALVs and the sea ice diatom *N. frigida*. The most likely source of the diatom in the deeper waters would be sedimentation and lateral (advective) transport of ice algae from upstream of our sampling effort, similar to the massive ice-algae community reported in the deep waters of the Central Arctic (Boetius et al., 2013). No corresponding deep water chlorophyll maximum was detected in our fluorescence profiles, suggesting that the reads originated from cysts or cells with low Chl *a* fluorescence, as reported for some diatoms (Ellegaard and Ribeiro, 2018). In addition, the near absence of *N. frigida* in the surface was evidence of a lack of vertical continuity between the surface and deep waters at a given station. Assuming an ice algal sinking rate of 2–20 m per day (Aumack and Juhl, 2015), it could take as few as 3 or as many as 30 days for ice algae released from ice to arrive at the depth of the PW. Following release from the ice, the algae would be displaced by the strong north to south currents in Nares Strait; the upper PML of Nares Strait has a mean flow of 0.15 m s^{-1}, but below 200 m the currents are much slower at <0.05 m s^{-1} (Münchow et al., 2007; Rabe et al., 2010). This means that the surface layer is moving south three times faster than the deeper waters. The distance between Ken 1 and Kane 1 is 1.68 degrees of latitude (ca. 180 km), and the ice algae possibly traveled from 14 to 41 days prior to reaching Kane Basin. The presence of *N. frigida* in the rRNA reads below 90 m suggests that the cells were still viable. However, the lack of a deep Chl *a* fluorescence signal would suggest they were present as ribosomal packed cysts (Blazewicz et al., 2013).

Community Selection

Apart from the North Water Polynya, productivity patterns in the Arctic have most widely been interpreted in terms of seasonality. A typical scenario begins with a deeply mixed water column, then as the water column becomes stratified the communities move from a pre-bloom to a bloom stage. A post-bloom stage follows when nutrients are depleted in the euphotic zone. The fall-winter stage, with low biomass, is driven by low light levels and water column mixing. Applying this conceptual model to the Nares Strait; Chl *a* and nutrient profiles from north to south were consistent with a pre-bloom in Kennedy Channel (Ken 1), followed by the beginning of an upper mixed layer biomass increase in Ken 3. We would have missed any surface bloom in Kane Basin because of our limited temporal coverage. Satellite images of the North Water and Nares Strait from 2014 showed a surface chlorophyll increase beginning in the south of Nares Strait, then moving north and east (Marchese et al., 2017). Consistent with these observations Kane Basin surface nutrient and chlorophyll concentrations would be assumed to have been depleted by early August at the time we sampled and the system was moving into a post-bloom stage.

However, the TS plots (**Figure 2**) suggested a more complex scenario, with solar warming and much fresher water persisting in the surface of Kane Basin, notably for stations 3–5 (**Supplementary Table S1**). In addition, the PML for those three stations showed signs of conductive warming to a depth of ca. 15 m (**Supplementary Figure S2**). The communities in the Kane Basin PML also clustered together, suggesting continued contact and exchange (Monier et al., 2015). To the North, the warm intrusion at 10 m in Kane 1 was consistent with water mass intrusions (warm salty water beneath cold fresh water) associated with cyclonic circulation within the Kane Basin. Such structure suggests that Kennedy Channel and Kane Basin are not a continuous north to south flow through system. The distinct biological communities found in Kennedy Channel compared to Kane Basin strongly argue that the two regions should not be treated as a continuum or single entity following a distance for time seasonal succession pattern.

Outflow shelves, including the Canadian Arctic Archipelago and the North Water in particular, have distinct seasonal production characteristics. Michel et al. (2015) suggested that regions should be put into four conceptual models based on initial nutrient inventories, degree of stratification and light availability due to latitude and ice flow. Briefly, different regions of the Canadian Arctic were classified as having the following characteristics: (1) High initial nutrient, and a highly stratified water column (HN–HS), with Barrow Strait as an example. (2) Low initial nutrients and high stratification (LN–HS) with most of the Beaufort Sea as an example. (3) High nutrients and high mixing (HN–HM) with the North Water, retreating ice edges and wind driven upwelling regions as examples. Finally, (4) variable nutrients and low light (VN–LL), which encompass extremely high latitudes or regions with thick persistent ice. The selectors for microbial species composition in the four conceptual models would differ, with larger diatoms generally favored in the regions with higher nutrient inventories and sufficient light (HN–HS and HN–HM). The seasonal progression of species and production are distinct in the four cases and the implication is that productivity and ecosystem function are constrained by hydrography and latitude. The same patterns cannot simply be displaced north, with consequences for upper trophic levels. An ongoing long productive season only occurs under the HN–HM regime such as seen in the North Water. The other three scenarios have a single peak in production, with the magnitude dependent on initial nutrient inventories, and light as an additional constraint for the VN–LL regions.

A closer examination of our indicator species suggests that the Michel et al.'s (2015) classification should be applied to Nares Strait. The euphotic zone Kennedy Channel and Kane Basin communities formed two distinct clusters consistent with geography and bathymetry. One exception was the 1 m sample from the most northern Kane Basin site which clustered with upper Kennedy Channel communities suggesting recent cold fresh ice melt surface waters. The question arises as to whether the VN–LL regime in the Kennedy Channel would ever resemble the LN–HS situation in Kane Basin. The much less robust pycnocline in Kennedy Channel does not resemble the LN–HS Beaufort Sea and Amundsen Gulf; the Beaufort Sea is highly stratified even in winter with low nutrients in the upper layers (Simpson et al., 2013). In contrast the high latitude and fast flow of Kennedy Channel means it will likely remain a VN–LL system. The microbial eukaryotic communities in the Kennedy Channel consisted mostly small celled arctic

species, including haptophytes, the arctic endemic *M. polaris* and *C. neogracilis* (**Figure 6**), which is a small non-chain forming diatom (Balzano et al., 2017). Because of large surface to volume ratios, small celled species have an advantage in both light and nutrient limited systems (Raven, 1998). The abundance of nutrients in Kennedy Channel suggests that light limitation due to recent ice cover and perhaps deep mixing was a primary selection agent for the community. The presence of some larger centric diatoms including Boreal–Arctic *Thalassiosira* species (Luddington et al., 2016) in both Kennedy Channel and Kane Basin is consistent with the beginnings of an initial (spring like) bloom in both systems, and not a spring to summer progression. These larger diatoms were recovered in both the rDNA and rRNA at the top of Kennedy Channel suggesting that these species were rapidly responding to increasing light levels (Kvernvik et al., 2018).

All water flowing out of Nares Strait goes over a narrow shallow 220 m sill, which tends to bring deeper PW nearer the surface as it enters Northern Baffin Bay. At the time of sampling in 2014, surface *f*CDOM concentrations at Stn 120 were typical of Pacific influenced waters in the Kane Basin (Kaiser et al., 2017), and did not resemble the PML in Nares Strait. This would suggest that much of the water, including near the surface of Stn 120 had an origin as deeper PW.

Stn 120 Northern North Water communities were sampled at the apex of the complex hydrography of Northern Baffin Bay (Lovejoy et al., 2002; Joli et al., 2018), which is influenced by two major current systems flowing in opposite directions. A strong southward flowing current moves water out of Baffin Bay along the Canadian coast, whereas the West Greenland current on the Greenland side flows north along the coast of Greenland (Bâcle et al., 2002). Because of the Coriolis effect this Northward flow turns left near the top of Northern Baffin Bay (Münchow et al., 2006, 2015) and the two water masses tend to interleave in the center. For example, complex TS profiles were reported at the same latitude in 2005 (Galand et al., 2009), where halocline intrusions were characterized by distinct archaeal phylotypes. In 2014, the cold water intrusion detected at 70–100 m did not resemble any of the water masses in Nares Strait (**Figure 2**) and would be consistent with lateral advection of water from elsewhere. The cold temperature suggests that it may have been be locally formed winter water, where brine is rejected as surface water freezes, creating dense cold saline water. The inconsistencies between the 71 and 100 m rRNA and rDNA communities at Stn 120 (**Figure 4**) would also suggest a changing environment with rDNA reflecting historical conditions and rRNA communities more reflective of the current environment. In this case, the mid-depth (70–100 m) communities were converging to resemble communities found closer to the surface. The low chlorophyll concentrations, high proportion of heterotrophic taxa, and high bacteria concentrations found at Stn 120 could indicate that overall the community was senescent (**Supplementary Tables S1, S2**). However, the high proportion Ctenophore reads suggest that top down selection of the community cannot be ruled out, but quantitative data or grazing studies are needed to verify such a hypotheses.

CONCLUSION

In conclusion, this study gave a first view of the microbial diversity in Nares Strait. We have shown that the Kennedy Channel and Kane Basin are distinct from each other and from the North Water. Given that local hydrography seemed to be the major species driver, we found little indication that Nares Strait will evolve into a high productivity region and replace the central importance of the North Water. Our study provides a baseline for future analysis and a new perspective of the *Pikialasorsuaq* ecoregion. Additional studies and monitoring are needed to evaluate the extent of future change in this high Arctic ecosystem.

SIGNIFICANCE STATEMENT

The Arctic Ocean has limited exchange with other oceans with Nares Strait, the most northern outflow gateway, contributing nutrients and freshwater to downstream ecosystems. Nares Strait is where a significant quantity of Arctic Water exits the Central Arctic Ocean and flows into the highly productive North Water Polynya. As Arctic ice formation and melt patterns change, Nares Strait is becoming biologically active earlier in the season. However virtually nothing is known about the phytoplankton and other protist communities in this northern gateway. Our north to south survey of these microbial eukaryotes revealed predominantly Pan-Arctic species. Two distinct communities were found in the upper sunlit waters, consistent with the hydrography of Nares Strait.

DATA AVAILABILITY

The datasets generated for this study can be found in the ENA under PRJEB24314 with sample data from ERS2074951 to ERS2075117.

AUTHOR CONTRIBUTIONS

CL and J-ÉT designed the study. NJ and CL collected the samples. NJ and MP carried out the laboratory work. DK, NJ, MP, and CL analyzed the data. J-ÉT contributed to the data. DK and CL wrote the manuscript. All authors commented on and contributed to the various versions of the manuscript.

FUNDING

The work was supported by the Natural Sciences and Engineering Research Council of Canada (NSERC) Discovery and Northern Supplement grants to CL and J-ÉT and the Fonds de Recherche du Québec – Nature et Technologies (FRQNT) supporting Québec-Océan. Ship time and logistic support was provided by ArcticNet, a Network of Centers of Excellence (Canada).

ACKNOWLEDGMENTS

This study is a contribution to ArcticNet. We thank P. Guillot for processing CTD data, and J. Gagnon and G. Deslongchamps for nutrient analysis. Support for sequencing was from the Plateforme d'Analyses Génomiques (IBIS, Université Laval), for data analysis from the Comput Canada, and for logistics from the officers and crew of the CCGS Amundsen are acknowledged. The data collected by the CCGS Amundsen were made available through the Amundsen Science program, supported by the Canada Foundation for Innovation and the NSERC.

SUPPLEMENTARY MATERIAL

The Supplementary Material for this article can be found online at: https://www.frontiersin.org/articles/10.3389/fmars.2019.00479/full#supplementary-material

FIGURE S1 | Bray–Curtis cluster analysis grouping the water masses based on the temperature, the salinity, and the Pacific Water contribution (see the text). The dot colors show a normalized representation of each of the three parameters, with blue for the minimum value through to red for the maximum value. The warmed and fresh surface water clustered apart.

FIGURE S2 | Depth profiles of temperature (black), Chl *a* (green), nitrate concentration (red l), and density (blue) at the seven stations sampled.

FIGURE S3 | Decision tree applied to each OTUs present in the Ken1 station to categorize them into each of the eight categories used in source tracking from the rarified data set (see the text). Below each category is the number of sequences and OTUs in the category.

FIGURE S4 | Depth profiles of the rDNA and rRNA fractions showing the relative proportion of sequences belonging to the categories defined from station Kennedy 1 following **Supplementary Figure S3**.

FIGURE S5 | Taxonomic contribution to the categories displayed in **Supplementary Figure S4**, for the rDNA and rRNA fraction. **(a)** "Ken1 All Depths rDNA" and "Ken1 All Depths rDNA and rRNA" categories. **(b)** "Ken1 aphotic rDNA" and "Ken1 aphotic rDNA and rRNA" categories. **(c)** "Ken1 photic rDNA" and "Ken1 photic rDNA and r RNA" categories. **(d)** "Ken1 rRNA only" category. **(e)** "Rare in Ken1" category and **(f)** "Not detected in Ken1" category.

TABLE S1 | Sample ID is the station from **Figure 1** main text and depth in meters (m), salinity (Sal) nitrate, phosphate, and silicate in micrometers, oxygen as percent saturation at depth and photosynthetically available radiation (PAR) as % attenuation relative to first surface reading, values <0.01% are not shown.

TABLE S2 | Additional contextual data. Trip depth is the actual depth (m) recorded as the sample bottle closed on the upward cast. The *f*CDOM (ppb) units refer to factory calibrations and Chl *a* concentrations (mg m^{-3}) estimated from relative fluorescence. Cell counts from FCM for bacteria ($\times 10^5$ cells ml^{-1}), both picophytoplankton (PPP and nanophytoplankton (NPP) in cells ml^{-1}.

TABLE S3 | Closest BLASTn hits, origins, and references were available for the 52 OTUs indicated in **Figures 6**, **7**.

REFERENCES

Ardyna, M., Gosselin, M., Michel, C., Poulin, M., and Tremblay, J.-É. (2011). Environmental forcing of phytoplankton community structure and function in the canadian high arctic: contrasting oligotrophic and eutrophic regions. *Mar. Ecol. Prog. Ser.* 442, 37–57. doi: 10.3354/meps09378

Aumack, C., and Juhl, A. (2015). Light and nutrient effects on the settling characteristics of the sea ice diatom *Nitzschia frigida*. *Limnol. Oceanogr.* 60, 765–776. doi: 10.1002/lno.10054

Bachy, C., López-García, P., Vereshchaka, A., and Moreira, D. (2011). Diversity and vertical distribution of microbial eukaryotes in the snow, sea ice and seawater near the North Pole at the end of the Polar Night. *Front. Microbiol.* 2:106. doi: 10.3389/fmicb.2011.00106

Bâcle, J., Carmack, E. C., and Ingram, G. R. (2002). Water column structure and circulation under the North Water during spring transition: April–July 1998. *Deep Sea Res. Part II Top. Stud. Oceanogr.* 49, 4907–4925. doi: 10.1016/s0967-0645(02)00170-4

Balzano, S., Marie, D., Gourvil, P., and Vaulot, D. (2012). Composition of the summer photosynthetic pico and nanoplankton communities in the beaufort sea assessed by T-RFLP and sequences of the 18S rRNA gene from flow cytometry sorted samples. *ISME J.* 6, 1480–1498. doi: 10.1038/ismej.2011.213

Balzano, S., Percopo, I., Siano, R., Gourvil, P., Chanoine, M., Marie, D., et al. (2017). Morphological and genetic diversity of Beaufort Sea diatoms with high contributions from the *Chaetoceros neogracilis* species complex. *J. Phycol.* 53, 161–187. doi: 10.1111/jpy.12489

Bauch, D., and Cherniavskaia, E. (2018). Water mass classification on a highly variable arctic shelf region: origin of Laptev Sea water masses and implications for the nutrient budget. *J. Geophys. Res.–Oceans* 123, 1896–1906. doi: 10.1002/2017jc013524

Blazewicz, S. J., Barnard, R. L., Daly, R. A., and Firestone, M. K. (2013). Evaluating rRNA as an indicator of microbial activity in environmental communities: limitations and uses. *ISME J.* 7, 2061–2068. doi: 10.1038/ismej.2013.102

Boetius, A., Albrecht, S., Bakker, K., Bienhold, C., Felden, J., Fernández-Méndez, M., et al. (2013). Export of algal biomass from the melting arctic sea ice. *Science* 339, 1430–1432. doi: 10.1126/science.1231346

Booth, B., Larouche, P., Bélanger, S., Klein, B., Amiel, D., and Mei, Z.-P. (2002). Dynamics of *Chaetoceros socialis* blooms in the North Water. *Deep Sea Res. Part II Top Stud. Oceanogr.* 49, 5003–5025. doi: 10.1016/s0967-0645(02)00175-3

Bushnell, B., Rood, J., and Singer, E. (2017). BBMerge – accurate paired shotgun read merging via overlap. *PLoS One* 12:e0185056. doi: 10.1371/journal.pone.0185056

Camacho, C., Coulouris, G., Avagyan, V., Ma, N., Papadopoulos, J., Bealer, K., et al. (2009). BLAST+: architecture and applications. *BMC Bioinformatics* 10:421. doi: 10.1186/1471-2105-10-421

Caporaso, G. J., Kuczynski, J., Stombaugh, J., Bittinger, K., Bushman, F. D., Costello, E. K., et al. (2010). QIIME allows analysis of high-throughput community sequencing data. *Nat. Methods* 7, 335–336. doi: 10.1038/nmeth.f.303

Chamnansinp, A., Li, Y., Lundholm, N., and Moestrup, Ø. (2013). Global diversity of two widespread, colony-forming diatoms of the marine plankton, *Chaetoceros socialis* (syn. *C. radians*) and *Chaetoceros gelidus* sp. nov. *J. Phycol.* 49, 1128–1141. doi: 10.1111/jpy.12121

Chazdon, R. L., Chao, A., Colwell, R. K., Lin, S.-Y., Norden, N., Letcher, S. G., et al. (2011). A novel statistical method for classifying habitat generalists and specialists. *Ecology* 92, 1332–1343. doi: 10.1890/10-1345.1

Coachman, L., and Aagaard, K. (1988). Transports through Bering Strait: annual and interannual variability. *J. Geophys. Res. Oceans* 93, 15535–15539. doi: 10.1029/jc093ic12p15535

Comeau, A. M., Li, W. K., Tremblay, J. -É., Carmack, E. C., and Lovejoy, C. (2011). Arctic ocean microbial community structure before and after the 2007 record sea ice minimum. *PLoS One* 6:e27492. doi: 10.1371/journal.pone.0027492

Daugbjerg, N., Norlin, A., and Lovejoy, C. (2018). *Baffinella frigidus* gen. et sp. nov. (Baffinellaceae fam. nov., Cryptophyceae) from Baffin Bay: morphology, pigment profile, phylogeny, and growth rate response to three abiotic factors. *J. Phycol.* 54, 665–680. doi: 10.1111/jpy.12766

Dixon, P. (2003). VEGAN, a package of R functions for community ecology. *J. Veg. Sci.* 14, 927–930. doi: 10.1111/j.1654-1103.2003.tb02228.x

Edgar, R. C. (2010). Search and clustering orders of magnitude faster than BLAST. *Bioinformatics* 26, 2460–2461. doi: 10.1093/bioinformatics/btq461

Ellegaard, M., and Ribeiro, S. (2018). The long-term persistence of phytoplankton resting stages in aquatic 'seed banks.'. *Biol. Rev.* 93, 166–183. doi: 10.1111/brv.12338

Galand, P. E., Lovejoy, C., Hamilton, A. K., Ingram, G. R., Pedneault, E., and Carmack, E. C. (2009). Archaeal diversity and a gene for ammonia oxidation are coupled to oceanic circulation. *Environ. Microbiol.* 11, 971–980. doi: 10.1111/j.1462-2920.2008.01822.x

Gonçalves-Araujo, R., Rabe, B., Peeken, I., and Bracher, A. (2018). High colored dissolved organic matter (CDOM) absorption in surface waters of the central-eastern Arctic Ocean: implications for biogeochemistry and ocean color algorithms. *PLoS One* 13:e0190838. doi: 10.1371/journal.pone.0190838

Granskog, M. A., Stedmon, C. A., Dodd, P. A., Amon, R. M., Pavlov, A. K., de Steur, L., et al. (2012). Characteristics of colored dissolved organic matter (CDOM) in the arctic outflow in the Fram Strait: assessing the changes and fate of terrigenous CDOM in the Arctic Ocean. *J. Geophys. Res. Oceans* 117:C12021. doi: 10.1029/2012jc008075

Grasshoff, K., Kremling, K., and Ehrhardt, M. (1999). *Methods of Seawater Analysis*, 3rd Edn. Hoboken, NY: John Wiley & Sons, 632.

Heide-Jørgensen, M., Burt, L. M., Hansen, R., Nielsen, N., Rasmussen, M., Fossette, S., et al. (2013). The significance of the North Water Polynya to arctic top predators. *Ambio* 42, 596–610. doi: 10.1007/s13280-012-0357-3

International Oceaographic Congress, SCOR, and IAPSOS. (2010). *The International Thermodynamic Equation of Seawater–2010: Calculation and use of Thermodynamic Properties*. Paris: UNESCO, 196.

Jackson, J. M., Lique, C., Alkire, M. B., Steele, M., Lee, C. M., Sethie, W. M., et al. (2014). On the waters upstream of Nares Strait, Arctic Ocean, from 1991 to 2012. *Cont. Shelf Res.* 73, 83–96. doi: 10.1016/j.csr.2013.11.025

Jennings, A., Sheldon, C., Cronin, T., Francus, P., Stoner, J., and Andrews, J. (2011). The holocene history of Nares Strait: transition from glacial bay to Arctic-Atlantic throughflow. *Oceanography* 24, 26–41. doi: 10.5670/oceanog.2011.52

Joli, N., Gosselin, M., Ardyna, M., Babin, M., Onda, D., Tremblay, J. -É., et al. (2018). Need for focus on microbial species following ice melt and changing freshwater regimes in a Janus Arctic Gateway. *Sci. Rep.* 8, 9405. doi: 10.1038/s41598-018-27705-6

Joli, N., Monier, A., Logares, R., and Lovejoy, C. (2017). Seasonal patterns in arctic prasinophytes and inferred ecology of *Bathycoccus* unveiled in an arctic winter metagenome. *ISME J.* 11, 1372–1385. doi: 10.1038/ismej.2017.7

Jones, P. E., Anderson, L. G., and Swift, J. H. (1998). Distribution of Atlantic and Pacific Waters in the upper Arctic Ocean: implications for circulation. *Geophys. Res. Lett.* 25, 765–768. doi: 10.1029/98gl00464

Kaiser, K., Benner, R., and Amon, R. (2017). The fate of terrigenous dissolved organic carbon on the Eurasian shelves and export to the North Atlantic. *J. Geophys. Res. Oceans* 122, 4–22. doi: 10.1002/2016jc012380

Kawai, Y. M., McLaughlin, F., Carmack, E., Nishino, S., and Shimada, K. (2008). Freshwater budget of the Canada Basin, Arctic Ocean, from salinity, $\delta^{18}O$, and nutrients. *J. Geophys. Res. Oceans* 113:C003858. doi: 10.1029/2006jc003858

Krishfield, R., Proshutinsky, A., Tateyama, K., Williams, W., Carmack, E., McLaughlin, F., et al. (2014). Deterioration of perennial sea ice in the Beaufort Gyre from 2003 to 2012 and its impact on the oceanic freshwater cycle. *J. Geophys. Res.Oceans* 119, 1271–1305. doi: 10.1002/2013jc008999

Kvernvik, A., Hoppe, C., Lawrenz, E., Prášil, O., Greenacre, M., Wiktor, J., et al. (2018). Fast reactivation of photosynthesis in arctic phytoplankton during the Polar Night. *J. Phycol.* 54, 461–470. doi: 10.1111/jpy.12750

Leblond, P. (1980). On the surface circulation in some channels of the Canadian Arctic Archipelago. *Arctic* 33, 189–197. doi: 10.2307/40509282

Liefer, J. D., Garg, A., Campbell, D. A., Irwin, A. J., and Finkel, Z. V. (2018). Nitrogen starvation induces distinct photosynthetic responses and recovery dynamics in diatoms and prasinophytes. *PLoS One* 13:e0195705. doi: 10.1371/journal.pone.0195705

Lovejoy, C. (2014). Changing views of arctic protists (marine microbial eukaryotes) in a changing Arctic. *Acta Protozool.* 53, 91–100. doi: 10.4467/16890027ap.14.009.1446

Lovejoy, C., Comeau, A., and Thaler, M. (2016). *Curated Reference Database of SSU rRNA for Northern Marine and Freshwater Communities of Archaea, Bacteria and Microbial Eukaryotes*. Quebec, QC: Nordicana D. doi: 10.5885/45409XD-79A199B76BCC4110

Lovejoy, C., Legendre, L., and Price, N. (2002). Prolonged diatom blooms and microbial food web dynamics: experimental results from an arctic polynya. *Aquat. Microb. Ecol.* 29, 267–278. doi: 10.3354/ame029267

Lovejoy, C., Massana, R., and Pedrós-Alió, C. (2006). Diversity and distribution of marine microbial eukaryotes in the Arctic Ocean and adjacent seas. *Appl. Environ. Microb.* 72, 3085–3095. doi: 10.1128/aem.72.5.3085-3095.2006

Lovejoy, C., and Potvin, M. (2011). Microbial eukaryotic distribution in a dynamic Beaufort Sea and the Arctic Ocean. *J. Plankton Res.* 33, 431–444. doi: 10.1093/plankt/fbq124

Lovejoy, C., Vincent, W. F., Bonilla, S., Roy, S., Martineau, M. J., Terrado, R., et al. (2007). Distribution, phylogeny, and growth of cold-adapted picoprasinophytes in Arctic Seas. *J. Phycol.* 43, 78–89. doi: 10.1111/j.1529-8817.2006.00310.x

Luddington, I. A., Lovejoy, C., and Kaczmarska, I. (2016). Species-rich meta-communities of the diatom order *Thalassiosirales* in the Arctic and northern Atlantic Ocean. *J. Plankton Res.* 38, 781–797. doi: 10.1093/plankt/fbw030

Majaneva, M., Rintala, J.-M., Piisilä, M., Fewer, D. P., and Blomster, J. (2012). Comparison of wintertime eukaryotic community from sea ice and open water in the Baltic Sea, based on sequencing of the 18S rRNA gene. *Polar Biol.* 35, 875–889. doi: 10.1007/s00300-011-1132-9

Makarewicz, A., Kowalczuk, P., Sagan, S., Granskog, M. A., Pavlov, A. K., Zdun, A., et al. (2018). Characteristics of chromophoric and fluorescent dissolved organic matter in the Nordic Seas. *Ocean Sci.* 14, 543–562. doi: 10.5194/os-14-543-2018

Marchese, C., Albouy, C., Tremblay, J. -É, Dumont, D., D'Ortenzio, F., Vissault, S., et al. (2017). Changes in phytoplankton bloom phenology over the North Water (NOW) Polynya: a response to changing environmental conditions. *Polar Biol.* 40, 1721–1737. doi: 10.1007/s00300-017-2095-2

Marie, D., Simon, N., Guillou, L., Partensky, F., and Vaulot, D. (2001). DNA/RNA analysis of phytoplankton by flow cytometry. *Curr. Protoc. Cytom.* 11, 11.12.1–11.12.14. doi: 10.1002/0471142956.cy1112s11

McKie-Krisberg, R. W. (2014). Phagotrophy by the picoeukaryotic green alga *Micromonas*: implications for Arctic Oceans. *ISME J.* 8, 1953–1961. doi: 10.1038/ismej.2014.16

Michel, C., Hamilton, J., Hansen, E., Barber, D., Reigstad, M., Iacozza, J., et al. (2015). Arctic Ocean outflow shelves in the changing Arctic: a review and perspectives. *Prog. Oceanogr.* 139, 66–88. doi: 10.1016/j.pocean.2015.08.007

Mitra, A., Flynn, K., Burkholder, J., Berge, T., Calbet, A., Raven, J., et al. (2014). The role of mixotrophic protists in the biological carbon pump. *Biogeosciences* 11, 995–1005. doi: 10.5194/bg-11-995-2014

Monier, A., Comte, J., Babin, M., Forest, A., Matsuoka, A., and Lovejoy, C. (2015). Oceanographic structure drives the assembly processes of microbial eukaryotic communities. *ISME J.* 9, 990–1002. doi: 10.1038/ismej.2014.197

Moore, G., and McNeil, K. (2018). The early collapse of the 2017 Lincoln Sea ice arch in response to anomalous sea ice and wind forcing. *Geophys. Res. Lett.* 45, 8343–8351. doi: 10.1029/2018gl078428

Münchow, A., Falkner, K. K., and Melling, H. (2007). Spatial continuity of measured seawater and tracer fluxes through Nares Strait, a dynamically wide channel bordering the Canadian Archipelago. *J. Mar. Res.* 65, 759–788. doi: 10.1357/002224007784219048

Münchow, A., Falkner, K. K., and Melling, H. (2015). Baffin Island and West Greenland current systems in northern Baffin Bay. *Prog. Oceanogr.* 132, 305–317. doi: 10.1016/j.pocean.2014.04.001

Münchow, A., and Melling, H. (2008). Ocean current observations from Nares Strait to the west of Greenland: interannual to tidal variability and forcing. *J. Mar. Res.* 66, 801–833. doi: 10.1357/002224008788064612

Münchow, A., Melling, H., and Falkner, K. K. (2006). An observational estimate of volume and freshwater flux leaving the arctic ocean through Nares Strait. *J. Phys. Oceanogr.* 36, 2025–2041. doi: 10.1175/jpo2962.1

Onda, D. F., Medrinal, E., Comeau, A. M., Thaler, M., Babin, M., and Lovejoy, C. (2017). Seasonal and interannual changes in ciliate and dinoflagellate species assemblages in the Arctic Ocean (Amundsen Gulf, Beaufort Sea, Canada). *Front. Mar. Sci.* 4:16. doi: 10.3389/fmars.2017.00016

Pavlov, A. K., Taskjelle, T., Kauko, H. M., Hamre, B., Hudson, S. R., Assmy, P., et al. (2017). Altered inherent optical properties and estimates of the underwater light

field during an Arctic under-ice bloom of *Phaeocystis pouchetii*. *J. Geophys. Res. Oceans* 122, 4939–4961. doi: 10.1002/2016jc012471

Preußer, A., Heinemann, G., Willmes, S., and Paul, S. (2015). Multi-decadal variability of polynya characteristics and ice production in the North Water Polynya by means of passive microwave and thermal infrared satellite imagery. *Remote Sens.* 7, 15844–15867. doi: 10.3390/rs71215807

Przytulska, A., Comte, J., Crevecoeur, S., Lovejoy, C., Laurion, I., and Vincent, W. (2016). Phototrophic pigment diversity and picophytoplankton in permafrost thaw lakes. *Biogeosciences* 13, 13–26. doi: 10.5194/bg-13-13-2016

Rabe, B., Münchow, A., Johnson, H., and Melling, H. (2010). Nares Strait hydrography and salinity field from a 3-year moored array. *J. Geophys. Res. Oceans* 115:C07010. doi: 10.1029/2009jc005966

Raven, J. (1998). The twelfth Tansley Lecture. Small is beautiful: the picophytoplankton. *Funct. Ecol.* 12, 503–513. doi: 10.1046/j.1365-2435.1998.00233.x

Renaut, S., Devred, E., and Babin, M. (2018). Northward expansion and intensification of phytoplankton growth during the early ice-free season in Arctic. *Geophys. Res. Lett.* 45, 10590–10598. doi: 10.1029/2018gl078995

Revell, L. J. (2011). phytools: an R package for phylogenetic comparative biology (and other things). *Methods Ecol. Evol.* 3, 217–223. doi: 10.1111/j.2041-210x.2011.00169.x

Riisgaard, K., Nielsen, T., and Hansen, P. (2015). Impact of elevated pH on succession in the arctic spring bloom. *Mar. Ecol. Prog. Ser.* 530, 63–75. doi: 10.3354/meps11296

Rognes, T., Flouri, T., Nichols, B., Quince, C., and Mahé, F. (2016). VSEARCH: a versatile open source tool for metagenomics. *Peerj* 4:e2584. doi: 10.7717/peerj.2584

Schloss, P. D., Westcott, S. L., Ryabin, T., Hall, J. R., Hartmann, M., Hollister, E. B., et al. (2009). Introducing mothur: open-source, platform-independent, community-supported software for describing and comparing microbial communities. *Appl. Environ. Microb.* 75, 7537–7541. doi: 10.1128/aem.01541-09

Simon, N., Foulon, E., Grulois, D., Six, C., Desdevises, Y., Latimier, M., et al. (2017). Revision of the genus *Micromonas* Manton et Parke (*Chlorophyta*, Mamiellophyceae), of the type species *M. pusilla (Butcher)* Manton & Parke and of the species *M. commoda* van Baren, Bachy and Worden and description of two new species based on the genetic and phenotypic characterization of cultured isolates. *Protist* 168, 612–635. doi: 10.1016/j.protis.2017.09.002

Simpson, K., Tremblay, J., and Price, N. (2013). Nutrient dynamics in the western Canadian Arctic. I. New production in spring inferred from nutrient drawdown in the Cape Bathurst Polynya. *Mar. Ecol. Prog. Ser.* 484, 33–45. doi: 10.3354/meps10275

Stamatakis, A. (2006). RAxML-VI-HPC: maximum likelihood-based phylogenetic analyses with thousands of taxa and mixed models. *Bioinformatics* 22, 2688–2690. doi: 10.1093/bioinformatics/btl446

Stasko, A., Bluhm, B. A., Michel, C., Archambault, P., Majewski, A., Reist, J., et al. (2018). Benthic-pelagic trophic coupling in an arctic marine food web along vertical water mass and organic matter gradients. *Mar. Ecol. Prog. Ser.* 594, 1–19. doi: 10.3354/meps12582

Svenning, J., Dalheim, L., Eilertsen, H., and Vasskog, T. (2019). Temperature dependent growth rate, lipid content and fatty acid composition of the marine cold-water diatom *Porosira glacialis*. *Algal Res.* 37, 11–16. doi: 10.1016/j.algal.2018.10.009

Thaler, M., Vincent, W. F., Lionard, M., Hamilton, A. K., and Lovejoy, C. (2017). Microbial community structure and interannual change in the last epishelf lake ecosystem in the North Polar region. *Front. Mar. Sci.* 3:275. doi: 10.3389/fmars.2016.00275

Vader, A., Marquardt, M., Meshram, A. R., and Gabrielsen, T. M. (2015). Key Arctic phototrophs are widespread in the Polar Night. *Polar Biol.* 38, 13–21. doi: 10.1007/s00300-014-1570-2

Vincent, R. F., and Marsden, R. F. (2010). An analysis of the dissolution of ice in Nares Strait using AVHRR imagery. *Atmosph. Ocean* 39, 209–222. doi: 10.1080/07055900.2001.9649677

Wollenburg, J., Katlein, C., Nehrke, G., Nöthig, E.-M., Matthiessen, J., Gladrow, W.-D., et al. (2018). Ballasting by cryogenic gypsum enhances carbon export in a *Phaeocystis* under-ice bloom. *Sci. Rep.* 8:7703. doi: 10.1038/s41598-018-26016-0

Conflict of Interest Statement: The authors declare that the research was conducted in the absence of any commercial or financial relationships that could be construed as a potential conflict of interest.

frontiers in Marine Science

ORIGINAL RESEARCH
published: 19 June 2020
doi: 10.3389/fmars.2020.00452

Sympagic Fauna in and Under Arctic Pack Ice in the Annual Sea-Ice System of the New Arctic

Julia Ehrlich[1,2], Fokje L. Schaafsma[3], Bodil A. Bluhm[4], Ilka Peeken[2], Giulia Castellani[2], Angelika Brandt[5,6] and Hauke Flores[2]*

[1] Centre of Natural History (CeNak), University of Hamburg, Hamburg, Germany, [2] Alfred Wegener Institute, Helmholtz Centre for Polar and Marine Research, Bremerhaven, Germany, [3] Wageningen Marine Research, Den Helder, Netherlands, [4] Institute of Arctic and Marine Biology, UiT – The Arctic University of Norway, Tromsø, Norway, [5] Senckenberg Research Institute and Natural History Museum, Frankfurt am Main, Germany, [6] Institute of Ecology, Diversity and Evolution, Goethe University, Frankfurt am Main, Germany

A strong decline and thinning of the Arctic sea-ice cover over the past five decades has been documented. The former multiyear sea-ice system has largely changed to an annual system and with it the dynamics of sea-ice transport across the Arctic Ocean. Less sea ice is reaching the Fram Strait and more ice and ice-transported material is released in the northern Laptev Sea and the central Arctic Ocean. This trend is expected to have a decisive impact on ice associated ("sympagic") communities. As sympagic fauna plays an important role in transmitting carbon from the ice-water interface to the pelagic and benthic food webs, it is important to monitor its community composition under the changing environmental conditions. We investigated the taxonomic composition, abundance and distribution of sea-ice meiofauna (here heterotrophs >10 μm; eight stations) and under-ice fauna (here metazoans >300 μm; fourteen stations) in Arctic 1.5 year-old pack ice north of Svalbard. Sampling was conducted during spring 2015 by sea-ice coring and trawling with a Surface and Under-Ice Trawl. We identified 42 taxa associated with the sea ice. The total abundance of sea-ice meiofauna ranged between 580 and 17,156 ind.m^{-2} and was dominated by Ciliophora (46%), Copepoda nauplii (29%), and Harpacticoida (20%). In contrast to earlier studies in this region, we found no Nematoda and few flatworms in our sea-ice samples. Under-ice fauna abundance ranged between 15 and 6,785 ind.m^{-2} and was dominated by Appendicularia (58%), caused by exceptionally high abundance at one station. Copepoda nauplii (23%), *Calanus finmarchicus* (9%), and *Calanus glacialis* (6%) were also very abundant while sympagic Amphipoda were comparatively rare (0.35%). Both sympagic communities showed regional differences in community composition and abundance between shelf and offshore stations, but only for the under-ice fauna those differences were statistically significant. Selected environmental variables moderately explained variations in abundances of both faunas. The results of this study are consistent with predictions of diversity shifts in the new Arctic.

Keywords: Arctic Ocean, Svalbard, sea-ice meiofauna, under-ice fauna, zooplankton, biodiversity, community composition, environmental conditions

OPEN ACCESS

Edited by:
Zhijun Dong,
Yantai Institute of Coastal Zone Research (CAS), China

Reviewed by:
Xiubao Li,
Hainan University, China
Juan Andrés López,
University of Alaska Fairbanks, United States

****Correspondence:***
Julia Ehrlich
julia.ehrlich@awi.de

Specialty section:
This article was submitted to Marine Evolutionary Biology, Biogeography and Species Diversity, a section of the journal Frontiers in Marine Science

Received: *02 March 2020*
Accepted: *22 May 2020*
Published: *19 June 2020*

Citation:
Ehrlich J, Schaafsma FL, Bluhm BA, Peeken I, Castellani G, Brandt A and Flores H (2020) Sympagic Fauna in and Under Arctic Pack Ice in the Annual Sea-Ice System of the New Arctic. Front. Mar. Sci. 7:452. doi: 10.3389/fmars.2020.00452

INTRODUCTION

Arctic pack ice is drift ice which moves with the agitation of winds and currents. It is either annual and reaches a maximum thickness of ∼2 m, or perennial with a thickness of 3–4 m (Haas, 2003; Kwok and Cunningham, 2015). Because sea-ice extent and thickness have been decreasing rapidly over the past five decades, the Arctic Ocean is gradually changing from a perennial sea-ice system to a system dominated by annual sea ice (Serreze et al., 2007; Comiso, 2012; Melnikov, 2018). This shift combined with associated ecosystem changes has coined the term 'The New Arctic' (Jeffries et al., 2013; Carmack et al., 2015; Granskog et al., 2020). More recently, changes in the Transpolar Drift were also characterized. Less sea ice is now reaching the Fram Strait and more ice and ice-transported material is released in the northern Laptev Sea and the central Arctic Ocean (Krumpen et al., 2019).

Sea ice provides a habitat for sympagic communities, which include microalgae and a diversity of heterotrophic protists and metazoans (Gradinger, 1999; David et al., 2015; Bluhm et al., 2018). Sympagic fauna comprises organisms that complete either their entire life cycle within the sea ice (autochthonous fauna) or spend at least part of their life cycle attached to the ice (allochthonous fauna) (Melnikov and Kulikov, 1980; Carey, 1985; Gulliksen and Lønne, 1989). Of these, the small heterotrophic organisms (>10 μm), which live in the brine channels and cavities within the sea-ice matrix, are referred to as sea-ice meiofauna. Some field studies have estimated the abundance and documented the distribution of sea-ice meiofauna in landfast ice (Carey and Montagna, 1982; Friedrich, 1997; Michel et al., 2002), but only few have focused on Arctic pack ice (Gradinger et al., 1992, 2005; Gradinger, 1999). While taxonomic composition of sea-ice meiofauna varies between regions, seasons and ice types, Harpacticoida, Nematoda, Rotifera, Acoela, other flatworms, and various nauplii are frequently occurring taxa (Bluhm et al., 2018). Loss and/or reduction of sea-ice meiofaunal taxa, however, has been reported from sea ice in the central Arctic Beaufort Gyre between the 1970s and 1980s and been related to sea-ice change (Melnikov et al., 2001). The highest sea-ice meiofauna densities are usually found in the bottom layer of the sea ice (Friedrich, 1997; Nozais et al., 2001; Marquardt et al., 2011). This is because the bottom layer has a high probability of colonization from pelagic and benthic fauna and is in free exchange with nutrients from the underlying seawater, which sustain the growth of ice algal food for many of these taxa (Arndt and Swadling, 2006). Ice algae can account for 50% of the primary production in the central Arctic Ocean in summer (Gosselin et al., 1997; Fernández-Méndez et al., 2015) and are a high-quality food source for the Arctic food web (Søreide et al., 2006, 2013; Falk-Petersen et al., 2009; Kohlbach et al., 2016). Sea-ice decline increases the light availability (Nicolaus et al., 2012) and thus the primary production over shelf areas (Arrigo et al., 2008; Ardyna et al., 2014; Arrigo and van Dijken, 2015), whereas primary production in the basins may remain low due to nutrient limitation caused by strong stratification through sea-ice melt (Bluhm and Gradinger, 2008; Tremblay and Gagnon, 2009; Tremblay et al., 2015). By grazing on ice algae, sea-ice meiofauna may represent an important link in the carbon transfer from the sea-ice to pelagic and benthic communities. Gradinger et al. (1999) and Nozais et al. (2001) analyzed the potential role of sea-ice meiofauna in controlling algal production, though they drew contradictory conclusions. Gradinger (1999) found significant positive correlations between ice-algal biomass and meiofauna abundance, indicating a strong trophic link between ice algae and sea-ice meiofauna. In contrast, Nozais et al. (2001) found that the grazing impact of sea-ice meiofauna on ice algae was negligible, suggesting a rather limited contribution of sea-ice meiofauna to the carbon flux in the food web.

Larger taxa such as Amphipoda, Calanoida, and Appendicularia are generally excluded from the narrow-channeled ice matrix but tend to concentrate under the ice (Carey, 1985; Gradinger and Bluhm, 2004; Bluhm et al., 2010). Amphipoda are the most studied organisms of this under-ice fauna (Poltermann et al., 2000; Beuchel and Lønne, 2002; Hop et al., 2011). They can regionally occur in high densities of >100 ind.m^{-2}, though decreasing densities have recently been suspected for the study area (Arctic Council Secretariat, 2016), and decreasing species number from the Beaufort Gyre (Melnikov et al., 2001). In contrast, the ice-association of Calanoida has gained much less attention and only few studies report on their species composition in the ice-water interface layer (Werner and Arbizu, 1999; David et al., 2015). Large copepod species are key drivers of the energy transfer through the Arctic marine ecosystem due to their high-energy lipid compounds and essential fatty acids (Søreide et al., 2010; Darnis et al., 2012; Kohlbach et al., 2016). There are three *Calanus* species in the Eurasian Arctic Ocean: *Calanus finmarchicus*, *Calanus glacialis*, and *Calanus hyperboreus*. They resemble one another morphologically, but differ in body size, reproductive strategy, life cycle, and distribution. While *C. hyperboreus* and *C. glacialis* are of true Arctic origin, *C. finmarchicus* is a boreal North Atlantic species (Conover, 1988; Auel and Hagen, 2002; Hirche and Kosobokova, 2007). In addition, *C. glacialis* and *C. hyperboreus* are dependent on ice algae as a food source at least during parts of their life cycle (Søreide et al., 2010; Kohlbach et al., 2016). In the past, under-ice fauna has mostly been sampled by divers (Arndt and Pavlova, 2005; Hop et al., 2011). This method provides a good small-scale resolution of sea-ice habitats, but does not provide insights into the large-scale spatial variability of the under-ice habitat. The SUIT used in this study overcomes that problem since it enables large-scale horizontal sampling of the 0–2 m surface layer, both under the sea ice and in the open water.

The community structure of sympagic fauna is related to ice age and under-ice topography (Hop et al., 2000; Hop and Pavlova, 2008; Flores et al., 2019). A further decline of sea ice may thus have strong effects on the composition, abundance, and biodiversity of sympagic fauna and, because of their role in the energy transfer to higher trophic levels (Budge et al., 2008), on the entire Arctic marine food web. Therefore, an accurate

Abbreviations: *A.*, *Apherusa*; *C.*, *Calanus*; chl *a*, chlorophyll *a*; CTD, Conductivity Temperature Depth probe; *H′*, Shannon diversity; ind., individuals; *J′*, Pielou's evenness; NMDS, non-metric multidimensional scaling; PCA, principal component analysis; PS, Polarstern; PVC, polyvinylchloride; S, taxa richness; SUIT, Surface and Under-Ice Trawl.

quantification of sympagic fauna in the Arctic Ocean along with environmental properties is crucial to provide a baseline for monitoring the effects of environmental changes on Arctic marine ecosystems. In this study, we combined two sampling methods to comprehensively cover a wide range of sympagic fauna from the Arctic Ocean pack ice. Sea-ice meiofauna was sampled by drilling ice cores on Arctic pack ice and under-ice fauna was sampled with the SUIT in the region of Atlantic Water inflow north of Svalbard during springtime 2015. Our study aimed to:

1. Provide a concurrent inventory of the community composition, biodiversity and abundance of sea-ice meiofauna and under-ice fauna, and
2. Identify key environmental variables of sea ice and the surface water that define in-ice and under-ice habitats and structure the different communities.

MATERIALS AND METHODS

Study Area

During the Polarstern expedition TRANSSIZ ('Transitions in the Arctic Seasonal Sea-Ice Zone,' PS92) from May 19 to June 28, 2015 the composition, abundance, and distribution of sea-ice meiofauna and under-ice fauna were examined. Samples were collected during eight ice stations and fourteen SUIT stations between 7.068–19.907°E and 81.007–82.211°N. Two of the eight sea-ice stations were located on the marginal shelf of north Svalbard (19 and 32), four in the Sophia Basin and on its slope (27, 31, 39, and 47), and two at the Yermak Plateau (43 and 46). In close proximity to each ice station a SUIT station was conducted. Five of the fourteen SUIT stations were located on the marginal shelf of north Svalbard (19 and 32), eight were located in the Sophia Basin and on its slope (27, 28, 31, 38, 39, 47, 48, and 49), and four on the Yermak Plateau (43, 44, 45, and 56) (**Figure 1**).

This region of the Arctic Ocean is characterized by a pronounced inflow of Atlantic Water along the West Spitsbergen Current and the Fram Strait branch. The latter is assumed to carry most of the oceanic heat into the Arctic Ocean (Rudels, 1987; Beszczynska-Möller et al., 2012; Rudels et al., 2013). Around 80°N the Atlantic Water inflow bifurcates due to topographic steering. Here, one part of the current propagates eastward while another part follows the topography around the Yermak Plateau. North of Svalbard the Atlantic Water is flowing close to the surface and thus contributing strongly to seasonal sea-ice melt and delays in the refreezing of the ice during fall (Rudels et al., 2004, 2013). In the past decades, observations in Fram Strait have revealed a warming of the Atlantic Water inflow into the Arctic Ocean. This warming trend reached its maximum in 2006 and has slightly decreased since then (Hughes et al., 2011; Beszczynska-Möller et al., 2012).

Environmental Parameters of Sea Ice at Ice Stations

At each ice station several ice cores were drilled for determination of environmental properties with a Kovacs corer (Kovacs Enterprise, Roseburg, OR, United States; inner diameter: 9 cm). To determine the chlorophyll *a* (chl *a*) concentration, one ice core was taken and the bottom 10 cm were cut into two sections of approximately 5 cm length. Those ice-core sections were then put into polyvinyl chloride (PVC) jars and 200 ml of 0.2 μm filtered seawater were added per 1 cm of ice core. Melting took place in a dark room at 4°C. After melting, the volume of the meltwater was determined and subsamples were filtered through Whatman GF/F filters. The filters were put into liquid nitrogen and kept at −80°C for later analysis. In the laboratories of the Alfred Wegener Institute, pigments including chl *a* were extracted from the filters with 100% Acetone and homogenized. The chl *a* concentration was then measured with high performance liquid chromatography (HPLC) as described in Tran et al. (2013) and calculated mean values of chl *a* concentration were used for further analyses. For ice-temperature measurements, one ice core was put into a PVC halfpipe immediately after coring and the temperature of the bottom 10 cm of the ice core was measured with a temperature probe (Testo 720) in 5 cm intervals. Mean values of those measurements were then calculated. In order to determine bulk salinity, one ice core was taken at each ice station and the bottom 10 cm section was cut off. The segment was put into a PVC jar and melted at 4°C in the dark. The salinity of the melted ice section was then measured with a salinometer (WTW Cond.3110) as described by Peeken (2016). Snow thickness was measured at 5 different points on each coring site by using a meter stick. Mean values were calculated and used for further analyses. Sea-ice thickness was measured using an ice thickness gauge (Kovacs Enterprise, Roseburg, OR, United States), which was lowered through one sea-ice meiofauna hole at each ice station.

Sampling and Processing of Sea-Ice Meiofauna

For sampling of sea-ice meiofauna, two replicate ice cores were drilled at each ice station with a Kovacs corer (Kovacs Enterprise, Roseburg, OR, United States; inner diameter: 9 cm) and the lowermost 10 cm of each ice core were cut off for further examination. The 10 cm ice-core sections were put separately into PVC jars. In the ship's laboratory 200 ml 0.2 μm filtered seawater were added per 1 cm of ice core to prevent the fauna from osmotic stress during melting (Garrison and Buck, 1986). Melting took place in a dark room at 4°C. After melting, the total volume was determined and the sample was then concentrated over 10 μm gauze and fixed in 4% buffered formaldehyde solution until later quantitative analysis in the laboratories of The Arctic University of Norway (UiT). The replicates of all eight ice stations were sorted under a stereo- microscope (Zeiss Discovery.V20) and identified to the lowest taxonomic level possible. Taxonomic names were verified for correctness and synonymy using the World Register of Marine Species (WoRMS[1]).

The number of individuals per liter of melted sea ice was determined by dividing the number of individuals in each sample by the volume of the sample (minus the added filtered seawater). From that the number of individuals per m^2 ($ind.m^{-2}$) was

[1]http://www.marinespecies.org

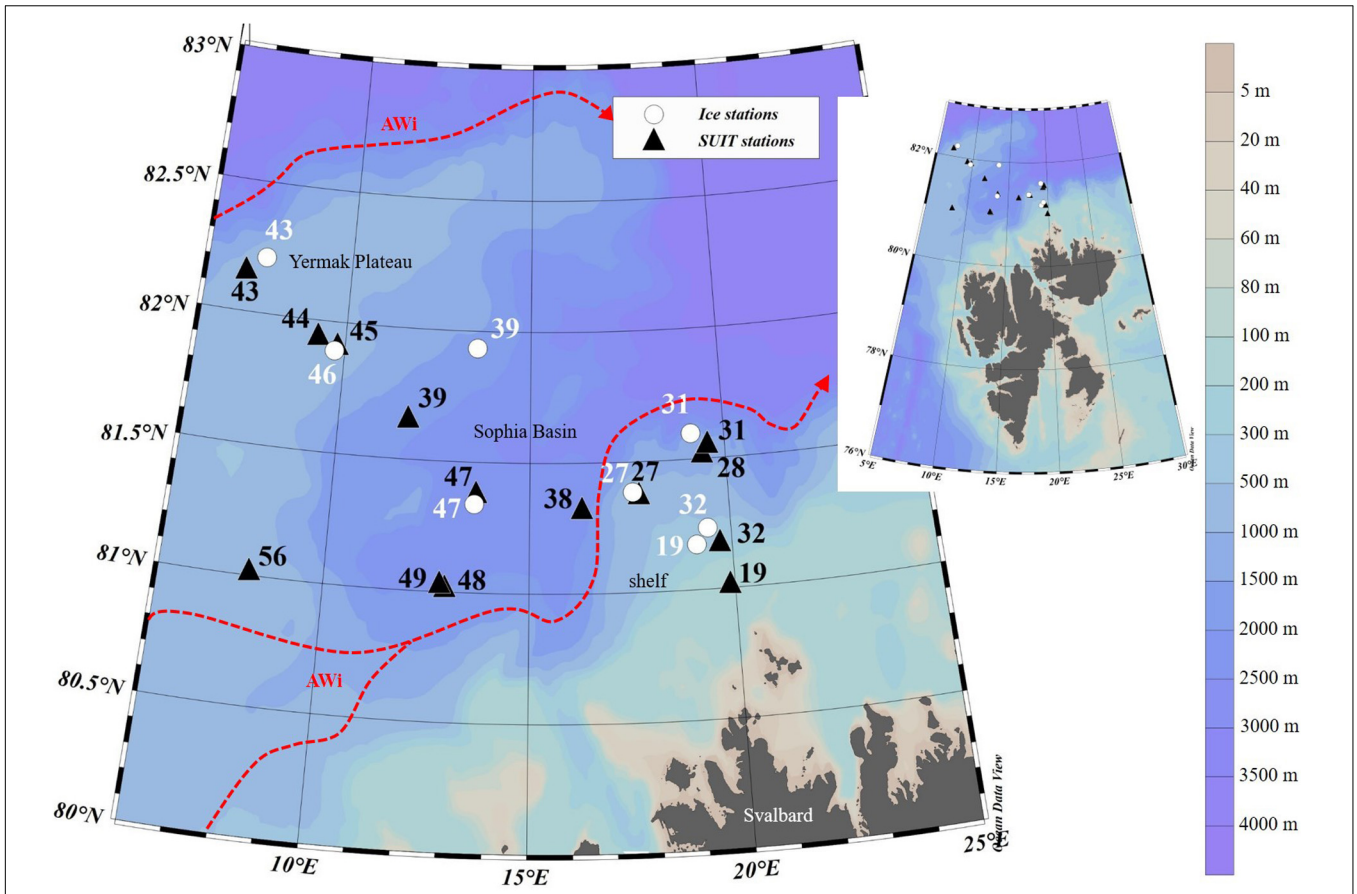

FIGURE 1 | Map of the sampled area north of Svalbard during the Polarstern expedition PS92 including the station numbers of ice and SUIT (Surface and Under-Ice Trawl) stations, the geographical regions, and the Atlantic Water inflow (AWi) originating from the West Spitsbergen Current (according to Renner et al., 2018). The map was created with Ocean Data View software version 5.1.7 (Schlitzer et al., 2018).

then calculated by multiplying by 100, by the height of the ice-core section in meters (0.1 m) and by an ice-to-water density conversion factor of 0.95 (Bluhm et al., 2018). An average was then calculated for the two replicates per station.

Environmental Parameters of Sea Ice and Under-Ice Water at SUIT Stations

An array of sensors was mounted on the SUIT frame in order to collect data on sea-ice and water properties (David et al., 2015; Lange et al., 2016; Castellani et al., in press). It contained an Acoustic Doppler Current Profiler (ADCP, Nortek Aquadopp®, Norway), which measured the velocity and direction of water passing through the net at a frequency of 2 MHZ, and a sampling interval of 1 s, and a CTD (CTD75 M, Sea & Sun Technology, Germany) with built-in fluorometer (Cyclops, Turner Designs, United States), which measured water temperature, salinity and surface water chl *a* concentration every 0.1 s. An altimeter (PA500/6-E, Tritech, United Kingdom) mounted on the CTD probe measured the distance between the net and the sea-ice underside. In combination with pressure data from the CTD, the distance to the sea-ice underside was used to derive ice thickness profiles over the entire SUIT haul (Lange et al., 2016; Castellani et al., in press). For examination of the ridge density the keels of ridges were detected along each profile by using the Rayleigh criterion (Rabenstein et al., 2010; Castellani et al., 2014). For all of the above mentioned parameters mean values were calculated. An observer on deck estimated the snow thickness visually during trawling. These estimates are presented as approximate ranges if variable and are therefore reported in **Table 1**, but were not included in further analyses. Some environmental data were not available at SUIT stations 31 and 32 due to failure of sensors.

Sampling and Processing of Under-Ice Fauna

Sampling of under-ice fauna was performed with the SUIT (van Franeker et al., 2009), which consisted of a steel frame with a 2 m × 2 m opening and two parallel, 15 m long nets attached. One net was a 0.3 mm mesh plankton net covering 0.5 m of the net opening, the other was a 7 mm half mesh covering 1.5 m of the net opening. As this study focused on mesozooplankton (0.3–20 mm), the net used to calculate the abundances of the under-ice fauna was the 0.3 mm zooplankton net. van Franeker et al. (2009), Flores et al. (2012), and David et al. (2015) provided a more detailed description of the SUIT. The catch was concentrated

TABLE 1 | Station table with the general characteristics of the ice stations.

Ice station	Cast number	Date	Lat (N)	Long (E)	Temp [°C]	Sal [PSU]	Chl *a* [$\mu g l^{-1}$]	Chl *a* [$\mu g m^{-2}$]	Btm depth [m]	Ice thick [m]	Snow thick [m]
19	6	28.05.15	81.17	19.13	−2.2	5.1	2.6	255	377	1.1	0.9
27	1	31.05.15	81.39	17.59	−1.6	3.9	2.3	227	877	1.2	0.3
31	2	03.06.15	81.60	19.15	−2.2	5.2	4.8	480	1349	1.2	0.4
32	4	06.06.15	81.24	19.43	−1.7	4.3	7.9	791	462	1.1	0.3
39	9	11.06.15	81.94	13.57	−2.0	5.9	4.7	470	1570	1.3	0.2
43	6	15.06.15	82.21	7.60	−1.4	5.2	2.0	199	806	1.1	0.3
46	3	17.06.15	81.89	9.73	−1.2	4.6	4.1	412	907	1.1	0.1
47	5	19.06.15	81.34	13.61	−1.2	1.7	5.3	529	2173	1.2	0.2

Lat, latitude; Long, longitude; Temp, temperature of the ice; Sal, salinity of the ice; Chl a, chlorophyll a concentration of the ice; Btm depth, bottom depth at ice station; Ice thick, ice thickness; Snow thick, snow thickness at coring site. Temp, Sal, Chl a, and Ice thick are for n = 1; Snow thick is for n = 5.

over a 100 μm sieve and a defined fraction (mostly one half of the original sample) was put in 4% buffered formaldehyde solution for preservation and later quantitative analysis. If the density was still high, the sample was split again with a plankton splitter prior to analysis. The samples of fourteen SUIT stations were sorted and identified to the lowest taxonomic level possible under a stereo- microscope coupled to a digital image analysis system (Leica Model M 205C, image analysis software LAR 4.2 or a Leica Discovery V8 with Axiocam) in the laboratories of the Alfred Wegener Institute. Taxonomic names were verified using the current classification of WoRMS[1]. Classification of *Calanus* spp. individuals to species level (*C. hyperboreus*, *C. glacialis*, and *C. finmarchicus*) was based on length measurements and stage determination according to Madsen et al. (2001). Abundances of ind.m^{-2} were calculated by multiplying the total number of individuals of each taxon in the sample by the respective splitting factor and dividing the result by the water volume sampled by the SUIT at the respective station (measured by the ADCP). The result was then multiplied by the height of the net (2 m) (David et al., 2015).

Data Analysis

A correlation based PCA (Mardia et al., 1979) with Euclidean distance measure was applied to both environmental datasets to reveal habitat typologies of the sea ice and the upper water column (Clarke and Warwick, 2001). Spearman's rank correlation coefficients were used to identify environmental variables with high collinearity (Clarke and Warwick, 2001; Zuur et al., 2007) in order to decide which variables to include in the respective PCA. If pairs of environmental variables had a Spearman's rank correlation coefficient >0.8, only one of the correlated variables was chosen for further analysis based on the relevance of this variable for the scientific question and the comparability to other studies (Zar, 1984). For the ice stations, six environmental variables were analyzed and four were retained for further statistical analysis (**Supplementary Table S1**). For the SUIT stations, seven environmental variables were analyzed and four were retained for further statistical analysis (**Supplementary Table S2**). The PCA was then applied to each normalized environmental dataset.

Three diversity indices were separately calculated for sea-ice meiofauna and under-ice fauna in order to investigate patterns of diversity over the sampled area: (1) Taxa richness (S) (the number of taxa observed per station), (2) Shannon diversity (H), and (3) Pielou's evenness (J') (Shannon and Weaver, 1963; Pielou, 1969). We note that these and subsequent analyses were done separately for sea-ice meiofauna and under-ice fauna communities, because gear types and mesh sizes are not directly comparable.

To visualize community similarity patterns of the sea-ice meiofauna and the under-ice fauna, NMDS (Shepard, 1962; Kruskal, 1964) based on a Bray–Curtis similarity matrix (Bray and Curtis, 1957) was applied to each data set. The four environmental variables selected for the PCA were fitted into the NMDS ordination. The generation of an NMDS is an iterative procedure. It compiles a plot by successively refining the positions of the points until they fit as closely as possible to the dissimilarity relations between the samples (Clarke and

Warwick, 2001). Thus, short distances of sampling sites in the NMDS plot indicate a high similarity in community structure, whereas sampling sites with low similarity are further apart in the ordination plot. The goodness-of-fit of NMDS plots was assessed by Shepard plots and stress values (Clarke and Warwick, 2001; Legendre and Legendre, 2012). A stress value of <0.05 was considered a very good representation with no prospect of misinterpretation (Clarke and Warwick, 2001). We applied the NMDS analysis with different transformations (none to 4th root) of the abundance datasets. The lowest stress values for both sea-ice meiofauna and under-ice fauna datasets were achieved by untransformed abundance data. Based on these untransformed abundance data an analysis of similarity (ANOSIM; Clarke and Ainsworth, 1993) was conducted to test for significant differences of community similarity between *a priori* defined geographical regions (shelf, Yermak Plateau and Sophia Basin with adjacent slope). Again, this analysis was separately performed for sea-ice meiofauna and under-ice fauna. Geographical regions were defined by a combination of water depth and geomorphological structures. Statistical analyses were conducted with the R software Version 3.5.1[2] (R Core Team, 2018) by using the packages: vegan (Oksanen et al., 2018), ggplot2 (Wickham, 2016), dplyr (Wickham and Ruiz, 2018), and scales (Wickham, 2018).

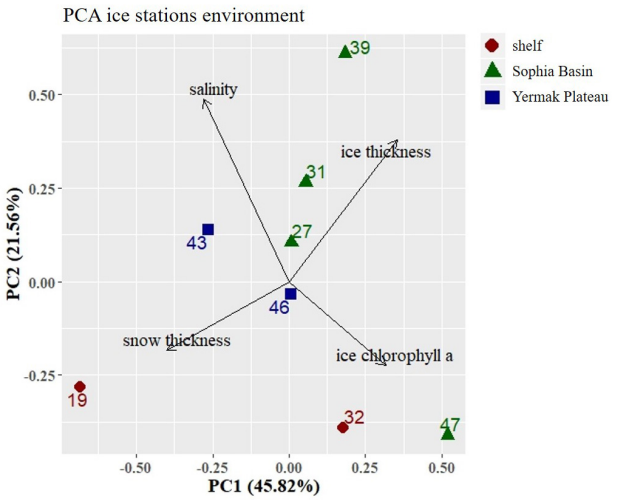

FIGURE 2 | Principal Component Analysis (PCA) plot of environmental parameters at the ice stations. Stations were color-coded according to geographical regions (shelf, Sophia Basin, and Yermak Plateau). Black arrows point into the direction of increasing values of environmental parameters in the ordination. Percentage values in axis annotations indicate the proportion of explained variance of the PCA.

RESULTS

Environmental Conditions at Ice Stations

The ice thickness of the sea-ice cores was very similar among stations and ranged between 1.07 m (station 19) and 1.25 m (station 39) with an average thickness of 1.16 m, reflecting first-year sea ice (**Table 1**). Snow thickness was highest at station 19 with 0.9 m while it ranged for the other stations between 0.13 and 0.4 m, with station 43 having the lowest snow thickness. On average, the stations had a snow thickness of 0.33 m across the sampled area (**Table 1**). The temperature of the sea-ice cores varied between −2.2°C (station 19) and −1.2°C (station 47) with an average temperature of −1.7°C (**Table 1**). Bulk salinity of the bottom 10 cm sea-ice sections stood out at station 47 with a PSU of 1.65. All the other stations ranged in their PSU between 3.88 (station 27) and 5.88 (station 39), with a mean salinity of 4.47 (**Table 1**). Sea-ice chl *a* concentration of the bottom 10 cm of the ice core varied from 199 μgm^{-2} (station 43) to 790 μgm^{-2} (station 32) with an average of 420 μgm^{-2} (**Table 1**).

In the PCA of environmental variables, 67% of variance could be explained by the first two components (**Figure 2**). The first axis (PC1) explained 46% of the variance and was mainly driven by snow thickness. Along this axis there was a distinction between the two shelf stations 19 and 32, with station 19 being strongly influenced by snow thickness (**Figure 2**). The second axis (PC2) explained 22% of the variance and was mainly associated with bulk salinity. Along this axis there was a noticeable, albeit not very strong, regional distinction between the shelf, the Sophia Basin with adjacent slope, and the Yermak Plateau stations (**Figure 2**).

[2]https://www.R-project.org/

Sea-Ice Meiofauna Biodiversity, Taxonomic Composition and Abundance

In total 10 sea-ice meiofauna taxa belonging to five phyla were identified in this study (**Tables 2**, **3** and **Figure 3**). Taxa richness (*S*) ranged from 2 to 8 and Shannon diversity index (H') ranged from 0.60 to 1.53 across ice stations (**Table 2**). The lowest *S* and *H*' were observed at stations in the Sophia Basin and on the Yermak Plateau (stations 39 to 47) (**Table 2**). The ice cores of these stations contained either only Harpacticoida and copepod nauplii (stations 39, 47) or these two taxa and Ciliophora (stations 43, 46) (**Figure 4**). Higher *S* and *H*' were observed at the stations on the Sophia Basin slope and the shelf of Svalbard with station 27 being the station with the highest *S* (8) and H' (1.53) (**Table 2**). Except for Amoebozoa, all phyla were present in the ice cores of this station (**Figure 4**). Pielou's evenness (J') ranged from 0.54 to 0.90 and did not strictly follow the pattern of *S* and H', though values were mostly higher further offshore where stations had low taxa richness and were dominated by Harpacticoida and copepod nauplii (**Table 2** and **Figure 4**). The lowest value of J' was reached at stations closer to the shelf, which were dominated by Ciliophora (**Table 2** and **Figure 4**).

Total abundances of sea-ice meiofauna ranged from 580 ind.m^{-2} (station 39) to 17,156 ind.m^{-2} (station 27) (**Table 2** and **Figure 4**). The most abundant taxon across all stations was Ciliophora with a maximum abundance of 8,562 ind.m^{-2} and an average contribution of 46% to the total sea-ice meiofauna abundance (**Table 3**). Second most abundant were copepod nauplii with a maximum abundance of 7,682 ind.m^{-2} and a share of 29%, and Harpacticoida with a maximum abundance of 4,609 ind.m^{-2} and a share of 20% to the total sea-ice meiofauna

TABLE 2 | List of total abundances and biodiversity indices for sea-ice meiofauna per station.

Sea-ice meiofauna/station	19	27	31	32	39	43	46	47
Total abundance [ind.m^{-2}]	14576	17156	8820	12130	580	3867	3610	6641
Taxa richness (*S*)	7	8	4	7	2	3	3	2
Shannon diversity (*H'*)	1.29	1.53	1.19	1.05	0.60	0.99	0.63	0.62
Pielou's evenness (*J'*)	0.66	0.74	0.86	0.54	0.87	0.90	0.58	0.89

TABLE 3 | List of sea-ice meiofauna taxa with mean abundance and frequency of occurrence across the sample area.

Sea-ice meiofauna taxon	Mean abundance [ind.m^{-2}]	*SD*	Range	Freq. of occurrence [%]	Relative abundance [%]
ARTHROPODA von Siebold, 1848					
Crustacea Brünnich, 1772					
Copepoda Milne Edwards, 1840					
Harpacticoida G.O. Sars, 1903	1710.56	1617.31	0–4609.38	0.88	20.31
Nauplii (copepoda)	2427.70	2336.31	167.41–7681.94	1.00	28.82
ROTIFERA Cuvier, 1817	106.16	216.24	0–593.22	0.25	1.26
CILIOPHORA not documented	3363.15	3414.98	0–8562.06	0.75	39.93
Oligotrichea Bütschli, 1887					
Tintinnina Kofoid and Campbell, 1929	482.75	575.19	0–1525.42	0.63	5.73
MYZOZOA Cavalier-Smith and Chao					
Dinoflagellata not documented					
Dinophyceae Fritsch, 1927					
Protoperidinium Bergh, 1881	123.47	228.84	0–512.13	0.25	1.47
Podolampas Stein, 1883	32.01	90.53	0–256.06	0.13	0.38
Polykrikos Bütschli, 1873 spp.	40.32	85.14	0–237.83	0.25	0.48
Gyrodinium Kofoid and Swezy, 1921	125.75	272.60	0–768.19	0.25	1.49
AMOEBOZOA Lühe, 1913, emend. Cavalier-Smith, 1998	10.59	29.96	0–84.75	0.13	0.13

"Ciliophora" values are excluding "Tintinnina". SD, standard deviation; Freq. of occurrence, frequency of occurrence.

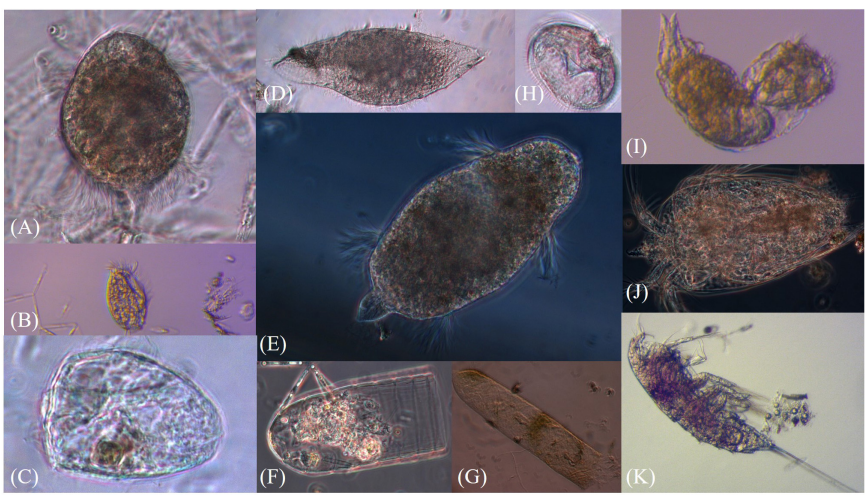

FIGURE 3 | Pictures of sea-ice meiofauna **(A–E)** Ciliophora, **(F,G)** Tintinnina, **(H)** *Protoperidinium* sp., **(I)** Rotifera, **(J)** Nauplius, **(K)** Harpacticoida. Photographs by Julia Ehrlich.

abundance (**Table 3**). The community structure showed some geographical or seasonal/temporal variability, since Rotifera, Dinophyceae, and Amoebozoa occurred solely at the four easternmost stations (stations 19–32) on the shelf of Svalbard and the slope of the Sophia Basin sampled early during the expedition (**Figure 4**). Those stations showed also a higher abundance of Ciliophora compared to the offshore stations (stations 39–47). The NMDS ordination of the sampling stations

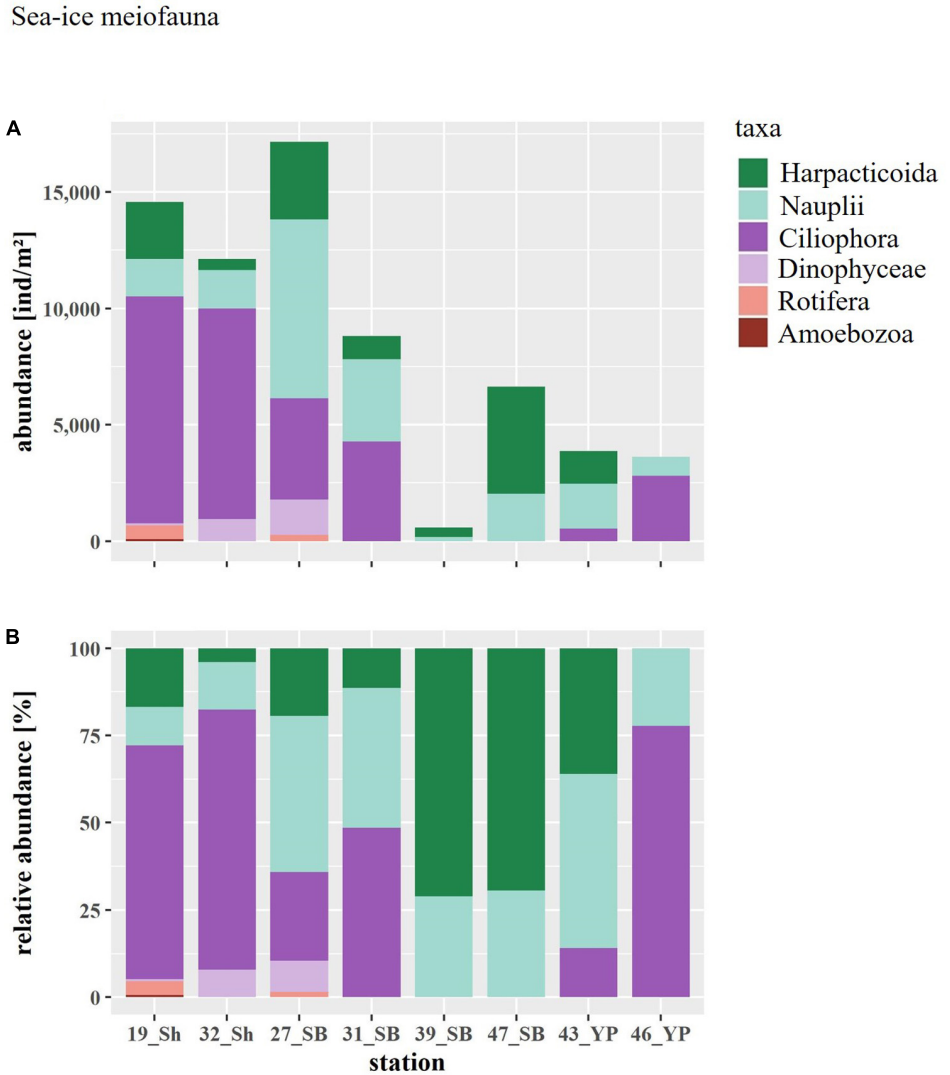

FIGURE 4 | (A) Abundance and **(B)** relative abundance of the sea-ice meiofauna at ice stations arranged by geographical region (Sh, shelf; SB, Sophia Basin; YP, Yermak Plateau).

along ordination axis 1 largely resembled gradual changes in community structure along a quasi-bathymetric gradient from the shelf to the Sophia Basin with adjacent slope and the Yermak Plateau stations (**Figure 5**). However, the conducted ANOSIM showed no significant difference in community similarity between the three regions shelf, Sophia Basin with slope and Yermak Plateau ($\alpha > 0.05$, $R = -0.075$, $p = 0.41$).

Environmental Conditions at SUIT Stations

The bottom depth of the SUIT stations varied considerably during this study from 188 m on the shelf (station 19) to 2,249 m in the Sophia Basin (station 38) (**Table 4**). The average ice coverage in the areas of the under-ice hauls was 51% (**Table 4**). Ice thickness ranged between 1.05 m (station 19) and 3.84 m (station 44), with a mean of 1.70 m across the sampled stations (**Table 4**). The density of sea-ice ridges was highest at station 39 with 11.4 ridges km^{-1} and lowest at station 19 with 1.4 ridges km^{-1}. The average ridge density was 4.9 ridges km^{-1} (**Table 4**). The temperature of the 0–2 m surface water varied between 1.3 and 1.8°C with an average of 1.6°C. Stations on the Svalbard shelf and slope of the Sophia Basin (stations 19, 27, and 28) had lower temperatures (1.3–1.4°C) than stations in the Sophia Basin and on the Yermak Plateau (39–56: 1.6–1.8°C) (**Table 4**). Salinity of the sampled SUIT stations ranged from 33.4 PSU (station 47) to 34.3 PSU (station 45) with a mean salinity of 33.8 PSU (**Table 4**). Chlorophyll *a* concentrations of the surface water varied widely between 540 $\mu g m^{-2}$ at station 43 and 21,158 $\mu g m^{-2}$ at station 47 with an average of 6,967 $\mu g m^{-2}$ (**Table 4**).

The first two components (PC1 and PC2) of the PCA explained 75% of the variance and showed a regional pattern (**Figure 6**). Stations located in the Sophia Basin and adjacent

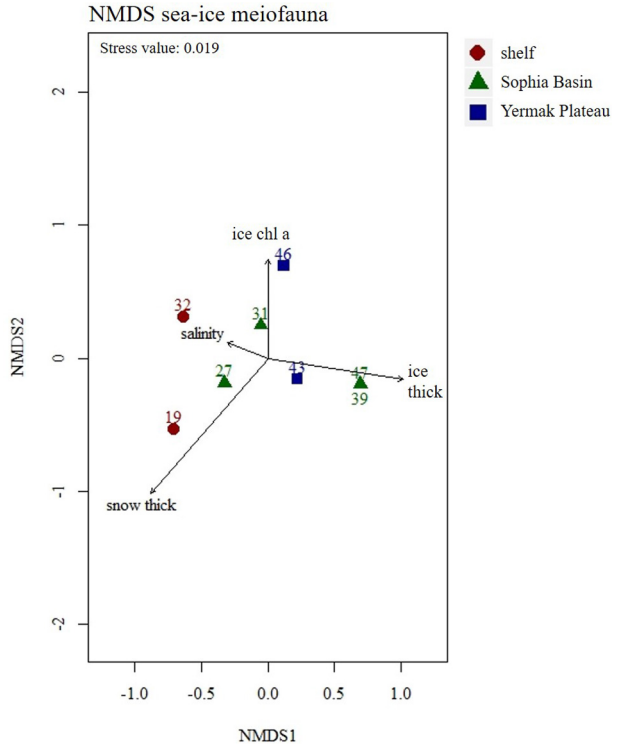

FIGURE 5 | Non-metric Multidimensional Scaling (NMDS) plot of sea-ice meiofauna abundances with four fitted environmental variables. Stations were color coded according to geographical regions (shelf, Sophia Basin, and Yermak Plateau). Ice thick, ice thickness; ice chl *a*, ice chlorophyll *a*; snow thick, snow thickness.

slope grouped together as did those over the Yermak Plateau (**Figure 6**). PC1 explained 50% of the variance and was mainly driven by bottom depth. Along this ordination axis there was a regional distinction between the shelf, the Sophia Basin with adjacent slope, and the Yermak Plateau stations (**Figure 6**). PC2 explained 25% of the variance and was mainly associated with ice thickness. Along this axis there was a clear separation of station 44 from all the other stations, which had an appreciably higher ice thickness than the other stations (**Figure 6**).

Under-Ice Fauna Biodiversity, Taxonomic Composition and Abundance

In total we identified 32 taxa of under-ice fauna from 8 phyla in this study (**Tables 5**, **6** and **Figure 7**). Species richness (*S*) ranged between 7 and 21 with no clear pattern among stations. For example, the lowest and the highest *S* were reached at stations 48 (7 taxa) and 49 (21 taxa), which were geographically closest to each other. Both stations were located in the southern part of the Sophia Basin and dominated by *C. finmarchicus* and *C. glacialis* (**Figure 8**). H' and J' ranged from 0.58 to 1.73 and from 0.21 to 0.80, respectively, again with no clear geographic pattern (**Table 5**). The highest H' and J' were reached at stations 27 and 31 on the slope of the Sophia Basin. Both stations were dominated by equally abundant *C. finmarchicus*, *C. glacialis*, *C. hyperboreus*, and

TABLE 4 | Station table with the general characteristics of the SUIT stations.

SUIT station	Cast number	Date	Lat (N)	Long (E)	Temp [°C]	Sal [PSU]	Chl *a* [$\mu g l^{-1}$]	Chl *a* [$\mu g m^{-2}$]	Btm depth [m]	Ice thick [m]	Snow thick [m]	Filtered vol [m^3]	Ridge dens [km^{-1}]
19	1	27.05.15	81.01	19.89	1.3	33.9	70.3	7032	189	1.1	0.1–0.2	1453	1.4
27	1	31.05.15	81.37	17.75	1.4	33.4	92.2	9218	828	1.1	0.1–0.4	1060	6.3
28	4	02.06.15	81.52	19.42	1.4	34.1	46.0	4600	928	1.3	0.3–0.4	841	4.4
31	1	03.06.15	81.55	19.57	NA	NA	NA	NA	1051	NA	0.2	424	NA
32	12	07.06.15	81.18	19.71	NA	NA	NA	NA	336	NA	0.2	403	NA
38	1	09.06.15	81.32	16.31	1.7	33.7	175.6	17560	2249	1.2	0.1–0.4	1025	4.8
39	17	12.06.15	81.65	11.82	1.8	33.8	9.1	906	1955	1.6	0.1–0.4	657	11.4
43	23	16.06.15	82.16	7.08	1.8	34.1	5.4	540	794	1.8	0.2–0.3	635	1.6
44	1	17.06.15	81.94	9.26	1.8	34.2	7.8	784	814	3.8	0.1–0.2	792	2.6
45	1	17.06.15	81.91	9.80	1.7	34.3	10.4	1044	922	1.8	0.1–0.3	588	3.4
47	1	19.06.15	81.38	13.65	1.7	33.4	211.6	21158	2139	1.5	0.1	551	5.2
48	1	21.06.15	81.02	12.95	1.5	33.5	56.7	5666	2047	1.7	0.1–0.2	1301	5.8
49	1	21.06.15	81.03	12.83	1.6	33.4	111.6	11164	2083	1.9	0.2–0.3	832	4.9
56	2	23.06.15	81.02	8.20	1.7	34.0	39.4	3940	849	2.3	0.05	656	7.2

Lat, latitude; Long, longitude; Temp, temperature of the surface water; Sal, salinity of the surface water; Chl a, chlorophyll a concentration of the surface water; Btm depth, bottom depth; Ice thick, ice thickness; Snow thick, snow thickness; Filtered vol, filtered water volume; Ridge dens, ridge density. Temp, Sal, and Chl a were measured every 0.1 s; Filtered vol was measured every 1 s; Temp, Sal, Chl a, Ice thick, and Ridge dens are averaged measurements over the SUIT transect.

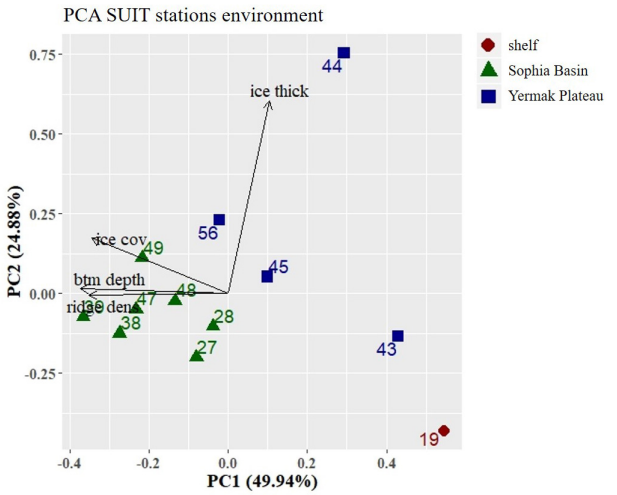

FIGURE 6 | Principal Component Analysis (PCA) plot of environmental parameters at the SUIT stations. Stations were color coded according to geographical regions (shelf, Sophia Basin, and Yermak Plateau). Black arrows point into the direction of increasing values of environmental parameters in the ordination. Percentage values in axis annotations indicate the proportion of explained variance of the PCA. Ice thick, ice thickness; ice cov, ice coverage; btm depth, bottom depth; ridge dens, ridge density.

nauplii. The lowest H' and J' were estimated for the shelf stations 19 and 32, which were dominated by copepod nauplii (**Table 5** and **Figure 8**).

Total abundances of under-ice fauna ranged from 15 ind.m^{-2} (station 44) to 6,785 ind.m^{-2} (station 32) (**Table 5**). The highest total abundances were found at stations in the center of the Sophia Basin (stations 38, 47, and 49) and at the single shelf station, with very high Appendicularia abundance (station 32) (**Figure 8**). The most abundant taxa were Appendicularia with a maximum abundance of 4,915 ind.m^{-2} and an average contribution of 58% to the total under-ice fauna abundance. The high share of Appendicularia to the overall abundance was due to their exceptionally high abundance (4,915 ind.m^{-2}) at station 32. At all other stations, their abundance ranged between 0 and 4 ind.m^{-2} (**Figure 8**). Except for station 32, all other stations were dominated by copepod nauplii with a maximum abundance of 1,747 ind.m^{-2} and a share of 23% to the total under-ice fauna abundance (55% if Appendicularia abundance at station 32 was excluded) (**Table 6** and **Figure 8**). Copepod nauplii were especially abundant at stations, which were sampled early during the expedition (stations 19–39). *C. finmarchicus* was the most abundant copepod species with abundances between 2 and 260 ind.m^{-2} contributing 9% to the total under-ice fauna abundance (20% if Appendicularia at station 32 excluded) (**Table 6** and **Figure 8**). *C. glacialis* ranged between 0.4 and 231 ind.m^{-2} contributing 6% (14% if Appendicularia at station 32 excluded), and *C. hyperboreus* ranged between 0.2 and 49 ind.m^{-2} contributing 2% (5% if Appendicularia at station 32 excluded) to total under-ice fauna abundance (**Table 6** and **Figure 8**). The remaining 27 taxa together made up 2% (6% if Appendicularia at station 32 excluded) of the total under-ice fauna abundance (**Table 6**). The three *Calanus* species were abundant at all fourteen stations and had a constantly high contribution to the under-ice fauna (**Figure 8**). Another taxon with high frequency of occurrence, but mostly low abundances (0–56 ind.m^{-2}) were Cirripedia, which made up 1% of the entire under-ice fauna (3% if Appendicularia at station 32 excluded) (**Table 6** and **Figure 8**). Cirripedia resembled the pattern of copepod nauplii that were mainly abundant at stations sampled early during the expedition (stations 27–39). The NMDS showed no clear separation of distinct communities based on taxa abundances (**Figure 9**). However, the ordination of the sampling stations along ordination axis 2 showed a gradual change in the community similarity from the shelf to the Sophia Basin with adjacent slope and the Yermak Plateau stations (**Figure 9**). This spatial community change was resembled in the conducted ANOSIM showed a significant difference in community similarity between the three regions shelf, Sophia Basin with slope and Yermak Plateau ($\alpha \leq 0.05$, $R = 0.26$, $p = 0.04$).

DISCUSSION

Sea-Ice Meiofauna

During this study, sea-ice meiofauna abundances ranged from 580 to 17,156 ind.m^{-2} in the pack ice north of Svalbard. This abundance range is consistent with that reported from pack ice in the same region two decades earlier (Gradinger et al., 1999). When excluding Ciliophora, which most ice biota studies from the Arctic Ocean do not include, the total abundances of sea-ice meiofauna in this study ranged between 580 and 13,827 ind.m^{-2}. This wide range of abundances is again similar to other pack-ice studies from the geographic area of our study (Schünemann and Werner, 2004; Bluhm et al., 2018) and has also been reported from other locations such as Baffin Bay and the Amerasian Basin (Nozais et al., 2001; Gradinger et al., 2005).

The taxonomic composition showed both similarities and differences to earlier sea-ice meiofauna studies. After Ciliophora, Harpacticoida and copepod nauplii were the most abundant groups, both of which have been consistently reported to occur in sea ice. Harpacticoida are common sea-ice residents and tolerant to extreme conditions such as freezing into solid ice for short periods (Damgaard and Davenport, 1994). Their capability to reproduce several times a year with no interruption during winter (Carey, 1992; Friedrich, 1997) may contribute to their high abundance in our and other studies. For pack ice in the region northwest of Svalbard, similar relative abundances for Copepoda (including Harpacticoida) were reported by Gradinger et al. (1999) and Schünemann and Werner (2004), but nauplii abundances were much lower in those studies. For the pan-Arctic, Bluhm et al. (2018) synthesized 23 studies on sea-ice meiofauna and estimated a mean abundance across all ice types and seasons of 341 ind.m^{-2} for Harpacticoida and 1,141 ind.m^{-2} for nauplii, recognizing that nauplii abundances are highly seasonal. Calanoid copepod nauplii

TABLE 5 | List of total abundances and biodiversity indices for under-ice fauna per station.

Under-ice fauna/station	19	27	28	31	32	38	39	43	44	45	47	48	49	56
Total abundance [ind.m^{-2}]	55	125	61	77	6785	277	25	27	15	57	216	39	548	186
Taxa richness (*S*)	15	9	10	11	14	13	8	10	7	10	17	21	7	11
Shannon diversity (*H'*)	0.58	1.73	1.71	1.93	0.69	1.62	1.58	1.23	1.31	1.21	1.38	1.34	0.99	1.02
Pielou's evenness (*J'*)	0.21	0.79	0.74	0.80	0.26	0.63	0.76	0.53	0.67	0.53	0.49	0.44	0.51	0.42

tend to be encountered in sea ice in highest abundances in springtime (Bluhm et al., 2018) matching the sampling time in this study. In addition, Nozais et al. (2001) suggested that copepods (including Harpacticoida and Cyclopoida) reproduce inside the bottom ice layer itself. Consistent with these findings we suggest that the high densities of nauplii were a result of successful reproduction of copepods inside the sea-ice in our study.

The taxonomic composition of the sea-ice meiofauna in this study, however, also shows some marked differences to earlier studies. Nematoda, Acoela, and platyhelminth flatworms (in earlier studies reported as 'Turbellaria') were among the most abundant taxa in earlier Arctic pack-ice studies (Gradinger, 1999; Nozais et al., 2001; Gradinger et al., 2005) including the region north of Svalbard (Gradinger et al., 1999; Schünemann and Werner, 2004), but neither of these taxa were observed in this study. Essentially the same pattern (absence of flatworms and nematodes except for a single ice core) was found in a parallel study in the same area that extended over six months comprising the entire ice-covered period (N-ICE data set in Bluhm et al., 2018; Granskog et al., 2018) suggesting our finding was not barely a bias of our limited sample size or the time point of our sampling. As Nematoda are thought to colonize the sea ice in shallow waters from the sediment, where they dominate the meiofauna of the benthic interstitial (Carey and Montagna, 1982), they are predominantly found in land-fast ice or pack ice formed on shallow shelves. So far, it was assumed that Nematoda are allochthonous and do not reproduce in sea ice (Riemann and Sime-Ngando, 1997). However, recently reproduction of Nematoda was reported from shallow Arctic land-fast ice of Alaska's north coast (Gradinger and Bluhm, 2020). Colonization patterns of ice fauna of benthic origin may change as climate driven sea-ice formation shifts. In a recent analysis of sea-ice meiofauna communities in different types of Arctic sea ice, Kiko et al. (2017) suggested that pack ice of the new Arctic will favor pelagic-sympagic species (e.g., Ciliophora) over benthic-sympagic species (e.g., Nematoda), because the now dominant first-year pack ice tends to form farther offshore and multi-year ice vanishes. For our study region, recent backtracking analyses suggest that less sea ice formed on the Siberian shelves now actually reaches the Fram Strait area (Krumpen et al., 2019). In addition, much of the ice in our research area was formed in the central Arctic Ocean (Krumpen et al., 2019). As a consequence, less sediment and, we suggest, less benthic-derived ice biota from shallow Siberian shelf areas may reached our research area. Satellite-backtracking data, which showed the origin of the specific ice floes sampled during this study, support that hypothesis (Krumpen, pers. communication). Finally, Rotifera only made up 1% of the sea-ice meiofauna abundance compared to a pan-Arctic average share of 22% (Bluhm et al., 2018) and even 33% to the pack-ice meiofauna north of Svalbard (Schünemann and Werner, 2004). According to Bluhm et al. (2018), Rotifera tend to get more abundant the later the season. Correspondingly, the early sampling season could explain the low abundance of Rotifera during this study. The abundance of sea-ice meiofauna is known to vary at least as much among seasons than regions typically reaching its peak by late spring/early summer (Schünemann and Werner, 2004; Bluhm et al., 2018). Thus, differences in abundances between studies are in part due to different seasons of sampling. A small fraction of the difference may also be explained by the fact that this study reports data from the bottom 10 cm while on average one-third of the abundance may be found outside this layer (Bluhm et al., 2018). However, inspection of the melted top 10 cm of our ice cores showed sea-ice meiofauna was absent from this layer.

Sea-ice chl *a* concentration can be used as an indicator for the prevalent food conditions in the pack ice for the dominant sympagic grazers in this study, Harpacticoida and copepod nauplii, who are known to feed on ice algae (Grainger and Hsiao, 1990; Gradinger and Bluhm, 2020). With a mean of 420 μg chl *a* m^{-2}, the chl *a* concentration was markedly lower than in a summer pack-ice study from the same region almost two decades earlier when it reached a mean of 1,200 μg chl *a* m^{-2} (Gradinger et al., 1999). It is possible that some of the ice algae were already flushed out of the ice, given the low bulk salinities (<5 PSU) and moderate temperatures of the sea ice, which indicated the onset of ice melting during this late spring expedition. Another explanation for the low chl *a* concentration could be the snow thickness, which resulted in extreme low irradiance under the ice as could be shown during this study for most of the ice stations (Massicotte et al., 2019). Sea-ice chl *a* concentration did not correlate with sea-ice meiofauna abundance, although in other studies this was the case (Gradinger, 1999; Nozais et al., 2001).

Both chl *a* concentration and sea-ice meiofauna abundance can vary by orders of magnitude on small spatial scales and representative sampling should encompass large sample sizes or sensor profiles (Lange et al., 2017). It is, therefore, possible that the sample size of this study was too small to disentangle patchiness effects from the potential relationship between ice algae and sea-ice meiofauna. Although ice coring can cause inherent biases, because of the potential to lose part of the bottom section and/or brine, it is the current standard method for assessing the community

TABLE 6 | List of under-ice fauna with mean abundance and frequency of occurrence across the sample area.

Under-ice fauna taxon	Mean abundance [ind.m^{-2}]	*SD*	Range	Freq. of occurrence [%]	Relative abundance [%]
ARTHROPODA von Siebold, 1848					
Crustacea Brünnich, 1772					
Copepoda Milne Edwards, 1840					
Harpacticoida G.O. Sars 1903	< 0.01	0.01	0–0.02	0.07	< 0.01
Tisbe Lilljeborg, 1853 spp.	0.01	0.03	0–0.12	0.21	< 0.01
Oithona Baird, 1843 sp.	0.17	0.62	0–2.34	0.21	0.03
Calanus hyperboreus Krøyer, 1838	11.52	13.39	0.20–49.21	1.00	1.90
Calanus glacialis Jaschnov, 1955	35.94	59.76	0.40–231.30	1.00	5.92
Calanus finmarchicus (Gunnerus, 1765)	51.60	69.94	2.05–260.83	1.00	8.51
Nauplii (Copepoda)	140.63	462.95	0–1746.59	0.79	23.18
Paraeuchaeta Scott, 1909 spp.	< 0.01	< 0.01	0–0.01	0.07	< 0.01
Metridia longa (Lubbock, 1854)	0.05	0.19	0–0.70	0.07	0.01
Clausocalanidae Giesbrecht, 1893	0.51	1.33	0–5.08	0.50	0.08
Malacostraca Latreille, 1802					
Amphipoda Latreille, 1806					
Themisto Guerin, 1825 spp.	0.12	0.47	0–1.75	0.14	0.02
Themisto libellula (Lichtenstein in Mandt, 1822)	0.11	0.31	0–1.17	0.43	0.02
Themisto abyssorum (Boeck, 1871)	0.02	0.07	0–0.25	0.14	< 0.01
Apherusa glacialis (Hansen, 1888)	1.90	2.37	0.06–7.52	1.00	0.31
Onisimus glacialis (G.O. Sars, 1900)	< 0.01	< 0.01	0–0.01	0.07	< 0.01
Eusirus Krøyer, 1845 spp.	< 0.01	0.01	0–0.05	0.07	< 0.01
Euphausiacea Dana, 1852					
Thysanoessa longicaudata Krøyer, 1846	0.06	0.13	0–0.46	0.36	0.01
Isopoda Latreille, 1817	0.01	0.03	0–0.12	0.21	< 0.01
Decapoda Latreille, 1802					
Zoaea larvae	0.01	0.04	0–0.16	0.14	< 0.01
Hexanauplia Oakley et al., 2013					
Cirripedia Burmeister, 1834	8.83	15.04	0–55.85	0.93	1.46
CHAETOGNATHA not documented	0.52	1.29	0–4.79	0.29	0.09
Sagittoidea not documented					
Eukrohnia hamata (Moebius, 1875)	1.07	1.24	0–2.90	0.71	0.18
Parasagitta elegans (Verrill,1873)	0.09	0.16	0–0.60	0.57	< 0.01
CHORDATA Haeckel, 1874					
Appendicularia Fol, 1874	351.57	1313.40	0–4914.82	0.29	57.96
Oikopleura Mertens, 1830 spp.	0.33	1.25	0–4.68	0.07	0.06
Osteichthyes larvae	0.01	0.05	0–0.19	0.07	< 0.01
MOLLUSCA not documented					
Gastropoda Cuvier, 1795					
Limacina helicina (Phipps, 1774)	< 0.01	< 0.01	0–0.01	0.14	< 0.01
Clione limacina (Phipps, 1774)	0.01	0.02	0–0,08	0.14	< 0.01
ANNELIDA incertae sedis					
Polychaeta Grube, 1850	0.15	0.33	0–1.12	0.36	0.02
Trochophora larvae	0.85	2.70	0–10.15	0.21	0.14
CNIDARIA Hatschek, 1888					
Hydrozoa Owen, 1843	< 0.01	< 0.01	0–0.01	0.07	< 0.01
XENACOELOMORPHA Philippe et al., 2011	0.51	1.26	0–4.22	0.29	0.08

"Chaetognatha" refers to individuals which could not be identified to species level. SD, standard deviation; Freq. of occurrence, frequency of occurrence.

structure of sea-ice meiofauna (Gradinger and Bluhm, 2009; Eicken et al., 2014). We recommend morphological studies such as this one to be combined with molecular approaches that are increasingly used for enhanced taxonomic resolution (Hardge et al., 2017; Marquardt et al., 2018; Pitusi, 2019).

Under-Ice Fauna

The overall mean abundance of under-ice fauna was 607 ind.m^{-2} during this study, which is one order of magnitude higher than in the only other SUIT study from the central Arctic Ocean from summer 2012 (David et al., 2015). The diversity of the under-ice fauna, however, was

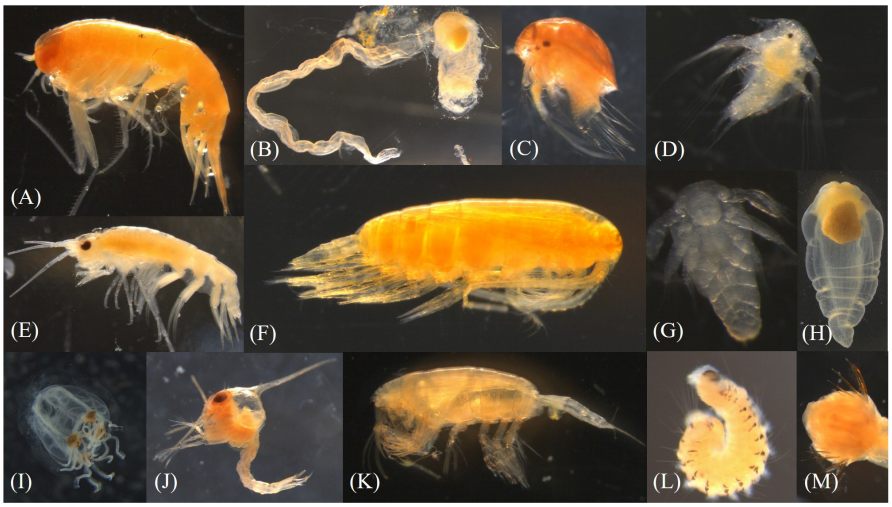

FIGURE 7 | Pictures of under-ice fauna **(A)** *Themisto* sp., **(B)** Appendicularia, **(C,D)** Cirripedia, **(E)** *Apherusa glacialis*, **(F)** *Calanus* sp., **(G)** Nauplius, **(H)** *Clione limacina*, **(I)** Hydrozoa, **(J)** Zoaea larvae, **(K)** *Paraeuchaeta* sp., **(L)** Polychaeta, **(M)** Chaetognatha (head). Photographs by Julia Ehrlich.

very much in accordance with studies from the Laptev Sea (Werner and Arbizu, 1999) and the central Arctic Ocean (David et al., 2015). Highest taxa richness and abundance of the under-ice fauna were found at stations with highest surface chl *a* values, though overall phytoplankton concentrations of the surface waters were relatively low compared to other studies (David et al., 2015; Castellani et al., in press).

It is well known that Crustacea such as Copepoda and Amphipoda can live associated with Arctic sea ice (Arndt and Swadling, 2006; Søreide et al., 2010; Hop et al., 2011). Apart from one occurrence of remarkably high abundance of Appendicularia (station 32), copepod nauplii and *Calanus* species were the most abundant and most frequent taxa across the sampled area. *C. finmarchicus*, the dominant *Calanus* species found in this study (**Figure 3**), is a boreal Atlantic species and is characteristic of the zooplankton community in Arctic areas with a strong inflow of Atlantic Water (Auel and Hagen, 2002; Rudels et al., 2013; Ehrlich, 2015). It shows a drastic decrease in abundance to <1 ind.m^{-2} toward the central deep basins (Kosobokova and Hirche, 2009; Kosobokova et al., 2011; David et al., 2015). *C. glacialis* and *C. hyperboreus* in turn are rather characteristic of Arctic conditions and dominated the under-ice fauna community in the central Arctic Ocean in other studies (Kosobokova and Hirche, 2000; David et al., 2015). As a well-known inhabitant of Arctic waters and an abundant species in first-year ice dominated environments (Werner and Auel, 2005) the high occurrence of *C. glacialis* in the present study is no surprise. In contrast to *C. finmarchicus*, this species reproduces in Arctic waters. Some studies predict a replacement of *C. glacialis* by the smaller and less energy-rich *C. finmarchicus* with increasing atlantification (Bonnet et al., 2005; Richardson, 2008; Polyakov et al., 2017). Potential consequences of that replacement for the Arctic ecosystem are not sufficiently assessed yet, but a recent study suggests it might not be as severe as previously assumed given the authors found copepod lipid content to be more related to habitat conditions than species identity (Renaud et al., 2018). The relatively low abundance of *C. hyperboreus* in this study can be explained by the fact that it is a high Arctic and deep water species, which occurs less in the meltwater layer underneath the ice (Hop et al., 2011). Both *C. glacialis* and *C. hyperboreus*, however, do use the under-ice environment as a nursing ground and time nauplii development with the springtime peak of primary production (Falk-Petersen et al., 2008; Kosobokova and Hirche, 2009; Søreide et al., 2010). High abundances of copepod nauplii under the ice, especially at the earlier sampled stations during this expedition, may have been related to spawning below the sea ice earlier in spring and to the release of nauplii from the sea ice.

Appendicularia are common in the Arctic Ocean (Kosobokova and Hirche, 2000; Auel and Hagen, 2002; Ershova and Kosobokova, 2019), but were not reported in such high abundance in the study region before. Mumm (1993) reported a relative abundance of 3% in the Nansen Basin in summer and similar ranges for Appendicularia were also reported from Kosobokova and Hirche (2000), and Ehrlich (2015) from the central Arctic Ocean. Similar to our study, David et al. (2015) reported a single station with a high abundance of Appendicularia in the ice-water interface layer from the central Arctic Ocean (52.6 ind.m^{-2}). Such isolated high abundances indicate a high patchiness under the sea ice. Maybe Appendicularia can make use of the increased primary production in the Arctic measured by Arrigo et al. (2008) and others, including under-ice blooms, which occur beneath annual sea ice (Assmy et al., 2017; Wollenburg et al., 2018). As Appendicularia are soft-bodied filter feeders and capable of responding faster to shifts in primary production than crustaceans

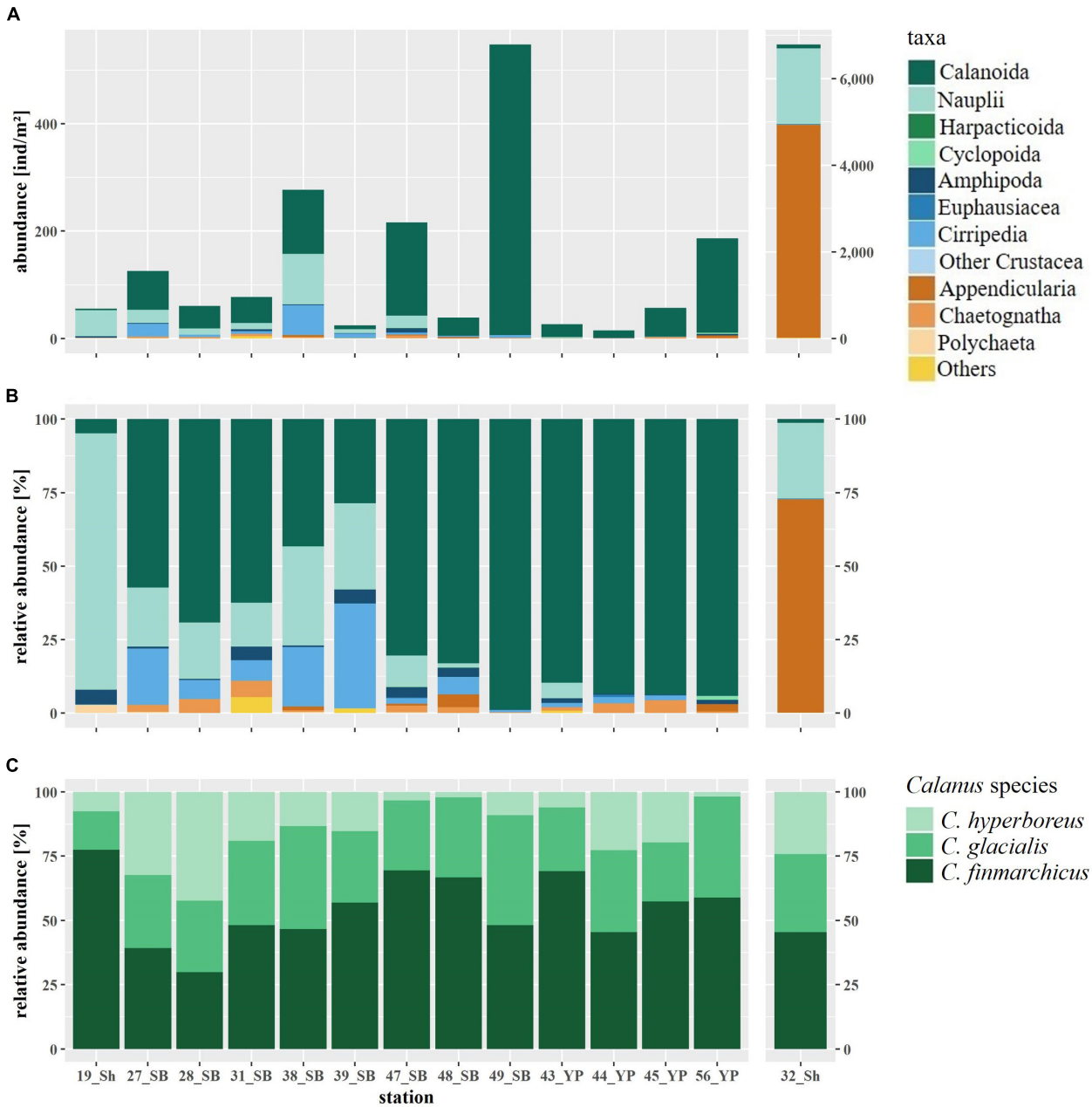

FIGURE 8 | (A) Abundance and **(B)** relative abundance of the under-ice fauna and **(C)** relative abundance of the three *Calanus* species at SUIT stations arranged by geographical region (Sh, shelf; SB, Sophia Basin; YP, Yermak Plateau). SUIT Station 32 has a different *y*-axis, because of high Appendicularia abundance. "Others" includes the rare taxa Hydrozoa, Osteichthyes larvae, Xenacoelomorpha, *Clione limacina*, *Limacina helicina*. "Other Crustacea" includes Isopoda and Zoaea larvae.

would (Hopcroft et al., 2005), their high abundance at one station might be a consequence of following a highly productive patch of water.

Amphipoda were rare in this study in comparison with their abundances in the under-ice fauna north of Svalbard almost three decades earlier (Lønne and Gulliksen, 1991). A more recent study from 2012 from the central Arctic Ocean, however, showed a similar range of sympagic Amphipoda abundance as the present study (David et al., 2015). An explanation for the decline of Amphipoda abundance could be that it seems to be positively related to the complexity of ice structures and the age of the ice (Bluhm et al., 2010; Hop et al., 2011; Bluhm et al., 2017). In the area north of Svalbard, multi-year ice has been declining dramatically since the mid-2000s

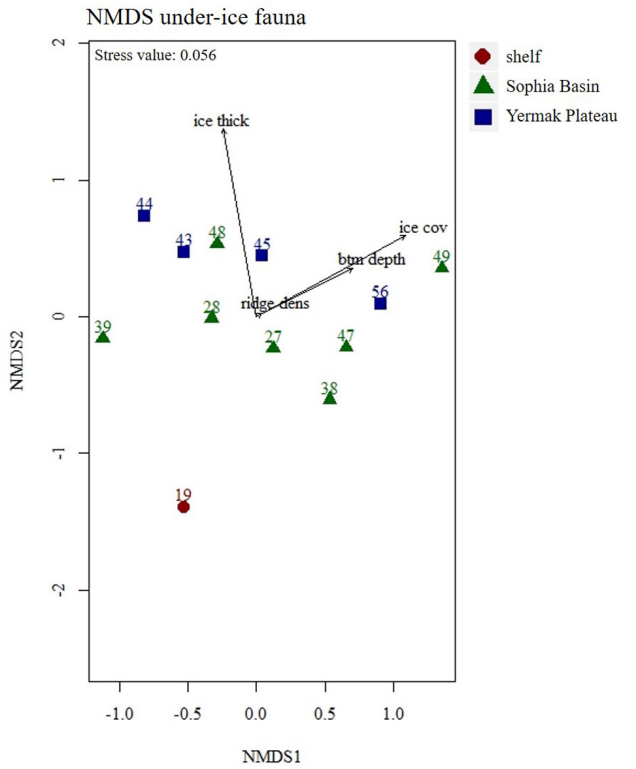

FIGURE 9 | Non-metric Multidimensional Scaling (NMDS) plot of under-ice fauna abundances with four fitted environmental variables. Stations were color coded according to geographical regions (shelf, Sophia Basin, and Yermak Plateau). Ice thick, ice thickness; ice cov, ice coverage; btm depth, bottom depth; ridge dens, ridge density.

(Polyakov et al., 2012; Perovich and Richter-Menge, 2015) and with it the abundance of sympagic Amphipoda (Bluhm et al., 2017). In our study, mainly ∼1.5 year-old sea ice (Peeken, 2016) covered the sampling area and might have been the reason for the low abundance of sympagic Amphipoda. *Apherusa glacialis* was the most abundant among the amphipod species and occurred at every station. This is in accordance with other studies (Werner and Auel, 2005; Hop et al., 2011; David et al., 2015). The species occurs under any ice type through the Arctic Ocean, though it is also found occasionally in the water column (Kunisch et al., 2020). As surface chl *a* concentration was very low during this study, the low abundance of *A. glacialis* might be related to food limitation. The larger amphipod species *Gammarus wilkitzkii* and *Eusirus* sp. were absent or very rare in the analyzed samples, but were actually found regularly, albeit in very low abundances in the larger (7 mm mesh) shrimp net of the SUIT (Schaafsma, pers. communication).

CONCLUSION

Although the results of this study show that the present taxa in the sea-ice and the under-ice water were in accordance with previous studies from this region, some relevant deviations in community composition have occurred. Some of the previously found sympagic taxa were conspicuously absent (e.g., Acoela, Platyhelminthes, and Nematoda) or rare (Rotifera, and ice Amphipoda) in our study area. This finding might reflect the changes in connectivity between the ice-producing shelf and the pack-ice areas in the last decades (Krumpen et al., 2019). The change from a multi-year to an annual sea-ice system means also a change from an ecosystem where a relatively constant community of sympagic fauna can establish over years to one where the community needs to reestablish annually and thus comprises more organisms from the pelagic habitat. This would apply especially to the sea-ice meiofauna, which is more tightly reflecting sea-ice processes, while the under-ice fauna is more influenced by water-mass processes. The under-ice community in part reflected the inflow of the Atlantic Water in this area. While Atlantic Water has in the past been below our sampled stratum, recent evidence documents decreased freshwater content from ice melt, because of less sea ice in the area, increased salinity, and enhanced mixing of Atlantic Water upward (Lind et al., 2018; Renner et al., 2018). Increased water temperatures might result in a further northward shift of Atlantic species, such as *C. finmarchicus* and will cause changes in the sympagic ecosystem by increasing competition for resources and space. Potential changes in sympagic community composition should be monitored to evaluate if occurrences of certain taxa such as Appendicularia are actually increasing and the trend of decreasing benthic-origin taxa continues. Consistent and increased taxonomic resolution (through molecular analysis, Hardge et al., 2017; Marquardt et al., 2018; Pitusi, 2019) is also recommended. Bio-physically coupled datasets should be prioritized to unequivocally link the reduction in the sea ice to change of sympagic fauna.

DATA AVAILABILITY STATEMENT

The datasets generated for this study are available on PANGAEA (Ehrlich et al., 2020a,b).

AUTHOR CONTRIBUTIONS

JE wrote the manuscript. AB, HF, and JE designed the sampling of this study. FS, GC, IP, and HF collected the samples of sea-ice meiofauna and under-ice fauna. JE and BB analyzed the sea-ice meiofauna samples. JE and FS analyzed the under-ice fauna samples. FS and IP contributed to the biological dataset. GC and FS contributed to the environmental dataset. AB contributed to the taxonomical accuracy of the manuscript. JE analyzed the data and prepared all figures and tables. BB, FS, and HF contributed to data interpretation. All authors contributed to the discussion of various versions of the manuscript.

FUNDING

JE was funded by the national scholarships "Promotionsstipendium nach dem Hamburger Nachwuchsfördergesetz (HmbNFG)" and "Gleichstellungsfond 2017 (4-GLF-2017)", both granted by the University of Hamburg. The German Academic Exchange Service (DAAD) and the graduate school "POLMAR" at Alfred Wegener Institute Bremerhaven supported JE's visit at The Arctic University of Norway's Institute of Arctic and Marine Biology. FS received support by Wageningen Marine Research, which is commissioned by the Netherlands Ministry of Agriculture, Nature and Food Quality (LNV) under its Statutory Research Task Nature & Environment WOT-04-009-047.04. The Netherlands Polar Programme (NPP), managed by the Dutch Research Council (NWO) funded this research under project nr. ALW 866.13.009. BB's contribution was under the framework of the Arctic Seasonal Ice Zone Ecology project, co-funded by UiT – The Arctic University of Norway and the Tromsø Research Foundation (Project Number 01vm/h15) and the Arctic ABC Project (Project Number #244319), funded by the Norwegian Research Council. IP, JE, GC, and HF were funded by the PACES (Polar Regions and Coasts in a Changing Earth System) programme of the Helmholtz Association and the expedition Grant No. AWI_PS92_00. HF, JE, and GC were part of the Helmholtz Association Young Investigators Groups *Iceflux*: Ice-ecosystem carbon flux in polar oceans (VH-NG-800).

ACKNOWLEDGMENTS

We thank the Captain and crew of Polarstern for their excellent support during the PS92 expedition. We are greatful for the technical help and great support during the work at sea and on the ice by team members Michiel van Dorssen and André Meijboom. We thank Ulrike Dietrich and Mischa Ungermann for their help with the sea-ice sampling. We thank Rolf Gradinger (UiT) for his support during the lab analysis of sea-ice meiofauna. The SUIT for this study was kindly provided by Jan Andries van Franeker (Wageningen Marine Research).

SUPPLEMENTARY MATERIAL

The Supplementary Material for this article can be found online at: https://www.frontiersin.org/articles/10.3389/fmars.2020.00452/full#supplementary-material

REFERENCES

Arctic Council Secretariat (2016). *Memo on the State of the Arctic Marine Biodiversity Report (SAMBR)*. Tromsø: Arctic Council Secretariat.

Ardyna, M., Babin, M., Gosselin, M., Devred, E., Rainville, L., and Tremblay, J. É (2014). Recent Arctic Ocean sea ice loss triggers novel fall phytoplankton blooms. *Geophys. Res. Lett.* 41, 6207–6212. doi: 10.1002/2014gl061047

Arndt, C. E., and Pavlova, O. (2005). Origin and fate of ice fauna in the Fram Strait and Svalbard area. *Mar. Ecol. Progr. Ser.* 301, 55–66. doi: 10.3354/meps301055

Arndt, C. E., and Swadling, K. M. (2006). Crustacea in arctic and antarctic sea ice: distribution, diet and life history strategies. *Adv. Mar. Biol.* 51, 197–315. doi: 10.1016/s0065-2881(06)51004-1

Arrigo, K. R., van Dijken, G., and Pabi, S. (2008). Impact of a shrinking Arctic ice cover on marine primary production. *Geophys. Res. Lett.* 35:L19603. doi: 10.1029/2008gl035028

Arrigo, K. R., and van Dijken, G. L. (2015). Continued increases in Arctic Ocean primary production. *Progr. Oceanogr.* 136, 60–70. doi: 10.1016/j.pocean.2015.05.002

Assmy, P., Fernández-Méndez, M., Duarte, P., Meyer, A., Randelhoff, A., Mundy, C. J., et al. (2017). Leads in Arctic pack ice enable early phytoplankton blooms below snow-covered sea ice. *Sci. Rep.* 7:40850.

Auel, H., and Hagen, W. (2002). Mesozooplankton community structure, abundance and biomass in the central Arctic Ocean. *Mar. Biol.* 140, 1013–1021. doi: 10.1007/s00227-001-0775-4

Beszczynska-Möller, A., Fahrbach, E., Schauer, U., and Hansen, E. (2012). Variability in Atlantic water temperature and transport at the entrance to the Arctic Ocean, 1997–2010. *ICES J. Mar. Sci.* 69, 852–863. doi: 10.1093/icesjms/fss056

Beuchel, F., and Lønne, O. (2002). Population dynamics of the sympagic amphipods *Gammarus wilkitzkii* and *Apherusa glacialis* in sea ice north of Svalbard. *Polar Biol.* 25, 241–250. doi: 10.1007/s00300-001-0329-8

Bluhm, B. A., and Gradinger, R. (2008). Regional variability in food availability for Arctic marine mammals. *Ecol. Appl.* 18, S77–S96.

Bluhm, B. A., Gradinger, R. R., and Schnack-Schiel, S. B. (2010). Sea ice meio-and macrofauna. *Sea Ice* 2, 357–393. doi: 10.1002/9781444317145.ch10

Bluhm, B. A., Hop, H., Vihtakari, M., Gradinger, R., Iken, K., Melnikov, I. A., et al. (2018). Sea ice meiofauna distribution on local to pan-Arctic scales. *Ecol. Evol.* 8, 2350–2364. doi: 10.1002/ece3.3797

Bluhm, B. A., Swadling, K. M., and Gradinger, R. (2017). "Sea ice as a habitat for macrograzers," in *Sea Ice*, Ed. D. N Thomas (Hoboken, NJ: Wiley), 394–414. doi: 10.1002/9781118778371.ch16

Bonnet, D., Richardson, A., Harris, R., Hirst, A., Beaugrand, G., Edwards, M., et al. (2005). An overview of *Calanus helgolandicus* ecology in European waters. *Progr. Oceanogr.* 65, 1–53. doi: 10.1016/j.pocean.2005.02.002

Bray, J. R., and Curtis, J. T. (1957). An ordination of the upland forest communities of southern Wisconsin. *Ecol. Monogr.* 27, 325–349. doi: 10.2307/1942268

Budge, S., Wooller, M., Springer, A., Iverson, S. J., McRoy, C., and Divoky, G. (2008). Tracing carbon flow in an arctic marine food web using fatty acid-stable isotope analysis. *Oecologia* 157, 117–129. doi: 10.1007/s00442-008-1053-7

Carey, A. Jr. (1985). *Sea Ice Biota*. Boca Raton, FL: CRC Press.

Carey, A. G. Jr. (1992). The ice fauna in the shallow southwestern Beaufort Sea. Arctic Ocean. *J. Mar. Syst.* 3, 225–236. doi: 10.1016/0924-7963(92)90002-p

Carey, A. G. Jr., and Montagna, P. A. (1982). Arctic Sea Ice Fauna1 Assemblage: First approach to description and source of the underice meiofauna. *Mar. Ecol. Progr. Ser.* 8, 1–8. doi: 10.3354/meps008001

Carmack, E., Polyakov, I., Padman, L., Fer, I., Hunke, E., Hutchings, J., et al. (2015). Toward quantifying the increasing role of oceanic heat in sea ice loss in the new Arctic. *Bull. Am. Meteorol. Soc.* 96, 2079–2105. doi: 10.1175/bams-d-13-00177.1

Castellani, G., Lüpkes, C., Hendricks, S., and Gerdes, R. (2014). Variability of A rctic sea-ice topography and its impact on the atmospheric surface drag. *J. Geophys. Res.* 119, 6743–6762. doi: 10.1002/2013jc009712

Castellani, G., Schaafsma, F., Arndt, S., Lange, B. A., Peeken, I., Ehrlich, J., et al. (in press). Large-scale variability of physical and biological sea-ice properties in polar oceans. *Front. Mar. Sci.*

Clarke, K., and Ainsworth, M. (1993). A method of linking multivariate community structure to environmental variables. *Mar. Ecol. Progr. Ser.* 92, 205–205.

Clarke, K. R., and Warwick, R. (2001). *Change in Marine Communities: An Approach to Statistical Analysis and Interpretation*. Plymouth: Primer-E Ltd.

Comiso, J. C. (2012). Large decadal decline of the Arctic multiyear ice cover. *J. Clim.* 25, 1176–1193. doi: 10.1175/jcli-d-11-00113.1

Conover, R. (1988). Comparative life histories in the genera *Calanus* and *Neocalanus* in high latitudes of the northern hemisphere. *Hydrobiologia* 167, 127–142. doi: 10.1007/978-94-009-3103-9_11

Damgaard, R., and Davenport, J. (1994). Salinity tolerance, salinity preference and temperature tolerance in the high-shore harpacticoid copepod *Tigriopus brevicornis*. *Mar. Biol.* 118, 443–449. doi: 10.1007/bf00350301

Darnis, G., Robert, D., Pomerleau, C., Link, H., Archambault, P., Nelson, R. J., et al. (2012). Current state and trends in Canadian Arctic marine ecosystems: II. Heterotrophic food web, pelagic-benthic coupling, and biodiversity. *Clim. Change* 115, 179–205. doi: 10.1007/s10584-012-0483-8

David, C., Lange, B., Rabe, B., and Flores, H. (2015). Community structure of under-ice fauna in the Eurasian central Arctic Ocean in relation to environmental properties of sea-ice habitats. *Mar. Ecol. Progr. Ser.* 522, 15–32. doi: 10.3354/meps11156

Ehrlich, J. (2015). *Diversity and Distribution Of High-Arctic Zooplankton in the Eurasian Basin in Late Summer 2012*. Hamburg: University of Hamburg/Alfred-Wegener-Institut.

Ehrlich, J., Schaafsma, F. L., Bluhm, B. A., Peeken, I., Castellani, G., Brandt, A., et al. (2020a). Sea-ice meiofauna (>10 μm) abundance in Arctic pack ice north of Svalbard during the Polarstern expedition PS92 in 2015. *PANGAEA*. doi: 10.1594/PANGAEA.915960

Ehrlich, J., Schaafsma, F. L., Bluhm, B. A., Peeken, I., Castellani, G., Brandt, A., et al. (2020b). Under-ice fauna abundance of Arctic pack ice north of Svalbard during the Polarstern expedition PS92 in 2015. *PANGAEA*. doi: 10.1594/PANGAEA.915961

Eicken, H., Bluhm, B. A., Collins, R. E., Haas, C., Ingham, M., Gradinger, R., et al. (2014). "Field techniques in sea-ice research," in *Cold Regions Science and Marine Technology*, Ed. H. H. Shen (Paris: EOLSS Publishers), 1–20.

Ershova, E. A., and Kosobokova, K. N. (2019). Cross-shelf structure and distribution of mesozooplankton communities in the East-Siberian Sea and the adjacent Arctic Ocean. *Polar Biol.* 42, 1353–1367. doi: 10.1007/s00300-019-02523-2522

Falk-Petersen, S., Leu, E., Berge, J., Kwasniewski, S., Nygård, H., Røstad, A., et al. (2008). Vertical migration in high Arctic waters during autumn 2004. *Deep Sea Res. Part II Top. Stud. Oceanogr.* 55, 2275–2284. doi: 10.1016/j.dsr2.2008.05.010

Falk-Petersen, S., Mayzaud, P., Kattner, G., and Sargent, J. R. (2009). Lipids and life strategy of Arctic Calanus. *Mar. Biol. Res.* 5, 18–39.

Fernández-Méndez, M., Katlein, C., Rabe, B., Nicolaus, M., Peeken, I., Bakker, K., et al. (2015). Photosynthetic production in the central Arctic Ocean during the record sea-ice minimum in 2012. *Biogeosciences* 12, 3525–3549. doi: 10.5194/bg-12-3525-2015

Flores, H., David, C., Ehrlich, J., Hardge, K., Kohlbach, D., Lange, B. A., et al. (2019). Sea-ice properties and nutrient concentration as drivers of the taxonomic and trophic structure of high-Arctic protist and metazoan communities. *Polar Biol.* 42, 1377–1395. doi: 10.1007/s00300-019-02526-z

Flores, H., Van Franeker, J. A., Siegel, V., Haraldsson, M., Strass, V., Meesters, E. H., et al. (2012). The association of Antarctic krill *Euphausia superba* with the under-ice habitat. *PLoS One* 7:e31775. doi: 10.1371/journal.pone.0031775

Friedrich, C. (1997). Ökologische Untersuchungen zur Fauna des arktischen Meereises. *Ber. zur Polarforschung* 246:211.

Garrison, D. L., and Buck, K. R. (1986). Organism losses during ice melting: a serious bias in sea ice community studies. *Polar Biol.* 6, 237–239. doi: 10.1007/bf00443401

Gosselin, M., Levasseur, M., Wheeler, P. A., Horner, R. A., and Booth, B. C. (1997). New measurements of phytoplankton and ice algal production in the Arctic Ocean. *Deep Sea Res. Part II Top. Stud. Oceanogr.* 44, 1623–1644. doi: 10.1016/s0967-0645(97)00054-4

Gradinger, R. (1999). Integrated abundance and biomass of sympagic meiofauna in Arctic and Antarctic pack ice. *Polar Biol.* 22, 169–177. doi: 10.1007/s003000050407

Gradinger, R., and Bluhm, B. (2009). "Assessment of the abundance and diversity of sea ice biota," in *Field Techniques for Sea-Ice Research*, eds H. Eicken, and M. Salganek (Fairbanks, AK: University of Alaska Press), 283.

Gradinger, R., and Bluhm, B. A. (2020). First analysis of an Arctic sea ice meiofauna food web based on abundance, biomass and stable isotope ratios. *Mar. Ecol. Progr. Ser.* 634, 29–43. doi: 10.3354/meps13170

Gradinger, R., Friedrich, C., and Spindler, M. (1999). Abundance, biomass and composition of the sea ice biota of the Greenland Sea pack ice. *Deep Sea Res. Part II Top. Stud. Oceanogr.* 46, 1457–1472. doi: 10.1016/s0967-0645(99)00030-2

Gradinger, R., Spindler, M., and Weissenberger, J. (1992). On the structure and development of Arctic pack ice communities in Fram Strait: a multivariate approach. *Polar Biol.* 12, 727–733.

Gradinger, R. R., and Bluhm, B. A. (2004). In-situ observations on the distribution and behavior of amphipods and Arctic cod (*Boreogadus saida*) under the sea ice of the High Arctic Canada Basin. *Polar Biol.* 27, 595–603.

Gradinger, R. R., Meiners, K., Plumley, G., Zhang, Q., and Bluhm, B. A. (2005). Abundance and composition of the sea-ice meiofauna in off-shore pack ice of the Beaufort Gyre in summer 2002 and 2003. *Polar Biol.* 28, 171–181. doi: 10.1007/s00300-004-0674-5

Grainger, E., and Hsiao, S. I. (1990). Trophic relationships of the sea ice meiofauna in Frobisher Bay. Arctic Canada. *Polar Biol.* 10, 283–292.

Granskog, M. A., Assmy, P., and Koç, N. (2020). "Emerging Traits of Sea Ice in the Atlantic Sector of the Arctic" in *Climate Change and the White World*, eds P. S. Goel, R. Ravindra, and S. Chattopadhyay (Berlin: Springer), 3–10. doi: 10.1007/978-3-030-21679-5_1

Granskog, M. A., Fer, I., Rinke, A., and Steen, H. (2018). Atmosphere-Ice-Ocean-Ecosystem processes in a thinner arctic sea ice regime: the norwegian young sea ICE (N-ICE2015) expedition. *J. Geophys. Res.* 123, 1586–1594. doi: 10.1002/2017jc013328

Gulliksen, B., and Lønne, O. J. (1989). Distribution, abundance, and ecological importance of marine sympagic fauna in the Arctic. *Rapp. PV Reun. Cons. Int. Explor. Mer.* 188, 133–138.

Haas, C. (2003). Dynamics versus thermodynamics: The sea ice thickness distribution. *Sea Ice* 1, 82–111. doi: 10.1002/9780470757161.ch3

Hardge, K., Peeken, I., Neuhaus, S., Lange, B. A., Stock, A., Stoeck, T., et al. (2017). The importance of sea ice for exchange of habitat-specific protist communities in the Central Arctic Ocean. *J. Mar. Syst.* 165, 124–138. doi: 10.1016/j.jmarsys.2016.10.004

Hirche, H.-J., and Kosobokova, K. (2007). Distribution of *Calanus finmarchicus* in the northern North Atlantic and Arctic Ocean—expatriation and potential colonization. *Deep Sea Res. Part II Top. Stud. Oceanogr.* 54, 2729–2747. doi: 10.1016/j.dsr2.2007.08.006

Hop, H., Mundy, C. J., Gosselin, M., Rossnagel, A. L., and Barber, D. G. (2011). Zooplankton boom and ice amphipod bust below melting sea ice in the Amundsen Gulf, Arctic Canada. *Polar Biol.* 34, 1947–1958. doi: 10.1007/s00300-011-0991-994

Hop, H., and Pavlova, O. (2008). Distribution and biomass transport of ice amphipods in drifting sea ice around Svalbard. *Deep Sea Res. Part II Top. Stud. Oceanogr.* 55, 2292–2307. doi: 10.1016/j.dsr2.2008.05.023

Hop, H., Poltermann, M., Lønne, O. J., Falk-Petersen, S., Korsnes, R., and Budgell, W. P. (2000). Ice amphipod distribution relative to ice density and under-ice topography in the northern Barents Sea. *Polar Biol.* 23, 357–367. doi: 10.1007/s003000050456

Hopcroft, R., Clarke, C., Nelson, R., and Raskoff, K. (2005). Zooplankton communities of the Arctic's Canada Basin: the contribution by smaller taxa. *Polar Biol.* 28, 198–206. doi: 10.1007/s00300-004-0680-7

Hughes, T., Bellwood, D., Baird, A., Brodie, J., Bruno, J., and Pandolfi, J. (2011). Shifting base-lines, declining coral cover, and the erosion of reef resilience: comment on Sweatman et al.(2011). *Coral Reefs* 30, 653–660. doi: 10.1007/s00338-011-0787-6

Jeffries, M. O., Overland, J. E., and Perovich, D. K. (2013). The arctic. *Phys. Today* 66:35.

Kiko, R., Kern, S., Kramer, M., and Mütze, H. (2017). Colonization of newly forming Arctic sea ice by meiofauna: a case study for the future Arctic? *Polar Biol.* 40, 1277–1288. doi: 10.1007/s00300-016-2052-5

Kohlbach, D., Graeve, M., Lange, B. A., David, C., Peeken, I., and Flores, H. (2016). The importance of ice algae-produced carbon in the central Arctic Ocean ecosystem: Food web relationships revealed by lipid and stable isotope analyses. *Limnol. Oceanogr.* 61, 2027–2044. doi: 10.1002/lno.10351

Kosobokova, K., and Hirche, H.-J. (2000). Zooplankton distribution across the Lomonosov Ridge, Arctic Ocean: species inventory, biomass and vertical structure. *Deep Sea Res. Part I Oceanogr. Res. Papers* 47, 2029–2060. doi: 10.1016/s0967-0637(00)00015-7

Kosobokova, K., and Hirche, H.-J. (2009). Biomass of zooplankton in the eastern Arctic Ocean–a base line study. *Progr. Oceanogr.* 82, 265–280. doi: 10.1016/j.pocean.2009.07.006

Kosobokova, K. N., Hopcroft, R. R., and Hirche, H.-J. (2011). Patterns of zooplankton diversity through the depths of the Arctic's central basins. *Mar. Biodivers.* 41, 29–50. doi: 10.1007/s12526-010-0057-9

Krumpen, T., Belter, H. J., Boetius, A., Damm, E., Haas, C., Hendricks, S., et al. (2019). Arctic warming interrupts the Transpolar Drift and affects long-range transport of sea ice and ice-rafted matter. *Sci. Rep.* 9:5459.

Kruskal, J. B. (1964). Nonmetric multidimensional scaling: a numerical method. *Psychometrika* 29, 115–129. doi: 10.1007/bf02289694

Kunisch, E. H., Bluhm, B. A., Daase, M., Gradinger, R., Hop, H., Melnikov, I. A., et al. (2020). Pelagic occurrences of the ice amphipod *Apherusa glacialis* throughout the Arctic. *J. Plankton Res.* 42, 73–86. doi: 10.1093/plankt/fbz072

Kwok, R., and Cunningham, G. (2015). Variability of Arctic sea ice thickness and volume from CryoSat-2. *Philos. Trans. R. Soc. A* 373:20140157.

Lange, B. A., Katlein, C., Castellani, G., Fernández-Méndez, M., Nicolaus, M., Peeken, I., et al. (2017). Characterizing spatial variability of ice algal chlorophyll a and net primary production between sea ice habitats using horizontal profiling platforms. *Front. Mar. Sci.* 4:349. doi: 10.3389/fmars.2017.00349

Lange, B. A., Katlein, C., Nicolaus, M., Peeken, I., and Flores, H. (2016). Sea ice algae chlorophyll *a* concentrations derived from under-ice spectral radiation profiling platforms. *J. Geophys. Res.* 121, 8511–8534. doi: 10.1002/2016jc011991

Legendre, P., and Legendre, L. F. (2012). *Numerical Ecology*. Amsterdam: Elsevier.

Lind, S., Ingvaldsen, R. B., and Furevik, T. (2018). Arctic warming hotspot in the northern Barents Sea linked to declining sea-ice import. *Nat. Clim. Change* 8, 634–639. doi: 10.1038/s41558-018-0205-y

Lønne, O., and Gulliksen, B. (1991). Sympagic macro-fauna from multiyear sea-ice near Svalbard. *Polar Biol.* 11, 471–477.

Madsen, S., Nielsen, T., and Hansen, B. (2001). Annual population development and production by *Calanus finmarchicus*, *C. glacialis* and *C. hyperboreus* in Disko Bay, western Greenland. *Mar. Biol.* 139, 75–83.

Mardia, K., Kent, J. T., and Bibby, J. M. (1979). *Multivariate Analysis*. San Francisco, CA: WordPress.

Marquardt, M., Kramer, M., Carnat, G., and Werner, I. (2011). Vertical distribution of sympagic meiofauna in sea ice in the Canadian Beaufort Sea. *Polar Biol.* 34, 1887–1900. doi: 10.1007/s00300-011-1078-y

Marquardt, M., Majaneva, S., Pitusi, V., and Søreide, J. E. (2018). Pan-Arctic distribution of the hydrozoan Sympagohydra tuuli? First record in sea ice from Svalbard (European Arctic). *Polar Biol.* 41, 583–588. doi: 10.1007/s00300-017-2219-8

Massicotte, P., Peeken, I., Katlein, C., Flores, H., Huot, Y., Castellani, G., et al. (2019). Sensitivity of phytoplankton primary production estimates to available irradiance under heterogeneous sea ice conditions. *J. Geophys. Res.* 124, 5436–5450. doi: 10.1029/2019jc015007

Melnikov, I. (2018). "Characterization of the Biodiversity of Modern Sea Ice in the North Pole Region," in *Doklady Earth Sciences*, Ed. N. S. Bortnikov (Berlin: Springer), 792–795. doi: 10.1134/s1028334x18060132

Melnikov, I., and Kulikov, A. (1980). "The cryopelagic fauna of the central Arctic basin," in *Biology of the central Arctic Basin*, eds M. E. Vinogradov, and I. A. Mel'nikov, (Moscow: Nauka), 97–111.

Melnikov, I. A., Zhitina, L. S., and Kolosova, H. G. (2001). The Arctic sea ice biological communities in recent environmental changes (scientific note). *Mem. Natl. Inst. Polar Rev. Spl. Issue* 54:409416.

Michel, C., Nielsen, T. G., Nozais, C., and Gosselin, M. (2002). Significance of sedimentation and grazing by ice micro-and meiofauna for carbon cycling in annual sea ice (northern Baffin Bay). *Aquatic Microb. Ecol.* 30, 57–68. doi: 10.3354/ame030057

Mumm, N. (1993). Composition and distribution of mesozooplankton in the Nansen Basin, Arctic Ocean, during summer. *Polar Biol.* 13, 451–461.

Nicolaus, M., Katlein, C., Maslanik, J., and Hendricks, S. (2012). Changes in Arctic sea ice result in increasing light transmittance and absorption. *Geophys. Res. Lett.* 39:L24501.

Nozais, C., Gosselin, M., Michel, C., and Tita, G. (2001). Abundance, biomass, composition and grazing impact of the sea-ice meiofauna in the North Water, northern Baffin Bay. *Mar. Ecol. Progr. Ser.* 217, 235–250. doi: 10.3354/meps217235

Oksanen, J., Blanchet, F., Friendly, M., Kindt, R., Legendre, P., McGlinn, D., et al. (2018). *vegan: Community Ecology Package. R package version 2.5-2.*

Peeken, I. (2016). The Expedition PS92 of the Research Vessel POLARSTERN to the Arctic Ocean in 2015. *Rep. Polar Mar. Res.* 694:153. doi: 10.2312/BzPM_0694_2016

Perovich, D. K., and Richter-Menge, J. A. (2015). Regional variability in sea ice melt in a changing Arctic. *Philos. Trans. R. Soc. A* 373:20140165.

Pielou, E. C. (1969). *An Introduction to Mathematical Ecology*. Hoboken, NJ: Wiley-Interscience.

Pitusi, V. (2019). *Seasonal Abundance and Activity of Sympagic Meiofauna in Van Mijenfjorden, Svalbard*. Tromsø: UiT Norges arktiske universitet.

Poltermann, M., Hop, H., and Falk-Petersen, S. (2000). Life under Arctic sea ice–reproduction strategies of two sympagic (ice-associated) amphipod species, Gammarus wilkitzkii and *Apherusa glacialis*. *Mar. Biol.* 136, 913–920. doi: 10.1007/s002270000307

Polyakov, I. V., Pnyushkov, A. V., Alkire, M. B., Ashik, I. M., Baumann, T. M., Carmack, E. C., et al. (2017). Greater role for Atlantic inflows on sea-ice loss in the Eurasian Basin of the Arctic Ocean. *Science* 356, 285–291. doi: 10.1126/science.aai8204

Polyakov, I. V., Walsh, J. E., and Kwok, R. (2012). Recent changes of Arctic multiyear sea ice coverage and the likely causes. *Bull. Am. Meteorol. Soc.* 93, 145–151. doi: 10.1175/bams-d-11-00070.1

R Core Team (2018). R: A Language and Environment for Statistical Computing. Vienna: R Foundation for Statistical Computing. Available online at: https://www.R-project.org/

Rabenstein, L., Hendricks, S., Martin, T., Pfaffhuber, A., and Haas, C. (2010). Thickness and surface-properties of different sea-ice regimes within the Arctic Trans Polar Drift: Data from summers 2001, 2004 and 2007. *J. Geophys. Res.* 115:C12.

Renaud, P. E., Daase, M., Banas, N. S., Gabrielsen, T. M., Søreide, J. E., Varpe, Ø, et al. (2018). Pelagic food-webs in a changing Arctic: a trait-based perspective suggests a mode of resilience. *ICES J. Mar. Sci.* 75, 1871–1881. doi: 10.1093/icesjms/fsy063

Renner, A., Sundfjord, A., Janout, M., Ingvaldsen, R., Beszczynska-Möller, A., Pickart, R., et al. (2018). Variability and redistribution of heat in the Atlantic Water boundary current north of Svalbard. *J. Geophys. Res.* 123, 6373–6391. doi: 10.1029/2018jc013814

Richardson, A. J. (2008). In hot water: zooplankton and climate change. *ICES J. Mar. Sci.* 65, 279–295. doi: 10.1093/icesjms/fsn028

Riemann, F., and Sime-Ngando, T. (1997). Note on sea-ice nematodes (Monhysteroidea) from Resolute Passage. Canadian high Arctic. *Pol. Biol.* 18, 70–75. doi: 10.1007/s003000050160

Rudels, B. (1987). *On the Mass Balance of the Polar Ocean, with Special Emphasis on the Fram Strait*. Tromsø: Norsk Polarinstitutt.

Rudels, B., Jones, E. P., Schauer, U., and Eriksson, P. (2004). Atlantic sources of the Arctic Ocean surface and halocline waters. *Polar Res.* 23, 181–208. doi: 10.3402/polar.v23i2.6278

Rudels, B., Schauer, U., Björk, G., Korhonen, M., Pisarev, S., Rabe, B., et al. (2013). Observations of water masses and circulation in the Eurasian Basin of the Arctic Ocean from the 1990s to the late 2000s. *OS Special Issue* 9, 147–169. doi: 10.5194/os-9-147-2013

Schlitzer, R., Anderson, R. F., Dodas, E. M., Lohan, M., Geibert, W., Tagliabue, A., et al. (2018). The GEOTRACES intermediate data product 2017. *Chem. Geol.* 493, 210–223.

Schünemann, H., and Werner, I. (2004). Seasonal variations in distribution patterns of sympagic meiofauna in Arctic pack ice. *Mar. Biol.* 146, 1091–1102. doi: 10.1007/s00227-004-1511-1517

Serreze, M. C., Holland, M. M., and Stroeve, J. (2007). Perspectives on the Arctic's shrinking sea-ice cover. *Science* 315, 1533–1536. doi: 10.1126/science.1139426

Shannon, C., and Weaver, W. (1963). The measurement theory of communication.

Shepard, R. N. (1962). The analysis of proximities: multidimensional scaling with an unknown distance function. I. *Psychometrika* 27, 125–140. doi: 10.1007/bf02289630

Søreide, J. E., Carroll, M. L., Hop, H., Ambrose, W. G. Jr., Hegseth, E. N., and Falk-Petersen, S. (2013). Sympagic-pelagic-benthic coupling in Arctic and Atlantic waters around Svalbard revealed by stable isotopic and fatty acid tracers. *Mar. Biol. Res.* 9, 831–850. doi: 10.1080/17451000.2013.775457

Søreide, J. E., Hop, H., Carroll, M. L., Falk-Petersen, S., and Hegseth, E. N. (2006). Seasonal food web structures and sympagic–pelagic coupling in the European

Arctic revealed by stable isotopes and a two-source food web model. *Progr. Oceanogr.* 71, 59–87. doi: 10.1016/j.pocean.2006.06.001

Søreide, J. E., Leu, E., Berge, J., Graeve, M., and Falk-Petersen, S. (2010). Timing of blooms, algal food quality and *Calanus glacialis* reproduction and growth in a changing Arctic. *Glob. Change Biol.* 16, 3154–3163.

Tran, S., Bonsang, B., Gros, V., Peeken, I., Sarda-Esteve, R., Bernhardt, A., et al. (2013). A survey of carbon monoxide and non-methane hydrocarbons in the Arctic Ocean during summer 2010. *Biogeosciences* 10, 1909–1935. doi: 10.5194/bg-10-1909-2013

Tremblay, J. -É, Anderson, L. G., Matrai, P., Coupel, P., Bélanger, S., Michel, C., et al. (2015). Global and regional drivers of nutrient supply, primary production and CO2 drawdown in the changing Arctic Ocean. *Progr. Oceanogr.* 139, 171–196. doi: 10.1016/j.pocean.2015.08.009

Tremblay, J. -É, and Gagnon, J. (2009). "The effects of irradiance and nutrient supply on the productivity of Arctic waters: a perspective on climate change," in *Influence of Climate Change on the Changing Arctic And Sub-Arctic Conditions*, Ed. J. Nihoul (Berlin: Springer), 73–93. doi: 10.1007/978-1-4020-9460-6_7

van Franeker, J. A., Flores, H., and Van Dorssen, M. (2009). *The Surface and Under Ice Trawl (SUIT). Frozen Desert Alive-The role of sea ice for Pelagic Macrofauna and Its Predators*. PhD thesis, University of Groningen, Groningen, 181–188.

Werner, I., and Arbizu, P. M. (1999). The sub-ice fauna of the Laptev Sea and the adjacent Arctic Ocean in summer 1995. *Polar Biol.* 21, 71–79. doi: 10.1007/s003000050336

Werner, I., and Auel, H. (2005). Seasonal variability in abundance, respiration and lipid composition of Arctic under-ice amphipods. *Mar. Ecol. Progr. Ser.* 292, 251–262. doi: 10.3354/meps292251

Wickham, H. (2016). *ggplot2: Elegant Graphics for Data Analysis*. Berlin: Springer.

Wickham, H. (2018). *Scales: Scale Functions for Visualization [WWW Document]*. Available online at: https://cran.r-project.org/package=scales (accessed May 5, 2019).

Wickham, H., and Ruiz, E. (2018). *dbplyr: A'dplyr'Back End for Databases. R package version 1*.

Wollenburg, J., Katlein, C., Nehrke, G., Nöthig, E.-M., Matthiessen, J., Wolf-Gladrow, D. A., et al. (2018). Ballasting by cryogenic gypsum enhances carbon export in a Phaeocystis under-ice bloom. *Sci. Rep.* 8, 1–9.

Zar, J. (1984). *Biostatistical Analysis*, 2nd Edn. Englewood Cliffs, NJ: Prentice-Hall.

Zuur, A., Ieno, E. N., and Smith, G. M. (2007). *Analyzing Ecological Data*. Berlin: Springer Science & Business Media.

Conflict of Interest: The authors declare that the research was conducted in the absence of any commercial or financial relationships that could be construed as a potential conflict of interest.

frontiers in Marine Science

ORIGINAL RESEARCH
published: 07 October 2020
doi: 10.3389/fmars.2020.554663

Abundance and Distributional Patterns of Benthic Peracarid Crustaceans From the Atlantic Sector of the Southern Ocean and Weddell Sea

Davide Di Franco[1,2], Katrin Linse[3], Huw J. Griffiths[3], Christian Haas[4], Hanieh Saeedi[1,2,5] and Angelika Brandt[1,2]*

[1] Department of Marine Zoology, Senckenberg Research Institute and Natural History Museum, Frankfurt, Germany, [2] Institute of Ecology, Diversity and Evolution, Goethe University Frankfurt, Frankfurt, Germany, [3] British Antarctic Survey, Cambridge, United Kingdom, [4] Alfred Wegener Institute for Polar and Marine Research, Bremerhaven, Germany, [5] Ocean Biodiversity Information System (OBIS), Frankfurt, Germany

OPEN ACCESS

Edited by:
Christian Marcelo Ibáñez, Andres Bello University, Chile

Reviewed by:
Aldo S. Pacheco, National University of San Marcos, Peru
Javier Sellanes, Catholic University of the North, Chile
Martin Thiel, Catholic University of the North, Chile

***Correspondence:**
Davide Di Franco
davide.di-franco@senckenberg.de

Specialty section:
This article was submitted to Marine Evolutionary Biology, Biogeography and Species Diversity, a section of the journal Frontiers in Marine Science

Received: *22 April 2020*
Accepted: *16 September 2020*
Published: *07 October 2020*

Citation:
Di Franco D, Linse K, Griffiths HJ, Haas C, Saeedi H and Brandt A (2020) Abundance and Distributional Patterns of Benthic Peracarid Crustaceans From the Atlantic Sector of the Southern Ocean and Weddell Sea. Front. Mar. Sci. 7:554663. doi: 10.3389/fmars.2020.554663

Climate change is influencing some environmental variables in the Southern Ocean (SO) and this will have an effect on the marine biodiversity. Peracarid crustaceans are one of the dominant and most species-rich groups of the SO benthos. To date, our knowledge on the influence of environmental variables in shaping abundance and species composition in the SO's peracarid assemblages is limited, and with regard to ice coverage it is unknown. The aim of our study was to assess the influence of sea ice coverage, chlorophyll-a, and phytoplankton concentrations on abundance, distribution and assemblage structure of peracarids. In addition, the influence of other physical parameters on peracarid abundance was assessed, including depth, temperature, salinity, sediment type, current velocity, oxygen, iron, nitrate, silicate and phosphate. Peracarids were sampled with an epibenthic sledge (EBS) in different areas of the Atlantic sector of the SO and in the Weddell Sea. Sampling areas were characterized by different regimes of ice coverage (the ice free South Orkney Islands, the seasonally ice-covered Filchner Trough and the Eastern Antarctic Peninsula including the Prince Gustav Channel which was formerly covered by a perennial ice shelf). In total 64766 individuals of peracarids were collected and identified to order level including five orders: Amphipoda, Cumacea, Isopoda, Mysidacea, and Tanaidacea. Amphipoda was the most abundant taxon, representing 32% of the overall abundances, followed by Cumacea (31%), Isopoda (29%), Mysidacea (4%), and Tanaidacea (4%). The Filchner Trough had the highest abundance of peracarids, while the South Orkney Islands showed the lowest abundance compared to other areas. Ice coverage was the main environmental driver shaping the abundance pattern and assemblage structure of peracarids and the latter were positively correlated with ice coverage and chlorophyll-a concentration.

We propose that the positive correlation between sea ice and peracarid abundances is likely due to phytoplankton blooms triggered by seasonal sea ice melting, which might increase the food availability for benthos. Variations in ice coverage extent and seasonality due to climate change would strongly influence the abundance and assemblage structure of benthic peracarids.

Keywords: the Weddell Sea, Southern Ocean, ice coverage, environmental variables, Peracarida, Crustacea, abundance, distribution pattern

INTRODUCTION

Peracarids play an important role in marine ecosystems; they can influence the structure and composition of benthic communities (Duffy and Hay, 2000) and they are an important converter of biomass and organic matter in the biogeochemical cycles (Karlson et al., 2007; Dunn et al., 2009). Burrows built by sediment-living peracarids allow oxygenated water to pass through the sediment layer, consequently promoting the mineralization of organic matter by other organisms (Pelegrí and Blackburn, 1994; Lehtonen and Andersin, 1998). Furthermore, peracarid crustaceans can also directly consume organic matter as deposit-feeders and also feed on dead organisms from the sea bottom as scavengers; the assimilated biomass can be then transferred to the higher trophic levels via direct consumption (Jeong et al., 2009; Thiel and Hinojosa, 2009; Duffy et al., 2012). Peracarids are also an important source of food for benthic organisms as well as pelagic fauna such as fish and squid (Mouat et al., 2001; Padovani et al., 2012; Xavier et al., 2020). For example, amphipods represent a large percentage in the diet of many Antarctic species, from benthic invertebrates such as the polynoid polychaete *Harmothoe spinosa*, to bentho- and bathy-pelagic predators such as cephalopods (e.g., *Galiteuthis glacialis*), notothenioid fish (e.g., *Notothenia coriiceps*), and megafaunal predators like penguins (e.g., *Eudyptes chrysolophus*), and baleen whales (e.g., *Balaenoptera borealis*) (Dauby et al., 2003). It has been estimated that about 60 million tons of amphipods are consumed every year within the Antarctic food web (Dauby et al., 2003).

Among invertebrates from the SO, Peracarida are one of the dominant and most species-rich groups of benthic fauna (De Broyer and Jazdzewski, 1996; Brandt et al., 2007b; De Broyer and Jazdzewska, 2014; De Broyer and Koubbi, 2014; Kaiser, 2014; Legezyńska et al., 2020). They show high levels of endemism, ranging from 51% (Cumacea) to 88% (Amphipoda) (Brandt, 2000; Brökeland et al., 2007). This might be because the SO's peracarids are characterized by low dispersal ability due to their reproductive biology (Brandt, 1999). Peracarids have undergone a long period of isolation during their evolution, which was strongly influenced by geological and climatic events over the last 40 Ma (Clarke and Crame, 1992; Lawver et al., 2011). During the Eocene-Oligocene, the opening of a seaway between Australia and East Antarctica and the subsequent opening of the Drake Passage in the Northern Antarctic Peninsula initiated the onset of the Antarctic Circumpolar Current (Lawver et al., 2011). The Antarctic Circumpolar Current is the largest current in the world and promoted the biogeographic isolation of the SO by forming a dispersal barrier for marine species (Barker et al., 2007). Furthermore, during the glacial period of the late Cenozoic, the variation in size and extent of the continental ice sheet influenced the benthic community by forcing the organisms to take refuge on the shelf, and/or to shift their distribution ranges into the deep sea (Thatje et al., 2005). Such events caused a reduced gene flow between the newly separated communities and enhanced speciation. As a result, new species from the deep sea could then recolonize the shallow waters following the glacial retreat (Brey et al., 1996; Hodgson et al., 2003). For example, recent studies showed that different families of isopods underwent multiple colonization events from the shelf to the deep sea; some hypotheses also supported these using molecular experiments (Brandt et al., 2007c; Raupach et al., 2009; Riehl et al., 2020). Cooling events likely caused the extinction of some groups of decapods in the SO (Thatje and Arntz, 2004; Aronson et al., 2009). Consequently, the lack of benthic predators such as lobsters or brachyuran crabs in Antarctica offered new ecological niches to the peracarid crustaceans (Brandt, 1999).

The success of the SO's peracarids can be further explained by their highly diverse lifestyle and feeding biology (Brökeland et al., 2007; Thiel and Hinojosa, 2009; Brusca et al., 2016). For example, mysidaceans are strictly distributed in the water column, isopods and amphipods have benthic, pelagic, or benthopelagic lifestyle (Brökeland et al., 2007). Isopods and amphipods are one of the most dominant components of the emerging benthos (Alldredge and King, 1985; Vallet and Dauvin, 2001; Kiljunen et al., 2020). They perform vertical migrations into the water column during the night, moving benthic resources to the pelagos, thus playing an important role in the benthic-pelagic coupling (Vallet and Dauvin, 2001; Pacheco et al., 2013; Kiljunen et al., 2020). Peracarids include mobile swimmers, bottom-dwelling, and sediment-living species feeding on a wide variety of different food sources. Besides being prey by themselves, they can also be predators, scavengers, suspension-feeders and, among isopods and amphipods (e.g., whale lice), there even are ectoparasites. Cumaceans and tanaidaceans represent a smaller range of lifestyles being more strictly related to the sediment type, they mainly include suspension-feeders and deposit-feeders, but also predators (Thiel and Hinojosa, 2009; Brusca et al., 2016). Despite their high abundance and dominance, the composition pattern of the orders of Peracarida along the SO is still far from being comprehensively understood.

Sediment characteristics and depth have been identified as the most important factors driving faunal abundance and composition patterns in the SO's peracarids (Brandt et al., 2007b; Rehm et al., 2007). In addition, temperature, oxygen, salinity,

primary productivity, and quantity of food influence their diversity and community structure (Brandt et al., 2007a; Ingels et al., 2012; Meyer-Löbbecke et al., 2014). Some of these factors in turn could be affected by sea-ice dynamics: the extent and duration of ice coverage affect the amount of light penetrating the water column, which can positively influence phytoplanktonic activity (Dayton et al., 1994; Runcie and Riddle, 2006; Clark et al., 2017). Moreover, ice melting can also influence the salinity of the upper water column (Haumann et al., 2016).

Apart from sea ice, SO's peracarids can also be affected by glacial ice, in particular by floating ice shelves, icebergs, or marine terminating glaciers. Ice shelves around Antarctica cover more than 1.561 million km^2 (Rignot et al., 2013; Smith et al., 2019) creating conditions of permanent limited light penetration and food depletion, which can last for millennia (Domack et al., 2005; Pudsey et al., 2006). Benthic communities living beneath the ice shelf rely on the lateral advection of food particles (Riddle et al., 2007; Gutt et al., 2011; Smith et al., 2019). Due to limited food and light, benthic communities that live under the ice shelves are more similar to those living in the deep sea (Rose et al., 2015). Icebergs calving from ice shelves can play an important role as a source of physical disturbance in shallow Antarctic benthic marine systems (Gutt and Starmans, 2001; Rack and Rott, 2004; Barnes and Souster, 2011). Iceberg scouring events are one of the main physical processes affecting shallow benthic communities which can be catastrophic (Gutt et al., 1996; Peck et al., 1999; Barnes and Souster, 2011; Valdivia et al., 2020). Iceberg calving events are episodic. Although, in the recent decades rising temperatures and in particular the regional warming along the Antarctic Peninsula caused destabilization leading to disintegration and break-up of several ice shelves (e.g., Larsen A and B and most recently Larsen C in the Eastern Antarctic Peninsula; Rott et al., 1996; Rack and Rott, 2003). Consequently, this caused an increase in the rate of iceberg calving events in the area (Rack and Rott, 2004; Massom et al., 2018).

Sea ice coverage (pack and fast ice) is characterized by strong seasonality, forming in winter and retreating or breaking out during austral summer, and it has a strong influence on the biota underneath. As aforementioned, during its retreat sea ice disperses and allows more light penetration into the upper water column, strongly increasing primary production and triggering phytoplankton blooms. Furthermore, when the ice melts, sea-ice biota are released and enhance the primary productivity and the organic matter input in the water column (e.g., fecal pellets produced by zooplankton). Released algae and fecal pellets can ultimately sink to the sea floor serving as food for the benthos, being able to reach also greater depths (Vanhove et al., 1995; Boetius et al., 2013; Wing et al., 2018). In addition, the land-fast sea ice along the coast prevents drifting icebergs from scouring the seabed (Smale et al., 2008; Smith, 2011; Collares et al., 2018).

Satellite observations show that the overall ice coverage in the Weddell Sea experienced a gradual increase since the early 1980s, particularly in summer. However, long-term trends are superimposed by large multi-year variability, with a recent strong decline beginning in 2016 (Parkinson, 2019; Vernet et al., 2019). The sea ice development is somewhat contradictory to the strong warming experienced by the Antarctic Peninsula region, which is considered one of the most rapidly warming regions of the world (Hansen et al., 2010).

In light of all this, improving our knowledge on composition and distribution of Antarctic benthic communities and their interactions with the environmental abiotic factors is important for prediction of the potential ecological impact induced by on-going climate change. The knowledge of its influence in shaping abundances and species composition in benthic communities of the deep sea is limited and in peracarid crustaceans still remains unknown. This study therefore aims to describe the composition of peracarid crustaceans in different areas of the Weddell Sea, and to investigate the importance of ice coverage and potential driving environmental variables on their abundance, distribution patterns and assemblage structure.

MATERIALS AND METHODS

Study Area

The peracarid samples were collected from different areas of the Atlantic sector of the SO, mainly in the Weddell Sea, during expeditions of the RRS *James Clark Ross* and RV *Polarstern* (**Figure 1**). The entire area of the Weddell Sea is dominated by the cyclonic Weddell Gyre, which branches off from the warmer and more saline Antarctic Circumpolar Current north of the Antarctic Peninsula going southwards into the Antarctic continental shelves (Fahrbach et al., 1995). In this area, colder deep and bottom waters (Weddell Sea Bottom Water) are produced, released into the gyre and transported back to the north along the Eastern Antarctic Peninsula. Another water mass that contributes to the formation of the Weddell Gyre is the Weddell Sea Deep Water, which originates by mixing processes between surface water masses and a component of the Antarctic Circumpolar Current, the Circumpolar Deep Water (Fahrbach et al., 1995; Vernet et al., 2019).

The expedition JR15005 with the RRS *James Clark Ross* worked at the South Orkney Islands in February-March 2016, a small archipelago located in the Northeast of the Antarctic Peninsula (**Figures 1A,B**, Griffiths, 2017). It is characterized by a great variability in the duration of ice coverage (Murphy et al., 1995; Meredith et al., 2011), the presence of the Antarctic Circumpolar Current in the north and the Weddell Sea Deep Water in the south (Meredith et al., 2011).

During the expedition JR17003a on the RRS *James Clarke Ross*, sampling was carried out in February–March 2018 in the Prince Gustav Channel, situated in the Eastern Antarctic Peninsula (**Figures 1A,C**) because the Larsen-C ice shelf, where iceberg A68 calved off in July 2017 (Hogg and Gudmundsson, 2017), could not be reached as originally planned due to heavy pack-ice conditions (Linse, 2018). The Prince Gustav Channel was formerly covered by ice shelf but in 1995, an almost total collapse of the ice shelf (Rott et al., 1998; Pudsey et al., 2001) exposed the area to new environmental conditions, leading to an increase in primary production (Bertolin and Schloss, 2009). The area, especially in the deeper parts, is characterized by drapes

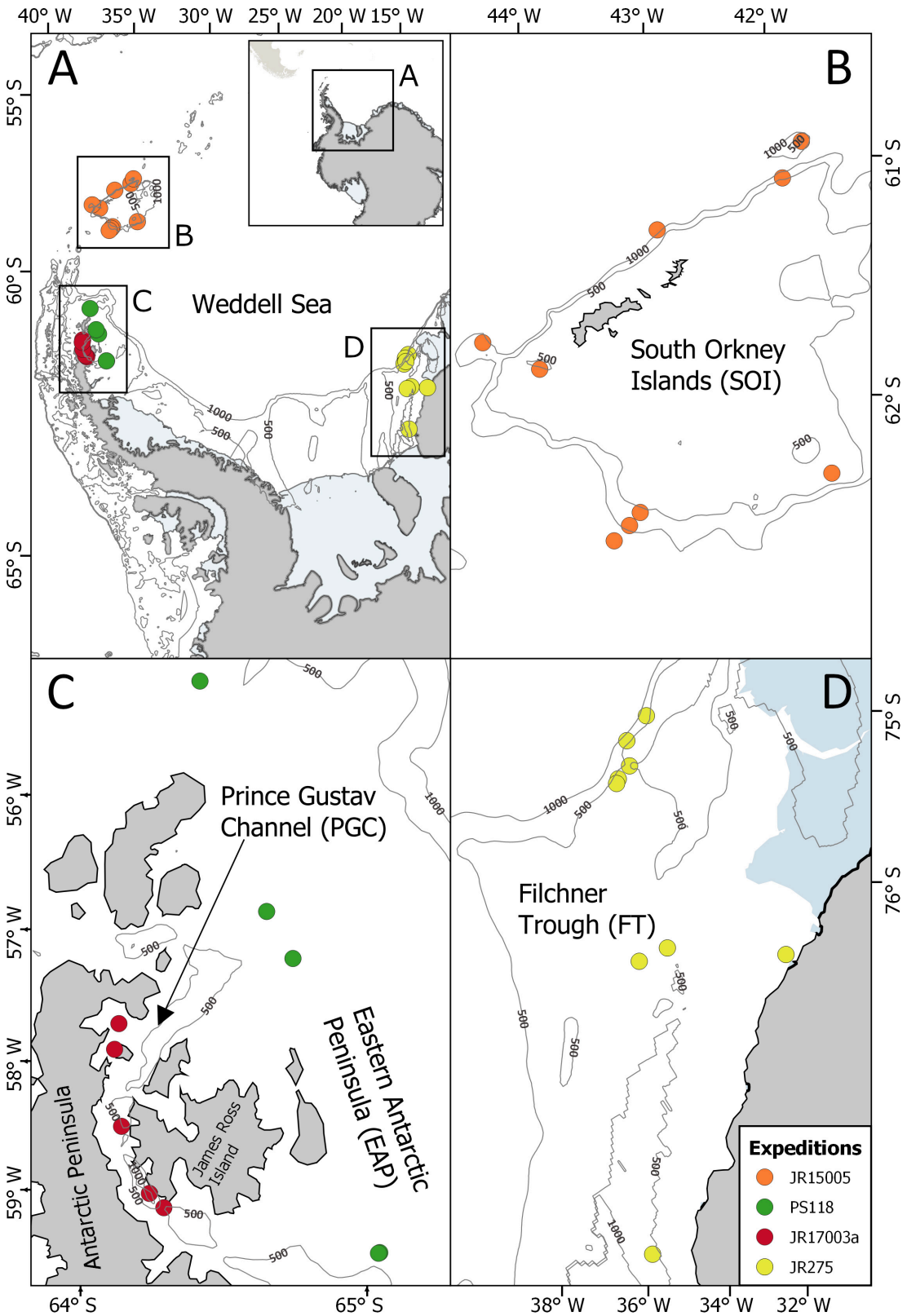

FIGURE 1 | Locations of the EBS stations sampled during the expeditions in the SO **(A)**; JR15005, South Orkney Island, SOI **(B)**; PS118, Eastern Antarctic Peninsula, EAP **(C)**; JR17003a, Prince Gustav Channel, PGC, **(C)**; JR275, Filchner Trough, FT, **(D)**.

of diatom-bearing glacial marine mud, which are typical of the presence of floating ice shelves (Pudsey et al., 2001).

The PS118 expedition of the RV *Polarstern* in February/March 2019 aimed to reach the Larsen-C ice shelf but also failed to reach this area as well due to very heavy sea-ice conditions (Dorschel, 2019). Therefore, sampling was done to the east of James Ross Island along the Eastern Antarctic Peninsula following a latitudinal gradient transect at an average depth of about 400 m from 63° to 64° south (**Figures 1AA,C**).

Previously, epibenthic sledge (EBS) samples were taken during the expedition JR275 on the RRS *James Clark Ross* (February–March 2012) in the Filchner Trough area (South-Eastern Weddell Sea), located in front of the Filchner Ice Shelf (**Figures 1A,D**) (Griffiths, 2012). The South-Eastern Weddell Sea is relatively inaccessible and under-sampled as it is mostly covered with perennial sea ice and is characterized by the presence of very large icebergs (Årthun et al., 2013; Darelius and Sallée, 2018). The sampled area, situated in the north of the Filchner Ice Shelf, is characterized by seasonality in the ice coverage (Yi et al., 2011) and is affected by super-cooled Ice Shelf Water. The latter originates from the Filchner Ice Shelf and flows northwards mixing with the Weddell Sea Bottom Water, contributing to the formation of the Weddell Gyre (Gordon et al., 2001). Ice Shelf Water and Weddell Sea Bottom Water are characterized by very low temperatures (with Ice Shelf Water reaching −2.3°C) and high level of oxygen concentration (Orsi et al., 1993; Makinson et al., 2011).

Sampling Protocol

During each expedition, peracarid crustaceans were collected using an EBS which consisted of a suprabenthic- and an epibenthic net with a mesh size of 500 μm (cod-ends 300 μm) and was deployed as described by Brenke (2005). The epibenthic net extended from 27 to 60 cm above the seafloor, while the suprabenthic net extended from 100 to 133 cm above the bottom. The sledge was provided with an opening-closing mechanism so that box supra- and epibenthic meshes would immediately close once the gear was lifted (Brenke, 2005). The deployment was carried out for 10 min at a mean velocity of about one knot. Trawling distances were then calculated on the basis of velocity of ship and winch from the start of the trawling until the sledge left the ground, following the equation #4 reported in Brenke (2005). Since the trawling distance between stations was not always the same, in order to compare the different stations, numbers of individuals where standardized to 1000 m haul distances (**Tables 1**, **2**).

In order to make station numbers more intuitive and easier to read, original station IDs were changed and reported in **Table 1** as "New Station ID." Nevertheless, original station names from each expedition were included as well (**Table 1**; "Original Station ID") to make our results comparable with published data in which the original names were used. A total of 28 EBS and 26 CTDs were deployed at 28 stations in the areas of the Filchner Trough (9 EBS/7 CTDs), the Prince Gustav Channel (5/5), the Eastern Antarctic Peninsula (4/4) and the South Orkney islands (9/9) (**Table 1**). CTD sensors attached to the EBS collected data about temperature and salinity, except for station F6 and F9 in the Filchner Trough. The characterization of the type of sediment was derived from the analysis of video footage, following the same protocol as in Brasier et al. (2018) for the geomorphologic classification (**Table 1**). Video footage was recorded using the Shallow Underwater Camera System during expeditions JR15005 and JR17003a, the Deep Water Camera System during JR275 and the Ocean Floor Observation and Bathymetry System during the expedition PS118 (**Table 1**).

On board samples were sieved with a mesh size of 300 μm and/or directly transferred into precooled (−20°C) 96% ethanol. All ethanol-preserved samples were then stored at −20°C for at least 48 h before further processing, to avoid DNA degradation. On board and later in the laboratory, ethanol-preserved peracarids were further sorted to order level. The number of individuals per sample was counted (raw data; **Supplementary Table 1**) and compared with the number of individuals standardized to 1000 m haul distance.

Environmental Data

Environmental data not collected during the expeditions were obtained from the "global environmental datasets for marine species distribution modeling" Bio-ORACLE[1] (Tyberghein et al., 2012; Assis et al., 2017) with a resolution of 5arcmin (0.0833°). The latter were compiled from combinations of satellite and *in situ* observations, gathering data for a period of 14 years (2000–2014; Assis et al., 2017).

The layers downloaded for the present paper included data about annual-mean value of chlorophyll-a (mg/m^3), current velocity (m^{-1}), oxygen concentration (mol/m^3), iron ($\mu mol/m^3$), nitrate (mol/m^3), silicate (mol/m^3), phosphate (mol/m^3), phytoplankton ($\mu mol/m^3$), primary production (g/m^3d^{-1}). All values referred only to the maximum depth at the sea bottom except for primary production which included only the pelagic data. Besides, ice concentration data (fractions from 0 to 1), salinity, and temperature (C°) were also downloaded in order to assess the reliability of Bio-ORACLE data in comparison with the CTD data. Bio-ORACLE data were used to replace the two missing values of CTD data of temperature and salinity in station F6 and F9 from the Filchner Trough. Ice concentration data from all study areas since the year 1978 were obtained from the meereisportal data base of the Alfred Wegener Institute[2] (Grosfeld et al., 2016). Ice concentration is given using the unit interval (fractions) from 0 to 1, where 0 indicates absence of ice and 1 indicates a completely ice-covered area.

Data Analysis

To determine the distribution patterns of the assemblage of peracarid crustaceans between stations and in relation to environmental variables, abundance data were analyzed by means of ordination analysis. Prior to analyses, a draftsman plot was used to check for multicollinearity between environmental variables and to assess the presence of heavily skewed ones. Heavily skewed variables were then transformed following Clarke and Gorley (2006). The following variables were removed:

[1]http://www.bio-oracle.org/

[2]meereisportal.de

TABLE 1 | Station list of analyzed EBS deployments ordered by depth, CTD and environmental data measured at seafloor.

Original station ID	New station ID	Date	Depth range	Latitude (S)	Longitude (W)	Haul	T	S	O2	Device	Sediment (%)		
			(m)	Start - End	Start - End	length (m)	(°C)	(psu)	(ml/l)		Soft	Hard	Biogenic
JR275	**JR275**									DWCS			
45	F1	22/02/2012	429 – 428	75° 45.72′ – 75° 45.85′	30° 26.56′ – 30° 27.08′	536	−1.96	34.66	–	✓	88.6	1.6	9.8
94	F2	29/02/2012	478 – 491	74° 41.51′ – 74° 41.36′	29° 29.27′ – 29° 29.05′	426	−1.75	34.40	–	✓	41.0	4.3	54.7
40	F3	21/02/2012	549 – 539	76° 10.01′ 76° 09.94′	27° 48.23′ – 27° 48.44′	508	−1.84	34.38	–	✓	65.7	0.2	34.1
50	F4	22/02/2012	583 – 587	75° 44.60′ – 75° 44.75′	31° 14.77′ – 31° 15.21′	684	−1.98	34.67	–	✓	69.8	2.3	5.5
89	F5	29/02/2012	642 – 657	74° 40.30′ – 74° 40.24′	29° 23.93′ – 29° 23.30′	575	−1.56	34.42	–	✓	16.3	13.8	70.0
23	F6	19/02/2012	654 – 656	77° 21.42′ – 77° 21.47′	35° 21.64′ – 35° 21.90′	701	–	–	–	–	–	–	–
99	F7	01/03/2012	977 – 963	74° 38.05′ – 74° 38.14′	29° 00.49′ – 28° 59.97′	741	0.18	34.60	–	✓	48.7	15.6	35.7
83	F8	28/02/2012	1582 – 1580	74° 29.12′ – 74° 29.08′	8° 46.48′ – 28° 47.08′	1172	0.33	34.67	–	✓	98.0	0.0	2.0
78	F9	26/02/2012	2021 – 2026	74° 24.28′ – 74° 24.39′	28° 05.09′ – 28° 04.62′	1251	–	–	–	✓	98.0	0.0	2.0
JR15005	**JR15005**									SUCS			
12	S1	02/03/2016	516 – 519	61° 31.85′ – 61° 31.80′	46° 55.89′ – 46° 56.20′	662	0.25	34.66	7.98	✓	100.0	0.0	0.0
133	S2	16/03/2016	527 – 521	60° 40.38′ – 60° 40.35′	42° 30.74′ – 42° 31.02′	670	0.34	34.67	7.96	✓	83.3	16.7	0.0
34	S3	06/03/2016	561 – 524	62° 09.61′ – 62° 09.45′	44° 58.92′ – 44° 59.00′	780	0.12	34.66	8.00	✓	80.2	19.8	0.0
115	S4	15/03/2016	588 – 590	60° 45.16′ – 60° 45.14′	42° 57.75′ – 42° 58.08′	780	0.07	34.66	8.02	✓	20.3	79.7	0.0
18	S5	03/03/2016	782 – 786	61° 32.20′ – 61° 32.08′	47° 07.99′ – 47° 08.24′	850	0.22	34.67	7.98	✓	88.1	11.9	0.0
103	S6	14/03/2016	788 – 817	60° 28.53′ – 60° 28.41′	44° 25.38′ – 44° 25.61′	819	0.09	34.66	8.01	✓	19.9	80.1	0.0
86	S7	12/03/2016	795 – 794	60° 13.07′ – 60° 13.11′	46° 44.54′ – 46° 44.87′	937	0.16	34.66	8.00	✓	100.0	0.0	0.0
57	S8	09/03/2016	798 – 835	60° 33.33′ – 60° 33.44′	46° 30.92′ – 46° 31.12′	898	0.23	34.65	7.98	✓	100.0	0.0	0.0
27	S9	04/03/2016	1461 – 1471	61° 31.92′ - 61° 31.80′	47° 23.49′ – 47° 23.68′	1456	−0.02	34.66	8.03	✓	100.0	0.0	0.0
JR17003a	**JR17003a**									SUCS			
53	P1	07/03/2018	470 – 445	63° 36.97′ – 63° 37.00′	57° 30.23′ – 57° 30.40′	508	−1.64	34.48	–	✓	28.4	62.5	5.7
35	P2	05/03/2018	787 – 727	64° 02.86′ – 64° 02.95′	58° 27.71′ – 58° 28.01′	937	−1.84	34.53	–	✓	3.1	0.1	0.1
34	P3	04/03/2018	843 – 850	64° 07.70′ – 64° 07.64′	58° 30.31′ – 58° 29.96′	851	−1.85	34.53	–	✓	90.5	2.4	7.4
47	P4	06/03/2018	874 – 872	63° 48.44′ – 63° 48.57′	58° 04.12′ – 58° 04.34′	898	−1.77	34.48	–	✓	99.0	0.2	0.9
5	P5	01/03/2018	1079 – 1081	63° 34.47′ – 63° 34.51′	57° 17.08′ – 57° 17.41′	937	−1.84	34.54	–	–	–	–	–
PS118	**PS118**									OFOBS			
9-5	E1	12/03/2019	403 – 401	64° 01.18′ – 64° 01.35′	55° 54.08′ – 55° 54.90′	459	−1.64	34.55	6.88	✓	99.0	0.7	0.3
38-9	E2	22/03/2019	428 – 427	63° 03.79′ – 63° 03.92′	54° 18.56′ – 54° 18.75′	579	−0.88	34.56	6.11	✓	94.6	4.4	1.0
6-5	E3	05/03/2019	432 – 433	64° 58.43′ – 64° 58.60′	57° 47.20′ – 57° 48.24′	854	−1.86	34.58	6.91	✓	97.0	1.4	1.7
6-6	E4	05/03/2019	438 – 438	64° 58.25′ – 64° 58.35′	57° 47.89′ – 57° 48.63′	640	−1.86	34.58	6.91	✓	97.0	1.4	1.7
12-7	E5	14/03/2019	445 – 444	63° 49.40′ - 63° 49.48′	55° 40.67′ – 55° 40.21′	334	−1.21	34.54	6.63	✓	98.8	0.5	0.7

SWCS, Shallow Underwater Camera System; DWCS, Deep Water Camera System; OFOBS, Ocean Floor Observation and Bathymetry System.

TABLE 2 | Standardized abundance of peracarid orders from all stations.

Taxon	Amphipoda	Cumacea	Isopoda	Mysidacea	Tanaidacea	Total
Station	**Standardized 1000 m trawl length**					
JR275						
F1	1681	5132	2073	274	56	9216
F2	2955	531	3085	33	164	6768
F3	1778	2081	963	646	384	5852
F4	1259	3466	1789	598	175	7287
F5	7555	553	5210	97	325	13740
F6	407	1083	531	150	23	2194
F7	1644	1254	1976	161	147	5182
F8	368	974	918	54	350	2664
F9	40	35	119	22	18	234
JR15005						
S1	195	59	142	11	33	440
S2	2249	63	213	4	9	2538
S3	739	1	253	6	33	1032
S4	823	18	326	12	10	1189
S5	259	49	218	0	74	600
S6	889	110	758	20	26	1803
S7	17	10	10	0	22	59
S8	2	3	2	0	2	9
S9	26	3	11	0	1	41
JR17003a						
P1	502	156	175	461	211	1505
P2	940	2930	653	186	106	4815
P3	612	1243	161	222	160	2398
P4	4018	2369	840	37	318	7582
P5	160	52	39	83	213	547
PS118						
E1	2815	1441	2699	619	1770	9344
E2	377	38	14	503	41	973
E3	269	184	303	75	68	899
E4	70	41	52	25	8	196
E5	2219	9823	7828	610	206	20686

phytoplankton, nitrate, oxygen, silicate. In addition, depth, chlorophyll-a, current velocity, iron and primary productivity were log transformed. When a couple of variables presented mutual Pearson correlation coefficients averaging more than 0.90 and less than −0.90, only one for each couple was selected for further analyses (**Supplementary Table 2**).

Ordinate analysis was performed using the non-metric multidimensional scaling (nMDS) based on Bray–Curtis dissimilarity matrix and on square rooted transformed abundance data in order to visualize dissimilarities in assemblages′ structure among samples. The similarity profile permutation test (SIMPROF) was used to visually identify significant dissimilarities among samples by superimposing significant SIMPROF clusters on nMDS plots. Principal Component Analysis (PCA) based on normalized environmental data was used to graphically represent correlations between peracarid assemblages and environmental parameters.

The BIOENV procedure (BEST) was used to identify the subset of variables that best explained the dissimilarity patterns observed. BIOENV computed a Spearman rank correlation (Rho) between the Bray–Curtis similarity matrix of peracarid's abundances and the similarity matrix of transformed and normalized environmental variables based on Euclidean distance. In order to examine the statistical significance of observed correlation, the global BEST match permutation test (999 permutations) was used.

The seriation with replication test of the RELATE routine was used to test whether the dissimilarity in assemblages' structure observed in the nMDS followed a sequential pattern of change. This analysis applies a Spearman rank correlation (Rho) between dissimilarities among samples and a perfect seriated model matrix based on a linear sequence of values equally spaced along a line (Clarke and Gorley, 2006). A Spearman rank correlation coefficient Rho close to one indicates high seriation,

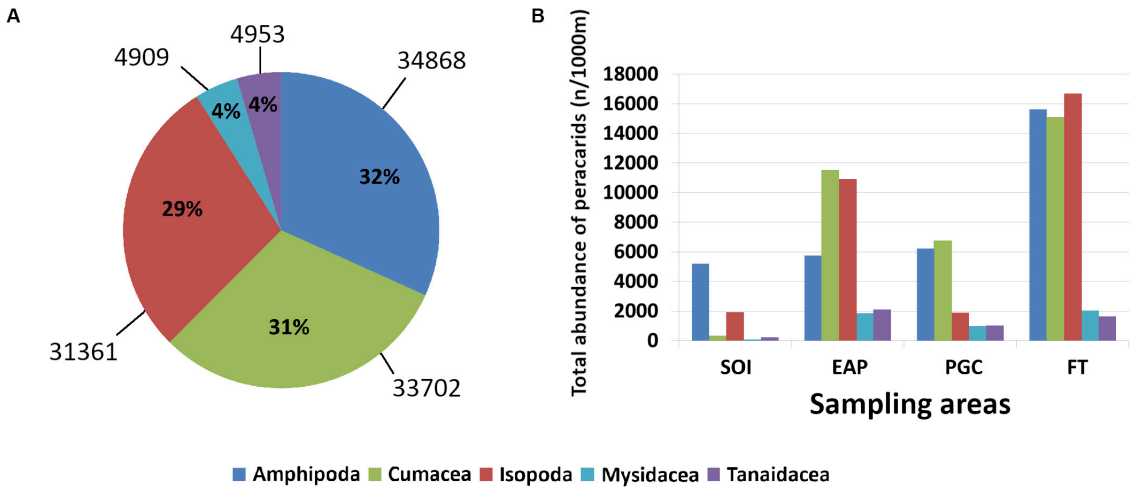

FIGURE 2 | Total relative abundance of peracarids **(A)**; total abundance of peracarids in each sampling area **(B)**. SOI, South Orkney Islands; EAP, Eastern Antarctic Peninsula; PGC, Prince Gustav Channel; FT, Filchner Trough.

while a coefficient Rho close to zero corresponds to the null hypothesis of no seriation. To reject the null hypothesis of a complete absence of seriation, a permutation test was applied to the matching coefficient (Rho; 999 permutations). The null hypothesis was rejected at a significance level of at least 1 in 10000 ($p < 0.0001$).

Ordination analysis including nMDS and PCA, BIOENV and RELATE analyses were performed using the multivariate software PRIMER v6 (Clarke and Gorley, 2006).

Ultimately, correlations between environmental variables and total peracarid abundances were analyzed by Pearson correlation analyses using the statistic software RStudio and the package "ggpubr" (Kassambara, 2017).

Statistical analyses by means of Pearson correlation were carried out on selected stations from the continental shelf (depth range 400–899 m) excluding those from the deep sea. The latter usually starts at about 200 m but in the SO where the continental shelf is usually deeper, it starts at a depth of 1000 m (Clarke, 2003). It was also shown that a shift between shelf and deep-sea isopod and sponge communities occurred only at about 1500 m in the Powell Basin (Brandt et al., 2007c). The depth range 400–899 m was chosen because it allowed us to have the larger dataset having the smallest difference in depth.

RESULTS

Peracarid Abundance

A total of 64766 peracarids were sorted and identified to order level, five orders were identified (Amphipoda, Cumacea, Isopoda, Mysidacea, Tanaidacea; **Table 2**). Standardized abundance data showed that the sampled areas had different levels of maximum abundance per station. Noteworthy was station F5 in the Filchner Trough which had the highest abundance with 13740 peracarid ind./1000 m haul, while abundance from station F9 was the lowest with only 234 ind./1000 m haul (**Table 2**).

In total, amphipods were the most abundant taxon with 34868 ind./1000 m haul, representing 32% of the total abundance, while Mysidacea and Tanaidacea were the least abundant with 4909 and 4953 ind./1000 m haul respectively, each only representing 4% of the total abundance (**Figure 2A**).

The number of individuals in each order of peracarids varied regardless of the depth in all sampling areas. In the Eastern Antarctic Peninsula, abundances from station E5 (445 m depth) were the highest with 20686 ind./1000 m haul, while abundances from station E4 (438 m) were only 196 ind./1000 m haul (**Table 2** and **Figure 3C**). The other stations from the same area and with similar depth showed a much lower number of peracarids (**Table 2** and **Figures 3A,E,G**).

The total abundance of the five peracarid orders varied between different areas. Whilst in the Filchner Trough amphipods, isopods, and cumaceans were similar in abundance, in the Prince Gustav Channel isopods were less abundant (**Figure 2B**). In the Eastern Antarctic Peninsula and in the South Orkney Islands the least abundant of these three taxa were the amphipods and cumaceans, respectively (**Figure 2B**).

One of the most striking results was the very high abundance of cumaceans at station E5 off the Eastern Antarctic Peninsula, dominating with 9823 ind./1000 m haul (**Figure 3C**), while at station S3 off the South Orkney Islands only one single ind./1000 m haul was found (**Table 2**). A similar trend was observed also for the other groups; although, none of them showed such high abundance in one single station. Cumaceans were also dominant at five of nine stations in the Filchner Trough and at two stations from the Prince Gustav Channel (**Figures 3E–H**).

Relative abundances showed different patterns between the different areas and regardless of depth. In the South Orkney Islands amphipods were the most dominant group, representing up to more than 80% of the total in the different stations (**Figure 3B**). A consistent relationship between depth and the abundance of amphipods was not observed. In the Eastern

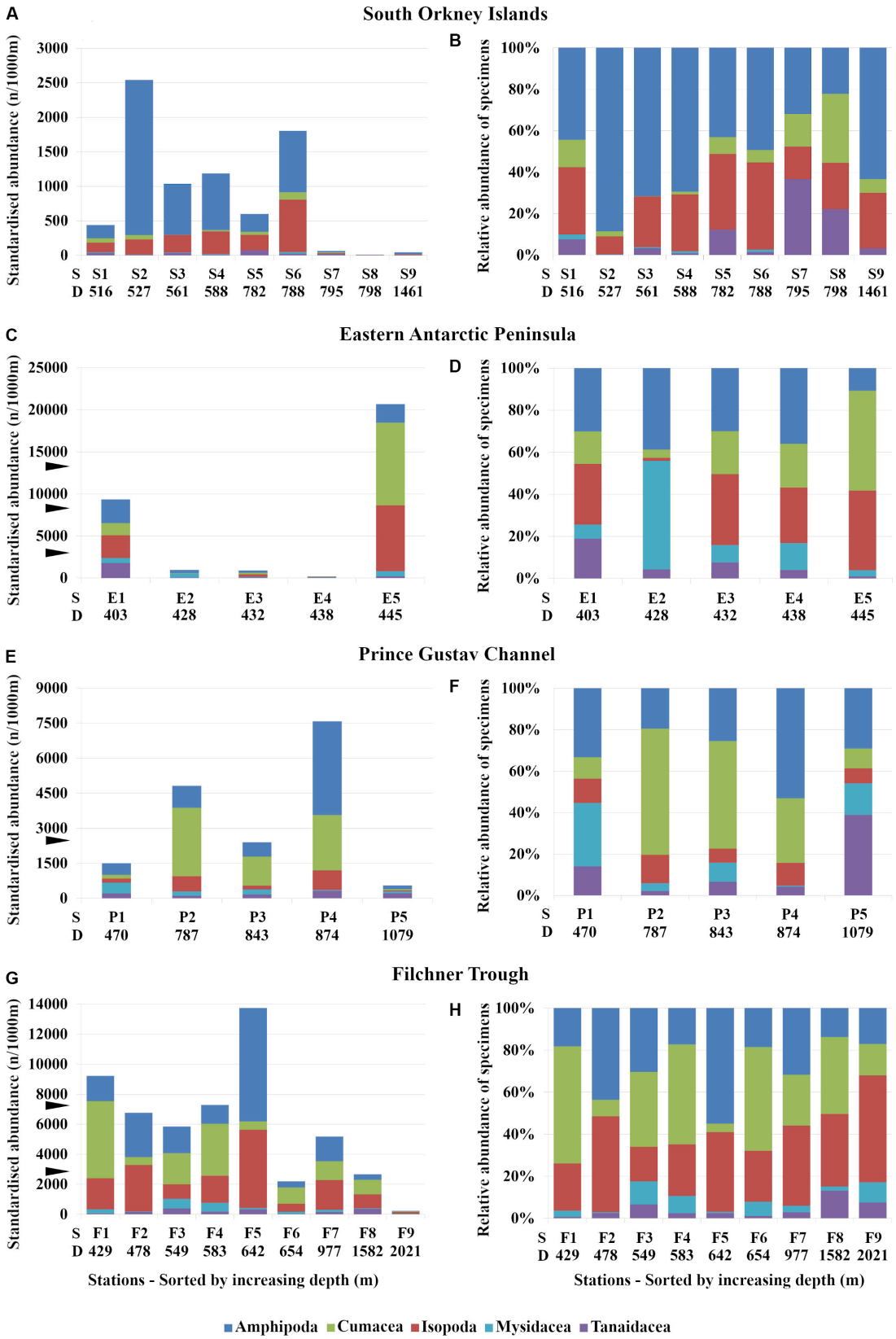

FIGURE 3 | Standard **(A,C,E,G)** and relative abundance **(B,D,F,H)** of peracarid orders in the study areas. **(A,B)** South Orkney Islands, **(C,D)** Eastern Antarctic Peninsula, **(E,F)** Prince Gustav Channel, **(G,H)** Filchner Trough. ►, maximum standardized abundance at comparative regions; S, station number; D, depth (m).

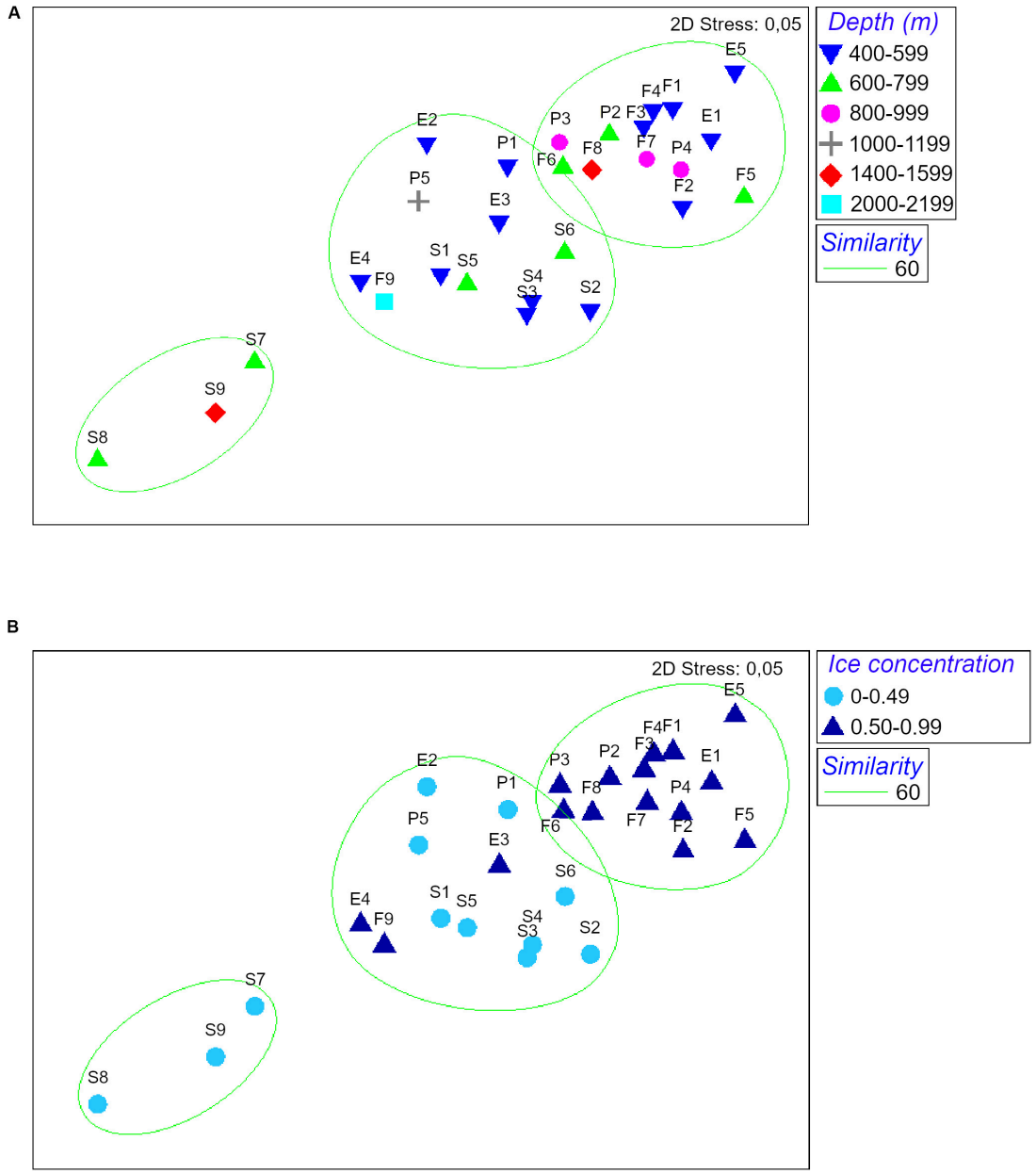

FIGURE 4 | nMDS of ice concentration and depth of peracarid assemblages from all stations. Depth is expressed in meters, ice concentration in fractions from 0 to 1 (where 0 indicates no ice coverage and 1 indicates complete ice coverage).

Antarctic Peninsula amphipods showed a similar pattern between stations (**Figure 3D**). In the Prince Gustav Channel, Cumacea were the dominant order, representing up to 61% of the total abundance among the different stations (**Figure 3F**). In the Filchner Trough almost all orders showed similar abundance patterns at all stations (**Figure 3H**).

Peracarid Assemblages and Environmental Variables

In order to assess the abundance, distribution patterns and assemblage structure of peracarids between the different stations and in relation to environmental variables, ordinate statistical analyses were performed.

The nMDS analysis showed a dissimilarity in assemblages' structure among sampling sites gradually increasing from low ice concentration (<0.5) to high ice concentration (>0.5). Stations S7, S8, S9 were very dissimilar compared to the rest of the cluster due to their extremely low abundances (59, 9 and 41 ind./1000 m haul, respectively; **Figure 4** and **Table 2**). In contrast, depth did not explain the patterns of dissimilarity in assemblages' structure observed. Stations from the same depth ranges were evenly distributed among the different clusters (**Figure 4**).

Principal Component Analysis produced a total of five principal components, the first three of which explained 80.1% of the total variance (eigenvalue > 1). Analysis of the eigenvectors showed that the major contribution in the first PCA axis (PC1) was given by phosphate concentration and temperature, while the predominant variables in the second axis (PC2) were salinity and primary productivity. Ice coverage and depth were the most significant variables in the third axis (PC3; **Table 3**; **Figure 5**). BIOENV analysis showed that the ice coverage was the variable which was most highly correlated with the similarity matrix derived from peracarid abundances ($p = 0.008$; $\rho = 0.334$). The presence of a gradual change of dissimilarities in assemblage's structure among samples with increasing/decreasing ice concentration was tested using the "seriation with replication" test implemented in the RELATE routine. The analysis showed a significant result ($p = 0.0001$; $\rho = 0.355$). The same test carried out on a depth gradient did not show any significant result ($p = 0.17$; $\rho = 0.077$).

Total abundance of peracarids from all the stations investigated in the present study (400–2021 m) decreased with depth ($R = -0.67$, $p = 0.033$; **Figure 6A** and **Table 4**). When the correlation was tested including only stations from the continental shelf (400–899 m) the result was not significant ($R = -0.82$, $p = 0.092$; **Table 4**), showing that the correlation between abundances and other environmental variables was not affected by the depth intervals (100 m) chosen in the analysis.

A negative correlation was found with increasing temperature and salinity ($R = -0.53$, $p = 0.013$ and $R = -0.52$, $p = 0.018$ respectively; **Figures 6C,E** and **Table 4**). Peracarids showed higher abundances at lower values of the two parameters. Conversely, peracarid abundances significantly increased with increasing ice and clorophyll concentration (**Figures 6B,D** and **Table 4**). No significant correlation with the other environmental parameters investigated in this study (current velocity, iron, phosphate, primary productivity; **Table 4**) was found.

When comparing Bio-ORACLE data with shipboard CTD measurements, both sources produced similar results.

TABLE 3 | Eigenvectors for the first five principal components (PCA) from environmental variables.

Variable	PC1	PC2	PC3	PC4	PC5
Depth	0.311	0.066	0.648	0.262	0.333
Ice	−0.36	0.038	0.554	0.225	−0.07
T	0.421	−0.294	0.101	−0.135	−0.211
S	0.227	−0.54	−0.039	0.265	0.474
Chl-a	−0.341	−0.098	0.371	−0.575	−0.019
Cv	0.226	0.455	−0.125	−0.424	0.607
Fe	−0.407	−0.174	−0.327	0.298	0.214
PO4	0.451	0.189	−0.036	0.124	−0.447
PP	−0.092	0.578	−0.02	0.42	0.032

PP, primary productivity; Chl-a, chlorophyll-a; S, salinity; T, temperature; Fe, iron; Cv, current velocity; PO4, phosphate; Ice, ice concentration.

DISCUSSION

Abundance of Peracarid Crustaceans

Results from this study showed that peracarid abundances varied in different study areas and between stations within the same area. Such a trend is in line with a previous study from the SO continental shelf, in which Kaiser et al. (2008) reported that total abundance of peracarids between different stations (South Sandwich Islands) ranged from 11 to 4123 ind./1000 m haul (samples collected with an EBS, the deepest station was about 1000 m). In our study, overall, shelf stations from the Filchner Trough showed much higher abundances compared to those recorded in the South Orkney Islands. A similar result was observed when comparing the Filchner Trough with the South Sandwich Islands (Kaiser et al., 2008). Total abundances of peracarids from the latter (4361 ind./1000 m haul) more closely resembled those from the South Orkney Islands (**Table 2**). The higher abundances in the Filchner Trough could be explained by the high frequencies of icebergs that can lead to more open water, broken-up ice, enhanced primary productivity and also impact benthic communities promoting the spread of opportunistic species, which in turn can become very abundant (Gerdes et al., 2003; Årthun et al., 2013). Our finding is in line with a previous study in which Brandt et al. (2007c) indicated an increase in abundance and species richness from the Scotia Arc area toward the Southern Weddell Sea.

Amphipods showed the highest relative abundance compared to other peracarid orders, which corresponds to previous studies where amphipods were also the most abundant group sampled in the SO (Brökeland et al., 2007; Kaiser et al., 2008). Nevertheless, a striking result was the high abundance recorded for cumaceans from many stations and from different areas (Filchner Trough, Prince Gustav Channel, Eastern Antarctic Peninsula). This is unusual, as in previous studies, cumaceans were rarely dominant, except for two stations sampled in the Ross Sea (Rehm et al., 2007).

Besides, the high relative abundance of cumaceans recorded in our study (31%) was never reported before. In Brandt (2001; Eastern Weddell Sea), they represented about 21%, in Brökeland et al. (2007; different areas of the SO) 16%, in Rehm et al. (2007; Ross Sea) 7%, in Kaiser et al. (2008; South Sandwich Islands) they represented only the 2% of the entire peracarid assemblage. The high abundance of cumaceans recorded in the present study may be explained by their life style. Cumaceans are inbenthic (only males move into the water column during circadial migrations; Mühlenhardt-Siegel, 2014), they specially occur in very fine and silty sediments which characterized most of the sampling sites.

Influence of Environmental Variables

Temperature, Salinity, Depth, Sediment Type

Previous studies that investigated the influence of environmental parameters on peracarid assemblages' abundance and composition in the SO mainly considered factors such as depth, salinity, temperature and sediment type. However, previous results did not always show the same patterns or correlations between peracarid assemblages and environmental parameters. Meyer-Löbbecke et al. (2014) suggested that salinity, temperature, chlorophyll-a, and depth might influence the

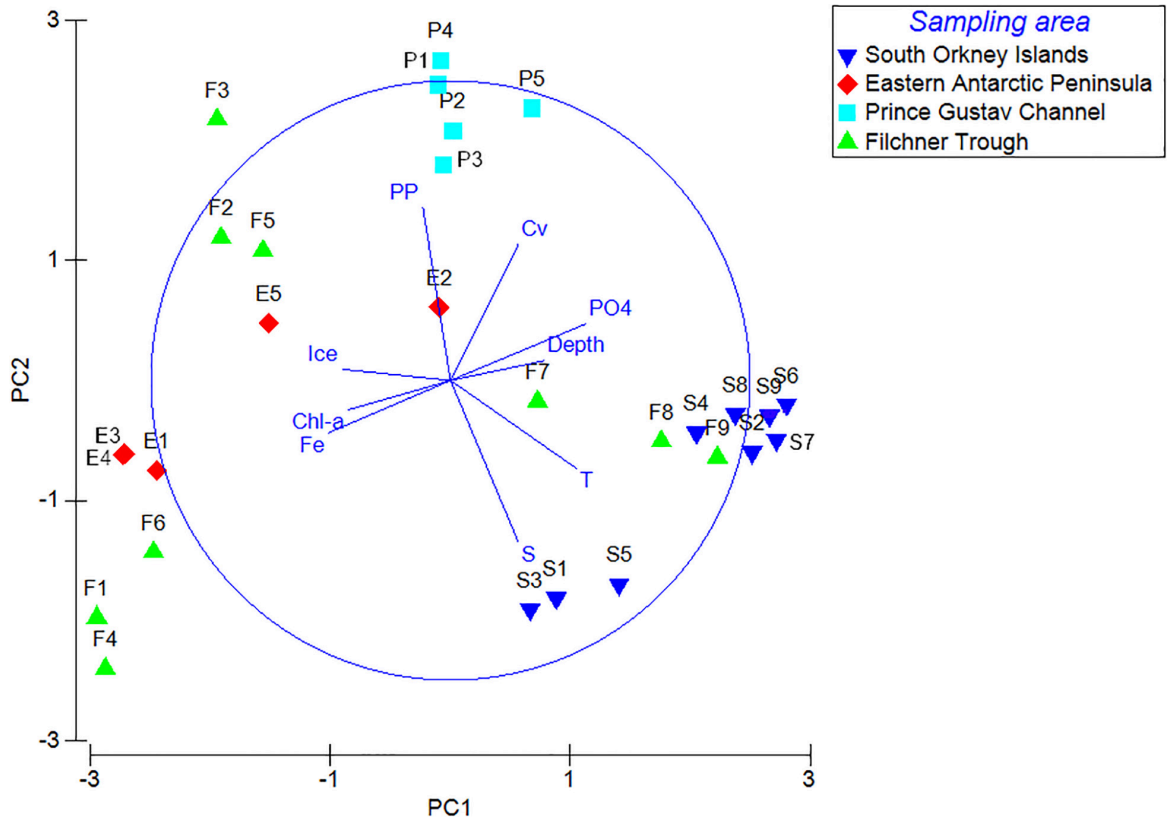

FIGURE 5 | Principal component analysis (PCA) of peracarid assemblages and environmental variables from all stations. PP, primary productivity; Chl, chlorophyll-a; S, salinity; T, temperature; Fe, iron; Cv, current velocity; PO4, phosphate; Ice, ice concentration.

number of isopod specimens and the isopod assemblages, while in Brandt et al. (2007a) depth was the main driver shaping the structure of isopod assemblages. These different results could be due to the fact that sampling was done in areas influenced by different water bodies and thus by different environmental conditions, besides the different number of stations and depth range. A full understanding of the dynamics governing the composition of benthic communities is difficult, since general distribution patterns can result from several different factors and from the spatial scales investigated (e.g., if local or regional scale; Kaiser et al., 2007).

In our study, the abundance of peracarids from all stations (depth range 400–2021 m) was negatively correlated with temperature, salinity, and depth. The negative correlation with the latter can be explained by a decrease in food availability and quality from shallower to deeper waters (Hessler, 1974; Gage and Tyler, 1991; Schnack-Schiel and Isla, 2005; Brökeland et al., 2007). The high number of peracarids recorded at stations from the deep sea showed that depth is not the only factor affecting food availability at the bottom (Brökeland et al., 2007). This possibly documents the importance of the Antarctic bottom-water production, which might enhance food availability in deeper waters (Brandt et al., 2007b). For example, in East Antarctica regions it was shown that downslope flow of Antarctic bottom-water rich in organic matter and generated in shelf polynyas can supply food to seafloor slope benthos (Jansen et al., 2018). It was shown to be also one of the key factors sustaining benthic communities from the continental shelf, down to about 900 m (Post et al., 2010).

Ice Coverage and Chlorophyll-a Concentration

In our study, ice concentration was the parameter which best explained the pattern of dissimilarity in assemblages' structure of peracarids. Dissimilarities among samples increased with decreasing percentage of ice concentration. In spite of the lack of studies in this regard in the Southern Ocean, the influence of sea ice on peracarid assemblages was reported in a previous study performed in the Northern Hemisphere (Greenland; Brandt, 1995). Composition, abundance and diversity of benthic peracarids reflected the availability of food (phytoplankton and ice algae) which was linked to the presence of a polynya and ice-edge primary production. The polynya opened in spring and enhanced the primary productivity of the area throughout the summer months. The increased primary productivity in the water column affects the benthos by the increasing amounts of organic matter reaching the seafloor. For example, Brandt (1995) linked the presence of high isopod abundances to the availability of fresh phytoplankton material on the seafloor, derived from phytoplankton blooms initiated by melting sea ice. In our study, noteworthy was the significant positive correlation observed

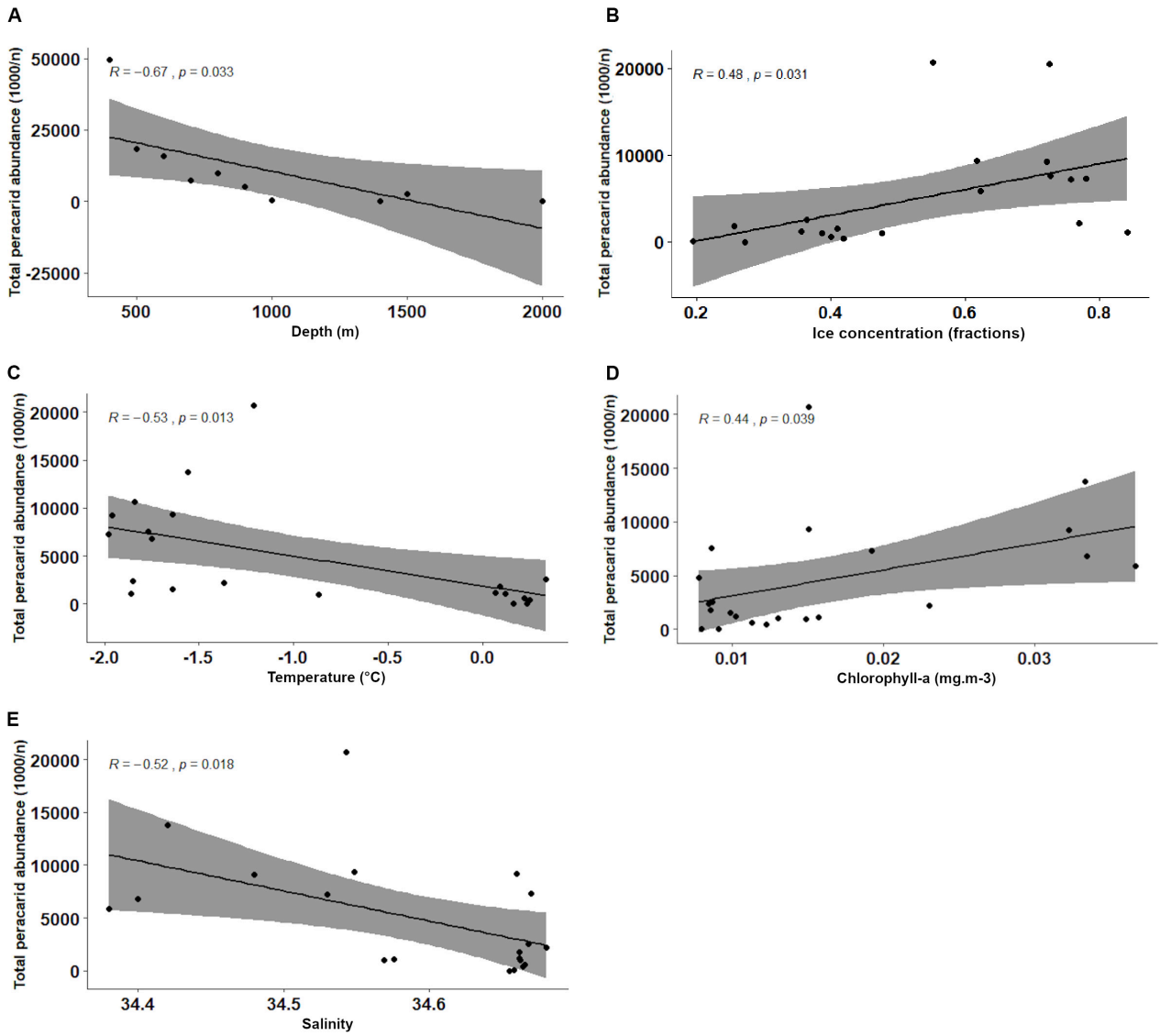

FIGURE 6 | Pearson's correlation analyses of peracarid abundances and environmental variables: depth **(A)**, ice concentration **(B)**, temperature **(C)**, chlorophyll-a **(D)**, salinity **(E)**.

between sea ice concentration and peracarid abundance and between chlorophyll-a and peracarid abundance. In the SO a previous study investigated the correlation between deep-sea isopod assemblage and chlorophyll-a concentration, although a clear pattern was not observed (Meyer-Löbbecke et al., 2014). An explanation for this result could be the use of surface chlorophyll-a in the analysis. The organic matter produced at the surface could be rapidly consumed by the zooplankton communities and in part also be laterally transferred by currents. Therefore, only a small amount of organic matter might reach the seafloor and be available for the benthic communities. A consideration of the concentration of chlorophyll-a and organic matter at the bottom might thus yield a more reliable result.

Mean sea ice concentration and peracarid abundances of continental shelf stations from present and previous studies combined (same sampling protocol and data standardization; Arntz and Gutt, 1999; Fütterer et al., 2003; Fahrbach, 2006; Linse, 2006; Brökeland et al., 2007; Kaiser et al., 2008) also showed a significant correlation. In contrast, the same analysis carried out at deeper stations did not show any significant result (**Table 4**). This suggests that benthic communities may be more strongly influenced by the presence of sea ice only within a certain depth range (up to about 1000 m from results of the present study). The reason could be the different response between deep-sea and shelf communities to seasonal organic inputs derived by the release of ice biota in the water column. Benthic shelf communities can show a quick response to the input of organic matter in productive shallow waters (Covazzi Harriague et al., 2007; Zhang et al., 2015); whereas, in the deep sea, results can be contrasting. Several studies showed that the benthic macrofauna

TABLE 4 | Pearson's correlation analyses of environmental variables and peracarid abundances.

Environmental	Present study		Present and previous studies	
Variables	***R***	***p* value**	***R***	***p*-value**
Depth (400–899 m)	−0.82	0.092	−0.86	0.061
Depth (400–2021 m)	−0.67	**0.033**	−0.66	**0.014**
Depth (400–6348 m)			−0.55	**0.011**
Se ice concentration 1978–2019	0.48	**0.031**		
Sea ice concentration Bio-ORACLE	0.44	**0.043**	0.53	**0.0023**
Sea ice concentration Bio-ORACLE (977–6348 m)			0.24	0.067
Temperature (CTD)	−0.53	**0.013**		
Temperature Bio-ORACLE + CTD	−0.47	**0.027**	−0.51	0.0037
Salinity (CTD)	−0.52	**0.018**		
Salinity Bio-ORACLE + CTD	−0.46	**0.033**	−0.42	**0.023**
Chlorophyll-a (max depth)	0.44	**0.039**	0.36	**0.045**
Current velocity	−0.098	0.66	−0.18	0.35
Iron	0.34	0.12	0.5	**0.0045**
Phosphate	−0.4	0.068	−0.08	0.67
Primary productivity	0.13	0.56	0.16	0.39

Significant results are highlighted in bold ($p < 0.05$).

from abyssal depths can quickly react to phytodetritus pulses (Sorbe, 1999; Aberle and Witte, 2003; Witte et al., 2003), although in other studies no clear response was observed (Pfannkuche, 1993; Gooday, 2002).

Concentration of chlorophyll-a in the water column can be influenced by sea ice, the break-up and melt of the latter might trigger phytoplankton blooms and enhance the production of sea-ice algae in the surrounding environment (Gradinger, 1996; Jin et al., 2007; Gradinger, 2009). In a previous study, it was also shown that the contribution of sea-ice algae to the general primary production in the water column increased in areas with more extensive ice coverage, reaching up to 57% of the total primary productivity in the ice of the Central Arctic Ocean (Leu et al., 2011). Besides, sea ice melting processes may cause a stabilization of the surface mixed layer, which can lead to higher primary production (Dunbar et al., 1998; Vernet et al., 2019) and thus higher abundances and more diverse benthic communities. In marginal sea ice zones or polynyas, higher abundances of benthic fauna were reported due to the enhanced primary productivity (Brandt, 1995, 1996; Fonseca and Soltwedel, 2007). This also proved true for peracarid assemblages from the continental shelf in the North Atlantic, where higher abundances were recorded in response to an increase in sedimentation of phytoplankton and ice algae to the sea floor (Brandt, 1995, 1996).

Sea ice retreat influences primary productivity also indirectly by the increase of open water areas whose ice-free surface is affected by wind action. During ice-free periods winds can change the depth of the mixed layer in the water column leading to a mixed-layer deepening, which in turn decreases the mean value of light available per water volume for phytoplankton photosynthesis, thus reducing the chlorophyll-a concentration (Ikeda, 1989; Dunbar et al., 1998; Montes-Hugo et al., 2009; Rainville et al., 2011). These results highlight the importance of seasonal ice coverage variations. Wlodarska-Kowalczuk et al. (2004) showed, for example, that areas characterized by seasonal ice coverage had higher abundances of the benthic macrofauna compared to areas characterized by perennial ice coverage. Moreover, the lack of sea ice break-up events strongly alters the benthic food-web structure, causing a shift on the diet of the benthic organisms (Michel et al., 2019).

Sea ice is characterized not only by seasonality but also by an interannual variability, which can drive changes in the annual rate of primary production in different regions of the SO (Arrigo et al., 2008). The latter authors showed an interannual variability in annual primary production in the Weddell Sea for the period range 1997–2006. They addressed higher annual primary production rates to anomalies in sea ice extent. Sea ice coverage around the Antarctic Peninsula has undergone a gradual increase during the last three decades and a strong decline starting from 2014 (Parkinson, 2019). In light of this, it is possible that the peracarid distribution pattern, abundance and assemblage structure observed in our study could be also explained by different sampling years (from 2012 to 2019), which may have experienced different interannual productivity rates due to changes in ice cover extent. Similarly, Meyer-Löbbecke et al. (2014) indicated the difference in sampling years as a possible factor explaining the different patterns observed in their study on isopod abundance.

CONCLUSION

Our study suggests that varying regimes of ice coverage and chlorophyll-a concentration strongly influence the abundance and assemblages' structure of benthic peracarids from the continental shelf of the SO. On one hand, the sea-ice break-up and retreat in summer is a key element for peracarid abundance and distribution since the ice-melting process releases a large amount of ice algae in the water column. These, in turn, increase the local primary productivity and thus enhance the amount of organic matter available for the benthic communities. On

the other hand, ice shelves with their continuous ice coverage allow the existence of a benthic fauna adapted to live in an environment characterized by very low sedimentation rate and which resembles that of the deep sea.

The retreat of sea ice and the disintegration of ice shelves caused by the increase of temperatures (Rott et al., 1996; Rack and Rott, 2003; Cook et al., 2016) can alter these equilibriums and impact the composition and abundance of the benthic fauna. Peracarid assemblages are subject to change drastically in the future due to such variations. Given the important role that peracarid crustaceans play among benthic communities, the complete retreat of sea ice and the consequent strong decrease of their abundance would negatively impact the benthic ecosystem. For a better understanding of interactions between sea-ice coverage and benthic communities, it is fundamental to study the ecological impact of such events on faunal compositions. Only if we understand these correlations might we be able to predict faunal alterations induced by climate change.

DATA AVAILABILITY STATEMENT

The raw data supporting the conclusions of this article will be made available by the authors, without undue reservation.

AUTHOR CONTRIBUTIONS

AB, KL, and HG developed and designed the study. DD, AB, KL, and HG collected the samples. DD, AB, and KL sorted the samples and identified the specimens to order level. CH provided the sea ice analyses. HS provided the environmental data and helped with the statistical analyses. DD prepared the figures and tables, performed the statistical analyses, and drafted the original manuscript which was revised and improved by AB, KL, HG, CH, and HS. All the authors contributed to the article and approved the submitted version.

FUNDING

DD and AB and their participation in the RV *Polarstern* expedition PS118 were funded by the Deutsche Forschungsgemeinschaft (DFG; Br1121/51-1). KL and HG are part of the British Antarctic Survey Polar Science for Planet Earth Programme. It was funded by the Natural Environment Research Council (NERC) (NC-Science), and included the funding for the RSS James Clark Ross expeditions JR275 and JR15005. The RSS *James Clark Ross* expedition JR17003a was funded by the NERC urgency grant NE/R012296/1. Multiyear ice data from 15/10/1978 to 15/03/2019 were obtained from https://www.meereisportal.de (grant: REKLIM-2013-04).

ACKNOWLEDGMENTS

We would like to thank the scientists and crew that were on board of the RRS *James Clark Ross* and the RV *Polarstern* expeditions, and the people who helped to collect the samples. We thank Oliver S. Ashford and Camille Moreau, who sorted the EBS samples to order level from the expeditions JR15005 and JR275, and Autumn Purser and the AWI OFOBS Team, who provided high quality images of the sea floor from the expedition PS118. We are grateful to Dilay Ergül, Katharina M. Krüger, Alexander H. Knorrn, Emily B. Riemer, Marissa Adler, and students of the Goethe University in Frankfurt who contributed to sort further samples to order and in peracarids to morphospecies level.

SUPPLEMENTARY MATERIAL

The Supplementary Material for this article can be found online at: https://www.frontiersin.org/articles/10.3389/fmars.2020.554663/full#supplementary-material

REFERENCES

Aberle, N., and Witte, U. (2003). Deep-sea macrofauna exposed to a simulated sedimentation event in the abyssal NE Atlantic: in situ pulse-chase experiments using 13C-labelled phytodetritus. *Mar. Ecol. Prog. Ser.* 251, 37–47. doi: 10.3354/meps251037

Alldredge, A. L., and King, J. M. (1985). The distance demersal zooplankton migrate above the benthos: implications for predation. *Mar. Biol.* 84, 253–260. doi: 10.1007/BF00392494

Arntz, W. E., and Gutt, J. (1999). "The expedition ANTARKTIS XV/3 (EASIZ II) of RV Polarstern in 1998," in *Berichte zur Polarforschung (Reports on Polar Research)*, Vol. 301, (Bremerhaven: Alfred Wegener Institute for Polar and Marine Research), 135–149. doi: 10.2312/BzP_0301_1999

Aronson, R. B., Moody, R. M., Ivany, L. C., Blake, D. B., Werner, J. E., and Glass, A. (2009). Climate change and trophic response of the Antarctic Bottom Fauna. *PLoS One* 4:e4385. doi: 10.1371/journal.pone.0004385

Arrigo, K. R., van Dijken, G. L., and Bushinsky, S. (2008). Primary production in the Southern Ocean, 1997–2006. *J. Geophys. Res.* 113:C08004. doi: 10.1029/2007JC004551

Årthun, M., Nicholls, K. W., and Boehme, L. (2013). Wintertime water mass modification near an Antarctic Ice Front. *J. Phys. Oceanogr.* 43, 359–365. doi: 10.1175/JPO-D-12-0186.1

Assis, J., Tyberghein, L., Bosch, S., Verbruggen, H., Serrão, E. A., and De Clerck, O. (2017). Bio-ORACLE v2.0: extending marine data layers for bioclimatic modelling. *Global Ecol. Biogeogr.* 27, 277–284. doi: 10.1111/geb.12693

Barker, P. F., Filippelli, G. M., Florindo, F., Martin, E. E., and Scher, H. D. (2007). Onset and role of the Antarctic circumpolar current. *Deep Sea Res. Part II Top. Stud. Oceanogr.* 54, 2388–2398. doi: 10.1016/j.dsr2.2007.07.028

Barnes, D. K. A., and Souster, T. (2011). Reduced survival of Antarctic benthos linked to climate-induced iceberg scouring. *Nat. Clim. Chang.* 1, 365–368. doi: 10.1038/nclimate1232

Bertolin, M. L., and Schloss, I. R. (2009). Phytoplankton production after the collapse of the Larsen A Ice Shelf, Antarctica. *Polar Biol.* 32, 1435–1446. doi: 10.1007/s00300-009-0638-x

Boetius, A., Albrecht, S., Bakker, K., Bienhold, C., Felden, J., Fernandez-Mendez, M., et al. (2013). Export of algal biomass from the melting Arctic sea ice. *Science* 339, 1430–1432. doi: 10.1126/science.1231346

Brandt, A. (1995). Peracarid fauna (Crustacea, Malacostraca) of the Northeast Water Polynya off Greenland: documenting close benthic-pelagic coupling in the Westwind Trough. *Mar. Ecol. Prog. Ser.* 121, 39–51. doi: 10.3354/meps121039

Brandt, A. (1996). Peracarid Crustaceans (Malacostraca) from a "time-series station" in the Westwind Trough of the New-Polynya (Greenland): a

benthic response to productivity? *Crustaceana* 69, 985–1004. doi: 10.1163/156854096X00420

Brandt, A. (1999). On the origin and evolution of Antarctic Peracarida (Crustacea, Malacostraca). *Sci. Mar.* 63, 261–274. doi: 10.3989/scimar.1999.63s1261

Brandt, A. (2000). Hypotheses on Southern Ocean peracarid evolution and radiation (Crustacea, Malacostraca). *Antarct. Sci.* 12, 269–275. doi: 10.1017/S095410200000033X

Brandt, A. (2001). Great differences in peracarid crustacean density between the Arctic and Antarctic deep sea. *Polar Biol.* 24, 785–789. doi: 10.1007/s003000100290

Brandt, A., Brix, S., Brökeland, W., Choudhury, M., Kaiser, S., and Malyutina, M. (2007a). Deep-sea isopod biodiversity, abundance, and endemism in the Atlantic sector of the Southern Ocean—Results from the ANDEEP I–III expeditions. *Deep Sea Res. Part II Top. Stud. Oceanogr.* 54, 1760–1775. doi: 10.1016/j.dsr2.2007.07.015

Brandt, A., De Broyer, C., De Mesel, I., Ellingsen, K. E., Gooday, A. J., Hilbig, B., et al. (2007b). The biodiversity of the deep Southern Ocean benthos. *Phil. Trans. R. Soc. B* 362, 39–66. doi: 10.1098/rstb.2006.1952

Brandt, A., Gooday, A. J., Brandão, S. N., Brix, S., Brökeland, W., Cedhagen, T., et al. (2007c). First insights into the biodiversity and biogeography of the Southern Ocean deep sea. *Nature* 447, 307–311. doi: 10.1038/nature05827

Brasier, M. J., Grant, S. M., Trathan, P. N., Allcock, L., Ashford, O., Blagbrough, H., et al. (2018). Benthic biodiversity in the South Orkney islands southern shelf marine protected area. *Biodiversity* 2018:148821. doi: 10.1080/14888386.2018.1468821

Brenke, N. (2005). An Epibenthic Sledge for operations on marine soft bottom and bedrock. *Mar. Technol. Soc. J.* 39, 10–21. doi: 10.4031/002533205787444015

Brey, T., Dahm, C., Gorny, M., Klages, M., Stiller, M., and Arntz, W. E. (1996). Do Antarctic benthic invertebrates show an extended level of eurybathy? *Antarct. Sci.* 8, 3–6. doi: 10.1017/S0954102096000028

Brökeland, W., Choudhury, M., and Brandt, A. (2007). Composition, abundance and distribution of Peracarida from the Southern Ocean deep sea. *Deep Sea Res. Part II Top. Stud. Oceanogr.* 54, 1752–1759. doi: 10.1016/j.dsr2.2007.07.014

Brusca, R. C., Moore, W., and Schuster, M. (2016). *Invertebrates*. Sunderland, MA: Sinauer Associated, Inc.

Clark, G. F., Stark, J. S., Palmer, A. S., Riddle, M. J., and Johnston, E. L. (2017). The roles of sea-ice, light and sedimentation in structuring shallow Antarctic benthic communities. *PLoS One* 12:e0173939. doi: 10.1371/journal.pone.0173939

Clarke, A. (2003). "The polar deep seas," in *Ecosystems of the Deep Oceans*, ed. P. A. Tyler (Amsterdam: Elsevier), 239–260.

Clarke, A., and Crame, A. (1992). The Southern Ocean benthic fauna and climate change: a historical perspective. *Phil. Trans. R. Soc. Lond. B* 338, 299–309. doi: 10.1098/rstb.1992.0150

Clarke, K. R., and Gorley, R. N. (2006). *PRIMER v6: User Manual/Tutorial*. Plymouth: *PRIMER-E*.

Collares, L. L., Mata, M. M., Kerr, R., Arigony-Neto, J., and Barbat, M. M. (2018). Iceberg drift and ocean circulation in the northwestern Weddell Sea, Antarctica. *Deep Sea Res. Part II Top. Stud. Oceanogr.* 149, 10–24. doi: 10.1016/j.dsr2.2018.02.014

Cook, A. J., Holland, P. R., Meredith, M. P., Murray, T., Luckman, A., and Vaughan, D. G. (2016). Ocean forcing of glacier retreat in the western Antarctic Peninsula. *Science* 353, 283–286. doi: 10.1126/science.aae0017

Covazzi Harriague, A., Albertelli, G., Bonomi, A., Fabiano, M., and Zunini-Sertorio, T. (2007). Pelagic–benthic coupling in a subtidal system of the North-Western Mediterranean. *Chem. Ecol.* 23, 263–277. doi: 10.1080/02757540701379527

Darelius, E., and Sallée, J. B. (2018). Seasonal outflow of Ice Shelf Water across the front of the Filchner Ice Shelf, Weddell Sea, Antarctica. *Geophys. Res. Lett.* 45, 3577–3585. doi: 10.1002/2017GL076320

Dauby, P., Nyssen, F., and Broyer, C. D. (2003). "Amphipods as food sources for higher trophic levels in the Southern Ocean: a synthesis," in *Antarctic Biology in a Global Context*, eds A. H. L. Huiskes, W. C. C. Gieskes, J. Rozema, R. M. L. Schorno, S. M. van der Vies, and W. J. Wolff (Leiden: Backhuys Publishers), 129–134. doi: 10.13140/RG.2.1.3879.0163

Dayton, P. K., Mordida, B. J., and Bacon, F. (1994). Polar marine communities. *Am. Zool.* 34, 90–99. doi: 10.1093/icb/34.1.90

De Broyer, C., and Jazdzewska, A. (2014). "Biogeographic patterns of Southern Ocean benthic amphipods," in *Biogeographic Atlas of the Southern Ocean*, eds C. De Broyer, P. Koubbi, H. J. Griffiths, B. Raymond, C. d'Udekem d'Acoz, A. Van de Putte, et al. (Cambridge: The Scientific Committee on Antarctic Research), 155–165. doi: 10.13140/RG.2.1.1716.3289

De Broyer, C., and Jazdzewski, K. (1996). Biodiversity of the Southern Ocean: towards a new synthesis for the Amphipoda (Crustacea). *Boll. Mus. Civ. Stor. Nat. Verona* 20, 547–568.

De Broyer, C., and Koubbi, C. P. (2014). *Biogeographic Atlas of the Southern Ocean*. Cambridge: Scientific Committee on Antarctic Research.

Domack, E., Duran, D., Leventer, A., Ishman, S., Doane, S., McCallum, S., et al. (2005). Stability of the Larsen B ice shelf on the Antarctic Peninsula during the Holocene epoch. *Nature* 436, 681–685. doi: 10.1038/nature03908

Dorschel, B. (2019). The expedition PS118 of the research vessel Polarstern to the Weddell Sea in 2019. *Berichte zur Polar Meeresforschung* 735:149.

Duffy, G. A., Horton, T., and Billett, D. S. M. (2012). Deep-sea scavenging amphipod assemblages from the submarine canyons of the Western Iberian Peninsula. *Biogeosciences* 9, 4861–4869. doi: 10.5194/bg-9-4861-2012

Duffy, J. E., and Hay, M. E. (2000). Strong impacts of grazing amphipods on the organization of a benthic community. *Ecol. Monogr.* 70, 237–263.

Dunbar, R. B., Leventer, A. R., and Mucciarone, D. A. (1998). Water column sediment fluxes in the Ross Sea, Antarctica: atmospheric and sea ice forcing. *J. Geophys. Res.* 103, 30741–30759. doi: 10.1029/1998JC900001

Dunn, R. J. K., Welsh, D. T., Jordan, M. A., Teasdale, P. R., and Lemckert, C. J. (2009). Influence of natural amphipod (Victoriopisa australiensis) (Chilton, 1923) population densities on benthic metabolism, nutrient fluxes, denitrification and DNRA in sub-tropical estuarine sediment. *Hydrobiologia* 628, 95–109. doi: 10.1007/s10750-009-9748-2

Fahrbach, E. (2006). The expedition ANTARKTIS-XXII/3 of the research vessel Polarstern in 2005. *Berichte zur Polar Meeresforschung* 533, 127–134. doi: 10.2312/BzPM_0533_2006

Fahrbach, E., Rohardt, G., Scheele, N., Schröder, M., Strass, V., and Wisotzki, A. (1995). Formation and discharge of deep and bottom water in the northwestern Weddell Sea. *J. Mar. Res.* 53, 515–538. doi: 10.1357/0022240953213089

Fonseca, G., and Soltwedel, T. (2007). Deep-sea meiobenthic communities underneath the marginal ice zone off Eastern Greenland. *Polar Biol.* 30, 607–618. doi: 10.1007/s00300-006-0220-8

Fütterer, D., Brandt, A., and Poore, G. (2003). The expeditions ANTARKTIS-XIX/3-4 of the research vessel POLARSTERN in 2002: (ANDEEP I and II: Antarctic benthic deep-sea biodiversity - colonization history and recent community patterns). *Berichte zur Polar Meeresforschung* 470, 66–71. doi: 10.2312/BzPM_0470_2003

Gage, J. D., and Tyler, P. A. (1991). *Deep-Sea Biology: A Natural History of Organisms at the Deep-Sea Floor*. Cambridge: Cambridge University Press.

Gerdes, D., Hilbig, B., and Montiel, A. (2003). Impact of iceberg scouring on macrobenthic communities in the high-Antarctic Weddell Sea. *Polar Biol.* 26, 295–301. doi: 10.1007/s00300-003-0484-1

Gooday, A. J. (2002). Biological responses to seasonally varying fluxes of organic matter to the ocean floor: a review. *J. Oceanogr.* 58, 305–332. doi: 10.1023/A:1015865826379

Gordon, A. L., Visbeck, M., and Huber, B. (2001). Export of Weddell Sea deep and bottom water. *J. Geophys. Res.* 106, 9005–9017. doi: 10.1029/2000JC000281

Gradinger, R. (1996). Occurrence of an algal bloom under Arctic pack ice. *Mar. Ecol. Prog. Ser.* 131, 301–305. doi: 10.3354/meps131301

Gradinger, R. (2009). Sea-ice algae: major contributors to primary production and algal biomass in the Chukchi and Beaufort Seas during May/June 2002. *Deep Sea Res. Part II Top. Stud. Oceanogr.* 56, 1201–1212. doi: 10.1016/j.dsr2.2008.10.016

Griffiths, H. J. (2012). *Cruise Report JR275*. Available online at: https://www.bodc.ac.uk (accessed February 20, 2020).

Griffiths, H. J. (2017). *Cruise Report JR15005*. Available online at: https://www.bodc.ac.uk (accessed February 20, 2020).

Grosfeld, K., Treffeisen, R., Asseng, J., Bartsch, A., Bräuer, B., Fritzsch, B., et al. (2016). Online sea-ice knowledge and data platform <www.meereisportal.de>. *Polarforschung* 85, 143–155. doi: 10.2312/polfor.2016.011

Gutt, J., Barratt, I., Domack, E., d'Udekem d'Acoz, C., Dimmler, W., Grémare, A., et al. (2011). Biodiversity change after climate-induced ice-shelf collapse in the Antarctic. *Deep Sea Res. Part II Top. Stud. Oceanogr.* 58, 74–83. doi: 10.1016/j.dsr2.2010.05.024

Gutt, J., and Starmans, A. (2001). Quantification of iceberg impact and benthic recolonisation patterns in the Weddell Sea (Antarctica). *Polar Biol.* 24, 615–619. doi: 10.1007/s003000100263

Gutt, J., Starmans, A., and Dieckmann, G. (1996). Impact of iceberg scouring on polar benthic habitats. *Mar. Ecol. Prog. Ser.* 137, 311–316. doi: 10.3354/meps137311

Hansen, J., Ruedy, R., Sato, M., and Lo, K. (2010). Global surface temperature change. *Rev. Geoph.* 48, 1–29. doi: 10.1029/2010RG000345

Haumann, F. A., Gruber, N., Münnich, M., Frenger, I., and Kern, S. (2016). Sea-ice transport driving Southern Ocean salinity and its recent trends. *Nature* 537, 89–92. doi: 10.1038/nature19101

Hessler, R. R. (1974). "The structure of deep benthic communities from central oceanic waters," in *The Biology of the Oceanic Pacific*, ed. C. B. Miller (Corvallis, OR: Oregon State University Press), 79–93.

Hodgson, D. A., McMinn, A., Kirkup, H., Cremer, H., Gore, D., Melles, M., et al. (2003). Colonization, succession, and extinction of marine floras during a glacial cycle: a case study from the Windmill Islands (east Antarctica) using biomarkers. *Paleoceanography* 18, 12. doi: 10.1029/2002PA000775

Hogg, A. E., and Gudmundsson, G. H. (2017). Impacts of the Larsen-C Ice Shelf calving event. *Nat. Clim. Chang.* 7, 540–542. doi: 10.1038/nclimate3359

Ikeda, M. (1989). A coupled ice-ocean mixed layer model of the marginal ice zone responding to wind forcing. *J. Geophys. Res.* 94, 9699. doi: 10.1029/JC094iC07p09699

Ingels, J., Vanreusel, A., Brandt, A., Catarino, A. I., David, B., De Ridder, C., et al. (2012). Possible effects of global environmental changes on Antarctic benthos: a synthesis across five major taxa. *Ecol. Evol.* 2, 453–485. doi: 10.1002/ece3.96

Jansen, J., Hill, N. A., Dunstan, P. K., McKinlay, J., Sumner, M. D., Post, A. L., et al. (2018). Abundance and richness of key Antarctic seafloor fauna correlates with modelled food availability. *Nat. Ecol. Evol.* 2, 71–80. doi: 10.1038/s41559-017-0392-3

Jeong, S. J., Yu, O. H., and Suh, H.-L. (2009). Reproductive patterns and secondary production of *Gammaropsis japonicus* (Crustacea, Amphipoda) on the seagrass *Zostera marina* of Korea. *Hydrobiologia* 623, 63–76. doi: 10.1007/s10750-008-9648-x

Jin, M., Deal, C., Wang, J., Alexander, V., Gradinger, R., Saitoh, S., et al. (2007). Ice-associated phytoplankton blooms in the southeastern Bering Sea. *Geophys. Res. Lett.* 34, L06612. doi: 10.1029/2006GL028849

Kaiser, S. (2014). "Antarctic and Sub-Antarctic isopod crustaceans (Peracarida, Malacostraca)," in *Biogeographic Atlas of the Southern Ocean*, eds C. De Broyer, P. Koubbi, H. J. Griffiths, B. Raymond, C. d'Udekem d'Acoz, A. Van de Putte, et al. (Cambridge: The Scientific Committee on Antarctic Research), 166–172.

Kaiser, S., Barnes, D. K. A., and Brandt, A. (2007). Slope and deep-sea abundance across scales: Southern Ocean isopods show how complex the deep sea can be. *Deep Sea Res. Part II Top. Stud. Oceanogr.* 54, 1776–1789. doi: 10.1016/j.dsr2.2007.07.006

Kaiser, S., Barnes, D. K. A., Linse, K., and Brandt, A. (2008). Epibenthic macrofauna associated with the shelf and slope of a young and isolated Southern Ocean island. *Antarct. Sci.* 20, 281–290. doi: 10.1017/S0954102008001107

Karlson, K., Hulth, S., and Rosenberg, R. (2007). Density of *Monoporeia affinis* and biogeochemistry in Baltic Sea sediments. *J. Exp. Mar. Biol. Ecol.* 344, 123–135. doi: 10.1016/j.jembe.2006.11.016

Kassambara, A. (2017). *ggpubr: "ggplot2" Based Publication Ready Plots*. Available online at: https://CRAN.R-project.org/package=ggpubr (accessed March 16, 2020).

Kiljunen, M., Peltonen, H., Lehtiniemi, M., Uusitalo, L., Sinisalo, T., Norkko, J., et al. (2020). Benthic-pelagic coupling and trophic relationships in northern Baltic Sea food webs. *Limnol.* Oceanogr. 9999, 1–17. doi: 10.1002/lno.11413

Lawver, L. A., Gahagan, L. M., and Dalziel, I. W. D. I. W. D. (2011). "A different look at gateways: drake passage and Australia/Antarctica," in *Special Publications*, eds J. B. Anderson and J. S. Wellner (Washington, DC: American Geophysical Union), 5–33. doi: 10.1029/2010SP001017

Legezyñska, J., De Broyer, C., and Wesławski, J. M. (2020). "Invasion of the poles," in *The Natural History of the Crustacea: Evolution and Biogeography of the Crustacea*, eds M. Thiel and G. Poore (New York, NY: Oxford University Press), 216–246.

Lehtonen, K. K., and Andersin, A.-B. (1998). Population dynamics, response to sedimentation and role in benthic metabolism of the amphipod *Monoporeia affinis* in an open-sea area of the northern Baltic Sea. *Mar. Ecol. Prog. Ser.* 168, 71–85.

Leu, E., Søreide, J. E., Hessen, D. O., Falk-Petersen, S., and Berge, J. (2011). Consequences of changing sea-ice cover for primary and secondary producers in the European Arctic shelf seas: timing, quantity, and quality. *Progr. Oceanogr.* 90, 18–32. doi: 10.1016/j.pocean.2011.02.004

Linse, K. (2006). *Cruise report JR144, JR145, JR146, JR147 and JR149*. Available online at: https://www.bodc.ac.uk (accessed February 20, 2020).

Linse, K. (2018). *Cruise report JR17003a*. Available online at: https://www.bodc.ac.uk (accessed February 20, 2020).

Makinson, K., Holland, P. R., Jenkins, A., Nicholls, K. W., and Holland, D. M. (2011). Influence of tides on melting and freezing beneath Filchner-Ronne Ice Shelf, Antarctica. *Geophys. Res. Lett.* 38:L06601. doi: 10.1029/2010GL046462

Massom, R. A., Scambos, T. A., Bennetts, L. G., Reid, P., Squire, V. A., and Stammerjohn, S. E. (2018). Antarctic ice shelf disintegration triggered by sea ice loss and ocean swell. *Nature* 558, 383–389. doi: 10.1038/s41586-018-0212-1

Meredith, M. P., Nicholls, K. W., Renfrew, I. A., Boehme, L., Biuw, M., and Fedak, M. (2011). Seasonal evolution of the upper-ocean adjacent to the South Orkney Islands, Southern Ocean: results from a "lazy biological mooring.". *Deep Sea Res. Part II Top. Stud. Oceanogr.* 58, 1569–1579. doi: 10.1016/j.dsr2.2009.07.008

Meyer-Löbbecke, A., Brandt, A., and Brix, S. (2014). Diversity and abundance of deep-sea Isopoda along the Southern Polar Front: results from the SYSTCO I and II expeditions. *Deep Sea Res. Part II Top. Stud. Oceanogr.* 108, 76–84. doi: 10.1016/j.dsr2.2014.06.006

Michel, L. N., Danis, B., Dubois, P., Eleaume, M., Fournier, J., Gallut, C., et al. (2019). Increased sea ice cover alters food web structure in East Antarctica. *Sci. Rep.* 9:8062. doi: 10.1038/s41598-019-44605-5

Montes-Hugo, M., Doney, S. C., Ducklow, H. W., Fraser, W., Martinson, D., Stammerjohn, S. E., et al. (2009). Recent changes in Phytoplankton communities associated with rapid regional climate change along the western Antarctic Peninsula. *Science* 323, 1470–1473. doi: 10.1126/science.1164533

Mouat, B., Collins, M. A., and Pompert, J. (2001). Patterns in the diet of *Illex argentinus* (Cephalopoda: Ommastrephidae) from the Falkland Islands jigging fishery. *Fish. Res.* 52, 41–49. doi: 10.1016/S0165-7836(01)00229-6

Mühlenhardt-Siegel, U. (2014). "Southern ocean Cumacea," in *Biogeographic Atlas of the Southern Ocean*, eds C. De Broyer, P. Koubbi, H. J. Griffiths, B. Raymond, C. d'Udekem d'Acoz, A. Van de Putte, et al. (Cambridge: The Scientific Committee on Antarctic Research), 181–184.

Murphy, E. J., Clarke, A., Symon, C., and Priddle, J. (1995). Temporal variation in Antarctic sea-ice: analysis of a long term fast-ice record from the South Orkney Islands. *Deep Sea Res. Part I Oceanogr. Res. Pap.* 42, 1045–1062. doi: 10.1016/0967-0637(95)00057-D

Orsi, A. H., Nowlin, W. D., and Whitworth, T. (1993). On the circulation and stratification of the Weddell Gyre. *Deep Sea Res. Part I Oceanogr. Res. Pap.* 40, 169–203. doi: 10.1016/0967-0637(93)90060-G

Pacheco, A. S., Goméz, G. E., and Riascos, J. M. (2013). First records of emerging benthic invertebrates at a sublittoral soft-bottom habitat in northern Chile. *Rev. Biol. Mar. Oceanogr.* 48, 387–392. doi: 10.4067/S0718-19572013000200018

Padovani, L. N., Viñas, M. D., Sánchez, F., and Mianzan, H. (2012). Amphipod-supported food web: *Themisto gaudichaudii*, a key food resource for fishes in the southern Patagonian Shelf. *J. Sea Res.* 67, 85–90. doi: 10.1016/j.seares.2011.10.007

Parkinson, C. L. (2019). A 40-y record reveals gradual Antarctic sea ice increases followed by decreases at rates far exceeding the rates seen in the Arctic. *Proc. Natl. Acad. Sci. U.S.A.* 116, 14414–14423. doi: 10.1073/pnas.1906556116

Peck, L., Brockington, S., Vanhove, S., and Beghyn, M. (1999). Community recovery following catastrophic iceberg impacts in a soft-sediment shallow-water site at Signy Island, Antarctica. *Mar. Ecol. Prog. Ser.* 186, 1–8.

Pelegrí, S. P., and Blackburn, T. H. (1994). Bioturbation effects of the amphipod *Corophium volutator* on microbial nitrogen transformations in marine sediments. *Mar. Biol.* 121, 253–258. doi: 10.1007/BF00346733

Pfannkuche, O. (1993). Benthic response to the sedimentation of particulate organic matter at the BIOTRANS station, 47°N, 20°W. *Deep Sea Res. Part II Top. Stud. Oceanogr.* 40, 135–149. doi: 10.1016/0967-0645(93)90010-K

Post, A. L., O'Brien, P. E., Beaman, R. J., Riddle, M. J., and De Santis, L. (2010). Physical controls on deep water coral communities on the George V Land slope, East Antarctica. *Antarct. Sci.* 22, 371–378. doi: 10.1017/S0954102010000180

Pudsey, C. J., Evans, J., Domack, E. W., Morris, P., and Valle, R. A. D. (2001). Bathymetry and acoustic facies beneath the former Larsen-A and Prince Gustav ice shelves, north-west Weddell Sea. *Antarct. Sci.* 13, 312–322. doi: 10.1017/S095410200100044X

Pudsey, C. J., Murray, J. W., Appleby, P., and Evans, J. (2006). Ice shelf history from petrographic and foraminiferal evidence, Northeast Antarctic Peninsula. *Quat. Sci. Rev.* 25, 2357–2379. doi: 10.1016/j.quascirev.2006.01.029

Rack, W., and Rott, H. (2003). "Further retreat of the northern Larsen Ice Shelf and collapse of Larsen B," in *Proceedings of the 16th International Workshop of the Forum for Research on Ice Shelf Processes (FRISP)*, (Bergen: University of Bergen).

Rack, W., and Rott, H. (2004). Pattern of retreat and disintegration of the Larsen B ice shelf, Antarctic Peninsula. *Ann. Glaciol.* 39, 505–510. doi: 10.3189/172756404781814005

Rainville, L., Lee, C., and Woodgate, R. (2011). Impact of wind-driven mixing in the Arctic Ocean. *Oceanography* 24, 136–145. doi: 10.5670/oceanog.2011.65

Raupach, M. J., Mayer, C., Malyutina, M., and Wägele, J.-W. (2009). Multiple origins of deep-sea Asellota (Crustacea: Isopoda) from shallow waters revealed by molecular data. *Proc. R. Soc. B* 276, 799–808. doi: 10.1098/rspb.2008.1063

Rehm, P., Thatje, S., Mühlenhardt-Siegel, U., and Brandt, A. (2007). Composition and distribution of the peracarid crustacean fauna along a latitudinal transect off Victoria Land (Ross Sea, Antarctica) with special emphasis on the Cumacea. *Polar Biol.* 30, 871–881. doi: 10.1007/s00300-006-0247-x

Riddle, M. J., Craven, M., Goldsworthy, P. M., and Carsey, F. (2007). A diverse benthic assemblage 100 km from open water under the Amery Ice Shelf, Antarctica. *Paleoceanography* 22:A1204. doi: 10.1029/2006PA001327

Riehl, T., Brandão, S. N., and Brandt, A. (2020). "Conquering the ocean depths over three geological eras," in *The Natural History of the Crustacea: Evolution and Biogeography of the Crustacea*, eds M. Thiel and G. Poore (New York, NY: Oxford University Press), 155–182.

Rignot, E., Jacobs, S., Mouginot, J., and Scheuchl, B. (2013). Ice-shelf melting around Antarctica. *Science* 341, 266–270. doi: 10.1126/science.1235798

Rose, A., Ingels, J., Raes, M., Vanreusel, A., and Arbizu, P. M. (2015). Long-term iceshelf-covered meiobenthic communities of the Antarctic continental shelf resemble those of the deep sea. *Mar. Biodiv.* 45, 743–762.

Rott, H., Rack, W., Nagler, T., and Skvarca, P. (1998). Climatically induced retreat and collapse of northern Larsen Ice Shelf, Antarctic Peninsula. *Ann. Glaciol.* 27, 86–92. doi: 10.3189/S0260305500017262

Rott, H., Skvarca, P., and Nagler, T. (1996). Rapid collapse of northern Larsen Ice Shelf, Antarctica. *Science* 271, 788–792. doi: 10.1126/science.271.5250.788

Runcie, J. W., and Riddle, M. J. (2006). Photosynthesis of marine macroalgae in ice-covered and ice-free environments in East Antarctica. *Eur. J. Phycol.* 41, 223–233. doi: 10.1080/09670260600645824

Schnack-Schiel, S. B., and Isla, E. (2005). The role of zooplankton in the pelagic-benthic coupling of the Southern Ocean. *Sci. Mar.* 69, 39–55. doi: 10.3989/scimar.2005.69s239

Smale, D. A., Brown, K. M., Barnes, D. K. A., Fraser, K. P. P., and Clarke, A. (2008). Ice ccour disturbance in Antarctic waters. *Science* 321, 371–371. doi: 10.1126/science.1158647

Smith, J. A., Graham, A. G. C., Post, A. L., Hillenbrand, C.-D., Bart, P. J., and Powell, R. D. (2019). The marine geological imprint of Antarctic ice shelves. *Nat. Commun.* 10:5635. doi: 10.1038/s41467-019-13496-5

Smith, K. L. (2011). Free-drifting icebergs in the Southern Ocean: an overview. *Deep Sea Res. Part II Top. Stud. Oceanogr.* 58, 1277–1284. doi: 10.1016/j.dsr2.2010.11.003

Sorbe, J. C. (1999). Deep-sea macrofaunal assemblages within the Benthic Boundary Layer of the Cap-Ferret Canyon (Bay of Biscay, NE Atlantic). *Deep Sea Res. Part II Top. Stud. Oceanogr.* 46, 2309–2329. doi: 10.1016/S0967-0645(99)00064-8

Thatje, S., and Arntz, W. E. (2004). Antarctic reptant decapods: more than a myth? *Polar Biol.* 27, 195–201. doi: 10.1007/s00300-003-0583-z

Thatje, S., Hillenbrand, C.-D., and Larter, R. (2005). On the origin of Antarctic marine benthic community structure. *Trends Ecol. Evol.* 20, 534–540. doi: 10.1016/j.tree.2005.07.010

Thiel, M., and Hinojosa, I. (2009). "Peracarida–amphipods, isopods, tanaidaceans & cumaceans," in *Marine Benthic Fauna of Chilean Patagonia: Illustrated Identification Guide*, eds V. Häussermann and G. Försterra (Santiago del Chile, CL: Nature in Focus), 671–738.

Tyberghein, L., Verbruggen, H., Pauly, K., Troupin, C., Mineur, F., and Clerck, O. D. (2012). Bio-ORACLE: a global environmental dataset for marine species distribution modelling. *Glob. Ecol. Biogeogr.* 21, 272–281. doi: 10.1111/j.1466-8238.2011.00656.x

Valdivia, N., Garrido, I., Bruning, P., Piñones, A., and Pardo, L. M. (2020). Biodiversity of an Antarctic rocky subtidal community and its relationship with glacier meltdown processes. *Mar. Env. Res.* 159, 104991. doi: 10.1016/j.marenvres.2020.104991

Vallet, C., and Dauvin, J.-C. (2001). Biomass changes and bentho-pelagic transfers throughout the Benthic Boundary Layer in the English Channel. *J. Plankton Res.* 23, 903–922. doi: 10.1093/plankt/23.9.903

Vanhove, S., Wittoeck, J., Desmet, G., Van den Berghe, B., Herman, R., Bak, R. P. M., et al. (1995). Deep-sea meiofauna communities in Antarctica: structural analysis and relation with the environment. *Mar. Ecol. Prog. Ser.* 127, 65–76. doi: 10.3354/meps127065

Vernet, M., Geibert, W., Hoppema, M., Brown, P. J., Haas, C., Hellmer, H. H., et al. (2019). The Weddell Gyre, Southern Ocean: present knowledge and future challenges. *Rev. Geophys.* 57, 623–708. doi: 10.1029/2018RG000604

Wing, S. R., Leichter, J. J., Wing, L. C., Stokes, D., Genovese, S. J., McMullin, R. M., et al. (2018). Contribution of sea ice microbial production to Antarctic benthic communities is driven by sea ice dynamics and composition of functional guilds. *Glob. Chang. Biol.* 24, 3642–3653. doi: 10.1111/gcb.14291

Witte, U., Wenzhöfer, F., Sommer, S., Boetius, A., Heinz, P., Aberle, N., et al. (2003). In situ experimental evidence of the fate of a phytodetritus pulse at the abyssal sea floor. *Nature* 424, 763–766. doi: 10.1038/nature01799

Wlodarska-Kowalczuk, M., Kendall, M. A., Marcin Weslawski, J., Klages, M., and Soltwedel, T. (2004). Depth gradients of benthic standing stock and diversity on the continental margin at a high-latitude ice-free site (off Spitsbergen, 79°N). *Deep Sea Res. Part I Oceanogr. Res. Pap.* 51, 1903–1914. doi: 10.1016/j.dsr.2004.07.013

Xavier, J. C., Cherel, Y., Boxshall, G., Brandt, A., Coffer, T., Forman, J., et al. (2020). *Crustacean Guide for Predator Studies in the Southern Ocean*. Cambridge: Scientific Committee on Antarctic Research, 255.

Yi, D., Zwally, H. J., and Robbins, J. W. (2011). ICESat observations of seasonal and interannual variations of sea-ice freeboard and estimated thickness in the Weddell Sea, Antarctica (2003–2009). *Ann. Glaciol.* 52, 43–51. doi: 10.3189/172756411795931480

Zhang, Q., Warwick, R. M., McNeill, C. L., Widdicombe, C. E., Sheehan, A., and Widdicombe, S. (2015). An unusually large phytoplankton spring bloom drives rapid changes in benthic diversity and ecosystem function. *Prog. Oceanogr.* 137, 533–545. doi: 10.1016/j.pocean.2015.04.029

Conflict of Interest: The authors declare that the research was conducted in the absence of any commercial or financial relationships that could be construed as a potential conflict of interest.

frontiers in Marine Science

ORIGINAL RESEARCH
published: 08 January 2021
doi: 10.3389/fmars.2020.595303

Annelid Fauna of the Prince Gustav Channel, a Previously Ice-Covered Seaway on the Northeastern Antarctic Peninsula

Regan Drennan[1,2], Thomas G. Dahlgren[3,4], Katrin Linse[5] and Adrian G. Glover[1]*

[1] Life Sciences Department, Natural History Museum, London, United Kingdom, [2] Ocean and Earth Science, University of Southampton, Southampton, United Kingdom, [3] NORCE Norwegian Research Centre, Bergen, Norway, [4] Department of Marine Sciences, University of Gothenburg, Gothenburg, Sweden, [5] British Antarctic Survey, Cambridge, United Kingdom

The Prince Gustav Channel is a narrow seaway located in the western Weddell Sea on the northeastern-most tip of the Antarctic Peninsula. The channel is notable for both its deep (>1200 m) basins, and a dynamic glacial history that most recently includes the break-up of the Prince Gustav Ice Shelf, which covered the southern portion of the channel until its collapse in 1995. However, the channel remains mostly unsampled, with very little known about its benthic biology. We present a preliminary account of the benthic annelid fauna of the Prince Gustav Channel in addition to samples from Duse Bay, a sheltered, glacier-influenced embayment in the northwestern portion of the channel. Samples were collected using an Agassiz Trawl, targeting megafaunal and large macrofaunal sized animals at depths ranging between 200–1200 m; the seafloor and associated fauna were also documented *in situ* using a Shallow Underwater Camera System (SUCS). Sample sites varied in terms of depth, substrate type, and current regime, and communities were locally variable across sites in terms of richness, abundance, and both taxonomic and functional composition. The most diverse family included the motile predator/scavenger Polynoidae, with 105 individuals in at least 12 morphospecies, primarily from a single site. This study provides first insights into diverse and spatially heterogeneous benthic communities in a dynamic habitat with continuing glacial influence, filling sampling gaps in a poorly studied region of the Southern Ocean at direct risk from climate change. These specimens will also be utilized in future molecular investigations, both in terms of describing the genetic biodiversity of this site and as part of wider phylogeographic and population genetic analyses assessing the connectivity, evolutionary origins, and demographic history of annelid fauna in the region.

Keywords: polychaeta, Weddell Sea, species checklist, Southern Ocean, benthic, morphology, taxonomy

OPEN ACCESS

Edited by:
Zhijun Dong,
Yantai Institute of Coastal Zone Research (CAS), China

Reviewed by:
Julian Gutt,
Alfred Wegener Institute Helmholtz Centre for Polar and Marine Research (AWI), Germany
Anja Schulze,
Texas A&M University at Galveston, United States

****Correspondence:***
Regan Drennan
r.drennan@nhm.ac.uk;
regan.drennan5@gmail.com

Specialty section:
This article was submitted to Marine Evolutionary Biology, Biogeography and Species Diversity, a section of the journal Frontiers in Marine Science

Received: *15 August 2020*
Accepted: *01 December 2020*
Published: *08 January 2021*

Citation:
Drennan R, Dahlgren TG, Linse K and Glover AG (2021) Annelid Fauna of the Prince Gustav Channel, a Previously Ice-Covered Seaway on the Northeastern Antarctic Peninsula. Front. Mar. Sci. 7:595303. doi: 10.3389/fmars.2020.595303

INTRODUCTION

Ice shelves are vast, floating platforms of ice that form where continental ice sheets meet the ocean, fringing much of the Antarctic coastline and covering over 30% of the Antarctic continental shelf (Barnes and Peck, 2008). Sub-ice shelf ecosystems thus constitute a significant portion of available benthic habitat in the Southern Ocean, though remain amongst the least known on the planet

due to general inaccessibility and are at a direct risk of being lost due to climate change. Ice shelves are extensive along both sides of the Antarctic Peninsula, covering approximately 120,000 km^2 of seafloor today (Cook and Vaughan, 2010). However, in recent decades the Antarctic Peninsula has experienced amongst some of the fastest regional warming on the planet (Vaughan et al., 2003), with substantial increases in both atmospheric and ocean temperatures (e.g., Meredith and King, 2005; Turner et al., 2005). These increases are largely thought to have contributed to the significant thinning, retreat and collapse of ice shelves along the Antarctic Peninsula over the past 60 years (Cook and Vaughan, 2010; Rignot et al., 2013; Etourneau et al., 2019), with significant losses including the collapse of the Larsen A and Prince Gustav Ice Shelves in 1995 (Rott et al., 1996), the Larsen B ice shelf in 2002 (Rack and Rott, 2004), and the calving of a massive 5,800 km^2 iceberg from the Larsen C Ice Shelf in 2017 (Marchant, 2017).

Until its collapse in the early 1990s, the Prince Gustav Ice Shelf (PGIS) was the most northerly ice shelf on the Antarctic Peninsula, spanning the southern portion of the Prince Gustav Channel (PGC) (see Ferrigno et al., 2006), a deep, narrow seaway located on the inner continental shelf of the northwestern Weddell Sea that separates James Ross Island from the northernmost tip of the Antarctic Peninsula (see **Figure 1**). Broadly categorized as a fjord (Camerlenghi et al., 2001), the PGC consists of a discontinuous u-shaped glacial trough with steep sided walls and three over-deepened basins (approximately 900 m, 1000 m, and 1200 m deep moving north to south), separated by two shallower sills (approximately 350 m and 600 m deep respectively) (Camerlenghi et al., 2001). The channel formed before the late Miocene and was progressively deepened by several advances of grounded glaciers during the Neogene and Quaternary periods (Nývlt et al., 2011), and with evidence of floating ice shelves from the end of the Pleistocene (Evans et al., 2005; Johnson et al., 2011).

In contemporary terms, the PGIS and other small ice shelves on the northeastern Antarctic Peninsula have been observed for a far longer period than many other Antarctic ice shelves; first visited over 170 years ago and mapped by the Swedish Antarctic Expedition 1901–1903 (Nordenskjöld and Andersson, 1905), these ice shelves are generally thought to have been in retreat since historical observations began, with the PGIS itself once contiguous with the Larsen A ice shelf until the mid 20th century (Cooper, 1997). In contrast to larger ice shelves that can remain stable over tens of thousands of years, these small northern ice shelves are at the climactic limit of ice shelf viability (Morris and Vaughan, 2003) and may therefore act as more sensitive indicators of recent climatic and oceanographic change (Pudsey et al., 2006), with evidence of periodic advance and retreat of ice shelves in the region throughout the Holocene, as demonstrated by several studies of data from sediment cores (e.g., Pudsey and Evans, 2001; Brachfeld et al., 2003; Pudsey et al., 2006). This includes a period of retreat during the mid-Holocene (∼5–2 ka) in which the PGIS was completely absent (Pudsey and Evans, 2001), though with break up and regrowth appearing to occur gradually over centuries as opposed to the decadal scale of changes to contemporary ice shelf extent (Pudsey et al., 2006).

Understanding the biology of previously ice covered habitats is important in the context of unprecedented ice loss along the Antarctic Peninsula. However, despite the dynamic glacial history of the channel, the biology of the PGC, both before and after ice shelf collapse, is virtually unknown. In May 2000, a number of geological and geophysical surveys of the PGC were conducted by the RVIB Nathaniel B. Palmer as part of a larger investigation of the seafloor exposed by the then recent 1995 break-up of the Larsen A ice shelf (Domack et al., 2001). Biological samples were also obtained from collected sediment, however, these sampling sites were restricted to the southern portion of the channel (see Blake, 2015). Furthermore, while a number of polychete specimens collected from this cruise have been included in several broader taxonomic publications (Blake, 2015, 2017, 2018), a summary of these samples and of the southern PGC benthic community is not currently available. In addition, no further biological investigations have taken place subsequent years, and the channel remains otherwise unsampled, which is not uncommon for the region, with the western Weddell Sea considered to be one of the most poorly sampled areas of the Southern Ocean (Griffiths et al., 2014).

Annelid worms, or polychetes, are amongst the most species rich groups in the Southern Ocean (Clarke and Johnston, 2003), and can represent a dominant component of Antarctic benthic assemblages in terms of both abundance and biomass (e.g., Gambi et al., 1997; Piepenburg et al., 2002; Hilbig et al., 2006; Sañé et al., 2012). Found across the Southern Ocean from intertidal to abyssal depths (Brandt et al., 2009), polychetes fill a diverse array of trophic guilds and functional groups on both hard and soft substrates (e.g., Gambi et al., 1997), and are thus both an important and informative group to consider when assessing the biology of Antarctic benthic ecosystems. The following report documents a preliminary overview of the benthic annelid fauna of the Prince Gustav Channel collected during the expedition JR17003a on board RSS *James Clark Ross* February–March 2018. Samples were collected using an Agassiz trawl from several sites along the northern portion of the channel including the deepest (>1200 m) basin of the PGC. In contrast to the more open channel, samples were additionally collected from Duse Bay, a sheltered, glacier influenced embayment located in the northwestern portion of the PGC. The aims of this study were to (1) characterize the annelid fauna of the PGC, a previously ice covered channel in the northwestern Weddell Sea and (2) examine spatial variation in annelid assemblages in this habitat by comparing samples from open and sheltered areas of the PGC.

MATERIALS AND METHODS

Sample Sites and Sample Collection

The annelid specimens examined in this study were collected using an Agassiz Trawl (AGT) during the expedition JR17003a on board the RRS *James Clark Ross* February–March 2018, which sampled the northern portion of the Prince Gustav Channel (PGC) situated on the northeastern tip of the Antarctic Peninsula. The three main sampling sites were as follows: (1)

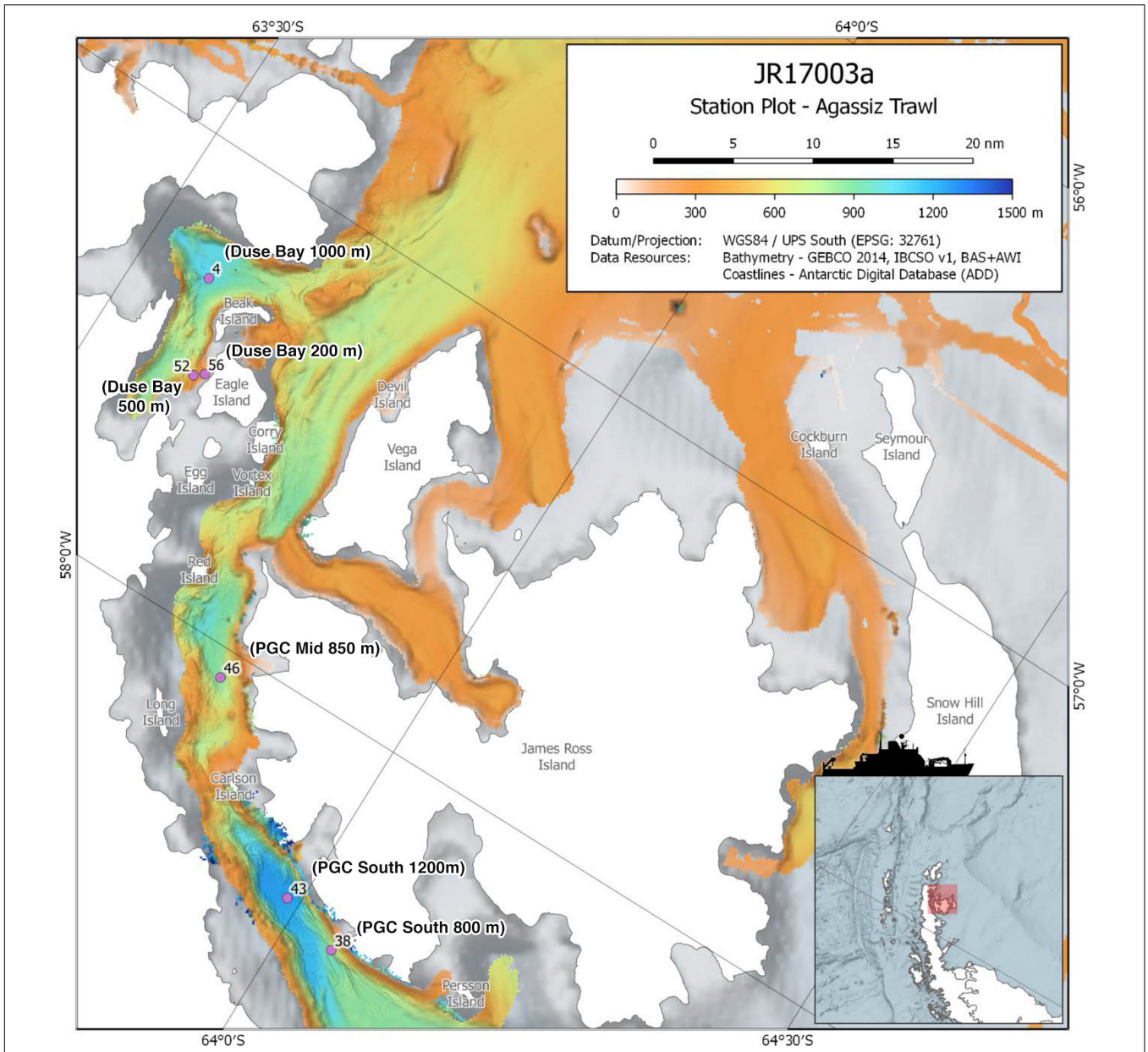

FIGURE 1 | Map of study area within the Prince Gustav Channel, showing the six Agassiz trawl sites, marked with event number and sample name. Modified from RRS *James Clark Ross* expedition JR17003a cruise report, accessible via https://www.bodc.ac.uk/resources/inventories/cruise_inventory/report/16954/. See Dreutter et al. (2020) for archived bathymetry data from the JR17003a expedition.

Duse Bay, a sheltered, glacier influenced bay located in the northwestern portion of the PGC; (2) PGC Mid, located in the main channel, including the second deepest basin of the PGC; (3) PGC South, the southernmost sample site, located in the main channel and including the deepest basin of the PGC (**Figure 1**).

Three trawling depths (200 m, 500 m, 800/1000 m) were initially planned for each of the main sampling sites, with an additional deep 1200 m trawl of the basin at PGC South. However, only at Duse Bay sites were all three trawling depths achieved, as 200 and 500 m sites in the channel proper were too influenced by boulders to deploy the AGT. In total, six successful AGT deployments between depths of 204 m and 1270 m were carried out across the three sites (**Figure 1** and **Table 1**) and sorted on board for benthic fauna. The AGT apparatus used comprised of a 1 cm mesh with a mouth width of 2 m, and once on the seabed was trawled at 1 knot for 5–10 min at each site. The AGT targeted macro- and megafaunal sized animals 1 cm and larger, though with some smaller animals additionally captured in the sediment retained in trawls.

A 'cold-chain' live sorting pipeline was followed on board, as outlined in detail in Glover et al. (2016). In summary, AGT

TABLE 1 | Details of Agassiz Trawl stations within the Prince Gustav Channel sampled during the expedition JR17003a.

Event no.	Site	Date	Decimal latitude	Decimal longitude	Max depth (m)	No. of individuals	No. of families	No. of morphospecies	H'	J'
56	Duse Bay 200 m	2018-03-07	−63.62531	−57.48627	203.85	48	10	13	1.99	0.77
52	Duse Bay 500 m	2018-03-07	−63.61614	−57.50349	483.01	99	19	32	2.76	0.80
4	Duse Bay 1000 m	2018-03-01	−63.57554	−57.29537	1080.63	260	8	10	0.95	0.41
46	PGC Mid 850 m	2018-03-06	−63.80603	−58.06523	869.95	126	8	21	2.33	0.76
38	PGC South 800 m	2018-03-05	−64.05515	−58.47654	868.42	41	11	19	2.45	0.83
43	PGC South 1200 m	2018-03-06	−63.98811	−58.42253	1271.42	24	3	4	0.84	0.60

H' = Shannon-Weiner diversity index, J' = Pielou's Evenness.

sub-samples were carefully washed on 300-micron sieves in cold filtered seawater (CFSW), and annelid specimens were picked from sieve residue, cleaned and maintained in CFSW, and relaxed in Magnesium Chloride solution prior to specimen photography. Specimens were imaged using Canon EOS600D cameras either with 100 mm Macro lens or through a Leica MZ7.5 microscope with SLR camera mount. Specimens were preliminary identified on-board to family level, numbered and recorded into a database, and fixed in 80% non-denatured ethanol. Samples that could not be fully sorted on board due to time restrictions were fixed in bulk for later sorting.

A Shallow Underwater Camera System (SUCS) (Nolan et al., 2017) comprised of a 1000 m fiber optic cable (allowing operation to ∼ 900 m) and a tripod-mounted HD camera system was deployed at twelve stations along the PGC, ranging in depth from 200–800 m. SUCS deployments typically involved three consecutive transects spaced 100 m apart, with each transect consisting of 10 photos taken at 10 m intervals. Photos consisted of high resolution stills (2448 × 2050 pixels) covering approximately 0.51 m^2 of seafloor (Almond, 2019). Four SUCS stations corresponded closely with AGT localities, providing a snapshot of the habitat heterogeneity in the vicinity of these samples and *in situ* images of some of the most common species encountered. A dataset of all JR17003a SUCS imagery can be accessed through the following doi: 10.5285/48DCEF16-6719-45E5-A335-3A97F099E451 (Linse et al., 2020).

Laboratory Sorting and Identification

In the laboratory, remaining bulk-fixed samples were sorted and all specimens were re-examined using a Leica M216 stereomicroscope, and key morphological characters were imaged using a fitted Canon EOS600D camera. Specimens were identified to the best possible taxonomic level using original literature, specimen keys, and comparison with type specimen material from NHM collections. Where named species identifications were not possible, specimens were described as a morphospecies where the voucher number of a representative specimen is used as an informal species name for all specimens deemed to be the same species as the representative individual, e.g., Polynoidae sp. NHM_228. Where named species identifications were uncertain, the open nomenclature 'cf.' was used as a precautionary approach along with a representative voucher number, e.g., *Antarctinoe* cf. *ferox* NHM_232. Where specimens were fragmented, only fragments that clearly bore heads were counted and included in abundance records, as standard practice.

Data Analysis

Specimen data were assembled into a Microsoft Excel database, and data visualization and analyses were carried out using the software R v.3.6.2 (R Core Team, 2019) and the R package 'vegan' v.2.5-6 (Oksanen et al., 2019). Local diversity was assessed for each site using the Shannon-Wiener diversity index (*H'*) and Pielou's evenness (*J')* (Shannon and Weaver, 1949; Pielou, 1969). Figures were assembled and edited using Microsoft PowerPoint and Adobe Photoshop software.

Specimen data are included as supplementary material (see **Supplementary Table 1**) and are also made available through the Global Biodiversity Information Facility (GBIF; http://www.gbif.org/) and Ocean Biogeographic Information Systems (OBIS; http://iobis.org/) databases via the SCAR Antarctic Biodiversity Portal (biodiversity.aq), accessible through the following doi: 10.15468/t223v4 (Drennan et al., 2020).

RESULTS

Sample Sites and SUCS Imagery

Four Shallow Underwater Camera System (SUCS) stations corresponded closely with the following AGT sample sites: Duse Bay 200 m, Duse Bay 500 m, PGC Mid 850 m, and PGC South 800 m (see **Figure 1**).

Duse Bay (**Figure 2A**), a sheltered bay located in the northwestern portion of the PGC, is influenced by several local glacier drainage basins (Ferrigno et al., 2006; Scambos et al., 2014); SUCS imagery at both 200 m (**Figures 2B,C**) and 500 m (**Figures 2D,E**). Duse Bay sites revealed substrate characterized by mud and soft sediments, though with the presence of coarser sediments and very small dropstones or gravel at the 200 m site. Additional SUCS deployments at 300 m and 400 m (not shown) show similar soft muddy substrates to the 500 m site. While SUCS imagery was not available for the deepest site at this locality, Duse Bay 1000 m, high abundances of burrowing subsurface deposit feeding polychetes in the families Sternaspidae and Maldanidae (see sections "Sample Overview," "Comparison of Sampling Sites") suggest that the substrate here similarly includes soft sediments.

Though also fed by a number of small outlet glaciers (Ferrigno et al., 2006; Scambos et al., 2014), the Prince Gustav Channel

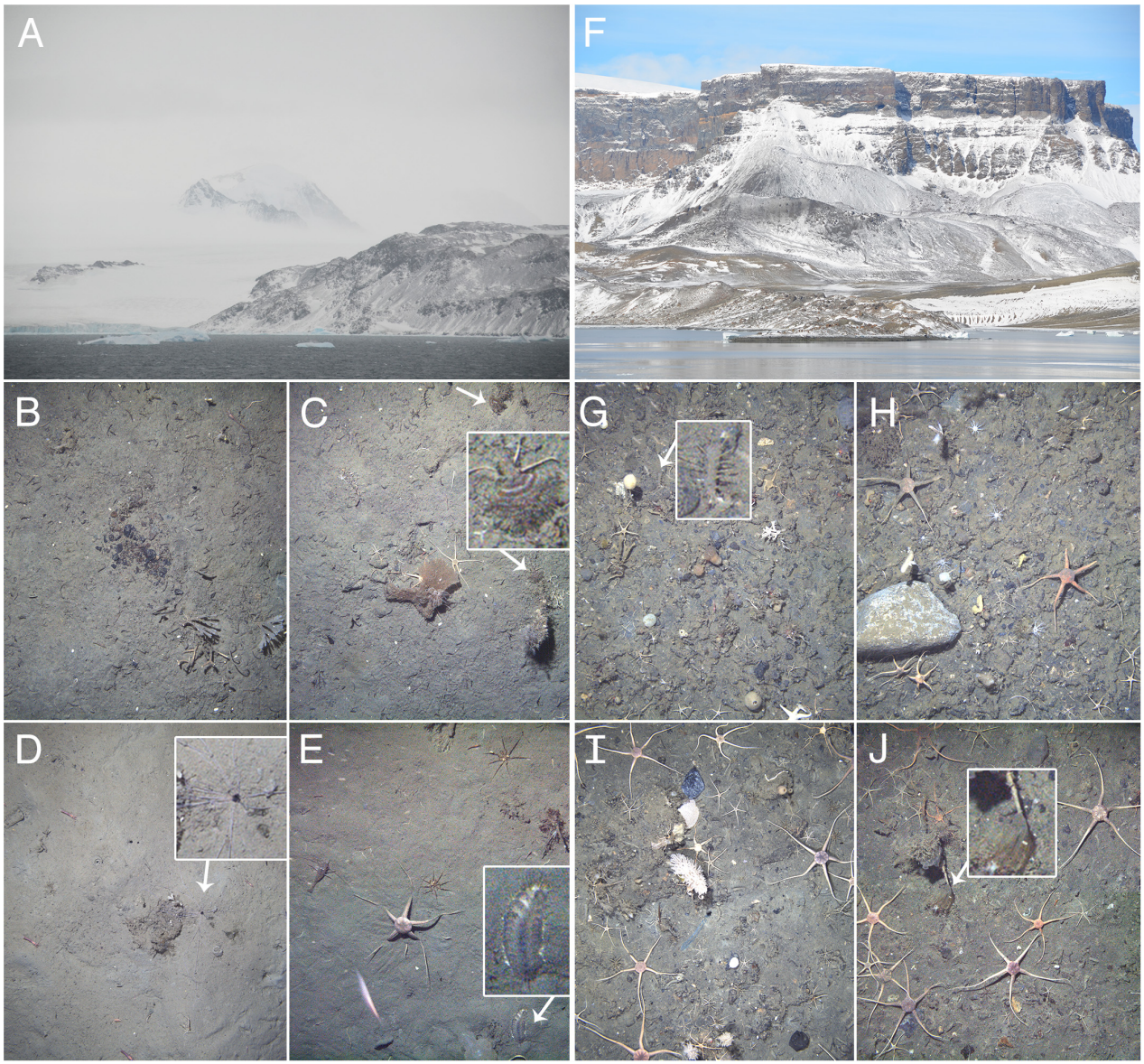

FIGURE 2 | Overview of sites within the Prince Gustav Channel (PGC) including Shallow-water camera system (SUCS) imagery of localities corresponding to AGT sampling sites. **(A–E)** Duse bay sites, **(F–J)** PGC sites. SUCS imagery for deepest sites (Duse Bay 1000 m and PGC South 1200 m) was not available due to depth limitations. **(A)** Above water image of Duse Bay (image credit Angelika Brandt); **(B)** SUCS event no. 15, Duse Bay 200 m site; **(C)** SUCS event no. 15, Duse Bay 200 m site, with detail of sabellidae polychete; **(D)** SUCS event no. 11, Duse Bay 500 m site, with detail of terebellid polychete; **(E)** SUCS event no. 11, Duse Bay 500 m site, with detail of polynoid polychete, possibly *Austrolaenilla antarctica* (see **Figure 4D**); **(F)** Above water image of the Prince Gustav Channel (image credit Angelika Brandt); **(G)** SUCS event no. 45, PGC Mid 850 m site, with detail of flabelligerid polychete, possibly *Flabegraviera mundata* (see **Figure 3B**); **(H)** SUCS event no. 45, PGC Mid 850 m site; **(I)** SUCS event no. 22, PGC South 800 m site; **(J)** SUCS event no. 22, PGC South 800 m site, with detail of sabellid polychete.

proper (**Figure 2F**) is more open than Duse Bay sites, with the narrow, steep-sided nature of channel allowing for a more energetic setting with high current speeds and tidal influence (e.g., Camerlenghi et al., 2001). SUCS imagery from the PGC Mid 850 m site (**Figures 2G,H**) revealed substrate dominated by gravel and small stones covered with a thin sediment, and with a number of small dropstones present. Imagery from PGC South 800 m site (**Figures 2I,J**) revealed compacted mud and sediment with coarse gravel, and the presence of both small and large dropstones. SUCS imagery from the deepest PGC site, PGC South 1200 m, was similarly unavailable, however an abundance of large surface deposit feeders in the family Flabelligeridae (see section "Comparison of Sampling Sites") suggest that some input of food-bearing sediment is occurring here, though with a notable absence of burrowing taxa.

A number of polychetes were visible *in situ* in SUCS imagery (**Figures 2C,D,E,G,J**) including several taxa that possibly correspond with morphospecies collected in AGT samples, such

as the flabelligerid *Flabegraviera mundata* (**Figures 2G**, **3B**) and the polynoid *Austrolaenilla antarctica* (**Figures 2E**, **4D**).

Sample Overview

In total, approximately 598 individual annelid specimens in roughly 57 morphospecies and at least 25 families were collected across all six AGT deployments (**Tables 1–3** and **Supplementary Table 1**). The preservation quality of the collected specimens was excellent, with many individuals recovered in full without fragmentation, and delicate features such as cirri and elytra often remaining intact (**Figures 3**, **4**). Of the morphospecies, 22 were identified to named species, while five were designated as "cf." and the remaining as morphospecies only (**Table 3**), due to a lack of appropriate taxonomic references and/or poor specimen condition. Morphospecies identified in this study will be subject to future molecular taxonomic and connectivity studies, which may change taxon assignments, for example through the use of genetic data as an error check for morphological assignments (e.g., Neal et al., 2018), and through the discovery of new taxa and cryptic diversity (e.g., Brasier et al., 2016).

The two most abundant species (**Table 3**) were the sternaspid *Sternaspis sendalli* (**Figure 3H**) with 176 individuals, and the maldanid *Maldane sarsi* (**Figure 3D**) with 121 individuals. If these two species are excluded from the total specimen count, the whole site ratio of individuals to morphospecies is reduced markedly to 301 individuals in 55 morphospecies. Notably, the majority of both of these species were found at a single site, Duse Bay 1000 m (**Table 3**).The most diverse group were scale worms in the family Polynoidae, with 10–12 morphospecies recorded (**Table 3** and **Figures 3I**, **4**), though with the majority, both in terms of richness and abundance, also found at a single site (**Table 2**). One polynoid individual (**Figure 4I**) was identified as a representative of the near-exclusively deep-sea subfamily Macellicephalinae (Neal et al., 2012).

Almost all specimens collected were considered benthic with only one individual recovered from a pelagic family, Tomopteridae. One specimen from the parasitic/commensal family Myzostomidae was recovered, though without an obvious host. Several examples of commensalism were also observed, including two individuals of the Polynoid *Polyeunoa laevis*, a known alcyonacean coral associate (Barnich et al., 2012), found living within coral branches (**Figure 3I**); individuals from the families Syllidae and Polynoidae were also found living within glass sponges (e.g., **Figure 4A**). The majority of specimens exceeded 1 cm in length, however individual animals ranged in size from several millimeters in families such as Cirratulidae, Dorvilleidae, and Ophelidae to between 15 and 18 cm long in families such as Maldanidae, Nephtyidae, and Terebellidae.

Comparison of Sampling Sites

As the size of the sampled area cannot be accurately determined, trawled sampling gear such as the Agassiz trawl are semi-quantitative in nature (Eleftheriou and Holme, 1984), and thus, reliable quantitative assessments and comparisons of abundance and diversity between sites within this study is not possible. However, trawls are efficient at sampling large areas and are useful in preliminary studies in terms of providing a broad qualitative overview of the distribution and structure of communities (Arnaud et al., 1998).

Each of the six sample sites varied in terms of abundance, morphospecies richness, Shannon-Wiener diversity, Pielou's evenness, and familial composition (**Tables 1–3** and **Figure 5**). Sites further varied in terms of the dominant functional group present, and the overall size classes of component specimens (**Figure 6**). Duse Bay sites in general had high proportions of burrowing specimens (**Figure 6**) with representatives of burrowing families such as Cirratulidae, Lumbrineridae (e.g., **Figure 4C**), and Maldanidae (e.g., **Figure 4D**) present at each site, though with overall taxonomic composition varying between individual sites (**Figure 5**). Sites in the channel proper varied somewhat more in terms of dominant taxa and functional groups (**Figures 5** and **6**).

Duse Bay 200 m, the shallowest site sampled, displayed moderate abundance and richness, relative to other sites, and possessed the highest proportion of suspension feeders with 25 individuals from the tube building family Sabellidae in two morphospecies. However, the majority of these consisted of 14 individuals of the morphospecies *Sabellidae* sp. NHM_272 (**Figure 3G**) that formed a single cluster of tubes on the end of a large empty tube, possibly belonging to the terebellid *Pista mirabilis* (**Figure 3K**) of which there were three individuals also present in the sample, up to 15 cm in length.

Duse Bay 500 m displayed relatively high abundances and the highest morphospecies and familial richness by considerable margin, with 32 morphospecies in 19 families across 99 individuals. The sample was dominated by burrowing taxa (**Figure 6**), with Maldanidae representing the most abundant family (36 individuals across three morphospecies), comprising mainly of *Maldane sarsi* (33 individuals) (**Figure 4D**). In addition to families not well represented at other sites such as Cirratulidae, many families such as Dorvilleidae, Hesionidae, Opheliidae, Orbiniidae, Paraonidae, and Scalibregmatidae were found exclusively at this site (**Table 2**). These families primarily included small, macrofaunal sized individuals approximately 1 cm in length or shorter. In contrast, the sample also included several notably large specimens, including an individual of the terebellid *Pista mirabilis* (**Figure 3K**) exceeding 18 cm in length, an anterior fragment of the large nephtyid *Aglaophamus trissophyllus* (**Figure 3E**) exceeding 15 cm in length, and six individuals of the large syllid *Trypanosyllis gigantea* (**Figure 3J**) (2.5–10 cm long) found living within a glass sponge.

Duse Bay 1000 m presented the highest abundances observed across all sites with 260 individuals, though as discussed in section "Sample Overview," this sample was primarily made up of two species, *Sternaspis sendalli* and *Maldane sarsi,* with richness otherwise relatively low with 10 morphospecies. While *M. sarsi* is moderate in size (∼2 mm wide though reaching lengths of up to 12 cm in the largest specimens), *S. sendalli* is small with most specimens not exceeding 1 cm in length – this site therefore displayed the highest proportion of small macrofaunal sized taxa (**Figure 6**). While *M. sarsi* was found at relatively high abundances in all but two sites (PGC Mid 850 m and PGC South

TABLE 2 | Number of individuals and morphospecies per polychete family (or higher taxonomic rank in the case of oligochaeta) sampled during cruise JR17003a.

Family (or higher)	Functional category	Total Site		Sites											
				Duse Bay 200 m		Duse Bay 500 m		Duse Bay 1000 m		PGC Mid 850 m		PGC South 800 m		PGC South 1200 m	
		No. ind.	*No. sp.*	*No. ind.*	*No. sp.*	*No. ind.*	*No. sp.*	*No. ind.*	*No. sp.*	*No. ind.*	*No. sp.*	*No. ind.*	*No. sp.*	*No. ind.*	*No. sp.*
Ampharetidae	tbsdf	5	1	2	1	2	1	–	–	–	–	1	1	–	–
Cirratulidae	b	10	4	2	1	7	4	1	1	–	–	–	–	–	–
Dorvilleidae	msom	5	1	–	–	5	1	–	–	–	–	–	–	–	–
Flabelligeridae	msdf	27	2	–	–	–	–	–	–	10	2	–	–	17	1
Hesionidae	msom	1	1	–	–	1	1	–	–	–	–	–	–	–	–
Lumbrineridae	b	12	2	1	1	6	2	4	1	–	–	1	1	–	–
Maldanidae	b	133	4	8	1	36	3	68	2	–	–	21	3	–	–
Myzostomidae	pa	1	1	–	–	–	–	–	–	–	–	1	1	–	–
Nephtyidae	msom	17	2	–	–	4	2	6	1	6	1	–	–	1	1
Oligochaeta	b	3	2	–	–	3	2	–	–	–	–	–	–	–	–
Opheliidae	b	6	2	–	–	6	2	–	–	–	–	–	–	–	–
Orbiniidae	b	4	1	–	–	4	1	–	–	–	–	–	–	–	–
Oweniidae	tbsdf	16	1	–	–	1	1	–	–	15	1	–	–	–	–
Paraonidae	b	1	1	–	–	1	1	–	–	–	–	–	–	–	–
Phyllodocidae	msom	5	3	1	1	–	–	1	1	3	3	–	–	–	–
Polynoidae	msom	105	12	2	2	3	3	6	2	82	10	6	5	6	2
Sabellidae	tbsf	29	2	25	2	2	1	–	–	1	1	1	1	–	–
Scalibregmatidae	b	1	1	–	–	1	1	–	–	–	–	–	–	–	–
Serpulidae	tbsf	1	1	–	–	1	1	–	–	–	–	–	–	–	–
Sternaspidae	b	176	1	2	1	–	–	173	1	–	–	1	1	–	–
Syllidae	msom	19	4	–	–	7	2	–	–	7	2	5	2	–	–
Terebellidae	tbsdf	11	5	4	2	2	2	1	1	2	1	2	2	–	–
Tomopteridae	pe	1	1	–	–	–	–	–	–	–	–	1	1	–	–
Travisiidae	b	1	1	–	–	–	–	–	–	–	–	1	1	–	–
Trichobranchidae	tbsdf	8	1	1	1	7	1	–	–	–	–	–	–	–	–
Total		598	57	48	13	99	32	260	10	126	21	41	19	24	4

A broad functional category based on shared functional traits such as life habit, motility and feeding behavior is also provided for each family: b (burrowing); msom (motile surface-dwelling omnivorous); msdf (motile surface-dwelling deposit-feeding); pe (pelagic); pa (parasitic); tbsdf (tube-building surface deposit-feeding); tbsf (tube-building suspension-feeding).

TABLE 3 | List of morphospecies identified from Agassiz Trawl samples collected on cruise JR17003a, with individual counts for each site provided.

Family (or higher)	Morphospecies	Taxon authority	Sites						Total
			DB 200 m	DB 500 m	DB 1000 m	PGCM 850 m	PGCS 800 m	PGCS 1200 m	
Ampharetidae	Ampharetidae sp. NHM_280		2	2	–	–	1	–	**5**
Cirratulidae	*Aphelochaeta* sp. NHM_301		–	3	–	–	–	–	**3**
	Chaetocirratulus andersenensis	Augener, 1932	2	1	–	–	–	–	**3**
	Cirratulidae sp. NHM_035		–	2	1	–	–	–	**3**
	Cirratulidae sp. NHM_317		–	1	–	–	–	–	**1**
Dorvilleidae	Protodorvillea sp. NHM_290		–	5	–	–	–	–	**5**
Flabelligeridae	***Brada mammillata***	Grube, 1877	–	–	–	1	–	17	**18**
	Flabegraviera mundata	Gravier, 1906	–	–	–	9	–	–	**9**
Hesionidae	Hesionidae sp. NHM_291		–	1	–	–	–	–	**1**
Lumbrineridae	***Augeneria tentaculata***	Monro, 1930	1	5	4	–	1	–	**11**
	Lumbrineridae sp. NHM_300		–	1	–	–	–	–	**1**
Maldanidae	***Lumbriclymenella robusta***	Arwidsson, 1911	–	1	–	–	5	–	**6**
	Maldane sarsi	Malmgren, 1865	8	33	67	–	13	–	**121**
	Maldanidae sp. NHM_125		–	–	1	–	3	–	**4**
	Maldanidae sp. NHM_302		–	2	–	–	–	–	**2**
Myzostomatidae	*Myzostoma* cf. *divisor* NHM_123	Grygier, 1989	–	–	–	–	1	–	**1**
Nephtyidae	***Aglaophamus trissophyllus***	Grube, 1877	–	3	6	6	–	1	**16**
	Aglaophamus sp. NHM_280F		–	1	–	–	–	–	**1**
Oligochaeta	Oligochaeta sp. NHM_287		–	2	–	–	–	–	**2**
	Oligochaeta sp. NHM_289		–	1	–	–	–	–	**1**
Opheliidae	***Ophelina breviata***	Ehlers, 1913	–	2	–	–	–	–	**2**
	Ophelina cf. *cylindricaudata*	Hansen, 1878	–	4	–	–	–	–	**4**
Orbiniiae	***Leitoscoloplos kerguelensis***	McIntosh, 1885	–	4	–	–	–	–	**4**
Oweniidae	Oweniidae sp. NHM_234C		–	1	–	15	–	–	**16**
Paraonidae	Paraonidae sp. NHM_295		–	1	–	–	–	–	**1**
Phyllodocidae	***Paranaitis bowersi***	Benham, 1927	1	–	1	1	–	–	**3**
	Phyllodocidae sp. NHM_234D		–	–	–	1	–	–	**1**
	Phyllodocidae sp. NHM_235D		–	–	–	1	–	–	**1**
Polynoidae	***Antarctinoe ferox***	Baird, 1865	–	1	1	7	1	–	**10**
	Antarctinoe cf. *ferox* NHM_232	Baird, 1865	–	–	–	39	–	1	**40**
	Antarctinoe spicoides	Hartmann-Schröder, 1986	–	–	–	1	–	–	**1**
	Austrolaenilla antarctica	Bergström, 1916	–	1	5	1	1	5	**13**
	Barrukia cristata	Willey, 1902	–	–	–	9	–	–	**9**
	Harmothoe fuligineum	Baird, 1865	–	–	–	18	1	–	**19**
	Harmothoe cf. *fuligineum* NHM_233	Baird, 1865	–	1	–	2	–	–	**3**
	Harmothoe cf. *fullo* NHM_330	Grube, 1878	1	–	–	–	–	–	**1**
	Macellicephalinae sp. NHM_234L		–	–	–	1	–	–	**1**
	Polyeunoa laevis	McIntosh, 1885	–	–	–	1	1	–	**2**
	Polynoidae sp. NHM_140D		1	–	–	–	2	–	**3**
	Polynoidae sp. NHM_228		–	–	–	3	–	–	**3**
Sabellidae	Sabellidae sp. NHM_272		19	2	–	1	1	–	**23**
	Sabellidae sp. NHM_332		6	–	–	–	–	–	**6**
Scalibregmatidae	Scalibregmatidae sp. NHM_281		–	1	–	–	–	–	**1**
Serpulidae	Serpulidae sp. NHM_280K		–	1	–	–	–	–	**1**
Sternaspidae	***Sternaspis sendalli***	Salazar-Vallejo, 2014	2	–	173	–	1	–	**176**
Syllidae	***Pionosyllis kerguelensis***	McIntosh, 1885	–	–	–	6	1	–	**7**
	Syllidae sp. NHM_140F		–	–	–	–	4	–	**4**

(Continued)

TABLE 3 | Continued

Family (or higher)	Morphospecies	Taxon authority	Sites						Total
			DB 200 m	DB 500 m	DB 1000 m	PGCM 850 m	PGCS 800 m	PGCS 1200 m	
	Syllidae sp. NHM_285		–	1	–	–	–	–	**1**
	Trypanosyllis gigantea	McIntosh, 1885	–	6	–	1	–	–	**7**
Terebellidae	***Leaena collaris***	Hessle, 1917	–	1	–	–	–	–	**1**
	Pista mirabilis	McIntosh, 1885	3	1	–	–	–	–	**4**
	Terebellidae sp NHM_142		–	–	1	–	1	–	**2**
	Terebellidae sp NHM_234P		–	–	–	2	1	–	**3**
	Terebellidae sp NHM_337		1	–	–	–	–	–	**1**
Tomopteridae	*Tomopteris* sp NHM_131		–	–	–	–	1	–	**1**
Travisiidae	***Travisia kerguelensis***	McIntosh, 1885	–	–	–	–	1	–	**1**
Trichobranchidae	Trichobranchidae sp. 280M		1	7	–	–	–	–	**8**

Taxa identified to named species are highlighted in bold. DB Duse Bay; PGC Prince Gustav Channel; M Mid; S South.

800 m), notably only a handful of *S. sendalli* were found at other sites despite being the most abundant species overall. Both species are burrowing deposit feeders, and Duse Bay 1000 m further presented the highest proportion of burrowing taxa across all sites (**Figure 6**). The remaining sample was primarily composed of medium to large sized motile scavenger/predator taxa including the large nephtyid *Aglaophamus trissophyllus,* the phyllodocid *Paranaitis bowersi* (**Figure 3F**) and the polynoids *Antarctinoe ferox* and *Austrolaenilla antarctica* (**Figures 4A,D**).

Sites in the channel proper were more variable. PGC Mid 850 m presented relatively high diversity and both the second highest abundance and richness of any site, with 126 individuals in 21 morphospecies, and is notable in that no burrowing taxa were present (**Figure 6**). While representatives of the family Polynoidae were present in small to moderate numbers across every site, PGC Mid 850 m is further notable in terms of a striking abundance and richness of polynoids with 82 individuals in at least 10 morphospecies (**Figures 3I**, **4A–I**), ranging in size from 2 cm to >6 cm. Other motile scavenger/predator taxa in Nephtyidae, Phyllodocidae, and Syllidae were also moderately abundant. Ten individuals in the motile surface deposit feeding family Flabelligeridae were also present at the site, including nine individuals of the species *Flabegraviera mundata* (**Figure 3B**), possibly visible *in situ* in SUCS imagery of this site (**Figure 2G**). Additionally, 15 individuals of an unidentified oweniid morphospecies, Oweniidae sp. NHM_234C, were present at this site, with the family being rare or absent entirely from other sites.

PGC South 800 m displayed relatively low abundance but moderate richness, with 41 individuals in 19 morphospecies, and was the only non-Duse Bay site with burrowing taxa, primarily comprised of the family Maldanidae (**Figures 5**, **6**) but also including representatives in families Lumbrineridae, Sternaspis and Travisiidae. The remaining taxa were mainly composed of motile surface scavenger/predators in families Polynoidae and Syllidae.

PGC South 1200 m was the deepest site sampled, with a maximum depth of 1270 m. The site displayed both the lowest abundance and richness of any site, with 24 individuals in four morphospecies, dominated by 17 individuals of the large (4–7 cm) flabelligerid *Brada mammillata* (**Figure 3A**), in addition to two species of polynoid (*Austrolaenilla antarctica* and *Antarctinoe* cf. *ferox* sp. NHM_232) and the nephtyid *Aglaophamus trissophyllus.* The site therefore was entirely composed of motile surface dwelling taxa, and further displayed the greatest proportion of large, megafaunal sized animals exceeding 5 cm (**Figure 6**).

Shannon-Wiener diversity indexes were lowest in the deepest stations, Duse Bay 1000 m and PGC South 1200 m (H' = 0.95 and 0.84, respectively) and highest at Duse Bay 500 m (H' = 2.75). Values for Pielou's Evenness were also lowest for the two deepest stations (J' = 0.41 and 0.60, respectively), ranging between J' = 0.76 and J' = 0.83 at the remaining sites.

DISCUSSION

General Overview

This study provides a first insight into the benthic annelid fauna of the Prince Gustav Channel, revealing locally variable communities in terms of abundance, richness, and both taxonomic and functional composition.

Fine scale habitat heterogeneity, for example in terms of substrate type and composition and the presence or absence of dropstones, can account for much of the variation observed in faunal composition in several previous studies of Antarctic shelf benthos, including investigations of the East Antarctic Shelf (Post et al., 2017), the Ross Sea (Cummings et al., 2006), King George Island (Quartino et al., 2001), and the South Orkney Islands (Brasier et al., 2018). In the present study, SUCS imagery at Duse Bay sites revealed substrate characterized by mud and soft sediments, reflected in high abundances of burrowing taxa at these sites, primarily subsurface deposit feeding families such as Maldanidae and Sternaspidae. Though SUCS imagery was not available for the deepest site (Duse Bay 1000 m), high abundances of these taxa suggest substrate also composed of soft sediments. Previous studies of Antarctic shelf annelids have found high abundances of subsurface deposit feeding taxa to

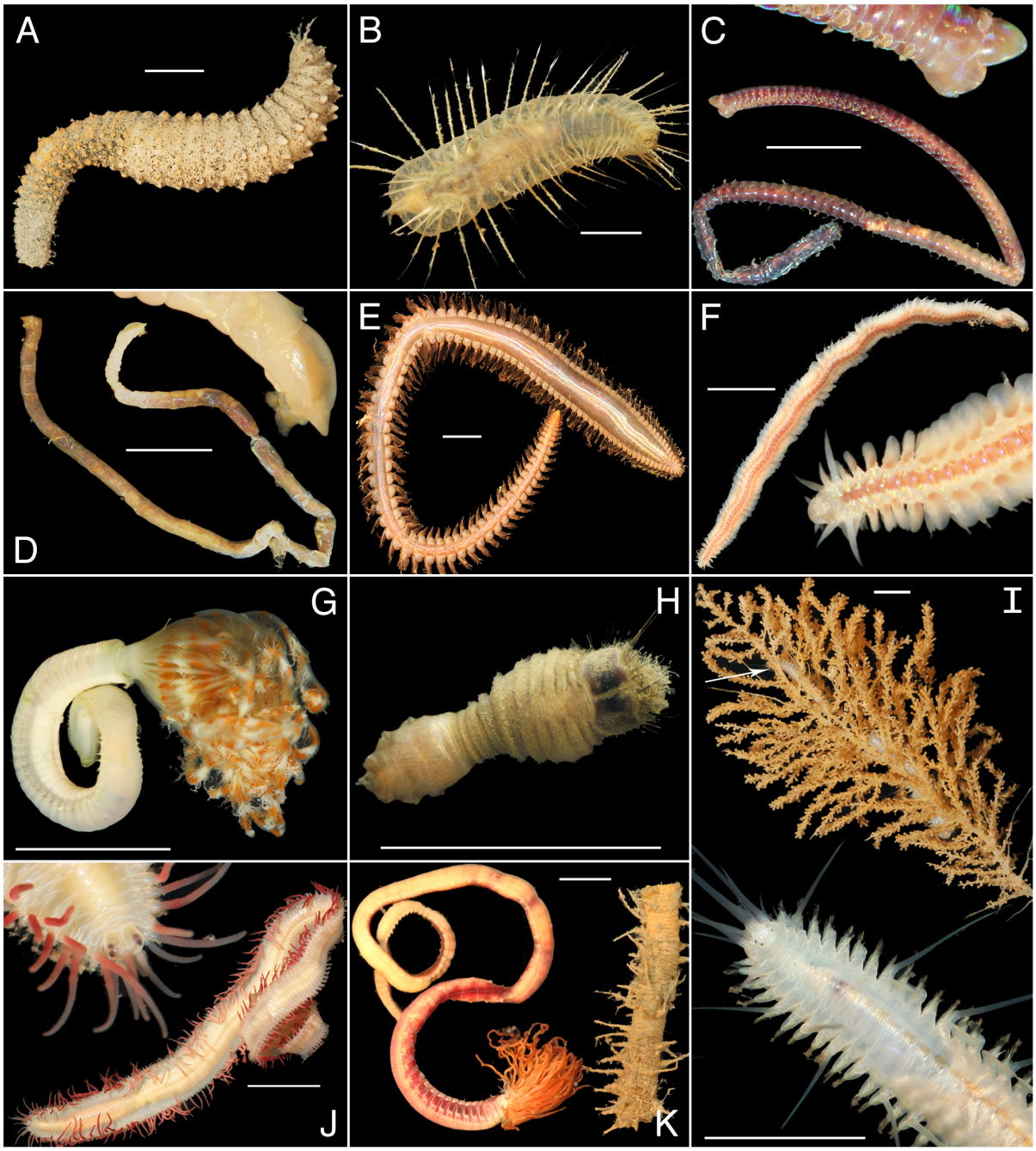

FIGURE 3 | Live specimen imagery taken on board the expedition JR17003a of several annelid species or morphospecies across a range of families collected by AGT trawls. **(A)** *Brada mammillata* (Flabelligeridae); **(B)** *Flabegraviera mundata* (Flabelligeridae); **(C)** *Augeneria tentaculata* (Lumbrineridae), whole specimen (bottom), with detail of prostomium (top); **(D)** *Maldane sarsi* (Maldanidae), whole specimen (bottom) with detail of prostomium (top); **(E)** *Aglaophamus trissophyllus* (Nephtyidae), **(F)** *Paranaitis bowersi* (Phyllodocidae), whole specimen (top) with detail of anterior (bottom); **(G)** Sabellidae sp. NHM_272; **(H)** *Sternaspis sendalli* (Sternaspidae); **(I)** *Polyeunoa laevis* (Polynoidae), whole specimen living within branches of coral (top) and detail of specimen anterior (bottom); **(J)** *Trypanosyllis gigantea* (Syllidae), whole specimen (bottom) with detail of anterior (top); **(K)** *Pista mirabilis* (Terebellidae) whole specimen (left) alongside portion of tube (right). All scale bars = 1 cm.

correspond with enhanced productivity and food availability in sediments (e.g., Neal et al., 2011). Duse Bay is a sheltered embayment influenced by a number of local outlet glaciers (Ferrigno et al., 2006; Scambos et al., 2014); in addition to the collapse of floating ice shelves, maritime glaciers along the Antarctic Peninsula have also experienced dramatic retreat in recent decades (Cook et al., 2005), with freshening and sedimentation events becoming more frequent due to increased

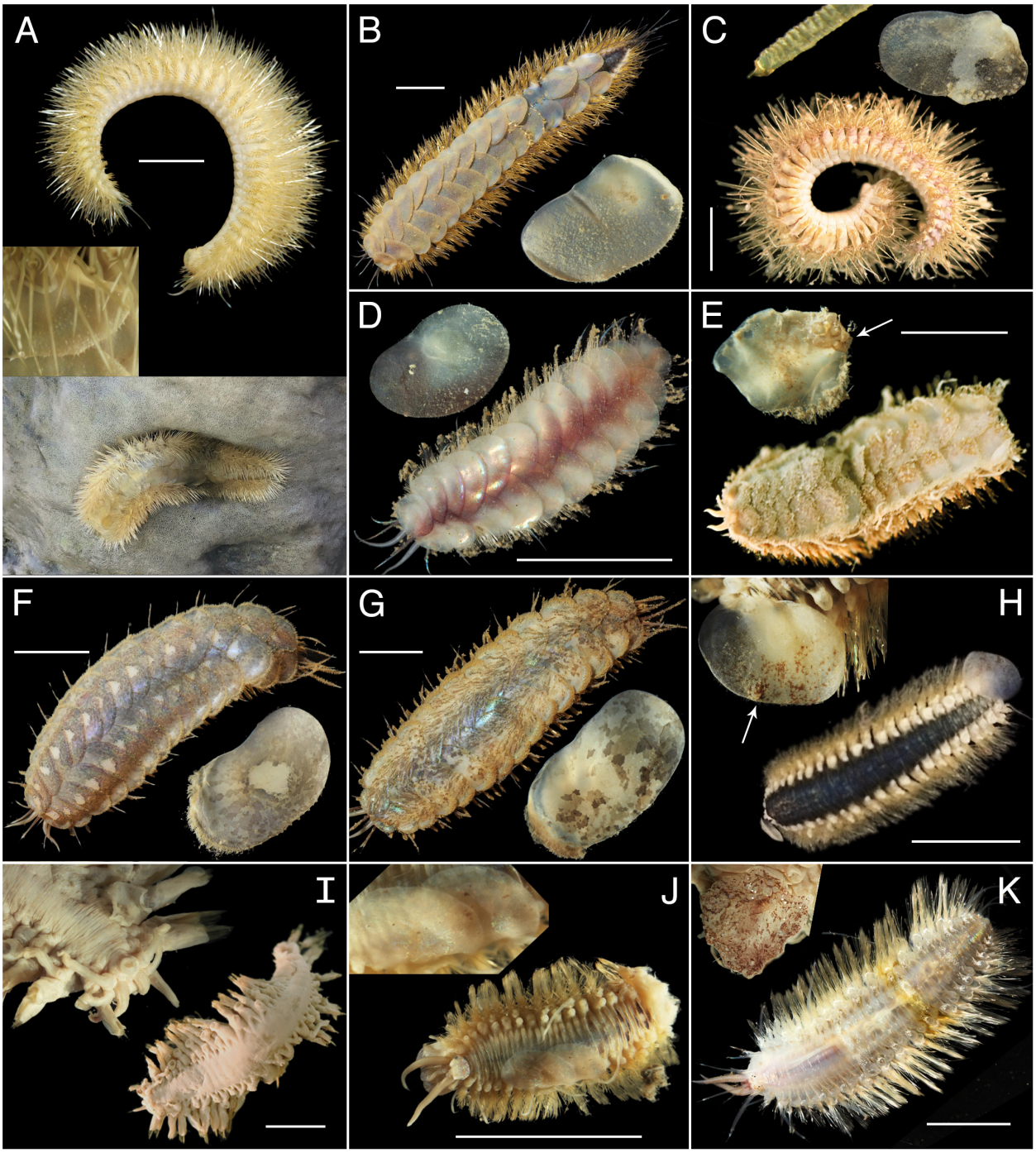

FIGURE 4 | Specimen imagery highlighting morphospecies diversity of the family Polynoidae collected JR17003a expedition. See also **Figure 3I**. **(A)** *Antarctinoe ferox* live image, lateral view (top), detail of elytra on preserved specimen (middle) and live, *in situ* image of specimen sitting in glass sponge; **(B)** *Antarctinoe* cf. *ferox* NHM_232, live image, with detail of midbody elytron (preserved); **(C)** *Antarctinoe spicoides*, preserved specimen, lateral view (bottom), detail of long notochaetal spine with pin tip (top left) and detail of midbody elytron (right); **(D)** *Austrolaenilla antarctica* live image, with detail of midbody elytron (preserved); **(E)** *Barrukia cristata*, preserved specimen, with detail of elytron with arrow highlighting large macrotubercles; F *Harmothoe* cf. *fuligineum* NHM_233, live image, with detail of elytron (preserved); **(G)** *Harmothoe fuligineum*, with detail of elytron; **(H)** *Harmothoe* cf. *fullo* NHM_330, preserved specimen, with detail of elytron, arrow highlighting mound on posterior margin; **(I)** Macellicephalinae sp. NHM_234L, preserved specimen, with detail of anterior (top left); **(J)** Polynoidae sp. NHM_140, preserved specimen, with detail of elytra; **(K)** Polynoidae sp. NHM_228, live image, with detail of elytron (preserved specimen, different individual to one shown in live image). All scale bars = 1 cm.

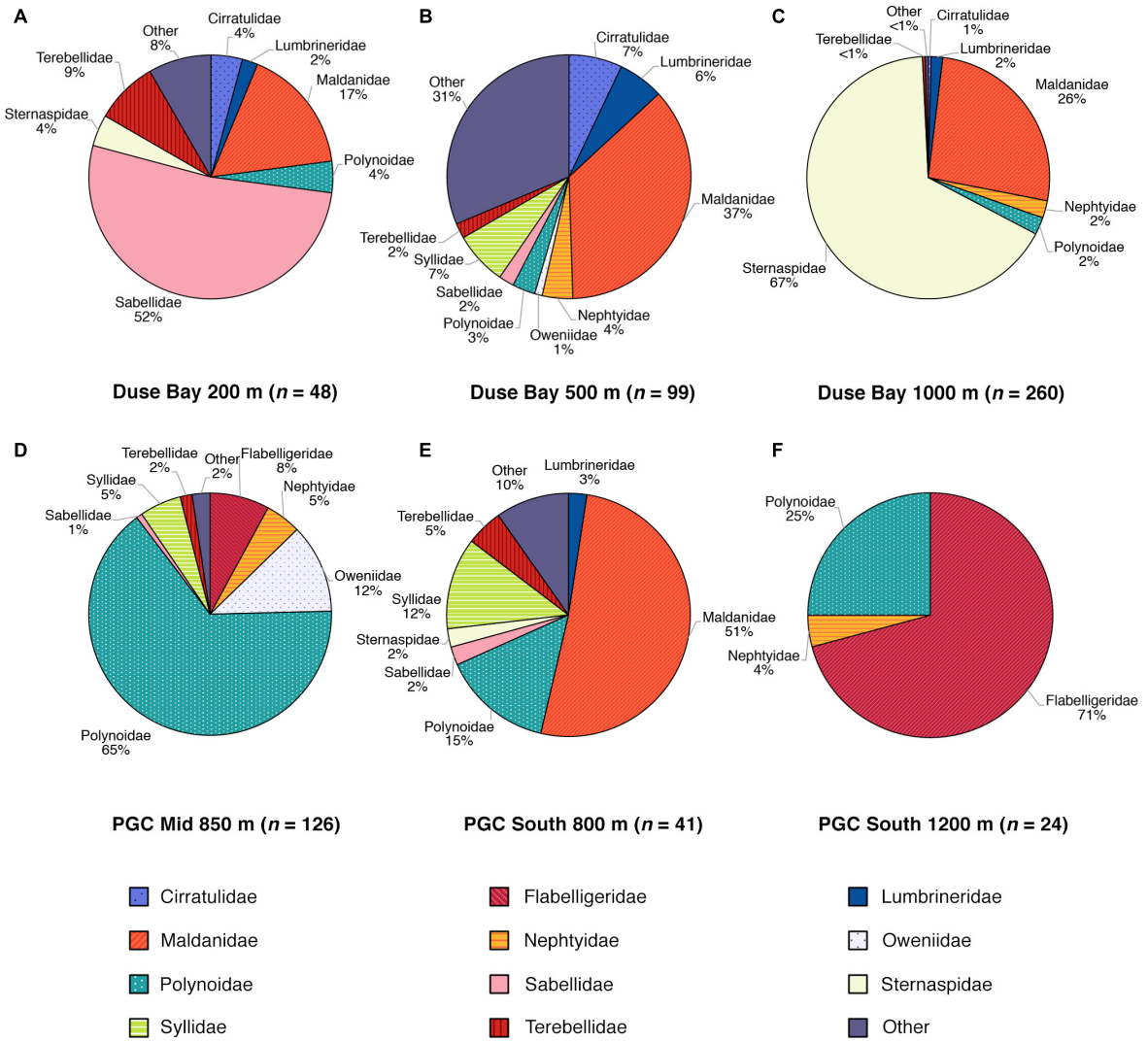

FIGURE 5 | Proportions of total specimen abundance by annelid family for each Agassiz Trawl sample site. **(A)** Duse Bay 200 m **(B)** Duse Bay 500 m **(C)** Duse Bay 1000 m **(D)** PGC Mid 850 m **(E)** PGC South 800 m **(F)** PGC South 1200 m. Families that had less than ten individuals across all sites (14 out of a total of 25 families) were combined into a single category, "other."

influxes of glacial meltwater and sediment runoff associated with glacial retreat (Smale and Barnes, 2008). These disturbances can affect adjacent benthic communities in a number of ways. For example, the presence of surface meltwater has been associated with nearshore phytoplankton blooms and increased primary productivity (Dierssen et al., 2002), and increased sedimentation with shifts in benthic community structures (Sahade et al., 2015), favoring soft substrate adapted taxa. Glacial input can also locally increase habitat complexity through the deposition of dropstones – land derived rock frozen into glacial ice that enter the sea via icebergs, which deposit the stones as they melt, providing hard substrata where they land (Smale and Barnes, 2008). Both large and small dropstones were visible throughout the channel where SUCS imagery was available, though in Duse Bay these were mainly restricted to the shallowest site (Duse Bay 200 m).

Glaciers that previously fed into the Prince Gustav Ice Shelf experienced accelerated ice loss and discharge into PGC embayments following the collapse of the ice shelf and its buttressing effect in 1995, though with a significant reduction in losses since 2013 (Rott et al., 2014, 2018). In addition to glacial input into the channel, the depth and north-south continuity of the PGC may further facilitate the flow of fine grained sediment and organic matter through the channel from adjacent shelf areas and more productive, seasonally open water, even during periods when the channel was covered by a floating ice shelf, which is possibly indicated by a measurable drape of diatom bearing sediment in the deepest parts of the channel, much thicker than for other glacial troughs in the region (Pudsey et al., 2001). This may have relevance to benthic communities in the channel today, as while the collapse of ice shelves exposed open water leading to massive increases in primary production in the

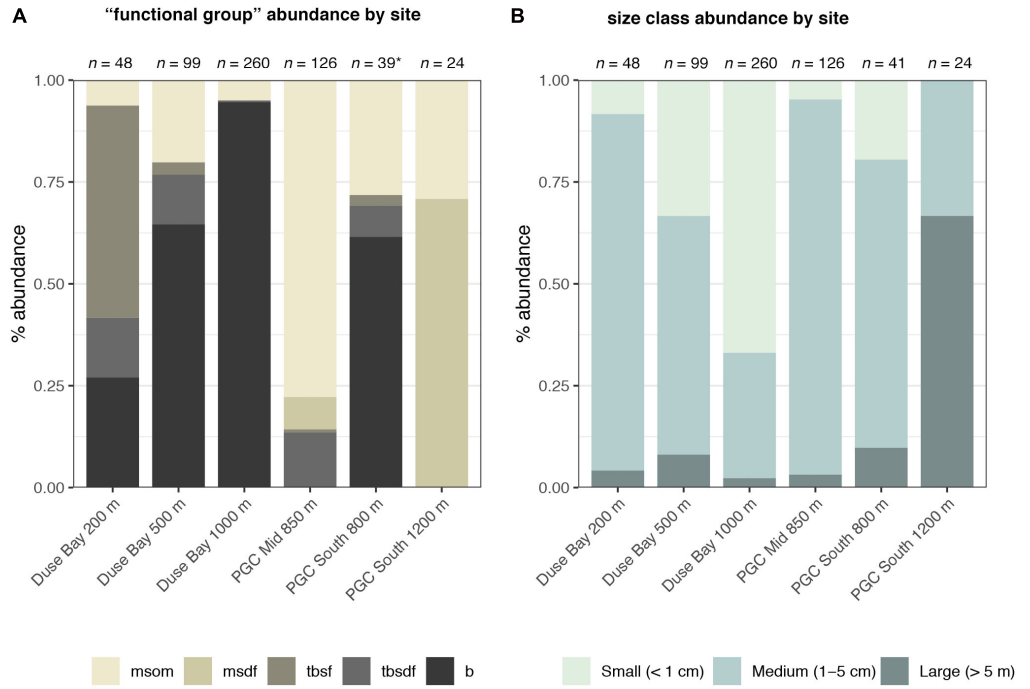

FIGURE 6 | Composition of annelid **(A)** "functional groups" and **(B)** size classes in terms of percentage abundance of individuals across all sampled AGT stations. **(A)** Polychete families were separated into broad functional categories based on shared functional traits such as life habit, motility and feeding behavior as follows: msom (motile surface-dwelling omnivorous); msdf (motile surface-dwelling deposit-feeding); tbsdf (tube-building surface deposit-feeding); tbsf (tube-building suspension-feeding); b (burrowing). See **Table 2** for list of functional groups by family. * Singleton specimens representing parasitic (pa) and pelagic (pe) functional groups (see **Table 2**) were excluded from PGC South 800 m. **(B)** Specimens were organized into general size classes as follows: small (less than 1 cm in length); medium (between 1–5 cm in length, or for long, slender taxa, less than 0.5 cm in width); large (exceeding 5 cm in length and 0.5 cm in width).

region (Bertolin and Schloss, 2009), the east coast of the Antarctic Peninsula experiences dense pack ice cover for much of the year, with pack ice in the channel occasionally lasting year round (Pudsey et al., 2006). Cut off from surface primary production, benthic communities beneath floating ice shelves are known to rely on the horizontal advection of food particles from open water as a primary food source (Riddle et al., 2007), with distance from the ice shelf edge a major factor in terms of the abundance, diversity and structure of sub-ice benthic communities (e.g., Riddle et al., 2007; Post et al., 2014).

In this study, SUCS imagery corresponding to sampled channel sites revealed higher proportions of hard substrate relative to Duse Bay sites, though with mud and compacted sediment present at PGC South 800 m (possibly reflected in an abundance of maldanids) and only a thin sediment drape at PGC Mid 850 m, the latter displaying remarkable abundance and diversity in the motile predator/scavenger family Polynoidae and the complete absence of sub-surface deposit feeding taxa. While SUCS imagery was not possible for the deepest basin of the channel, PGC South 1200 m, previous acoustic investigations have shown that the deeper parts of the channel are filled by a measurable sediment drape (Pudsey et al., 2001). The benthic fauna of this site was distinct from other samples with the lowest richness, abundance, and diversity, entirely dominated by large motile megafauna, primarily in the surface deposit feeding family Flabelligeridae but also including predator/scavenger families Polynoidae and Nephtyidae. In a comparative study of depth zonation in polychete communities from Scotia and Amundsen seas, deep glacial troughs up to 1500 m deep in the inner shelf of the glacier-influenced Pine Island Bay in the Amundsen Sea were dominated by motile predator/scavengers such as Polynoidae and Nephtyidae and deposit feeding families (both surface and subsurface) at 500 m depth horizons; deeper sites were entirely dominated by the former with a complete absence of deposit feeders (Neal et al., 2018). The basins of the PGC are amongst a number of deep glacial troughs that exceed depths of 800 m in the greater Larsen A area, though are distinct in having a much thicker drape of diatom bearing sediment than other troughs in the region, suggesting that the bathymetry of the channel facilitates the advection of food bearing particles from more productive waters through the channel and to these troughs (Pudsey et al., 2001). This could possibly support deposit feeding communities in the deep basins of the PGC, however comparative samples from other troughs in the region are not available.

In the Amundsen Sea, Antarctic Circumpolar Deep water is known to intrude onto the inner shelf of Pine Island Bay (Thoma et al., 2008), connecting the shelf troughs with deep water and acting as a potential source of the deep-water species found in these troughs (e.g., Kaiser et al., 2009; Riehl and Kaiser, 2012; Linse et al., 2013), including polynoids in the deep sea sub-family Macellicephalinae (Neal et al., 2012, 2018).

An individual of this subfamily was collected in the present study from PGC Mid 850 m site. On the continental shelf of the greater Larsen region, glacial troughs running out to the continental shelf break allow for the inflow of Modified Weddell Deep Water, a derivative of Circumpolar Deep Water, onto the shelf and toward the coast and ice shelf fronts (Nicholls et al., 2004), though it is unknown whether this could similarly act as a source of deep sea taxa on the western Weddell shelf without comparative faunistic studies with deep Weddell communities.

Southern Ocean polychetes are typically reported to have wide depth ranges (Schüller, 2011), however this notion is beginning to be challenged, with recent comparative investigations finding depth to be one of the main factors structuring shelf and slope polychete communities (Neal et al., 2018). As the sample size in this study was small and qualitative, and with three sampling depths only achieved at Duse Bay sites, any effects of depth are difficult to discern. In a separate analysis of the 12 SUCS deployments taken throughout the channel on the JR17003a expedition from depths ranging from 200 m to 850 m, heterogeneity and complexity was found to decrease with depth, with the most complex and heterogeneous sites found at the southern-most sample sites (Almond, 2019).

Without comparable baseline records from the Prince Gustav Channel, either before or directly after ice shelf collapse, any effects of ice loss on the benthos of the channel are similarly difficult to discern. Based on historical records, the maximum northern extent of the Prince Gustav Ice shelf in contemporary terms would have extended to just south of the PGC South 1200 m sampling site (Cooper, 1997; Ferrigno et al., 2006). Sites in this study therefore would have been just proximal to the ice shelf rather than directly covered by it, however the effects of this are similarly unknown.

Sampling Biases and Comparability

The Agassiz Trawl is best suited for collecting large epifauna or large infauna at or close to the sediment surface interface, and can be hindered by very rocky substrate, hence why 200 m and 500 m trawls in the main channel were not possible due to the influence of boulders. This may explain why the sample site with the largest dropstones, PGC South 800 m, displayed relatively low abundances despite moderately high morphospecies richness. The nature of the trawl further limits the collection of smaller encrusting species, and larger numbers of small infaunal species than otherwise targeted can occasionally be collected when the trawl becomes embedded in soft sediment (Brasier et al., 2018), as likely occurred at Duse Bay 500 m site, which displayed the highest diversity and highest overall familial and morphospecies richness, largely from small infaunal taxa.

Placing these results in wider comparative terms is difficult due to the above sampling biases and general qualitative nature of the AGT, in addition to the range of sampling devices and different spatial and bathymetric scales used by previous benthic sampling projects. The majority of Antarctic macrobenthic abundance and diversity assessments have been carried out using grabs and corers (Linse et al., 2007), including the only previous biological sampling effort of the Prince Gustav Channel in 2000 (see Blake, 2015), and a number of large-scale assessments of Antarctic polychete diversity (e.g., Hilbig et al., 2006; Neal et al., 2011; Parapar et al., 2011). Coring devices, which are considered more quantitative than dragged gear at the cost of area sampled, may only have a low degree of species overlap with sledged or trawled sampling gear even at the same site (Hilbig, 2004). Several large Antarctic polychete studies have collected samples using an epibenthic sledge (EBS) (e.g., Schüller et al., 2009; Neal et al., 2018), however while the EBS is similarly a dragged sampling gear, it targets a smaller size class of fauna than the Agassiz trawl, again limiting comparability. The standardized use of multiple gear types at any one station is an efficient method of getting a comprehensive impression of the benthic fauna of an area, particularly where seafloor is sparsely colonized (Hilbig, 2004). Core and EBS samples were also taken during the JR17003a expedition and will be incorporated in future taxonomic studies using an integrative taxonomy approach (Glover et al., 2016), whereby morphological assessments are streamlined by molecular barcoding, and will provide a more holistic and comparable account of polychete diversity in the Prince Gustav Channel. However, AGT samples provide a good preliminary overview of the megafaunal and larger macrofaunal communities of the channel.

Antarctic AGT-based sampling efforts that are broadly comparable include the second expedition of the Ecology of the Antarctic Sea Ice Zone (EASIZ) program on board the RV Polarstern in 1998, in which 11 AGT trawls from depths ranging from 230 m–2070 m, primarily from the continental shelf and slope of the southeastern Weddell Sea, were sorted to family level (Arntz and Gutt, 1999). If excluding single locally abundant species such as *Sternaspis sendalli* at Duse Bay 1000 m, then the EASIZ AGT samples are broadly similar to the samples of this study in terms of total annelid abundances and familial richness, ranging from 28–101 individuals and 5–17 families per trawl[1]. However, familial composition does differ somewhat, with Syllidae and Terebellidae amongst the most dominant families numerically, and families such as Maldanidae scarce relative to PGC samples. Furthermore, families that are moderately common in the EASIZ samples such as Glyceridae and Nereididae are totally absent from the PGC AGT samples. Maximum abundances also tended to be lower, with 43 syllid individuals the maximum recorded abundance in a single family for a single trawl, in contrast to individual counts of up to 173, 81, and 70 for Sternaspidae, Polynoidae, and Maldanidae respectively in PGC samples.

Closer to the PGC, several AGT trawls were taken from seabed formerly covered by Larsen A and B ice shelves during the expedition ANT-XXIII/8 RV on the Polarstern 2006/2007 (Gutt, 2008) as part of a larger study investigating the biodiversity of the then recently uncovered seabed (Gutt et al., 2011). Macrofaunal presence/absence data published show that several

[1]Excluding the deepest trawl that consisted of mud, which was sieved entirely through a 0.5 mm mesh screen, resulting in a maximum abundance of 2427 individuals in 20 families.

named species identified in the current study were also present in these samples, such as *Antarctinoe ferox, Antarctinoe spicoides, Austrolaeniella antarctica, Flabelligera mundata* (synonym of *Flabegraviera mundata*), *Harmothoe fuligineum, Harmothoe fullo, Maldane sarsi and Pista mirabilis* (Gutt et al., 2010), 12 and 5 years after the collapse of the Larsen A and B ice shelves. The large flabelligerid *Flabegraviera mundata*, found at relatively high abundances at PGC Mid 850 m, is also thought to have been observed under the Amery Ice shelf, East Antarctica, 100 km from open water (as *Flabelligera mundata*) (Riddle et al., 2007), however it is a relatively common species in the Southern Ocean with an assumed circumpolar distribution (though see section "Morphological Limitations and Future Molecular Work").

Morphological Limitations and Future Molecular Work

This study provides a good preliminary assessment of polychete communities in the Prince Gustav channel in terms of broad dominant functional groups present and taxonomic composition at the family level. The turnover in community structure and diversity is important to understand in a wider perspective; significantly increased burial of organic carbon caused by loss of ice cover and increased primary production has recently been reported from Antarctic areas (Barnes, 2015; Fogwill et al., 2020; Pineda-Metz et al., 2020; Rogers et al., 2020) but the role of the faunal response to changed nutrient availability and sedimentation rates are not known (Smith and DeMaster, 2008; Gogarty et al., 2020). However, diversity at the species level can be difficult to assess based on morphological identification alone.

Many of the named species identified in this study are considered to have widespread, circum-Antarctic distributions and broad depth ranges – a phenomenon well reported both for Southern Ocean polychetes and for Antarctic benthos in general (Schüller, 2011). The increasing use of molecular methods such as DNA barcoding in Antarctic sampling however is beginning to challenge this traditional notion (Grant et al., 2011), with numerous studies finding that many previously widespread species across several phyla are instead composed of cryptic species complexes (see Riesgo et al., 2015 and references therein) – morphologically similar yet genetically distinct species. In 2016, DNA barcoding of 16 Antarctic polychete morphospecies found evidence of cryptic diversity in over half the morphospecies examined, including taxa identified in the present study, such as *Aglaophamus trissophyllus* and *Maldane sarsi* (Brasier et al., 2016), suggesting that assessment based on morphology alone may significantly underestimate true species diversity. More recently, evidence of cryptic diversity has been found in Southern Ocean lineages of the polynoid *Polyeunoa laevis* (Bogantes et al., 2020), a taxon also present in the JR17003a samples.

A further consideration is the fact that traditional faunal lists and taxonomic identification literature available for Southern Ocean polychetes are considered to be outdated (Neal et al., 2018), with the presence of several globally widespread taxa with Northern Hemisphere type localities questionable. For example, the supposed cosmopolitan *Maldane sarsi* and its Antarctic subspecies *Maldane sarsi antarctica* Arwidsson, 1911 have both been reported from throughout the Southern Ocean (e.g., Hartman, 1966, 1967) – while the stem and subspecies differ primarily by color and gland pattern, these are not considered to be robust taxonomic characters (Wang and Li, 2016). However, Brasier et al. (2016) found that DNA barcode data of morphospecies identified as *M. sarsi* collected from Scotia and Amundsen seas differed from barcodes of *M. sarsi* collected from the stem species' type locality in northwestern Europe. The authors subsequently assigned their Antarctic morphospecies to *M. sarsi antarctica*, questioning whether the subspecies should be investigated as a separate morpho- or cryptic species given the genetic difference and geographic distance from the parent species, and querying the presence of the parent species in the Southern Ocean altogether. *Maldane sarsi* was amongst the most common morphospecies collected in the present study, with all morphotypes assigned to the parent taxon as a conservative approach until further assessment.

Annelids are also prone to fragmentation, and morphology cannot account for missing characters from damaged or incomplete specimens that could otherwise identify or delimit species. Although the preservation quality in the current study was high, the samples still included many posteriorly incomplete or damaged individuals, in addition to fragments without heads that were not included at all, but could be potentially be identified using DNA.

However, morphology can also overestimate species diversity. For example, the only two species of sternaspid polychetes described from the Southern Ocean, *Sternaspis sendalli* and *Sternaspis monroi,* were recently synonymized (the latter now the junior synonym) based on a molecular investigation that found little genetic structure between the two despite considerable variation in diagnostic morphological characters (Drennan et al., 2019). Furthermore, Polynoidae, the most morphospecies rich family in the current study, can display considerable degrees of intraspecific variation yet remain a single genetic species, as in the case of *Harmothoe imbricata* (Linnaeus, 1767) from waters off Scandinavia and Svalbard, which has at least ten distinct color morphs yet little genetic variation (Nygren et al., 2011). Additionally, juvenile polychetes can also show marked morphological differences from adult counterparts, and thus can often be misidentified as separate species when using morphology alone (Neal et al., 2014).

While molecular-based taxonomy can allow for a faster, statistically-rigorous assessment of diversity (though with its own caveats, see Riesgo et al., 2015), morphological assessments are still necessary in terms of providing information on life history, ecology, and ecosystem function, in addition to linking molecular results to described species and traditional pre-molecular taxonomic literature, and are a requisite for useful field identification guides (Glover et al., 2016). Molecular taxonomy should thus complement rather than supplant existing taxonomic methods (Bucklin et al., 2011).

The morphospecies identified in the present study will be subject to future molecular taxonomic and connectivity analyses, which will include the DNA barcoding of all specimens; additional annelid specimens collected from the PGC sampling sites on the expedition JR170003a using both Epibenthic Sledge (EBS) and multi-corer sampling gear will also be included in these analyses. This will allow for a more thorough and comparable assessment of annelid diversity in the channel, for example through assessments of cryptic diversity and as an error check for morphological assignments. Furthermore, while the number of molecular investigations of Southern Ocean fauna have rapidly expanded in recent decades (Grant et al., 2011; Riesgo et al., 2015), major gaps in taxonomic and geographic coverage in terms of genetic data still exist, with annelids poorly represented relative to other groups such as Mollusca and Arthropoda (Riesgo et al., 2015), and regions of the Southern Ocean such as the Western Weddell Sea rarely sampled at all (Griffiths et al., 2014). Future molecular investigations of these samples will aid in filling these sampling gaps and will be included as part of wider phylogeographic and population genetic analyses assessing the connectivity, demographic history, and evolutionary origins of annelid fauna in this ice-influenced region. Understanding how the benthos of the Southern Ocean evolved and persisted through past environmental change over multimillion year timescales can provide insight into their resilience against current and future climactic change (Lau et al., 2020) and could inform current glacial and climactic models by providing an independent biological line of evidence for past ice sheet behavior (Strugnell et al., 2018).

CONCLUSION

This study provides a good snapshot of diverse benthic communities in a habitat with a dynamic recent glacial history and continuing glacial influence, which may be relevant to future habitats if present rates of ice loss and retreat along the Antarctic Peninsula continue. In addition, these specimens begin to fill sampling gaps in a poorly sampled region of the Southern Ocean and will be utilized in future molecular investigations, both in terms of assessing the genetic diversity of the channel and as part of wider phylogeographic and population genetic analyses of annelid fauna in this ice-influenced region. Curating accurate taxonomic and distributional data provides a necessary and important baseline for monitoring ecosystems and understanding current and future environmental change, while insights into the evolutionary history of the Southern Ocean benthos can help inform current climatic debate.

The channel is of further interest as its southern portion (south of 64°N) is currently included within the margins of a proposed Marine Protected Area for the Weddell Sea, presented in 2014 to the Commission for the Conservation of Antarctic Marine Living Resources (CCAMLR), though as of 2018 has not yet been agreed upon (UN Ocean Conference, 2018). Increased knowledge of the fauna of this region may contribute to future decisions in regards to conservation policy implementation for the Weddell Sea area.

DATA AVAILABILITY STATEMENT

The original contributions presented in the study are included in the article and in **Supplementary Material**; the specimen biodiversity data generated in this study are publicly available online via the SCAR Antarctic Biodiversity Portal (biodiversity.aq) and can be accessed through the following doi: 10.15468/t223v4. A dataset of all JR17003a expedition Shallow Underwater Camera System (SUCS) imagery is available at doi: 10.5285/48DCEF16-6719-45E5-A335-3A97F099E451. Further inquiries can be directed to the corresponding author.

AUTHOR CONTRIBUTIONS

KL, AG, and TD developed and designed the study. AG, TD, and KL collected the samples. AG and TD sorted the samples and identified the specimens to family level in the field. RD performed morphological taxonomic analysis and identification of samples in the laboratory, prepared the figures and tables, performed analyses and drafted the original manuscript, which was critically revised by and improved by two reviewers. All authors contributed to the article and approved the submitted version.

FUNDING

This work was supported by the National Environment Research Council grants: RD has support by the NERC INSPIRE DTP (NE/S007210/1). KL is part of the British Antarctic Survey's Polar Science for Planet Earth Programme (NC-Science). TD was funded by the Norwegian Research Centre NORCE and the RSS James Clark Ross expedition JR17003a was funded by the NERC urgency grant NE/R012296/1 and enabled the participation of KL, AG, and TD.

ACKNOWLEDGMENTS

We would like to thank the Master and crew of RRS James Clark Ross and the scientific and technical participants of JR17003a for their support. Special thanks to Simon Dreuter for providing the bathymetric map. A special thank you also to Anton Van de Putte for their great assistance and guidance throughout the process of publishing data through biodiversity.aq. The fieldwork in the western Weddell Sea during JR17003a was undertaken under the permit No. 43/2017 issued by the Foreign and Commonwealth Office, London to section 3 of the Antarctic Act 1994.

SUPPLEMENTARY MATERIAL

The Supplementary Material for this article can be found online at: https://www.frontiersin.org/articles/10.3389/fmars.2020.595303/full#supplementary-material

REFERENCES

Almond, P. (2019). *Benthic Assemblage and Habitat Heterogeneity in the Prince Gustav Channel of the Antarctic Peninsula*. Master's thesis, Newcastle University, Newcastle Upon Tyne.

Arnaud, P. M., López, C. M., Olaso, I., Ramil, F., Ramos-Esplá, A. A., and Ramos, A. (1998). Semi-quantitative study of macrobenthic fauna in the region of the South Shetland Islands and the Antarctic Peninsula. *Polar Biol.* 19, 160–166. doi: 10.1007/s003000050229

Arntz, W., and Gutt, J. (1999). The expedition ANTARKTIS XV/3 (EASIZ II) of RV "Polarstern" in 1998. *Ber. Polarforsch.* 301:229.

Barnes, D., and Peck, L. (2008). Vulnerability of Antarctic shelf biodiversity to predicted regional warming. *Clim. Res.* 37, 149–163. doi: 10.3354/cr00760

Barnes, D. K. A. (2015). Antarctic sea ice losses drive gains in benthic carbon drawdown. *Curr. Biol.* 25, R789–R790. doi: 10.1016/j.cub.2015.07.042

Barnich, R., Gambi, M. C., and Fiege, D. (2012). Revision of the genus Polyeunoa McIntosh, 1885 (Polychaeta, Polynoidae). *Zootaxa* 3523, 25–38. doi: 10.11646/zootaxa.3523.1.3

Bertolin, M. L., and Schloss, I. R. (2009). Phytoplankton production after the collapse of the Larsen A Ice Shelf, Antarctica. *Polar Biol.* 32, 1435–1446. doi: 10.1007/s00300-009-0638-x

Blake, J. A. (2015). New species of Scalibregmatidae (annelida, polychaeta) from the East Antarctic Peninsula including a description of the ecology and post-larval development of species of *Scalibregma* and *Oligobregma*. *Zootaxa* 4033, 57–93. doi: 10.11646/zootaxa.4033.1.3

Blake, J. A. (2017). Polychaeta orbiniidae from antarctica, the southern ocean, the abyssal pacific ocean, and off South America. *Zootaxa* 4218, 1–145. doi: 10.11646/zootaxa.4218.1.1

Blake, J. A. (2018). Bitentaculate Cirratulidae (Annelida, Polychaeta) collected chiefly during cruises of the R/V Anton Bruun, USNS Eltanin, USCG Glacier, R/V Hero, RVIB Nathaniel B. Palmer, and R/V Polarstern from the Southern Ocean, Antarctica, and off Western South A. *Zootaxa* 4537, 1–130. doi: 10.11646/zootaxa.4537.1.1

Bogantes, V. E., Whelan, N. V., Webster, K., Mahon, A. R., and Halanych, K. M. (2020). Unrecognized diversity of a scale worm, *Polyeunoa laevis* (Annelida: Polynoidae), that feeds on soft coral. *Zool. Scr.* 49, 236–249. doi: 10.1111/zsc.12400

Brachfeld, S., Domack, E., Kissel, C., Laj, C., Leventer, A., Ishman, S., et al. (2003). Holocene history of the Larsen - A Ice Shelf constrained by geomagnetic paleointensity dating. *Geology* 31, 749–752. doi: 10.1130/G19643.1

Brandt, A., Linse, K., and Schüller, M. (2009). Bathymetric distribution patterns of Southern Ocean macrofaunal taxa: bivalvia, Gastropoda, Isopoda and Polychaeta. *Deep Sea Res. Part I Oceanogr. Res. Pap.* 56, 2013–2025. doi: 10.1016/J.DSR.2009.06.007

Brasier, M. J., Grant, S. M., Trathan, P. N., Allcock, L., Ashford, O., Blagbrough, H., et al. (2018). Benthic biodiversity in the South Orkney Islands Southern Shelf Marine Protected Area. *Biodiversity* 19, 5–19. doi: 10.1080/14888386.2018.1468821

Brasier, M. J., Wiklund, H., Neal, L., Jeffreys, R., Linse, K., Ruhl, H., et al. (2016). DNA barcoding uncovers cryptic diversity in 50% of deep-sea Antarctic polychaetes. *R. Soc. Open Sci.* 3:160432. doi: 10.1098/rsos.160432

Bucklin, A., Steinke, D., and Blanco-Bercial, L. (2011). DNA Barcoding of marine Metazoa. *Annu. Rev. Mar. Sci.* 3, 471–508. doi: 10.1146/annurev-marine-120308-080950

Camerlenghi, A., Domack, E., Rebesco, M., Gilbert, R., Ishman, S., Leventer, A., et al. (2001). Glacial morphology and post-glacial contourites in northern Prince Gustav Channel (NW Weddell Sea, Antarctica). *Mar. Geophys. Res.* 22, 417–443. doi: 10.1023/A:1016399616365

Clarke, A., and Johnston, N. M. (2003). Antarctic marine benthic diversity. *Oceanogr. Mar. Biol. Ann. Rev.* 41, 47–114. doi: 10.1201/9780203180570-8

Cook, A. J., Fox, A. J., Vaughan, D. G., and Ferrigno, J. G. (2005). Retreating glacier fronts on the Antarctic Peninsula over the past half-century. *Science* 308, 541–544. doi: 10.1126/science.1104235

Cook, A. J., and Vaughan, D. G. (2010). Overview of areal changes of the ice shelves on the Antarctic Peninsula over the past 50 years. *Cryosphere* 4, 77–98. doi: 10.5194/tc-4-77-2010

Cooper, A. P. R. (1997). Historical observations of Prince Gustav Ice Shelf. *Polar Rec.* 33, 285–294. doi: 10.1017/S0032247400025389

Cummings, V., Thrush, S., Norkko, A., Andrew, N., Hewitt, J., Funnell, G., et al. (2006). Accounting for local scale variability in benthos: implications for future assessments of latitudinal trends in the coastal Ross Sea. *Antarct. Sci.* 18, 633–644. doi: 10.1017/s0954102006000666

Dierssen, H. M., Smith, R. C., and Vernet, M. (2002). Glacial meltwater dynamics in coastal waters west of the Antarctic peninsula. *Proc. Natl. Acad. Sci. U.S.A.* 99, 1790–1795. doi: 10.1073/pnas.032206999

Domack, E., Leventer, A., Gilbert, R., Brachfeld, S., Ishman, S., Camerlenghi, A., et al. (2001). Cruise reveals history of Holocene Larsen Ice Shelf. *Eos* 82, 13–13. doi: 10.1029/01EO00009

Drennan, R., Wiklund, H., Rouse, G. W., Georgieva, M. N., Wu, X., Kobayashi, G., et al. (2019). Taxonomy and phylogeny of mud owls (Annelida: Sternaspidae), including a new synonymy and new records from the Southern Ocean, North East Atlantic Ocean and Pacific Ocean: challenges in morphological delimitation. *Mar. Biodivers.* 49, 2659–2697. doi: 10.1007/s12526-019-00998-0

Drennan, R., Dahlgren, T. G., Linse, K., and Glover, A. G. (2020). Annelid Fauna of the Prince Gustav Channel, a previously ice-covered seaway on the northeastern Antarctic Peninsula - Data. SCAR - AntOBIS. *Occur. Dataset* 2020, 12–14. doi: 10.15468/t223v4 accessed via GBIF.org on 2020-12-14

Dreutter, S., Dorschel, B., and Linse, K. (2020). Swath sonar bathymetry data of RRS JAMES CLARK ROSS during cruise JR17003a with links to multibeam raw data. *PANAGAEA* 2020:EM122. doi: 10.1594/PANGAEA.916177

Eleftheriou, A., and Holme, N. A. (1984). "Macrofauna techniques," in *Methods for the Study of Marine Benthos*, eds N. A. Holme, et al. (Oxford: Blackwell Scientific Publications), 140–216.

Etourneau, J., Sgubin, G., Crosta, X., Swingedouw, D., Willmott, V., Barbara, L., et al. (2019). Ocean temperature impact on ice shelf extent in the eastern Antarctic Peninsula. *Nat. Commun.* 10:304. doi: 10.1038/s41467-018-08195-6

Evans, J., Pudsey, C. J., ÓCofaigh, C., Morris, P., and Domack, E. (2005). Late Quaternary glacial history, flow dynamics and sedimentation along the eastern margin of the Antarctic Peninsula Ice Sheet. *Quat. Sci. Rev.* 24, 741–774. doi: 10.1016/j.quascirev.2004.10.007

Ferrigno, J. G., Cook, A. J., Foley, K. M., Williams, R. S., Jr., Swithinbank, C., Fox, A. J., et al. (2006). *Coastal-Change and Glaciological Map of the Trinity Peninsula Area and South Shetland Islands, Antarctica—1843–2001: U.S. Geological Survey Geologic Investigations Series Map I–2600–A, 1 map sheet, 32-p.* Cambridge: British Antarctic Survey.

Fogwill, C. J., Turney, C. S. M., Menviel, L., Baker, A., Weber, M. E., Ellis, B., et al. (2020). Southern Ocean carbon sink enhanced by sea-ice feedbacks at the Antarctic Cold Reversal. *Nat. Geosci.* 13, 489–497. doi: 10.1038/s41561-020-0587-0

Gambi, M. C., Castelli, A., and Guizzardi, M. (1997). Polychaete populations of the shallow soft bottoms off Terra Nova Bay (Ross Sea, Antarctica): distribution, diversity and biomass. *Polar Biol.* 17, 199–210. doi: 10.1007/s003000050123

Glover, G. A., Dahlgren, G. T., Wiklund, H., Mohrbeck, I., and Smith, R. C. (2016). An End-to-End DNA Taxonomy Methodology for Benthic Biodiversity Survey in the Clarion-Clipperton Zone, Central Pacific Abyss. *J. Mar. Sci. Eng.* 4:2. doi: 10.3390/jmse4010002

Gogarty, B., McGee, J., Barnes, D. K. A., Sands, C. J., Bax, N., Haward, M., et al. (2020). Protecting Antarctic blue carbon: as marine ice retreats can the law fill the gap? *Clim. Policy* 20, 149–162. doi: 10.1080/14693062.2019.1694482

Grant, R. A., Griffiths, H. J., Steinke, D., Wadley, V., and Linse, K. (2011). Antarctic DNA barcoding; a drop in the ocean? *Polar Biol.* 34, 775–780. doi: 10.1007/s00300-010-0932-7

Griffiths, H., Van de Putte, A., Danis, B., De Broyer, C., Koubbi, P., Raymond, B., et al. (2014). "The data behind the Biogeographic Atlas of the Southern Ocean," in *Proceedings of the EPIC32014 XXXIII SCAR Open Science Conference*, Auckland.

Gutt, J. (2008). The expedition ANTARKTIS-XXIII/8 of the research vessel "Polarstern" in 2006/2007. *Ber. Polar Meeresforsch.* 569, 48–56.

Gutt, J., Barratt, I., Domack, E. W., d'Udekem d'Acoz, C., Dimmler, W., Grémare, A., et al. (2010). Macro benthos in surface sediments sampled during POLARSTERN cruise ANT-XXIII/8. *PANGAEA*. doi: 10.1594/PANGAEA.718106. In supplement to: Gutt et al. (2011).

Gutt, J., Barratt, I., Domack, E., d'Udekem d'Acoz, C., Dimmler, W., Grémare, A., et al. (2011). Biodiversity change after climate-induced ice-shelf collapse in the Antarctic. *Deep Sea Res. Part II* 58, 74–83. doi: 10.1016/j.dsr2.2010.05.024

Hartman, O. (1966). Polychaeta Myzostomidae and Sedentaria of Antarctica. *Antartic Res. Ser.* 7, 1–155. doi: 10.1029/AR007

Hartman, O. (1967). *Polychaetous Annelids Collected by the USNS Eltanin and Staten Island Cruises, Chiefly from Antarctic Seas*. Los Angeles, CA: University of Southern California.

Hilbig, B. (2004). Polychaetes of the deep Weddell and Scotia Seas – Composition and zoogeographical links. *Deep Sea Res. Part II Top. Stud. Oceanogr.* 51, 1817–1825. doi: 10.1016/j.dsr2.2004.07.015

Hilbig, B., Gerdes, D., and Montiel, A. (2006). Distribution patterns and biodiversity in polychaete communities of the Weddell Sea and Antarctic Peninsula area (Southern Ocean). *J. Mar. Biolog. Assoc.* 86, 711–725. doi: 10.1017/s0025315406013610

Johnson, J. S., Bentley, M. J., Roberts, S. J., Binnie, S. A., and Freeman, S. P. H. T. (2011). Holocene deglacial history of the northeast Antarctic Peninsula - A review and new chronological constraints. *Quat. Sci. Rev.* 30, 3791–3802. doi: 10.1016/j.quascirev.2011.10.011

Kaiser, S., Barnes, D. K. A., Sands, C. J., and Brandt, A. (2009). Biodiversity of an unknown Antarctic Sea: assessing isopod richness and abundance in the first benthic survey of the Amundsen continental shelf. *Mar. Biodivers.* 39, 27–43. doi: 10.1007/s12526-009-0004-9

Lau, S. C. Y., Wilson, N. G., Silva, C. N. S., and Strugnell, J. M. (2020). Detecting glacial refugia in the Southern Ocean. *Ecography* 43, 1639–1656. doi: 10.1111/ecog.04951

Linse, K., Brandt, A., Bohn, J. M., Danis, B., De Broyer, C., Ebbe, B., et al. (2007). Macro- and megabenthic assemblages in the bathyal and abyssal Weddell Sea (Southern Ocean). *Deep Sea Res. Part II Top. Stud. Oceanogr.* 54, 1848–1863. doi: 10.1016/J.DSR2.2007.07.011

Linse, K., Griffiths, H. J., Barnes, D. K. A., Brandt, A., Davey, N., David, B., et al. (2013). The macro- and megabenthic fauna on the continental shelf of the eastern Amundsen Sea, Antarctica. *Cont. Shelf Res.* 68, 80–90. doi: 10.1016/j.csr.2013.08.012

Linse, K., Grant, S., Whittle, R., Reid, W., McKenzie, M., Federwisch, L., et al. (2020). *Benthic Seafloor Images from Prince Gustav Channel and Duse Bay, Eastern Antarctic Peninsula, March 2018 (Version 1.0) [Data set]*. Cambridge: British Antarctic Survey.

Marchant, J. (2017). Giant iceberg's split exposes hidden ecosystem. *Nature* 549, 443–443. doi: 10.1038/549443a

Meredith, M. P., and King, J. C. (2005). Rapid climate change in the ocean west of the Antarctic Peninsula during the second half of the 20th century. *Geophys. Res. Lett.* 32:L19604. doi: 10.1029/2005GL024042

Morris, E. M., and Vaughan, D. G. (2003). "Spatial and temporal variation of surface temperature on the Antarctic peninsula and the limit of viability of ice shelves," in *Antarctic Peninsula Climate Variability: Historical and Paleoenvironmental Perspectives*, eds E. Domack, A. Levente, A. Burnet, R. Bindschadler, P. Convey, and M. Kirby (Washington, DC: American Geophysical Union), 61–68. doi: 10.1029/ar079p0061

Neal, L., Barnich, R., Wiklund, H., and Glover, A. G. (2012). A new genus and species of Polynoidae (Annelida, Polychaeta) from Pine Island Bay, Amundsen Sea, Southern Ocean—a region of high taxonomic novelty. *Zootaxa* 3542, 80–88. doi: 10.11646/zootaxa.3542.1.4

Neal, L., Linse, K., Brasier, M. J., Sherlock, E., and Glover, A. G. (2018). Comparative marine biodiversity and depth zonation in the Southern Ocean: evidence from a new large polychaete dataset from Scotia and Amundsen seas. *Mar. Biodivers.* 48, 581–601. doi: 10.1007/s12526-017-0735-y

Neal, L., Mincks Hardy, S., Smith, C., and Glover, A. (2011). Polychaete species diversity on the West Antarctic Peninsula deep continental shelf. *Mar. Ecol. Prog. Ser.* 428, 119–134. doi: 10.3354/meps09012

Neal, L., Wiklund, H., Muir, A. I., Linse, K., and Glover, A. G. (2014). The identity of juvenile Polynoidae (Annelida) in the Southern Ocean revealed by DNA taxonomy, with notes on the status of *Herdmanella gracilis* Ehlers sensu Augener. *Mem. Mus. Vic.* 71, 203–216. doi: 10.24199/j.mmv.2014.71.16

Nicholls, K. W., Pudsey, C. J., and Morris, P. (2004). Summertime water masses off the northern Larsen C Ice Shelf, Antarctica. *Geophys. Res. Lett.* 31:L09309. doi: 10.1029/2004GL019924

Nolan, E. T., Barnes, D. K. A., Brown, J., Downes, K., Enderlein, P., Gowland, E., et al. (2017). Biological and physical characterization of the seabed surrounding Ascension Island from 100–1000 m. *J. Mar. Biolog. Assoc.* 97, 647–659. doi: 10.1017/S0025315417000820

Nordenskjöld, O. G., and Andersson, J. G. (1905). *Antarctica*. London: Hurst and Blackett.

Nygren, A., Norlinder, E., Panova, M., and Pleijel, F. (2011). Colour polymorphism in the polychaete *Harmothoe imbricata* (Linnaeus, 1767). *Mar. Biol. Res.* 7, 54–62. doi: 10.1080/17451001003713555

Nývlt, D., Košler, J., Mlcoch, B., Mixa, P., Lisá, L., Bubík, M., et al. (2011). The mendel formation: evidence for late miocene climatic cyclicity at the northern tip of the Antarctic Peninsula. *Palaeogeogr. Palaeoclimatol. Palaeoecol.* 299, 363–384. doi: 10.1016/j.palaeo.2010.11.017

Oksanen, J., Guillaume Blanchet, F., Friendly, M., Kindt, R., Legendre, P., McGlinn, D., et al. (2019). *vegan: Community Ecology Package*. Available online at: https://cran.r-project.org/package=vegan (accessed July 9, 2020).

Parapar, J., López, E., Gambi, M. C., Núñez, J., and Ramos, A. (2011). Quantitative analysis of soft-bottom polychaetes of the Bellingshausen Sea and Gerlache Strait (Antarctica). *Polar Biol.* 34, 715–730. doi: 10.1007/s00300-010-0927-4

Pielou, E. C. (1969). *An Introduction to Mathematical Ecology*. New York, NY: Wiley.

Piepenburg, D., Schmid, M. K., and Gerdes, D. (2002). The benthos off King George Island (South Shetland Islands, Antarctica): further evidence for a lack of a latitudinal biomass cline in the Southern Ocean. *Polar Biol.* 25, 146–158. doi: 10.1007/s003000100322

Pineda-Metz, S. E. A., Gerdes, D., and Richter, C. (2020). Benthic fauna declined on a whitening Antarctic continental shelf. *Nat. Commun.* 11:2226. doi: 10.1038/s41467-020-16093-z

Post, A. L., Galton-Fenzi, B. K., Riddle, M. J., Herraiz-Borreguero, L., O'Brien, P. E., Hemer, M. A., et al. (2014). Modern sedimentation, circulation and life beneath the Amery Ice Shelf, East Antarctica. *Cont. Shelf Res.* 74, 77–87. doi: 10.1016/J.CSR.2013.10.010

Post, A. L., Lavoie, C., Domack, E. W., Leventer, A., Shevenell, A., and Fraser, A. D. (2017). Environmental drivers of benthic communities and habitat heterogeneity on an East Antarctic shelf. *Antarct. Sci.* 29, 17–32. doi: 10.1017/S0954102016000468

Pudsey, C. J., and Evans, J. (2001). First survey of Antarctic sub–ice shelf sediments reveals mid-Holocene ice shelf retreat. *Geology* 29, 787–790. doi: 10.1130/0091-7613(2001)029<0787:fsoasi>2.0.co;2

Pudsey, C. J., Evans, J., Domack, E. W., Morris, P., and Del Valle, R. A. (2001). Bathymetry and acoustic facies beneath the former Larsen-A and Prince Gustav ice shelves, north-west Weddell Sea. *Antarct. Sci.* 13, 312–322. doi: 10.1017/S095410200100044X

Pudsey, C. J., Murray, J. W., Appleby, P., and Evans, J. (2006). Ice shelf history from petrographic and foraminiferal evidence, Northeast Antarctic Peninsula. *Quat. Sci. Rev.* 25, 2357–2379. doi: 10.1016/j.quascirev.2006.01.029

Quartino, M. L., Klöser, H., Schloss, I. R., and Wiencke, C. (2001). Biomass and associations of benthic marine macroalgae from the inner Potter Cove (King George Island, Antarctica) related to depth and substrate. *Polar Biol.* 24, 349–355. doi: 10.1007/s003000000218

R Core Team (2019). *R: A Language and Environment for Statistical Computing*. Vienna: R Foundation for Statistical Computing.

Rack, W., and Rott, H. (2004). Pattern of retreat and disintegration of the Larsen B ice shelf, Antarctic Peninsula. *Ann. Glaciol.* 39, 505–510. doi: 10.3189/172756404781814005

Riddle, M. J., Craven, M., Goldsworthy, P. M., and Carsey, F. (2007). A diverse benthic assemblage 100 km from open water under the Amery Ice Shelf, Antarctica. *Paleoceanography* 22:PA1204. doi: 10.1029/2006PA001327

Riehl, T., and Kaiser, S. (2012). Conquered from the deep sea? A new deep-sea isopod species from the Antarctic shelf shows pattern of recent colonization. *PLoS One* 7:e49354. doi: 10.1371/journal.pone.0049354

Riesgo, A., Taboada, S., and Avila, C. (2015). Evolutionary patterns in Antarctic marine invertebrates: an update on molecular studies. *Mar. Genomics* 23, 1–13. doi: 10.1016/J.MARGEN.2015.07.005

Rignot, E., Jacobs, S., Mouginot, J., and Scheuchl, B. (2013). Ice-shelf melting around Antarctica. *Science* 341, 266–270. doi: 10.1126/science.1235798

Rogers, A. D., Frinault, B. A. V., Barnes, D. K. A., Bindoff, N. L., Downie, R., Ducklow, H. W., et al. (2020). Antarctic Futures: an assessment of climate-driven changes in ecosystem structure, function, and service

provisioning in the Southern Ocean. *Annu. Rev. Mar. Sci.* 12, 87–120. doi: 10.1146/annurev-marine-010419-011028

Rott, H., Abdel Jaber, W., Wuite, J., Scheiblauer, S., Floricioiu, D., Van Wessem, J. M., et al. (2018). Changing pattern of ice flow and mass balance for glaciers discharging into the Larsen A and B embayments, Antarctic Peninsula, 2011 to 2016. *Cryosphere* 12, 1273–1291. doi: 10.5194/tc-12-1273-2018

Rott, H., Floricioiu, D., Wuite, J., Scheiblauer, S., Nagler, T., and Kern, M. (2014). Mass changes of outlet glaciers along the Nordensjköld Coast, northern Antarctic Peninsula, based on TanDEM-X satellite measurements. *Geophys. Res. Lett.* 41, 8123–8129. doi: 10.1002/2014GL061613

Rott, H., Skvarca, P., and Nagler, T. (1996). Rapid collapse of northern Larsen Ice Shelf, Antarctica. *Science* 271, 788–792. doi: 10.1126/science.271.5250.788

Sahade, R., Lagger, C., Torre, L., Momo, F., Monien, P., Schloss, I., et al. (2015). Climate change and glacier retreat drive shifts in an Antarctic benthic ecosystem. *Sci. Adv.* 1:e1500050. doi: 10.1126/sciadv.1500050

Sañé, E., Isla, E., Gerdes, D., Montiel, A., and Gili, J. M. (2012). Benthic macrofauna assemblages and biochemical properties of sediments in two Antarctic regions differently affected by climate change. *Cont. Shelf Res.* 35, 53–63. doi: 10.1016/j.csr.2011.12.008

Scambos, T. A., Berthier, E., Haran, T., Shuman, C. A., Cook, A. J., Ligtenberg, S. R. M., et al. (2014). Detailed ice loss pattern in the northern Antarctic Peninsula: widespread decline driven by ice front retreats. *Cryosphere* 8, 2135–2145. doi: 10.5194/tc-8-2135-2014

Schüller, M. (2011). Evidence for a role of bathymetry and emergence in speciation in the genus Glycera (Glyceridae, Polychaeta) from the deep Eastern Weddell Sea. *Polar Biol.* 34, 549–564. doi: 10.1007/s00300-010-0913-x

Schüller, M., Ebbe, B., and Wägele, J. W. (2009). Community structure and diversity of polychaetes (Annelida) in the deep Weddell Sea (Southern Ocean) and adjacent basins. *Mar. Biodivers.* 39, 95–108. doi: 10.1007/s12526-009-0009-4

Shannon, C. E., and Weaver, W. (1949). *The Mathematical Theory of Communication*. Urbana, IL: University of Illinois.

Smale, D. A., and Barnes, D. K. A. (2008). Likely responses of the Antarctic benthos to climate-related changes in physical disturbance during the 21st century, based primarily on evidence from the West Antarctic Peninsula region. *Ecography* 31, 289–305. doi: 10.1111/j.0906-7590.2008.05456.x

Smith, C. R., and DeMaster, D. J. (2008). Preface and brief synthesis for the FOODBANCS volume. *Deep Sea Res. Part II Top.* 55, 2399–2403. doi: 10.1016/j.dsr2.2008.08.001

Strugnell, J. M., Pedro, J. B., and Wilson, N. G. (2018). Dating Antarctic ice sheet collapse: proposing a molecular genetic approach. *Quat. Sci. Rev.* 179, 153–157. doi: 10.1016/j.quascirev.2017.11.014

Thoma, M., Jenkins, A., Holland, D., and Jacobs, S. (2008). Modelling Circumpolar Deep Water intrusions on the Amundsen Sea continental shelf, Antarctica. *Geophys. Res. Lett.* 35:L18602. doi: 10.1029/2008GL034939

Turner, J., Colwell, S. R., Marshall, G. J., Lachlan-Cope, T. A., Carleton, A. M., Jones, P. D., et al. (2005). Antarctic climate change during the last 50 years. *Int. J. Climatol.* 25, 279–294. doi: 10.1002/joc.1130

UN Ocean Conference (2018). *Marine Protected Area in the Weddell-Sea, Antarctica*. Available online at: https://oceanconference.un.org/commitments/?id=16038 (accessed May 1, 2020).

Vaughan, D. G., Marshall, G. J., Connolley, W. M., Parkinson, C., Mulvaney, R., Hodgson, D. A., et al. (2003). Recent rapid regional climate warming on the Antarctic Peninsula. *Clim. Change* 60, 243–274. doi: 10.1023/A:1026021217991

Wang, Y., and Li, X. (2016). A new *Maldane* species and a new Maldaninae genus and species (Maldanidae, Annelida) from coastal waters of China. *ZooKeys* 2016, 1–16. doi: 10.3897/zookeys.603.9125

Conflict of Interest: The authors declare that the research was conducted in the absence of any commercial or financial relationships that could be construed as a potential conflict of interest.

frontiers in Marine Science

ORIGINAL RESEARCH
published: 28 January 2021
doi: 10.3389/fmars.2021.614496

In-situ Image Analysis of Habitat Heterogeneity and Benthic Biodiversity in the Prince Gustav Channel, Eastern Antarctic Peninsula

Peter M. Almond[1], Katrin Linse[2], Simon Dreutter[3], Susie M. Grant[2], Huw J. Griffiths[2], Rowan J. Whittle[2], Melanie Mackenzie[4] and William D. K. Reid[1]**

[1] School of Natural and Environmental Sciences, Newcastle University, Newcastle upon Tyne, United Kingdom, [2] British Antarctic Survey, Cambridge, United Kingdom, [3] Alfred Wegener Institute, Bremerhaven, Germany, [4] Museums Victoria, Melbourne, VIC, Australia

OPEN ACCESS

Edited by:
Wei-Jen Chen, National Taiwan University, Taiwan

Reviewed by:
Karine Olu, Institut Français de Recherche pour l'Exploitation de la Mer (IFREMER), France
Ann Vanreusel, Ghent University, Belgium

***Correspondence:**
Peter M. Almond
p.almond@newcastle.ac.uk
William D. K. Reid
william.reid@newcastle.ac.uk

Specialty section:
This article was submitted to Marine Evolutionary Biology, Biogeography and Species Diversity, a section of the journal Frontiers in Marine Science

Received: *06 October 2020*
Accepted: *06 January 2021*
Published: *28 January 2021*

Citation:
Almond PM, Linse K, Dreutter S, Grant SM, Griffiths HJ, Whittle RJ, Mackenzie M and Reid WDK (2021) In-situ Image Analysis of Habitat Heterogeneity and Benthic Biodiversity in the Prince Gustav Channel, Eastern Antarctic Peninsula. Front. Mar. Sci. 8:614496. doi: 10.3389/fmars.2021.614496

Habitat heterogeneity is important for maintaining high levels of benthic biodiversity. The Prince Gustav Channel, on the Eastern Antarctic Peninsula, is characterized by an array of habitat types, ranging from flat, mud-dominated sheltered bays to steep and rocky exposed slopes. The channel has undergone dramatic environmental changes in recent decades, with the southern end of the channel permanently covered by the Prince Gustav Ice Shelf until it completely collapsed in 1995. Until now the marine benthic fauna of the Prince Gustav Channel has remained unstudied. A shallow underwater camera system and Agassiz trawl were deployed at different locations across the channel to collect information on habitat type and heterogeneity, benthic community composition and macrofaunal biomass. The texture of the seafloor was found to have a significant influence on the benthos, with hard substrates supporting higher abundances and diversity. Suspension and filter feeding organisms, including porifera, crinoids, and anthozoans, were strongly associated with hard substrates, with the same being true for deposit feeders, such as holothurians, and soft sediments. Habitat heterogeneity was high across the Prince Gustav Channel, particularly on a local scale, and this was significant in determining patterns of benthic composition and abundance. Other physical variables including depth and seafloor gradient played significant, interactive roles in determining composition potentially mediated through other processes. Sites that were once covered by the Prince Gustav Ice Shelf held distinct and unique communities, suggesting that the legacy of the ice shelf collapse may still be reflected in the benthos. Biomass estimations suggest that critical thresholds of vulnerable marine ecosystem indicator taxa, as defined by the Commission for the Conservation of Antarctic Marine Living Resources, have been met at multiple locations within the Prince Gustav Channel, which has implications for the future establishment of no take zones and marine protected areas within the region.

Keywords: vulnerable marine ecosystem, habitat heterogeneity, benthic biodiversity, global climate change, ice shelf, marine protect area, Antarctic

INTRODUCTION

The Antarctic continental shelf and slope is characterized by a highly diverse benthos that displays high levels of endemism and spatial variability (Convey et al., 2014). All main types of macrobenthic communities, in particular suspension and mobile or deposit feeders, can occur all around the Southern Ocean, which suggests that their distribution on a regional and local scale is likely unpredictable and assumed to be shaped by complex biological and physical interactions (Gutt et al., 2013). Measuring species and biological diversity on the Antarctic shelf is notoriously difficult as a result of high community patchiness and complex hierarchical scales of spatial variation (Thrush et al., 2006). Additionally, sampling gaps limit our understanding of the processes at work (Griffiths, 2010). Current biodiversity estimates come either from regions which vary from small, well-sampled locations such as King George Island or the South Orkney Islands to areas like the Amundsen Sea, which spans a large area but where no fauna had been collected prior to 2008 (Kaiser et al., 2009). The development of statistical and modeling methods using the to-date knowledge on all known or described Antarctic species are also useful in the development of biodiversity estimates (Gutt et al., 2004). Constraining interactions between physical and biological variables is vital for understanding drivers of Antarctic biodiversity and enabling development of predictive ecological models (Convey et al., 2014). Physical datasets are available across larger scales than biological observations, with broad-scale bathymetric, geomorphological, temperature, sea ice patterns, and more available from observations and satellite data (Post et al., 2014). Thus, physical datasets provide an opportunity to build predictive models of species distributions and diversity if significant relationships can be established. Such models can be significant for guiding Southern Ocean ecosystem management, including the selection and monitoring of Marine Protected Areas (MPAs).

Habitat heterogeneity and substrate characteristics have been found to be important determinants of benthic community composition in the South Orkney Islands, Ross Sea, and East Antarctica (Cummings et al., 2006; Post et al., 2017; Brasier et al., 2018), while in other regions the relationship between the benthos and substrate is less consistent (Gutt et al., 2016). These patterns vary between regions, and there is little if any clear evidence relationships between biodiversity and depth, latitude or environmental parameters that can be applied to benthos across the whole Southern Ocean (Brandt et al., 2007). In addition to developing broad-scale biodiversity models, it is important to consider the significance of fine-scale variability and its impact on biological communities. The complex interplay of different biological and physical factors creates habitat patchiness at a range of scales that significantly enhance biological diversity on the Antarctic shelf on both a local and regional scale (Gutt and Piepenburg, 2003). The impacts of variations in physical determiners are mediated by the biological characteristics and life history traits of the local fauna, including mode of dispersal, growth rate, and functional role (Gutt and Koltun, 1995).

The Commission for the Conservation of Antarctic Marine Living Resources (CCAMLR) is responsible for the management of fisheries and conservation of marine ecosystems throughout the Southern Ocean. Part of CCAMLR's remit is the identification and protection of Vulnerable Marine Ecosystems (VMEs) to protect benthic habitats from the adverse impacts of bottom fishing activities (CCAMLR, 2009a; Parker and Bowden, 2010). To facilitate this, CCAMLR developed a classification of VME indicator organisms (CCAMLR, 2009b), taxa deemed potentially vulnerable to the impacts of bottom fishing. Conservation Measures dictate that when specific thresholds of VME taxa biomass are met, specifically 10 kg of biomass per 1200 m longline, these areas will be defined as "VME Risk Area" and are then to be closed to fishing activities until management decisions can be determined by the Commission (CCAMLR, 2009a). Several previous studies based on the Antarctic shelf and slope have provided data on VME biomass that have been useful for the notification of VME Risk Areas, as week as the development of protected areas within the region (Parker and Bowden, 2010; Lockhart and Hocevar, 2018).

The Prince Gustav Channel (PGC) is located at the north-eastern tip of the Antarctic Peninsula, defined by the Peninsula itself to the west and James Ross Island to the east. The channel extends to the Antarctic Sound and Andersson Island to the north, including Eagle Island and the associated Duse Bay, and reaches Cape Obelisk at the very south. The south region of the channel was covered by the Prince Gustav Ice Shelf, which was more than 15 nautical miles across and included Ross Bay and part of James Ross Island (Cook and Vaughan, 2010). The ice shelf began to collapse in the mid-19th century, and by 1995 the PGC was completely open throughout its length during the austral summer (Cooper, 1997). By these same estimates, the ice shelf still permanently covered the sea at Cape Obelisk as recently as 1989, making this a relatively newly uncovered area of seafloor. The southern part of the channel was included in a proposed Weddell Sea MPA presented to CCAMLR in 2016 (Teschke et al., 2016). CCAMLR has not yet reached an agreement on the proposal.

The goal of the present research was to investigate the benthic community of the PGC and how these relate to aspects of habitat complexity and heterogeneity. Specifically, the aims were to: (1) describe the physical habitat characteristics and overall structure of the benthos at sites across the PGC; (2) investigate how these communities vary across different regions and depths; (3) establish the physical variables that are associated with differences in community structure (4) investigate the abundance and distribution associated with VME taxa. This study represents the first assessment of the benthic community of the PGC. It provides an opportunity to assess the implications for conservation and management for this section of the Weddell Sea and establish a baseline for assessing the impacts of future biological or environmental changes that occur in the region.

MATERIALS AND METHODS

Data Collection

In 2018, the RSS *James Clark Ross* expedition JR17003a sampled four sites within the PGC and one site north of the PGC in the vicinity of Andersson Island between 63°30′S and

64°8′S (**Figure 1**; **Table 1**). Before deployment of the Shallow Underwater Camera System (SUCS) and Agassiz Trawl (AGT), multibeam bathymetry data were collected to ascertain seafloor topography, slope gradient, and suitability for deployment of these sampling gears. The sampling covered depths between 200 and 1200 m, although not all depths were sampled at each location because of either ice cover or unsuitable seafloor topography (**Table 1**). The SUCS is a tethered drop-camera system with an HD camera and live feed back to the ship. The system allows the capture of high-resolution images (2448 × 2050 pixels) covering 0.51 m^2 of seafloor. It was deployed 12 times across the five locations (**Table 1**). Each deployment was at a unique depth within that location and consisted of three transects of 10 photos. Each photo within a transect was taken 10 m apart. At the end of each transect the SUCS was moved 100 m to begin the next. The direction of the transects was determined by the wind direction and topography. In some cases, not all the transects could be completed because of icebergs in close vicinity to the vessel or problems with the gear. The AGT was deployed six times across three locations, all of which were also sampled using the SUCS (**Table 1**). The AGT had a mouth width of 2 m and a mesh size of 1 cm. It was trawled at 1 knot for 2–10 min. These provided reference specimens to help identify species in the SUCS images. Five trawls were identified to the lowest possible taxonomic level and sorted during the cruise while the final trawl was fixed in bulk in 99.8% absolute ethanol and sorted at a later date. The wet weight (biomass) of all different taxa was assessed on board using calibrated scales. Topography and presence of pack-ice meant that not all locations where SUCS sampling was undertaken had a corresponding AGT sample.

Image Analysis

All organisms in each SUCS image were identified to the lowest possible taxonomic level, or to morphospecies, dependent on resolution of the images and cross-checked where possible with taxa identified from the AGT trawls at the corresponding location and depth. Some biological material was unidentifiable to phyla but distinguishable as VME species, for example

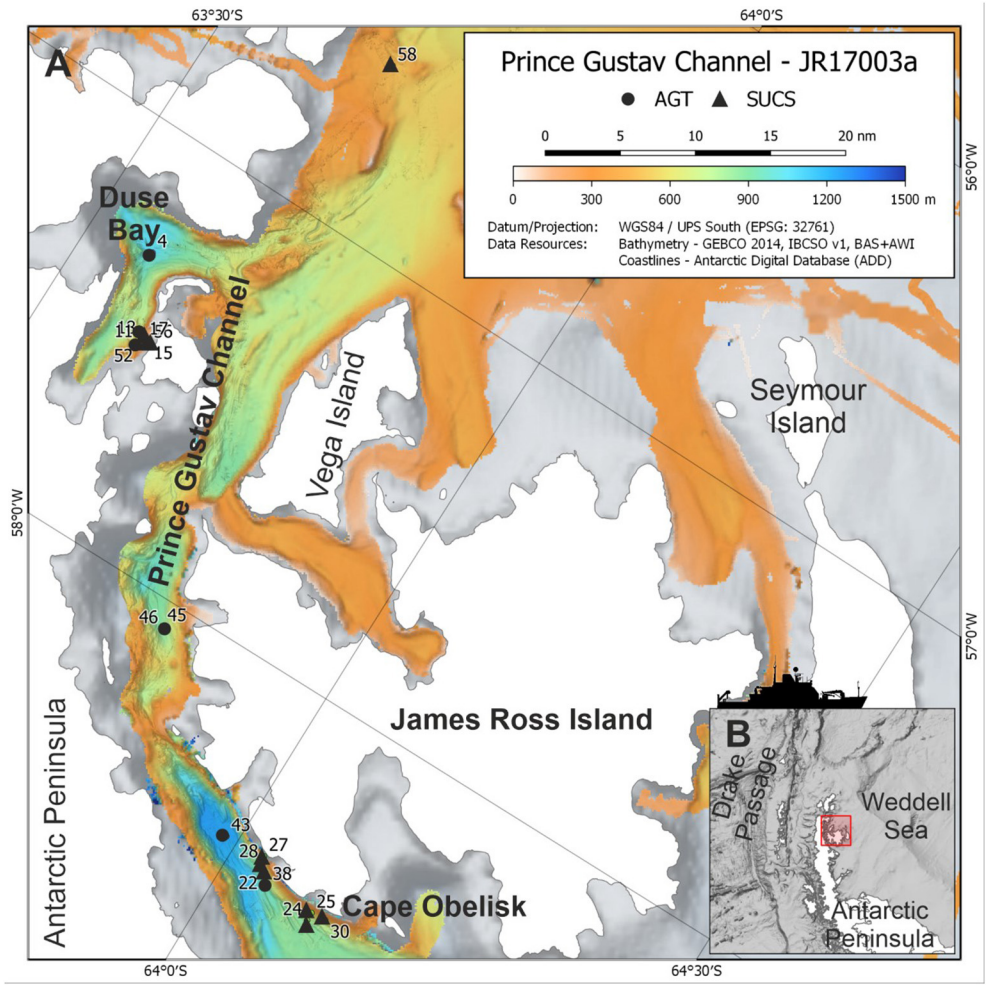

FIGURE 1 | Map of study area. **(A)** Station locations of SUCS and AGT deployments during JR17003a, including event deployment numbers. **(B)** Position of the Prince Gustav Channel on the Antarctic Peninsula in the Southern Ocean. Bathymetry data archived from Dreutter et al. (2020).

TABLE 1 | Station details for SUCS and AGT deployments.

Region	Station number SUCS/ AGT* Deployment	Depth[a]	Latitude[b]	Longitude[b]	Transects/No. of photos (SUCS)	Trawl time in minutes (AGT)	Date
Duse Bay	11	500 m	−63.6154	−57.4976	3/30	-	02/03/2018
	15	200 m	−63.6243	−57.4821	3/30	-	02/03/2018
	17	300 m	−63.619	−57.4848	3/30	-	02/03/2018
	18	400 m	−63.6154	−57.4869	3/30	-	02/03/2018
	4*	1000 m	−63.5755	−57.2954	-	10	01/03/2018
	52*	500 m	−63.6161	−57.5035	-	5	07/03/2018
	56*	200 m	−63.6253	−57.4863	-	2	07/03/2018
Prince Gustav Channel Mid							
	45	850 m	−63.8044	−58.0632	3/29	-	06/03/2018
	46*	850 m	−63.8082	−58.0677	-	5	06/03/2018
Prince Gustav Channel–South							
	22	800 m	−64.0412	−58.4526	3/26	-	03/03/2018
	27	200 m	−64.0333	−58.4185	3/30	-	04/03/2018
	28	500 m	−64.0363	−58.4328	3/30	-	04/03/2018
	38*	800 m	−64.0552	−58.4765	-	5	05/03/2018
	43*	1200 m	−63.9881	−58.4225	-	5	06/03/2018
Cape Obelisk							
	24	800 m	−64.111	−58.4995	3/30	-	03/03/2018
	25	500 m	−64.1108	−58.4777	3/30	-	03/03/2018
	30	400 m	−64.128	−58.4750	3/30	-	04/03/2018
Andersson Island							
	58	500 m	−63.6846	−56.5787	3/30	-	06/03/2018

**AGT; [a]General station depth, [b]Coordinates for start of first transect (SUCS) and net reaching the seafloor (AGT).*

branched or budding fragments which were identifiable as cnidarian or bryozoan species. These individuals were classed as "VME unidentifiable." Length-weight relationships were used to estimate VME biomass present in the SUCS imagery, derived from measurements of specimens collected from the South Orkney Islands (Brasier et al., 2018). SUCS images were used to investigate the relationships between habitat type and community structure. The percentage cover of different substrate types in each image was recorded. Substrate was classified as either mud, sand, gravel, pebbles, cobbles, boulders (which included dropstones) or bedrock, based on size classifications from Sedimentary Petrology: An Introduction to the Origin of Sedimentary Rocks (Tucker, 1991). Substrate size classifications were adjusted to align with the image size on screen using the known SUCS field of view (0.51 m^2). Each image was assigned a texture, based on the dominating substrate type in each image, with mud and sand classified as "Soft" and all others as "Hard." Biogenic substrate was also determined as percentage cover of each photo. Biogenic substrate refers to any ecosystem engineering organisms that create a three-dimensional structure that contributes to the given habitat. This included organisms such as Porifera, tube forming polychaeta and Ascidians, Cnidaria and Bryozoa.

Data Analysis

Data analysis was performed in RStudio, version 1.3.1056. All organisms observed in the SUCS images and AGT were totalled and converted into proportion of total catch to allow for comparison of proportional catch between gear type. As the sample size was relatively low, no significant statistical analysis was carried out on AGT data. The observable taxa in each image of the SUCS were counted and an ANOVA was used to test the difference among sample sites within the PGC. Diversity measures (Simpson's index and Shannon-Weiner index) were calculated for each photo using the total number of individuals and the total number of different taxa present in any given photo using the Vegan package for R (Oksanen et al., 2011). These measures were chosen as each can be used to infer different information about the community, and both can be viewed as appropriate representations in marine systems (Washington, 1984). While Shannon-Weiner represents a combination of both species richness and equitability in distribution among a sample, Simpson's is weighted toward more abundant species in a sample, thereby giving an impression of species dominance within a system. Estimated VME biomass over 1200 m^2 (the area used by CCAMLR to define a VME Risk Area) (CCAMLR, 2009a) was calculated using the known area of the SUCS field of view (0.51 m^2), where wet weight over 1200 m^2 = (average weight × 1.961) × 1200.

Beta-diversity and the degree to which benthic habitat characteristics were associated with the benthos were analyzed using a combination of correspondence analysis (CA) and canonical correspondence analysis (CCA) using the Vegan package for R. The CA site scores from the ordination represent

the similarity between sites. The result is that two sites with similar CA scores have a very similar composition of benthic fauna whereas those with widely different CA scores contain a very different collection of benthic fauna. Any major trend in the first axis represents the degree to which the benthic community turns over along an environmental gradient. The CA scores are used as a measure of beta-diversity. The beta-diversity estimates will be based on the images from the SUCS so will represent the epibenthic fauna that are visible. A structural equational model (SEM) was used to determine the direct and indirect effects of physical variables on beta-diversity. SEMs are a regression-based approach to evaluating causal links between multiple variables in a multivariate system (Lefcheck, 2016). This approach allows variables to function as both predictors and responses within a single model allowing the identification of indirect effects and the testing of specific hypotheses on the interactions between these variables. The SEM was constructed using the R-package piecewiseSEM (Lefcheck, 2016), which allows for the inclusion of non-normally distributed response variables and random effects that account for non-independence in the data. CA1 and CA2 axis scores were used as proxies to represent beta-diversity. The SEM had two indirect pathways, which flow from depth and slope angle to substrate cover and on to CA1 and CA2 scores. Depth and slope angle also have direct pathways to CA1 and CA2, which allow evaluation of whether any depth or slope related change are due to changes in the indirect pathways or due to a different unmeasured variable. A second SEM was used to investigate the indirect and direct effects of slope, depth, and substrate cover on predicted VME biomass. Indirect pathways flowing from depth and slope gradient to biomass were evaluated, as were the corresponding direct pathways. Regression coefficients were standardized using scaling by standard deviation, accomplished using the formula

$$\beta\text{std} = \beta * (\text{sdx}/\text{sdy}),$$

where β is the coefficient, x is the predictor variable and y is the response variable. Non-significant pathways were removed, and the model Akaike information criterion (AIC) were checked, with the model with the lowest AIC being selected. The model fit of the SEMs were tested by the test of direct separation (Lefcheck, 2016). If the *p*-value is >0.05, then the model adequately fits the hypothesized causal network with no important paths missing.

RESULTS

Physical Characteristics of the Seafloor

Substrate type and habitat complexity varied across all 12 SUCS deployments sites (**Figure 2**). Soft, muddy sediments dominated the seafloor at all depths at Duse Bay (95.6%), Cape Obelisk (91.4%), and Andersson Island (96.2%) (**Table 2**), making the habitat at these sites highly homogenous. An increase in hard substrates was observed at the PGC Mid and PGC South sites where mud only covered an average of 13% of the seafloor. These "hard" sites were instead dominated by a wider variety of harder and coarser sediments, predominantly gravel (38.7%), pebbles (21.8%), and bedrock (11.6%), making these regions more heterogenous in nature. Boulders could be found sporadically across all depths within PGC South, PGC Mid and Cape Obelisk, but were absent from most of Duse Bay and the Andersson Island site. PGC South 200 m had the highest occurrence of boulders, which covered an average of 19.3% of the seafloor. Boulders were also found in small amounts (0.4%) at Duse Bay 200 m. Biogenic substrate could be found at all 12 deployment sites. PGC South 200 m had the highest proportions of biogenic cover (16.7%), while Duse Bay 400 m had the lowest (0.6%). All other sites had biogenic cover within this range. Depth ranges within each transect were generally small (<30 m). Slope gradient remained below 10° at all transects in Duse Bay, PGC Mid, Cape Obelisk, and Andersson Island, with the majority of these transects carried out on a slope <5°. PGC South had much higher slope gradients, peaking at 22° on a transect at 800 m.

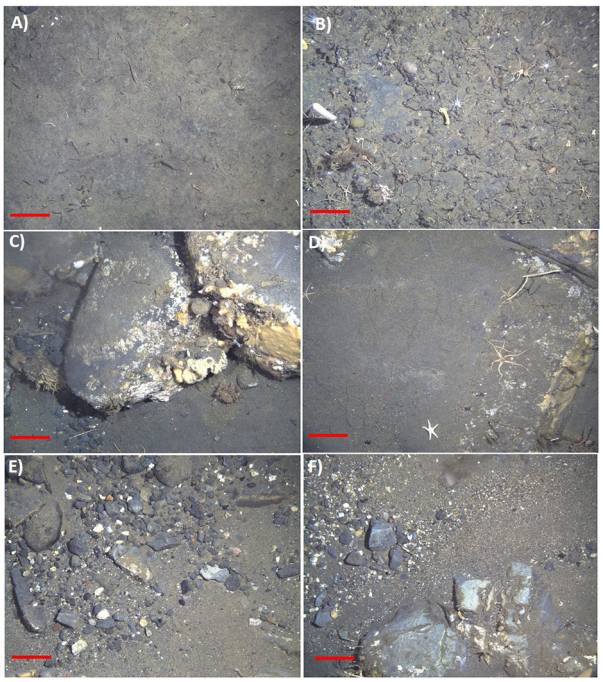

FIGURE 2 | Examples of *in-situ* SUCS images showing different substrate classifications. **(A)** Mud dominated, **(B)** gravel and small pebbles above exposed bedrock, **(C)** boulders/dropstones, **(D)** sandy bottom with some exposed boulders, **(E)** gravel and small pebbles, and **(F)** mixture of sand, gravel, pebbles, and cobbles. Scale bars represent 10 cm.

Benthic Assemblage

A total of 11,396 individuals from eight known phyla were identified from the SUCS imagery (**Table 3**). Ophiuroids were the most common taxa by abundance, representing 40.63% of the total number of individuals recorded. Pycnogonids were the next most abundant taxon, representing 15.51% of the total number. The AGTs sampled a total of 5351 individuals, of which 34.57% were ophiuroids and 17.83% were pycnogonids. Relative proportions of taxa between the sampling gears were mostly consistent, although VME taxa such as bryozoans, soft corals,

TABLE 2 | Mean % cover per photo of substrate size classifications by region/depth set.

Region	Depth (m)	Benthic substrate							
		Mud	Sand	Gravel	Pebbles	Cobbles	Boulders	Bedrock	Biogenic
Duse Bay	200	86.1	4.0	2.3	1.3	0.1	0.4	0	5.8
Duse Bay	300	98.4	0	0	0.1	0.1	0.4	0	1.4
Duse Bay	400	98.9	0	0.4	0	0	0	0	0.6
Duse Bay	500	99.0	0	0	0.2	0	0	0	0.9
PGC-S	200	0	6.7	48.1	5.5	1.3	2.1	19.3	16.7
PGC-S	500	22.1	0.6	38.4	15.1	1.9	3.6	8.0	9.2
PGC-S	800	0.8	0.8	68.4	5.1	0.8	0.6	18.9	4.5
PGC-M	850	29.2	0	0	61.3	1.4	2.0	0.1	5.9
Cape Obelisk	400	90.3	0	0.5	0.7	0.3	1.3	0	7.3
Cape Obelisk	500	91.8	0	1.3	1.4	0.9	0.3	0	4.5
Cape Obelisk	800	92.1	0	0.4	1.0	0.3	0.4	3.2	2.5
Andersson Island	500	96.2	0	0	0	0	0	0	3.7

Biogenic cover accounts for bioconstructors which act as habitat-forming substrate, including Porifera, tube forming Polychaeta, Bryozoa, and Anthozoa. PGC, Prince Gustav Channel; S, South; M, Mid.

hydrozoans, and poriferans were underrepresented in the AGT catch, while bivalves, holothurians, echinoids, and hemichordates were underrepresented in the SUCS. In total 11 VME taxonomic categories were observed from SUCS imagery and 13 from the AGT. Several VME taxa were absent from the SUCS imagery, including brachiopods, chemosynthetic species (e.g., decapods, bivalves, and tubeworms), acorn barnacles, stalked crinoids, basket stars, and the scallop *Adamussium colbecki*. Brachiopods and acorn barnacles were present, but rare, in the AGT sample. VME abundance varied significantly between sites (**Table 4**). The highest abundances of VME taxa were found at PGC South and Mid, with its peak at PGC South 200 m (33.17 ± 12.18), while the lowest abundances were at Duse Bay 400 and 500 m (1.47 ± 1.59 and 1.93 ± 3.86, respectively). VME biomass was also greatest at PGC South, with a combined total of 30.07 kg across the three sampled depths. VME biomass was dominated by Porifera in both the AGT and SUCS samples, accounting for 73.64 and 42.52% of biomass, respectively. For 10 out of the 12 sampled sites, estimated VME biomass over 1200 m^2 exceeded the 10 kg threshold set out by CCAMLR to define a VME Risk Area (**Table 5**).

From the SUCS imagery alone, benthic community structure varied greatly between regions (**Figure 3**), and there were significant differences in the numbers of organisms observed between deployment sites (**Table 4**). PGC South had the highest mean numbers of individuals per photo at its three sampled depths (65.32 ± 19.22, 58.97 ± 17.39, and 56.38 ± 17.39 at 800, 500, and 200 m, respectively). The PGC Mid 850 m site contained an average of 39.93 ± 9.66 individuals per photo, while all other regions had <30. The lowest average abundances were found at Duse Bay 400 m (13.93 ± 4.67) and Andersson Island 500 m (18.53 ± 5.52). On average hard substrates were inhabited by nearly double the number of taxa (11.31 ± 3.78 compared to 6.38 ± 2.8) and more than double the number of individuals (53.63 ± 24.77 compared to 21.03 ± 12.55) as soft substrates. Diversity as measured by Shannon-Weiner index was significantly greater on hard substrata, while there was no significance in Simpson's diversity between textures (**Figure 4**). This suggests that diversity in the sense of species richness and evenness of those species was greater on hard habitats, there was little change in the dominance of relative taxa between the two.

Region and substrate texture appeared to have a greater role in determining benthic community composition along CA1 than depth while CA2 appeared to be more related to depth (**Figure 5**). The first two axes of the CA explained 45% of the observed variation (CA1 = 36% and CA2 = 9%). The Andersson Island and Duse Bay communities show greater variation along CA1 compared to the other regions. The majority of the CA1 scores for Andersson Island and Duse Bay were negative. Cape Obelisk, PGC South, and PGC Mid all had positive CA1 scores except for only a few samples (**Figure 5**). Substrate texture also appeared to be important along CA1 as the hard substrate scores were all positive, apart from four images, while the soft substrate sites were distributed along the entire CA1 axis. The variability in CA2 scores increased with increasing CA1 scores. The majority of CA2 scores for Cape Obelisk were positive except for a few samples. This was the opposite for PGC South and PGC Mid. There appeared to be some relationship between CA2 scores and depth, albeit weak. The majority of samples taken at 200 and 850 m had negative CA2 scores, while those sampled at 400 and 800 m had mainly positive CA2 scores.

Substrate cover, slope angle, and depth together accounted for 52% of variation observed in the CCA which was related to benthic community composition of the SUCS images (**Figure 6**). High variance inflation factors (>10) were observed for slope gradient, cobbles, and bedrock. The CCA sites scores indicated that gravel, boulders, and bedrock and slope were all positively related to the benthos at PGC South whilst negatively related to Duse Bay and PGC Mid. Mud was an important determinant for Duse Bay and Cape Obelisk benthic communities which were further separated by depth (**Figure 6A**). The CCA species scores revealed that suspension feeding holothurians and crinoids were

TABLE 3 | All taxa observed and identified from SUCS imagery and AGT, including relative proportion of total observation/catch.

Phyla	Taxa	SUCS		AGT	
		Total counted	% of total	Total counted	% of total
Annelida	Polychaeta	220	1.93	329	6.15
	Clitellata	0	0	2	0.04
Arthropoda	Decapoda	214	1.88	39	0.73
	Euphausiacea	0	0	3	0.06
	Amphipoda	170	1.49	83	1.55
	Isopoda	4	0.04	31	0.58
	Mysidacea	645	5.65	20	0.37
	Pycnogonida	1768	15.51	954	17.83
Brachiopoda	Brachiopoda	0	0	4	0.07
Bryozoa	Bryozoans	567	4.98	17	0.32
Cephalorhyncha	Cephalorhyncha	0	0	9	0.17
Chordata	Actinopterygii	50	0.44	8	0.15
	Ascidiacea	453	3.98	120	2.24
Cnidaria	Actiniaria	27	0.24	28	0.52
	Alcyonacea	544	4.77	25	0.47
	Pennatulacea	9	0.08	1	0.02
	Scleractinia	14	0.12	0	0
	Hydroidozoa	649	5.69	75	1.40
Echinodermata	Asteroidea	39	0.34	32	0.60
	Crinoidea	95	0.83	22	0.41
	Echinoidea	118	1.04	466	8.71
	Holothuroidea	161	1.41	236	4.41
	Ophiuroidea	4630	40.63	1850	34.57
Hemichordata	Hemichordata	0	0	500	9.34
Mollusca	Bivalvia	0	0	173	3.23
	Gastropoda	72	0.63	46	0.86
	Scaphopoda	53	0.47	33	0.62
	Cephalopoda	1	0.01	0	0
	Polyplacophora	0	0	5	0.09
Nemertea	Nemertea	0	0	20	0.37
Porifera	Porifera	379	3.33	94	1.76
Sipuncula	Sipuncula	0	0	5	0.09
Unidentified VME	Unidentified VME	514	4.51	121	2.26
Total		11396		5351	

strongly associated with an increase in slope gradient and hard substrates such as cobbles, boulders and gravel, while suspension feeding annelids, anthozoans, bryozoans, porifera, hydrozoans, and ascidians were more closely associated with bedrock (**Figure 6B**). Deposit feeding annelids, holothurians, and ophiuroids were associated with mud. Abundance varied significantly for 11 of the 18 identified higher classifications that were tested (**Table 4**). All 11 saw their peak in abundance within the PGC South region. For Anthozoa, Ascidiacea, Bryozoa, Echinoidea, Hydroidilina, Porifera, and Scaphopoda this was at 200 m, although for the latter this may not be meaningful as Scaphopoda are infaunal so will rarely be identified using SUCS imagery. Crinoidea and Holothuridea were highest in abundance at 500 m, while Pycnogonida were highest in abundance at 800 m. Pycnogonida were also characterized by a very patchy abundance, reaching their highest abundance at an average of 23.04 ± 8.99 per photo, while at most sites this remained below five. Crinoidea and Echinoidea were also patchy in abundance, being among the few groups to not occur at every site.

The SEM investigating the effects of depth, gradient and substrate on CA1 and CA2 score was found to represent the data well (Fisher C = 4.49, $p = 0.098$, df = 9). There was a significant indirect pathway between slope gradient and CA1 score, mediated through its direct influence on substrate cover (**Figure 7**; **Table 6**). The relationship between gradient and hard substrate cover was positive while the relationship between gradient and soft substrate cover was negative. Hard substrate cover had a positive influence on CA1 score, while soft cover

TABLE 4 | Mean number of individuals identified at each location in the Prince Gustav Channel.

Region	Duse Bay				PGC-S			PGC-M	Cape Obelisk			Anderson Island
Depth (m)	**200**	**300**	**400**	**500**	**200**	**500**	**800**	**850**	**400**	**500**	**800**	**500**
Taxa												
Actinopterygii	0.12 ± 1.19	0.08 ± 1	0.07 ± 0.09	0.03 ± 0.08	0.72 ± 1.1	0.65 ± 1.12	0.69 ± 1.29	0.07 ± 0.74	0.59 ± 0.99	0.2 ± 1.51	0.07 ± 0.33	0.2 ± 0.47
Amphipoda	0.52 ± 1.16	0.9 ± 1.14	0.43 ± 0.67	0.27 ± 0.44	1.31 ± 1.34	0.73 ± 1.03	0.2 ± 0.49	0.62 ± 0.81	0.3 ± 0.59	0.31 ± 0.59	0.2 ± 0.6	0.1 ± 0.21
Annelida	0.21 ± 0.55	0.33 ± 1.45	0.17 ± 0.45	0.07 ± 0.12	2.28 ± 3.41	1.67 ± 1.51	0.2 ± 0.49	0.55 ± 0.67	0.97 ± 0.98	0.48 ± 0.81	0.47 ± 1.15	0.13 ± 0.34
Anthozoa	**1.72 ± 1**	**0.17 ± 0.37**	**0.23 ± 0.5**	**0.27 ± 0.51**	**7.86 ± 7.56**	**3.93 ± 3.16**	**2 ± 3.61**	**1.38 ± 1.19**	**1.73 ± 1.05**	**1.24 ± 1.87**	**0.63 ± 1.25**	**0.37 ± 0.66**
Ascidiacea	**3.72 ± 7.65**	**0.77 ± 1.82**	**0.13 ± 0.43**	**0.6 ± 2.3**	**4.1 ± 5.38**	**1.8 ± 2.33**	**0.56 ± 1.3**	**1.14 ± 1.91**	**0.77 ± 1.26**	**0.59 ± 0.62**	**0.83 ± 1.95**	**0.33 ± 0.94**
Asteroidea	0.03 ± 0.18	0.07 ± 0.25	0.07 ± 0.25	0.03 ± 0.18	0.17 ± 0.32	0.2 ± 0.54	0.12 ± 0.32	0.17 ± 0.46	0.13 ± 0.34	0.17 ± 0.73	0.07 ± 0.25	0.07 ± 0.25
Bryozoa	**2.69 ± 3**	**1.47 ± 1.76**	**0.17 ± 0.45**	**0.23 ± 0.67**	**5.07 ± 4.25**	**4.7 ± 3.62**	**1.28 ± 2.66**	**1.59 ± 1.59**	**1.23 ± 2.03**	**0.59 ± 1.08**	**0.57 ± 1.87**	**0.5 ± 0.92**
Crinoidea	**0 ± 0**	**0 ± 0**	**0 ± 0**	**0 ± 0**	**0.59 ± 1.03**	**1.3 ± 1.39**	**0.08 ± 0.27**	**0 ± 0**	**0.67 ± 1.11**	**0.51 ± 0.72**	**0.03 ± 0.07**	**0 ± 0**
Decapoda	1 ± 1.46	1.47 ± 1.41	0.7 ± 0.94	0.73 ± 0.85	1.14 ± 0.34	0.5 ± 0.76	0.2 ± 0.4	0.27 ± 0.25	0.8 ± 0.83	0.83 ± 1.24	0.2 ± 0.4	0.57 ± 0.8
Echinoidea	**0 ± 0**	**0 ± 0**	**0 ± 0**	**0 ± 0**	**2.9 ± 3.94**	**0.4 ± 1.17**	**0 ± 0**	**0.38 ± 0.61**	**0.2 ± 0.4**	**0.03 ± 0.18**	**0 ± 0**	**0 ± 0**
Gastropoda	0.01 ± 0.12	0.03 ± 0.09	0.03 ± 0.18	0.01 ± 0.11	0.69 ± 1.39	0.9 ± 1.07	0.88 ± 1.18	0.03 ± 0.18	0.03 ± 0.1	0.04 ± 0.09	0.03 ± 1	0.07 ± 0.11
Holothuroidea	**0.24 ± 0.82**	**0.3 ± 0.64**	**0.1 ± 0.3**	**0.07 ± 0.25**	**0.52 ± 1.1**	**2.13 ± 3.39**	**0.52 ± 0.59**	**1.17 ± 1.26**	**0.43 ± 0.99**	**0.1 ± 0.3**	**0.23 ± 0.42**	**0.03 ± 0.17**
Hydroidilina	**1.09 ± 1.14**	**0.53 ± 0.88**	**0.7 ± 0.97**	**0.7 ± 1.13**	**7.34 ± 8.24**	**3.9 ± 3.13**	**2.12 ± 3.52**	**2.03 ± 1.38**	**1.17 ± 1.04**	**0.52 ± 0.67**	**0.7 ± 0.86**	**0.9 ± 1.19**
Mysida	0.93 ± 1.11	0.7 ± 0.86	2.4 ± 1.89	1.9 ± 1.76	2.69 ± 1.74	3.23 ± 2.25	0.72 ± 1.04	0.38 ± 0.72	1.5 ± 1.31	1.34 ± 1.11	3.2 ± 2.23	2.77 ± 1.41
Ophiuroidea	**15.28 ± 9.75**	**17.27 ± 8.84**	**7.17 ± 4.27**	**10.9 ± 9.23**	**11.62 ± 10.96**	**11.47 ± 5.44**	**30.56 ± 11.53**	**24.17 ± 8.86**	**9.73 ± 6.81**	**2.93 ± 2.48**	**8.13 ± 5.64**	**9.1 ± 3.76**
Porifera	**1.62 ± 2.96**	**0.43 ± 0.88**	**0.1 ± 0.4**	**0.13 ± 0.42**	**4.97 ± 4.84**	**1.97 ± 2.83**	**0.52 ± 1.14**	**1.55 ± 1.35**	**0.33 ± 0.6**	**0.55 ± 0.88**	**0.27 ± 0.63**	**0.3 ± 0.53**
Pycnogonida	**0.34 ± 0.6**	**0.5 ± 0.85**	**5.2 ± 1.3**	**0.77 ± 0.96**	**0 ± 0**	**15.53 ± 9.17**	**23.04 ± 8.99**	**1.72 ± 2.29**	**5.2 ± 3.38**	**2.66 ± 3.05**	**8.47 ± 4.89**	**2.57 ± 1.99**
Scaphopoda	**0 ± 0**	**0 ± 0**	**0 ± 0**	**0 ± 0**	**0.31 ± 0.59**	**0.67 ± 1.04**	**0.88 ± 0.77**	**0.07 ± 0.25**	**0 ± 0**	**0 ± 0**	**0 ± 0**	**0 ± 0**
VME	**10.24 ± 15.16**	**2.63 ± 3.57**	**1.47 ± 1.59**	**1.93 ± 3.86**	**33.17 ± 12.18**	**19.5 ± 12.8**	**8.24 ± 12.18**	**10.59 ± 4.06**	**7.67 ± 6.01**	**5.24 ± 4.43**	**3.8 ± 6.28**	**3.17 ± 3.32**
Overall	**29.07 ± 23.39**	**24.3 ± 8.3**	**13.93 ± 4.67**	**16.63 ± 10.95**	**56.38 ± 17.39**	**58.97 ± 17.39**	**65.32 ± 19.22**	**39.93 ± 9.66**	**27.53 ± 10.13**	**14.76 ± 6.04**	**25.07 ± 10.46**	**18.53 ± 5.52**

ANOVA was used to test differences among locations for each taxa with significant ($p < 0.05$) differences indicated in bold. Taxa with <30 individuals identified in total are not included. PGC, Prince Gustav Channel; S, South; M, Mid.

TABLE 5 | Estimated VME taxa wet weight over 1200 m^2 (kg) using mean weights determined for each taxa from AGT data per SUCS deployment site.

Region	Depth (m)	VME Taxa							
		Ascidacea	Bryozoa	Cidaroidea	Cnidaria	Porifera	Polychaeta, Serpulidae	Unidentified VME	Total
Duse Bay	200	20.35	12.65	0.50	11.91	106.86	0	0.53	152.84
Duse Bay	300	9.13	1.91	0	4.70	45.80	0	1.07	62.61
Duse Bay	400	1.66	0.59	0	25.50	15.27	0	2.14	25.50
Duse Bay	500	1.67	0.59	0	3.25	3.56	0	0	9.06
PGC-S	200	137.02	8.53	0	46	178.1	1.38	45.44	416.45
PGC-S	500	107.95	7.94	0	66.54	137.39	2.99	50.25	373.06
PGC-S	800	79.72	6.18	0	36.83	103.81	1.44	28.22	256.20
PGC-M	850	79.89	4.18	0	24.67	125.29	0	30.41	264.45
Cape Obelisk	400	15.78	5.44	0.54	33.29	14.25	1.49	50.23	108.74
Cape Obelisk	500	8.30	2.50	0.27	17.37	25.44	1.10	27.80	82.78
Cape Obelisk	800	7.89	0.74	0	5.25	8.65	1.70	1.60	25.82
Andersson Island	500	1.66	2.21	0	1.50	3.05	0	1.07	9.49

Red totals exceed CCAMLR's guidelines of 10 kg per 1200 m^2 longline haul, suggesting they should be classified as VME high risk areas. PGC, Prince Gustav Channel; S, South; M, Mid.

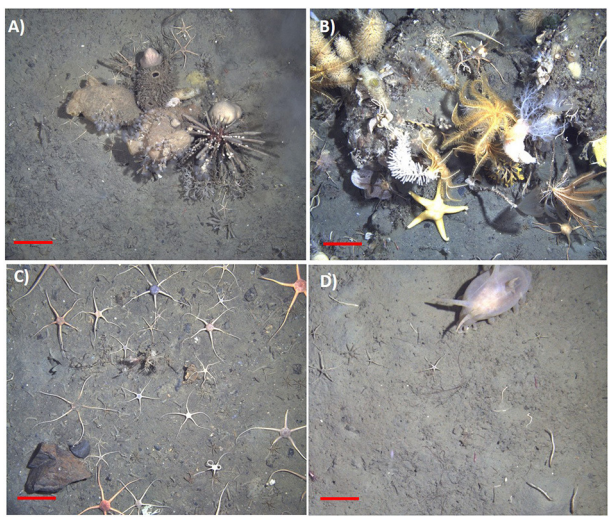

FIGURE 3 | Examples of *in-situ* SUCS images of common benthic communities and taxa. **(A)** Biogenic habitat forming taxa including poriferan species and the pencil spine urchin cidaroid, **(B)** species associated with hard substrata including crinoid species, and suspension feeding dendrochirotid holothurians, cnidarians, and annelids, **(C)** ophiuroid dominated community (cf. *Ophionotus victoriae*), and **(D)** deposit feeding holothurian *Protelpidia murrayi* in a mud dominated area. Scale bars represent 10 cm.

had a negative one. This suggests that the CA1 scores represent a gradient of soft to hard substrate that is influencing community structure, while depth does play a smaller yet still significant role. Contrary to what was expected, a significant direct association between seafloor gradient and CA2 score was found. This suggests seafloor gradient is influencing community structure via a different unmeasured variable. Depth had no association with abiotic substrate cover. Depth did have a positive direct influence on CA1 and a greater influence on CA2 but was negatively related to biogenic substrate cover. The cover of biogenic substrate had a direct negative influence on CA2. The CA2 scores likely represent a gradient of biogenic cover and depth. This suggests that some taxa are potentially physiologically depth limited, or an unmeasured variable is mediating this process. The SEM investigating the direct and indirect effects of slope gradient, depth, and substrate cover on VME biomass was a good fit for the data (Fisher C = 6.51, $P = 0.072$, df = 6). Seafloor gradient had a significant indirect effect on biomass, mediated through its influence on substrate cover (**Figure 8**; **Table 6**). Gradient had a negative relationship with soft substrate, while soft substrate had a negative relationship with biomass. The reverse was true of the relationship between gradient and hard substrate and between hard substrate and biomass. Cumulatively, seafloor gradient therefore has a strong, positive relationship with predicted biomass. Contrary to the predicted outcomes, depth had a direct, negative influence on biomass. This suggests that some VME taxa observed are either physiologically depth-limited or influenced by an unmeasured variable that is itself mediated by depth. It is also possible the full depth range within the channel has not been adequately sampled to properly identify depth trends.

DISCUSSION

Our work found that benthic faunal composition was heavily influenced by the substrate type available, with greater abundances and diversity associated with hard, rocky substrate. This was often associated with the physiology and functional group of different taxa. Depth and seafloor gradient had direct and indirect effects on community structure, often mediated through their influence on habitat forming organisms and substrate type. High numbers of VME taxa were identified, and VME biomass was strongly associated with hard substrate and shallower depths.

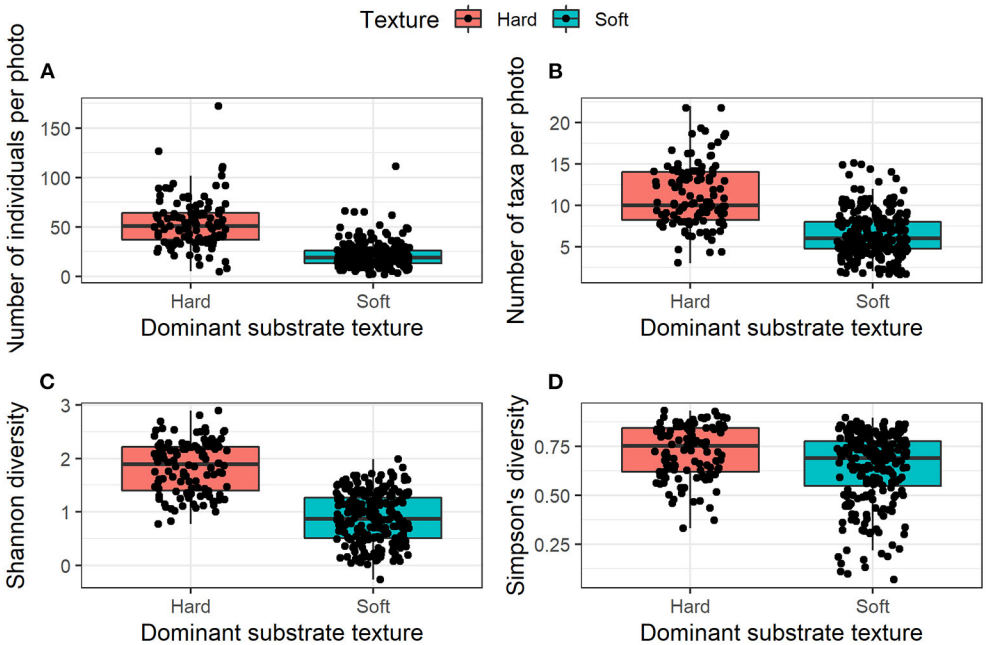

FIGURE 4 | Mean number of individuals and taxa present per SUCS image and mean diversity indices per photo according to substrate texture. **(A)** Mean number of individuals per image, **(B)** Mean number of taxa per image, **(C)** Mean diversity (Shannon-Weiner Index), and **(D)** Mean diversity (Simpson's Index).

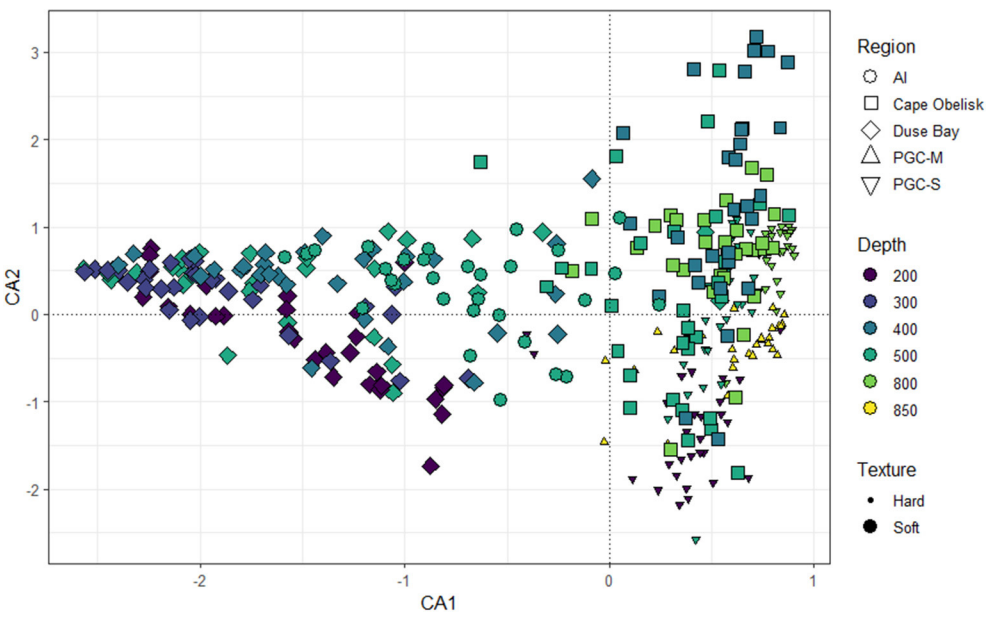

FIGURE 5 | Correspondence Analysis (CA) of benthic community structure according to region, depth, and substrate texture. CA1 and CA2 axis together explain 45% of observed variation.

Benthic Assemblages and Physical Variables

The influence of physical environmental variables such as substrate type, substrate texture, and depth have frequently been associated with the distribution and structure of benthic communities around the Antarctic continental shelf and slope. Substrate texture and type in particular have been found to play significant roles in structuring epifaunal communities in other regions around the Antarctic Peninsula, including the South Orkney Islands and King George Island (Quartino et al., 2001; Brasier et al., 2018). Similar results have been found in east Antarctica (Post et al., 2011) and in the Ross Sea, where

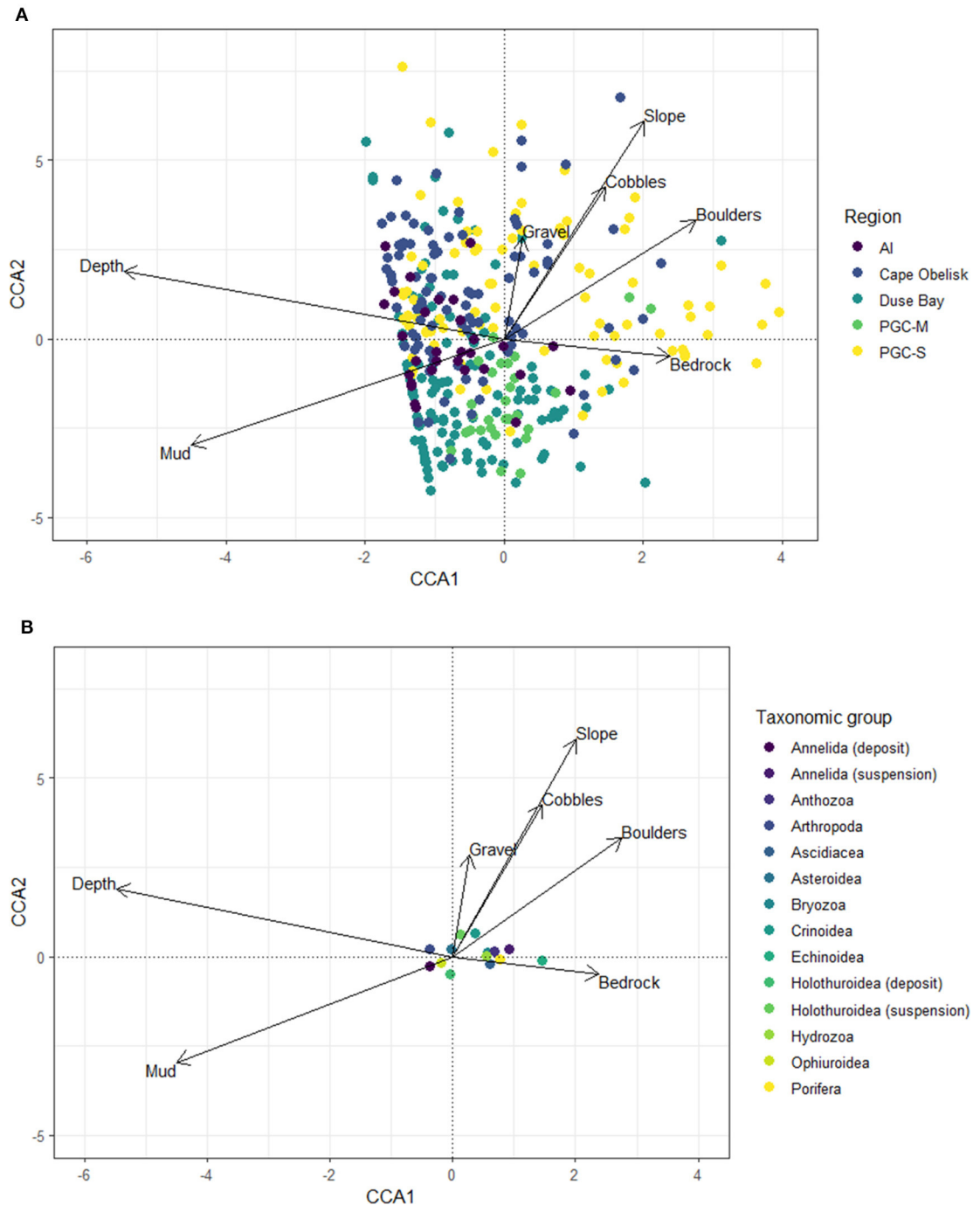

FIGURE 6 | Canonical Correspondence Analysis (CCA) of community assemblage and environmental variables including substrate cover, depth, and seafloor slope gradient. Organisms are grouped into higher taxonomic classifications and functional groups were necessary. **(A)** Site scores. **(B)** Taxon scores.

substrate type and composition explained 66% of the variation observed in shallow water macrofaunal communities (Cummings et al., 2006). Coarse substrates are preferential for most filter or suspension feeders, as it often provides hard surface for attachment and an elevated position which enhances the capture success rate of these functional groups (Muschenheim, 1987). Conversely, finer, siltier sediments provide a food resource for both facultative and obligate deposit feeders (Gutt, 1990). This is reflected in the PGC, where deposit feeding holothurians and annelids were strongly associated with muddy sediments. Although, it is likely that the diversity and abundance of these taxonomic groups will be underestimated because the analysis

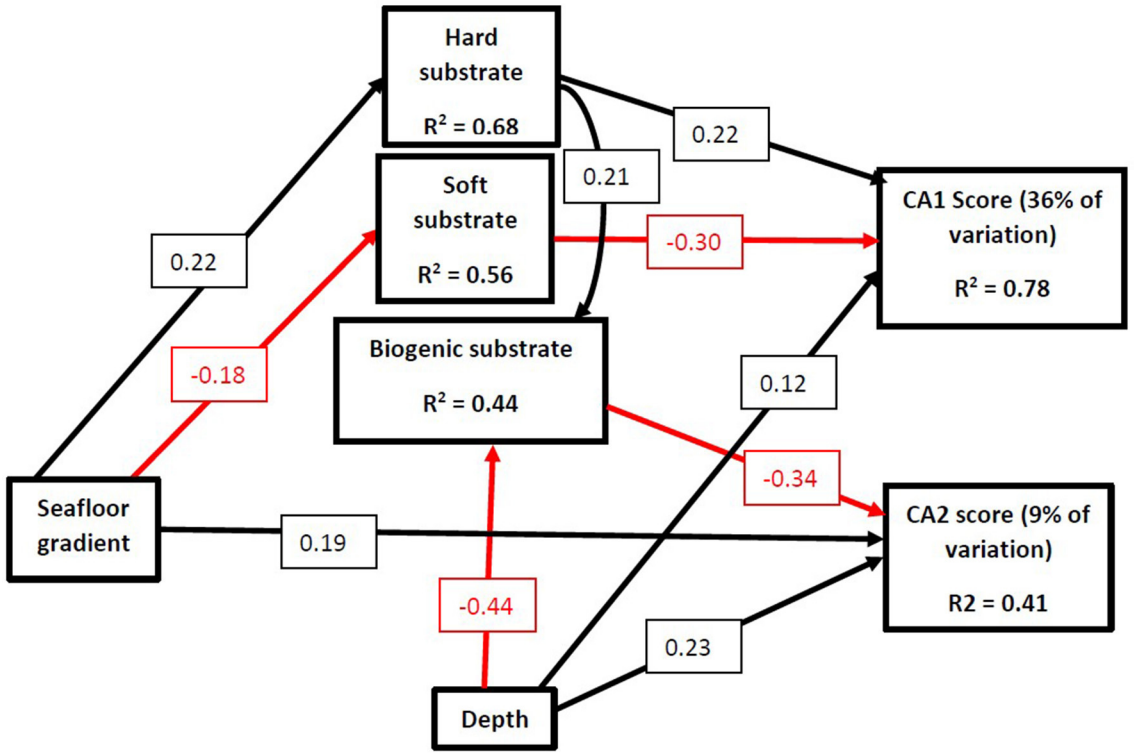

FIGURE 7 | Structural equational model (SEM) exploring the relationships between seafloor gradient, depth, substrate cover, and community structure as measured by CA1 and CA2 axis scores. Arrows represent unidirectional relationships among variables, with black arrows denoting positive relationships and red arrows depicting negative ones. Only significant pathways ($P \leq 0.05$) are displayed. The standardized regression coefficient is given in the associated box. R^2s for component models are given in the boxes of the response variable. Model incorporates random effect of Region. Hard substrate represents the combined cover of gravel, cobbles, pebbles, boulders, and bedrock. Soft substrate represents the combined cover of sand and mud.

is based on images of the benthic communities rather than a combination of infaunal and epifaunal sampling. Suspension feeders such as some cnidarians and crinoids were associated with rocky habitats. As in this present study, abundance, biomass, and taxonomic epifaunal diversity are often found to be greater in areas of coarse, hard substrates than in areas of finer sediments. This was the case in east Antarctica, where boulders and cobbles were associated with significant increases in faunal abundance (Post et al., 2017) and in deeper communities (c. 1000 m) in the Weddell Sea (Jones et al., 2007).

It has been suggested that differences in diversity could be related to the abundance of suspension feeding taxa that prefer hard substrates being highly diverse in Antarctic waters (Gutt and Starmans, 1998). The resolution of taxonomic data available from SUCS imagery prevents analysis of the exact number of epifaunal species present, but greater diversity amongst hard substrates of deep water corals has been found off the Antarctic Peninsula when identified to genus level (Roberts and Hirshfield, 2004). In the PGC, those areas dominated by harder substrates were also characterized by increased habitat heterogeneity. The higher diversity observed at these sites may therefore be a result of fauna characteristic of both coarse and fine sediment being able to occupy the same space, as more ecological niches and functional groups are provided for. The association of sessile invertebrates and hard substrates likely has a cumulative effect on the diversity of these assemblages. High diversity and abundance of taxa found on hard substrates is enhanced by the three-dimensional surface created by the organisms themselves, particularly Porifera, some anthozoans, and bryozoans, which form complex habitats for other invertebrates. This is reflected in the SEM which suggests biogenic cover played a significant role in determining overall community structure. Other studies have noted the positive correlations between overall abundance and diversity and the presence of ecosystem engineers such as large sponges, gorgonians, and bryozoans (Gutt and Shickan, 1998; Gutt and Starmans, 1998). It is also possible that limitations inherent in the SUCS imagery means biodiversity in soft sediment areas cannot be reliably estimated. Epifauna that periodically burrow and infauna will be underestimated or not observed using SUCS imagery. This may explain the observed underrepresentation of bivalves, hemichordates, echinoids, and holothurians in the SUCS data compared to the AGT data. Previous studies have noted higher than expected levels of diversity among infaunal communities in soft sediment areas, including in the South Shetland Islands and the Antarctic shelf in general (Gallardo, 1987; Lovell and Trego, 2003). It is possible that this may be the case in the PGC. However, this cannot be confirmed in the present study.

TABLE 6 | Summary of all direct pathways investigated using structural equation models and the hypothesis underpinning the expected relationship between predictor and response variables.

Predictor variable	Response variable	Hypothesis	Outcome	Standardized regression coefficient
Depth	Biogenic cover	Depth will have no direct significant impact on community structure (Dayton et al., 1982)	Increase in depth = decrease in cover of biogenic substrate	−0.44
	Hard substrate	Depth will have no direct significant impact on substrate cover	No direct significant pathway	-
	Soft substrate	Depth will have no direct significant impact on substrate cover	No direct significant pathway	-
	CA1 score	Depth will have no direct significant impact on community structure (Dayton et al., 1982)	Increase in depth = increase in CA1 score	0.12
	CA2 score	Depth will have no direct significant impact on community structure (Dayton et al., 1982)	Increase in depth = increase in CA2 score	0.23
	VME biomass	Depth will have no direct significant impact on community structure (Dayton et al., 1982)	Increase in depth = decrease in VME biomass	−0.43
Seafloor gradient	Biogenic cover	Seafloor gradient will have no direct significant impact on community structure	No direct significant pathway	-
	Hard substrate	Seafloor gradient will affect sedimentation rates, with lower gradients resulting in greater cover of soft, fine sediments (Post et al., 2020)	Increase in slope gradient = increase in rocky substrate cover	0.22
	Soft substrate	Seafloor gradient will affect sedimentation rates, with lower gradients resulting in greater cover of soft, fine sediments (Post et al., 2020)	Increase in slope gradient = decrease in mud cover	−0.18
	CA1 score	Seafloor gradient will have no direct significant impact on community structure	No direct significant pathway	-
	CA2 score	Seafloor gradient will have no direct significant impact on community structure	Increase in slope gradient = increase in CA2 score	0.19
	VME biomass	Seafloor gradient will have no direct significant impact on community structure, and therefore VME biomass	No direct significant pathway	-
Biogenic cover	CA1 score	Biogenic cover will significantly affect community structure due to the role of bioconstructors in creating additional habitat (Gutt and Starmans, 1998)	No direct significant pathway	-
	CA2 score	Biogenic cover will significantly affect community structure due to the role of bioconstructors in creating additional habitat (Gutt and Starmans, 1998)	Increase in cover of biogenic substrate = decrease in CA2 score	−0.34
Hard substrate	CA1 score	Substrate type will significantly affect community composition (Post et al., 2017)	Increase in rocky substrate cover = increase in CA1 score	0.22
	CA2 score	Substrate type will significantly affect community composition (Post et al., 2017)	No direct significant pathway	-
	Biogenic cover	Substrate type will significantly affect community composition (Post et al., 2017)	Increase in hard substrate cover = increase in biogenic cover	0.21
	VME biomass	An increase in rocky cover will result in greater VME biomass (Brasier et al., 2018)	Increase in rocky substrate cover = increase in VME biomass	0.3
Soft substrate	CA1 score	Substrate type will significantly affect community composition (Post et al., 2017)	Increase in mud cover = decrease in CA1 score	−0.3
	CA2 score	Substrate type will significantly affect community composition (Post et al., 2017)	No direct significant pathway	-
	VME biomass	An increase in mud cover will result in a decrease in VME biomass (Brasier et al., 2018)	Increase in mud cover = decrease in VME biomass	−0.61

Regression coefficients were standardized using scaling by standard deviation. CA1 and CA2 axis scores act as a proxy for community structure.

Community composition was influenced by depth and seafloor gradient in the PGC, albeit not as significantly as substrate type and often through indirect effects. Gutt and Starmans (1998) found that some variation in the benthos could be explained by a combination of these two factors. While several studies have highlighted the role of depth in determining benthic

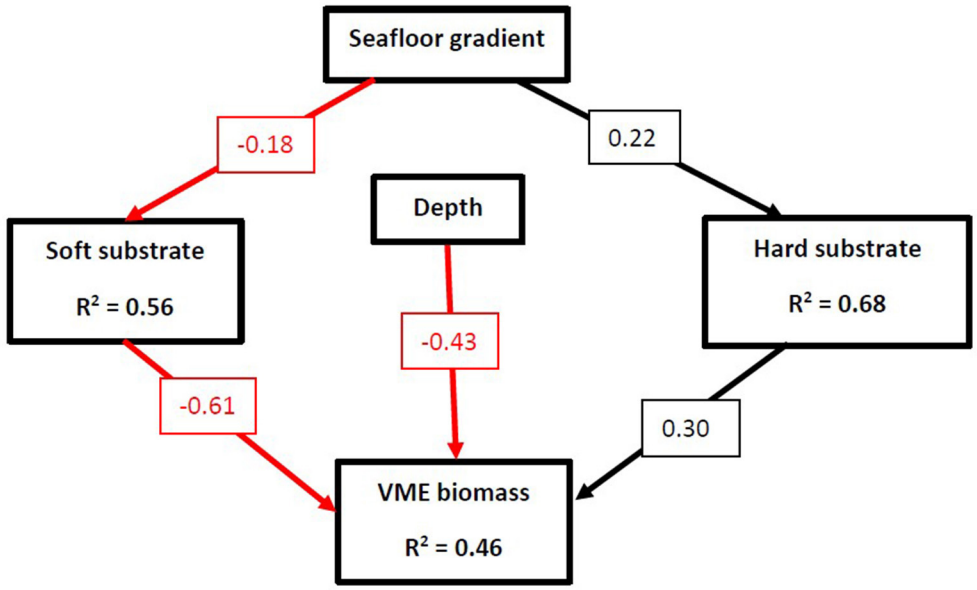

FIGURE 8 | Structural equational model (SEM) exploring the relationships between slope angle, depth, substrate cover, and estimated VME biomass. Arrows represent unidirectional relationships among variables, with black arrows denoting positive relationships and red arrows depicting negative ones. Only significant pathways ($P \leq 0.05$) are displayed. The standardized regression coefficient is given in the associated box. R^2s for component models are given in the boxes of the response variable. Model incorporates random effect of Region. Hard substrate represents the combined cover of gravel, cobbles, pebbles, boulders, and bedrock. Soft substrate represents the combined cover of sand and mud.

composition (Post et al., 2017; Neal et al., 2018), others suggest that the influence of depth is either non-existent or limited to indirectly effecting the benthos through its mediating impact on other physical variables (Brandt et al., 2007; Jones et al., 2007). After the mass-wasting of benthic communities caused during the Cenozoic glacial period, it is thought that the continental shelf was predominantly recolonised by deep-water organisms with wide bathymetric tolerances (Thatje et al., 2005). This legacy is still evident today, and as a result depth is typically regarded as less important in controlling species distributions than in many other areas (Dayton et al., 1982). Thus, any direct change in abundance and diversity with depth is likely related to a reduction in organic matter available to the benthos (Lampitt et al., 2001). The influence of seafloor gradient on the benthos has not been as thoroughly studied, although in this present study its influence was limited to its effect on substrate cover. Flatter gradients result in greater sedimentation accumulation and the dominance of fine sediments (Post et al., 2020), as evidenced in the present study through the high inflation factors between gradient and some hard substrates, which will in turn influence both the texture of the habitat and the accumulation of particulate matter available for deposit feeders.

The relative influence of physical environmental variables depends on the scale of investigation. Previous studies of the Antarctic shelf have highlighted the problems associated with using large-scale, regional patterns to predict benthic abundance and distribution. Variations in habitat and substrate on the local, often sub-meter, scale have significant impacts on overall diversity (Cummings et al., 2006; Post et al., 2017). Studies that consider variations in the small-scale also often result in stronger distinctions between assemblages than those that use larger geomorphic units (Douglass et al., 2014; Brasier et al., 2018). Gutt et al. (2012) argue that broad patterns in environmental variables can be used to explain variation at larger scales (>2 km), whereas fewer variables explain variation at finer scales. These variations are likely explained by non-measured variables as well as biological interactions and traits. The influence of small-scale heterogeneity in determining community composition, particularly in areas dominated by muddy sediments, is evident in this study. Dropstones in particular are a noted small-scale physical feature that act as important habitats and enhance diversity among sessile invertebrates in both the Antarctic and Arctic (Thrush et al., 2010). It has been suggested that dropstones act as important stepping stones for the dispersal and connectivity of communities that rely on hard substrates (Post et al., 2017), and given that most of the Antarctic shelf is dominated by muddy sediments (Smith et al., 2006), their potential importance for the overall biodiversity of a system cannot be underestimated. A higher level of connectivity between hard substrate-preferring taxa may also be reflected in the PGC data, evidenced by the high levels of similarity between the communities found at PGC South and Mid, especially when compared to the soft sites of Duse Bay and Cape Obelisk, which despite sharing similar sediment characteristics supported different communities. This suggests small scale heterogeneity is particularly important in muddy, soft sedimented habitats where local variation can greatly impact benthic abundance and diversity.

Changes in annual and seasonal sea ice cover must be considered when investigating benthic community structure. In the eastern Weddell Sea, benthic abundance, and biomass decreased by up to two thirds and composition shifted from suspension to deposit feeders as a result of sea ice increases between 1988 and 2014 (Pineda-Metz et al., 2020). In the present study, the communities found occupying all depths at Cape Obelisk were distinctly unique from the communities found elsewhere in the PGC. It is possible that the communities here are still experiencing the legacy of the Prince Gustav ice shelf, which permanently covered Cape Obelisk as recently as 1989 (Cooper, 1997). Fauna characteristic of a system that has undergone change from an oligotrophic sub-ice shelf ecosystem to a productive shelf ecosystem are often unique to these systems, and it has been suggested that some benthic communities can take 150–200 years to reach complete recolonization following exposure to the sea surface (Gutt et al., 2010). These fauna can vary from pioneer organisms such as demosponges and juvenile cnidaria to taxa more typical of advanced stages of recolonization such as sponges, compound ascidians, and unique bryozoans. While higher numbers of ascidians and porifera were found at Cape Obelisk compared to its muddy counterparts, resolution of the SUCS imagery and the lack of AGT data from this region prevents analysis down to species level.

The range and distribution patterns of different taxa are highly dependent on both life history and evolutionary history (Barnes and Griffiths, 2007; Convey et al., 2014). Some groups, such as pycnogonids, show a global hotspot of biodiversity within the Southern Ocean, and when examined on a regional scale have distinct local hotspots (Griffiths et al., 2011). This was observed at PGC South 800 m, where their abundance reached a significant peak. Polychaetes, similar to pycnogonids, are represented at higher than average levels in Antarctica (Barnes and Peck, 2008). At the South Shetlands Islands, polychaetes were found to compose up to 61% of the total macrobenthic abundance (Gutt and Starmans, 1998). Polychaetes were also among the predominating organisms at King George Island (Arnaud et al., 1986), and despite also being located around the Antarctic Peninsula, these patterns were not reflected in the PGC, where polychaete abundance remained relatively low throughout. However, this is reflective of the individuals observed on the seafloor and infaunal samples may provide a different perspective. Ophiuroids were the most dominant taxa found across all sites and among both substrate types. This has been observed around much of the Antarctic shelf. In east Antarctica, ophiuroids represent high proportions of overall observed taxa, sometimes up to 50% (Post et al., 2017), although the proportional abundance of ophiuroids is greater in this current study than in others that have occurred around the Peninsula (Grange and Smith, 2013; Brasier et al., 2018). This dominance is unsurprising, as ophiuroids, as well as other echinoderms such as echinoids, are generally considered ubiquitous in the Southern Ocean and can thrive across large depth ranges and on both hard and soft substrate (Thrush et al., 2006). Overall abundance per m^2 was greater in the PGC than in many similar studies around the Antarctic shelf and continental slope (**Table 7**), including the Antarctic Peninsula shelf and fjords (Sumida et al., 2008; Grange and Smith, 2013). Abundance was however lower than in the Weddell Sea shelf (Gutt and Starmans, 1998). It is likely that the full extent of benthic distribution and diversity cannot be assessed completely. More AGTs would be necessary so that the sample size is meaningful enough to carry out more robust analysis on the catch data. The SUCS also has some inherent limitations. The SUCS is a downward facing camera, meaning it can only land on flat surfaces. This prevents certain regions such as steep slopes, boulders, and canyons from being studied due to their topography. These habitats are often considered diversity hotspots (Robert et al., 2015; Fernandez-Arcaya et al., 2017), meaning these potentially diverse regions are difficult to sample.

VME Taxa

The relationship between benthic community composition and environmental characteristics is complex with many variables contributing to differences in community composition and the spatial structure of biodiversity (Convey et al., 2014). Given the current international effort to establish a representative system of MPAs in the Southern Ocean it is important to continue to investigate the relationship between both broad and local scale physical surrogates that could be used to infer high levels of biodiversity, VME locations, and potential MPA sites.

Abundances of VME taxa were greatest within the PGC South sites, and VME biomass was characterized by an increase association with rocky cover and a decrease with mud cover. This is unsurprising because of the high number of hard substrate-preferring suspension and filter feeders that are classified as VME taxa (CCAMLR, 2009b). VMEs have been found in lower abundances on soft sediment compared to hard elsewhere around the Antarctic Peninsula (Lockhart and Jones, 2008; Brasier et al., 2018). Depth had a negative influence on VME biomass, which is likely related to organic flux and food availability due to the functional nature of many VME taxa (Jansen et al., 2018). Slope gradient played an indirect role in influencing biomass, mediated through its effect on substrate cover. While the SEM presented in the present study may be useful in predicting biomass in specific regions, the overall impact of variables on VME taxa will likely be highly area specific (Parker and Bowden, 2010). More data are required on the relationship between seafloor gradient and VME taxa in order to check the validity of this model for other regions of the Antarctic shelf and continental slope.

VME Risk Area thresholds are projected to have been met in all sites with the exceptions of Andersson Island and Duse Bay 500 m. The projected wet weights over 1200 m^2 in the current study may have implications for the development of future conservation measures across the Antarctic Peninsula as a whole and the PGC in particular. Several previous studies have provided evidence of VME thresholds being met in the northwestern Antarctic Peninsula region (Lockhart and Jones, 2008; Parker and Bowden, 2010), which have led to the notification and designation of new VME Risk Areas by CCAMLR. As in the present study, VME biomass is often driven by porifera, and in some cases the wet weight of porifera alone has been enough to exceed thresholds and make areas high risk (Brasier et al., 2018). This threshold may therefore be severely biased toward "heavy"

TABLE 7 | Comparison of abundance and key taxa based on photographic studies at comparative depths on Antarctica's continental shelf.

Location	Depth range (m)	Abundance of macrofauna (m^2)	Most abundant taxa	References
East Antarctic Peninsula, Prince Gustav Channel	173–880	32.5	Ophiuroidea, Pycnogonida	Present study
South-eastern Weddell Sea, shelf	99–1243	46	Ophiuroidea, Bryozoa	Gutt and Starmans, 1998
North-eastern Weddell Sea, Fimbul Ice Shelf	245–510	2.6	Ophiuroidea, Polychaeta	Jones et al., 2007
Wilkes Land, Sabrina Coast	274–896	19.3	Ophiuroidea, Polychaeta	Post et al., 2017
Amundsen Sea, Beakley Glacier	171–561	0.38	Echinodermata, Anthozoa	Starmans et al., 1999
West Antarctic Peninsula, shelf	526–641	0.5	Holothuridea, Anthozoa	Sumida et al., 2008
West Antarctic Peninsula, fjords	436–725	26	Polychaeta, Amphipoda	Grange and Smith, 2013

Mean abundances of macrofauna are shown.

taxa, namely porifera, such that communities of lighter taxa stand little to no chance of meeting these criteria and being adequately protected. This concern is reflected in the present study, as the two sites that do not meet this threshold are also characterized by disproportionately lower porifera biomass. It is possible that VME abundance or diversity, rather than biomass, may be a better way to define this threshold for certain taxa.

CCAMLR defined its VME thresholds on the basis of using actual longline haul data rather than imagery. In previous studies seafloor imagery has provided direct evidence of the presence of VME taxa where there was insufficient or no actual catch data (Jones and Lockhart, 2011; Lockhart and Hocevar, 2018). In the present study, various VME taxa such as bryozoans, gorgonians, porifera, and hydrozoans were underrepresented in the AGT sample. Similar results were found in Brasier et al. (2018), who found an AGT hauled lower biomass and abundance than predicted by SUCS imagery within the South Orkney region. This does suggest that some of the present study sites may not contain enough biomass to exceed the threshold on longline hauling alone. Trawls and longlines are highly destructive compared to image-based types of analysis, and often are not needed, especially when sampling in recently disturbed or vulnerable areas (Bowden, 2005). A switch from longline bycatch based to camera-based evidence, and instead focusing on species richness, diversity or abundance, may both reduce damage to the habitat and reduce bias toward organisms with greater biomass. Additionally, all sites within the proposed Weddell Sea MPA (Teschke et al., 2016), that is, all sites south of 64°S, exceeded the projected 10 kg of VME taxa per 1200 m^2. This includes all SUCS deployments in PGC South and Cape Obelisk. This additional information on VME taxa in the region could be used to further support the case for a Weddell Sea MPA.

CONCLUSIONS

Benthic assemblages in the PGC were dominated across all regions by ophiuroids, regardless of depth or substrate texture. Abundance and diversity were greater on hard substrata, and the cover of rocky substrate played a significant role in increasing VME biomass. Overall average abundance of organisms across the PGC was greater than in many other studies on the Antarctic shelf, including other locations around the Antarctic Peninsula. The legacy of the Prince Gustav ice shelf may be still be reflected in the epibenthic community, although higher taxonomic resolution would be required to confirm this. Seafloor gradient and depth played significant roles in determining epibenthic community composition and VME biomass. Although more research and focused sampling of softer sediments is required to assess the infauna contribution to the regional diversity. It is likely that variables such as food availability, organic flux, and biological interactions are important in determining the structure of the benthic community, but these factors are beyond the scope of this present study. The PGC hosts large amounts of VME taxa, and further study of the region may be crucial in determining the future management strategy of not just the eastern Antarctic Peninsula region but potentially the wider Weddell Sea.

DATA AVAILABILITY STATEMENT

The datasets presented in this study can be found in online repositories. The images used in the analysis have been deposited with the UK Polar Data Centre (Linse et al., 2020).

ETHICS STATEMENT

Ethical review and approval was not required for the animal study because ethical approval for this study was undertaken through the Preliminary Environmental Assessment by British Antarctic Survey. No experimentation or animal husbandry was planned, which required ethical approval. The study was designed to collect invertebrate macrofauna not vertebrate animals or cephalopod. All fish ($n = 8$) were killed following appropriate guidelines.

AUTHOR CONTRIBUTIONS

PA, KL, and WR developed and designed the study. KL, MM, RW, SG, and WR collected the samples. PA, MM, KL, and HG identified habitats and the specimens to highest possible taxonomic level. HG provided environmental data and helped with the statistical analyses. SD provided bathymetry data and site maps. PA prepared the figures

and tables, performed the statistical analyses, and drafted the original manuscript which was critically revised and improved by KL, WR, HG, SG, SD, RW, and MM. All authors contributed to the article and approved the submitted version.

FUNDING

PA and WR are funded by Newcastle University. KL, HG, SG, and RW are part of the British Antarctic Survey Polar Science for Planet Earth Programme funded by The Natural Environment Research Council (NERC) [NC-Science]. The RSS *James Clark Ross* expedition JR17003a and participation of KL, WR, RW, MM, and SG were funded by the NERC urgency grant NE/R012296/1. MM was also funded by Museums Victoria.

ACKNOWLEDGMENTS

We are grateful to the master and crew of RRS *James Clark Ross*, and the AME staff at BAS for tremendous logistic and shipboard support during the fieldwork in the Southern Ocean. We thank our colleagues on board of JR17003a for their company during hours of SUCS deployments. The fieldwork in the western Weddell Sea during JR17003a was undertaken under the permit No. 43/2017 issued by the Foreign and Commonwealth Office, London to section 3 of the Antarctic Act 1994.

REFERENCES

Arnaud, P. M., Jazdzewski, K., Presler, P., and Sicinski, J. (1986). Preliminary survey of benthic invertebrates collected by Polish Antarctic Expeditions in Admiralty Bay (King George Island, South Shetland Islands, Antarctica). *Pol. Polar Res.* 7, 7–24.

Barnes, D. K. A., and Griffiths, H. J. (2007). Biodiversity and biogeography of southern temperate and polar bryozoans. *Global Ecol. Biogeogr.* 17, 84–99. doi: 10.1111/j.1466-8238.2007.00342.x

Barnes, D. K. A., and Peck, L. S. (2008). Vulnerability of Antarctic shelf biodiversity to predicted regional warming. *Clim. Res.* 37, 149–163. doi: 10.3354/cr00760

Bowden, D. A. (2005). Quantitative characterization of shallow marine benthic assemblages at Ryder Bay, Adelaide Island, Antarctica. *Mar. Biol.* 146, 1235–1249. doi: 10.1007/s00227-004-1526-0

Brandt, A., Gooday, A. J., Brandão, S. N., Brix, S., Brökeland, W., Cedhagen, T., et al. (2007). First insights into the biodiversity and biogeography of the Southern Ocean deep sea. *Nature* 447, 307–311. doi: 10.1038/nature05827

Brasier, M. J., Grant, S. M., Trathan, P. N., Allcock, L., Ashford, O., Blagbrough, H., et al. (2018). Benthic biodiversity in the South Orkney Islands Southern Shelf Marine Protected Area. *Biodiversity* 19, 5–19. doi: 10.1080/14888386.2018.1468821

CCAMLR (2009a). *Conservation Measure 22-07. Interim Measure for Bottom Fishing Activities Subject to Conservation Measure 22-06 Encountering Potential Vulnerable Marine Ecosystems in the Convention Areas. Schedule of Conservation Measure in Force 2017/18.* Hobart, TAS: CCAMLR.

CCAMLR (2009b). *CCAMLR VME Taxa Classification Guide Version 2009.* Hobart, TAS: CCAMLR.

Convey, P., Chown, S. L., Clarke, A., Barnes, D. K. A., Bokhorst, S., Cummings, V., et al. (2014). The spatial structure of Antarctic biodiversity. *Ecol. Monogr.* 84, 203–204. doi: 10.1890/12-2216.1

Cook, A. J., and Vaughan, D. G. (2010). Overview of areal changes of the ice shelves on the Antarctic Peninsula over the past 50 years. *Cryosphere* 4, 77–98. doi: 10.5194/tc-4-77-2010

Cooper, A. P. R. (1997). Historical observation of Prince Gustav ice shelf. *Polar Rec.* 33, 285–294. doi: 10.1017/S0032247400025389

Cummings, V., Thrush, S., Norkko, A., Andrew, N., Hewitt, J., Funnell, G., et al. (2006). Accounting for local scale variability in the benthos: implications for future assessments of latitudinal trends in the coastal Ross Sea. *Antarct. Sci.* 18, 633–644. doi: 10.1017/S0954102006000666

Dayton, P. K., Newman, W. A., and Oliver, J. (1982). The vertical zonation of the deep-sea Antarctic acorn barnacle, Bathylasma corolliforme (Hoek): experimental transplants from the shelf into shallow water. *J. Biogeogr.* 9, 95–109. doi: 10.2307/2844695

Douglass, L. L., Turner, J., Grantham, H. S., Kaiser, S., Constable, A., Nicoll, R., et al. (2014). A hierarchal classification of benthic biodiversity and assessment of protected areas in the Southern Ocean. *PLoS ONE* 7:e10551. doi: 10.1371/journal.pone.0100551

Dreutter, S., Dorschel, B., and Linse, K. (2020). Swath sonar bathymetry data of RRS JAMES CLARK ROSS during cruise JR17003a with links to multibeam raw data, EM122. *PANAGAEA*.

Fernandez-Arcaya, U., Ramirez-Llodra, E., Aguzzi, J., Allcock, A. L., Davies, J. S., Dissanayake, A., et al. (2017). Ecological role of submarine canyons and need for canyon conservation: a review. *Front. Mar. Sci.* 4:00005. doi: 10.3389/fmars.2017.00005

Gallardo, V. A. (1987). The sublittoral macrofaunal benthos of the Antarctic shelf. *Environ. Int.* 13, 71–81. doi: 10.1016/0160-4120(87)90045-6

Grange, L. J., and Smith, C. R. (2013). Megafaunal communities in rapidly warming fjords along the west Antarctic Peninsula: hotspots of abundance and beta diversity. *PLoS ONE* 8:e77917. doi: 10.1371/journal.pone.0077917

Griffiths, H. J. (2010). Antarctic marine biodiversity–what do we know about the distribution of life in the Southern Ocean? *PLoS ONE* 5:e11683. doi: 10.1371/journal.pone.0011683

Griffiths, H. J., Arango, C. P., Munilla, T., and Mcinnes, S. J. (2011). Biodiversity and biogeography of Southern Ocean pycnogonids. *Ecography* 34, 616–627. doi: 10.1111/j.1600-0587.2010.06612.x

Gutt, J. (1990). New Antarctic holothurians (Echinodermata)–II. *Four* species of the orders Aspidochirotida, Elasipodida, and Apodida. *Zool. Scr.* 19, 119–127. doi: 10.1111/j.1463-6409.1990.tb00244.x

Gutt, J., Barratt, I., Domack, E., d'Acoz, C. D., Dimmler, W., Gremare, A., et al. (2010). Biodiversity change after climate-induced ice-shelf collapse in the Antarctic. *Deep-Sea Res. Pt. II.* 58, 74–83. doi: 10.1016/j.dsr2.2010.05.024

Gutt, J., David, B., Isla, E., and Piepenburg, D. (2016). High environmental variability and steep biological gradients in the waters off the northern Antarctic Peninsula: Polarstern expedition PS81 (ANT-XXIX/3). *Polar Biol.* 39, 761–764. doi: 10.1007/s00300-016-1937-7

Gutt, J., Griffiths, H. J., and Jones, C. D. (2013). Circumpolar overview and spatial heterogeneity of Antarctic macrobenthic communities. *Mar. Biodivers.* 43, 481–487. doi: 10.1007/s12526-013-0152-9

Gutt, J., and Koltun, V. M. (1995). Sponges of the Lazarev and Weddell Sea, Antarctica: explanations for their patchy occurrence. *Antarct. Sci.* 19, 165–182. doi: 10.1017/S0954102007000247

Gutt, J., and Piepenburg, D. (2003). Scale-dependent impact on diversity of Antarctic benthos caused by groundings of icebergs. *Mar. Ecol. Prog. Ser.* 253, 77–83. doi: 10.3354/meps253077

Gutt, J., and Shickan, T. (1998). Epibiotic relationships in the Antarctic benthos. *Antarct. Sci.* 10, 398–405. doi: 10.1017/S0954102098000480

Gutt, J., Sirenko, B. I., Smirnov, I. S., and Arntz, W. E. (2004). How many macrozoobenthic species might inhabit the Antarctic shelf? *Antarct. Sci.* 16, 11–16. doi: 10.1017/S0954102004001750

Gutt, J., and Starmans, A. (1998). Structure and biodiversity of megabenthos in the Weddell and Lazarev Seas (Antarctica): ecological role of physical parameters and biological interactions. *Polar Biol.* 20, 229–247. doi: 10.1007/s003000050300

Gutt, J., Zurell, D., Bracegirdle, T. J., Cheung, W., Clark, M. S., Convey, P. et al. (2012). Correlative and dynamic species distribution modelling for ecological

predictions in the Antarctic: a cross-disciplinary concept. *Polar Res*. 31:11091. doi: 10.3402/polar.v31i0.11091

Jansen, J., Hill, N. A., Dunstan, P. K., McKinlay, J., Sumner, M. D., Post, A. L., et al. (2018). Abundance and richness of key Antarctic seafloor fauna correlates with modelled food availability. *Nat. Ecol. Evol.* 2, 71–80. doi: 10.1038/s41559-017-0392-3

Jones, C. D., and Lockhart, S. J. (2011). Detecting vulnerable marine ecosystems in the Southern Ocean using research trawls and underwater imagery. *Mar. Policy* 35, 732–736. doi: 10.1016/j.marpol.2011.02.004

Jones, D. O. B., Bett, B. J., and Tyler, P. A. (2007). Depth-related changes to density, diversity, and structure of benthic megafaunal assemblages in the Fimbul ice shelf region, Weddell Sea, Antarctica. *Polar Biol.* 20, 1579–1592. doi: 10.1007/s00300-007-0319-6

Kaiser, S., Barnes, D. K. A., Sands, C. J., and Brandt, A. (2009). Biodiversity of an unknown Antarctic Sea: assessing isopod richness and abundance in the first benthic survey of the Amundsen continental shelf. *Mar. Biodivers.* 39. 27–43. doi: 10.1007/s12526-009-0004-9

Lampitt, R. S., Bett, B. J., Kiriakoulakis, K., Popova, E. E., Ragueneau, O., and Vangriesheim, A. (2001). Material supply to the abyssal seafloor in the northeast Atlantic. *Prog. Oceanogr*. 50, 27–63. doi: 10.1016/S0079-6611(01)00047-7

Lefcheck, J. S. (2016). piecewiseSEM: piecewise structural equation modelling in R for ecology, evolution, and systematics. *Methods Ecol. Evol*. 7, 573–579. doi: 10.1111/2041-210X.12512

Linse, K., Grant, S., Whittle, R., Reid, W., McKenzie, M., Federwisch, L., et al. (2020). *Benthic seafloor images from Prince Gustav Channel and Duse Bay, Eastern Antarctic Peninsula, March 2018 (Version 1.0) [Data set]*. UK Polar Data Centre, Natural Environment Research Council, UK Research and Innovation. doi: 10.5285/48DCEF16-6719-45E5-A335-3A97F099E451

Lockhart, S., and Hocevar, J. (2018). "Evidence of vulnerable marine ecosystems documented via submarine in the Antarctic Sound and Gerlache Strait (Subarea 48.1)," in *CCAMLR WG-EMM-18/35* (Hobart, TAS).

Lockhart, S. J., and Jones, C. D. (2008). Biogeographic patterns of the benthic invertebrate megafauna on shelf areas within the Southern Ocean Atlantic sector. *CCAMLR Sci.* 15, 167–192.

Lovell, L. L., and Trego, K. D. (2003). The epibenthic megafaunal and benthic infaunal invertebrates of Port Foster, Deception Island (South Shetland Islands, Antarctica). *Deep-Sea Res. Pt. II*. 50, 1799–1819. doi: 10.1016/S0967-0645(03)00087-0

Muschenheim, D. K. (1987). The dynamics of near-bed seston flux and suspension-feeding benthos. *J. Mar. Res*. 45, 473–496. doi: 10.1357/002224087788401098

Neal, L., Linse, K., Brasier, M. J., Sherlock, E., and Glover, A. G. (2018). Comparative marine biodiversity and depth zonation in the Southern Ocean: evidence from a new large polychaete dataset from Scotia and Amundsen seas. *Mar. Biodivers*. 48, 581–601. doi: 10.1007/s12526-017-0735-y

Oksanen, J., Blanchet, F. G., Kindt, R., Legendre, P., O'Hara, R. B., Henry, M., et al. (2011). *vegan: Community Ecology Package. R Package Version 1.17–10*. Vienna: R Foundation for Statistical Computing.

Parker, S. J., and Bowden, D. A. (2010). Identifying taxonomic groups vulnerable to bottom longline fishing gear in the Ross Sea region. *CCAMLR Sci.* 17, 105–127.

Pineda-Metz, S. E. A., Gerdes, D., and Richter, C. (2020). Benthic fauna declined on a whitening Antarctic continental shelf. *Nat. Commun*. 11:2226. doi: 10.1038/s41467-020-16093-z

Post, A. L., Beaman, R. J., O'Brien, P. E., Eléaume, M., and Riddle, M. J. (2011). Community structure and benthic habitats across the George V Shelf, East Antarctica: trends through space and time. *Deep-Sea Res. Pt. II.* 58, 105–118. doi: 10.1016/j.dsr2.2010.05.020

Post, A. L., Lavoie, C., Domack, E. W., Leventer, A., Shevenell, A., and Fraser, A. D. (2017). Environmental drivers of benthic communities and habitat heterogeneity on an East Antarctic shelf. *Antarct. Sci.* 29, 17–32. doi: 10.1017/S0954102016000468

Post, A. L., Meuers, A. J. S., Fraser, A. D., Meiners, K. M., Ayers, J., Bindoff, N. L., et al. (2014). "Chapter 14. environmental setting." in *Biogeographic Atlas of the Southern Ocean*. Cambridge: Scientific Committee on Antarctic Research, 46–64.

Post, A. L., O'Brien, P. E., Edwards, S., Carroll, A. G., Malakoff, K., Armand, L. K., et al. (2020). Upper slope processes and seafloor ecosystems on the Sabrina continental slope, East Antarctica. *Mar. Geol.* 422:e106091. doi: 10.1016/j.margeo.2019.106091

Quartino, M. L., Klöser, H., Schloss, I. R., and Wiencke, C. (2001). Biomass and associations of benthic marine macroalgae from the inner Potter Cove (King George Island, Antarctica) related to depth and substrate. *Polar Biol.* 24, 349–355. doi: 10.1007/s003000000218

Robert, K., Jones, D. O. B., Tyler, P. A., Van Rooij, D., and Huvenne, V. A. I. (2015). Finding the hotspots within a biodiversity hotspot: fine-scale biological predictions within a submarine canyon using high-resolution acoustic mapping techniques. *Mar. Ecol.* 36, 1256–1276. doi: 10.1111/maec.12228

Roberts, S., and Hirshfield, M. (2004). Deep-sea corals: out of sight, but no longer out of mind. *Front. Ecol. Environ*. 2, 123–130. doi: 10.1890/1540-9295(2004)002[0123:DCOOSB]2.0.CO;2

Smith, C. R., Mincks, S., and DeMaster, D. J. (2006). A synthesis of bentho-pelagic coupling on the Antarctic shelf: food banks, ecosystem inertia, and global climate change. *Deep-Sea Res. Pt. II*. 53, 875–894. doi: 10.1016/j.dsr2.2006.02.001

Starmans, A., Gutt, J., and Arntz, W. E. (1999). Mega-epibenthic communities in Arctic and Antarctic shelf areas. *Mar. Biol.* 135, 269–280. doi: 10.1007/s002270050624

Sumida, P. Y. G., Bernardino, A. F., Stedall, V. P., Glover, A. G., and Smith, C. R. (2008). Temporal changes in benthic megafaunal abundance and composition across the West Antarctic Peninsula shekf: results from video surveys. *Deep-Sea Res. Pt. II*. 55, 2465–2477. doi: 10.1016/j.dsr2.2008.06.006

Teschke, K., Beaver, D., Bester, M., Bombosch, A., Bornemann, H., Brandt, A., et al. (2016). *Scientific Background Document in Support of the Development of a CCAMLR MPA in the Weddell Sea (Antarctica)–Version 2016–Part A: General Context of the Establishment of MPAs and Background Information on the Weddell Sea MPA Planning Area*. WG-EMM-16/01, CCAMLR.

Thatje, S., Hillenbrand, C. D., and Larter, R. (2005). On the origin of Antarctic marine benthic community structure. *Trends Ecol. Evol*. 20, 534–540. doi: 10.1016/j.tree.2005.07.010

Thrush, S., Dayton, P., Cattaneo-Vietti, R., Chiantore, M., Cummings, V., Andrew, N., et al. (2006). Broad-scale factors influencing the biodiversity of coastal benthic communities of the Ross Sea. *Deep-Sea Res. Pt. II*. 53, 959–971. doi: 10.1016/j.dsr2.2006.02.006

Thrush, S. F., Hewitt, J. E., Cummings, V. J., Norkko, A., and Chiantore, M. (2010). β-diversity and species accumulation in Antarctic coastal benthos: influence of habitat, distance, and productivity on ecological connectivity. *PLoS ONE* 5:e11899. doi: 10.1371/journal.pone.0011899

Tucker, M. (1991). *Sedimentary Petrology: An Introduction to the Origin of Sedimentary Rocks*. Oxford: Blackwell Sciences Ltd.

Washington, H. G. (1984). Diversity, biotic, and similarity indices: a review with special relevance to aquatic ecosystems. *Water Res*. 18, 653–694. doi: 10.1016/0043-1354(84)90164-7

Conflict of Interest: The authors declare that the research was conducted in the absence of any commercial or financial relationships that could be construed as a potential conflict of interest.

frontiers in Marine Science

ORIGINAL RESEARCH
published: 15 February 2021
doi: 10.3389/fmars.2021.642040

Breaking All the Rules: The First Recorded Hard Substrate Sessile Benthic Community Far Beneath an Antarctic Ice Shelf

Huw J. Griffiths[1], Paul Anker[1], Katrin Linse[1], Jamie Maxwell[1,2], Alexandra L. Post[3], Craig Stevens[4,5], Slawek Tulaczyk[6] and James A. Smith[1]*

[1] British Antarctic Survey, Cambridge, United Kingdom, [2] Ryan Institute, National University of Ireland Galway, Galway, Ireland, [3] Geoscience Australia, Canberra, ACT, Australia, [4] National Institute of Water and Atmospheric Research, Wellington, New Zealand, [5] Department of Physics, University of Auckland, Auckland, New Zealand, [6] Earth and Planetary Sciences, University of California, Santa Cruz, Santa Cruz, CA, United States

OPEN ACCESS

Edited by:
Christian Marcelo Ibáñez, Andres Bello University, Chile

Reviewed by:
Sebastian Rosenfeld, University of Magallanes, Chile
Javier Sellanes, Catholic University of the North, Chile

***Correspondence:**
Huw J. Griffiths
hjg@bas.ac.uk

Specialty section:
This article was submitted to Marine Evolutionary Biology, Biogeography and Species Diversity, a section of the journal Frontiers in Marine Science

Received: *15 December 2020*
Accepted: *18 January 2021*
Published: *15 February 2021*

Citation:
Griffiths HJ, Anker P, Linse K, Maxwell J, Post AL, Stevens C, Tulaczyk S and Smith JA (2021) Breaking All the Rules: The First Recorded Hard Substrate Sessile Benthic Community Far Beneath an Antarctic Ice Shelf. Front. Mar. Sci. 8:642040. doi: 10.3389/fmars.2021.642040

The seafloor beneath floating ice shelves accounts roughly a third of the Antarctic's 5 million km^2 of continental shelf. Prior to this study, our knowledge of these habitats and the life they support was restricted to what has been observed from eight boreholes drilled for geological and glaciological studies. The established theory of sub-ice shelf biogeography is that both functional and taxonomic diversities decrease along a nutrient gradient with distance from the ice shelf front, resulting in a depauperate fauna, dominated by mobile scavengers and predators toward the grounding line. Mobile macro-benthic life and mega-benthic life have been observed as far as 700 km under an ice shelf. New observations from two boreholes in the Filchner-Ronne Ice Shelf challenge the idea that sessile organisms reduce in prevalence the further under the ice you go. The discovery of an established community consisting of only sessile, probably filter feeding, organisms (sponges and other taxa) on a boulder 260 km from the ice front raises significant questions, especially when the local currents suggest that this community is somewhere between 625 km and 1500 km in the direction of water flow from the nearest region of photosynthesis. This new evidence requires us to rethink our ideas with regard to the diversity of community types found under ice shelves, the key factors which control their distribution and their vulnerability to environmental change and ice shelf collapse.

Keywords: dropstone, oligotrophic, borehole, sponge (Porifera), Filchner-Ronne Ice Shelf, Weddell Sea

INTRODUCTION

Antarctic continental shelf benthos is often dominated by large, sessile, filter feeding communities (Gutt et al., 2013). These have been shaped by millennia of cold and highly seasonal conditions driven by glacial cycles, annual sea ice formation and melt, and the impacts of iceberg scour. The huge flux of food coming from the plankton above, driven by the summer melt and continuous daylight, allow these communities to thrive and achieve very high levels of biomass (Griffiths, 2010).

TABLE 1 | Details of Antarctic Ice Shelf boreholes that have seafloor images, including those with living organisms.

Site	Year	Region	Latitude	Longitude	Depth (m)	Ice Thickness (m)	Water Column (m)	Distance from open water (km)	Substrate	Benthic Fauna	Pelagic/mobile Fauna	References
J9	1977	Ross	82°22.5′S	168°37.5′W	597	420	237	430	Clay/silt	Amphipods, isopod, fish	Mysid	Lipps et al., 1979; Bruchhausen et al., 1979
Jutulgryta	1991	Fimbulisen	71°18.6′S	0°17.2′E	–	11	391	140	Clean dropstones and muddy matrix	–	–	Østerhus and Orheim, 1994
AM01b	2003	Amery	69°25.86′S	71°26.77′E	775	479	361	100	Silt and sand	Sponges, hydroids, polychetes, bivalves, bryozoans, ascidians, polychetes, holothurians, echinoids, gastropod	Krill, amphipods, fish or squid	Riddle et al., 2007
AM03	2005	Amery	70°33.67′S	70°19.93′E	1254	722	617	200	Clay/silt	Holothurian or flabelligerid polychete, ophiuroid, echinoid, possible sponge	–	Post et al., 2014
AM04	2006	Amery	69°53.97′S	70°17.42′E	931	603	399	160	clay/silt	Polychetes, echinoid, sediment mounds	Medusa, krill, amphipods	Post et al., 2014
SCINI	2008	Ross	78°13.2′S	164°14.1′E	188	1.1–20	188	80	Fine sediment and dropstones	Polychete, ophiuroids, cerianthid anemones, octocoral, bryozoans, porifera, chordates, arthropods, mollusks	–	Kim, 2019
Site 1	2012	Langhovde Glacier	69°12.15′S	39°49.3′E	–	400	10 to 25	2.5	Silt and rocks	Large isopod c.f. *Glyptonotus antarcticus*, fish	krill	Sugiyama et al., 2014

(Continued)

TABLE 1 | Continued

Site	Year	Region	Latitude	Longitude	Depth (m)	Ice Thickness (m)	Water Column (m)	Distance from open water (km)	Substrate	Benthic Fauna	Pelagic/mobile Fauna	References
WGZ-1	2015	Ross	84°19.5′S	163°40′W	600	755	10	700	Glaciomarine diamicton	Amphipods, zoarcid and notothenioid fish	Medusoid and ctenophorid jellies	Kingslake et al., 2018
FSW1	2016	Filchner	80°26.12′S	44°25.88′W	1215	853	471	260	Rock on silt	Single glass sponge	–	New findings
FSW2	2016	Filchner	80°28.87′S	44°11.32′W	1233	872	472	260	Boulder and silt	Stalked sponge, non-stalked sponges, unidentified stalked taxa, filamentous taxa	–	New findings
FSE1	2016	Filchner	80°58.44′S	41°26.92′W	1306	891	528	305	Small clasts and fine sediment	–	–	New findings
FSE2	2016	Filchner	81°04.55′S	40°49.65′W	1142	387	442	320	Small clasts and fine sediment	–	Ctenophore	New findings
FNE1	2016	Filchner	78°33.85′S	38°05.25′W	1104	597	588	27	Small clasts and fine sediment	–	–	New findings
HWD2	2017	Ross	80°39.5′S	174°27.68′E	741	367.5	428	300	∼5-cm clasts and fine mud	Fish, ophiuroid, possible infauna burrows	Krill, ctenophore, chaetognath, amphipod	Stevens et al., 2020

FIGURE 1 | Antarctic ice shelf borehole locations with seafloor images. Details for each location can be found in **Table 1**. New records with life present from this study are marked with a star, boreholes where life was observed with a black circle and where no life was observed or reported with a white circle. R-FIS, Ronne-Filchner Ice Shelf; RIS, Ross Ice Shelf; AIS, Amery Ice Shelf.

This contrasts sharply with the areas beneath the floating ice shelves, which are hidden from daylight and often far from areas of primary productivity (Ingels et al., 2021).

Ice shelves cover roughly a third of the Antarctic's 5 million km^2 of continental shelf (Ingels et al., 2018). The Ronne-Filchner Ice Shelf, in the Weddell Sea, is the second largest Antarctic ice shelf, accounting for ∼28% of the total area under ice shelves, covering around 420,000 km2 of seabed. Further north on the East Antarctic Peninsula, the collapses of the Larsen A and Larsen B ice-shelves, in 1995 and 2002, and the recent high-profile calving of the giant iceberg, A-68, from Larsen C, have highlighted how little we know about the habitat beneath these floating ice shelves.

Our knowledge of the biological communities beneath these ice shelves is limited to sparse observations through boreholes and scientific expeditions that investigated the sites of Larsen A and B at least 5 years after their collapse (Ingels et al., 2021). Current theory suggests a gradient in abundance and community type exists under ice shelves with distance from open water. Sessile suspension-feeders are believed to be restricted to areas of inflow, close to the ice shelf front, with deposit-feeders and detritivores, feeding on ever more limited food, further under the ice shelf (Ingels et al., 2018).

These borehole records are the result of images captured as part of geological and glaciological sampling which happened to record images of the seafloor life beneath the ice shelves. To date, the furthest "inland" from the ice shelf front where life has been observed is 700 km from the Ross Ice Shelf front (**Table 1**). To put this in perspective that is over 64 times the depth of the Mariana Trench in distance from any known primary productivity. The WISSARD Program observed amphipods and fish at the seafloor and pelagic gelatinous organisms in the cavity beneath the Whillans Ice Stream (Kingslake et al., 2018), but there was no evidence of benthic organisms or for bioturbation in the sediment cores. Similarly, the Ross Ice Shelf Project (1977-78) used baited traps and cameras to observe mobile fauna such as numerous amphipods, two fish and an isopod; however, no live sessile organisms were recorded (Bruchhausen et al., 1979; Lipps et al., 1979). Sediment samples obtained from the borehole, ∼475 km from the Ross Ice Shelf front, also contained the dead remains of meiofaunal foraminifera, bivalves, gastropods, ostracods, and possible polychete tubes but did not find any living infauna. The 2017 Aotearoa New Zealand Ross Ice Shelf Program drilled a borehole in the middle of the ice shelf, some 300 km from the shelf front (Stevens et al., 2020). In addition to multiple pelagic organisms, they observed an ophiuroid, a benthic fish, and what appeared to be infaunal burrows.

Multiple boreholes have been drilled through the Amery Ice Shelf at varying distances from the ice front. In 2003, a downward facing camera system investigated a borehole (AM01b) 100 km from the ice shelf front (**Table 1** and **Figure 1**) and observed a diverse assemblage comparable with coastal, sea ice-dominated locations or deeper water communities (Riddle et al., 2007). Observed taxa were dominated by sessile suspension feeders such as bryozoans, ascidians, polychetes, hydroids, bivalves, and sponges, as well as mobile fauna such as echinoids, flabelligerid worms, holothurians, and gastropods (Riddle et al., 2007). A less diverse and more sparse community was found in 2005 by cameras in a borehole 200 km in from the Amery Ice Shelf front (AM03), recording mobile deposit feeders and evidence of potential suspension/filter feeders (Post et al., 2014). In 2006, a further borehole (AM04) revealed a surface-living benthic polychete, a heart urchin, and polychete tubes 160 km from the Amery Ice Shelf front (**Table 1**). All Amery Ice Shelf observations recorded evidence of krill and amphipods in the water column, with multiple observations of medusa at AM04. The overall distribution of life beneath the Amery appears to be strongly controlled by ocean circulation, with richer and more diverse taxa associated with nutrient-rich inflowing currents and more impoverished seafloor coinciding with nutrient-poor outflow (Post et al., 2014).

Other studies have sampled narrower ice shelves or regions nearer to the ice shelf front. The most diverse fauna recorded came from the Ross Sea, 80 km inland from the ice front (Kim, 2019). They observed eight different phyla and a high biomass of organisms. Observations from only 2.5 km landward of the Langhovde Glacier ice front yielded only a single large isopod crustacean and a fish (Sugiyama et al., 2014). Not all boreholes have resulted in observations of benthic organisms. An expedition to the Fimbul Ice Shelf in 1991 found a seafloor of mud

and dropstones, but no visible life, 140 km from the ice shelf front (Østerhus, 1994).

Whilst the studies beneath the Amery and Ross Ice Shelf have been transformative to our understanding of sub-ice-shelf ecosystems, the paucity of information from other ice shelves undoubtedly means we are missing vital information about the diversity and structure of sub-ice-shelf habitats. Such information is important for our understanding of how ice shelf collapse might affect these communities and our interpretation of ice shelf history from sediment records. Here we present the first observations of the sub-ice shelf fauna of the Filchner-Ronne Ice Shelf (FRIS) and discuss its significance in relation to previous records elsewhere.

MATERIALS AND METHODS

Access holes were drilled through the 387–890 m thick Filchner Ice Shelf (FIS) during the austral summer of 2015–2016 and 2016–2017 (**Figure 2**) using the British Antarctic Survey (BAS) hot water drill system (Makinson and Anker, 2014). Water column and seabed imagery was obtained using a GoPro HERO4

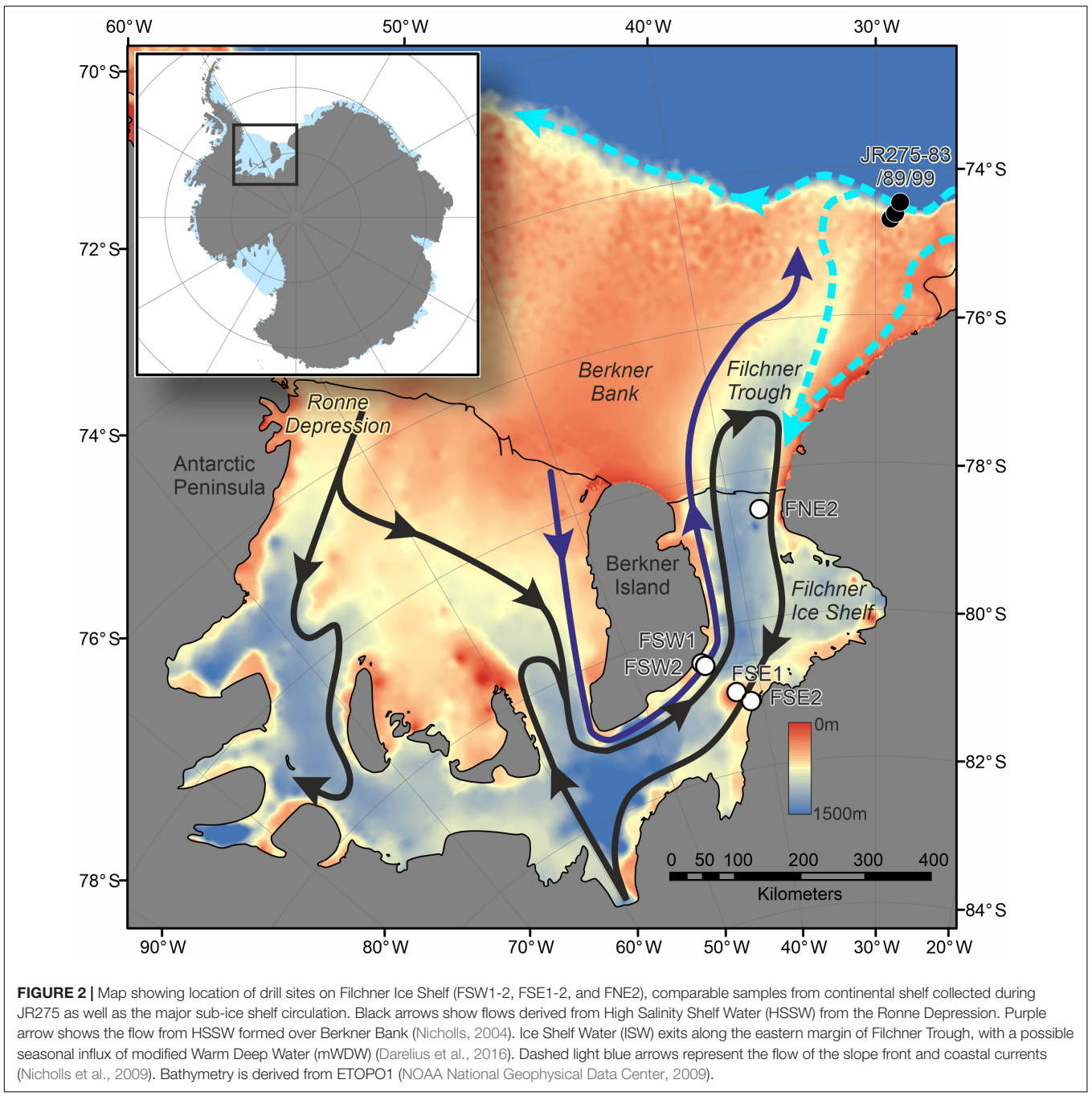

FIGURE 2 | Map showing location of drill sites on Filchner Ice Shelf (FSW1-2, FSE1-2, and FNE2), comparable samples from continental shelf collected during JR275 as well as the major sub-ice shelf circulation. Black arrows show flows derived from High Salinity Shelf Water (HSSW) from the Ronne Depression. Purple arrow shows the flow from HSSW formed over Berkner Bank (Nicholls, 2004). Ice Shelf Water (ISW) exits along the eastern margin of Filchner Trough, with a possible seasonal influx of modified Warm Deep Water (mWDW) (Darelius et al., 2016). Dashed light blue arrows represent the flow of the slope front and coastal currents (Nicholls et al., 2009). Bathymetry is derived from ETOPO1 (NOAA National Geophysical Data Center, 2009).

video camera, protected within an off-the-shelf pressure housing that was mounted above a BAS-modified UWITEC gravity corer. The GoPro recorded video at 30 frames per second, with a 1080 p resolution and a fixed ISO of 1600. Conductivity-temperature-depth (CTD) profiles were additionally obtained using a Seabird SBE49 with estimated accuracies of 0.004°C and 0.005, for temperature and salinity, respectively (Huhn et al., 2018).

Drill sites FSW1 and FSW2 (**Figures 1**, **2** and **Table 1**) are located on the western margin of FIS close to Berkner Island, 260 km from the ice shelf front, in a region where the ice shelf base is experiencing no significant melting or freezing (Makinson et al., 2011). Sites FSW1 and FSW2 are on the opposite side of the Filchner Trough, over 300 km from the ice shelf front. Drill site FNE2 was located on the northern end of the FIS in an area of inflow, only 27 km from the ice shelf front (**Figures 1**, **2** and **Table 1**).

The primary location of our observations is FSW2, where the ice shelf and water column are 872 and 472 m, respectively (**Figures 1**, **2** and **Table 1**). Despite multiple attempts to obtain a sediment core at FSW2, the corer hit a large sub-rounded boulder which is black/gray in color that was found to host a diverse benthic fauna (see **Supplementary Video**). Inspection of available video footage suggests that the boulder is mafic (gabbro?). Possible source regions include the Pensacola Mountains, which is part of an extensive Middle Jurassic igneous province related to and emplaced just prior to Gondwana break-up (Ford, 1976; Ferris et al., 1998). The Dufek Massif, for example, consists of well-layered pyroxene gabbro that contains abundant magnetite in higher levels that is visually similar to the boulder imaged here (Ford, 1976). We assume that the boulder has been transported by the ice shelf, eventually melting out at the drill site. In this context, a source in the Dufek Massif would make sense as the drill site lies directly downstream of this mountain range.

The hydrography of site FSW2 is dominated by inflow of cold High Salinity Shelf Water (HSSW; **Figure 1**) which forms along Berkner Bank or is re-circulated, originally entering the cavity via Ronne Depression (Ronne Trough) (Nicholls et al., 2009). The water column is characterized by two well-mixed zones, the upper 100 m below the ice shelf base and in the 250 m thick layer above the bottom (Huhn et al., 2018). Potential temperature (θ) close to the ice shelf base is cold (−2.49°C), although this is still warmer than the *in situ* freezing temperature at this depth. The bottom layer is warmer (−2.2°C) and more saline (34.61) (Huhn et al., 2018). Ice Shelf Water exits Filchner Trough along the eastern margin, which is also characterized by the re-circulation of HSSW and seasonal input of modified Warm Deep Water (**Figure 2**) (Darelius et al., 2016; Nachtsheim et al., 2019). Currents at FSW2 are likely to be strong with model estimates of up to 0.25 m s^{-1} (Daae et al., 2020) and carry with them a visible particulate load of silt-sized detritus. It is unclear if this is entirely terrigenous or whether it also includes a biogenic component.

The dimensions of the boulder and associated fauna were estimated by comparison with those of the corer which had a maximum radius of 11 cm and a height of 75 cm.

RESULTS

The boulder below FSW2 is located at a depth of 1,233 m and approximately 260 km from the modern calving margin of FIS (measured as a straight line through water). However, this is in the opposite direction of the main flow of HSSW (Nicholls, 2004). Following the two main sources of HSSW would put the boulder at > 1500 km from FIS front (following HSSW from the Ronne Depression) or > 625 km from Ronnie Ice Shelf front (following HSSW formed over Berkner Bank) (**Figure 2**).

The boulder itself is approximately 96 cm long by 69 cm wide and around 75 cm high. Fauna is largely concentrated on the sides of the boulder (**Figure 3**). The upper surface of the boulder seems to have a patchy coating of sediment of a similar color to the surrounding substrate The surrounding sediments show ripples formed by currents but there is no visible evidence of infauna or mobile epifauna.

The fauna associated with the boulder can be categorized into three main types of suspension feeders: a stalked sponge, non-stalked sponges, and unidentifiable stalked taxa (possible sponges, ascidians, hydroids, barnacles, cnidarian, or polychetes). It is also possible that the stalked sponge and/or stalked taxa might be carnivorous sponges, similar to Cladorhizidae. Only one confirmed stalked sponge (**Figure 3E**) was observed at a length of approximately 8.9 cm; 15 non-stalked sponges were observed around the edges of the boulder, the largest of which was 6.64 cm wide by 4 cm tall. Unidentifiable stalked taxa were the most numerous group, accounting for 58% of all observed individuals (22 individuals), the longest of which was estimated to be ∼6.6 cm long (**Table 2**). **Figure 3B** shows evidence of filamentous organisms of around 1 cm in length which could not be identified further but are possibly bacterial mats or hydroids. The upper surface of the boulder (**Figure 3F**) may also have a covering of filamentous organisms coated by the sediment layer but none of the images available had high enough resolution to investigate this.

A single, smaller rock with one non-stalked sponge on the surface was observed from under the nearby FSW1 borehole. No other benthic or pelagic life was seen, but the camera did not get as near to this rock as it did to the boulder in FSW2 so the images were not of comparable detail or scale. No benthic animals were observed on the seafloor at FNE2, FSE1 or FSE2. There was a single pelagic ctenophore observed in the borehole water at FSE2.

TABLE 2 | Counts of taxa observed on the boulder found at FSW2 (for location of transects refer to **Figure 3**).

Transect	Length (cm)	Stalked sponge	Non-stalked sponge	Unidentified stalked taxa	Filamentous organisms
A	40		4	1	
B	26			2	Many
C	10		3	1	
D	15		3	4	
E	28	1	5	14	
F	15				

The substrate was similar at each of these locations and consisted of fine-grained sediments and scattered pebble-sized clasts. From the video footage, the sediment, and bubbles from the corer at FNE2 are seen to be moved rapidly by a strong horizontal current.

DISCUSSION

Under ice shelf assemblages are generally believed to resemble the communities of the oligotrophic deep sea, subsisting on advected food particles (Ingels et al., 2018). The few previous examples of these communities from boreholes have all been from soft substrates or glacial sediments (Bruchhausen et al., 1979; Lipps et al., 1979; Riddle et al., 2007; Post et al., 2014; Sugiyama et al., 2014; Kingslake et al., 2018; Kim, 2019; Stevens et al., 2020). This is the first recorded observation of an *in situ* hard substrate sessile community beneath an ice shelf. The discovery of this suspension feeding community 260 km under a floating ice shelf in an area of outflow is remarkable in itself and goes against the existing paradigm (Ingels et al., 2018). Even though the prevailing current at FSW2 was strong, it was flowing in the wrong direction to connect the location directly to the nearest open water at the point of measurement (**Figure 2**). Instead, the currents suggest that this community is somewhere between 625 and 1500 km from the nearest region of photosynthesis. The effect of seasonality and pulses in the currents of the region (Darelius and Sallée, 2018) is unknown given that we do not yet know where the food comes from or how often they feed, but may significantly impact these communities, their feeding, and their recruitment.

Previous borehole records, excluding the new records from Filchner Ice Shelf (FSW1 and 2), show a general decrease in overall diversity and in the prevalence of sessile organisms with increasing distance from the ice shelf front (**Figure 4**). These data support the theory that in these oligotrophic environments mobile taxa are dominant (Ingels et al., 2018), with no sessile fauna previously observed from greater than 200 km under an ice shelf. The new findings from FSW1 and 2 go against this trend, with only sessile organisms present, but agree with the general trend of lower diversity at phylum level. The absence of any observed deposit feeding infauna or mobile epifauna on the sediments surrounding the boulder contrasts with existing theory (Ingels et al., 2018) and the dominance of these groups in the Amery and Ross Sea bore holes (Bruchhausen et al., 1979; Lipps et al., 1979; Riddle et al., 2007; Post et al., 2014; Kingslake et al., 2018; Kim, 2019; Stevens et al., 2020).

The abundance of organisms on the boulder is higher than would be expected so far from a source of primary production (Ingels et al., 2018) and is comparable with large dropstones in the seasonal sea ice regimes of the fjords of the West Antarctic Peninsula (Ziegler et al., 2017) or the Filchner Trough (~450 km north of the ice shelf front, see **Figure 2** and **Supplementary Figure 1**). However, the taxonomic and functional diversity is much lower than for the dropstones of the Peninsula (Ziegler et al., 2017) or the outer Filchner Trough (**Supplementary Figure 1**).

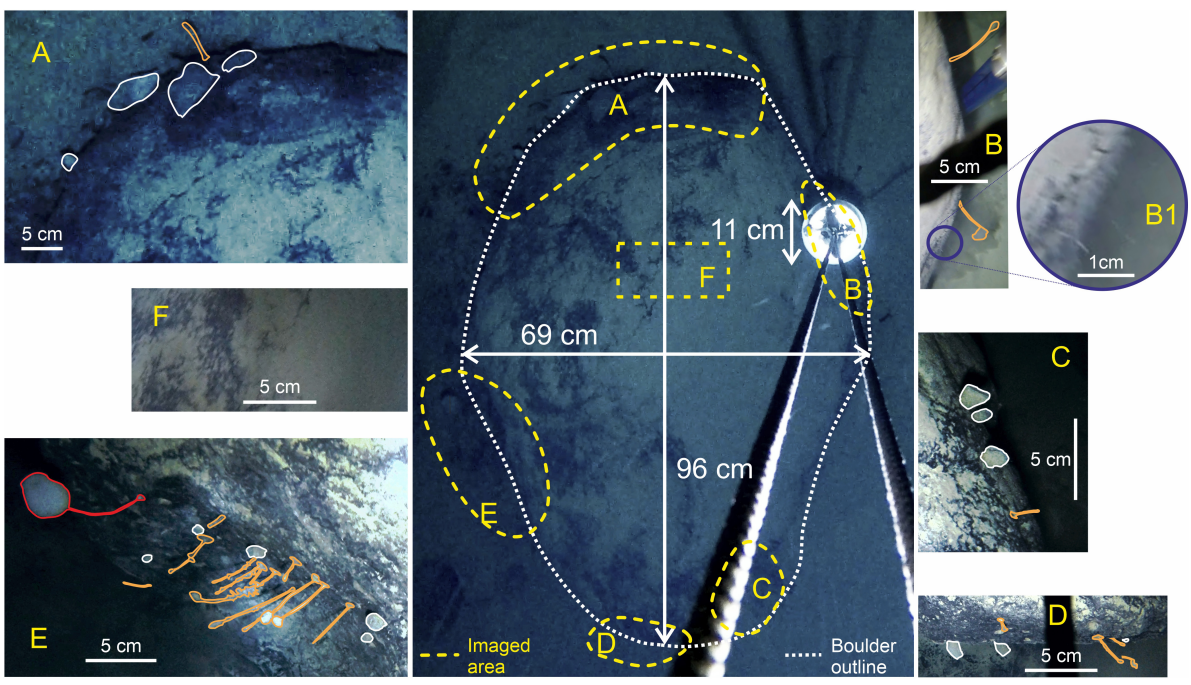

FIGURE 3 | Dimensions and close-ups of the boulder, highlighting where life is clearly visible **(A–E)** and the top of the boulder where no obvious life is visible **(F)**. The taxa visible on the boulder: Red, large stalked sponge; White, sponge; Orange, stalked taxa [possible sponge, ascidians, hydroid, barnacles, cnidaria (e.g., tubularia), and polychetes].

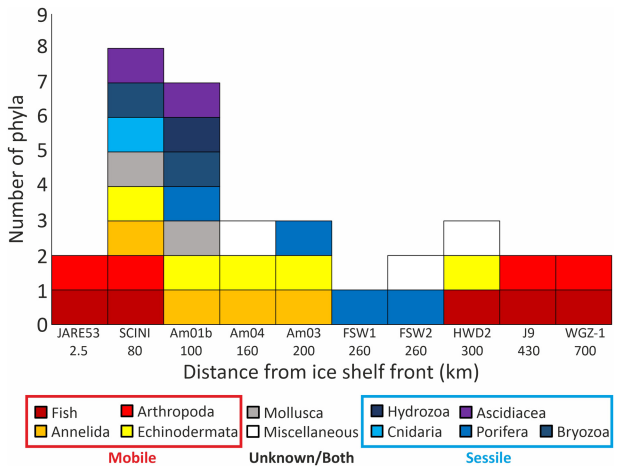

FIGURE 4 | Counts of phyla observed at each borehole with increasing distance from the ice shelf front, boreholes with no observed life are excluded. Miscellaneous, unidentifiable living organisms or evidence of infaunal activity.

The existence of this sessile and probable suspension feeding community so far under the ice shelf raises many ecological questions that cannot be fully answered given our current state of knowledge:

What Species Are Present and Are They Endemic to This Environment?

While it is reasonable to assume that many of the organisms visible are sponges, it is impossible to tell if they are glass sponges, demosponges, or calcareous. Antarctica has high percentages of endemic species from all groups of sponges (Downey et al., 2012), and species level identification would require physical specimens and genetic material. The uncertainty around the identity the other stalked and filamentous taxa lies in the lack of detail obtainable from the video. However, they are sessile and have not been observed at any other previous borehole locations. Given the inherent complexity of obtaining physical samples (except for mobile fauna caught in baited traps) future studies could use environmental DNA (eDNA) techniques on water and sediment samples to identify taxa. The origin of these communities is unknown and the advection of larvae might well play a role, it is also possible that given the huge physical extent of these regions that a specialist endemic fauna, similar in function to that of the oligotrophic deep sea, may have evolved *in situ*.

How Old Is This Community?

The time frame for survival of this community is unlikely to be limited by biology, assuming a sufficient food supply, with some living sponges estimated to be thousands of years old (Folkers and Rombouts, 2020). However, exposed dropstones are ephemeral in nature, especially in regions of high sedimentation. FSW2 is in a region of strong currents and no significant melt, meaning low sedimentation compared with regions nearer the grounding line or with slower currents. This could mean that the boulder would remain exposed for a long time, as evidenced by the very thin and patchy layer of sediment on the surface with areas of exposed rock, especially on the left-hand side of the image (**Figure 3**). If this is indeed an endemic and specialized community, for long-term survival it could "island hop" between dropstones, like hydrothermal vent communities between active vents (Tyler and Young, 2003) or between whale falls (Smith et al., 2017). It could also be continuously recruited from a more stable hard substrate region upstream, such as the flanks of Berkner Island or sheltered parts of the edge of the continent.

How Often Does the Community Feed and What Is the Source of Its Food?

Although these organisms observed on the boulder at FSW2 were all sessile, without physical specimens it is impossible to know their true mode of nutrition. At least some of these animals might be carnivorous sponges. Southern Ocean species represent ∼20% of all known carnivorous sponges and they are often found in oligotrophic bathyal regions or on isolated seamounts (Goodwin et al., 2017). Chemosynthesis is believed to play a role in some sub-ice shelf trophic pathways. Methane and hydrogen sulfide associated with cold seeps are suggested as a source of energy beneath the former Larsen B Ice Shelf (Domack et al., 2005), although no typically chemotrophic organisms have been observed through any of the boreholes to date. Nutrients and organic matter can also come from beneath the grounded ice sheet with subglacial water discharge (Gerringa et al., 2012; Death et al., 2014; Vick-Majors et al., 2020) or from sediment melting out of basal ice (Neuhaus et al., 2020).

How Common Are These Hard Substrate Sub-Ice Shelf Communities?

Given that this is the first hard sub-ice shelf substrate habitat observed, we have no estimate for the density, distribution, longevity, or size range of sub-ice shelf dropstones and boulders. Such a census would require the use of autonomous technology with downward facing sensors surveying the under-ice shelf environment. Large boulders, ca. 1 m in diameter and larger, were found to account for about 0.1 volume% of Alpine glacial till (Felletti and Pietro Beretta, 2009). This likely represents an overestimate for glaciomarine sub-ice-shelf sediments in Antarctica which can be reasonably expected to be more fine-grained than Alpine glacial till. But it does suggest that large boulders can be spaced at the bottom of sub-ice shelf cavities at intervals as short as 1 km, or greater.

This study shows that there are regions where suitably stable hard substrate (suited for sessile fauna) coincides with currents that are sufficiently powerful to advect food from open waters. However, in other localities, such as FNE2, that are far closer (27 km) to the ice shelf front and experience significant currents showed no sign of life at all. To really understand sub-ice shelf communities, we need to combine information on both suitable oceanography and substrate. Other locations might provide one of these factors but not the other. The grounding line, for instance, may have a higher number of rocks, but may provide a poor food source or a higher sedimentation rate, burying the rocks more rapidly. These results demonstrate the potential

for finding other similar communities elsewhere under large Antarctic ice shelves. We cannot currently pinpoint the exact location of similar habitats, future high-resolution modeling of sub-ice shelf oceanography and topography will enable us to target further investigation.

In the case of WGZ-1 (Kingslake et al., 2018), being very close to the grounding line the factor that might prevent sessile fauna from becoming established is the rainout of debris from the melting ice base. Sediment deposition rates may be as high as a few centimeters per year. The water column is also heavily loaded with suspended fine sediment which would inhibit filter feeding organisms which tend to favor regions of low inorganic turbidity (Turner, 2009). Near to grounding lines, these factors may be as important as the distance from the open ocean, if not more so. This is supported by the fact that mobile predators, scavengers, and detritivores (amphipods and fish) were observed 700 km from the ice front, suggesting that the absence of sessile macroscopic benthic may not be from a lack of food but potentially because of the high sediment flux. The sedimentary material raining out of the ice base does contain organic matter (at a level of per mils by weight), and there may be organic material coming from beneath the ice sheet (Vick-Majors et al., 2020).

How Does the Existence of This Community Inform Our Knowledge of the Physical Environment and Regime Under the Ronne-Filchner Ice Shelf and Other Ice Shelves?

Our findings also suggest that sub-ice shelf oceanographic conditions that are capable of providing a food source may be more widespread than previously thought. The presence of a sessile community 260 km from the ice shelf front supports the possibility that diatoms or other advected organic material are traveling far beneath the ice shelf. This has major implications for the study of glaciology and Antarctic marine geology, as the presence and composition of these marine microfossils in the sedimentary record have traditionally been used to determine presence/absence of paleo-ice shelves, as well as the proximity to the open-ocean (Smith et al., 2019).

What Would Become of These Communities in the Event of Ice Shelf Collapse?

These findings may be evidence of an Antarctic sub-ice shelf hard substrate benthic community that is well adapted to a low food supply, which makes it particularly vulnerable to the effects of ice shelf collapse and associated changes in productivity regimes. However, if this community turns out to be a restricted subset of the more general Weddell Sea hard substrate community, then it would be logical to assume that ice shelf loss would allow the community to thrive and succession would result in a community resembling that of the sea ice zone (**Supplementary Figure 1**). In the smaller Larsen A and B regions, the shift to more open water conditions with high local primary productivity was rapid (Ingels et al., 2018). The Larsen A and B communities are believed to be derived from the nearby shelf communities restricted by limited food availability. This is also reflected in many of the boreholes, with mobile fish, echinoderms, and arthropods, recognizable from the sea ice zone, being the only fauna observed on soft or glacial sediments (Bruchhausen et al., 1979; Kingslake et al., 2018; Stevens et al., 2020).

The first observation of a hard substrate community far under an ice shelf demonstrates that dropstones and boulders must play a similarly significant role in these regions as they do in the rest of the Southern Ocean acting as islands of hard substrate in a sea of mud (Ziegler et al., 2017). The biological and physical attributes that allow this community to survive, despite our current theories, suggest that these communities are either better connected to the outside world than we can currently explain or that the organisms themselves represent highly specialized extreme oligotrophic adaptation.

Given that our combined knowledge of *in situ* under ice shelf habitats (more than 1.5 million km^2) is drawn from 10 discrete observations covering a total area comparable to that of a tennis court, it should not come as a surprise that we are still discovering previously unseen types of sub-ice shelf communities far from open water. These findings raise more questions than they answer, highlighting the need for a concerted international effort to systematically observe, sample, and quantify these communities; their wider role in the Southern Ocean; and their physiological adaptations to this extreme environment. These observations challenge our understanding of what types of organisms can survive so far from daylight and have wider implications with regard to the evolution of the first complex organisms on earth, in particular through the "snowball earth" period, astrobiology, and the survival of polar organisms during more recent glacial maxima.

DATA AVAILABILITY STATEMENT

The original contributions presented in the study are included in the article/**Supplementary Material**, further inquiries can be directed to the corresponding author/s.

AUTHOR CONTRIBUTIONS

JS and PA collected the seabed imagery in Antarctica. HG analyzed the images and compared with other studies. CS and ST provided images and data for comparison. HG wrote the manuscript with contributions from JS, PA, KL, AP, JM, CS, and ST. All authors have contributed to previous versions and approved the final, submitted version.

FUNDING

HG, PA, KL, and JS are part of the British Antarctic Survey's Polar Science for Planet Earth Program (NC-Science). Images from Filchner were obtained using the UK Natural Environment Research Council grant number NE/L013770/1, Ice shelves in

a warming world: Filchner Ice Shelf system, Antarctica. JM is funded by the Irish Research Council GOIPG/2019/4020. AP is funded by Geoscience Australia. CS is funded by the New Zealand Antarctic Research Institute Ross Ice Shelf Program and the New Zealand Antarctic Science Platform (ASP). ST was funded by NSF-OPP award 0838947 as part of the Whillans Ice Stream Subglacial Access Drilling (WISSARD) project supported by the ANDRILL drilling team at the University of Nebraska, Lincoln, and by logistics provided by the United States Antarctic Program.

ACKNOWLEDGMENTS

The fieldwork on the Filchner Ice Shelf in 2015–2016 was undertaken under the permit 45/2015 issued by the Foreign and Commonwealth Office, London, to section 3 of the Antarctic Act 1994. We would like to thank everyone at the Alfred Wegener Institute (AWI) and the British Antarctic Survey (BAS) who supported the FISP and FISS drilling campaigns 2015/2016 and 2016/2017 by logistics and funding. The 2017 Ross Ice Shelf borehole was made possible by Antarctica New Zealand and the Victoria of University of Wellington Antarctic Research Centre.

SUPPLEMENTARY MATERIAL

The Supplementary Material for this article can be found online at: https://www.frontiersin.org/articles/10.3389/fmars.2021.642040/full#supplementary-material

Supplementary Figure 1 | Comparable images of JR275 from open water (seasonal sea ice) sites for comparison with the fauna observed on the boulder.

Supplementary Video | Video taken at the seafloor beneath borehole FSW2 in the Weddell Sea beneath the Ronne-Filchner Ice Shelf. Visible in the video are multiple sessile organisms attached to a large boulder.

REFERENCES

Bruchhausen, P. M., Raymond, J. A., Jacobs, S. S., Devries, A. L., Thorndike, E. M., and Dewitt, H. H. (1979). Fish, crustaceans, and the sea floor under the ross ice shelf. *Science* 203, 449–451. doi: 10.1126/science.203.4379.449

Daae, K., Hattermann, T., Darelius, E., Mueller, R. D., Naughten, K. A., Timmermann, R., et al. (2020). Necessary conditions for warm inflow toward the Filchner Ice Shelf, Weddell Sea. *Geophy. Res. Lett*. 47, 1–11. doi: 10.1029/2020gl089237

Darelius, E., Fer, I., and Nicholls, K. W. (2016). Observed vulnerability of Filchner-Ronne Ice Shelf to wind-driven inflow of warm deep water. *Nat. Commun*. 7:12300.

Darelius, E., and Sallée, J. B. (2018). Seasonal outflow of ice shelf water across the front of the Filchner Ice Shelf, Weddell Sea, Antarctica. *Geophys. Res. Lett*. 45, 3577–3585. doi: 10.1002/2017gl076320

Death, R., Wadham, J. L., Monteiro, F., Le Brocq, A. M., Tranter, M., Ridgwell, A., et al. (2014). Antarctic ice sheet fertilises the Southern Ocean. *Biogeosciences* 11, 2635–2643. doi: 10.5194/bg-11-2635-2014

Domack, E., Ishman, S., Leventer, A., Sylva, S., Willmott, V., and Huber, B. (2005). A chemotrophic ecosystem found beneath Antarctic Ice Shelf. *EOS Transact. Am. Geophys. Union* 86:269. doi: 10.1029/2005eo290001

Downey, R. V., Griffiths, H. J., Linse, K., and Janussen, D. (2012). Diversity and distribution patterns in high southern latitude sponges. *PLoS One* 7:e41672. doi: 10.1371/journal.pone.0041672

Felletti, F., and Pietro Beretta, G. (2009). Expectation of boulder frequency when tunneling in glacial till: a statistical approach based on transition probability. *Eng. Geol.* 108, 43–53. doi: 10.1016/j.enggeo.2009.06.006

Ferris, J., Johnson, A., and Storey, B. (1998). Form and extent of the Dufek intrusion, Antarctica, from newly compiled aeromagnetic data. *Earth Planet Sci. Lett*. 154, 185–202. doi: 10.1016/s0012-821x(97)00165-9

Folkers, M., and Rombouts, T. (2020). *Sponges Revealed: A Synthesis of Their Overlooked Ecological Functions Within Aquatic Ecosystems. YOUMARES 9 – The Oceans: Our Research, Our Future*. Cham: Springer, 181–193. doi: 10.1007/978-3-030-20389-4-9

Ford, A. B. (1976). *Stratigraphy of the Layered Gabbroic Dufek Intrusion, Antarctica*. Washington, D.C.: US Government Printing Office, 36. doi: 10.3133/b1405d

Gerringa, L. J. A., Alderkamp, A. C., Laan, P., Thuróczy, C. E., De Baar, H. J. W., Mills, M. M., et al. (2012). Iron from melting glaciers fuels the phytoplankton blooms in Amundsen Sea (Southern Ocean): iron biogeochemistry. *Deep Sea Res. 2 Top. Stud. Oceanogr*. 7, 16–31. doi: 10.1016/j.dsr2.2012.03.007

Goodwin, C. E., Berman, J., Downey, R. V., and Hendry, K. R. (2017). Carnivorous sponges (Porifera : Demospongiae : Poecilosclerida : Cladorhizidae) from the drake passage (Southern Ocean) with a description of eight new species and a review of the family Cladorhizidae in the Southern Ocean. *Inverteb. Syst.* 31, 37–64. doi: 10.1071/is16020

Griffiths, H. J. (2010). Antarctic marine biodiversity–what do we know about the distribution of life in the Southern Ocean? *PLoS One* 5:e11683. doi: 10.1371/journal.pone.0011683

Gutt, J., Griffiths, H. J., and Jones, C. D. (2013). Circumpolar overview and spatial heterogeneity of Antarctic macrobenthic communities. *Mar. Biodivers*. 43, 481–487. doi: 10.1007/s12526-013-0152-9

Huhn, O., Hattermann, T., Davis, P. E. D., Dunker, E., Hellmer, H. H., Nicholls, K. W., et al. (2018). Basal melt and freezing rates from first noble gas samples beneath an ice shelf. *Geophy. Res. Lett*. 45, 8455–8461. doi: 10.1029/2018gl079706

Ingels, J., Aronson, R. B., and Smith, C. R. (2018). The scientific response to Antarctic ice-shelf loss. *Nat. Clim. Chang*. 8, 848–851. doi: 10.1038/s41558-018-0290-y

Ingels, J., Aronson, R. B., Smith, C. R., Baco, A., Bik, H. M., Blake, J. A., et al. (2021). Antarctic ecosystem responses following ice-shelf collapse and iceberg calving: science review and future research. *Wiley Interdiscip. Rev*. 12:e682. doi: 10.1002/wcc.682

Kim, S. (2019). Complex life under the McMurdo Ice Shelf, and some speculations on food webs. *Antarct. Sci*. 31, 80–88. doi: 10.1017/s0954102018000561

Kingslake, J., Scherer, R. P., Albrecht, T., Coenen, J., Powell, R. D., Reese, R., et al. (2018). Extensive retreat and re-advance of the West Antarctic ice sheet during the holocene. *Nature* 558, 430–434. doi: 10.1038/s41586-018-0208-x

Lipps, J. H., Ronan, T. E. Jr., and Delaca, T. E. (1979). Life below the ross ice shelf, antarctica. *Science* 203, 447–449. doi: 10.1126/science.203.4379.447

Makinson, K., and Anker, P. G. D. (2014). The BAS ice-shelf hot-water drill: design, methods and tools. *Ann. Glaciol*. 55, 44–52. doi: 10.3189/2014aog68a030

Makinson, K., Holland, P. R., Jenkins, A., Nicholls, K. W., and Holland, D. M. (2011). Influence of tides on melting and freezing beneath Filchner-Ronne Ice Shelf, Antarctica. *Geophys. Res. Lett*. 38:L06601. doi: 10.1029/2010gl046462

Nachtsheim, D. A., Ryan, S., Schröder, M., Jensen, L., Chris Oosthuizen, W., Bester, M. N., et al. (2019). Foraging behaviour of Weddell seals (*Leptonychotes weddellii*) in connection to oceanographic conditions in the southern Weddell Sea. *Prog. Oceanogr*. 173, 165–179. doi: 10.1016/j.pocean.2019.02.013

Neuhaus, S. U., Tulaczyk, S. M., Stansell, N. D., Coenen, J. J., Scherer, R. P., Mikucki, J. A., et al. (2020). Did Holocene climate changes drive West Antarctic grounding line retreat and re-advance? *Cryosph. Discuss* [Preprint]. doi: 10.5194/tc-2020-308

Nicholls, K. W. (2004). Interannual variability and ventilation timescales in the ocean cavity beneath Filchner-Ronne Ice Shelf, Antarctica. *J. Geophy. Res*. 109:C04014. doi: 10.1029/2003jc002149

Nicholls, K. W., Østerhus, S., Makinson, K., Gammelsrød, T., and Fahrbach, E. (2009). Ice-ocean processes over the continental shelf of the southern Weddell Sea, Antarctica: a review. *Rev. Geophy*. 47:RG3003. doi: 10.1029/2007rg000250

NOAA National Geophysical Data Center (2009). *ETOPO1 1 Arc-Minute Global Relief Model. NOAA National Centers for Environmental Information* (accessed March 4, 2019).

Østerhus, S. (1994). *Report of the Norwegian Antarctic Research Expedition 1991/1992* Tromsø: Norsk polarinstitutt.

Østerhus, S., and Orheim, O. (1994). Oceanographic and glaciologic investigations through Jutulgryta, Fimbulisen in the 1991/92 season. *Norsk Polarinst. Meddel.* 124, 21–28.

Post, A. L., Galton-Fenzi, B. K., Riddle, M. J., Herraiz-Borreguero, L., O'Brien, P. E., Hemer, M. A., et al. (2014). Modern sedimentation, circulation and life beneath the Amery Ice Shelf, East Antarctica. *Cont. Shelf Res.* 74, 77–87. doi: 10.1016/j.csr.2013.10.010

Riddle, M. J., Craven, M., Goldsworthy, P. M., and Carsey, F. (2007). A diverse benthic assemblage 100 km from open water under the Amery Ice Shelf, Antarctica. *Paleoceanography* 22:PA1204. doi: 10.1029/2006pa001327

Smith, C. R., Amon, D. J., Higgs, N. D., Glover, A. G., and Young, E. L. (2017). Data are inadequate to test whale falls as chemosynthetic stepping-stones using network analysis: faunal overlaps do support a stepping-stone role. *Proc. Biol. Sci.* 284, 1–16. doi: 10.1098/rspb.2017.1281

Smith, J. A., Graham, A. G. C., Post, A. L., Hillenbrand, C.-D., Bart, P. J., and Powell, R. D. (2019). The marine geological imprint of Antarctic ice shelves. *Nat. Commun.* 10:5635.

Stevens, C., Hulbe, C., Brewer, M., Stewart, C., Robinson, N., Ohneiser, C., et al. (2020). Ocean mixing and heat transport processes observed under the ross ice shelf control its basal melting. *Proc. Natl. Acad. Sci. U.S.A.* 117, 16799–16804. doi: 10.1073/pnas.1910760117

Sugiyama, S., Sawagaki, T., Fukuda, T., and Aoki, S. (2014). Active water exchange and life near the grounding line of an Antarctic outlet glacier. *Earth Planet. Sci. Lett.* 399, 52–60. doi: 10.1016/j.epsl.2014.05.001

Turner, J. (2009). *Antarctic Climate Change and the Environment: A Contribution to the International Polar Year 2007-2008*. Cambridge: Scientific Committee on Antarctic Research.

Tyler, P. A., and Young, C. M. (2003). Dispersal at hydrothermal vents: a summary of recent progress. *Hydrobiologia* 503, 9–19. doi: 10.1023/b:hydr.0000008492.53394.6b

Vick-Majors, T., Achberger, A., Michaud, A., and Priscu, J. (2020). "Metabolic and taxonomic diversity in antarctic subglacial environments," in *Life in Extreme Environments: Insights in Biological Capability: Ecological Reviews*, eds G. Di Prisco, H. Edwards, J. Elster, and A. Huiskes (Cambridge: Cambridge University Press), 279–296. doi: 10.1017/9781108683319.016

Ziegler, A. F., Smith, C. R., Edwards, K. F., and Vernet, M. (2017). Glacial dropstones: islands enhancing seafloor species richness of benthic megafauna in West Antarctic Peninsula fjords. *Mar. Ecol. Prog. Ser.* 583, 1–14. doi: 10.3354/meps12363

Conflict of Interest: The authors declare that the research was conducted in the absence of any commercial or financial relationships that could be construed as a potential conflict of interest.

frontiers in Marine Science

ORIGINAL RESEARCH
published: 18 February 2021
doi: 10.3389/fmars.2021.593566

Whole Community Metatranscriptomes and Lipidomes Reveal Diverse Responses Among Antarctic Phytoplankton to Changing Ice Conditions

Jeff S. Bowman[1], Benjamin A. S. Van Mooy[2], Daniel P. Lowenstein[2], Helen F. Fredricks[2], Colleen M. Hansel[2], Rebecca Gast[2], James R. Collins[2,3], Nicole Couto[1] and Hugh W. Ducklow[4]*

[1] Scripps Institution of Oceanography, University of California, San Diego, San Diego, CA, United States, [2] Woods Hole Oceanographic Institution, Woods Hole, MA, United States, [3] School of Oceanography, University of Washington, Seattle, WA, United States, [4] Lamont-Doherty Earth Observatory, Columbia University, Palisades, NY, United States

OPEN ACCESS

Edited by:
Anne Helene Solberg Tandberg, University Museum of Bergen, Norway

Reviewed by:
Xiubao Li, Hainan University, China
Ken G. Ryan, Victoria University of Wellington, New Zealand

***Correspondence:**
Jeff S. Bowman
jsbowman@ucsd.edu

Specialty section:
This article was submitted to Marine Evolutionary Biology, Biogeography and Species Diversity, a section of the journal Frontiers in Marine Science

Received: *10 August 2020*
Accepted: *29 January 2021*
Published: *18 February 2021*

Citation:
Bowman JS, Van Mooy BAS, Lowenstein DP, Fredricks HF, Hansel CM, Gast R, Collins JR, Couto N and Ducklow HW (2021) Whole Community Metatranscriptomes and Lipidomes Reveal Diverse Responses Among Antarctic Phytoplankton to Changing Ice Conditions. Front. Mar. Sci. 8:593566. doi: 10.3389/fmars.2021.593566

The transition from winter to spring represents a major shift in the basal energy source for the Antarctic marine ecosystem from lipids and other sources of stored energy to sunlight. Because sea ice imposes a strong control on the transmission of sunlight into the water column during the polar spring, we hypothesized that the timing of the sea ice retreat influences the timing of the transition from stored energy to photosynthesis. To test the influence of sea ice on water column microbial energy utilization we took advantage of unique sea ice conditions in Arthur Harbor, an embayment near Palmer Station on the western Antarctic Peninsula, during the 2015 spring–summer seasonal transition. Over a 5-week period we sampled water from below land-fast sea ice, in the marginal ice zone at nearby Palmer Station B, and conducted an ice removal experiment with incubations of water collected below the land-fast ice. Whole-community metatranscriptomes were paired with lipidomics to better understand how lipid production and utilization was influenced by light conditions. We identified several different phytoplankton taxa that responded similarly to light by the number of genes up-regulated, and in the transcriptional complexity of this response. We applied a principal components analysis to these data to reduce their dimensionality, revealing that each of these taxa exhibited a strikingly different pattern of gene up-regulation. By correlating the changes in lipid concentration to the first principal component of log fold-change for each taxa we could make predictions about which taxa were associated with different changes in the community lipidome. We found that genes coding for the catabolism of triacylglycerol storage lipids were expressed early on in phytoplankton associated with a *Fragilariopsis kerguelensis* reference transcriptome. Phytoplankton associated with a *Corethron pennatum* reference transcriptome occupied an adjacent niche, responding favorably to higher light conditions than *F. kerguelensis*. Other diatom and dinoflagellate taxa had distinct transcriptional profiles and correlations to lipids, suggesting diverse ecological strategies during the polar winter–spring transition.

Keywords: Antarctica, phytoplankton, lipids, metatranscriptomics, Palmer LTER project

INTRODUCTION

The western Antarctic Peninsula is a region characterized by a highly dynamic sea ice regime. Seasonal and higher frequency shifts in sea ice cover are superimposed on large, inter-annual variations in ice thickness and extent. In the coastal zone this variability coincides with the zone of highest biological productivity, setting the stage for strong physical control of biological processes that enable the region's rich marine ecosystem (Bowman et al., 2016). During the winter–spring seasonal transition, sea ice rapidly advects in and out of the shallow coastal zone. This sea ice impacts phytoplankton communities by limiting light penetration into the surface ocean and stabilizing the surface mixed layer. Though sea ice cover leads to a shallow mixed layer, a scenario conducive to a strong spring bloom, it also decreases the light available to drive photosynthesis. In regions of highly variable sea ice cover phytoplankton must respond to rapidly changing light conditions independent of the circadian rhythms available to coordinate metabolic responses in lower latitude oceans.

Phytoplankton utilize a number of strategies to survive periods of prolonged darkness. While some utilize cysts or resting spores, and are thus metabolically inactive, others rely on lipid or carbohydrate energy stores to survive periods of prolonged darkness. Recent analysis of the translational response of *Fragilariopsis cylindrus*, a model sea ice diatom, to prolonged darkness suggests regulation of multiple systems to sustain cell function and enable a fast response to light (Kennedy et al., 2019). Specifically, those authors identified an increase in proteins diagnostic of catabolic processes including glycolysis, the Entner–Doudoroff pathway, and the tricarboxylic acid cycle. Significantly, however, proteins that are necessary for photosynthesis and related anabolic functions were not necessarily less abundant during prolonged darkness. This suggests an adaptation to the extreme seasonal cycle of light and dark based on a fast response to light. As soon as the photon flux is sufficient to drive the photosynthetic machinery *F. cylindrus* is able to undergo primary production (PP); there is no need to expend additional resources retooling the cell's molecular machinery.

Lipids are a key component for the survival of phytoplankton in the dark, but these compounds and their derivatives play important roles beyond energy storage (Collins et al., 2018). While triacylglycerols (TAGs) are primarily involved in energy storage, phospholipids, including phosphatidylcholine (PC), phosphatidylethanolamine (PE), and phosphatidylglycerol (PG), are key components of cell membranes. Free fatty acids (FFA) are rare in healthy cells, and, thus, are indicative of cell degradation. Oxidized FFA (i.e., oxylipins) can be deleterious to bacterial growth (Edwards et al., 2015). The glycolipids sulfoquinovosyldiacylglycerol (SQDG), digalactosyldiacylglycerol (DGDG), along with PG, are the primary structural lipids associated with the chloroplast.

The community lipidome can change on scales much shorter than seasonal. Recent work in the North Pacific subtropical gyre revealed a diel cycle in TAGs, with these compounds being synthesized during the day and catabolized at night (Becker et al., 2018). Given the complexity of light during the polar winter–spring seasonal transition, with day length and sea ice cover interacting in unpredictable ways, we sought to identify major contributors to the lipidome and patterns in lipid synthesis and catabolism through a coupled metatranscriptomic and lipidomic study. We made use of unusual sea ice conditions during the 2015 Austral spring to investigate the response of Antarctic phytoplankton to changing light conditions. Samples were collected from below sea ice, the marginal ice zone, and microcosms to identify different physiological responses to variable conditions associated with the winter–spring transition. Although metatranscriptomes are easily disaggregated into their component transcriptomes by mapping to references, it is much more difficult to assign lipids to specific phytoplankton (except for lipids that are uniquely produced by a given taxonomic group). To overcome this limitation we used principal components analysis (PCA) as a dimension reduction technique, correlating changes in lipid concentration to principal components describing up- or down-regulated genes for each reference phytoplankton transcriptome. This approach allowed us to identify key phytoplankton taxa responding to our experimental conditions, and different lipid utilization strategies employed by these phytoplankton during the Antarctic winter–spring seasonal transition.

MATERIALS AND METHODS

Ethics Statement

Written informed consent was obtained from the individuals for the publication of any potentially identifiable images or data included in this article.

Experimental Design and Sampling

Persistent land-fast sea ice in Arthur Harbor allowed us to establish an ice station at 64.77253°S and 64.05411°W, on November 4, 2015 (**Figure 1A**). On November 10, 2015 we initiated a microcosm experiment to simulate the effects of ice removal and concomitant exposure to sunlight. Using a peristaltic pump and acid-washed tubing we filled 12 × 10 L acid-washed carboys with seawater from the ice station (**Figure 1B**). The carboys were transported to an outdoor recirculating incubator (**Figure 1C**) and shaded with screening to approximate light conditions at 10 m with no sea ice cover (approximately 30% irradiance as determined with a LI-COR Spear sensor for November 21, 2014 at Station B) (**Supplementary Figure 1**). As a control, three carboys were covered with additional layers of screening to maintain light levels below an estimated 1% irradiance, which was similar to under the sea ice. Three carboys each were sampled on November 11 (24 h; day 1), November 13 (72 h; day 3), and November 18 (192 h; day 8) (**Figure 1E**). On November 18 we also sampled the three dark controls.

PAR profiles were collected from the Ice Station on November 4 (6 days prior to T_0) and November 15 (day 5), and from Station B on November 17 (day 7). Profiles were collected with a LI-COR 193 against a LI-COR 193 surface reference. Care was taken to position the casts on the

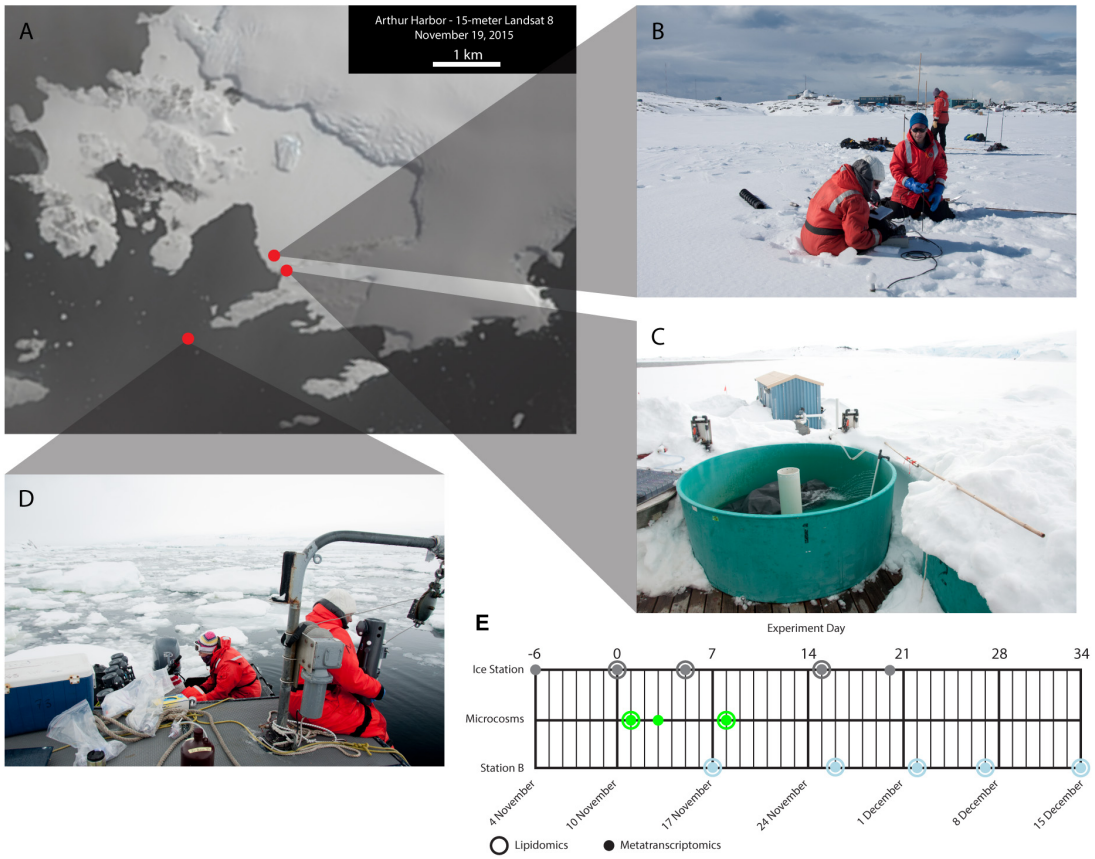

FIGURE 1 | Site descriptions and experimental time-line. **(A)** Landsat imagery (15 m resolution) of southern Anvers Island on November 19, 2015. The landfast sea ice in Arthur Harbor is readily apparent. Red circles indicate the location of the Ice Station **(B)**, Palmer Station and the outdoor incubators **(C)**, and Palmer LTER Station B **(D)**. **(E)** Experimental time-line showing when samples were collected for lipidomics and metatranscriptomics for each sampling location. Note that the Ice Station day 0 sample is also the day 0 sample for the microcosms.

unshadowed side of the Zodiac (for Station B) and ice sampling team (Ice Station).

Concurrent with the ice removal experiment, seawater samples were collected from the Ice Station on November 4, November 15, November 25, and November 30 (**Figure 1E**), at which time the ice was deemed too unstable for travel. At each sampling opportunity an ice core was removed with a Sipre-type corer. Acid-washed peristaltic pump tubing secured to a bamboo pole was inserted into the ice to a depth of 1 m below the ice surface. For the metatranscriptomes, a field-portable peristaltic pump was used to filter water onto sterile 47 mm 0.2 μm Durapore filters (PALL). Immediately after filtering, the filter was inserted into a bead-beating tube pre-loaded with RNeasy PowerWater kit (Qiagen) buffer #1 and 10 μL 2-betamercaptoethanol (Sigma). The tube was inverted to fully coat the filter surface, and the filters were placed on ice and protected from sunlight until extraction within 4 h of sampling.

For lipidomics, the peristaltic pump was used to fill acid-washed polycarbonate bottles. Care was taken to shade the bottles during collection and transport. Within 4 h the samples were filtered on 47 mm diameter, 0.2 μm pore size, hydrophilic PVDF membranes (Millipore) under gentle vacuum. The membranes were flash frozen in liquid nitrogen and stored in a −80°C freezer.

Samples were collected from the Palmer Long Term Ecological Research project (PAL-LTER) Station B, located at approximately 64.78205°S and 64.07934°W, on November 22, November 26, December 2, December 7, and December 15 (**Figures 1A,D**). Samples were collected by peristaltic pump from a Zodiac, at 5 m depth, following the same methods employed for sampling at the ice station.

RNA extraction followed the manufacturers recommended protocol, including DNase treatment. RNA was quantified using the Qubit HS RNA kit (Invitrogen). Parallel samples were collected for DNA and extracted using the DNeasy PowerWater kit (Qiagen), quantification was carried out using the Qubit HS DNA kit (Invitrogen). Measurements for chlorophyll *a*, bacterial production (BP), PP, and fluorescence induction and relaxation (FIRe) were carried out by the Palmer Long Term Ecological Research Program using the standard methods available on the Palmer LTER DataZoo (Palmer LTER Science Team, 2021).

Sequencing and Sequence Processing

Sequencing was carried out via PE sequencing on the Illumina HiSeq platform at either the Joint Genome Institute (12 samples) or the UC San Diego IMG Genomics core facility (64 samples). Demultiplexed reads were merged and quality controlled with the Paired-End reAd mergeR (PEAR) (Stamatakis et al., 2014), using a *p*-value of 0.01, minimum PHRED score of 33, and eliminating merged reads <100 bp in length.

Merged, quality controlled reads were mapped to reference transcriptomes of the Marine Microbial Eukaryotic Transcriptome Sequencing Project (MMETSP) (Keeling et al., 2014) and reference genomes from GenBank with an extension of the paprica bioinformatics pipeline (i.e., paprica-mt) (Bowman and Ducklow, 2015a,b). In brief, reference bacterial, archaeal, and viral genomes were downloaded from GenBank, and reference eukaryotic transcriptomes were downloaded from MMETSP, on February 1, 2017. All unique genes coding for a product with an Enzyme Commission (EC) number were identified and concatenated in a database, along with the taxonomic information of the originating genome or transcriptome, and the name of the gene product. BWA (Langmead et al., 2009) was used to search all query reads against this database. The BWA output in SAM format was parsed to create a tab-delimited file of query reads, best mapped reference sequence, and taxonomy and gene product of the reference sequence.

Lipid Extraction and Quantification

Biomass captured on the PVDF filters was extracted using a modification of the Bligh and Dyer (1959) method as described in Popendorf et al. (2013). Total lipid extracts were stored under argon at −80°C prior to analysis. We analyzed the lipids using high performance liquid chromatography and high-resolution accurate-mass mass spectrometry (HPLC/HRAM-MS). The HPLC/HRAM-MS method was based on Hummel et al. (2011) with minor modifications, including electrospray source conditions, as described by Collins et al. (2016). We processed the data with R-based CAMERA (Kuhl et al., 2012), LOBSTAHS (Collins et al., 2016), and xcms (Smith et al., 2006; Tautenhahn et al., 2008; Benton et al., 2010) packages as described by Collins et al. (2016, 2018) and Becker et al. (2018). Downstream analysis focused on the following lipid classes: monogalactosyldiacylglycerol (MGDG; a chloroplast lipid), sulfoquinovosyldiacylglycerol (SQDG; a chloroplast lipid), digalactosyldiacylglycerol (DGDG; a chloroplast lipid), PE (a phospholipid), PG (a phospholipid), PC (a phospholipid), Diacylglyceryl hydroxymethyl-trimethylalanine (DGTA; a betaine lipid), Diacylglyceryl carboxyhydroxy-methylcholine (DGCC; a betaine lipid), TAG, and FFA.

Data Analysis

For each sample and reference transcriptome/genome, the unique EC numbers were tallied to produce tables of transcript abundance. This approach allowed an independent comparison of each reference transcriptome/genome between replicate libraries for select samples. To make this comparison we employed DESeq2 (Love et al., 2014); differentially expressed transcripts are described as those with a p-value < 0.05 in a Wald test. p-Values reflect Holm–Bonferroni correction for multiple-comparisons as is the default in DESeq2. This experiment was designed such that ice station samples were the initial condition, followed by samples from Station B, then the microcosm incubations. Where comparisons were made within each of these groups, the initial condition was that which occurred first in the time series.

To identify which reference transcriptomes responded similarly to changing environmental conditions we applied PCA to the differential expression data for all points of comparison. PCA was applied to each reference independently. The step was important for dimension reduction; the PCA effectively collapsed one dimension of the data allowing us to compare all reference transcriptomes for all points of comparison in only two dimensions. Transcriptomes with similar magnitudes in the first principal component (PC1) according to a simprof analysis based on Euclidean distance (in deference to positive and negative values) and hierarchical clustering were considered to have a similar response to changing environmental conditions. To explore specific gene expression patterns within each group we then considered the contribution of each enzyme (cos^2) to PC1.

To relate the lipidomes to the transcriptomes we constructed a correlation matrix based on Pearson's correlation coefficient (r). For each transcriptome, PC1 was correlated with the change in lipid concentration between each sample. The resulting matrix was organized according to hierarchical clustering based on Euclidean distances (in deference to the positive and negative values).

All statistical analyses were carried out in R v3.6 (R Core Team, 2014) using R Studio and R Studio Server. The simprof analysis was carried out using the "simprof" function in package clustsig (Whitaker and Christman, 2014). For the PCA analysis, the cos^2 values were extracted using the "get_pca_var" function from the factoextra package (Kassambara and Mundt, 2017).

RESULTS

Ecophysiology

Chlorophyll *a* values responded quickly to the microcosm treatment (**Figure 2A**). Initial (T_0) samples for the microcosms and ice station samples were 0.23 mg m^{-3} on November 10, 2015. At the time of the final sampling on November 25, 2015 (day 15), the ice station had risen to 0.63 mg m^{-3}. By contrast, after only 7 days the microcosms had increased to 1.20 mg m^{-3} (mean of three replicates, SD = 0.50 mg m^{-3}). At Station B the values increased from 0.52 mg m^{-3} on day 17 to 2.08 mg m^{-3} on day 34. The PP values largely followed the pattern set by chlorophyll *a*, increasing from initial values of 1.71 mg C m^{-3} d^{-1} at the ice station and mesocosm T_0 samples to 41.75 mg C m^{-3} d^{-1} in the microcosms on day 8 (mean of three replicates, SD = 26.93 mg C m^{-3} d^{-1}) (**Figure 2B**). One exception was the Ice Station day 20 value, which jumped to 24.05 mg C m^{-3} from 6.03 mg C m^{-3} d^{-1} on day 15. Bacterial production values followed PP values with no indication of a lag (**Figure 2C**). These values ranged from 3.34 pmol leucine l^{-1} h^{-1}

on day 6 at Station B to 19.95 pmol leucine l^{-1} h^{-1} on day 20 at the Ice Station. For all ecophysiology parameters, only single values are available for most time-points from the Ice Station and all time-points from Station B.

Fluorescence induction and relaxation parameters measured included F_v/F_m (a key indicator of photosynthetic efficiency), ρ_{PSII} (the cross-sectional absorption area of photosystem II), and ρ (the reaction center connectivity). F_v/F_m remained relatively stable at the Ice Station over the course of the experiment (**Figure 2D**). The high light associated with the microcosms induced rapid perturbations in this parameter, with F_v/F_m falling from 0.46 on day 0 to 0.41 on day 3, before recovering to 0.50 on day 8. Overall the Station B samples were lower than either the Ice Station or microcosm values, and increased over the course of the experiment from 0.26 on day 6 to 0.41 on day 16. ρ_{PSII} declined over the course of the microcosms, from 440 to 302 (**Figure 2E**). ρ_{PSII} was consistently higher at the Ice Station than at Station B. For the microcosms, ρ followed an inverse relationship to F_v/F_m, falling from a day 0 value of 0.26 to 0.09 on day 1, before recovering to 0.25 on day 3 (**Figure 2F**). At the start of the experiment ρ was higher at the Ice Station than at Station B, these values converged near 0.08 by day 16.

On November 4 (6 days prior to T_0) the 1% irradiance depth at the Ice Station was estimated to be 1.25 m (**Supplementary Figure 1**). On day 5 it was not possible to get a clean value for the uppermost portion of the water column and we could not estimate the depth of the 1% light level. The shape of the profile, however, suggests a similar value to that estimated for November 4. The lowest irradiance values observed for Station B on day 7 was 17.0%. The irradiance at 5 m depth (the sampling depth for our Station B metatranscriptomes) was 51.7%.

Metatranscriptome Results

We produced 76 merged sequence libraries with a minimum quality score of 33, ranging in size from 3,492,999 to 104,508,538 (mean = 4.94×10^7, SD = 2.49×10^7). The fraction of reads mapped to a reference transcriptome/genome for each sample ranged from 13.06 to 81.87% (mean = 48.48%, SD = 13.48%). All sequence data is available from the NCBI SRA at BioProject PRJNA494856, and a flat file of differentially expressed genes is provided as **Supplementary Table 1**. Heatmaps for each enzyme in the paprica-mt database that had significant $\log_2$ fold-change differences for one or more reference transcriptomes are provided as a **Supplementary Material**.

We identified 93 reference genomes/transcriptomes with significantly differentially expressed genes. Of these, 37 had differentially expressed genes for all points of comparison. These were primarily eukaryotic reference transcriptomes from the MMETSP, but included one prokaryotic reference genome; GCF_000012305.1 (*Psychrobacter arcticus* 273-4). The prokaryotic genome was not considered further in our analysis. The remaining reference transcriptomes included 23 members of Bacillariophyta (diatoms), 10 Dinophyta (dinoflagellates), 1 Ascomycota (fungi), 1 Ochrophyta (a chrysophyte or golden algae), and 1 Sarcomastigophora (**Table 1**). Each reference transcriptome could represent a range of more or less closely related phytoplankton present in the system. Here, when we refer to a reference transcriptome by name we are referring to the collection of phytoplankton with gene transcripts that mapped to that reference transcriptome. This approach does not imply a close evolutionary relationship between the reference and environmental phytoplankton. For brevity the strain name of each reference transcriptome is included only at first use.

To assess general growth and the photosynthetic response to changing conditions we considered the expression patterns of genes coding for DNA polymerase (EC 2.7.7.7), Photosystem I enzymes (EC 1.97.1.12), Photosystem II enzymes (EC 1.10.3.9), and ribulose bisphosphate carboxylase/oxygenase (RUBISCO, EC 4.1.1.39). The regulation of genes coding for DNA polymerase was highly variable (**Supplementary Figure 2**), however, diatoms associated with three reference transcriptomes had the strongest response to the microcosm experiments: MMETSP0169 (*Corethron pennatum* L29A3), MMETSP0910 (*Thalassiosira rotula* GSO102), and MMETSP0733 (*Fragilariopsis kerguelensis* L26-C5). *F. kerguelensis* initially up-regulated genes coding for DNA polymerase between microcosm day 0 and day 1, then down-regulated these genes after day 1. By contrast *C. pennatum* generally up-regulated these genes throughout the microcosm experiment, and in comparisons between earlier and later experimental time-points.

Photosystem I (**Supplementary Figure 3**) and II (**Supplementary Figure 4**) expression patterns were dominated by dinoflagellates. While most phytoplankton associated with the reference transcriptomes up-regulated Photosystem I over the course of the microcosm experiment, and in comparisons between earlier and later experimental time-points, MMETSP1367 (*Symbiodinium* sp. C1) and MMETSP0503 (*Heterocapsa rotundata* SCCAP-K-0483) strongly down-regulated the genes coding for Photosystem I at the start of the microcosms. A similar pattern was observed for Photosystem II, though MMETSP0796 (*Pyrodinium bahamense* RCC2770) and MMETSP0228 (*Protoceratium reticulatum* CCCM535 = CCMP1889) had a strong transcriptional response, and generally up-regulated Photosystem II in response to conditions associated with higher light levels. It should be noted that here we have retained the MMETSP nomenclature for the *Symbiodinium* reference transcriptomes, however, *Symbiodinium* C1 is now a member of the genus *Cladocopium* (LaJeunesse et al., 2018).

Dinoflagellates also dominated the expression pattern of genes coding for RUBISCO (**Supplementary Figure 5**). MMETSP1036 (*Azadinium spinosum* 3D9), MMETSP0258 (*Amphidinium carterae* CCMP1314), and *Symbiodinium* sp. C1 strongly up-regulated these genes in response to conditions of higher light. A large number of diatoms also significantly up- or down-regulated the genes coding for RUBISCO over the course of the experiment, albeit at lower levels than the dinoflagellates.

The total number of differentially expressed genes for a given reference and comparison ranged between 1 and 328 (**Figure 3**). We consider this value as the *response complexity* of the reference genome/transcriptome for the point of comparison. Hierarchical clustering of response complexity for the eukaryotic reference transcriptomes identified 19 significant clusters according to a

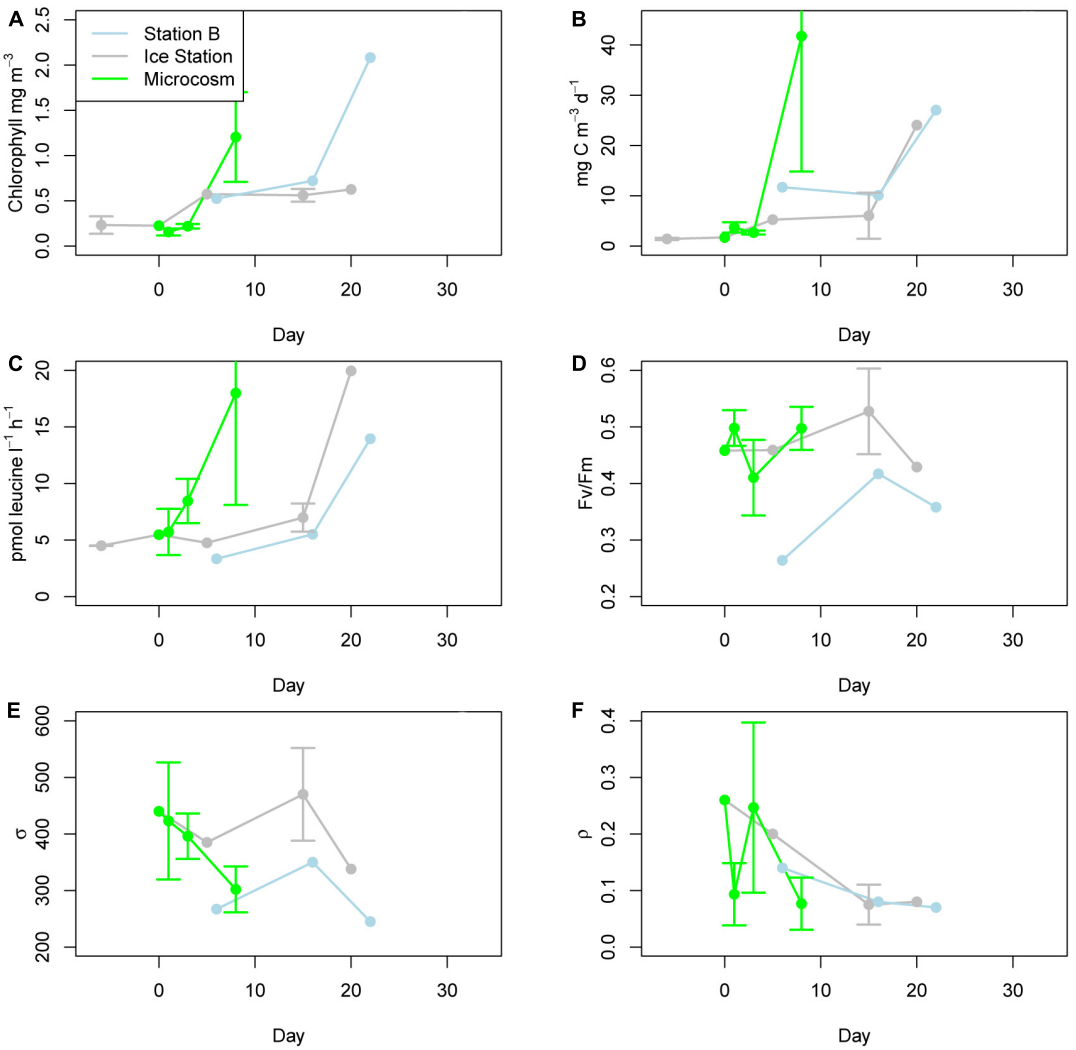

FIGURE 2 | Ecophysiology. **(A)** Chlorophyll *a* concentrations for Station B (located in the marginal ice zone), the Ice Station, and microcosms. **(B)** Primary production according to H-$^{14}CO_3$ uptake. **(C)** Bacterial production as determined from the uptake of ^{3}H-leucine. **(D)** F_v/F_m as determined by fluorescence induction and relaxation (FIRe). **(E)** σ_{PSII}, a measure of the absorption cross-sectional area for photosystem II as determined by FIRe. **(F)** ρ, a measure of reaction center connectivity as determined by FIRe. Ecophysiology parameters for Station B and the Ice Station represent a single measurement, as provided by the Palmer LTER project. Values for the microcosms on days 1, 3, and 8 represent the means of triplicates.

simprof analysis. Three reference transcriptomes stood out as having high response complexity; *F. kerguelensis*, *C. pennatum*, and *T. rotula*, with the latter two forming a statistically significant cluster. These reference transcriptomes also had the strongest DNA polymerase signal across the microcosm portion of the experiment. The greatest response complexity was observed for *F. kerguelensis* between Ice Station day 5 (November 15) and Station B day 7 (November 17), and between Ice Station day 5 and Station B day 27 (December 7).

For Ice Station day 5 to Station B day 7, the comparison of greatest response complexity for *F. kerguelensis*, several genes relevant to lipid metabolism were significantly down-regulated (**Supplementary Table 1**). These included long-chain-3-hydroxyacyl-CoA dehydrogenase (EC 1.1.1.211; normalized $\log_2$ fold-change −7.41), 2,4-dienoyl-CoA reductase (EC 1.3.1.34; normalized $\log_2$ fold-change −6.26), triacylglycerol lipase (3.1.1.3; normalized $\log_2$ fold-change −5.31), and 3-oxoacyl-(acyl-carrier-protein) reductase (EC 1.1.1.100; normalized $\log_2$ fold-change −5.11). A gene coding for sphingolipid 4-desaturase (EC 1.14.19.17; normalized $\log_2$ fold-change 4.00) was significantly up-regulated. Of these, only 2,4-dienoyl-CoA reductase was similarly down-regulated by *T. rotula*, and none were significantly up- or down-regulated by *C. pennatum*.

In contrast to response complexity we defined *response strength* as the summed fold-change for all differentially expressed genes for a given reference and comparison (**Figure 4**). Hierarchical clustering of response strength identified 23 significant clusters according to a simprof analysis, with *F. kerguelensis* and *C. pennatum* responding most strongly to changing conditions. To identify which references responded

TABLE 1 | Reference transcriptomes with reads mapped for all points of comparison.

Accession	Name	Phylum	PC1 % variance
MMETSP0009	*Grammatophora oceanica* CCMP410	Bacillariophyta	26.4
MMETSP0010	*Corethron hystrix* 308	Bacillariophyta	19.2
MMETSP0105	*Acanthoeca*-like sp. 10tr	Sarcomastigophora	50.3
MMETSP0139	*Pseudo-nitzschia australis* 10249-10-AB	Bacillariophyta	23.6
MMETSP0160	*Odontella sinensis* Grunow 1884	Bacillariophyta	21.6
MMETSP0169	*Corethron pennatum* L29A3	Bacillariophyta	18.0
MMETSP0228	*Protoceratium reticulatum* CCCM535 (CCMP 1889)	Dinophyta	39.7
MMETSP0232	*Debaryomyces hansenii* J26	Ascomycota	39.8
MMETSP0258	*Amphidinium carterae* CCMP1314	Dinophyta	47.9
MMETSP0270	*Scrippsiella trochoidea* CCMP3099	Dinophyta	39.0
MMETSP0418	*Astrosyne radiata* 13vi08-1A	Bacillariophyta	29.1
MMETSP0503	*Heterocapsa rotundata* SCCAP-K-0483	Dinophyta	36.7
MMETSP0578	*Skeletonema grethea* CCMP1804	Bacillariophyta	22.5
MMETSP0603	*Skeletonema menzelii* CCMP793	Bacillariophyta	22.7
MMETSP0724	*Amphiprora* sp. CCMP467	Bacillariophyta	18.3
MMETSP0733	*Fragilariopsis kerguelensis* L26-C5	Bacillariophyta	32.8
MMETSP0794	*Stephanopyxis turris* CCMP815	Bacillariophyta	26.3
MMETSP0796	*Pyrodinium bahamense* pbaha01	Dinophyta	38.6
MMETSP0850	*Pseudo-nitzschia fraudulenta* WWA7	Bacillariophyta	22.3
MMETSP0878	*Thalassiosira weissflogii* CCMP1336	Bacillariophyta	22.0
MMETSP0910	*Thalassiosira rotula* GSO102	Bacillariophyta	18.0
MMETSP1032	*Lingulodinium polyedra* CCMP1738	Dinophyta	35.0
MMETSP1036	*Azadinium spinosum* 3D9	Dinophyta	37.2
MMETSP1039	*Skeletonema marinoi* FE7	Bacillariophyta	20.7
MMETSP1057	*Cyclotella meneghiniana* CCMP338	Bacillariophyta	19.5
MMETSP1059	*Thalassiosira* sp. FW	Bacillariophyta	21.6
MMETSP1064	*Aulacoseira subarctica* CCAP 1002/5	Bacillariophyta	29.1
MMETSP1065	*Amphiprora paludosa* CCMP125	Bacillariophyta	22.2
MMETSP1070	*Minutocellus polymorphus* NH13	Bacillariophyta	25.6
MMETSP1103	*Paraphysomonas bandaiensis* Caron Lab Isolate	Ochrophyta	24.9
MMETSP1110	*Symbiodinium* sp. CCMP421	Dinophyta	40.5
MMETSP1322	*Minutocellus polymorphus* RCC2270	Bacillariophyta	23.4
MMETSP1362	*Leptocylindrus danicus* CCMP1856	Bacillariophyta	26.3
MMETSP1367	*Symbiodinium* sp. C1	Dinophyta	39.7
MMETSP1370	*Symbiodinium* sp. C15	Dinophyta	42.6
MMETSP1437	*Eucampia antarctica* CCMP1452	Bacillariophyta	20.3

similarly to changing conditions we considered the magnitude of each sample comparison in PC1.

principal component 1 accounted for between 18.0 and 50.3% of variance across the points of comparison for all reference transcriptomes (**Table 1**; mean = 29.0%, SD = 9.2%). Using the magnitude of each sample comparison in PC1, we identified 23 distinct clusters of reference transcriptomes when organized by response to environmental gradients (normalized magnitude of points of comparison in PC1) (**Supplementary Figure 6**). Although they did not form a statistically significant cluster, the 10 dinoflagellate references formed a coherent group. These references showed a strong positive expression response for the Ice Station day 20 samples in comparison to the microcosms, and a strong negative expression response for the Station B day 7 samples when compared to the day 8 microcosms (November 18). It is important to recognize that the magnitude in PC1 for a given sample comparison only considers the degree of response according to $\log_2$ fold-change, it does not imply that similar genes are being up- or down-regulated. The three reference transcriptomes with the largest response strength (*F. kerguelensis* and *C. pennatum*) and complexity (*F. kerguelensis*, *C. pennatum*, and *T. rotula*) clustered separately from one another in the PC1 magnitude analysis, though *C. pennatum* clustered with MMETSP0139 (*Pseudo-nitzschia australis* 1024910AB), and *F. kerguelensis* clustered with MMETSP0105 (*Acanthoeca* sp. 10tr).

To take a closer look at the three reference transcriptomes that exhibited the highest response complexity (*T. rotula*, *F. kerguelensis*, and *C. pennatum*) we considered the transcripts for each reference with the highest $\cos^2$ values for PC1 (**Figure 5**). These transcripts were presumed to contribute strongest to the transcriptional response described by PC1. Each of these

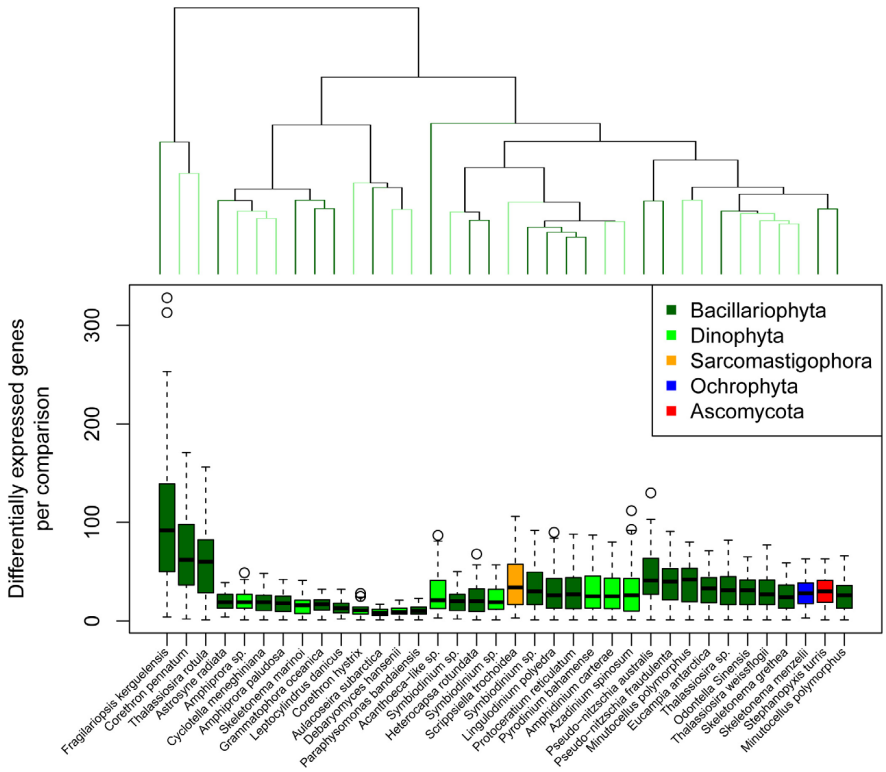

FIGURE 3 | Transcriptional response complexity. Transcriptional response complexity was determined as the number of genes in each reference transcriptomes determined to be differentially expressed between two points of comparison. The dendrogram at the top of the plot indicates similarity according to the number of unique genes differentially expressed between points of comparison but does not consider the identify of those genes. Significant clusters are indicated by alternating light and dark green color.

references had a different transcriptional profile according to $\cos^2$, with the largest $\cos^2$ values associated with *Ficus kerguenlensis*. For that reference, contributions to PC1 were led by transcripts coding for phosphoenolpyruvate carboxykinase (EC 4.1.1.49), 3-hydroxyacyl-CoA dehydrogenase (EC 1.1.1.35), and triacylglycerol lipase (EC 3.1.1.3). Transcripts contributing most to PC1 for *T. rotula* coded for a hypothetical protein, a glutathione amide-dependent peroxidase (EC 1.11.1.17), malate dehydrogenase (EC 1.1.1.37), and cell division protein FtsH (EC 3.6.4.3). For *C. pennatum*, major contributors to PC1 included UDP-glucuronate decarboxylase (EC 4.1.1.35), proline dehydrogenase (EC 1.5.5.2), fatty acid desaturase (EC 1.14.19.3), and acyl-lipid omega-6 desaturase (EC 1.14.19.22).

Lipid Distribution and Correlation With Metatranscriptomes

Triacylglycerols were the most abundant lipid class, followed by FFA (**Figure 6** and **Supplementary Figures 7**, **8**). TAGs rapidly increased in the microcosms, from 1847.3 pM at T_0 (November 10) to 10,252.6 pM at the end (day 8). Over the same period, TAGs also increased at the Ice Station, reaching 11,132.3 pM on day 15. TAG concentrations at Station B reached 11,327.9 pM that same day, and increased by more than fourfold to 53,391.4 pM on day 34. At T_0 the dominant TAGs were 48:2 and 48:1. For the microcosms, by day 8 the dominant TAG was 52:9, while at the end of the sampling period the dominant TAGs at Station B were 50:6, 52:6, and 52:7 (**Supplementary Figure 7**).

Free fatty acids were the next most abundant lipid class (**Figure 6**) and exhibited a more variable distribution (**Supplementary Figure 8**). FFAs increased only slightly from 4409.3 pMol at the start of the microcosm experiment to 4901.2 pMol at the end of the experiment (day 8). Over the same period FFA increased at the Ice Station to 5697.5 pMol on day 5 (November 15), but then decreased to 3802.2 on day 15. FFA initially declined at Station B, from 7509.9 pMol on day 6 to 6233.1 pMol on day 15, however, FFA increased dramatically at Station B after day 15, ending at 36,632.8 pMol on day 34. Initially the dominant FFA was 18:0, however, 20:5 was the most abundant FFA in the microcosms by day 8, and this FFA was also dominant at Station B after day 22 (**Supplementary Figure 8**).

To look for correlations between changes in lipid concentration (Δlipid) and gene expression, we evaluated Pearson's *r* for Δlipid and PC1 for all reference transcriptomes (**Figure 7A**). Mean variance in Δlipid explained by PC1 ranged from 10.41% for *C. pennatum* and 0.53% for *T. rotula* GSO102. *C. pennatum* and Aulacoseira subarctica yielded the strongest correlations between PC1 and Δlipid (**Figures 7C–F**), ranging from $r = 0.57$ for MGDG 24:0 (**Figure 7C**) to $r = -0.71$ for DGCC 37:0 (**Figure 7D**). Clustering the reference transcriptomes by

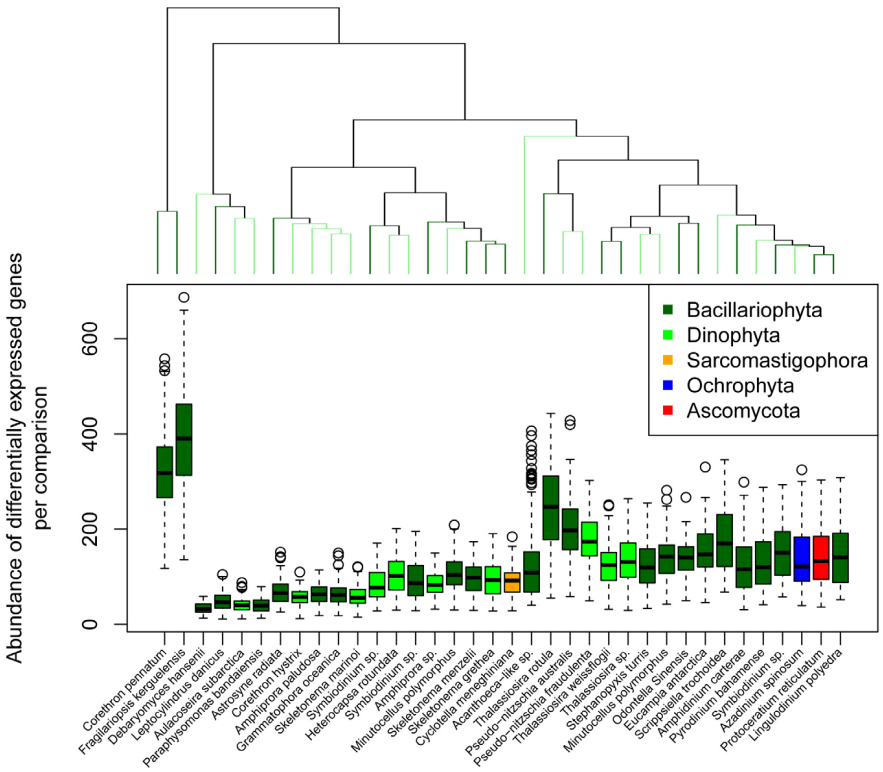

FIGURE 4 | Transcriptional response strength. Transcriptional response strength was determined as the summed, normalized $\log_2$ fold-change for all significantly differentially expressed genes in each reference transcriptome between two points of comparison. The dendrogram at the top of the plot indicates similarity according to the total number of transcripts associated with differentially expressed genes between points of comparison but does not consider the identify of those genes. Significant clusters are indicated by alternating light and dark green color.

r yielded two groups. One group, exemplified by *P. australis* 1024910AB, *F. kerguelensis*, and *C. pennatum*, was characterized by largely negative correlations with PC1, except for FFA and select DGCC lipids (**Figure 7A**). The other group was exemplified by MMETSP1362 (*Leptocylindrus danicus* CCMP1856), MMETSP1057 (*Cyclotella meneghiniana* CCMP338), and *Aulacoseira subarctica* CCAP1002-5. These had largely positive correlations between Δlipid and PC1, and weak or negative correlations between FFA and PC1.

DISCUSSION

Dynamic light conditions are associated with the winter to spring seasonal transition in the coastal Antarctic. Superimposed on the steady increase in irradiance associated with solar declination and day length are variable-term variations in irradiance caused by sea ice cover. We observed that the development of the spring phytoplankton bloom was significantly impeded by sea ice cover at our ice station, with only a slight increase in chlorophyll *a* over the observational period. Nonetheless, the concentration of TAGs increased at the ice station from day 0 to day 15, consistent with the downregulation of the gene coding for triacylglycerol lipase (EC 3.1.1.3) in *F. kerguelensis* and increasing PP. Combined with the up-regulation of genes coding for DNA polymerase, this suggests that *F. kerguelensis* was acclimated to the extreme low light conditions present and actively undergoing PP at the Ice Station throughout the experimental period.

This early transcriptional activity suggests a diverse lipid utilization strategy by the phytoplankton associated with the *F. kerguelensis* transcriptome. *F. kerguelensis* was by far the most transcriptionally active reference for the gene coding triacylglycerol lipase. Although the gene was generally down-regulated from earlier to later season samples, and from the Ice Station to Station B, it was up-regulated in the microcosms on days 1, 3, and 8 in comparison with day 0. One possible explanation is that *F. kerguenlensis* had become photoinhibited within 24 h of exposure to high light conditions, and reverted to lipid catabolism for energy. There is strong evidence for photoinhibition in the microcosms by day 1. Although F_v/F_m increased slightly before dropping on day 3, ρ, a measure of reaction center connectivity, dropped sharply.

Other members of the phytoplankton community responded quickly to the simulated removal of ice and release from light limitation. Within 192 h, chlorophyll *a* concentration had more than doubled, TAG lipid concentrations had reached parity with those observed at Station B the day prior (despite the up-regulation of triacylglycerol lipase by *F. kerguelensis*), and the transcriptional response was dominated by a mixed diatom community. Diatoms represented by the reference

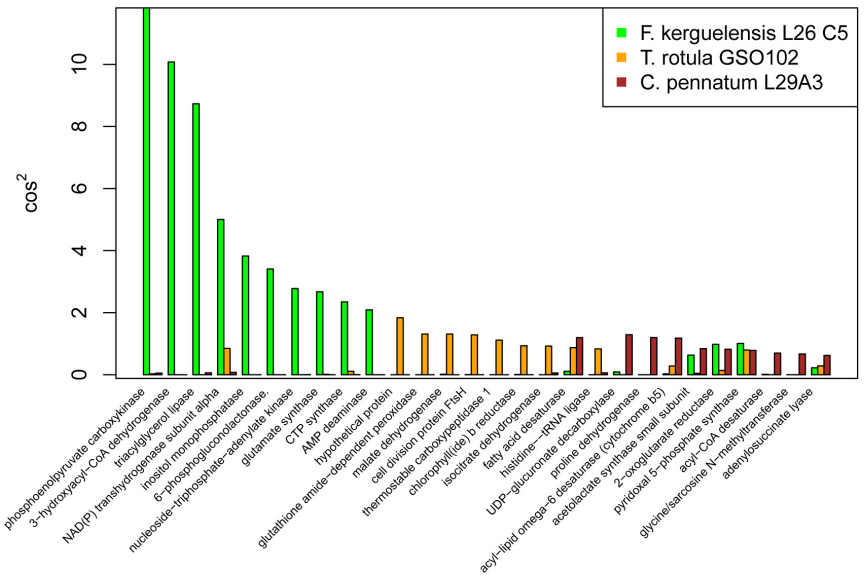

FIGURE 5 | Major transcriptional response associated with the first principal component (PC1) for *Fragilariopsis kerguelensis*, *Thalassiosira rotula*, and *Corethron pennatum*. The cos^2 metric is a measure of the contribution of each variable to a PC. The higher the cos^2 value, the greater the contribution of that variable.

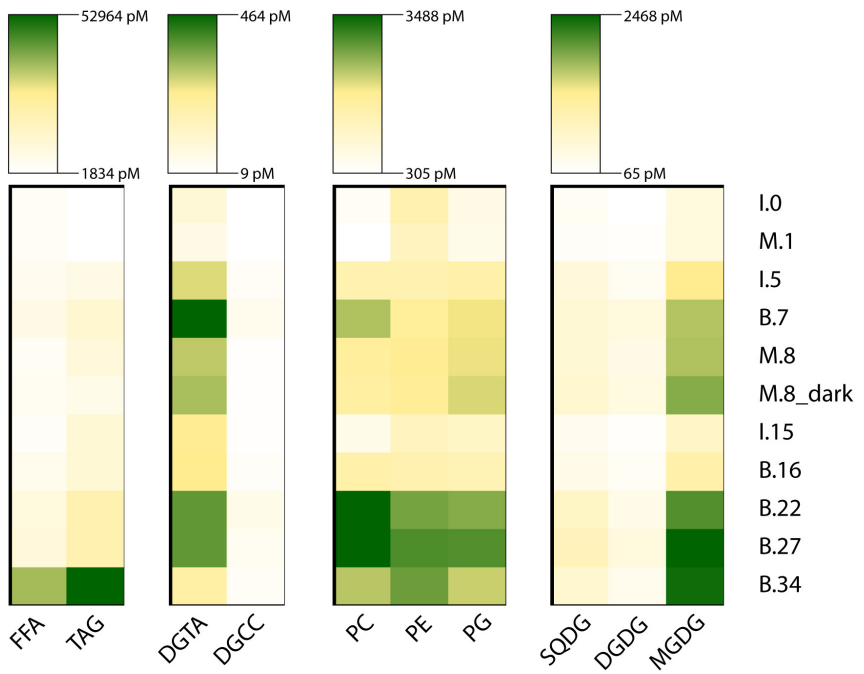

FIGURE 6 | The abundance of major lipid classes during the experiment. The rows are sampling point, where the letter indicates experimental condition (I, ice station; M, microcosm; B, Station B), the number indicates days since the start of the experiment on November 10, 2015. The lipids are grouped according to abundance (TAG and FFA) and physiological role (DGTA and DGCC; PC, PE, and PG; SQDG, DGDG, and MGDG). Due to the large difference in abundance between groups each group is scaled differently.

transcriptomes *T. rotula*, *F. kerguelensis*, and *C. pennatum* were observed to have the strongest and most complex transcriptional response to changing environmental conditions. The specific response, however, and underlying transcriptional patterns varied widely across these references. As seen by the magnitude in PC1 for these points of comparison (**Figure 7B**), *C. pennatum* responded strongest to the experimental conditions in the microcosms, with high values for the transition from Ice Station day −6 and day 0 samples to the microcosm day 8 and Station B day 16 samples. We consider the phytoplankton associated

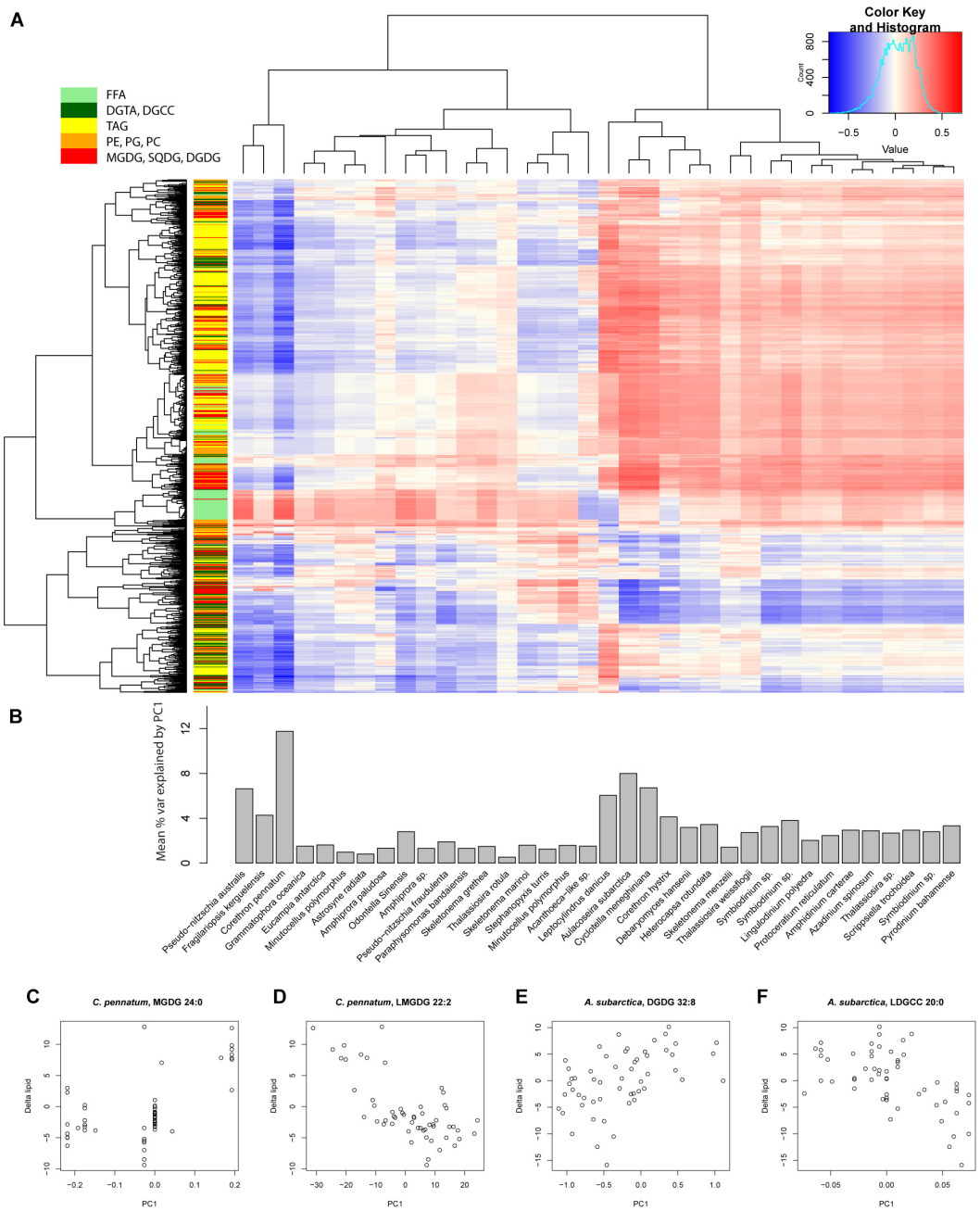

FIGURE 7 | Correlation between the first principal component (PC1) and individual lipids for each reference transcriptome. **(A)** Matrix of Pearson's correlation coefficient (*r*) for each lipid and PC1 for all reference transcriptomes. Columns and rows of the correlation matrix are organized according to hierarchical clustering based on Euclidean distance. Row colorbar indicates the class of lipid. FFA, free fatty acid; DGTA, Diacylglyceryl hydroxymethyl-trimethylalaninee; DGCC, Diacylglyceryl hydroxymethyl-trimethylalaninee; TAG, triacylglycerol; PE, phosphatidylethanolamine; PG, phosphatidylglycerol; PC, phosphatidylcholine; MGDG, monogalactosyldiacylglycerol; SQDG, sulfoquinovosyldiacylglycerol; DGDG, digalactosyldiacylglycerol. **(B)** Barplot of mean % variance explained for all lipids by PC1 for each reference transcriptome. Calculated by taking the mean of r^2 for each column in **(A)**. These values are distinct from the variance explained by PC1 for the transcriptome data described by the principal components. **(C–F)** Scatterplots of Δlipid and PC1 for the highest r^2 values for *Corethron pennatum* (MMETSP0169) and *Aulacoseira subarctica* (MMETSP1064). These two reference transcriptomes had the highest mean % variance explained by PC1.

with the *C. pennatum* reference transcriptome as high light specialists capable of rapidly responding to a stable light regime. Based on the % variance in lipid concentration explained by PC1 (**Figure 7B**), *C. pennatum* was also the dominant driver of the composition of the lipidome over the course of the experiment. Overall, our analysis suggests that the lipidome and transcriptome were only weakly connected. This may reflect a more complex and transient transcriptional regulation of the

lipidome that is not easily detected by correlation, or alternate modes of regulation.

In contrast to *C. pennatum*, *F. kerguelensis* down-regulated the genes coding for DNA polymerase between the microcosm day 1 and day 8 samples, but up-regulated them between the Ice Station day 0 and Station B samples. Similarly, *F. kerguelensis* had a neutral or down-regulated response to these conditions in genes coding for Photosystems I and II. This is consistent with the idea of *F. kerguelensis*-associated phytoplankton as low-light specialists, capable of early-season growth below sea ice and within the marginal ice zone, but inhibited in the higher light regime represented by the microcosm experiments.

The phytoplankton associated with the *T. rotula* reference transcriptome may represent an intermediate case. Like *F. kerguelensis*, *T. rotula* responded strongly in comparisons between Ice Station day 0 and Station B days 27 and 34. Unlike *F. kerguelensis*, *T. rotula* showed an early positive growth response to the microcosm conditions through up-regulation of the genes coding for DNA polymerase. This regulation was not sustained over the course of the microcosm experiments, however, and could represent an effort to repair damage brought on by the rapid increase in light, or a quick transition from a preferential to inhibiting photon dose.

Transcripts associated with several dinoflagellates were observed over the course of the experiment. The dinoflagellate references exhibited similar transcriptional response strength and complexity, and low mean % variance explained by PC1 (**Figure 7B**), suggesting a weak connection to the lipidome. Although very few studies have evaluated the ecological role of dinoflagellates along the WAP, they are thought to form blooms (Schofield et al., 2017) and to play a significant role in the regional carbon budget (Lin et al., 2017). Dinoflagellates are well known for their unusual modes of transcriptional regulation, which can lead to a reduced transcriptional response to changing environmental conditions. Because our analysis considered only the $\log_2$ fold-change of significantly differentially expressed genes, the role of dinoflagellates may be underrepresented in this study. Despite this potential issue, dinoflagellate associated transcripts for PSI, PSII, and RUBISCO dominated transcriptional responses to increased light. This suggests that they are not poised to take immediate advantage of available light, as the diatoms may be, perhaps because they are able to supplement their nutritional needs during low light conditions through mixotrophic grazing.

Our findings come with two important caveats. One is that the true composition of the community does not necessarily reflect the mapping of reads to our reference transcriptomes, however, many of the references mapped are expected members of the WAP phytoplankton assemblage. *F. kerguelensis*, *C. pennatum*, and *T. rotula* in particular have been observed in the region or in coastal Antarctica. *T. rotula* is highly cosmopolitan (Whittaker et al., 2012), while *C. pennatum* and *F. kerguelensis* have previously been observed in WAP phytoplankton blooms (Lange et al., 2007; Świło et al., 2016). It is important to note that the model sea ice diatom *F. cylindrus*, a known low-light specialist with broad distribution in the Antarctic, is not present in the MMETSP database. Thus, read recruitment to *F. kerguelensis* could represent the presence of *F. cylindrus*. Other species not present in our database may also have been present in our samples. To work around this we focused our analysis on the specific response of those taxa we were able to observe.

The second caveat is that transcriptional response to the day 8 dark control in our microcosm experiments is very similar to that of the day 8 treatment. The amount of screening needed to achieve a 1% irradiance level was determined experimentally with the PAR meter, however, it was not possible to verify this light level after the carboys had been screened. Thus we suspect light leakage resulted in a higher light level than anticipated. Although we do not know what range of light was represented by our treatment and control, the expected wide difference in irradiance yet similar response points to the broad niche defined by "normal" light levels.

Here we used a novel analytical approach to couple two high-dimensional datasets. Although our findings are inferential, and further experiments will be required to confirm the changes in gene expression and lipid composition that we observed for different reference transcriptomes, we have identified phytoplankton responding to different light levels brought on by variable sea ice conditions. Putative low light and high light specialists had distinct transcriptional signatures, and impacts on the community lipidome. As sea ice cover along the western Antarctic Peninsula continues to change on annual and decadal scales, we expect these changes to impact the composition of the phytoplankton community, and the concentration and composition of the lipidome. Because of the ecological role played by lipids, which function as key sources of energy, as signaling molecules, and even toxins, we expect these changes to have wider ecosystem ramifications during the critical winter–spring seasonal transition.

DATA AVAILABILITY STATEMENT

The datasets presented in this study can be found in online repositories. The names of the repository/repositories and accession number(s) can be found below: NCBI BioProject, PRJNA494856.

ETHICS STATEMENT

Written informed consent was obtained from the individuals for the publication of any potentially identifiable images or data included in this article.

AUTHOR CONTRIBUTIONS

JB and JC designed the study with input from HD, BV, and NC. JB, JC, and NC carried out the sampling with assistance from CH. DL, HF, and BV contributed the lipidomics analysis. JB carried out the metatranscriptomics analysis and drafted the initial version of the manuscript. RG and CH contributed discussions of protist physiology and enzyme functions. All authors edited the manuscript.

FUNDING

JB was supported by NSF-OPP 1641019, NSF-OPP 1846837, and the Simons Foundation Early Career Marine Microbial Investigator program. BV, DL and JC were supported by NSF (OPP-1543328 and OCE-1756254). CH was supported by NSF OCE-1355720. The Palmer LTER project is support by NSF-OPP 1440435. A small-scale Community Sequencing Project (CSP) award from the DOE Joint Genome Institute supported part of the sequencing effort.

ACKNOWLEDGMENTS

We would like to thank Ashley Goncalves and Chelsea Farischon for assistance with sampling at Palmer Station, and the Palmer Station logistics personnel for their dedication during the 2015–2016 season. Satellite imagery in support of this project (see **Figure 1A**) was kindly provided by the Polar Geospatial Center.

SUPPLEMENTARY MATERIAL

The Supplementary Material for this article can be found online at: https://www.frontiersin.org/articles/10.3389/fmars.2021.593566/full#supplementary-material

Supplementary Figure 1 | PAR profiles for Station B and the Ice Station.

Supplementary Figure 2 | Differential expression of genes coding for DNA polymerase. Only significant values are shown, all other values are represented as 0.

Supplementary Figure 3 | Differential expression of genes coding for Photosystem I. Only significant values are shown, all other values are represented as 0.

Supplementary Figure 4 | Differential expression of genes coding for Photosystem II. Only significant values are shown, all other values are represented as 0.

Supplementary Figure 5 | Differential expression of genes coding for RUBISCO. Only significant values are shown, all other values are represented as 0.

Supplementary Figure 6 | The magnitude of each point of comparison in the first principal component (PC1) of each reference transcriptome. Reference transcriptomes and points of comparison are organized by hierarchical clustering based on Euclidean distance. For the reference transcriptomes only, significant clusters as determined by simprof analysis are indicated by alternating light and dark green colors. Reference transcriptomes that fall in the same cluster, or that clustered more closely, can be interpreted as responding to similar changes in environmental conditions. The nature of the transcriptional response, however, is likely different (and can be evaluated through an analysis of cos^2). The row names in the heatmap describe the two sample points being compared. The letter describes the sample type (M, microcosm; B, Station B; I, Ice Station) and the number describes the experimental day (days from day 0).

Supplementary Figures 7–14 | bye Heatmaps of abundance for the 50 most abundant lipids for all analyzed lipid classes.

REFERENCES

Becker, K. W., Collins, J. R., Durham, B. P., Groussman, R. D., White, A. E., Fredricks, H. F., et al. (2018). Daily changes in phytoplankton lipidomes reveal mechanisms of energy storage in the open ocean. *Nat. Commun.* 9:5179. doi: 10.1038/s41467-018-07346-z

Benton, H. P., Want, E. J., and Ebbels, T. M. D. (2010). Correction of mass calibration gaps in liquid chromatography-mass spectrometry metabolomics data. *Bioinformatics* 26, 2488–2489. doi: 10.1093/bioinformatics/btq441

Bligh, E. G., and Dyer, W. J. (1959). A rapid method of total lipid extraction and purification. *Can. J. Biochem. Physiol.* 37.

Bowman, J., and Ducklow, H. (2015a). Microbial communities can be described by metabolic structure: a general framework and application to a seasonally variable, depth-stratified microbial community from the coastal West Antarctic Peninsula. *PLoS One* 10:e0135868.

Bowman, J., and Ducklow, H. (2015b). *paprica*. Available online at: https://github.com/bowmanjeffs/paprica.

Bowman, J. S., Vick-Majors, T. J., Morgan-Kiss, R. M., Takacs-Vesbach, C., Ducklow, H. W., and Priscu, J. C. (2016). Microbial community dynamics in two polar extremes: the lakes of the mcmurdo dry valleys and the west antarctic peninsula marine ecosystem. *Bioscience* 66, 830–847.

Collins, J. R., Edwards, B. R., Fredricks, H. F., and Van Mooy, B. A. S. (2016). LOBSTAHS: an adduct-based lipidomics strategy for discovery and identification of oxidative stress biomarkers. *Anal. Chem.* 88, 7154–7162. doi: 10.1021/acs.analchem.6b01260

Collins, J. R., Fredricks, H. F., Bowman, J. S., Ward, C. P., Moreno, C., Longnecker, K., et al. (2018). The molecular products and biogeochemical significance of lipid photooxidation in West Antarctic surface waters. *Geochim. Cosmochim. Acta* 232, 244–264. doi: 10.1016/j.gca.2018.04.030

Edwards, B. R., Bidle, K. D., and Van Mooy, B. A. S. (2015). Dose-dependent regulation of microbial activity on sinking particles by polyunsaturated aldehydes: implications for the carbon cycle. *Proc. Natl. Acad. Sci. U.S.A.* 112:201422664. doi: 10.1073/pnas.1422664112

Hummel, J., Segu, S., Li, Y., Irgang, S., Jueppner, J., and Giavalisco, P. (2011). Ultra performance liquid chromatography and high resolution mass spectrometry for the analysis of plant lipids. *Front. Plant Sci.* 2:54. doi: 10.3389/fpls.2011.00054

Kassambara, A., and Mundt, F. (2017). *factoextra: Extract and Visualize the Results of Multivariate Data Analyses*. Available online at: https://cran.r-project.org/package=factoextra (accessed April 01, 2020).

Keeling, P. J., Burki, F., Wilcox, H. M., Allam, B., Allen, E. E., Amaral-Zettler, L. A., et al. (2014). The marine microbial eukaryote transcriptome sequencing project (MMETSP): illuminating the functional diversity of eukaryotic life in the oceans through transcriptome sequencing. *PLoS Biol.* 12:e1001889. doi: 10.1371/journal.pbio.1001889

Kennedy, F., Martin, A., Bowman, J. P., Wilson, R., and McMinn, A. (2019). Dark metabolism: a molecular insight into how the Antarctic sea-ice diatom Fragilariopsis cylindrus survives long-term darkness. *New Phytol.* 223, 675–691. doi: 10.1111/nph.15843

Kuhl, C., Tautenhahn, R., Bottcher, C., Larson, T. R., and Neumann, S. (2012). CAMERA: an integrated strategy for compound spectra extraction and annotation of liquid chromatography/mass spectrometry data sets. *Anal. Chem.* 84, 283–289. doi: 10.1021/ac202450g

LaJeunesse, T. C., Parkinson, J. E., Gabrielson, P. W., Jeong, H. J., Reimer, J. D., Voolstra, C. R., et al. (2018). Systematic revision of Symbiodiniaceae highlights the antiquity and diversity of coral endosymbionts. *Curr. Biol.* 28, 2570.e6–2580.e6. doi: 10.1016/j.cub.2018.07.008

Lange, P. K., Tenenbaum, D. R., De Santis Braga, E., and Campos, L. S. (2007). Microphytoplankton assemblages in shallow waters at Admiralty Bay (King George Island, Antarctica) during the summer 2002-2003. *Polar Biol.* 30, 1483–1492. doi: 10.1007/s00300-007-0309-8

Langmead, B., Trapnell, C., Pop, M., and Salzberg, S. L. (2009). Ultrafast and memory-efficient alignment of short DNA sequences to the human genome. *Genome Biol.* 10:R25. doi: 10.1186/gb-2009-10-3-r25

Lin, Y., Cassar, N., Marchetti, A., Moreno, C., Ducklow, H., and Li, Z. (2017). Specific eukaryotic plankton are good predictors of net community production in the Western Antarctic Peninsula. *Sci. Rep.* 7, 1–11. doi: 10.1038/s41598-017-14109-1

Love, M. I., Huber, W., and Anders, S. (2014). Moderated estimation of fold change and dispersion for RNA-seq data with DESeq2. *Genome Biol.* 15:550. doi: 10.1186/s13059-014-0550-8

Palmer LTER Science Team (2021). *Palmer LTER Datazoo*. Available online at: http://pal.lternet.edu/data.

Popendorf, K. J., Fredricks, H. F., and Van Mooy, B. A. S. (2013). Molecular ion-independent quantification of polar glycerolipid classes in marine plankton using triple quadrupole MS. *Lipids* 48, 185–195. doi: 10.1007/s11745-012-3748-0

R Core Team (2014). *R: A Language and Environment for Statistical Computing*. Available online at: http://www.r-project.org/ (accessed December 1, 2012).

Schofield, O., Saba, G., Coleman, K., Carvalho, F., Couto, N., Ducklow, H., et al. (2017). Decadal variability in coastal phytoplankton community composition in a changing West Antarctic Peninsula. *Deep Sea Res. Part I Oceanogr. Res. Pap.* 124, 42–54. doi: 10.1016/j.dsr.2017.04.014

Smith, C. A., Want, E. J., O'Maille, G., Abagyan, R., and Siuzdak, G. (2006). XCMS: processing mass spectrometry data for metabolite profiling using nonlinear peak alignment, matching, and identification. *Anal. Chem.* 78, 779–787. doi: 10.1021/ac051437y

Stamatakis, A., Zhang, J., and Kobert, K. (2014). PEAR: a fast and accurate Illumina Paired-End reAd mergeR. *Bioinformatics* 30, 614–620. doi: 10.1093/bioinformatics/btt593

Świło, M., Majewski, W., Minzoni, R. T., and Anderson, J. B. (2016). Diatom assemblages from coastal settings of West Antarctica. *Mar. Micropaleontol.* 125, 95–109. doi: 10.1016/j.marmicro.2016.04.001

Tautenhahn, R., Bottcher, C., and Neumann, S. (2008). Highly sensitive feature detection for high resolution LC/MS. *BMC Bioinformatics* 9:504. doi: 10.1186/1471-2105-9-504

Whitaker, D., and Christman, M. (2014). *clustsig: Significant Cluster Analysis*. Available online at: http://cran.r-project.org/package=clustsig (accessed March 1, 2016).

Whittaker, K. A., Rignanese, D. R., Olson, R. J., and Rynearson, T. A. (2012). Molecular subdivision of the marine diatom Thalassiosira rotula in relation to geographic distribution, genome size, and physiology. *BMC Evol. Biol.* 12:209. doi: 10.1186/1471-2148-12-209

Conflict of Interest: The authors declare that the research was conducted in the absence of any commercial or financial relationships that could be construed as a potential conflict of interest.

frontiers in Marine Science

ORIGINAL RESEARCH
published: 24 March 2021
doi: 10.3389/fmars.2021.640050

Winter Carnivory and Diapause Counteract the Reliance on Ice Algae by Barents Sea Zooplankton

Doreen Kohlbach[1], Katrin Schmidt[2], Haakon Hop[1], Anette Wold[1], Amalia Keck Al-Habahbeh[1], Simon T. Belt[2], Matthias Woll[3], Martin Graeve[3], Lukas Smik[2], Angus Atkinson[4] and Philipp Assmy[1]*

[1] Norwegian Polar Institute, Fram Centre, Tromsø, Norway, [2] School of Geography, Earth and Environmental Sciences, University of Plymouth, Plymouth, United Kingdom, [3] Alfred Wegener Institute, Helmholtz Centre for Polar and Marine Research, Bremerhaven, Germany, [4] Plymouth Marine Laboratory, Plymouth, United Kingdom

The Barents Sea is a hotspot for environmental change due to its rapid warming, and information on dietary preferences of zooplankton is crucial to better understand the impacts of these changes on food-web dynamics. We combined lipid-based trophic marker approaches, namely analysis of fatty acids (FAs), highly branched isoprenoids (HBIs) and sterols, to compare late summer (August) and early winter (November/December) feeding of key Barents Sea zooplankters; the copepods *Calanus glacialis*, *C. hyperboreus* and *C. finmarchicus* and the amphipods *Themisto libellula* and *T. abyssorum*. Based on FAs, copepods showed a stronger reliance on a diatom-based diet. Phytosterols, produced mainly by diatoms, declined from summer to winter in *C. glacialis* and *C. hyperboreus*, indicating the strong direct linkage of their feeding to primary production. By contrast, *C. finmarchicus* showed evidence of year-round feeding, indicated by the higher winter carnivory FA ratios of 18:1(n-9)/18:1(n-7) than its larger congeners. This, plus differences in seasonal lipid dynamics, suggests varied overwintering strategies among the copepods; namely diapause in *C. glacialis* and *C. hyperboreus* and continued feeding activity in *C. finmarchicus*. Based on the absence of sea ice algae-associated HBIs (IP_{25} and $IPSO_{25}$) in the three copepod species during both seasons, their carbon sources were likely primarily of pelagic origin. In both amphipods, increased FA carnivory ratios during winter indicated that they relied strongly on heterotrophic prey during the polar night. Both amphipod species contained sea ice algae-derived HBIs, present in broadly similar concentrations between species and seasons. Our results indicate that sea ice-derived carbon forms a supplementary food rather than a crucial dietary component for these two amphipod species in summer and winter, with carnivory potentially providing them with a degree of resilience to the rapid decline in Barents Sea (winter) sea-ice extent and thickness. The weak trophic link of both zooplankton taxa to sea ice-derived carbon in our study likely reflects the low abundance and quality of ice-associated carbon during late summer and the inaccessibility of algae trapped inside the ice during winter.

Keywords: *Calanus*, *Themisto*, Barents Sea, sea ice, carbon sources, trophic markers, polar night

OPEN ACCESS

Edited by:
Anne Helene Solberg Tandberg, University Museum of Bergen, Norway

Reviewed by:
Anja Schulze, Texas A&M University at Galveston, United States
Mariana Díaz-Santana-Iturrios, Andres Bello University, Chile

****Correspondence:***
Doreen Kohlbach
doreen.kohlbach@npolar.no

Specialty section:
This article was submitted to Marine Evolutionary Biology, Biogeography and Species Diversity, a section of the journal Frontiers in Marine Science

Received: *10 December 2020*
Accepted: *02 March 2021*
Published: *24 March 2021*

Citation:
Kohlbach D, Schmidt K, Hop H, Wold A, Al-Habahbeh AK, Belt ST, Woll M, Graeve M, Smik L, Atkinson A and Assmy P (2021) Winter Carnivory and Diapause Counteract the Reliance on Ice Algae by Barents Sea Zooplankton. Front. Mar. Sci. 8:640050. doi: 10.3389/fmars.2021.640050

INTRODUCTION

In Arctic marine ecosystems, primary and secondary production, and subsequently its availability to higher trophic levels, are subject to a strong seasonality (Wassmann and Slagstad, 1993; Weydmann et al., 2013). Zooplankton in the Barents Sea are well adapted to interannual and seasonal environmental changes and fluctuations in food supply, from a low sea-ice cover or open water conditions and high incident irradiance during the summer months ranging to a consolidated sea-ice cover and extremely low light levels during the winter period (Conover and Huntley, 1991; Hagen, 1999; Bandara et al., 2016). Despite great inter-annual variability (Årthun et al., 2012; Herbaut et al., 2015), especially during the winter months (December throughout February), the Barents Sea has experienced a strong decline in sea-ice extent and concentration over the last decades, mostly due to higher water temperatures (Onarheim and Årthun, 2017; Barton et al., 2018; Årthun et al., 2019).

During spring and early summer, the Barents Sea is highly productive (Stramska and Bialogrodzka, 2016), particularly in the marginal ice zone (MIZ) (Falk-Petersen et al., 2007). However, productivity varies significantly depending on oceanographic conditions, nutrient concentrations and sea-ice cover (Sakshaug and Slagstad, 1992; Falk-Petersen et al., 2000b; Reigstad et al., 2002; Hop et al., 2019). Nevertheless, phytoplankton carbon is generally considered to be sufficient to meet the energetic requirements of the food web (Verity et al., 2002; Tamelander et al., 2006; Wassmann et al., 2006; Kohlbach et al., 2021). Additionally, sea ice-associated (sympagic) primary production can provide an alternative or supplemental source of carbon for some zooplankton taxa, early in the season (Søreide et al., 2008; Gradinger, 2009) and also during summer (Scott et al., 1999; Assmy et al., 2013; Kohlbach et al., 2016, 2021; Brown et al., 2017). During winter, primary production levels in the water column (Kvernvik et al., 2018) and in sea ice are practically zero (Mikkelsen et al., 2008), and the ice algal biomass trapped in internal ice layers might be difficult to access for grazers (Van Leeuwe et al., 2018). Compared to sea ice in the Arctic Ocean, the Barents Sea winter sea-ice is relatively thin and has been identified as being particularly affected by sea-ice loss (Francis and Hunter, 2007; Onarheim and Årthun, 2017). The reduced expansion of winter sea ice and continuing thinning of the ice cover has consequences for winter-active species that depend on the sympagic habitat for shelter and foraging (Hop et al., 2000; Poltermann, 2001; Werner and Gradinger, 2002; Werner and Auel, 2005), but little is known about the impact on food-web interactions.

Zooplankton are a vital link between primary production and higher tropic levels, and information on their lifestyle and feeding behavior is crucial to understand the functioning of marine ecosystems under present conditions and future change (Falk-Petersen et al., 2007; Atkinson et al., 2012; Pecuchet et al., 2020). The lower trophic levels of the Barents Sea food-web are dominated by *Calanus* copepods (Aarflot et al., 2018), with *C. glacialis* being dominant in Arctic shelf waters and the boreal *C. finmarchicus* in the warmer Atlantic sector. Both of these species are generally more abundant in the sampling region (**Figure 1**) than the larger *C. hyperboreus* that prefers deeper

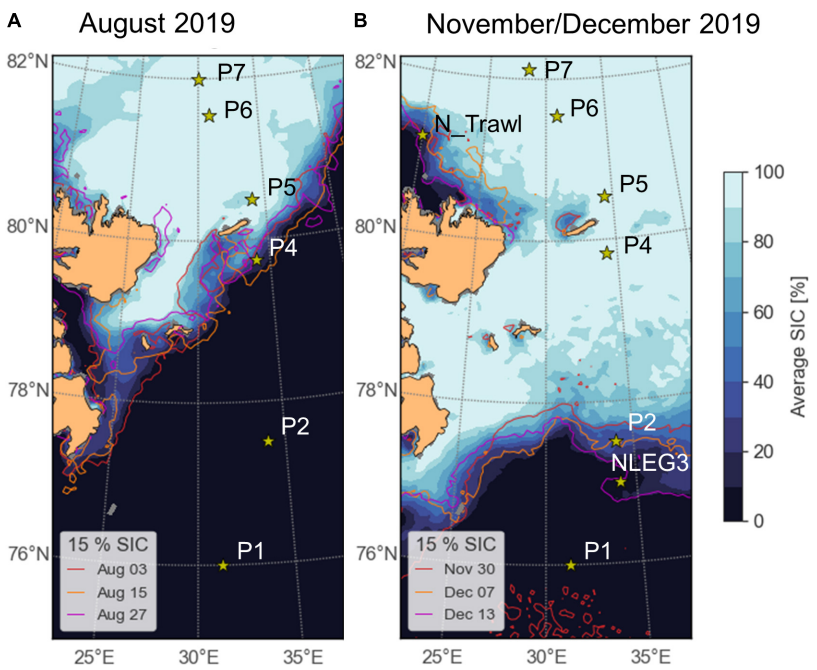

FIGURE 1 | Sampling area with sampling stations during Nansen Legacy cruises **(A)** Q3 (polar day, August 2019) and **(B)** Q4 (polar night, November/December 2019). Sea-ice concentrations (*SIC*%) are shown for the beginning, mid and end of sampling for each sampling campaign, respectively. *SIC* data acquired from Bremen University (http://www.iup.uni-bremen.de:8084/amsr2/) (Spreen et al., 2008). More detailed information on sampling stations can be found in Kohlbach et al. (2021).

water masses (Hirche and Mumm, 1992; Hirche, 1997). *Themisto* amphipods, such as *T. libellula* and *T. abyssorum*, are major contributors to the macrozooplankton biomass in the study region (Dalpadado et al., 2001; Havermans et al., 2019). Both taxa serve as important prey for fish, seabirds and whales (Hop and Gjøsæter, 2013; Jakubas et al., 2016; Haug et al., 2017; Eriksen et al., 2020), but show significant differences in life-history strategies and feeding modes.

During winter, some Arctic zooplankton switch from herbivorous to omnivorous or carnivorous diets (Werner and Auel, 2005), while others rely at least partly on their lipid stores built up during the productive season (Hagen and Auel, 2001). The latter is the case for diapausing *Calanus* copepods (Falk-Petersen et al., 2009; Choi et al., 2020), and has also been described for Antarctic calanoid copepods (Atkinson, 1998). Governed by their energy reserves, *Calanus hyperboreus*, for example, has the ability to reproduce during winter (Melle and Skjoldal, 1998; Hirche, 2013; Halvorsen, 2015), in contrast to *C. finmarchicus*, which is not able to reproduce successfully in the high Arctic (Hirche and Kosobokova, 2007). Besides decreasing their metabolic activity, there are indications that Arctic *Calanus* spp. remain actively feeding also during winter (Søreide et al., 2008; Hobbs et al., 2020) with a possible increase in carnivory (Cleary et al., 2017), which would be in line with the recently suggested surprisingly high biological activity during the Arctic polar night (Berge et al., 2015, 2020). Early in the season, ice-associated food can be an important carbon source for the reproduction of *Calanus glacialis* while pelagic production is still low (Wold et al., 2011; Daase et al., 2013; Durbin and Casas, 2014), and all three *Calanus* species rely on phytoplankton (mostly diatoms) during summer (Campbell et al., 2009). The potential importance of sea-ice algae for copepods that do not perform diapause during winter is unclear (Cleary et al., 2017); thus far, information on their carbon source composition during the dark period is mostly restricted to late autumn (Scott et al., 2000) and the winter-spring transition (Wold et al., 2011). Other species with a more omnivorous/carnivorous lifestyle, such as *Themisto* amphipods, are less impacted by the lower algal productivity and can thus remain active during winter (Hagen and Auel, 2001; Kraft et al., 2013); they have a pelagic lifestyle but are often encountered at the sea ice-water interface (David et al., 2015) and are capable of utilizing sympagic carbon (Wang et al., 2015; Kohlbach et al., 2016, 2021).

Most polar zooplankton are opportunistic feeders with a pronounced dietary plasticity (e.g., Berge et al., 2020), capable of utilizing carbon of different origin and from multiple trophic positions. Thus, some can switch from a pelagic lifestyle during summer to a stronger reliance on sympagic food sources during winter, as illustrated for Antarctic copepods and amphipods (Kohlbach et al., 2018). A similar seasonal change from pelagic to sympagic carbon source composition could be expected for Arctic crustaceans, provided they feed to some extent throughout the winter and can actually access the ice-associated carbon. Preferred dietary sources of marine animals and their seasonality can be elucidated from the composition of lipid-based trophic markers (Leu et al., 2020). Their stability when transferred along the marine food chain makes them valuable trophic proxies in disentangling food-web relationships and revealing the importance of varying carbon sources (e.g., Scott et al., 1999; Iverson, 2009). Certain fatty acids (FAs), called trophic marker FAs, are produced by (pelagic and sympagic) diatoms [e.g., 16:1(n-7), 20:5(n-3)] and others by (pelagic and sympagic) dinoflagellates [18:4(n-3), 22:6(n-3)] (Dalsgaard et al., 2003), and can thus indicate the importance of diatom- versus dinoflagellate-derived food in a consumer. FAs can be incorporated into membrane lipids for the structural support of cell membranes and somatic growth, while others can be used as energy reserves in the form of storage lipids (Stübing et al., 2003; Falk-Petersen et al., 2009; Parrish, 2009; Ruess and Müller-Navarra, 2019). When food is abundant, marine animals accumulate large lipid reserves, which can be utilized for energy-intensive reproduction processes and to ensure survival during periods when food is not sufficiently abundant (Lee et al., 2006). Thus, the distribution of membrane and storage lipids in an animal's body can give information on their nutritional condition and overwintering strategies (Kattner et al., 1994). Highly branched isoprenoid (HBI) lipids and sterols can further complement food-web studies (e.g., Schmidt et al., 2018; Kohlbach et al., 2021). Different HBIs allow for the differentiation of sympagic (IP_{25} and $IPSO_{25}$) and pelagic (HBIs III and IV) carbon (Belt et al., 2012; Brown and Belt, 2012; Belt, 2018), whereas phyto- and animal-derived sterols allow conclusions about the degree of carnivory of a species (Drazen et al., 2008; Ruess and Müller-Navarra, 2019).

Based on the absence of sea ice algae-produced HBIs in their carbon pool, *Calanus* copepods collected during August 2019 in the Barents Sea had no verifiable trophic interaction with the sea-ice system, while these sea ice-produced metabolites were detected in *Themisto* amphipods during this period of the year (Kohlbach et al., 2021). Building on these previous results, the present study aims to assess species-specific changes in lipid content and lipid-based trophic markers indicating diet-source variability of these invertebrates during the transition from late summer (August 2019) to early winter (November/December 2019).

MATERIALS AND METHODS

Sampling

As a contribution to the Norwegian Nansen Legacy project (arvenetternansen.com), samples were collected during the summer expedition Q3 (5 to 27 August 2019) and the winter expedition Q4 (28 November to 17 December 2019) onboard RV *Kronprins Haakon* in the northern Barents Sea (**Table 1** and **Figure 1**). During Q3, sampling was carried out from south to north, while on Q4 the transect was sampled from north to south. Detailed information about sampling during Q3 can be found in Kohlbach et al. (2021).

During Q3, *Calanus* copepods (*C. glacialis* Jaschnov, 1955; *C. hyperboreus* Krøyer, 1838; *C. finmarchicus* Gunnerus, 1770) and *Themisto* amphipods (*Themisto libellula* Liechtenstein, 1822; *T. abyssorum* Boeck, 1870) were collected at six stations

TABLE 1 | Station information for RV *Kronprins Haakon* seasonal Nansen Legacy cruises Q3 during August 2019 and Q4 during November/December 2019 in the Barents Sea.

Station #	Date of sampling (2019)	
	Q3	Q4
P1	08/08	13/12
NLEG 3		11/12
P2	11/08	10/12
P4	14/08	08/12
P5_ice		06/12
P5	15/08, 16/08	06/12
P6_ice	17/08	
P6	18/08	05/12
P7_ice	20/08	02/12
P7	20/08, 21/08	01/12
N_TRAWL		30/11

Detailed information on sampling stations can be found in Kohlbach et al. (2021).

(Kohlbach et al., 2021) and during Q4 at eight stations (**Table 1** and **Figure 1**) with MIK nets (1200 μm with 500 μm cod end), WP3 nets (1000 μm), Macroplankton trawls (multiple mesh sizes, 8 mm bottom of the net), Bongonets (180 μm), Multinets (180 μm) and WP2 nets (90 μm). Samples were sorted into species (**Supplementary Figures 1,2**) and stage/size groups (**Table 2**) onboard the ship and immediately frozen at −80°C until further processing. The different *Calanus* species were differentiated based on morphology and prosome lengths according to Kwasniewski et al. (2003). Small species/individuals were pooled by stage/size group in order to obtain sufficient sample material for analyses (**Table 2**).

During Q3, pelagic particulate organic matter (PPOM) was collected at six stations (P1, P2, P4, P5, P6, and P7) with Niskin bottles attached to a CTD rosette at the depth of the chlorophyll (Chl) *a* maximum (between 14 and 73 m). During Q4, water samples were collected at five stations (P1, P4, P5, P6, and P7) at 20 m depth. Volumes of 1.2 to 3 L of seawater were filtered via a vacuum pump through pre-combusted Whatman GF/F filters (3 h, 550°C) and PPOM filters were stored at −80°C until further processing. Chlorophyll *a* concentrations reached up to 2.6 μg L^{-1} during summer and were generally below 0.05 μg L^{-1} during winter (Vader et al., 2021).

During both sampling campaigns, ice-associated POM (IPOM) was collected at two stations, respectively, (Q3: P6_ice, P7_ice; Q4: P5_ice, P7_ice). The bottom 10 cm of the ice cores were melted in the dark without the addition of filtered seawater. For each sample, between 570 and 640 mL of melted ice sample was filtered by a vacuum pump through pre-combusted 47 mm GF/F filters and filters were stored at −80°C until further processing. Mean Chl *a* concentrations (n = 2 each) in the bottom 3 cm of the sea ice were higher during the summer sampling (P6_ice: 0.4 μg L^{-1}, P7_ice: 2.3 μg L^{-1}) compared to the winter ice cores (P5_ice: 0.04 μg L^{-1}, P7_ice: 0.3 μg L^{-1}; Vader et al., 2021).

TABLE 2 | Zooplankton collected during the RV *Kronprins Haakon* expeditions Q3 (August 2019) and Q4 (November/December 2019) in the Barents Sea.

Species	Stage/sex or length group (mm)*		Ind. per sample		Dry weight/ ind. (mg)**		Total lipids/ dry weight (%)**	
	Q3	Q4	Q3	Q4	Q3	Q4	Q3	Q4
Calanus glacialis	CIV, CV, AF	CV, AF, AM	5 to 31	10 to 25	–	0.7 to 1.2 (0.9 ± 0.2)	–	12.0 to 38.2 (27.2 ± 10.6)
Calanus hyperboreus	CIV, CV, AF	CV, AF, AM	4 to 22	5 to 12	2.2 to 6.2 (3.7 ± 1.4)	2.4 to 6.5 (4.2 ± 1.4)	4.0 to 45.9 (29.7 ± 15.7)	3.2 to 40.0 (31.1 ± 10.5)
Calanus finmarchicus	CIV, CV, AF	CIV, CV	8 to 30	30		0.3 to 0.4 (0.4 ± 0.1)	–	34.9 to 43.4 (38.6 ± 3.0)
Themisto libellula	5–10, 10–20	10–20, 20–30, 30–40	2 to 8	1 to 3	1.2 to 6.1 (3.5 ± 2.0)	12.0 to 115.5 (43.4 ± 29.4)	4.3 to 11.9 (8.8 ± 3.2)	3.3 to 19.7 (10.8 ± 4.2)
Themisto abyssorum	5–10, 25–30	0–10, 10–20	3 to 25	3 to 8	0.7 to 17.1 (11.2 ± 7.3)	2.9 to 12.8 (7.6 ± 5.3)	16.5 to 19.3 (18.2 ± 1.3)	5.7 to 11.5 (7.6 ± 2.0)

Values are presented as range, with mean ± SD in brackets.
AF, adult female; AM, adult male; CIV and CV, copepodid stages IV and V.
**Copepods measured from base of rostrum to the tip of the last prosome segment; amphipods measured from base of rostrum to end of urosome.*
***Individuals used for lipid class and fatty acid analyses. For n see **Supplementary Table 2**.*

Lipid Classes and Fatty Acids

Lipid classes and FAs were analyzed at the Alfred Wegener Institute, Bremerhaven, Germany. Details on sample preparation, analysis and lab equipment can be found in Kohlbach et al. (2021). Briefly, total lipids were extracted from the freeze-dried samples using a modified procedure from Folch et al. (1957) with dichloromethane/methanol (2:1, v/v). Lipid class analysis of the zooplankton was performed directly on the extracted lipids (Graeve and Janssen, 2009) via high performance liquid chromatography. Lipids were separated into neutral (= storage lipids) and polar lipid classes (= membrane lipids; **Supplementary Table 1**).

Total lipids were converted into fatty acid methyl esters (FAMEs) by transesterification in methanol, containing 3% concentrated sulfuric acid, and separated via gas chromatography (Kattner and Fricke, 1986). Total lipids were estimated using an internal standard (C23:0). FAs are expressed by the nomenclature A:Bn-X, where A represents the number of carbon atoms, B the amount of double bonds, and X gives the position of the first double bond starting from the methyl end of the carbon chain. The proportions of individual FAs are expressed as mass percentage of the total FA content.

Dry weights and percentage total lipids per dry weight are summarized in **Table 2**.

To study changes in carbon-source composition of the zooplankton species from summer to winter, we investigated relative proportions of marker FAs that can inform about carbon-source preferences of the consumers. The FAs 16:1(n-7), 16:4(n-1), and 20:5(n-3) are mainly produced by diatoms (= diatom-associated FAs), and the FAs 18:4(n-3) and 22:6(n-3) (= dinoflagellate-associated FAs) are predominantly produced by dinoflagellates and the prymnesiophyte *Phaeocystis* (Falk-Petersen et al., 1998; Reuss and Poulsen, 2002; Dalsgaard et al., 2003). FA ratios of 16:1(n-7)/16:0, ΣC16/ΣC18 and 20:5(n-3)/22:6(n-3) $>$ 1 can indicate a dominance of diatom-produced versus dinoflagellate-produced carbon in an algal community or carbon pool of a consumer. *Calanus* spp. biosynthesize the monounsaturated long-chained FAs 20:1 and 22:1 (all isomers), which then can indicate the importance of *Calanus* spp. as a food source for a consumer (Sargent and Falk-Petersen, 1988; Falk-Petersen et al., 1990). The FA 18:1(n-7) derives from the elongation of 16:1n-7 in algae (Falk-Petersen et al., 1990) whereas 18:1(n-9) can be produced by the consumers (Graeve et al., 1994; Nyssen et al., 2005), and ratios of 18:1(n-9)/18:1(n-7) (carnivory index) can further inform about the degree of carnivory in a consumer (Graeve et al., 1997; Falk-Petersen et al., 2000a; Auel et al., 2002).

PPOM was analyzed on triplicates for each station (Q3: total n = 18, Q4: total n = 15). Q3 IPOM was analyzed on duplicates (total n = 4) and Q4 IPOM on individual samples (total n = 2).

Highly Branched Isoprenoids and Sterols

Highly branched isoprenoids and sterols were analyzed at the University of Plymouth, United Kingdom. Details on sample preparation, analysis and lab equipment can be found in Kohlbach et al. (2021). Briefly, total lipids were extracted with chloroform/methanol (2:1, v/v) and saponified with 20% potassium hydroxide in water/methanol (1:9, v/v). Non-saponifiable lipids were purified by open column chromatography (SiO_2). The sea ice algae-associated HBIs IP_{25} (m/z 350.3) and $IPSO_{25}$ (m/z 348.3), and the pelagic HBIs III and IV (m/z 346.3), were analyzed by gas chromatography mass spectrometry (GC-MS). HBIs were quantified by integrating individual ion responses in single-ion monitoring mode, and normalizing these to the corresponding peak area of the internal standard and an instrumental response factor obtained from purified standards (Belt et al., 2012).

Sterols were eluted from the same silica column using hexane:methylacetate (4:1,v/v). Sterol fractions were derivatized using N,O-bis(trimethylsilyl)trifluoroacetamide (BSTFA) and analyzed by GC-MS. Individual sterols were identified by comparison of the mass spectra of their trimethylsilyl-ethers with published data (Belt et al., 2018). The main identifiable sterols were those commonly synthesized by plants (hereafter: phytosterols): brassicasterol (24-methylcholesta-5,22E-dien-3β–ol; m/z 470), sitosterol (24-ethylcholest-5-en-3β–ol; m/z 396), chalinasterol (24-methylcholesta-5,24(28)-dien-3β–ol; m/z 470) and campesterol (24-methylcholest-5-en-3β–ol; m/z 382) and those that are synthesized by both plants and animals (hereafter: zoosterols): cholesterol (Cholest-5-en-3β–ol; m/z 458), desmosterol (Cholesta-5,24-dien-3β–ol; m/z 343) and dehydrocholesterol (Cholesta-5,22E-dien-3β–ol; m/z 327).

Statistical Analyses

Statistical significance of differences in trophic markers between summer and winter in POM and the zooplankton were assessed using unpaired Student's t-tests. A statistical threshold of $\alpha = 0.05$ was chosen, and results with $p \leq 0.05$ were considered significant. All measures of statistical variation are reported as means $\pm$1 SD. Prior to statistical analysis, the data were verified for normality of distribution. For testing, lipid class and FA data were transformed by applying an arcsine square root function to meet normality requirements for parametric statistics (Legendre and Legendre, 2012). All statistical analyses and data visualization were run in R v.3.4.3 (R Core Team, 2017), using the R package ggplot2 (Wickham, 2016).

RESULTS

Variability in Zooplankton Lipid Class Composition

In all species, the relative proportions of the neutral lipids, mainly wax esters (WEs) and triacylglycerols (TAGs), during summer (mean 66% in *T. libellula* to 97% in *C. hyperboreus*) and winter (mean 79% in *T. libellula* to 98% in *C. hyperboreus*) exceeded the proportions of the polar lipids, mainly phosphatidylethanolamines (PEs) and phosphatidylcholines (PCs) during summer (mean 3% in *C. hyperboreus* and *C. finmarchicus* to 34% in *T. libellula*) and winter (mean 2% in *C. hyperboreus* to 21% in *T. libellula*). The lipid content of the *Calanus* copepods consisted almost entirely of WEs during both seasons (mean $\geq$79%; **Figure 2**). In *T. libellula*, WEs and TAGs

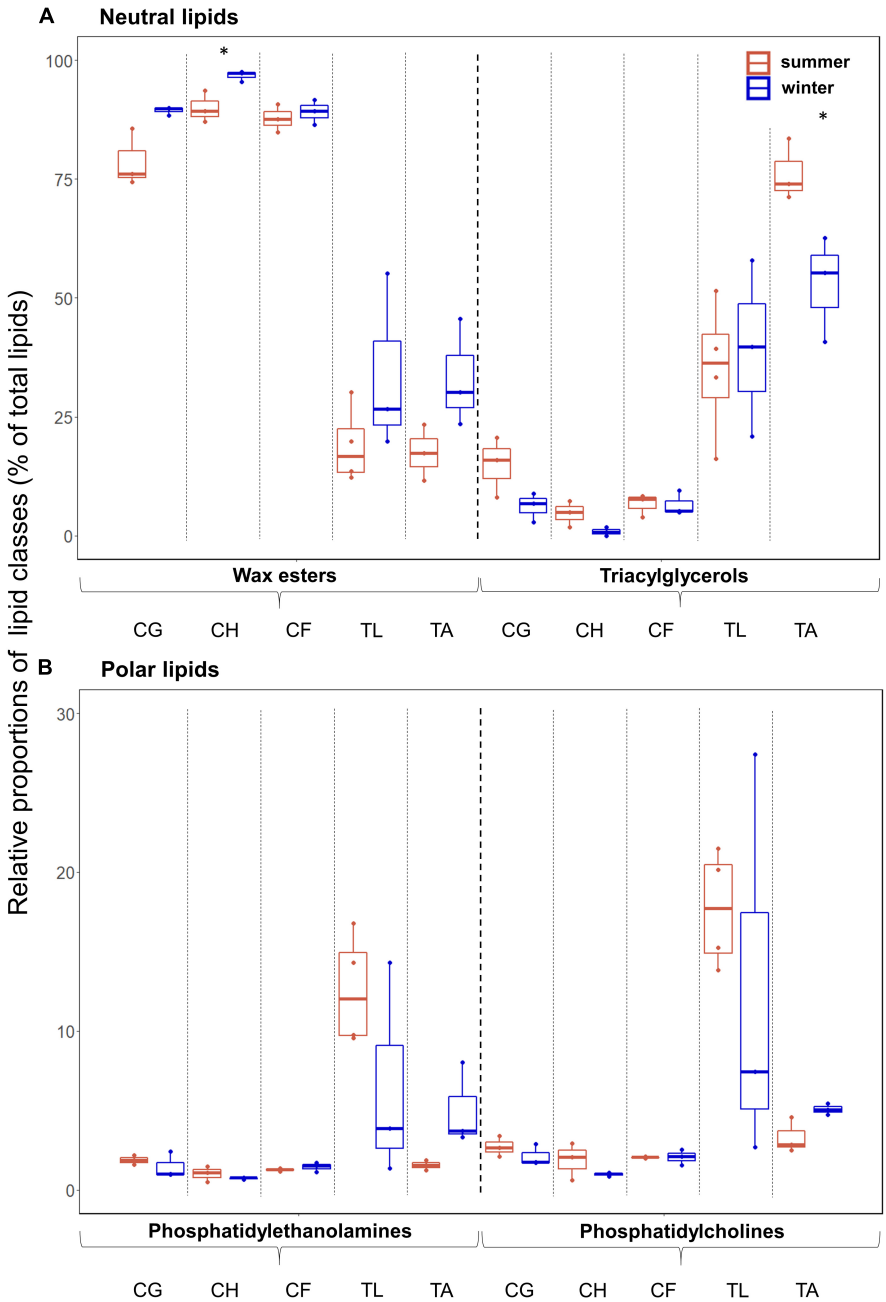

FIGURE 2 | Lipid class composition (as % of total lipids) during summer (Q3) and winter (Q4) in the zooplankton. **(A)** Neutral lipids and **(B)** polar lipids in the copepods *Calanus glacialis* (CG; Q3: $n = 3$, Q4: $n = 3$), *C. hyperboreus* (CH; Q3: $n = 3$, Q4: $n = 3$), *C. finmarchicus* (CF; Q3: $n = 3$, Q4: $n = 3$), and the amphipods *Themisto libellula* (TL; Q3: $n = 4$, Q4: $n = 3$) and *T. abyssorum* (TA; Q3: $n = 3$, Q4: $n = 3$). Horizontal bars in the box plots indicate median proportional values. Upper and lower edges of the boxes represent the approximate 1st and 3rd quartiles, respectively. Vertical error bars extend to the lowest and highest data value inside a range of 1.5 times the inter-quartile range, respectively (R Core Team, 2017). Individual datapoints are represented by the dots. Statistical differences between seasons are marked with an asterisk: $^{*}p \leq 0.05$, $^{**}p \leq 0.01$, $^{***}p \leq 0.001$.

contributed equally to the neutral lipid fraction in winter, while in *T. abyssorum,* TAGs had higher relative contributions than WEs during both summer and winter (**Figure 2A**). In all species, the proportions of WEs were higher during winter compared to summer (significant difference in *C. hyperboreus*). In contrast, proportions of TAGs were higher during summer compared to winter in all species except for *T. libellula* (significant difference in *T. abyssorum*). The relative contributions of the polar lipids PC and PE showed no significant seasonal differences within each species, but were somewhat higher during winter compared to summer in *T. abyssorum* (**Figure 2B**). Relative proportions of individual lipid classes can be found in **Supplementary Table 1**.

Variability in FA Composition

Pelagic and Ice-Associated Particulate Organic Matter (PPOM and IPOM)

During summer, the sum of diatom-associated FAs 16:1(n-7), 16:4(n-1), and 20:5(n-3) was on average more than twice as high in IPOM (mean 43%) compared to PPOM (mean 18%), whereas the sum of dinoflagellate-associated FAs 18:4(n-3) and 22:6(n-3) was on average more than four times higher in PPOM (mean 17%) than in IPOM (mean 4%; **Figure 3**). During winter, the sum of diatom-associated FAs was slightly higher in PPOM (mean 12%) than in IPOM (mean 9%), and the sum of dinoflagellate-associated FAs was on average nine times higher in PPOM (mean 9%) compared to IPOM (mean 1%).

In both PPOM and IPOM, seasonal variability in FA profiles was mainly driven by differences in trophic marker FAs. In PPOM, all marker FAs, except for 16:1(n-7), had higher relative proportions during summer compared to winter, with significant differences in the diatom-associated FA 20:5(n-3) and the dinoflagellate-associated FA 18:4(n-3) (**Figure 3**). The averaged sum of dinoflagellate-associated FAs in PPOM was about twice as high during summer compared to winter. In IPOM, the same pattern was observed, with significantly higher proportions of the diatom-associated FA 16:4(n-1) and the dinoflagellate-associated FA 22:6(n-3) in summer compared to winter. Moreover, the diatom-associated FA 16:1n-7 dominated the IPOM FA profile during summer (mean 36%), whereas during winter, the relative proportions of the marker FAs were more evenly distributed (**Figure 3**). In summer, the averaged sum of diatom-associated FAs in IPOM was about five times higher than in winter, and the sum of dinoflagellate-associated FAs was four times higher. Relative proportions of individual FAs can be found in **Supplementary Table 2**.

Zooplankton

Overall, differences in diatom-associated FAs were more pronounced than differences in dinoflagellate-associated FAs among the zooplankton (**Figures 4A,B**). Among all species, *C. hyperboreus* had the most stable fatty acid composition when transitioning from summer to winter conditions (**Figure 4**), and variability in FAs was not as pronounced as in the other species. In most species, the relative proportions of the diatom-associated FAs 16:4(n-1) (except for *T. libellula*) and 20:5(n-3) (except for *C. hyperboreus*) were significantly higher in summer than in winter (**Figure 4A**). There was no clear seasonal pattern apparent for the relative proportions of the two dinoflagellate-associated FAs. For example, in *C. glacialis* (**Figure 4B**; summer: mean 7%, winter: mean 4%) and *T. abyssorum* (summer: mean 8%, winter: mean 3%), the dinoflagellate-associated FA 18:4(n-3) had higher levels during summer, while in *C. finmarchicus*, this FA had higher levels during winter (summer: mean 5%, winter: mean 9%). The dinoflagellate-associated FA 22:6(n-3) had significantly higher levels in *T. libellula* collected during summer (mean 19%) compared to winter (mean 8%; **Figure 4B**), while in all other species seasonal differences in this FA were insignificant. Mean relative proportions of calanoid copepod-associated FAs were higher in winter (26.5 ± 8.4%) compared to summer (10.7 ± 2.2%) in *T. libellula*, but remained seasonally unchanged in *T. abyssorum* (19.9 ± 3.8 and 21.0 ± 4.8%, respectively). Relative proportions of individual FAs can be found in **Supplementary Table 2**.

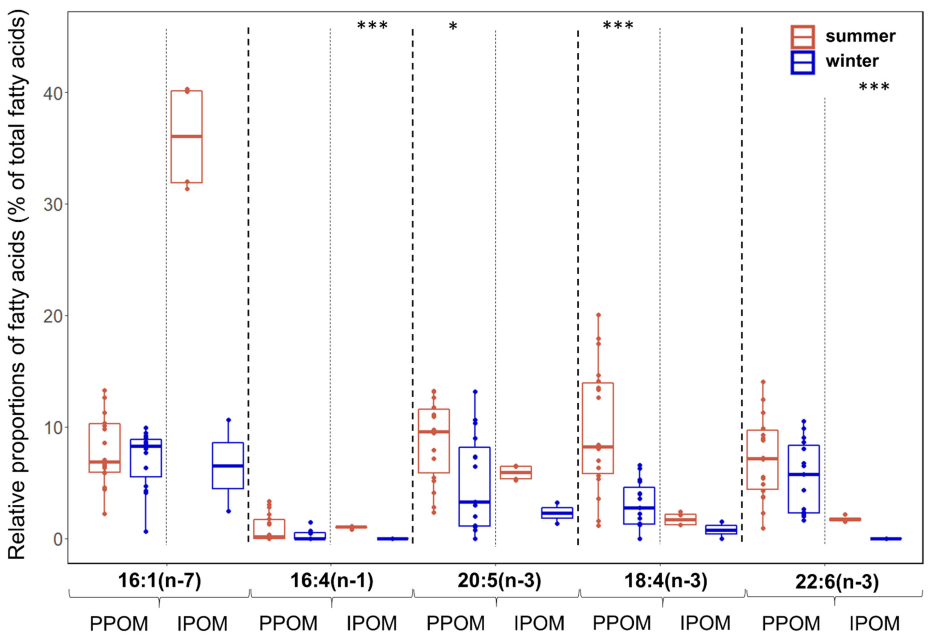

FIGURE 3 | Relative proportions (as % of total fatty acids-FAs) of diatom- [16:1(n-7), 16:4(n-1), 20:5(n-3)] and dinoflagellate-associated marker FAs [18:4(n-3), 22:6(n-3)] during summer (Q3) and winter (Q4) in pelagic particulate organic matter (PPOM) (Q3: *n* = 15, Q4: *n* = 18) and ice-associated particulate organic matter (IPOM) (Q3: *n* = 4, Q4: *n* = 2). Box plot design is described in **Figure 2**.

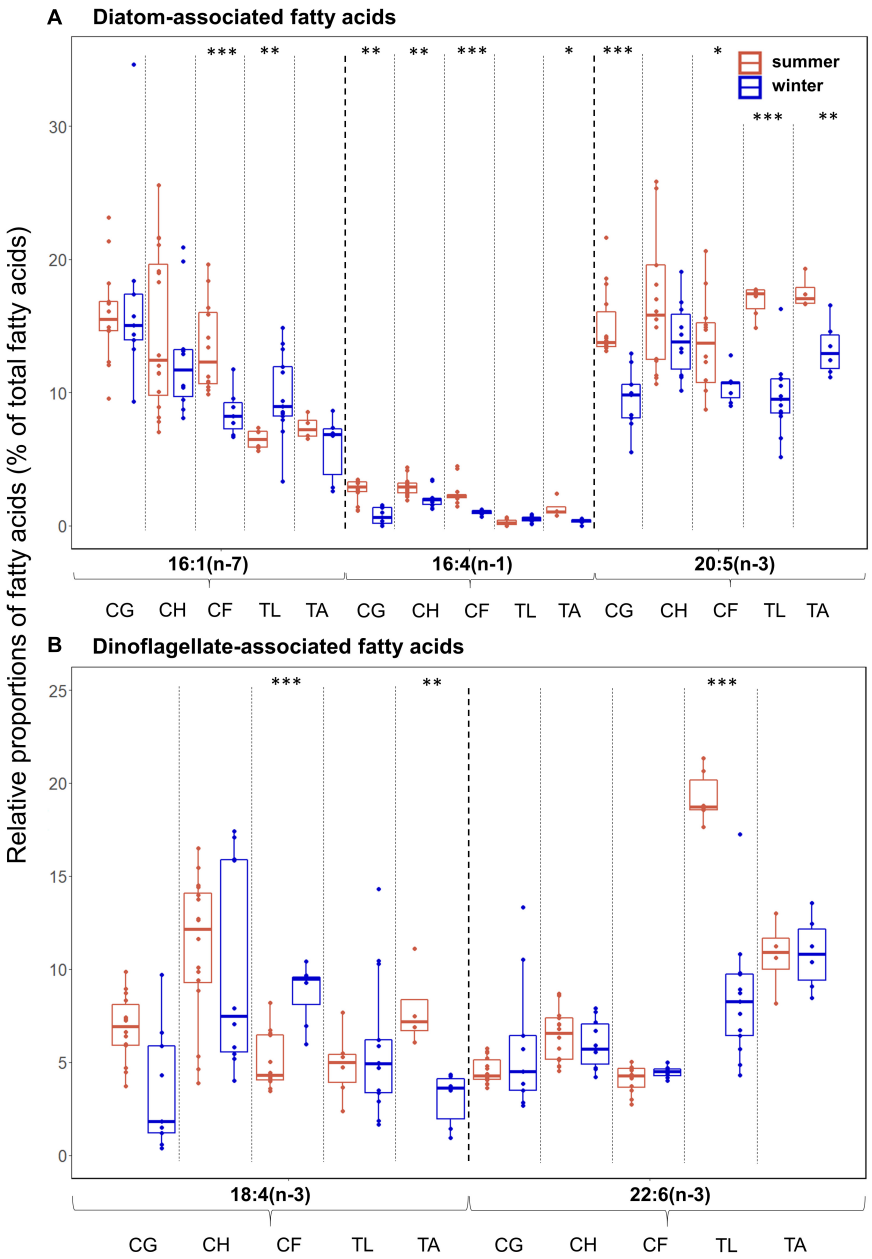

FIGURE 4 | Relative proportions (as % of total fatty acids-FAs) of **(A)** diatom- [16:1(n-7), 16:4(n-1), 20:5(n-3)] and **(B)** dinoflagellate-associated marker FAs [18:4(n-3), 22:6(n-3)] during summer (Q3) and winter (Q4) in the copepods *Calanus glacialis* (CG; Q3: *n* = 14, Q4: *n* = 9), *C. hyperboreus* (CH; Q3: *n* = 16, Q4: *n* = 10) and *C. finmarchicus* (CF; Q3: *n* = 12, Q4: *n* = 7) and the amphipods *Themisto libellula* (TL; Q3: *n* = 6, Q4: *n* = 13) and *T. abyssorum* (TA; Q3: *n* = 4, Q4: *n* = 6). Box plot design is described in **Figure 2**.

Based on the diatom/dinoflagellate marker FA ratios, *Calanus* spp. had a stronger diatom signal than amphipods during both seasons (**Table 3**). Based on the ratio 18:1(n-9)/18:1(n-7), the degree of carnivory increased from summer to winter in *C. finmarchicus* and both *Themisto* species, while the ratio 16:1(n-7)/16:0 simultaneously decreased in *C. finmarchicus* and *T. abyssorum*. The ratio 20:5(n-3)/22:6(n-3) decreased in *C. glacialis*, *C. finmarchicus* and *T. abyssorum* from summer to winter (**Table 3**).

Variability in HBI and Sterol Composition

In both seasons, PPOM and all three *Calanus* species did not contain detectable quantities of the sea ice algae-associated HBIs IP_{25} and $IPSO_{25}$ (**Figure 5A**). In both amphipod species, mean sea ice algae-associated HBI concentrations were slightly higher in winter compared to summer. Mean concentrations of the pelagic/MIZ HBIs III and IV were slightly lower in winter than in summer in *C. glacialis*, *C. hyperboreus*, and *T. libellula*, but

TABLE 3 | Trophic marker fatty acid ratios (mean ± SD) in copepods and amphipods during summer (Q3) and winter (Q4).

Parameter	Description	*Calanus glacialis*		*Calanus hyperboreus*		*Calanus finmarchicus*		*Themisto libellula*		*Themisto abyssorum*	
		Q3	Q4	Q3	Q4	Q3	Q4	Q3	Q4	Q3	Q4
16:1(n-7)/16:0	Diatom/ Dinoflagellate-associated FA	2.4 ± 0.6	2.9 ± 1.3	4.6 ± 1.8	4.0 ± 1.3	1.4 ± 0.4	0.8 ± 0.2	0.5 ± 0.1	1.0 ± 0.4	0.9 ± 0.3	0.5 ± 0.2
ΣC16/ΣC18		1.9 ± 0.5	2.5 ± 1.1	1.3 ± 0.7	1.3 ± 0.8	2.4 ± 0.7	1.3 ± 0.2	0.9 ± 0.1	0.9 ± 0.2	0.9 ± 0.1	0.8 ± 0.2
20:5(n-3)/22:6(n-3)		3.4 ± 1.0	2.0 ± 0.9	2.7 ± 1.2	2.5 ± 0.9	3.3 ± 0.7	2.3 ± 0.2	0.9 ± 0.1	1.2 ± 0.3	1.7 ± 0.5	1.2 ± 0.1
18:1(n-9)/18:1(n-7)	Carnivory index	4.8 ± 1.6	3.8 ± 0.8	2.7 ± 0.7	2.9 ± 0.6	4.1 ± 1.1	8.4 ± 1.3	3.5 ± 0.2	4.8 ± 1.3	5.1 ± 0.7	6.4 ± 1.1

Sample size is presented in ***Supplementary Table 2****.*

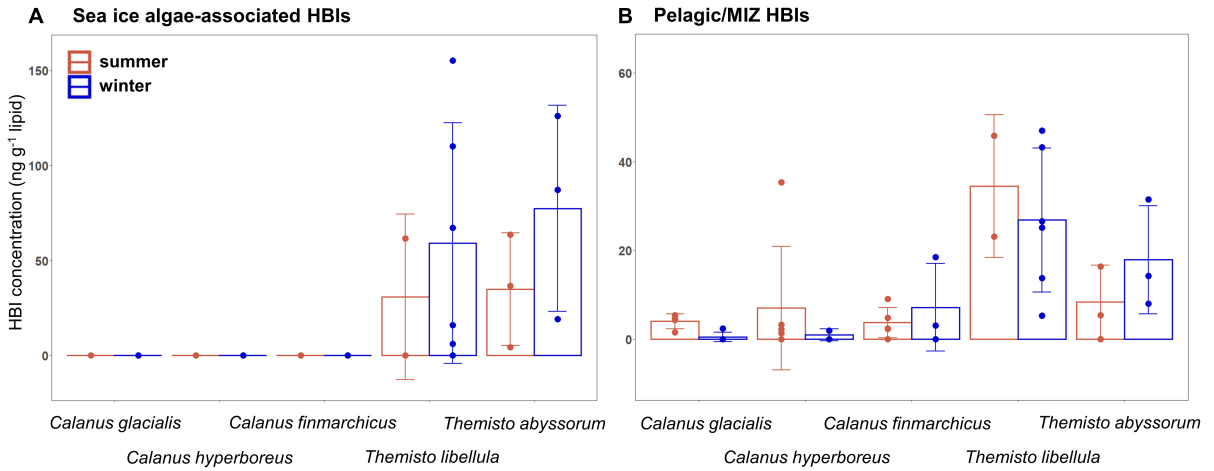

FIGURE 5 | Concentrations of **(A)** sea ice algae-associated and **(B)** pelagic/MIZ highly branched isoprenoids (HBIs; mean ± SD ng g^{-1} lipid) in copepods and amphipods during summer (Q3) and winter (Q4). Individual datapoints are represented by the dots. Sample size is presented in **Table 4**.

lower in summer than in winter in *C. finmarchicus* and *T. abyssorum* (**Figure 5B**).

The mean ratio of zoosterols/phytosterols increased in all zooplankton species from summer to winter (**Table 4**), but there was large variability in individual sterols among the zooplankton between the seasons. In *C. glacialis*, all phyto- and zoosterols, except for cholesterol, had higher averaged values in summer compared to winter (**Figure 6A**). In *C. hyperboreus*, chalinasterol content in winter was about 30% of that in summer, while averaged levels of the other phytosterols were more similar between the seasons, and all zoosterols were higher during winter (**Figure 6B**). In *C. finmarchicus*, all phytosterols and zoosterols had higher averaged levels in winter than in summer (**Figure 6C**). All phytosterols, except for brassicasterol, were similar in summer and winter in *T. libellula* (**Figure 6D**), while in *T. abyssorum*, all phytosterols were less abundant in winter than in summer (**Figure 6E**). In both amphipods, the zoosterol content was relatively stable between the seasons.

TABLE 4 | Ratios of the relative values of zoosterols/phytosterols (mean ± SD) in copepods and amphipods during summer (Q3) and winter (Q4).

Species	Zoosterols/phytosterols			
	n	Q3	*n*	Q4
Calanus glacialis	4	93.2 ± 15.6	5	117.8 ± 13.1
Calanus hyperboreus	6	77.7 ± 15.9	2	109.1 ± 2.6
Calanus finmarchicus	5	92.5 ± 15.8	3	140.4 ± 61.6
Themisto libellula	2	122.3 ± 62.5	6	257.3 ± 138.9
Themisto abyssorum	3	66.0 ± 66.9	3	98.4 ± 32.5

n, number of samples analyzed across the sampling area.

DISCUSSION

All five species showed, to a varying degree, seasonal changes in their composition of lipid classes and lipid-based trophic markers, reflecting differences in life history and food composition between the more productive summer and low-level food availability during winter. Species that are utilizing their lipid storage during winter, such as *Calanus* spp., are typically rich in WEs. These constitute often more than 70% of their lipid mass (**Figure 2A**), providing

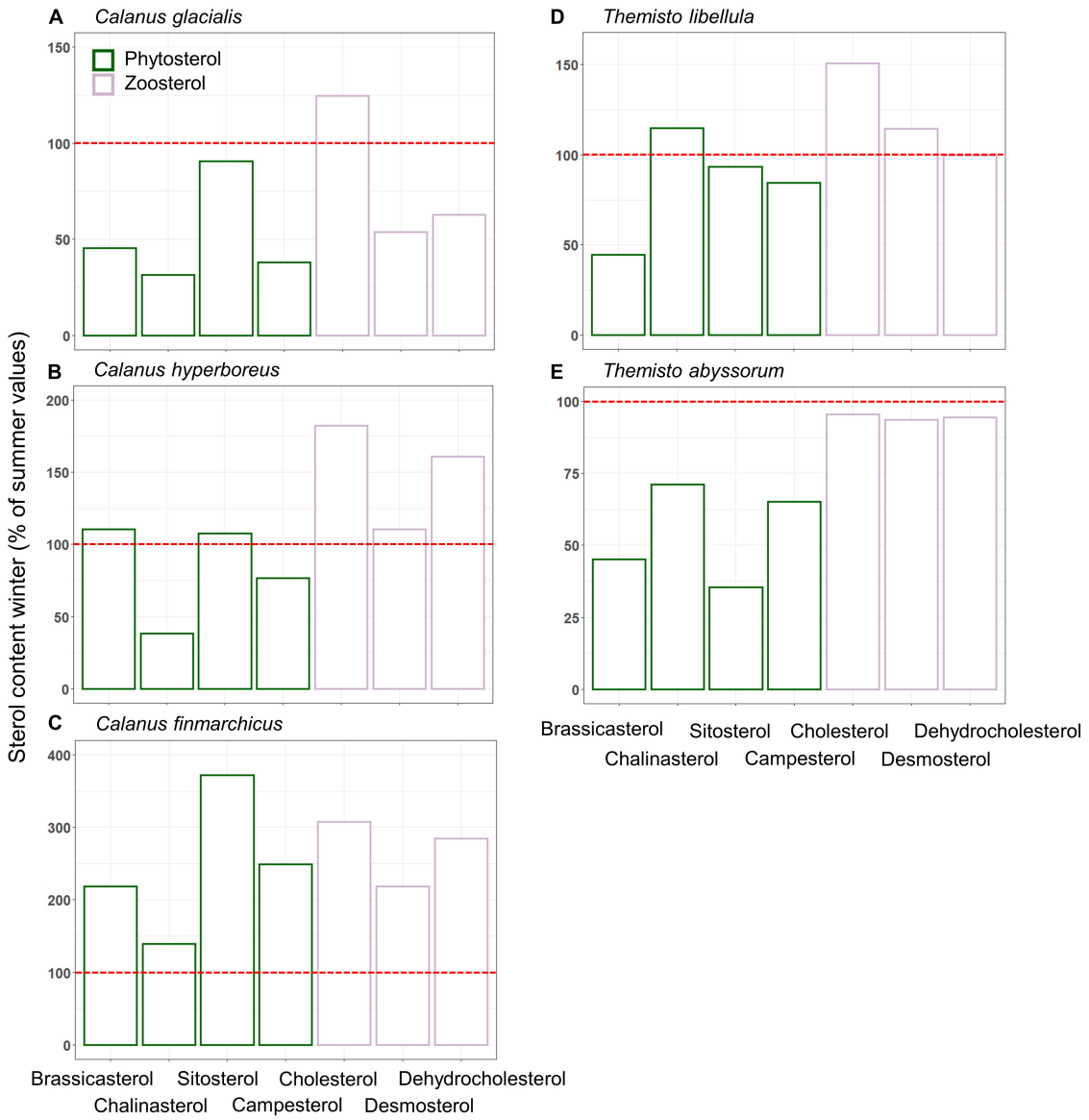

FIGURE 6 | Relative proportions of phyto-and zoosterols (mean ± SD%) represented by green and purple bars, respectively, during winter (Q4) related to summer (Q3) in *Calanus* spp. **(A–C)** and *Themisto* spp. **(D,E)**. Percentages are based on average sterol-content values from both sampling campaigns. The red line highlights 100%, i.e., same proportions of sterols during summer and winter. Sample size is presented in **Table 4**.

a store of long-chained FAs and alcohols with a high density of energy (Graeve and Kattner, 1992; Falk-Petersen et al., 2009). By contrast, TAGs are metabolized faster, and often dominate the lipid reservoir of non-dormant species, such as *Themisto* spp. (**Figure 2A**; Albers et al., 1996; Lee et al., 2006).

Calanus Copepods

Congruent with other studies (Kattner et al., 1989; Scott et al., 2000; Falk-Petersen et al., 2009), *C. hyperboreus* had the highest WE levels (mean 97% in summer and 90% in winter related to total lipids) among the copepods during both seasons, which can be attributed to their superior ability to synthesize and store high-energy long-chained FAs and alcohols (20:1 and 22:1 isomers) (Ackman et al., 1974; Sargent and Falk-Petersen, 1988). In comparison with the other two *Calanus* species, *C. hyperboreus* showed similar FA composition and FA marker ratios during the polar day and night (**Table 3** and **Figure 4**). Moreover, the total lipid content per dry weight was similar between summer and winter in *C. hyperboreus* (**Table 2**), indicating that this species was in similar body condition between the seasons and well adapted to the food-poor winter conditions.

In *C. glacialis* and *C. hyperboreus*, WE levels were higher in winter than in summer (**Figure 2A**), reflecting the significance of long-term storage lipids for successful overwintering in

species that are directly dependent on the highly seasonal algal production (Albers et al., 1996; Lee et al., 2006; Falk-Petersen et al., 2009). Concomitantly, relative proportions of the faster metabolized TAGs decreased in these species in December, likely already utilized in the days and weeks prior to the winter sampling. In *C. finmarchicus* by contrast, the relative proportions of individual neutral and polar lipids varied little from summer to winter, indicating species-specific differences in seasonal lipid dynamics among the copepods (**Figures 2A,B** and **Supplementary Table 1**).

As found before (Søreide et al., 2008; Cleary et al., 2017), the marker FA ratios suggested the importance of diatom- over dinoflagellate-associated carbon in the diets of all three *Calanus* species during both seasons (**Table 3**). In *C. glacialis* and *C. hyperboreus*, the overall phytosterol content declined from late summer to early winter (**Figures 6A,B**), most noticeably in chalinasterol, however, variability across the sampling area was large. The decrease in phytosterols in *C. glacialis* and *C. hyperboreus* was not evident in *C. finmarchicus*, further pointing to differences in overwintering activity and strategies between the *Calanus* species. However, phyto- and zoosterol contents varied largely between the sampling stations within one species so that differences between the species might not only be species-specific but also driven by spatial variability. Pelagic HBIs were also slightly lower in *C. glacialis* and *C. hyperboreus* during winter (**Figure 5B**). Given that diatoms are the major producers of marine sterols (Stonik and Stonik, 2015; Jaramillo-Madrid et al., 2019), these changes likely reflected a shift away from intake of fresh phytoplankton during summer, as the primary production declined. The lower proportions of the diatom-associated FAs 16:4(n-1) and 20:5(n-3) in winter compared to summer in all three copepods (**Figure 4A**) further reflected the seasonal decrease in diatom contribution to their diet (lower Chl *a* concentrations in water column and sea ice, lower proportions of diatom-associated FAs in PPOM and IPOM; **Figure 3**).

In *C. finmarchicus*, the carnivory index 18:1(n-9)/18:1(n-7) and the averaged ratio of zoosterols to phytosterols were higher in winter than in summer (**Tables 3**, **4**). The other two *Calanus* species also showed higher ratios of zoosterols/phytosterols during winter, but ratios of 18:1(n-9)/18:1(n-7) varied little between the seasons in *C. hyperboreus* and were even lower in winter compared to summer in *C. glacialis* (**Tables 3**, **4**). While proportions of 18:1(n-9) can potentially increase during starvation (Graeve et al., 1997), these species-specific differences could also indicate that the *C. finmarchicus* investigated in our study were actually active during the winter sampling, which was also reported for *Calanus* spp. in Svalbard fjords (Daase et al., 2018), and relied more on degraded heterotrophic material or heterotrophic prey due to the low quantity and quality of POM during winter (Søreide et al., 2008; Hobbs et al., 2020). For example, winter-active *C. glacialis* may be able to prey on small copepods, and their eggs and nauplii that are available during winter (Hobbs et al., 2020), as well as early life stages of chaetognaths or ctenophores (Cleary et al., 2017). *Calanus* individuals that were not able to accumulate enough lipids during the productive season might be required to stay active during winter (Hobbs et al., 2020), and search for food near the surface or ice-water interface (Pedersen et al., 1995), while individuals with large lipid stores can descend into deeper water layers where food but also predators are scarce (Wold et al., 2011; Freese et al., 2017; Schmid et al., 2018; Kvile et al., 2019). Seasonal changes in the trophic markers can, to some degree also reflect ontogenetic differences in the copepods, and consequently feeding behavior and food composition driven by size or possibly sex. The samples collected during summer contained individuals of the copepodid stages CIV and CV as well as female adults, and the samples collected during winter contained stages CIV, CV, female, and male individuals (**Table 2**), however, due to the low sample size of each life stage it is not possible to reveal the influence of ontogenetic variability in this study.

Failure to detect the sea ice algae-associated HBIs in all three *Calanus* species during both seasons (**Figure 5A**) suggests that their carbon sources were likely predominantly of pelagic origin. Ice algae can be essential for reproduction and development of early *Calanus* life stages in spring (Niehoff et al., 2002; Søreide et al., 2010; Daase et al., 2013), but abundant pelagic food during spring and summer, large lipid reservoirs and dormancy during winter possibly render alternative or additional ice-associated carbon sources unnecessary. However, the known HBI-producing ice algal taxa *Haslea* and *Pleurosigma* (Brown et al., 2014a,b; Limoges et al., 2018) are not usually amongst the major ice algal species, and indeed were not detected in the sea-ice communities during both seasons (or their abundances were below the detection limit of the Utermöhl settling method). This is in agreement with previous taxonomic studies showing that the known IP_{25}-producing species (*Haslea crucigeroides*, *H. spicula*, *H. kjellmanii*, and *Pleurosigma stuxbergii* var *rhomboides*) typically represent <1% of the sea ice diatom assemblages in Svalbard waters (von Quillfeldt, 2000). Therefore, we cannot rule out the possibility that the copepods were grazing on sea-ice algae containing HBI producers, but which were below the detection limit or were grazing on non-HBI-producing ice algal taxa. We should emphasize, however, that both amphipods and other pelagic zooplankton such as the filter-feeding pteropods *Clione limacina* and *Limacina helicina* contained sympagic HBIs during summer (Kohlbach et al., 2021), pointing to differences in feeding depth layers and/or feeding mechanisms between the taxa, and showing that HBI-producing diatoms were present at some point in the sampling area.

Themisto Amphipods

The two pelagic amphipods varied in their lipid class (**Figures 2A,B**) and FA compositions (**Figures 4A,B**) as well as seasonal variability of these parameters, which supports the notion that the two species differ in their lipid storage modes, carbon source composition and consequently their trophic interactions within the Arctic food web (Auel et al., 2002).

During both seasons, concentrations of pelagic HBIs were higher (**Figure 5B**), whereas 18:1(n-9)/18:1(n-7) carnivory ratios were lower in *T. libellula* compared to *T. abyssorum* (**Table 3**),

suggesting that *T. abyssorum* occupied a higher trophic level than *T. libellula*, in agreement with the literature (Auel et al., 2002). In both amphipod species, heterotrophic prey had a greater contribution to their food composition in winter versus summer based on the higher carnivory ratios of 18:1(n-9)/18:1(n-7) and zoosterols to phytosterol ratios (**Tables 3**, **4**). To some extent, the observed seasonal differences likely reflect ontogenetic changes in carbon and prey composition (Noyon et al., 2012), e.g., in *T. libellula* from early life stages during summer (average dry weight 3.5 mg ind.$^{-1}$) to larger predatory *T. libellula* individuals during winter (average dry weight 43.4 mg/ind^{-1}).

The significantly higher relative proportions of the marker FA 18:4(n-3) in *T. abyssorum* during summer (**Figure 4B**) reflected the higher concentrations and availability of dinoflagellates and/or *Phaeocystis*, in agreement with higher relative proportions of 18:4(n-3) in summer PPOM compared to winter PPOM (**Figure 3**), and further suggests the greater importance of phytoplankton and flagellate-based prey in their diet during the polar day. Our results correspond to previous studies (Mayzaud and Boutoute, 2015), suggesting continuous, more carnivorous, feeding during winter for both species (Dale et al., 2006; Kraft et al., 2013).

In both amphipods, WE levels were higher during winter (**Figure 2A**), pointing to an increased predation on wax ester-rich species during the polar night. In the case of *T. libellula*, these seasonal differences in WEs as well as calanoid copepod-associated FAs reflected the greater importance of *Calanus* copepods in their winter diet (**Supplementary Table 2**). Significantly higher levels of the diatom-associated FA 16:1(n-7), an important contributor to the FA pool of *Calanus* spp., in *T. libellula* during winter further highlights the significance of these copepods for the successful overwintering of *T. libellula*. The significantly higher relative proportions of the polyunsaturated FAs (PUFAs) 20:5(n-3) and 22:6(n-3) in *T. libellula* in summer compared to winter (**Figures 4A,B**) could again point to ontogenetic differences in feeding habits, as the rather omnivorous younger stages (length group 5–20 mm) collected during summer probably fed more intensely on PUFA-rich phytoplankton/ice algae than the mostly carnivorous adult stages of *T. libellula* (length group 10–40 mm) (Noyon et al., 2009, 2012). However, these PUFAs are mainly incorporated into polar lipids (Stübing et al., 2003), and lower PUFA concentrations in *T. libellula* in winter might be explained by the larger proportion of storage lipids during the polar night (**Supplementary Table 1**).

In *T. abyssorum*, zooplankton other than *Calanus* spp. might have been equally important prey items due to similar relative proportions of calanoid copepod-associated FAs in both seasons. *Calanus* copepods are generally an important food item for both amphipods (Auel et al., 2002; Dalsgaard et al., 2003; Marion et al., 2008; Noyon et al., 2009), but *T. abyssorum* has been reported to also prey on other copepods such as *Metridia* and appendicularians (Dalpadado et al., 2008). Information on feeding modes and diet composition during the polar night is generally scarce, but during summer and autumn, *T. abyssorum* has been found to have a greater diversity of food items in comparison to *T. libellula* which fed mostly on copepods (Auel et al., 2002; Dalpadado et al., 2008). For carnivorous species, such as the two hyperiid amphipods, seasonality in primary production has a less severe impact on their feeding behavior in comparison to herbivorous copepods since their preferred prey is basically available throughout the year (Hagen and Auel, 2001; Hirche and Kosobokova, 2011).

Themisto libellula is associated with Arctic waters, while *T. abyssorum* is more abundant in subarctic (Atlantic) waters. Moreover, *T. libellula* has been observed to be distributed closer to the surface (<50 m) which could give them easier access to sea ice-associated prey than *T. abyssorum* that has a more mesopelagic lifestyle (>200 m) (Dalpadado et al., 2001; Auel et al., 2002; Dalpadado, 2002). However, concentrations of sea ice algae-associated HBIs were similar between the two species (**Figure 5A**), only slightly higher in *T. abyssorum*, indicating an at least comparable trophic relationship to the ice-associated ecosystem for both species. The lack of sea ice algae-associated HBIs in the copepods further reveals that both amphipod species obtained sympagic metabolites by feeding on other sympagic prey. The presence versus absence of sea ice-derived HBIs in amphipods and copepods, respectively, likely reflects differences in their feeding location (under ice versus water column) and/or feeding behavior. Furthermore, it is possible that the juvenile amphipods during summer were feeding on sinking ice algal aggregates in the mid-water column (marine snow), as suggested for pteropods and appendicularians (Kohlbach et al., 2021), as young Arctic and Antarctic *Themisto* have been observed to feed partly on phytoplankton (Noyon et al., 2012; Watts and Tarling, 2012). Sea ice algae-associated HBIs were somewhat more concentrated in the winter compared to the summer *Themisto* spp., but concentrations varied strongly among the individuals (**Figure 5A**). On one hand, this could again reflect ontogenetic differences in food composition, but could on the other hand, be the result of the very opportunistic feeding style of these amphipods (Havermans et al., 2019).

Highly branched isoprenoids concentrations in Barents Sea fauna during winter, spanning pelagic and benthic invertebrates and fish, were in a similar order of magnitude as in our study (**Figures 5A,B**; Brown et al., 2015). Compared to HBI concentrations in Antarctic krill *Euphausia superba*, however, the levels of both sea ice algae-associated and pelagic HBIs in the amphipods were distinctly lower in our study. This could reflect hemispheric differences in the abundance of HBI-producing algae as for example Arctic diatoms producing IP_{25} have, despite their ubiquitous distribution throughout the Arctic, a relatively low contribution (< 5%) to the overall sympagic diatom community (Brown et al., 2014b). Given the low level of sea ice-associated primary production and that the available ice algae are not accessible for grazers during winter, HBIs detected in the winter samples could also, to some degree, reflect the importance of benthic food sources for the amphipods as HBI-producing diatoms have been found to be present in benthic sediments and bottom waters rather than sea ice and upper water layers during winter (Brown et al., 2015). Both amphipod species have been

observed close to the seafloor (Vinogradov, 1999), however, the extent that they rely on benthic food sources remains unclear.

CONCLUSION

During some periods of the year, sea ice algae can serve as a valuable carbon source for ice-associated grazers and subsequently their predators, both in the Arctic (Wang et al., 2015, 2016; Kohlbach et al., 2016, 2019) and the Antarctic marine environment (Kohlbach et al., 2017, 2018; Bernard et al., 2018; Schmidt et al., 2018). Yet, in both late summer and early winter, the trophic link between *Calanus* copepods and the ice-associated ecosystem was weak in our study area. This suggests that (a) during summer, phytoplankton and pelagic prey are sufficient to meet the energetic requirements of the copepods and (b) diapause or the decrease in metabolic activity as well as the presence of accumulated lipids during winter counteract the reliance on ice algae. Furthermore, in the case of the (likely) winter-active *C. finmarchicus*, plasticity in feeding behavior and carbon source composition enables successful survival, seemingly without the utilization of sympagic carbon. In the *Themisto* amphipods, relatively similar concentrations of sea ice-associated metabolites in their lipid pool between the seasons and ontogenetic life stages suggest that sympagic carbon was more important, possibly obtained from benthic food sources, but still likely not critical for their overwintering in the Barents Sea. Rather than diapause, carnivory helped sustain these amphipods during the polar night.

DATA AVAILABILITY STATEMENT

The original contributions presented in the study are included in the article/**Supplementary Material**, further inquiries can be directed to the corresponding author/s.

AUTHOR CONTRIBUTIONS

AW and AKA-H conducted the sampling. HH and PA provided sampling logistics. PA, HH, and DK developed the study design. DK was the main author of this manuscript and accomplished the fatty acid laboratory analyses and data evaluation. MW carried out lipid class analysis with support of MG. KS accomplished the HBI and sterol analysis and data evaluation with the help of LS, SB, and AA. MG and SB provided laboratory materials, methodological expertise, and laboratory space. Data analyses and figure assemblage was done by DK with the help of the other authors. All authors contributed significantly to data interpretation and to the writing of the manuscript.

FUNDING

This work was funded by the Research Council of Norway through the project The Nansen Legacy (RCN #276730). Contributions by KS, SB, and AA were funded by the UK's Natural Environment Research Council MOSAiC-Thematic project SYM-PEL: "Quantifying the contribution of sympagic versus pelagic diatoms to Arctic food webs and biogeochemical fluxes: application of source-specific highly branched isoprenoid biomarkers" (NE/S002502/1).

ACKNOWLEDGMENTS

We thank the captain and the crew of RV *Kronprins Haakon* for their excellent support at sea during the Nansen Legacy seasonal cruises Q3 and Q4. We would like to thank Kasia Dmoch (IOPAN) for her help with zooplankton sorting during Q3, and Sinah Müller and Valeria Adrian (AWI) with their help with the fatty acid laboratory analyses. We thank Øyvind Lundesgaard (NPI) for his help creating the sea-ice map. We thank the editor Anne Helene Tandberg and the two reviewers for providing helpful comments and suggestions during the review process.

SUPPLEMENTARY MATERIAL

The Supplementary Material for this article can be found online at: https://www.frontiersin.org/articles/10.3389/fmars.2021.640050/full#supplementary-material

REFERENCES

Aarflot, J. M., Skjoldal, H. R., Dalpadado, P., and Skern-Mauritzen, M. (2018). Contribution of *Calanus* species to the mesozooplankton biomass in the Barents Sea. *ICES J. Mar. Sci.* 75, 2342–2354. doi: 10.1093/icesjms/fsx221

Ackman, R. G., Linke, B. A., and Hingley, J. (1974). Some details of fatty acids and alcohols in the lipids of North Atlantic copepods. *J. Fish. Res. Board Can.* 31, 1812–1818. doi: 10.1139/f74-233

Albers, C. S., Kattner, G., and Hagen, W. (1996). The compositions of wax esters, triacylglycerols and phospholipids in Arctic and Antarctic copepods: evidence of energetic adaptations. *J. Mar. Chem.* 55, 347–358. doi: 10.1016/S0304-4203(96)00059-X

Årthun, M., Eldevik, T., and Smedsrud, L. H. (2019). The role of Atlantic heat transport in future Arctic winter sea ice loss. *J. Clim.* 32, 3327–3341. doi: 10.1175/JCLI-D-18-0750.1

Årthun, M., Eldevik, T., Smedsrud, L. H., Skagseth, Ø, and Ingvaldsen, R. B. (2012). Quantifying the influence of Atlantic heat on Barents Sea ice variability and retreat. *J. Clim.* 25, 4736–4743. doi: 10.1175/JCLI-D-11-00466.1

Assmy, P., Ehn, J. K., Fernández-Méndez, M., Hop, H., Katlein, C., Sundfjord, A., et al. (2013). Floating ice-algal aggregates below melting Arctic sea ice. *PLoS One* 8:e76599. doi: 10.1371/journal.pone.0076599

Atkinson, A. (1998). Life cycle strategies of epipelagic copepods in the Southern Ocean. *J. Mar. Syst.* 15, 289–311. doi: 10.1016/S0924-7963(97)00081-X

Atkinson, A., Ward, P., Hunt, B. P. V., Pakhomov, E. A., and Hosie, G. W. (2012). An overview of Southern Ocean zooplankton data: abundance, biomass, feeding and functional relationships. *CCAMLR Sci.* 19, 171–218.

Auel, H., Harjes, M., Da Rocha, R., Stübing, D., and Hagen, W. (2002). Lipid biomarkers indicate different ecological niches and trophic relationships of the Arctic hyperiid amphipods *Themisto abyssorum* and *T. libellula*. *Polar Biol.* 25, 374–383. doi: 10.1007/s00300-001-0354-7

Bandara, K., Varpe, Ø, Søreide, J. E., Wallenschus, J., Berge, J., and Eiane, K. (2016). Seasonal vertical strategies in a high-Arctic coastal zooplankton community. *Mar. Ecol. Prog. Ser.* 555, 49–64. doi: 10.3354/meps11831

Barton, B. I., Lenn, Y.-D., and Lique, C. (2018). Observed Atlantification of the Barents Sea causes the polar front to limit the expansion of winter sea ice. *J. Phys. Oceanogr.* 48, 1849–1866. doi: 10.1175/JPO-D-18-0003.1

Belt, S. T. (2018). Source-specific biomarkers as proxies for Arctic and Antarctic sea ice. *Org. Geochem.* 125, 277–298. doi: 10.1016/j.orggeochem.2018.10.002

Belt, S. T., Brown, T. A., Sanz, P. C., and Rodriguez, A. N. (2012). Structural confirmation of the sea ice biomarker IP_{25} found in Arctic marine sediments. *Environ. Chem. Lett.* 10, 189–192. doi: 10.1007/s10311-011-0344-0

Belt, S. T., Brown, T. A., Smik, L., Assmy, P., and Mundy, C. J. (2018). Sterol identification in floating Arctic sea ice algal aggregates and the Antarctic sea ice diatom *Berkeleya adeliensis*. *Org. Geochem.* 118, 1–3. doi: 10.1016/j.orggeochem.2018.01.008

Berge, J., Daase, M., Hobbs, L., Falk-Petersen, S., Darnis, G., and Søreide, J. E. (2020). "Zooplankton in the polar night," in *Polar Night Marine Ecology*, eds J. Berge, G. Johnsen, and J. H. Cohen (Cham: Springer), 113–159.

Berge, J., Daase, M., Renaud, P. E., Ambrose, W. G. Jr., Darnis, G., Last, K. S., et al. (2015). Unexpected levels of biological activity during the polar night offer new perspectives on a warming Arctic. *J. Curr. Biol.* 25, 2555–2561. doi: 10.1016/j.cub.2015.08.024

Bernard, K. S., Gunther, L. A., Mahaffey, S. H., Qualls, K. M., Sugla, M., Saenz, B. T., et al. (2018). The contribution of ice algae to the winter energy budget of juvenile Antarctic krill in years with contrasting sea ice conditions. *ICES J. Mar. Sci.* 76, 206–216. doi: 10.1093/icesjms/fsy145

Brown, T. A., Assmy, P., Hop, H., Wold, A., and Belt, S. T. (2017). Transfer of ice algae carbon to ice-associated amphipods in the high-Arctic pack ice environment. *J. Plankton Res.* 39, 664–674. doi: 10.1093/plankt/fbx030

Brown, T. A., and Belt, S. T. (2012). Identification of the sea ice diatom biomarker IP_{25} in Arctic benthic macrofauna: direct evidence for a sea ice diatom diet in Arctic heterotrophs. *Polar Biol.* 35, 131–137. doi: 10.1007/s00300-011-1045-7

Brown, T. A., Belt, S. T., and Cabedo-Sanz, P. (2014a). Identification of a novel di-unsaturated C_{25} highly branched isoprenoid in the marine tube-dwelling diatom *Berkeleya rutilans*. *Environ. Chem. Lett.* 12, 455–460. doi: 10.1007/s10311-014-0472-4

Brown, T. A., Belt, S. T., Tatarek, A., and Mundy, C. J. (2014b). Source identification of the Arctic sea ice proxy IP_{25}. *Nat. Commun.* 5:4197. doi: 10.1038/ncomms5197

Brown, T. A., Hegseth, E. N., and Belt, S. T. (2015). A biomarker-based investigation of the mid-winter ecosystem in Rijpfjorden, Svalbard. *Polar Biol.* 38, 37–50. doi: 10.1007/s00300-013-1352-2

Campbell, R. G., Sherr, E. B., Ashjian, C. J., Plourde, S., Sherr, B. F., Hill, V., et al. (2009). Mesozooplankton prey preference and grazing impact in the western Arctic Ocean. *Deep Sea Res. II* 56, 1274–1289. doi: 10.1016/j.dsr2.2008.10.027

Choi, H., Ha, S.-Y., Lee, S., Kim, J.-H., and Shin, K.-H. (2020). Trophic dynamics of zooplankton before and after Polar Night in the Kongsfjorden (Svalbard): evidence of trophic position estimated by $\delta^{15}N$ analysis of amino acids. *Front. Mar. Sci.* 7:489. doi: 10.3389/fmars.2020.00489

Choquet, M., Kosobokova, K., Kwaśniewski, S., Hatlebakk, M., Dhanasiri, A. K., Melle, W., et al. (2018). Can morphology reliably distinguish between the copepods *Calanus finmarchicus* and *C. glacialis*, or is DNA the only way? *Limnol. Oceanogr. (Methods)* 16, 237–252. doi: 10.1002/lom3.10240

Cleary, A. C., Søreide, J. E., Freese, D., Niehoff, B., and Gabrielsen, T. M. (2017). Feeding by *Calanus glacialis* in a high arctic fjord: potential seasonal importance of alternative prey. *ICES J. Mar. Sci.* 74, 1937–1946. doi: 10.1093/icesjms/fsx106

Conover, R. J., and Huntley, M. (1991). Copepods in ice-covered seas—distribution, adaptations to seasonally limited food, metabolism, growth patterns and life cycle strategies in polar seas. *J. Mar. Syst.* 2, 1–41. doi: 10.1016/0924-7963(91)90011-I

Daase, M., Falk-Petersen, S., Varpe, Ø, Darnis, G., Søreide, J. E., Wold, A., et al. (2013). Timing of reproductive events in the marine copepod *Calanus glacialis*: a pan-Arctic perspective. *Can. J. Fish. Aquat. Sci.* 70, 871–884. doi: 10.1139/cjfas-2015-0333

Daase, M., Kosobokova, K., Last, K. S., Cohen, J. H., Choquet, M., Hatlebakk, M., et al. (2018). New insights into the biology of *Calanus* spp. (Copepoda) males in the Arctic. *Mar. Ecol. Prog. Ser.* 607, 53–69. doi: 10.3354/meps12788

Dale, K., Falk-Petersen, S., Hop, H., and Fevolden, S.-E. (2006). Population dynamics and body composition of the Arctic hyperiid amphipod *Themisto libellula* in Svalbard fjords. *Polar Biol.* 29, 1063–1070. doi: 10.1007/s00300-006-0150-5

Dalpadado, P. (2002). Inter-specific variations in distribution, abundance and possible life-cycle patterns of *Themisto* spp. (Amphipoda) in the Barents Sea. *Polar Biol.* 25, 656–666. doi: 10.1007/s00300-002-0390-y

Dalpadado, P., Borkner, N., Bogstad, B., and Mehl, S. (2001). Distribution of *Themisto* (Amphipoda) spp. in the Barents Sea and predator-prey interactions. *ICES J. Mar. Sci.* 58, 876–895. doi: 10.1006/jmsc.2001.1078

Dalpadado, P., Yamaguchi, A., Ellertsen, B., and Johannessen, S. (2008). Trophic interactions of macro-zooplankton (krill and amphipods) in the Marginal Ice Zone of the Barents Sea. *Deep Sea Res. II* 55, 2266–2274. doi: 10.1016/j.dsr2.2008.05.016

Dalsgaard, J., St. John, M., Kattner, G., Müller-Navarra, D., and Hagen, W. (2003). Fatty acid trophic markers in the pelagic marine environment. *Adv. Mar. Biol.* 46, 227–237. doi: 10.1016/S0065-2881(03)46005-7

David, C., Lange, B., Rabe, B., and Flores, H. (2015). Community structure of under-ice fauna in the Eurasian central Arctic Ocean in relation to environmental properties of sea-ice habitats. *Mar. Ecol. Prog. Ser.* 522, 15–32. doi: 10.3354/meps11156

Drazen, J. C., Phleger, C. F., Guest, M. A., and Nichols, P. D. (2008). Lipid, sterols and fatty acid composition of abyssal holothurians and ophiuroids from the North-East Pacific Ocean: food web implications. *Comp. Biochem. Physiol. B Biochem. Mol. Biol.* 151, 79–87. doi: 10.1016/j.cbpb.2008.05.013

Durbin, E. G., and Casas, M. C. (2014). Early reproduction by *Calanus glacialis* in the Northern Bering Sea: the role of ice algae as revealed by molecular analysis. *J. Plankton Res.* 36, 523–541. doi: 10.1093/plankt/fbt121

Eriksen, E., Benzik, A. N., Dolgov, A. V., Skjoldal, H. R., Vihtakari, M., Johannesen, E., et al. (2020). Diet and trophic structure of fishes in the Barents Sea: the Norwegian-Russian program "Year of stomachs" 2015–establishing a baseline. *Prog. Oceanogr.* 183:102262. doi: 10.1016/j.pocean.2019.102262

Falk-Petersen, S., Hagen, W., Kattner, G., Clarke, A., and Sargent, J. (2000a). Lipids, trophic relationships, and biodiversity in Arctic and Antarctic krill. *Can. J. Fish. Aquat. Sci.* 57, 178–191. doi: 10.1139/f00194

Falk-Petersen, S., Hop, H., Budgell, W. P., Hegseth, E. N., Korsnes, R., Løyning, T. B., et al. (2000b). Physical and ecological processes in the marginal ice zone of the northern Barents Sea during the summer melt period. *J. Mar. Syst.* 27, 131–159. doi: 10.1016/S0924-7963(00)00064-6

Falk-Petersen, S., Hopkins, C. C. E., and Sargent, J. R. (1990). "Trophic relationships in the pelagic, Arctic food web," in *Trophic Relationships in the Marine Environment*, eds M. Barnes and R. N. Gibson (Aberdeen: Aberdeen University Press), 315–333.

Falk-Petersen, S., Mayzaud, P., Kattner, G., and Sargent, J. R. (2009). Lipids and life strategy of Arctic *Calanus*. *Mar. Biol. Res.* 5, 18–39. doi: 10.1080/17451000802512267

Falk-Petersen, S., Pavlov, V., Timofeev, S., and Sargent, J. R. (2007). "Climate variability and possible effects on arctic food chains: the role of *Calanus*," in *Arctic Alpine Ecosystems and People in a Changing Environment*, eds J. B. Ørbæk, R. Kallenborn, I. Tombre, E. N. Hegseth, and S. Falk-Petersen (Berlin: Springer), 147–166.

Falk-Petersen, S., Sargent, J. R., Henderson, J., Hegseth, E. N., Hop, H., and Okolodkov, Y. B. (1998). Lipids and fatty acids in ice algae and phytoplankton from the Marginal Ice Zone in the Barents Sea. *Polar Biol.* 20, 41–47. doi: 10.1007/s003000050274

Folch, J., Lees, M., and Sloane Stanley, G. H. (1957). A simple method for the isolation and purification of total lipides from animal tissues. *J. Biol. Chem. (Baltim.)* 226, 497–509.

Francis, J. A., and Hunter, E. (2007). Drivers of declining sea ice in the Arctic winter: a tale of two seas. *Geophys. Res. Lett.* 34:L17503. doi: 10.1029/2007GL030995

Freese, D., Søreide, J. E., Graeve, M., and Niehoff, B. (2017). A year-round study on metabolic enzymes and body composition of the Arctic copepod *Calanus glacialis*: implications for the timing and intensity of diapause. *Mar. Biol.* 164:3. doi: 10.1007/s00227-016-3036-2

Gradinger, R. R. (2009). Sea-ice algae: major contributors to primary production and algal biomass in the Chukchi and Beaufort Seas during

May/June 2002. *Deep Sea Res. II* 56, 1201–1212. doi: 10.1016/j.dsr2.2008.10.016

Graeve, M., Hagen, W., and Kattner, G. (1994). Herbivorous or omnivorous? On the significance of lipid compositions as trophic markers in Antarctic copepods. *Deep Sea Res. I* 41, 915–924. doi: 10.1016/0967-0637(94)90083-3

Graeve, M., and Janssen, D. (2009). Improved separation and quantification of neutral and polar lipid classes by HPLC–ELSD using a monolithic silica phase: application to exceptional marine lipids. *J. Chromatogr. B* 877, 1815–1819. doi: 10.1016/j.jchromb.2009.05.004

Graeve, M., and Kattner, G. (1992). Species-specific differences in intact wax esters of *Calanus hyperboreus* and *C. finmarchicus* from Fram Strait- Greenland Sea. *Mar. Chem.* 39, 269–281. doi: 10.1016/0304-4203(92)90013-Z

Graeve, M., Kattner, G., and Piepenburg, D. (1997). Lipids in Arctic benthos: does the fatty acid and alcohol composition reflect feeding and trophic interactions? *Polar Biol.* 18, 53–61. doi: 10.1007/s003000050158

Hagen, W. (1999). Reproductive strategies and energetic adaptations of polar zooplankton. *Invertebr. Reprod. Dev.* 36, 25–34. doi: 10.1080/07924259.1999.9652674

Hagen, W., and Auel, H. (2001). Seasonal adaptations and the role of lipids in oceanic zooplankton. *Zoology* 104, 313–326. doi: 10.1078/0944-2006-00037

Halvorsen, E. (2015). Significance of lipid storage levels for reproductive output in the Arctic copepod *Calanus hyperboreus*. *Mar. Ecol. Prog. Ser.* 540, 259–265. doi: 10.3354/meps11528

Haug, T., Falk-Petersen, S., Greenacre, M., Hop, H., Lindstrøm, U., and Meier, S. (2017). Trophic level and fatty acids in harp seals compared with common minke whales in the Barents Sea. *Mar. Biol. Res.* 13, 919–932. doi: 10.1080/17451000.2017.1313988

Havermans, C., Auel, H., Hagen, W., Held, C., Ensor, N. S., and Tarling, G. A. (2019). Predatory zooplankton on the move: *Themisto* amphipods in high-latitude marine pelagic food webs. *Adv. Mar. Biol.* 82, 51–92. doi: 10.1016/bs.amb.2019.02.002

Herbaut, C., Houssais, M.-N., Close, S., and Blaizot, A.-C. (2015). Two wind-driven modes of winter sea ice variability in the Barents Sea. *Deep Sea Res. I* 106, 97–115. doi: 10.1016/j.dsr.2015.10.005

Hirche, H.-J. (1997). Life cycle of the copepod *Calanus hyperboreus* in the Greenland Sea. *Mar. Biol.* 128, 607–618. doi: 10.1007/s002270050127

Hirche, H.-J. (2013). Long-term experiments on lifespan, reproductive activity and timing of reproduction in the Arctic copepod *Calanus hyperboreus*. *Mar. Biol.* 160, 2469–2481. doi: 10.1007/s00227-013-2242-4

Hirche, H.-J., and Kosobokova, K. N. (2007). Distribution of *Calanus finmarchicus* in the northern North Atlantic and Arctic Ocean—expatriation and potential colonization. *Deep Sea Res. II* 54, 2729–2747. doi: 10.1016/j.dsr2.2007.08.006

Hirche, H.-J., and Kosobokova, K. N. (2011). Winter studies on zooplankton in Arctic seas: the Storfjord (Svalbard) and adjacent ice-covered Barents Sea. *Mar. Biol.* 158, 2359–2376. doi: 10.1007/s00227-011-1740-5

Hirche, H.-J., and Mumm, N. (1992). Distribution of dominant copepods in the Nansen Basin, Arctic Ocean, in summer. *Deep Sea Res. A* 39, S485–S505. doi: 10.1016/S0198-0149(06)80017-8

Hobbs, L., Banas, N. S., Cottier, F. R., Berge, J., and Daase, M. (2020). Eat or sleep: availability of winter prey explains mid-winter and spring activity in an Arctic *Calanus* population. *Front. Mar. Sci.* 7:744. doi: 10.3389/fmars.2020.541564

Hop, H., Assmy, P., Wold, A., Sundfjord, A., Daase, M., Duarte, P., et al. (2019). Pelagic ecosystem characteristics across the Atlantic water boundary current from Rijpfjorden, Svalbard, to the Arctic Ocean during summer (2010–2014). *Front. Mar. Sci.* 6:181. doi: 10.3389/fmars.2019.00181

Hop, H., and Gjøsæter, H. (2013). Polar cod (*Boreogadus saida*) and capelin (*Mallotus villosus*) as key species in marine food webs of the Arctic and the Barents Sea. *Mar. Biol. Res.* 9, 878–894. doi: 10.1080/17451000.2013.775458

Hop, H., Poltermann, M., Lønne, O. J., Falk-Petersen, S., Korsnes, R., and Budgell, W. P. (2000). Ice amphipod distribution relative to ice density and under-ice topography in the northern Barents Sea. *Polar Biol.* 23, 357–367. doi: 10.1007/s003000050456

Iverson, S. J. (2009). "Tracing aquatic food webs using fatty acids: from qualitative indicators to quantitative determination," in *Lipids in Aquatic Ecosystems*, eds M. Kainz, M. T. Brett, and M. T. Arts (New York, NY: Springer), 281–308.

Jakubas, D., Wojczulanis-Jakubas, K., Boehnke, R., Kidawa, D., Błachowiak-Samołyk, K., and Stempniewicz, L. (2016). Intra-seasonal variation in zooplankton availability, chick diet and breeding performance of a high Arctic planktivorous seabird. *Polar Biol.* 39, 1547–1561. doi: 10.1007/s00300-015-1880-z

Jaramillo-Madrid, A. C., Ashworth, J., Fabris, M., and Ralph, P. J. (2019). Phytosterol biosynthesis and production by diatoms (Bacillariophyceae). *Phytochem* 163, 46–57. doi: 10.1016/j.phytochem.2019.03.018

Kattner, G., and Fricke, H. S. G. (1986). Simple gas-liquid chromatographic method for the simultaneous determination of fatty acids and alcohols in wax esters of marine organisms. *J. Chromatogr. A* 361, 263–268. doi: 10.1016/S0021-9673(01)86914-4

Kattner, G., Graeve, M., and Hagen, W. (1994). Ontogenetic and seasonal changes in lipid and fatty acid/alcohol compositions of the dominant Antarctic copepods *Calanus propinquus, Calanoides acutus* and *Rhincalanus gigas*. *Mar. Biol.* 118, 637–644. doi: 10.1007/BF00347511

Kattner, G., Hirche, H. J., and Krause, M. (1989). Spatial variability in lipid composition of calanoid copepods from Fram Strait, the Arctic. *Mar. Biol.* 102, 473–480. doi: 10.1007/BF00438348

Kohlbach, D., Ferguson, S. H., Brown, T. A., and Michel, C. (2019). Landfast sea ice-benthic coupling during spring and potential impacts of system changes on food web dynamics in Eclipse Sound, Canadian Arctic. *Mar. Ecol. Prog. Ser.* 627, 33–48. doi: 10.3354/meps13071

Kohlbach, D., Graeve, M., Lange, B. A., David, C., Peeken, I., and Flores, H. (2016). The importance of ice algae−produced carbon in the central Arctic Ocean ecosystem: food web relationships revealed by lipid and stable isotope analyses. *Limnol. Oceanogr.* 61, 2027–2044. doi: 10.1002/lno.10351

Kohlbach, D., Graeve, M., Lange, B. A., David, C., Schaafsma, F. L., van Franeker, J. A., et al. (2018). Dependency of Antarctic zooplankton species on ice algae−produced carbon suggests a sea ice−driven pelagic ecosystem during winter. *Glob. Change Biol.* 24, 4667–4681. doi: 10.1111/gcb.14392

Kohlbach, D., Hop, H., Wold, A., Schmidt, K., Smik, L., Belt, S. T., et al. (2021). Multiple trophic markers trace dietary carbon sources in Barents Sea zooplankton during late summer. *Front. Mar. Sci.* 7:610248. doi: 10.3389/fmars.2020.610248

Kohlbach, D., Lange, B. A., Schaafsma, F. L., David, C., Vortkamp, M., Graeve, M., et al. (2017). Ice algae-produced carbon is critical for overwintering of Antarctic krill *Euphausia superba*. *Front. Mar. Sci.* 4:310. doi: 10.3389/fmars.2017.00310

Kraft, A., Berge, J., Varpe, Ø, and Falk-Petersen, S. (2013). Feeding in Arctic darkness: mid-winter diet of the pelagic amphipods *Themisto abyssorum* and *T. libellula*. *Mar. Biol.* 160, 241–248. doi: 10.1007/s00227-012-2065-8

Kvernvik, A. C., Hoppe, C. J. M., Lawrenz, E., Prášil, O., Greenacre, M., Wiktor, J. M., et al. (2018). Fast reactivation of photosynthesis in arctic phytoplankton during the polar night. *J. Phycol.* 54, 461–470. doi: 10.1111/jpy.12750

Kvile, K. Ø, Ashjian, C., and Ji, R. (2019). Pan-Arctic depth distribution of diapausing *Calanus* copepods. *Biol. Bull.* 237, 76–89. doi: 10.1086/704694

Kwasniewski, S., Hop, H., Falk-Petersen, S., and Pedersen, G. (2003). Distribution of *Calanus* species in Kongsfjorden, a glacial fjord in Svalbard. *J. Plankton Res.* 25, 1–20. doi: 10.1093/plankt/25.1.1

Lee, R. F., Hagen, W., and Kattner, G. (2006). Lipid storage in marine zooplankton. *Mar. Ecol. Prog. Ser.* 307, 273–306. doi: 10.3354/meps307273

Legendre, P., and Legendre, L. (2012). *Numerical Ecology*, 3rd Edn. Amsterdam: Elsevier, 24.

Leu, E., Brown, T. A., Graeve, M., Wiktor, J. M., Hoppe, C. J. M, Chierici, M., et al. (2020). Spatial and temporal variability of ice algal trophic markers-with recommendations about their application. *J. Mar. Sci. Eng.* 8:676. doi: 10.3390/jmse8090676

Limoges, A., Masse, G., Weckström, K., Poulin, M., Ellegaard, M., Heikkilä, M., et al. (2018). Spring succession and vertical export of diatoms and IP_{25} in a seasonally ice-covered high Arctic fjord. *Front. Earth Sci.* 6:226. doi: 10.3389/feart.2018.00226

Marion, A., Harvey, M., Chabot, D., and Brêthes, J.-C. (2008). Feeding ecology and predation impact of the recently established amphipod, *Themisto libellula*, in the St. Lawrence marine system, Canada. *Mar. Ecol. Prog. Ser.* 373, 53–70. doi: 10.3354/meps07716

Mayzaud, P., and Boutoute, M. (2015). Dynamics of lipid and fatty acid composition of the hyperiid amphipod *Themisto*: a bipolar comparison with special emphasis on seasonality. *Polar Biol.* 38, 1049–1065. doi: 10.1007/s00300-015-1666-3

Melle, W., and Skjoldal, H. R. (1998). Reproduction and development of *Calanus finmarchicus*, *C. glacialis* and *C. hyperboreus* in the Barents Sea. *Mar. Ecol. Prog. Ser.* 169, 211–228. doi: 10.3354/meps169211

Mikkelsen, D. M., Rysgaard, S., and Glud, R. N. (2008). Microalgal composition and primary production in Arctic sea ice: a seasonal study from Kobbefjord (Kangerluarsunnguaq), West Greenland. *Mar. Ecol. Prog. Ser.* 368, 65–74. doi: 10.3354/meps07627

Niehoff, B., Madsen, S., Hansen, B., and Nielsen, T. (2002). Reproductive cycles of three dominant *Calanus* species in Disko Bay, West Greenland. *Mar. Biol.* 140, 567–576. doi: 10.1007/s00227-001-0731-3

Nielsen, T. G., Kjellerup, S., Smolina, I., Hoarau, G., and Lindeque, P. (2014). Live discrimination of *Calanus glacialis* and *C. finmarchicus* females: can we trust phenological differences? *Mar. Biol.* 161, 1299–1306. doi: 10.1007/s00227-014-2419-5

Noyon, M., Gasparini, S., and Mayzaud, P. (2009). Feeding of *Themisto libellula* (Amphipoda Crustacea) on natural copepods assemblages in an Arctic fjord (Kongsfjorden, Svalbard). *Polar Biol.* 32, 1559–1570. doi: 10.1007/s00300-009-0655-9

Noyon, M., Narcy, F., Gasparini, S., and Mayzaud, P. (2012). Ontogenic variations in fatty acid and alcohol composition of the pelagic amphipod *Themisto libellula* in Kongsfjorden (Svalbard). *Mar. Biol.* 159, 805–816. doi: 10.1007/s00227-011-1856-7

Nyssen, F., Brey, T., Dauby, P., and Graeve, M. (2005). Trophic position of Antarctic amphipods- enhanced analysis by a 2-dimensional biomarker assay. *Mar. Ecol. Prog. Ser.* 300, 135–145. doi: 10.3354/meps300135

Onarheim, I. H., and Årthun, M. (2017). Toward an ice−free Barents Sea. *Geophys. Res. Lett.* 44, 8387–8395. doi: 10.1002/2017GL074304

Parrish, C. C. (2009). "Essential fatty acids in aquatic food webs," in *Lipids in Aquatic Ecosystems*, eds M. Kainz, M. T. Brett, and M. T. Arts (New York, NY: Springer), 309–326.

Pecuchet, L., Blanchet, M.-A., Frainer, A., Husson, B., Jørgensen, L. L., Kortsch, S., et al. (2020). Novel feeding interactions amplify the impact of species redistribution on an Arctic food web. *Glob. Change Biol.* 26, 4895–4906. doi: 10.1111/gcb.15196

Pedersen, G., Tande, K., and Ottesen, G. O. (1995). Why does a component of *Calanus finmarchicus* stay in the surface waters during the overwintering period in high latitudes?' *J. Mar. Sci.* 52, 523–531. doi: 10.1016/1054-3139(95)80066-2

Poltermann, M. (2001). Arctic sea ice as feeding ground for amphipods–food sources and strategies. *Polar Biol.* 24, 89–96. doi: 10.1007/s003000000177

R Core Team (2017). *R: A Language and Environment for Statistical Computing*. Vienna: R Foundation for Statistical Computing.

Reigstad, M., Wassmann, P., Wexels Riser, C., Øygarden, S., and Rey, F. (2002). Variations in hydrography, nutrients and chlorophyll *a* in the marginal ice-zone and the central Barents Sea. *J. Mar. Syst.* 38, 9–29. doi: 10.1016/S0924-7963(02)00167-7

Reuss, N., and Poulsen, L. (2002). Evaluation of fatty acids as biomarkers for a natural plankton community. A field study of a spring bloom and a post-bloom period off West Greenland. *Mar. Biol.* 141, 423–434. doi: 10.1007/s00227-002-0841-6

Ruess, L., and Müller-Navarra, D. (2019). Essential biomolecules in food webs. *Front. Ecol. Evol.* 7:269. doi: 10.3389/fevo.2019.00269

Sakshaug, E., and Slagstad, D. (1992). Sea ice and wind: effects on primary productivity in the Barents Sea. *Atmos. Ocean* 30, 579–591. doi: 10.1080/07055900.1992.9649456

Sargent, J. R., and Falk-Petersen, S. (1988). "The lipid biochemistry of calanoid copepods," in *Biology of Copepods*, eds G. A. Boxshall and H. K. Schminke (Dordrecht: Springer), 101–114.

Schmid, M. S., Maps, F., and Fortier, L. (2018). Lipid load triggers migration to diapause in Arctic *Calanus* copepods- insights from underwater imaging. *J. Plankton Res.* 40, 311–325. doi: 10.1093/plankt/fby012

Schmidt, K., Brown, T. A., Belt, S. T., Ireland, L. C., Taylor, K. W. R., Thorpe, S. E., et al. (2018). Do pelagic grazers benefit from sea ice? Insights from the Antarctic sea ice proxy $IPSO_{25}$. *Biogeosciences* 15, 1987–2006. doi: 10.5194/bg-15-1987-2018

Scott, C. L., Falk-Petersen, S., Sargent, J. R., Hop, H., Lønne, O. J., and Poltermann, M. (1999). Lipids and trophic interactions of ice fauna and pelagic zooplankton in the marginal ice zone of the Barents Sea. *Polar Biol.* 21, 65–70. doi: 10.1007/s003000050335

Scott, C. L., Kwasniewski, S., Falk-Petersen, S., and Sargent, J. R. (2000). Lipids and life strategies of *Calanus finmarchicus, Calanus glacialis* and *Calanus hyperboreus* in late autumn, Kongsfjorden, Svalbard. *Polar Biol.* 23, 510–516. doi: 10.1007/s003000000114

Søreide, J. E., Falk-Petersen, S., Hegseth, E. N., Hop, H., Carroll, M. L., Hobson, K. A., et al. (2008). Seasonal feeding strategies of *Calanus* in the high-Arctic Svalbard region. *Deep Sea Res. II* 55, 2225–2244. doi: 10.1016/j.dsr2.2008.05.024

Søreide, J. E., Leu, E., Berge, J., Graeve, M., and Falk-Petersen, S. (2010). Timing of blooms, algal food quality and *Calanus glacialis* reproduction and growth in a changing Arctic. *Glob. Change Biol.* 16, 3154–3163. doi: 10.1111/j.1365-2486.2010.02175.x

Spreen, G., Kaleschke, L., and Heygster, G. (2008). Sea ice remote sensing using AMSR−E 89−GHz channels. *J. Geophys. Res. (Oceans)* 113:C02S03. doi: 10.1029/2005JC003384

Stonik, V., and Stonik, I. (2015). Low-molecular-weight metabolites from diatoms: structures, biological roles and biosynthesis. *Mar. Drugs* 13, 3672–3709. doi: 10.3390/md13063672

Stramska, M., and Bialogrodzka, J. (2016). Satellite observations of seasonal and regional variability of particulate organic carbon concentration in the Barents Sea. *Oceanologia* 58, 249–263. doi: 10.1016/j.oceano.2016.04.004

Stübing, D., Hagen, W., and Schmidt, K. (2003). On the use of lipid biomarkers in marine food web analyses: an experimental case study on the Antarctic krill, *Euphausia superba*. *Limnol. Oceanogr.* 48, 1685–1700. doi: 10.4319/lo.2003.48.4.1685

Tamelander, T., Renaud, P. E., Hop, H., Carroll, M. L., Ambrose, W. G. Jr., and Hobson, K. A. (2006). Trophic relationships and pelagic–benthic coupling during summer in the Barents Sea Marginal Ice Zone, revealed by stable carbon and nitrogen isotope measurements. *Mar. Ecol. Prog. Ser.* 310, 33–46. doi: 10.3354/meps310033

Vader, A., Amundsen, R., Marquardt, M., and Bodur, Y. (2021). Chlorophyll A and phaeopigments, Nansen Legacy. *Nor. Mar. Data Centre* (in press). doi: 10.21335/NMDC-1477580440

Van Leeuwe, M. A., Tedesco, L., Arrigo, K. R., Assmy, P., Campbell, K., Meiners, K. M., et al. (2018). Microalgal community structure and primary production in Arctic and Antarctic sea ice: a synthesis. *Elementa* 6:4. doi: 10.1525/elementa.267

Verity, P. G., Wassmann, P., Frischer, M. E., Howard-Jones, M. H., and Allen, A. E. (2002). Grazing of phytoplankton by microzooplankton in the Barents Sea during early summer. *J. Mar. Syst.* 38, 109–123. doi: 10.1016/S0924-7963(02)00172-0

Vinogradov, G. M. (1999). Deep-sea near-bottom swarms of pelagic amphipods *Themisto*: observations from submersibles. *Sarsia* 84, 465–467. doi: 10.1080/00364827.1999.10807352

von Quillfeldt, C. H. (2000). Common diatom species in Arctic spring blooms: their distribution and abundance. *Bot. Mar.* 43, 499–516. doi: 10.1515/BOT.2000.050

Wang, S. W., Budge, S. M., Iken, K., Gradinger, R. R., Springer, A. M., and Wooller, M. J. (2015). Importance of sympagic production to Bering Sea zooplankton as revealed from fatty acid-carbon stable isotope analyses. *Mar. Ecol. Prog. Ser.* 518, 31–50. doi: 10.3354/meps11076

Wang, S. W., Springer, A. M., Budge, S. M., Horstmann, L., Quakenbush, L. T., and Wooller, M. J. (2016). Carbon sources and trophic relationships of ice seals during recent environmental shifts in the Bering Sea. *Ecol. Appl.* 26, 830–845. doi: 10.1890/14-2421

Wassmann, P., Reigstad, M., Haug, T., Rudels, B., Carroll, M. L., Hop, H., et al. (2006). Food webs and carbon flux in the Barents Sea. *Prog. Oceanogr.* 71, 232–287. doi: 10.1016/j.pocean.2006.10.003

Wassmann, P., and Slagstad, D. (1993). Seasonal and annual dynamics of particulate carbon flux in the Barents Sea. *Polar Biol.* 13, 363–372. doi: 10.1007/BF01681977

Watts, J., and Tarling, G. A. (2012). Population dynamics and production of *Themisto gaudichaudii* (Amphipoda, Hyperiidae) at South Georgia, Antarctica. *Deep Sea Res. II* 59, 117–129. doi: 10.1016/j.dsr2.2011.05.001

Werner, I., and Auel, H. (2005). Seasonal variability in abundance, respiration and lipid composition of Arctic under-ice amphipods. *Mar. Ecol. Prog. Ser.* 292, 251–262. doi: 10.3354/meps292251

Werner, I., and Gradinger, R. (2002). Under-ice amphipods in the Greenland Sea and Fram Strait (Arctic): environmental controls and seasonal patterns below the pack ice. *Mar. Biol.* 40, 317–326. doi: 10.1007/s00227-001-0709-1

Weydmann, A., Søreide, J. E., Kwaśniewski, S., Leu, E., Falk-Petersen, S., and Berge, J. (2013). Ice-related seasonality in zooplankton community composition in a high Arctic fjord. *J. Plankton Res.* 35, 831–842. doi: 10.1093/plankt/fbt031

Wickham, H. (2016). *ggplot2: Elegant Graphics for Data Analysis*. Berlin: Springer. doi: 10.1007/978-0-387-98141-3

Wold, A., Darnis, G., Søreide, J. E., Leu, E., Philippe, B., Fortier, L., et al. (2011). Life strategy and diet of *Calanus glacialis* during the winter–spring transition in Amundsen Gulf, south-eastern Beaufort Sea. *Polar Biol.* 34, 1929–1946. doi: 10.1007/s00300-011-1062-6

Conflict of Interest: The authors declare that the research was conducted in the absence of any commercial or financial relationships that could be construed as a potential conflict of interest.

frontiers in Marine Science

ORIGINAL RESEARCH
published: 06 April 2021
doi: 10.3389/fmars.2021.629787

Ross Sea Benthic Ecosystems: Macro- and Mega-faunal Community Patterns From a Multi-environment Survey

Vonda J. Cummings[1], David A. Bowden[1], Matthew H. Pinkerton[1], N. Jane Halliday[1] and Judi E. Hewitt[2,3]*

[1] National Institute of Water and Atmospheric Research, Wellington, New Zealand, [2] National Institute of Water and Atmospheric Research, Hamilton, New Zealand, [3] Department of Statistics, University of Auckland, Auckland, New Zealand

The Ross Sea, Antarctica, is amongst the least human-impacted marine environments, and the site of the world's largest Marine Protected Area. We present research on two components of the Ross Sea benthic fauna: mega-epifauna, and macro-infauna, sampled using video and multicore, respectively, on the continental shelf and in previously unsampled habitats on the northern continental slope and abyssal plain. We describe physical habitat characteristics and community composition, in terms of faunal diversity, abundance, and functional traits, and compare similarities within and between habitats. We also examine relationships between faunal distributions and ice cover and productivity, using summaries of satellite-derived data over the decade prior to our sampling. Clear differences in seafloor characteristics and communities were noted between environments. Seafloor substrates were more diverse on the Slope and Abyss, while taxa were generally more diverse on the Shelf. Mega-epifauna were predominantly suspension feeders across the Shelf and Slope, with deposit feeder-grazers found in higher or equal abundances in the Abyss. In contrast, suspension feeders were the least common macro-infaunal feeding type on the Shelf and Slope. Concordance between the mega-epifauna and macro-infauna data suggests that non-destructive video sampling of mega-epifauna can be used to indicate likely composition of macro-infauna, at larger spatial scales, at least. Primary productivity, seabed organic flux, and sea ice concentrations, and their variability over time, were important structuring factors for both community types. This illustrates the importance of better understanding bentho-pelagic coupling and incorporating this in biogeographic and process-distribution models, to enable meaningful predictions of how these ecosystems may be impacted by projected environmental changes. This study has enhanced our understanding of the distributions and functions of seabed habitats and fauna inside and outside the Ross Sea MPA boundaries, expanding the baseline dataset against which the success of the MPA, as well as variability and change in benthic communities can be evaluated longer term.

Keywords: Antarctica, benthic community, sea ice, productivity, environmental change, marine protected area, functional traits

OPEN ACCESS

Edited by:
Katrin Linse,
British Antarctic Survey (BAS),
United Kingdom

Reviewed by:
Santiago Pineda Metz,
Alfred Wegener Institute, Helmholtz Centre for Polar and Marine Research (AWI), Germany
Jan Jansen,
University of Tasmania, Australia

****Correspondence:***
Vonda J. Cummings
vonda.cummings@niwa.co.nz

Specialty section:
This article was submitted to Marine Evolutionary Biology, Biogeography and Species Diversity, a section of the journal Frontiers in Marine Science

Received: *16 November 2020*
Accepted: *01 March 2021*
Published: *06 April 2021*

Citation:
Cummings VJ, Bowden DA, Pinkerton MH, Halliday NJ and Hewitt JE (2021) Ross Sea Benthic Ecosystems: Macro- and Mega-faunal Community Patterns From a Multi-environment Survey. Front. Mar. Sci. 8:629787. doi: 10.3389/fmars.2021.629787

INTRODUCTION

Climate change is considered the greatest anthropogenic threat to Antarctic ecosystems (Gutt et al., 2020). Antarctica and its biota are highly sensitive to environmental changes, due in part to the biota's narrow tolerance range to a number of environmental features (e.g., temperature; Peck, 2005; Pörtner et al., 2007; Peck et al., 2010). Warming, and its influence on sea ice dynamics is anticipated to reduce sea ice coverage and alter ocean circulation, affecting key processes such as biogeochemical and nutrient cycling and increasing primary production (e.g., Stammerjohn et al., 2008, 2012; Jacobs and Giulivi, 2010). Convey et al. (2014) found that ice cover, ice scour, salinity, and productivity are the most important determinants of marine habitat and community level diversity at smaller spatial scales. This view is supported by data from the Ross Sea shelf and coastal areas (e.g., Thrush et al., 2006; Kröger and Rowden, 2008; Dayton et al., 2013; Rowden et al., 2015). Along with impacts of ocean acidification (Orr et al., 2005; Aronson et al., 2011), effects of climate change on species composition, productivity, phenology and predator-prey interactions in these changing environments are considered imminent (Doney et al., 2012). Indeed, sea ice retreat and ocean warming along the Western Antarctic Peninsula has already resulted in increased algal blooms (Moreau et al., 2015), and changes in the distributions of krill (Steinberg et al., 2015), penguins (Ducklow et al., 2013), and king crabs (Smith et al., 2012; Griffiths et al., 2013) in recent decades.

Interannual variability in Southern Ocean primary production is strongly controlled by changes in sea ice cover (Arrigo et al., 2008, 2015), which also regulates particle flux to the seafloor (Isla, 2016; Deppeler and Davidson, 2017; Henley et al., 2020). The influence of productivity on benthic biomass and abundance in food limited Antarctic ecosystems has been repeatedly demonstrated (e.g., Brey and Clarke, 1993). Suspension feeders in particular have been shown to respond quickly to decreases in productivity associated with reductions in sea ice (Pineda-Metz et al., 2020) due to their more direct link to pelagic production than other feeding guilds (e.g., Smith et al., 2006; Dayton et al., 2013; Sumida et al., 2014). Patterns in the distributions of benthos (abundance, community composition, functional groups) will likely reflect sea ice conditions and water circulation and provide a strong correlative tool for changes in food supply over time (Thrush and Cummings, 2011; Dayton et al., 2019; Kim et al., 2019).

The Ross Sea is a large Antarctic embayment centered at 180° S. Its continental shelf – the largest and widest in Antarctica – covers 466,000 km^2, with an average depth of 530 m and a depth range of 200–1200 m (Smith et al., 2012). Despite commercial hunting of whales and seals in the 19th and 20th centuries, and toothfish in the 21st, the Ross Sea is amongst the least human-impacted marine environments worldwide, due largely to its remoteness, intense seasonality, and extensive ice cover (e.g., Halpern et al., 2008), which make access difficult. The Ross Sea shelf has been sampled by biologists, geologists, and oceanographers since the earliest days of Antarctic exploration and consequently has a relatively well-known benthic fauna by comparison with other regions of the Antarctic (Bullivant, 1959; Bullivant and Dearborn, 1967; Dayton et al., 1974; Barry et al., 2003; Cummings et al., 2010; Barnes et al., 2011). In places, this fauna is rich and the area is considered a 'biodiversity hotspot' (Clarke and Johnston, 2003). The benthic biota of the Ross Sea slope and abyssal environments, however, have had little scientific study (Arntz et al., 1994; Clarke and Johnston, 2003; Brandt et al., 2007). In December 2018, the world's largest marine protected area (MPA) (CCAMLR, 2016) was established in the Ross Sea region, encompassing shelf, slope, seamount, and abyssal environments. Documenting baseline information on the composition, distribution and functioning of ecological communities within the MPA boundaries is a priority for understanding how well the MPA meets its objectives of conserving ecological structure and function, protecting representative portions of benthic environments, and protecting rare or vulnerable seabed habitats (CCAMLR, 2016). A key aspect of the MPA is that it should enable a scientific research and monitoring program that will improve understanding of the effects of natural and anthropogenic change on the ecosystem (CCAMLR, 2016). A fundamental requirement for any understanding of such change is baseline information about the current status of key ecosystem components.

Here, we present research on two components of the Ross Sea benthic fauna: mega-epifauna, and macro-infauna, sampled at sites on the continental shelf, northern continental slope and the abyssal plain during New Zealand's International Polar Year research voyage (RV *Tangaroa*). This research builds and expands on earlier studies of benthic fauna in the Ross Sea by extending sampling beyond the continental shelf to deeper, previously unsampled habitats. We examine patterns in diversity, abundance, and function across the three major environments: (1) continental shelf; (2) continental slope, and (3) abyssal plain. In these three areas, we also explore relationships between the presence of mega-epifauna and macro-infauna to local habitat characteristics. We are particularly interested in the extent to which spatial patterns in benthic community composition concur between mega- and macrofaunal groups, with the aim of assessing whether surface dwelling mega-epifauna can be used to indicate likely composition of the more cryptic (and difficult to sample) macro-infauna.

Relationships between benthic communities and broader spatial and temporal patterns in sea ice conditions were also examined. Sea ice cover in the western Ross Sea increased between 1979 and 2016, with a longer ice-covered season, a later sea ice retreat (∼1 month) and an earlier advance (∼1–2 months) (Stammerjohn and Maksym, 2017). Since 2017, with 2 years of low ice cover, these trends are no longer statistically significant (except for in autumn) (Maksym, 2019). Against this backdrop of change, we provide an initial assessment of the influence of sea ice conditions in conjunction with changes to primary production and organic flux to the seabed, on benthic community characteristics (abundance, composition).

MATERIALS AND METHODS

Sample Collection and Processing

Mega-epifaunal and macro-infaunal assemblages, and substrate characteristics were investigated at 21 sites across the Ross Sea continental shelf (eight sites), northern continental slope (10 sites), and northern abyssal plain (three sites) in February 2008 (**Figure 1** and **Table 1**). At 15 of these sites ('Core' sites, prefix 'C'), one towed camera transect, one beam trawl tow, and one or two multicorer deployments were conducted. At the remaining six sites ('Demersal' sites, prefix 'D') only the towed camera and the beam trawl were deployed. Towed camera transects and beam trawl samples were analyzed for the identities and abundances of mega-epifauna (>ca. 50 mm), and categorical descriptors of substrate type. Multicorer samples were analyzed for macro-infaunal (>300 μm) assemblages and sediment characteristics. Details of the sampling devices, and methods used for determination of the different community components, are provided below.

Mega-Epifauna

Camera transects were run using NIWA's Deep Towed Imaging System (Hill, 2009; Bowden and Jones, 2016) configured with a high definition digital color video camera (HD1080i format) angled forward at 45° and a vertically orientated digital still image camera (Canon 10 MP DSLR). Transects were of 1 h duration at target speed of 0.25–0.5 ms^{-1} and a target altitude above the seabed of 2–3 m. Video was recorded continuously and still images were taken automatically at 15 s intervals. The seabed position of DTIS was recorded continuously in real time using an ultra-short baseline (USBL) acoustic tracking system (Simrad HPR410). Total seabed area imaged by video during each transect ranged from 1,800 to 3,000 m^2, depending on realized tow speed. After the camera transect, a single beam trawl tow (4 m wide, 25 mm cod-end mesh) of approximately 10 min bottom time at 1.0 – 1.5 ms^{-1} tow speed was completed at each site, following the track of the towed camera transect where possible.

Counts of benthic taxa and substrate information were derived from laboratory reviews of the full length of each video transect by analysts using Ocean Floor Observation Protocol software (OFOP, Huetten and Greinert, 2008), with the high-resolution still images and beam trawl specimens used as references for taxonomic identifications. Substratum type was recorded continuously on an eight-category scale from 'Bedrock' to 'Muddy sediment' and expressed as percentages of the full transect distance after correcting for any sections of the transect in which the seabed was not visible (e.g., because of excessive altitude, or contact with the seabed). All visible benthic fauna (>ca. 50 mm) were identified to the finest practicable taxonomic level and counted. Each individual was recorded as a separate observation and logged with its position on the seabed (latitude and longitude), depth, and the substrate type. Densities for each taxon were standardized as the number of individuals 1000 m^{-2} along the whole transect. Both unitary and clonal fauna were recorded as counts, which may underestimate abundance of smaller and more abundant clonal taxa, especially bryozoans, hydroids, and some sponges (i.e., those with indeterminate growth form).

Benthic taxa from the beam trawl were identified to operational taxonomic groups at sea, weighed individually, and preserved using appropriate methods for each taxon (either 90% ethanol, 4% buffered formalin, or frozen). Preserved specimens were later identified to finer taxonomic levels (species, genus, family) by an international network of taxonomists coordinated by the NIWA Invertebrate Collection in New Zealand. Densities for each taxon were calculated as the total number of specimens standardized to the number of individuals 1000 m^{-2} of seabed.

Macro-infauna

Macro-infauna and sediments were sampled at 13 of the 15 Core sites (**Table 1**) using an Ocean Instruments MC-800 multicorer. The multicorer was deployed with either 4 or 8 individual core tubes (96 mm internal diameter), depending on substratum type. For most sites, only one core was processed for macrofauna from each shelf and slope site, but 5–7 cores were processed from each abyssal site. Cores (110 mm deep) were sieved (300 μm mesh) to remove fine sediments, residues preserved in 4% buffered formalin solution, and all retained fauna were identified and enumerated. Non-living biogenic material (e.g., sponge spicules and bryozoan and shell fragments) in each macro-infaunal core was dried and weighed and the amount of sponge spicule material was classified on a categorical scale from 0 (none) to 3 (abundant).

Sediment samples (top 50 mm of cores) were stored frozen and in the dark until analysis. In the laboratory, samples were homogenized prior to determination of particle size distribution, pigment (chlorophyll *a* and phaeophytin) concentrations, total organic content, and calcium carbonate ($CaCO_3$) content. Chlorophyll *a* was extracted from freeze dried sediments by boiling in 90% ethanol. The extract was measured spectrophotometrically and an acidification step was included to separate degradation products (phaeophytin) from chlorophyll *a* (Sartory, 1982). Sediments for particle size analysis were digested in 6% hydrogen peroxide for 48 h to remove organic matter and dispersed using Calgon. A combination of sieving and analysis on a Galai particle analyzer (Galai Cis-100; Galai Productions Ltd, Midgal Haemek, Israel) was then used to calculate percentage volumes for the various size fractions. Organic content was determined by drying the sediment at 60°C for 48 h, followed by combustion at 400°C for 5.5 h, while $CaCO_3$ content was determined using a CO_2 vacuum-gasometric method with ±1% accuracy (Jones and Kaiteris, 1983).

Faunal Functional Traits

To identify the relative predominance of faunal feeding type (suspension feeders, deposit feeder-grazers, or predator-scavengers) and, for macro-infauna only, living position (surface, top 2 cm of sediment or deeper-sediment dwellers) within and between areas/environments. The taxon lists for each faunal group data set were examined and trait modalities were assigned using a combination of literature information, advice from taxonomic experts and our own observations. Because taxa can exhibit more than one feeding type or living position, 'fuzzy coding' (*sensu* Chevenet et al., 1994) was applied to allow the species to vary in the degree in which it exhibited affinity to a specific modality within the feeding and living position trait

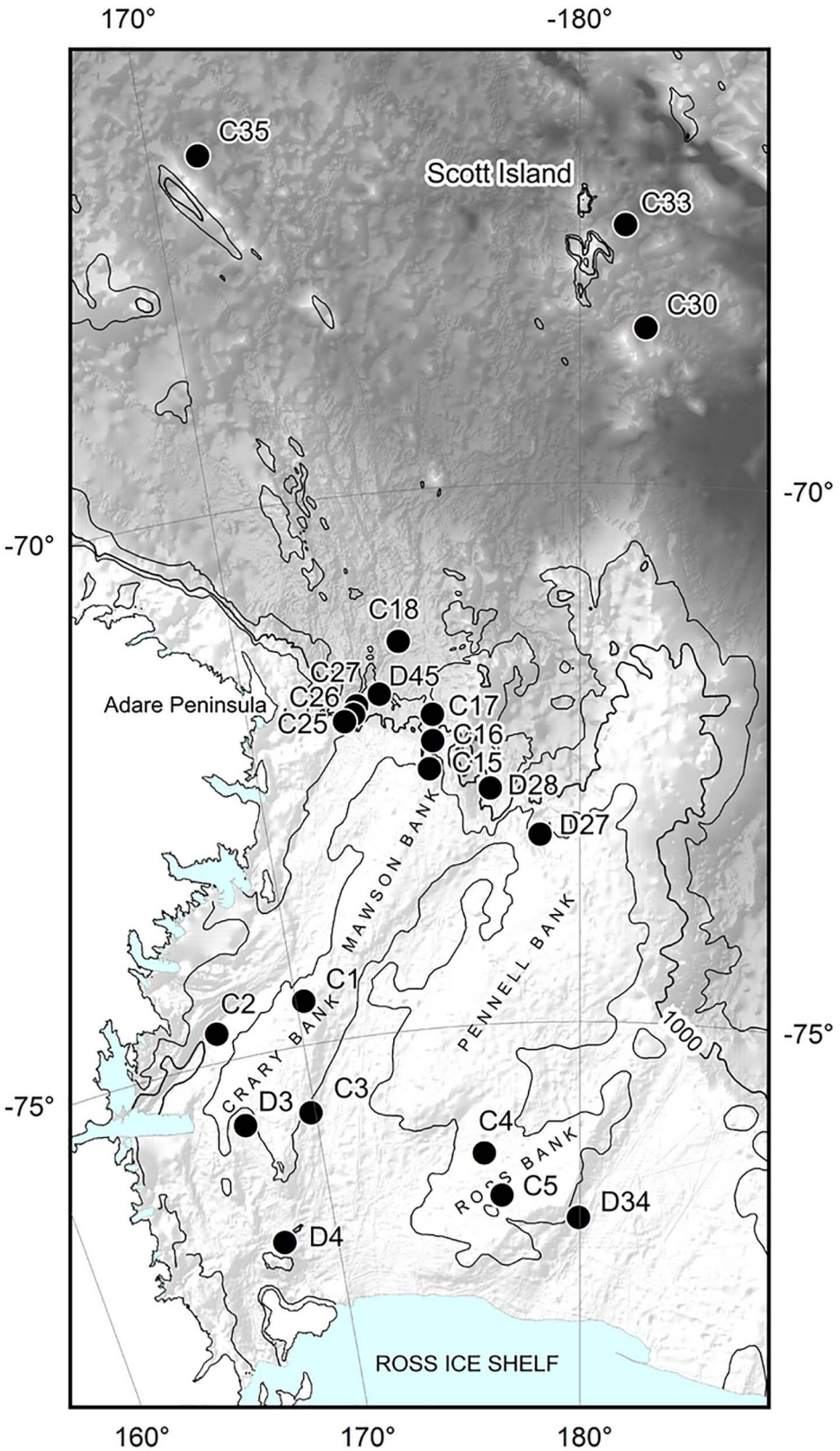

FIGURE 1 | Sites sampled for benthic invertebrates during the NZ IPY-CAML voyage to the Ross Sea (TAN0802) in Jan-Apr 2008. C prefix sites: towed camera, beam trawl, and multicorer; D prefix sites: towed camera and beam trawl only. Hill shade bathymetry from IBSCO v1, isobaths at 500, 1000, and 2000 m.

TABLE 1 | Details of benthic sampling sites.

Environment	Site	Longitude (°)	Latitude (°)	Depth (m)			Faunal groups sampled
				Maximum	Minimum	Mean	
Continental shelf	C1	170.27083 E	74.58885 S	286	283	286	I, E
	C2	167.03842 E	74.73285 S	886	831	893	I, E
	C3	169.83000 E	75.62802 S	532	511	580	I, E
	C4	176.26125 E	76.19980 S	450	445	442	I, E
	C5	176.81882 E	76.59780 S	370	360	364	I, E
	D3	167.32117 E	75.62417 S	460	460	470	E
	D4	167.83600 E	76.77500 S	705	705	698	E
	D34	179.95033 E	76.83283 S	665	665	662	E
Continental slope	C15	175.33318 E	72.58890 S	479	470	472	E
	C16	175.50653 E	72.32996 S	980	971	967	I, E
	C17	175.55897 E	72.08564 S	1620	1600	1599	I, E
	C18	174.72779 E	71.38790 S	2283	2214	2209	I, E
	C25	172.90433 E	72.07550 S	536	510	514	I, E
	C26	173.19950 E	72.01726 S	822	807	815	I, E
	C27	173.31891 E	71.94094 S	1570	1534	1510	E
	D45	174.03300 E	71.85567 S	1957	1957	1960	E
	D27	178.72367 E	73.24817 S	774	774	778	E
	D28	177.19367 E	72.80533 S	1368	1368	1374	E
Abyssal plain	C30	178.33380 W	68.56317 S	3245	3198	3225	I, E
	C33	178.89632 W	67.62379 S	3553	3475	3545	I, E
	C35	171.14914 E	66.72817 S	3419	3382	3402	I, E

C prefix denotes Core sites, D prefix denotes Demersal sites. Maximum, minimum, and mean depths across all sampling methods are given for each site. I, macro-infauna; E, mega-epifauna.

categories. The probability of a species exhibiting a particular trait was allocated, with allocation across a single trait category summing to 1 (see Hewitt et al., 2008, 2018 for specifics on how probabilities were generated). The fuzzy probability of a species exhibiting a specific trait modality, multiplied by the abundance the species displayed, then partitions the abundance of species that exhibit more than one modality across the traits. The resulting functional trait data were assessed in two ways: (i) the number of taxa with a particular trait ('taxa weighted trait'), and (ii) the number of individuals with a given trait ('abundance weighted trait'). The latter was calculated by multiplying the fuzzy probability by the abundance of each taxon to provide an abundance weighted measure of each trait.

Sea Ice Conditions, Productivity, and Seabed Flux

Sea ice concentration data for the region were derived from satellite measurements. We used data from the Scanning Multichannel Microwave Radiometer (SMMR) on the Nimbus-7 satellite and from the Special Sensor Microwave/Imager (SSM/I) sensors on the Defense Meteorological Satellite Program's (DMSP) -F8, -F11, and -F13 satellites. Measurements from the Special Sensor Microwave Imager/Sounder (SSMIS) aboard DMSP-F17 are also included. The data set has been generated using the Advanced Microwave Scanning Radiometer – Earth Observing System (AMSR-E) Bootstrap Algorithm with daily varying tie-points (Cavalieri et al., 1990/2007).

The monthly time series was also used to calculate spatial maps of the proportions of time present of four sea ice types: ice free, marginal ice zone, open pack ice, and close pack ice. Areas of ocean are usually taken to be "ice-free" if the proportion of the sea covered with ice within a given area is less than about 10–15% (e.g., Comiso, 2003; Arrigo and van Dijken, 2004). Here, we use 15% as the limit. Sea ice concentrations between 15–40% are typically associated with "marginal ice zone" conditions, while concentrations between 40–70% are typically "open pack" conditions, and concentrations over about 70% are usually "close pack" conditions (Comiso, 1983, 1995; Cavalieri et al., 1984; Gloersen and Cavalieri, 1986).

Net primary production (mg C m^{-2} d^{-1}) was derived using the Vertically Generalized Production Model (VGPM; Behrenfeld and Falkowski, 1997) sourced from www.science.oregonstate.edu/ocean.productivity/. This model incorporates data on near surface Chlorophyll *a* (Chl *a*) and sea surface temperature (SST). Near surface concentration of Chl *a* (mg m^3) was estimated from the default (case 1) processing of MODIS-Aqua (version R2018.0) and SeaWiFS (version R2018.0) satellite sensors, blended using overlap period 2002–2010 (NASA Goddard Space Flight Center, Ocean Ecology Laboratory, and Ocean Biology Processing Group., 2018a,b). The Chl *a* and VGPM data sets span the period September 1997 to August 2018, but only data in the decade before benthic sampling were used here (1998–2008). The SST dataset used was the Optimum Interpolation Sea Surface Temperature (OISST), version 2, which is based on satellite measurements by the Advanced Very High Resolution Radiometer series, operated

by the National Oceanic and Atmospheric Administration, United States (Reynolds et al., 2002).

Downward vertical flux of particulate organic matter at the seabed (mg C m^{-2} d^{-1}) was estimated based on net primary production in the surface mixed layer (VGPM), with export fraction and flux attenuation factor with depth obtained by refitting sediment trap and thorium-based measurements to environmental data (VGPM, SST) as Lutz et al. (2007) and Law et al. (2017) and using data from Cael et al. (2018).

The above data were analyzed for the time period 1998 to 2008; i.e., encompassing the 10 years up to the time of the benthic sample collection. All sea ice and productivity data were projected onto a circumpolar, polar stereographic grid with nominal 9 km resolution. For five variables (% sea ice concentration, Chl *a*, SST, VGPM, seabed flux), monthly climatologies were generated by averaging all data in a given calendar month. Monthly resolution was chosen as shorter timespans lead to large data gaps. The pixel value of the monthly composites was used to calculate annual means. We consider a year the period from July to June (e.g., data for 1998 corresponds to July 1997 to June 1998). The long-term (i.e., 10 years) mean and standard deviation values were calculated from the annual averages, so that the standard deviations represent the variability between years. Mean and standard deviations (between years) were also calculated from the proportions of time with a given type of sea ice (% of time ice free, or with marginal, open pack, or close pack ice).

Statistical Analyses

Community Analyses

Mega-epifauna (from DTIS video) and macro-infauna assemblage data were analyzed to identify spatial patterns in assemblages between and within environments (Shelf, Slope, Abyssal plain). For each faunal group separately, total numbers of taxa and individuals were calculated and similarities in community composition among sites were visualized using non-metric multidimensional scaling ordinations (MDS: PrimerE, Clarke and Warwick, 2001) of Bray–Curtis similarity matrices calculated from both untransformed and presence-absence transformed faunal abundance data. These two data treatments have been used throughout out our analyses; together they provide complementary information by emphasizing the importance of dominant and rare species, respectively. Where no major differences were observed between the two data treatments, only the raw results are presented. The individual taxa contributing to the community differences between environments were identified using the similarity percentages procedure, SIMPER (Primer E).

The PERMANOVA routine in PrimerE was used to quantify differences in benthic community structure between environments (Shelf, Slope, and Abyss) indicated in the MDS, and the significance of these differences using pairwise comparisons. *P*-values were obtained using 999 permutations. Because PERMANOVA is sensitive to differences in multivariate dispersion among groups, the PERMDISP routine in PRIMER was used to test for homogeneity of dispersion, also using pairwise comparisons.

Comparison of patterns across faunal groups

Spatial patterns in community composition between the mega-epifauna (from DTIS video) and macro-infauna were compared using a matrix correlation method (RELATE, Clarke and Warwick, 2001; Somerfield et al., 2002). For mega-epifauna only, data from the two sampling methods (DTIS video vs beam trawl) were also compared at this stage to assess any influence of gear type on spatial patterns. Similarity matrices were calculated for each of the faunal data sets (mega-epifauna DTIS, mega-epifauna beam trawl, and macro-infauna) using Bray–Curtis distance as a measure of similarity between pairs of samples. Spearman's rho (ρ) correlations between these similarity matrices were then calculated using RELATE. The analyses were run using untransformed and presence-absence faunal data to assess the relative contributions of species richness and abundance to concordance between patterns.

Community composition for the mega-epifaunal (DTIS video) and macro-infaunal data sets was initially investigated across all samples to determine whether patterns observed in the similarity matrices were alike for the two faunal components. The similarity matrices compared were of the same type (e.g., untransformed compared with untransformed, and presence-absence with presence-absence). After this initial comparison, each data set was divided into shelf, slope and abyssal plain sites to determine whether any common patterns detected between the faunal data sets at the scale of the entire survey area were similar within and between the shelf, slope and abyssal habitats separately.

Because RELATE provides only a single correlation value describing the relationship between two matrices, it cannot be used to test for interactions among variables directly. To explore this further, a three stage partial canonical ordination was used (CANOCO, Ter Braak and Smilauer, 1998). In the first stage, Correspondence Analysis (CA) was used to reduce the multivariate composition of the macro-infauna and mega-epifauna data (separately) to a few dimensions. This analysis was based on untransformed data and down weighted to reduce the influence of rare species and thus highlight general inter-sample differences (note that this procedure does not change the abundance of common species). Next, dummy variables were constructed to represent each of the two areas (shelf and slope) and the interaction between them and used in Canonical Correspondence Analysis (CCA) where the macro-infauna data was predicted by the sample scores from the CA of the mega-epifauna and the dummy variables. Finally, we established whether consistent relationships occurred between the macro-infauna data and the mega-epifauna CA scores, and whether or not these were a direct result of depth, by re-running the CCAs with the effect of depth partialed out.

Sea Ice, Productivity and Seabed Flux, and Community Characteristics

To investigate the relative importance of the sea ice and productivity-associated variables on community composition and feeding traits (i.e., taxa and abundance weighted traits), distance-based linear models were run (DistLM, McArdle and Anderson, 2001) based on Bray–Curtis dissimilarities calculated

from untransformed macro-infaunal and mega-epifaunal data, and using step-wise selection based on the adjusted R^2 criterion. Thirteen variables were included in the initial model (i.e., mean and SD for: % sea ice concentration; % seabed flux; % of time ice free, or with close pack- or marginal ice; VGPM). The % of time with open pack ice and concentration of Chl *a* were both excluded due to their high correlations with close pack ice and VGPM, respectively. Depth was included as a starting condition in all models so that the influence of other variables could be evaluated after allowing for the effect of depth. Distance-based Redundancy Analysis ordinations (dbRDA, Legendre and Anderson, 1999) of the fitted values of the selected models were created, to visualize the strength and direction of the relationships between community composition and individual environmental variables.

RESULTS

General Site Descriptions – Substrata

Substrata at sites on the Shelf were mostly muddy sediments, with occasional glacial drop-stones (recorded as 'boulders' in the video analysis, **Figure 2A**). Analyses of multicores showed that Shelf sediments consisted predominantly of fine sand, with varying amounts of medium sand and silt (**Figure 2B** and **Supplementary Table 1**). The deepest shelf site, C2 in the Drygalski Basin, contained a significant amount of pebble (17%; **Figure 2B** and **Supplementary Table 1**). The Shelf site cores contained the most sponge material of all areas (**Supplementary Table 1**).

Slope substrata were more heterogeneous than those on the shelf, comprising a mixture of gravel, cobbles and sand, with smaller proportions of shell hash and boulder. The volume of coarser sediment and biogenic material was highest on the Slope (**Figure 2B** and **Supplementary Table 1**). The seafloor at two upper-slope sites on the shelf break east of Cape Adare (C25 and C26) were predominantly fragments of stylasterid hydro-coral skeleton. The cores from these sites had a distinctive coarse layer of coral fragments overlying finer sediment, and also contained gastropod and bivalve shells. At the base of the slope (sites D27 and C18) substrata were mostly fine muddy sediments.

The Abyssal sites consisted of muddy sediments with varying amounts of boulder, cobble and, particularly at site C33 east of Scott Island, dark basaltic gravels (**Figure 2A**). These muddy

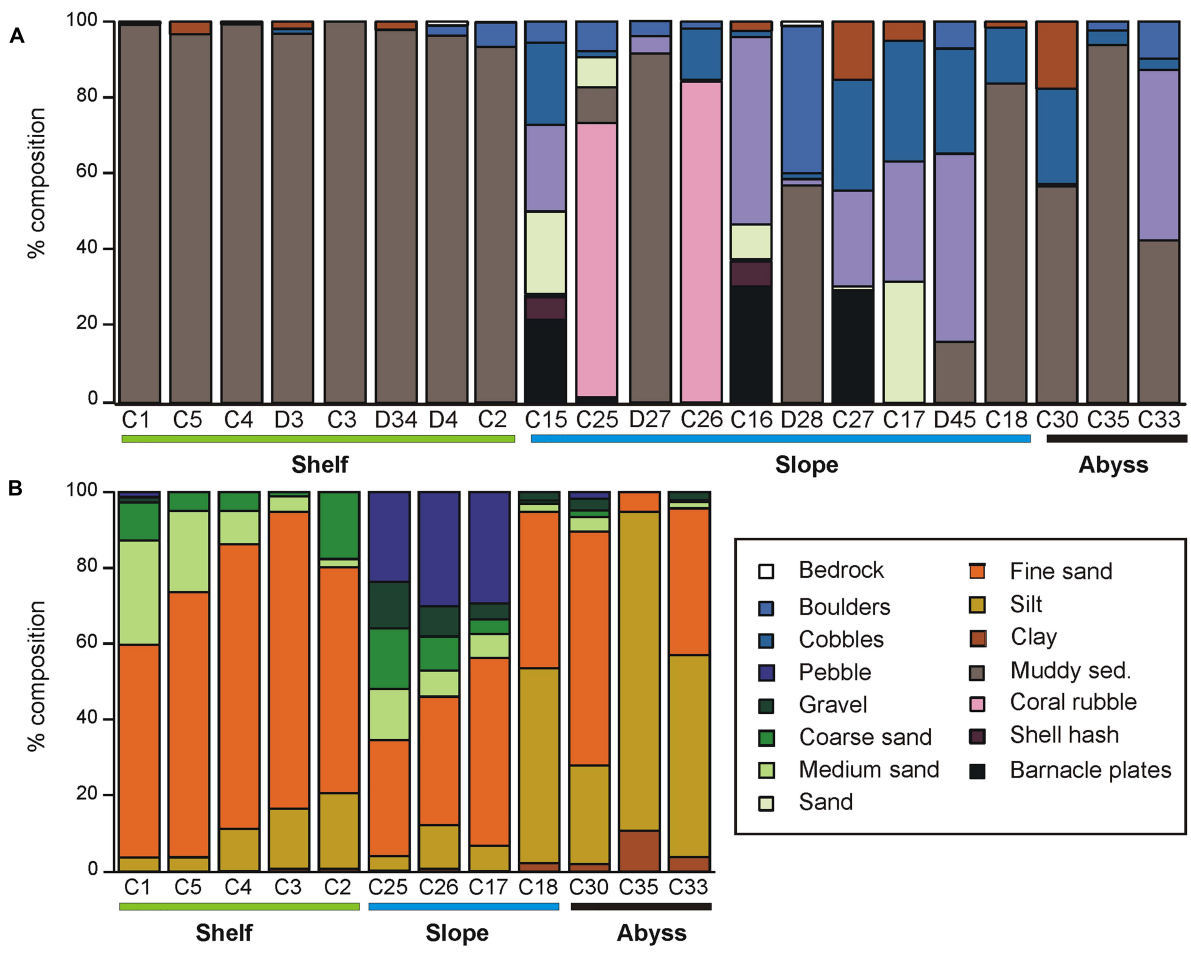

FIGURE 2 | (A) Substrate type determined for Core and Demersal sites from DTIS video, and **(B)** grain size composition of the multi-core sampled sediments at each Core station. Stations are grouped by environment (Shelf, Slope, Abyss), and, within each environment, are arranged from shallowest to deepest (left to right).

sediments were predominantly silt and fine sand, with some clay, and contained relatively little biogenic material (**Figure 2A** and **Supplementary Table 1**).

Sediment organic content ranged from 0.8 to 3.1% and did not differ between environments (**Supplementary Table 1**). In contrast, sediment pigment concentrations were considerably higher on the Shelf (1.84 – 7.28 μg phaeophytin g^{-1} sediment) than on either the Slope or Abyssal plain ($<<$ 1 μg phaeophytin g^{-1} sediment). Chl *a* was only detected at two sites; C1 and C2 on the continental shelf ($\leq$0.43 μg g^{-1} sediment). $CaCO_3$ content of the sediments was generally very low (0.04 – 2.67%), with the exception of the two shelf-break Slope sites C25 and C26 (43 and 38%, respectively; **Supplementary Table 1**).

General Site Descriptions – Fauna

For mega-epifauna 48,818 individuals, representing 261 taxa across 11 phyla, were identified from DTIS video transects, while 61,399 individuals representing 592 taxa across were identified from beam trawl samples. One hundred and twenty-seven macro-infaunal taxa (ranging from species to phyla) and 1230 individuals were recorded from the 48 multicore samples analyzed for this study.

Mega-Epifauna

On the continental shelf, mega-epifaunal assemblages were comprised of 53–101 taxa and from 448 to nearly 3000 individuals 1000 m^{-2} (**Figures 3A,B**, respectively). Communities were characterized by bryozoans, gorgonian and pennatulacean octocorals, comatulid crinoids, sponges (demosponges and hexactinellids), hydroids, anthozoans (cerianthids and anemones), and ascidians; all of which are suspension feeding taxa. The highest densities of fauna were recorded at site C4, where bryozoans dominated. At the two deepest Shelf sites, C2 and D4, deposit feeding taxa, primarily holothuroids constituted a greater proportion of the community, but suspension feeders in the form of hexactinellid sponges, pennatulaceans, and large solitary athecate hydroids were also common.

On the continental slope, by contrast, numbers of taxa and abundances were lower (27 – 45 taxa, 104 – 405 individuals 1000 m^{-2} **Figures 3A,B**) and there were fewer sessile suspension feeding taxa. Asteroids, demosponges, and anemones were the most consistent characterizing taxa (highest similarity values) across all Slope sites. However, natant decapod crustaceans were conspicuous at deeper sites and stylasterid hydrocorals dominated at the shallow Shelf break site on the westernmost cross-slope transect in the Cape Hallett and Cape Adare region (Site C25).

At the Abyssal sites, numbers of taxa were similar to those on the Slope (23 – 42 taxa 1000 m^{-2}; **Figure 3A**), but overall densities were lower than in the other environments (18 – 141 individuals 1000 m^{-2}; **Figure 3B**). Deposit-feeding holothuroids were the most abundant mega-epifauna. Anemones, echinoids, ophiuroids, isopods, asteroids and natant decapods were consistently found, albeit at lower densities.

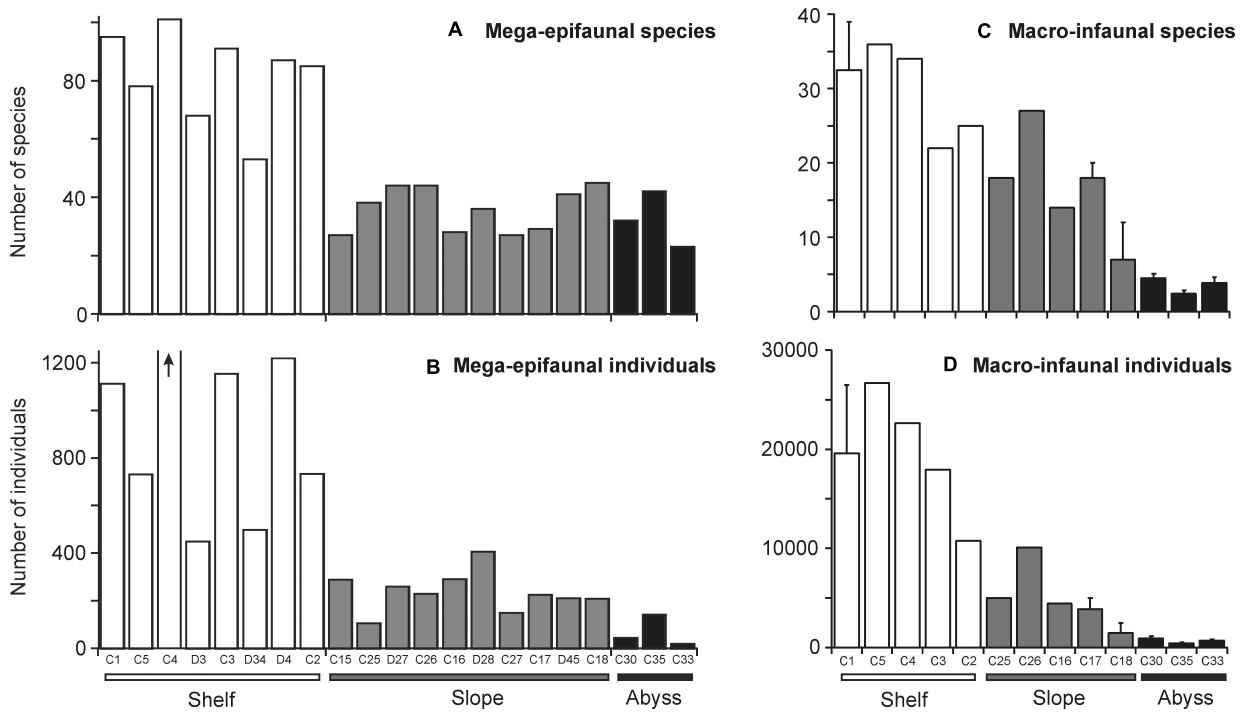

FIGURE 3 | Total number of **(A)** mega-epifaunal and **(C)** macro-infaunal species and **(B,D)** individuals found at each site. Sites are arranged in order of increasing depth (left to right) within the "Shelf," "Slope," and "Abyss" categories. The arrow on **(B)** indicates number of individuals at Site C4 was off the scale (2959 individuals). Standard error bars on some macro-infaunal sites indicate where multiple stations were sampled at that Core site. Note the different y-axes scales on comparable plots.

Macro-Infauna

Polychetes were the most diverse macro-infaunal taxonomic group overall (47 taxa) and, along with nematodes, accounted for half and one quarter of the total number of individuals collected (658 and 321 specimens), respectively.

The continental shelf sites had from 22 to 39 taxa, and the most individuals (10,776 – 26,664 individuals m^{-2}) of all areas (**Figures 3C,D**). The assemblages were all dominated by nematodes, in varying abundances (2,487 – 8,487 individuals m^{-2}). The small suspension feeding bivalve *Thyasira debilis* was the second most abundant taxon at sites C5 and C4 (4,421 and 2,487 individuals m^{-2}, respectively). Ostracoda, and the deposit feeding polychete grouping Cirratulidae were common at three of the five shelf sites (ostracods at C1, C5, and C4, with 2,072, 1,796, and 691 individuals m^{-2}, respectively; cirratulids at C5, C3, and C4, with 1,382, 967, and 829 individuals m^{-2}, respectively).

All of the Slope sites featured Isopoda spp. (276 – 1,105 individuals m^{-2}) which was the most common taxon at C18 and the second most abundant taxon at C16, C17, and C26. Nematodes were also the most abundant taxa at two of the slope sites, C17 and C25 (691 and 829 individuals m^{-2}, respectively), and featured at C26 (967 individuals m^{-2}). Numbers of taxa and individuals were intermediate between those of the Shelf and Abyss sites (**Figures 3C,D**).

Abyssal sites were characterized by very low numbers of individuals and taxa (**Figures 3C,D**), with Cirratulidae the most common taxa at C30 (average 161 individuals m^{-2}), and oligochaetes (predator/scavengers) the most abundant taxa at C33 and C35 (124 and 81 individuals m^{-2}, respectively). Isopoda spp. were the second or third most abundant taxa at these sites. Nematodes were the second most common taxa at C30, with 80 individuals m^{-2} on average.

Comparisons of Faunal Characteristics Across Environments

Numbers of mega-epifaunal taxa and overall sample abundances were higher at sites on the Shelf than on either the Slope or Abyssal plain but were comparable between Slope and Abyssal sites (**Figures 3A,B**). Macro-infauna were also more species-rich and considerably more abundant on the Shelf than on either the Slope or Abyssal plain (**Figures 3C,D**); additionally, numbers of taxa and individuals were higher in the Slope sites compared to the Abyssal sites. Macro-infauna taxon-richness and abundance showed a strong inverse relationship with depth (R^2 = 0.92 and 0.86, respectively; **Figure 4B**), with similar but weaker relationships for mega-epifauna (R = 0.64 and 0.53, respectively; **Figure 4A**).

MDS ordinations revealed distinct groupings of sites by environments (**Figure 5**). For mega-epifauna untransformed data, all Shelf sites and four of the easternmost Slope sites grouped together and were distinct from the remaining Slope sites and the Abyssal sites (**Figure 5A**). However, dissimilarities were generally very high (>70%; **Supplementary Table 2**), with the exception of Slope sites C16, C17, D27, and D28 (**Figure 5A**), among which dissimilarities were ≤50% (**Supplementary Table 2**). Dissimilarity between mega-epifaunal assemblages in the three large-scale environments was high (>80%), particularly in comparisons involving the abyssal environments (i.e., shelf vs.

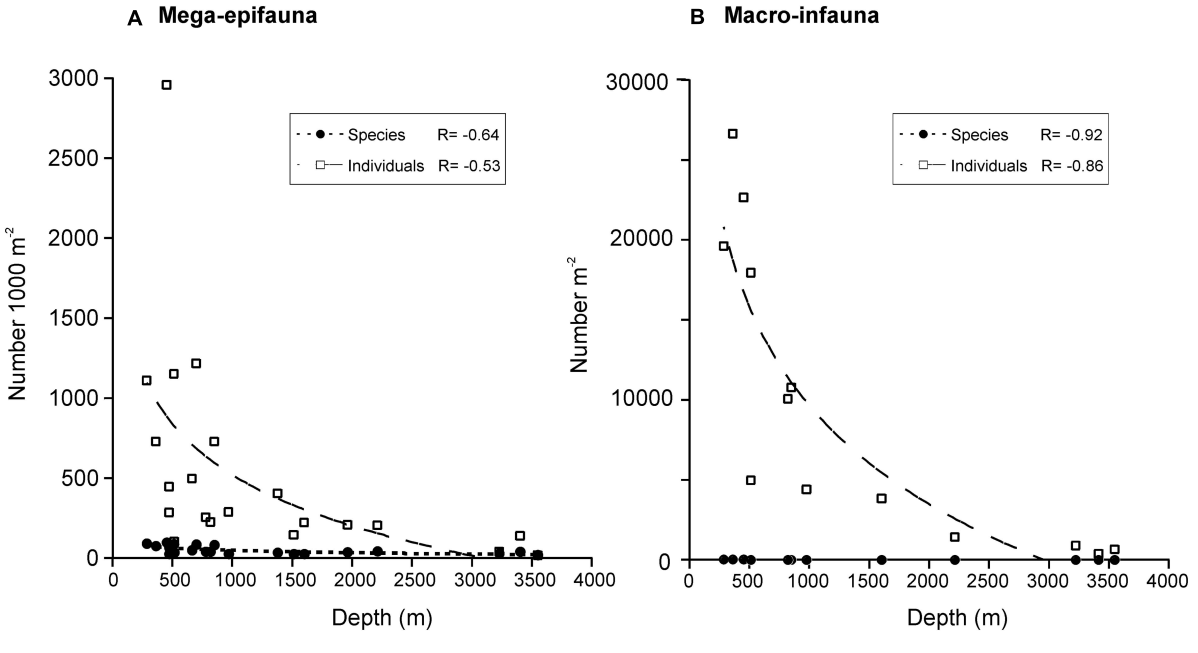

FIGURE 4 | Relationship between depth and number of **(A)** mega-epifaunal and **(B)** macro-infaunal taxa and individuals. Curves are logarithmic fits and correlation coefficients (R) are shown for each. Mega-epifaunal data from DTIS video footage.

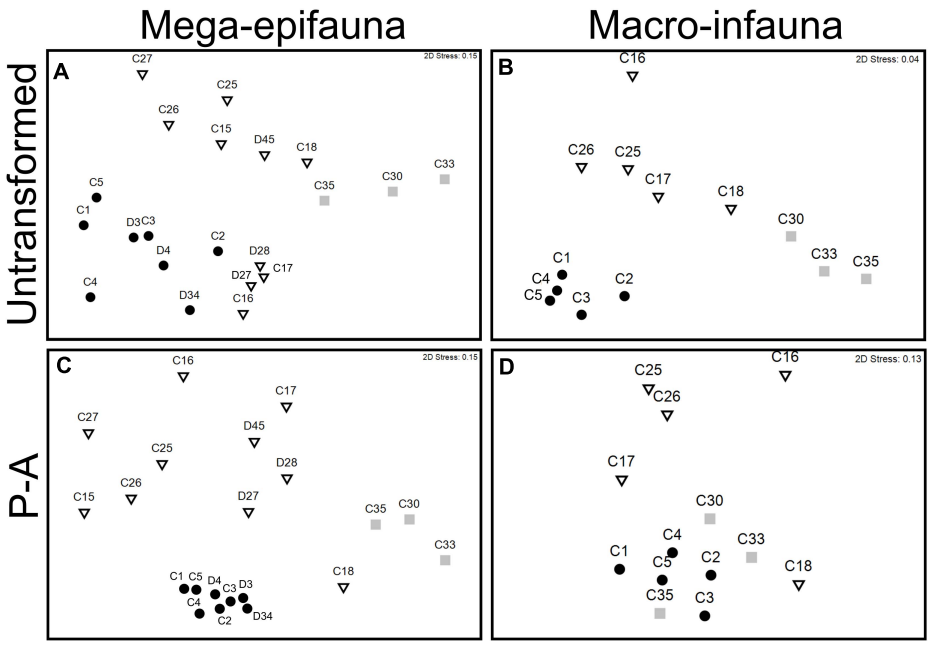

FIGURE 5 | MDS ordinations of mega-epifaunal and macro-infaunal community similarity between sampling sites on the continental shelf (circles), continental slope (triangles), and abyss (squares). Data are untransformed (**A,B**), and presence-absence transformed (P-A, **C,D**) abundance values from seabed video transects (mega-epifauna) and multicorer (macro-infauna) samples. Distances represent Bray–Curtis similarities among sites.

slope = 80.34%, abyss vs. shelf = 90.85%, abyss vs. slope = 87.25% **Supplementary Table 2**).

In the mega-epifauna MDS based on presence-absence transformed data (**Figure 5C**) there was strong clustering of Shelf site communities, and strong dissimilarities between these and all other sites, indicating pronounced differences in taxonomic composition between on- and off-shelf faunas. Comparable ordinations using data from the beam trawl samples showed broadly similar relationships (not shown here).

Macro-infaunal communities from the Shelf, Slope, and Abyssal plain were, like the mega-epifauna, clearly separated in ordination space (untransformed MDS, **Figure 5B**). Closer examination of the species comprising the assemblages in the different environments (using SIMPER analysis of the untransformed data; **Supplementary Table 3**) revealed considerably lower % dissimilarity between core sites on the Shelf (37 – 73%) than that within either the Slope (61 – 90%) or Abyss (80 – 83%). The stations comprising each of the abyssal core sites exhibited very low similarity (15 – 27%), indicating there were strong differences in community composition between stations/within sites. Only one slope and one shelf Core site had sufficient replication to test within-site similarity, and in both cases, these were higher than those of the abyssal stations (slope C17, 36%; shelf C1, 43%). MDS using presence/absence transformed data shows higher similarity of the Abyssal sites to the Shelf sites, reflecting occurrence of some wide-spread taxa (**Figures 5B** cf. **D**).

These observations of differences in mega-epifaunal and macro-infaunal community structure between environments are supported by statistical significance of the PERMANOVA analyses (**Table 2**). Significant differences were found between environments for almost all mega-epifauna and macro-infaunal comparisons, regardless of the data transformation treatment (**Tables 3A,B**). The exception was the comparison between Slope and Abyssal macro-infauna communities using presence-absence (p = 0.106; **Table 3B**), reflecting the fact that the deepest Slope sites are at similar depths to the Abyssal sites. PERMDISP pairwise comparisons of variability between environments were significantly different only for the mega-epifaunal presence/absence transformed data, in which the Slope data were significantly more variable than those from the Abyss and the Shelf (**Table 3A** and **Figure 5C**). This is expected because the Slope sites span a depth range from Shelf to Abyss and an environmental gradient across the shelf-break front.

Functional Traits

Across the Shelf and Slope stations, mega-epifauna were predominantly suspension feeding taxa (**Figure 6**). In the Abyss, deposit feeder-grazers were found in higher or equal abundances. For macro-infauna in contrast, suspension feeding taxa were the least common feeding type at all Shelf stations, and at all but one of the five Slope stations (i.e., C26, C16–C18; **Figure 6**). Deposit feeder-grazers were found in relatively high proportions at the three shallowest Shelf sites (C1, C5, and C4; 0.45–0.50), and equal numbers of deposit-grazer and predator-scavenger taxa were noted at C3 and C2 (**Figure 6**). There was no clear pattern of feeding type across the Abyssal sites, although fewer predator/scavenger taxa were found here.

TABLE 2 | Results of PERMANOVA analyses testing for differences in benthic community composition between environments, for **(A)** mega-epifauna taxon identity data, **(B)** macro-infauna taxon identity data, **(C)** mega-epifauna feeding traits, and **(D)** macro-infauna feeding traits.

	Source	df	SS	MS	Pseudo-F	*P*	Perms
(A) Mega-epifauna							
Raw	Habitat	2	19022	9510.8	2.7882	**0.001**	999
	Residuals	18	61400	3411.1			
	Total	20	80422				
p/a	Habitat	2	18044	9022.2	5.0155	**0.001**	997
	Residuals	18	32380	1798.9			
	Total	20	50424				
(B) Macro-infauna							
Raw	Habitat	2	20673	10336.0	4.7402	**0.001**	984
	Residuals	10	21806	2180.6			
	Total	12	42478				
p/a	Habitat	2	8646.7	4323.3	2.2706	**0.001**	987
	Residuals	10	19041	1904.1			
	Total	12	27688				
(C) Mega-epifauna feeding traits							
Abundance weighted trait	Habitat	2	19941	9970.4	16.544	**0.001**	992
	Residuals	10	6026.7	602.67			
	Total	12	25967				
Taxa weighted trait	Habitat	2	9062.1	4531	24.949	**0.001**	99
	Residuals	18	3269	181.61			
	Total	20	12331				
(D) Macro-infauna feeding traits							
Abundance weighted trait	Habitat	2	19941	9970.4	16.544	**0.001**	992
	Residuals	10	6026.7	602.67			
	Total	12	25967				
Taxa weighted trait	Habitat	2	12475	6237.6	19.729	**0.001**	990
	Residuals	10	3161.7	316.17			
	Total	12	15637				

raw, untransformed data; p/a, presence–absence transformed data.
For C and D, data are untransformed.
df, degrees of freedom; SS, sum of squares; MS, mean square; Perms, unique permutations.
Significant p-values are indicated in bold.

When weighted by abundance, these patterns become less obvious – the Shelf and Slope macro-infaunal assemblages were both predominantly deposit feeder-grazers and predator-scavengers, with the exception of the shallowest slope site (C26) which had considerably more suspension feeders (**Figure 6**). No one feeding type predominated across all Abyssal stations.

Significant differences between all environments for mega-epifauna and macro-infauna feeding traits were found using PERMANOVA, both when examining taxa- and trait-weighted abundance (**Tables 2**, **3**). There were no differences in trait variability between communities from the environments being compared, as indicated by PERMDISP (**Table 3**).

Across all stations and environments, there were relatively few macro-infauna taxa residing deeper in the sediments (below 2 cm; <0.5) (**Supplementary Figure 1**). At all Shelf sites, 0.4 – 0.5 of taxa found were top 2 cm dwellers, while on the Slope the majority were surface dwelling taxa (except at the two deepest sites, C17 and C18). A combination of top 2 cm and surface-dwellers were most common at the Abyssal sites. Weighting by abundance accentuated the predominance of top 2 cm-dwellers on the Shelf and of surface dwellers on the Slope (**Supplementary Figure 1**).

Concordance of Faunal Group Spatial Patterns

RELATE tests comparing patterns from the two benthic faunal groups across all sampling sites and environments showed significant concordance in all comparisons (**Table 4**). The strongest concordance was found using untransformed abundance data ($\rho = 0.749$, $P = 0.001$), and the weakest using presence-absence data ($\rho = 0.326$, $P = 0.020$) (**Table 4**).

When Shelf and Slope environments were analyzed independently, concordance was weaker than for comparisons across all sampling areas and was significant only for the slope (**Table 4**, untransformed data only). A comparison between mega-epifaunal assemblage characteristics sampled by video or by beam trawl also showed strong and significant concordance, for all data transformations ($\rho > 0.675$, $P = 0.010$; **Table 4**).

The first two axes of the CA ordination of the untransformed DTIS-based mega-epifauna data explained 14.5 and 12.5% of the variance in assemblage composition, with a further 11 and 10% explained by the third and fourth axes, respectively, and a total of 48% explained across four axes. For macro-infauna, the first two axes explained 21 and 15% of the total variance, respectively, with a total of 53% explained by all four axes.

There was a significant relationship between the untransformed macro-infaunal data and the DTIS video mega-epifaunal CA scores, even with the effect of depth partialed out ($p = 0.008$, community composition variation explained = 42%; **Supplementary Table 4**). Depth by itself explained only 9% of the variability in community composition ($p = 0.092$).

Sea Ice, Productivity and Seabed Flux, and Community Characteristics

Community Structure

Mega-epifaunal community structure was best explained in the DistLM analysis by five variables in addition to depth: the standard deviation of ice-free time (*iceFree_sd*, 11.5%); mean water-column productivity (*vgpm_mean*, 9.9%); mean flux of primary production to the seabed (*flux_mean*, 7.9%); mean marginal sea-ice duration (*marginal_mean*, 4.3%), and the standard deviation of water-column productivity (*vgpm_sd*, 3.9%) (**Figure 7A**; untransformed ordination; **Supplementary Table 5**). Depth alone explained 6.8% of variance. The total explained variance was 48.9. Shelf sites were strongly distinguished from slope and abyssal sites primarily by higher productivity and to a lesser extent by mean marginal ice duration. Within each set of these broad groupings of sites (i.e., Shelf versus Slope and Abyss), individual sites were distributed along an axis defined by the variability of ice-free duration (*iceFree_sd*) and mean flux to the seabed (*flux_mean*).

TABLE 3 | Results of pairwise comparisons from PERMANOVA and PERMDISP analyses, testing for differences in benthic community composition between environments, for **(A)** mega-epifauna taxon identity data, **(B)** macro-infauna taxon identity data, **(C)** mega-epifauna feeding traits, and **(D)** macro-infauna feeding traits.

		PERMANOVA			PERMDISP	
	Comparison	***t***	***P***	**Perms**	***t***	***P***
(A) Mega-epifauna taxon identity data						
Raw	Shelf vs. Slope	1.7794	**0.001**	986	1.3855	0.230
	Shelf vs. Abyss	1.7217	**0.006**	165	1.1345	0.632
	Slope vs. Abyss	1.4705	**0.008**	275	1.9225	0.354
p/a	Shelf vs. Slope	2.2818	**0.001**	989	8.6054	**0.001**
	Shelf vs. Abyss	3.0044	**0.007**	165	0.3630	0.847
	Slope vs. Abyss	1.8166	**0.004**	277	6.382	**0.002**
(B) Macro-infauna taxon identity data						
Raw	Shelf vs. Slope	2.1164	**0.007**	126	2.7356	0.091
	Shelf vs. Abyss	2.7172	**0.026**	56	0.0261	1.000
	Slope vs. Abyss	1.8222	**0.016**	56	3.2803	0.058
p/a	Shelf vs. Slope	1.7875	**0.010**	126	2.9225	0.059
	Shelf vs. Abyss	1.4038	**0.027**	56	0.7170	0.654
	Slope vs. Abyss	1.2243	0.106	56	2.5025	0.072
(C) Mega-epifauna feeding trait data						
Abundance weighted trait	Shelf vs. Slope	3.6032	**0.001**	986	0.4853	0.697
	Shelf vs. Abyss	3.3535	**0.009**	165	0.6890	0.628
	Slope vs. Abyss	3.0223	**0.005**	281	1.1441	0.362
Taxa weighted trait	Shelf vs. Slope	5.9432	**0.001**	993	1.3989	0.225
	Shelf vs. Abyss	5.4893	**0.008**	165	0.3029	0.832
	Slope vs. Abyss	3.1930	**0.009**	279	0.6370	0.536
(D) Macro-infauna feeding trait data						
Abundance weighted trait	Shelf vs. Slope	3.4658	**0.006**	126	1.8206	0.173
	Shelf vs. Abyss	6.6410	**0.018**	56	0.5467	0.742
	Slope vs. Abyss	3.0671	**0.017**	56	1.0941	0.462
Taxa weighted trait	Shelf vs. Slope	2.4851	**0.016**	126	1.9362	0.119
	Shelf vs. Abyss	8.4393	**0.020**	56	0.5938	0.605
	Slope vs. Abyss	3.8158	**0.018**	56	1.1077	0.584

raw, untransformed data; p/a, presence–absence transformed data; Perms, unique permutations.
Significant p-values are indicated in bold.

The westernmost Slope sites, at the outflow of the Drygalski Trough off the Adare Peninsula, together with deepest slope sites and the abyssal sites, were correlated with higher mean seabed flux and lower variability in ice-free duration than the eastern slope sites, where ice-free duration was more variable and flux was lower.

Macro-infaunal community structure was best explained by six variables in addition to depth: mean water-column productivity (*vgpm_mean*, 18.2%); mean flux of primary production to the seabed (*flux_mean*, 9.2%); mean ice-free time (*iceFree_mean*, 5.9%); the standard deviation of marginal sea-ice duration (*marginal_sd*, 5.2%), and the standard deviation of close pack-ice duration (*closePack_sd*, 4.7%) (**Figure 7B**; untransformed ordination; **Supplementary Table 6**). Depth alone explained 29.2% of the variance and the total explained variance was 78.5%. Shelf, slope, and abyssal sites formed three distinct groupings, with the separation of abyssal sites from the others explained primarily by depth, and the distinction between shelf and slope sites explained by higher productivity (*vgpm_mean*), seabed flux (*flux_mean*), and longer ice-free duration (*iceFree_mean*). Separation among Shelf sites was associated primarily with differences in these same three variables (productivity, flux, and ice-free duration) but for the Slope sites depth was the dominant variable.

Feeding Traits

Mega-epifaunal abundance weighted feeding traits were best explained in the DistLM analysis by five variables: the mean flux of primary production to the seabed (*flux_mean*, 20.3%), standard deviation of water-column productivity (*vgpm_sd*, 12.6%); standard deviation of ice-free time (*iceFree_sd*, 5.9%); mean water-column productivity (*vgpm_mean*, 2.8%); mean sea-ice (*Seaice_mean*, 2.2%) (**Figure 8A** and **Supplementary Table 7**). Depth explained 26.2% of variance. The total explained variance was 62.6%. Patterns of abundance weighted feeding traits showed the Shelf, Slope, and Abyss were all clearly distinguished from each other (**Figure 8A** and **Supplementary Table 7**). Shelf and Abyssal sites were characterized by higher mean flux of primary production to

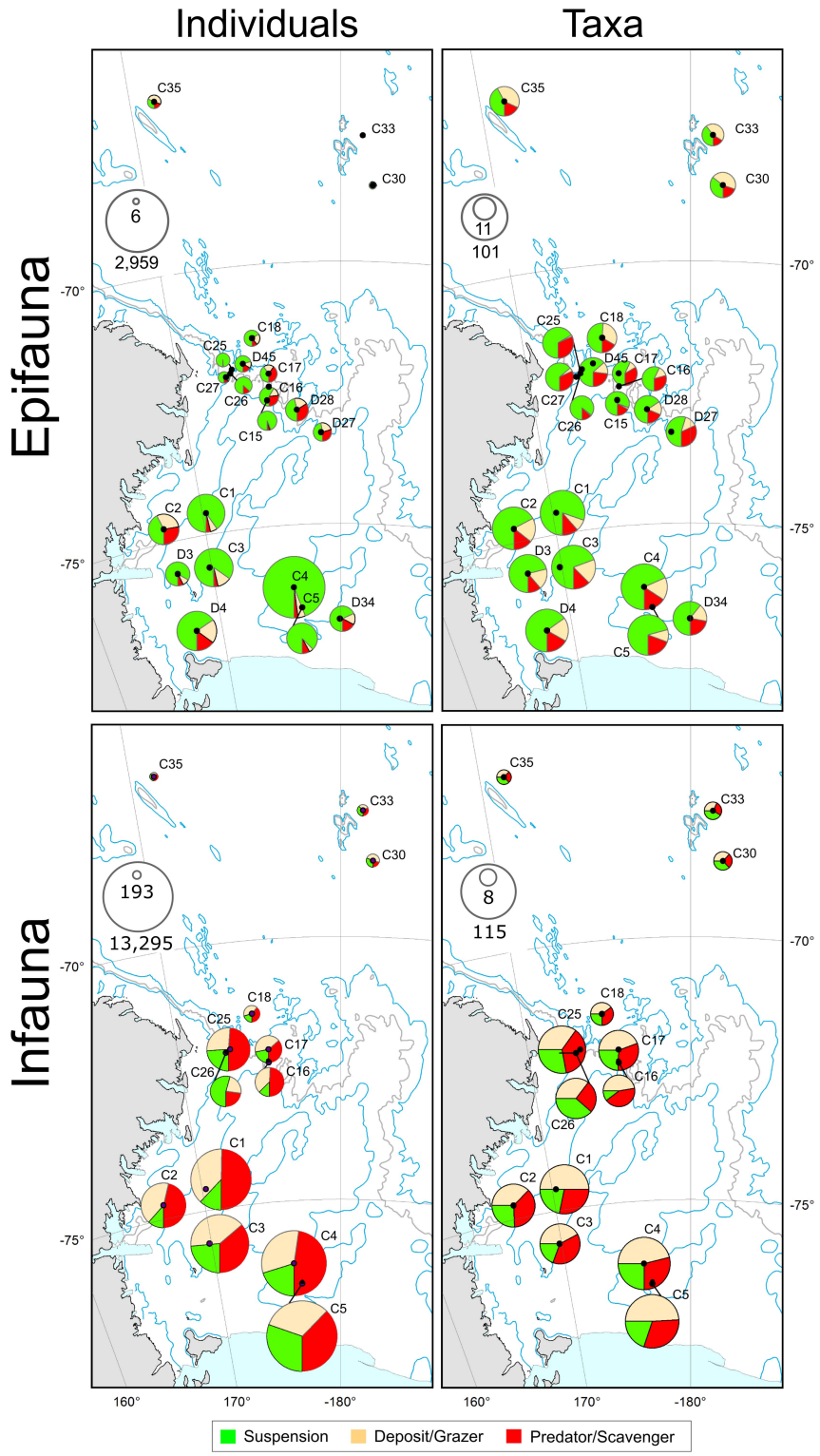

FIGURE 6 | Feeding modes of mega-epifauna **(top panels)** and macro-infauna **(bottom panels)** represented in terms of the number of individuals **(left)** and the number of taxa **(right)** exhibiting each of three feeding modes: suspension feeders; deposit-feeders or grazers; and predators/scavengers. Pie symbol diameters are scaled in proportion to the total number of individuals (see inset max-min scales: epifauna, individuals 1000 m^{-2}; infauna, individuals m^{-2}) or taxa recorded at each site, and segments indicate the relative occurrence of each feeding category. For Mega-epifauna individuals, proportions of suspension feeders, predator-scavengers, and deposit-grazers at the Abyssal sites were: C30: 0.37, 0.23, 0.40, C33: 0.16, 0.11, 0.73; C35: 0.32, 0.20, 0.48, respectively. For macro-infauna individuals proportions were C30: 0.31, 0.48, 0.21, C33: 0.37, 0.26, 0.38; C35: 0.38, 0.29, 0.34, respectively.

TABLE 4 | Patterns of community composition change between all sampling sites across all environments, and within the Shelf and Slope only.

Environment	Faunal components	Treatment	ρ	*P*
All	Macro-infauna vs. mega-epifauna	Raw	0.749	**0.001**
		p/a	0.326	**0.020**
Shelf	Macro-infauna vs. mega-epifauna	Raw	0.529	0.113
	Macro-infauna vs. mega-epifauna	p/a	−0.195	0.580
Slope	Macro-infauna vs. mega-epifauna	Raw	0.673	**0.027**
	Macro-infauna vs. mega-epifauna	p/a	0.671	0.087
All	Mega-epifauna: video vs. beam trawl	Raw	0.726	**0.010**
		p/a	0.675	**0.010**

Results of concordance analysis between data derived from macro-infauna and mega-epifauna. Mega-epifauna data are from video transects. A comparison between mega-epifauna data derived from DTIS video and from beam trawl is also given. Spearman's rho correlations (ρ) and probabilities are from the RELATE procedure in PRIMER-E and are derived from 9,999 random permutations of sample order.
Raw, untransformed; p/a, presence/absence.
Significant P-values are shown in bold.

the seabed, water column productivity (mean and standard deviation), and to a lesser extent by standard deviation of ice-free time.

Macro-infaunal abundance weighted feeding traits were explained in the DistLM analysis by many variables, the most important of which was the mean flux of primary production to the seabed (*flux_mean*, 16.2%), followed by the standard deviation of close pack-ice duration (*iceClosePack_sd,* 6.5%) (**Figure 8B** and **Supplementary Table 8**). Depth explained 59.0% of the total 91.4% variance explained. The many other variables with small contributions to this total included the mean and standard deviation of ice free time (*iceFree_mean*, 3.5%; *iceFree_sd* 1.2%), standard deviation of sea ice (*seaIce_sd,* 2.8%), the mean and standard deviation of marginal sea-ice duration (*iceMarginal_mean* 1.8%, *iceMarginal_sd* 1.2%), *flux_sd* 1.4%, mean and standard deviation of water-column productivity (*vgpm_mean* 1.3%, *vgpm_sd* 0.8%).

DISCUSSION

This study adds to our knowledge of the composition, spatial variability, and drivers of benthic invertebrate community structure and function in the Ross Sea Shelf, Slope, and Abyssal environments. We have provided new information on these communities and habitats, particularly in deep slope and abyssal areas, shown that patterns in mega-epifaunal assemblages can be used to indicate likely composition of the more cryptic (and difficult to sample) macro-infaunal assemblages at large spatial scales, and demonstrated the influence of sea ice conditions, primary production and organic flux to the seabed on benthic community characteristics (abundance, composition). Below we describe these findings and discuss their relevance to monitoring of the Ross Sea Marine Protected Area.

Variations in Benthic Habitat and Community Composition Within and Between Environments

Our eight Shelf sites spanned mean depths from 286 to 893 m, while the ten Slope and three Abyssal sites encompassed areas from 472 to 2209 m and 3225 to 3545 m, respectively. The Abyssal sites are only slightly deeper than the >3000 m used to define abyssal depths (**Table 1**). Our data support the expected decline in faunal diversity from the Shelf to the Abyss (e.g., Convey et al., 2014), a pattern that was particularly strong for macro-infauna (**Figure 4**).

We found clear differences between the Shelf, Slope, and Abyssal environments in community characteristics and their environmental drivers. In comparing these environments, it is important to note that they are located at markedly different latitudes; i.e., the Abyssal sites (68.5–66.7^{o}S) were significantly further north than the Slope sites (72.5 to 71.3^{o}S), with the Shelf sites from 76.8 to 74.5^{o}S (**Table 1** and **Figure 1**).

Seafloor substrata at Shelf sites contained predominantly soft sediments at the large scale (1000 m^{-2}), which our small scale (m^{-2}) sampling identified as mostly fine sand (**Figure 2**). Slope substrates were very heterogeneous at both scales and consisted mostly of coarser substrate/sediment fractions and higher volumes of biogenic material, including shell hash, barnacle plates and coral rubble (**Figure 2**). Perhaps surprisingly, the Abyssal substrates were even more heterogeneous than the Shelf substrates; with boulders and cobbles scattered amongst silt and fine sand (**Figure 2**). This may reflect the deposition of glacial drop-stones and scour material from the last glacial maximum, or the close proximity of these sites to seamounts (Bowden et al., 2011; Clark and Bowden, 2015). Earlier surveys in the deep Southern Ocean noted a high frequency of drop-stones amongst soft muds (e.g., Bullivant, 1959; Brandt et al., 2007).

Sediment organic content was very low < 3.1% (**Supplementary Table 1**) across all environments. These values are within the range of those found at selected shelf areas (<750 m deep) from another study in the north-western Ross Sea (<3.5%, Cummings et al., 2010). Sediment phaeophytin concentrations were considerably higher on the Shelf (1.84 – 7.28 μg phaeophytin g^{-1} sediment) than in the deeper Slope or Abyssal sites (<<1 μg phaeophytin g^{-1} sediment), reflecting the reduced flux of algal material from surface to deeper waters.

The apparently higher substrate diversity on the Slope (see **Figure 2**), did not translate to greater species diversity: mega-epifaunal abundances and numbers of taxa were higher on the Shelf than on the Slope or Abyssal plain (**Figures 3A,B**), and shelf assemblages were distinct from those at the other environments in multivariate analyses (**Figure 5**). Mega-epifauna were predominantly suspension feeders across the Shelf and Slope stations, with highest densities of suspension feeders found at the shallower bank sites (C4 and C1). In the Abyss deposit feeder-grazers were found in higher or equal abundances (**Figure 6**). Bryozoans, sponges, and crinoids were the major conspicuous groups on banks, but even in the deep basins sponges, crinoids, and pennatulaceans were abundant. In their study of Ross Sea Shelf sites spanning depths from 270 to

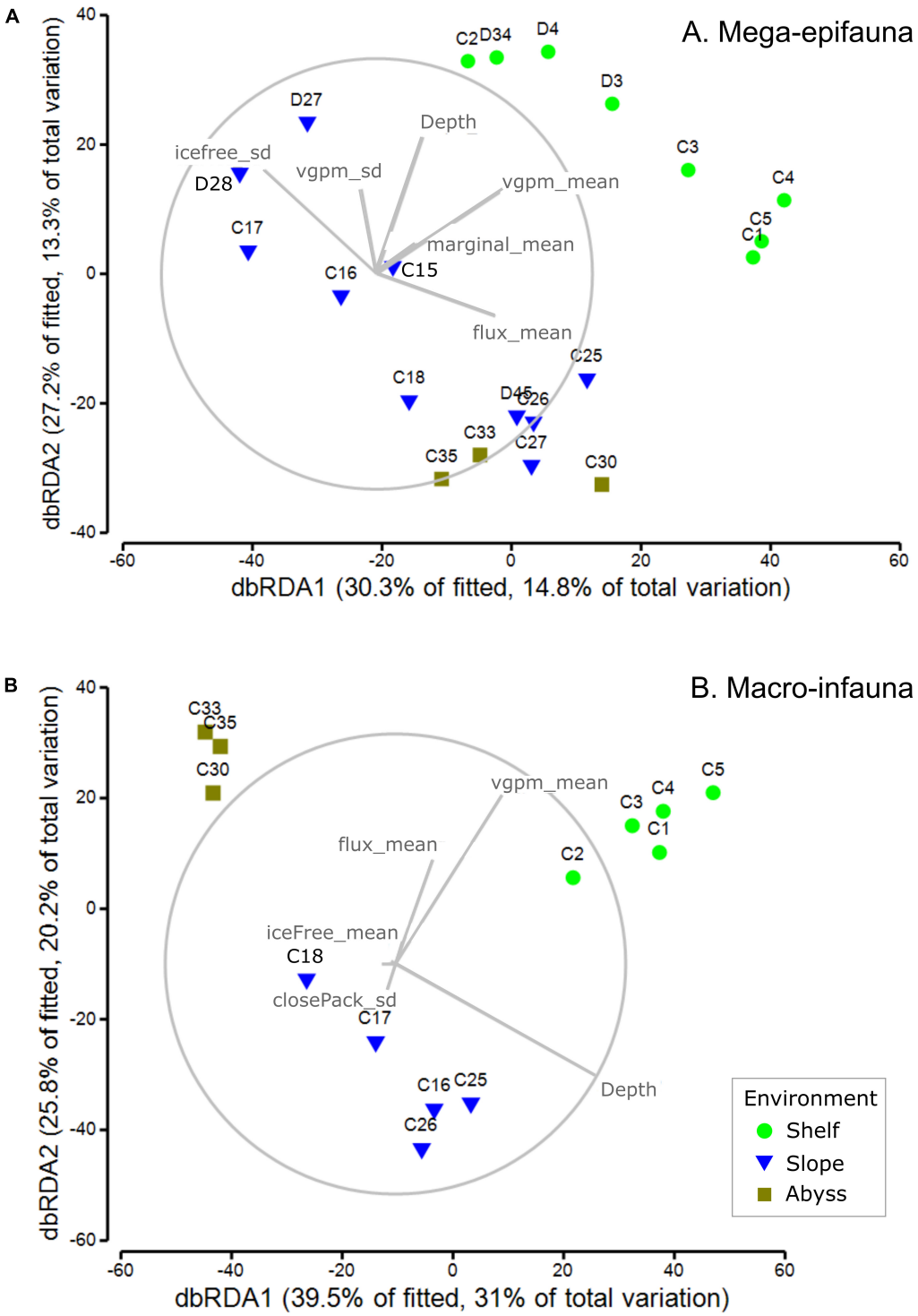

FIGURE 7 | dbRDA ordinations community composition of **(A)** mega-epifaunal and **(B)** macro-infaunal at each site. Vector overlays indicate the strength and direction of the relationships between sea ice- and productivity-associated environmental variables on the dispersion of samples in the ordination. DistLM outputs are provided in **Supplementary Tables 2**, **3**, respectively.

1173 m, Barry et al. (2003) also found that suspension feeding mega-epifauna were more dominant in the shallow waters, with deposit feeders most abundant at the deepest sites. Our data show an increase in the abundance of deposit-feeding taxa at deeper shelf sites for mega-epifauna (**Figure 6**, sites C2, D4, D34) but not for macro-infauna.

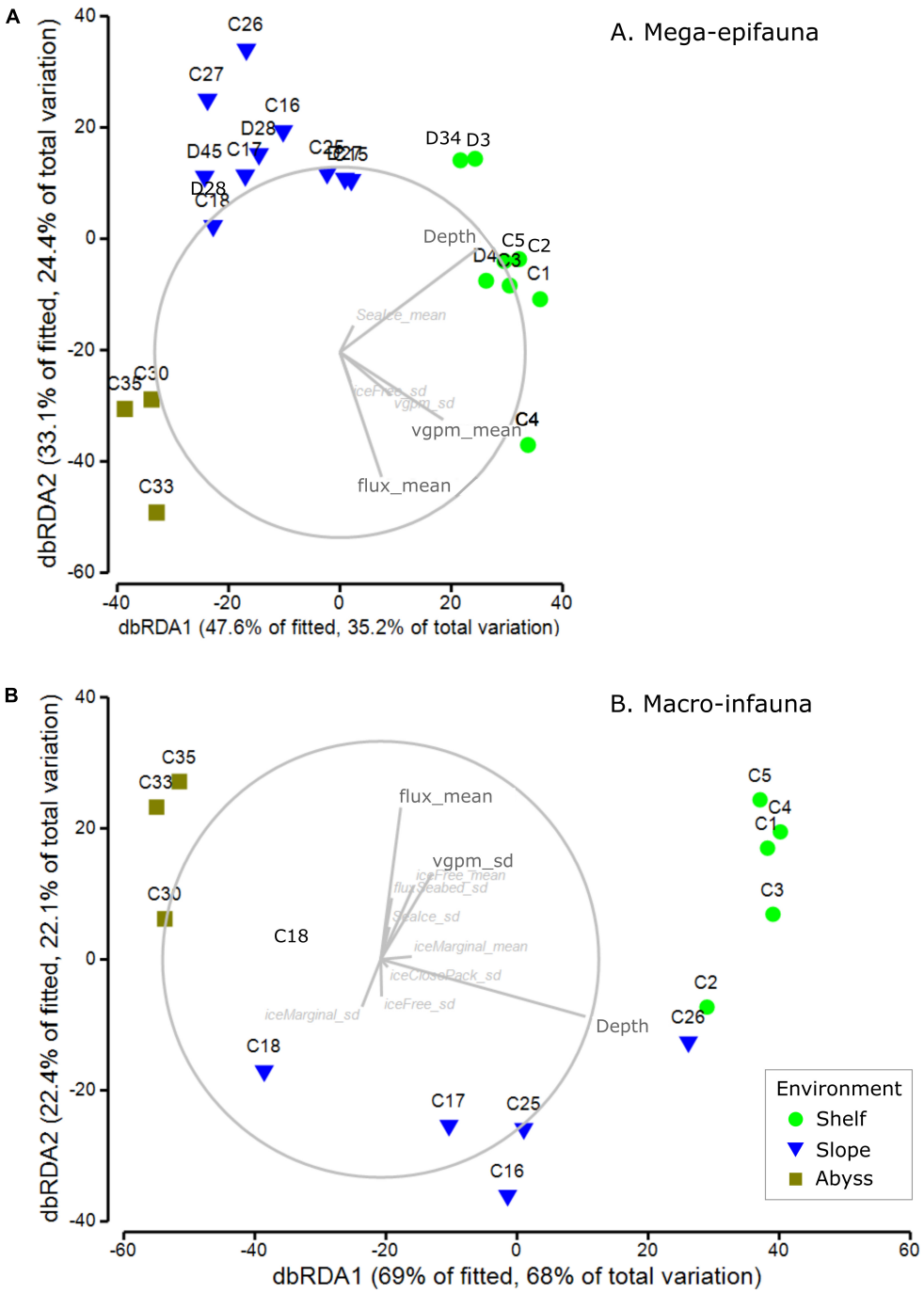

FIGURE 8 | dbRDA ordinations of abundance weighted feeding traits of **(A)** mega-epifaunal and **(B)** macro-infaunal, at each site. Vector overlays indicate the strength and direction of the relationships between sea ice- and productivity-associated environmental variables on the dispersion of samples in the ordination. DistLM outputs are provided in **Supplementary Tables 7**, **8**, respectively.

Mega-epifaunal assemblages on the continental Shelf are distinct from those on the Slope and in the Abyss in our analyses, aligning with well-documented general characteristics of Antarctic continental shelf fauna, including the predominance of sessile suspension feeders, particularly bryozoans, sponges and comatulid crinoids and the absence of decapod crustaceans (Clarke and Johnston, 2003; Clarke et al., 2004). These characteristics are thought to result from environmental conditions in the present, including the extremely cold, stable, seawater temperatures (Frederich et al., 2001) and absence of riparian sedimentation (Aronson and Blake, 2001), but also from historical events, particularly the episodic defaunation of

continental shelf areas during glacial maxima (Clarke and Crame, 1992). The distinct character of the shelf fauna is emphasized by the gradient of assemblage change from sites on the shelf break down to abyssal depths. Despite greater variation in substrate types among the slope sites (**Figure 2**) and a broad depth range, conditions on the shelf are sufficiently different to maintain a distinct fauna.

Distinct macro-infaunal assemblages were observed between all three environments and, like the mega-epifauna, taxa were generally more diverse on the Shelf (**Figure 3**). Abundances were higher there than on either the Slope or Abyssal plain, and in the Slope sites compared to the Abyssal sites (**Figure 3**). In contrast to the mega-epifauna, suspension feeders were the least common macro-infaunal feeding type on the Shelf and Slope (**Figure 6**). On the Shelf, deposit feeder-grazers and predator-scavengers were most common. There was no clear pattern of feeding type across the Abyssal sites, although fewer predator/scavengers were found there. Sea ice conditions in an area over time may influence the feeding types of the taxa present. Analysis of benthic macrofaunal community data spanning 26 years on the north eastern Weddell Sea shelf found a decrease in suspension feeders, an increase in deposit feeders, and an overall decline in biomass, in association with an increasing trend of sea ice cover, which the authors' attributed to reduced productivity and vertical flux of organic matter (Pineda-Metz et al., 2020).

While both faunal groups showed distinct clustering of assemblages from each environment in the MDS ordinations, clear separation between sites within environments was also apparent (**Figure 5**). Comparison of the ordinations derived from presence/absence transformed *vs.* raw data indicate considerable similarity in mega-epifaunal taxa comprising the Shelf site assemblages (**Figure 5C** vs. **5A**) and, for macro-infauna, closer clustering of Shelf sites with some Abyssal sites (**Figure 5D** vs. **5B**). The latter is primarily due to the occurrence of cirratulids and nematodes at Shelf sites and at Abyssal sites C30 and C35. Assemblage variability among Shelf sites was less than that among Slope or Abyssal sites, as shown by the closer grouping (lower dispersion) of Shelf sites in the MDS ordinations (**Figure 5**). This can be explained by the Slope sites encompassing greater ranges of environmental variables and habitats than the Shelf sites; most obviously, they extend over a greater depth range than the Shelf sites.

Concordance of Spatial Patterns in Mega-Epifauna and Macro-Infauna Benthic Community Composition

To explore whether surface dwelling mega-epifauna can be used to indicate likely composition of the cryptic (and more difficult to sample) macro-infauna, we examined the extent to which mega-epifauna and macro-infaunal patterns in benthic communities co-occur. Results show that patterns of assemblage variability across the whole study area are largely similar (concordant) regardless of which faunal fraction is examined. Thus, the same general patterns are seen whether we look at mega-epifauna or macro-infauna. However, despite the significance of these relationships, the strength of the correlations between faunal fractions varied. Correlations between macro-infauna and mega-epifauna were stronger for quantitative comparisons ($\rho = 0.749$ for untransformed data; **Table 4**) than for that using presence-absence data. This suggests that the concordance between faunal fractions is influenced by both assemblage composition and changes in abundance.

A comparative analysis of benthic infauna (collected using multibox corer) and epifauna (obtained from imagery) in the southern Weddell Sea similarly found comparable spatial distribution patterns (Pineda-Metz and Gerdes, 2018), suggesting this pattern may be widespread in the Southern Ocean. The generally strong concordance between macro-infauna and mega-epifauna patterns across our entire study area suggests that these elements of the fauna are responding to similar environmental constraints at this scale (e.g., large-scale differences in organic content, benthic production, hydrodynamic conditions). This relationship remained strong within the Slope environment but was moderate (and non-significant) on the Shelf ($p < 0.05$; **Table 4**), suggesting that generalizations across faunal groups in terms of how we explain observed patterns might only be appropriate at larger spatial scales. In other words, while we might be able to predict macro-infaunal communities on the basis of mega-epifaunal data at the scale of environments (e.g., between Shelf and Slope), this would not be reliable for sites within one of these environments (e.g., discriminating macro-infaunal communities between sites on the Shelf on the basis of the mega-epifaunal community). Concordance was also strong for comparisons between video and beam trawl mega-epifauna data across all three environments (**Table 4**), indicating that patterns of assemblage similarity between sites at the largest spatial scale of the survey can be summarized effectively by reference to either data set.

Environmental Conditions – Explaining Benthic Community Characteristics

The importance of sea ice conditions, their influence on productivity – and so on flux of organic material to the seafloor (Smith et al., 2006; Arrigo et al., 2015; Isla, 2016) – as a driver of benthic community structure and function is well recognized (e.g., Cummings et al., 2018; Pineda-Metz et al., 2019), even at depths far below the surface (Gutt et al., 2019). Incorporating spatial and temporal variability in sea ice concentrations and conditions, rather than just an average concentration, is important in understanding different distribution patterns, particularly as the extent, timing and duration of sea ice break out will affect the magnitude and timing of primary production (e.g., Gutt et al., 2012; Ingels et al., 2012; Kim et al., 2018). We assessed the influence of various concentrations of sea ice [from an overall average, to ice free (concentrations < 15%), marginal (15-40%), and close pack (>70%)], and summarized these over the 10 years period prior to our sampling. For each site, we calculated the mean time these conditions were experienced, and the variability around these means. Results for general community composition revealed that the % of time a site was ice free or experienced marginal ice was important for both mega-epifauna and macro-infauna,

although when the mean values were highlighted as important for one community type, the variability (SD) was identified for the other (**Figure 7** and **Supplementary Tables 2**, **3**). Other key explanatory variables for both community groups were mean VGPM (net primary production; particularly for macro-infauna) and seabed flux (downward vertical flux of particulate organic matter at the seabed). The variability (SD) in VGPM was also identified for mega-epifauna, and variability in the % of time of close pack ice was also important for the macro-infaunal model (**Figure 7**). Combinations of these same variables (Flux mean, VGPM mean and SD, and ice free time SD) were important for the mega-epifauna feeding traits, where the shelf and slope had high percentages of suspension feeders, and the abyss had equal or higher numbers of deposit feeder-grazers (**Figure 8**). In contrast, many different environmental variables explained the distribution of macro-infaunal abundance-weighted feeding traits, which is perhaps reflected in the mixture of feeding types found on the Slope and Abyss and the low predominance of suspension feeders on the Shelf (**Figure 8**).

Sea ice conditions and concentrations are correlated with and strongly influence primary production and flux (both physically, and in the calculation of these variables). These findings point to the importance of formally including and considering the drivers of food supply in analyses explaining existing benthic community distributions, and especially when predicting consequences of future environmental change.

We also found strong correlations of simple assemblage variables (number of taxa and individuals; **Figure 4**) and changes in assemblage composition (**Figures 7**, **8**), with depth. Across the Southern Ocean, deep sea faunal composition differs from that on the Shelf (Brandt et al., 2007, 2012). For example, there is a general decline in the number of some macrofaunal groups (bivalves, gastropods, polychetes) from the Shelf to the Slope, followed by stable, lower numbers at greater depth (Brandt et al., 2009). However, the relationship with depth is not consistent among groups (e.g., isopods increase in abundance from the Slope to the Abyss; Ellingsen et al., 2007), and Brandt et al. (2007) comment that there is rarely any clear relationship of biodiversity pattern with depth (or indeed latitude or environmental parameters). This is particularly apparent from previous analyses of Shelf faunal assemblages in the Ross Sea (Cummings et al., 2010), despite the broad depth range sampled (i.e., 50 – 750 m). As noted above, our data show distinct, tight clustering of Shelf assemblages for mega-epifauna and macro-infauna, but more variation in assemblages within the Slope and Abyssal environments (e.g., **Figure 5**). In fact, some of the same macro-infaunal species characterize both the Shelf and Abyssal sites (presence-absence ordination; **Figure 5D**). Several ecologically important variables, notably pressure, light, and the availability of food, co-vary with depth (Levin et al., 2001), and it is likely that these and other important environmental factors (e.g., hydrodynamic conditions) will be influential in determining distributions (e.g., Pineda-Metz et al., 2019). Past colonization history will also be key (e.g., Thatje, 2012).

It is also highly probable that biotic interactions between faunal classes contribute to concordant patterns of distribution. For instance, the activities of, and habitats provided by, mega-epifauna might affect macro-infaunal community composition, and will be but one factor influencing the types and living positions of infaunal taxa (e.g., **Supplementary Figure 1**; Gutt, 2006). When the effect of depth was removed from the concordance analyses, the relationship between macro-infauna and mega-epifauna remained significant.

Ross Sea MPA

The Ross Sea MPA was established in December 2018 to enhance understanding of the effects of fishing and climate change on a valued high latitude marine ecosystem, and is the focus of an on-going research and monitoring program (CCAMLR, 2016; Dunn et al., 2017; Parker and Dunn, 2018). The sites sampled in this study span areas of interest to the Ross Sea MPA: all of the Shelf sites sampled (C1 – C5, D3, D4, and D34) fall within General Protection Zone 1 (GPZ I); Slope sites straddle the boundary of GPZ I off the Adare Peninsula, including cross-Shelf-break sites within GPZ I (C25, C26, and C27) and outside the MPA in an area of high fishing intensity for toothfish (C15, C16, C17, D27, D28); the Abyssal sites include one that lies within GPZ I (adjacent to Admiralty Seamount), and two that lie just outside of GPZ III (encompassing Scott Island and associated features). The data presented in this paper are from a 2008 voyage, conducted over a decade after the toothfish fishery was first established in 1995 and a decade before the MPA was established. These data analyses can aid our understanding of the distributions of seabed habitats and fauna inside and outside the Ross Sea MPA boundaries, and along with information from earlier studies (e.g., Bullivant and Dearborn, 1967; Barry et al., 2003; Kröger and Rowden, 2008; Bowden et al., 2011; Clark and Bowden, 2015), contribute to an expanding baseline of data against which the success of the MPA, and variability and change in benthic communities can be evaluated. A broader analysis, combining all available benthic community data from earlier Ross Sea studies (abundance, diversity, and feeding traits) with information on sea ice and productivity trends, would be a valuable addition to understanding the status of benthic habitats in the MPA.

CONCLUSION

Net primary productivity and seabed organic flux, along with sea ice concentrations and variability over time are important structuring factors for both mega- and macro-infaunal communities (e.g., Pineda-Metz et al., 2020). Even though the influence of sea ice conditions on surface productivity occurs far above the seafloor, we have demonstrated their influence on benthic communities (e.g., Jansen et al., 2018a). This illustrates the importance of better understanding bentho-pelagic coupling in this region, and the need to consider water circulation and currents (not considered here, and not always well resolved at small-intermediate scales) and so the dispersal, distribution and flux of this surface derived food source (e.g., Jansen et al., 2018b). Future changes in Ross Sea sea ice conditions, circulation patterns and ocean chemistry are predicted as a result of climate change and ocean acidification that will alter these important variables, and will in turn, significantly affect

ecosystem dynamics. Monitoring these factors longer term will be key to understanding natural variability and trends in benthic ecosystems. Their inclusion, along with biological information (e.g., species dispersal modes and potential, inter- and intraspecific interactions, community dynamics), in biogeographic distribution and process-based models, will also enable meaningful predictions of how these ecosystems may be impacted by future projected environmental changes.

DATA AVAILABILITY STATEMENT

The original contributions presented in the study are included in the article/**Supplementary Material**, further inquiries can be directed to the corresponding author/s.

AUTHOR CONTRIBUTIONS

VC and DB designed the sampling and sample processing and analyses. NH coordinated the macroinvertebrate processing and constructed the functional traits data set. MP analyzed the satellite sea ice and productivity components. JH and DB conducted the statistical analyses. VC planned and wrote the initial manuscript, with input from JH and DB. All the authors edited and approved the final version.

FUNDING

Data collection for this research was funded by the New Zealand Government under the New Zealand International Polar Year-Census of Antarctic Marine Life Project (IPY2007-01). The write up and analyses were funded by NIWA Coasts and Oceans SSIF.

ACKNOWLEDGMENTS

We thank the officers and crew of *RV Tangaroa* and the science staff on the 2008 *RV Tangaroa* voyage to the Ross Sea (IPY-CAML) for their help with sample collection and processing on board. Sincere thanks are due to the many international expert taxonomists who examined and verified invertebrate identifications, and to Peter Marriott (NIWA) for his contribution to the functional trait analyses. Thanks to the reviewers for their constructive comments that improved the manuscript, and the editor for the opportunity to contribute to this topic.

SUPPLEMENTARY MATERIAL

The Supplementary Material for this article can be found online at: https://www.frontiersin.org/articles/10.3389/fmars.2021.629787/full#supplementary-material

REFERENCES

Arntz, W. E., Brey, T., and Gallardo, V. A. (1994). Antarctic zoobenthos. *Oceanogr. Mar. Biol.* 32, 241–304.

Aronson, R. B., and Blake, D. B. (2001). Global climate change and the origin of modern benthic communities in Antarctica. *Am. Zool.* 41, 27–39. doi: 10.1093/icb/41.1.27

Aronson, R. B., Thatje, S., McClintock, J. B., and Hughes, K. A. (2011). Anthropogenic impacts on marine ecosystems in Antarctica. *Ann. N. Y. Acad. Sci.* 1223, 82–107. doi: 10.1111/j.1749-6632.2010.05926.x

Arrigo, K. R., and van Dijken, G. L. (2004). Annual changes in sea-ice, chlorophyll a, and primary production in the Ross Sea, Antarctica. *Deep Sea Res. 2 Top. Stud. Oceanogr.* 51, 117–138. doi: 10.1016/j.dsr2.2003.04.003

Arrigo, K. R., van Dijken, G. L., and Bushinsky, S. (2008). Primary production in the Southern Ocean, 1997–2006. *J. Geophys. Res.* 113:C08004. doi: 10.1029/2007JC004551

Arrigo, K. R., Van Dijken, G. L., and Strong, A. L. (2015). Environmental controls of marine productivity hot spots around Antarctica. *J. Geophys. Res. Oceans* 120, 5545–5565. doi: 10.1002/2015jc010888

Barnes, D. K. A., Kuklinski, P., Jackson, J. A., Keel, G. W., Morley, S. A., and Winston, J. E. (2011). Scott's collections help reveal accelerating marine life growth in Antarctica. *Curr. Biol.* 21, R147–R148. doi: 10.1016/j.cub.2011.01.033

Barry, J. P., Grebmeier, J. M., Smith, J., and Dunbar, R. B. (2003). Oceanographic versus seafloor-habitat control of benthic megafaunal communities in the S.W. Ross Sea, Antarctica. *Antarct. Res. Ser.* 78, 327–354. doi: 10.1029/078ars21

Behrenfeld, M. J., and Falkowski, P. G. (1997). Photosynthetic rates derived from satellite-based chlorophyll concentration. *Limnol. Oceanogr.* 42, 1–20. doi: 10.4319/lo.1997.42.1.0001

Bowden, D. A., and Jones, D. O. B. (2016). "Towed cameras," in *Biological Sampling in The Deep Sea*, eds M. R. Clark, A. A. Rowden, and M. Consalvey (Chichester: Wiley & Sons Ltd), 260–284. doi: 10.1002/9781118332535.ch12

Bowden, D. A., Schiaparelli, S., Clark, M. R., and Rickard, G. J. (2011). A lost world? Archaic crinoid-dominated assemblages on an Antarctic seamount. *Deep Sea Res. 2 Top. Stud. Oceanogr.* 58, 119–127. doi: 10.1016/j.dsr2.2010.09.006

Brandt, A., De Broyer, C., Ebbe, B., Ellingsen, K. E., Gooday, A. J., and Janussen, D. (2012). "Southern Ocean deep benthic biodiversity," in *Antarctic Ecosystems: An Extreme Environment in a Changing World*, 1st Edn, eds A. D. Rogers, N. M. Johnston, E. J. Murphy, and A. Clarke (Chichester: Blackwell Publishing Ltd), 291–334.

Brandt, A., Gooday, A. J., Brandao, S. N., Brix, S., Brökeland, W., Cedhagen, T., et al. (2007). First insights into the biodiversity and biogeography of the Southern Ocean deep sea. *Nature* 447, 307–311. doi: 10.1038/nature05827

Brandt, A., Linse, K., and Schüller, M. (2009). Bathymetric distribution patterns of Southern Ocean macrofaunal taxa: Bivalvia, Gastropoda, Isopoda and Polychaeta. *Deep Sea Res. 1* 56, 2013–2025. doi: 10.1016/j.dsr.2009.06.007

Brey, T., and Clarke, A. (1993). Population dynamics of marine benthic invertebrates in Antarctic and Subantarctic environments: are there unique adaptations? *Antarct. Sci.* 5, 253–266. doi: 10.1017/s0954102093000343

Bullivant, J. S. (1959). An oceanographic survey of the Ross Sea. *Nature* 184, 422–423. doi: 10.1038/184422a0

Bullivant, J. S., and Dearborn, J. H. (1967). *The fauna of the Ross Sea. Part 5. General accounts, station lists, and benthic ecology*. New Zealand Oceanographic Institute memoirs No. 32. Wellington: New Zealand Dept. of Scientific and Industrial Research. 77.

Cael, B. B., Bisson, K., and Follett, C. (2018). Can rates of ocean primary production and biological carbon export be related through their probability distributions? *Global Biogeochem. Cycles* 32, 954–970. doi: 10.1029/2017GB005797

Cavalieri, D., Gloerson, P., and Zwally, J. (1990/2007). "DMSP SSM/I daily polar gridded sea-ice concentrations, 1997 to 2006," in *Digital Media*, eds J. Maslanik, J. Stroeve, C. O. Boulder, National Snow, and Ice Data Center. Available online at: https://nsidc.org/data/NSIDC-0079/versions/3 (accessed June, 2018).

Cavalieri, D. J., Campbell, W. J., and Gloersen, P. (1984). Determination of sea ice parameters with the NIMBUS 7 SMMR. *J. Geophys. Res.* 89, 5355–5369. doi: 10.1029/jd089id04p05355

CCAMLR (2016). *Conservation Measure 91-05 (2016): Ross Sea Region Marine Protected Area*. Unpublished document. Hobart, TAS: CCAMLR.

Chevenet, F., Doledec, S., and Chessel, D. (1994). A fuzzy coding approach for the analysis of long-term ecological data. *Freshw. Biol.* 31, 295–309. doi: 10.1111/j.1365-2427.1994.tb01742.x

Clark, M. R., and Bowden, D. A. (2015). Seamount biodiversity: high variability both within and between seamounts in the Ross Sea region of Antarctica. *Hydrobiologia* 761, 161–180. doi: 10.1007/s10750-015-2327-9

Clarke, A., Aronson, R. B., Crame, J. A., Gil, J. M., and Blake, D. B. (2004). Evolution and diversity of the benthic fauna of the Southern Ocean continental shelf. *Antarct. Sci.* 16, 559–568. doi: 10.1017/s0954102004002329

Clarke, A., and Crame, J. A. (1992). The Southern Ocean benthic fauna and climate change–a historical perspective. *Philos. Trans. R. Soc. Lond. B Biol. Sci.* 338, 299–309. doi: 10.1098/rstb.1992.0150

Clarke, A., and Johnston, N. M. (2003). Antarctic marine benthic diversity. *Oceanogr. Mar. Biol.* 41, 47–114.

Clarke, K. R., and Warwick, R. M. (2001). *Change in Marine Communities: An Approach to Statistical Analysis*, 2nd Edn. Plymouth: PRIMER-E Ltd.

Comiso, J. C. (1983). Sea ice effective microwave emissivities from satellite passive microwave and infrared observations. *J. Geophys. Res.* 88, 7686–7704. doi: 10.1029/jc088ic12p07686

Comiso, J. C. (1995). *SSM/I Sea Ice Concentrations Using the Bootstrap Algorithm*. NASA Report 1380. Washington, D.C: National Aeronautics and Space Administration.

Comiso, J. C. (2003). "Large-scale characteristics and variability of the global sea ice cover," in *Sea Ice: An Introduction to its Physics, Chemistry, Biology and Geology*, eds D. N. Thomas and G. S. Dieckmann (Oxford: Blackwell Science), 112–142. doi: 10.1002/9780470757161.ch4

Convey, P., Chown, S. L., Clarke, A., Barnes, D. K. A., Bokhorst, S., Cummings, V., et al. (2014). The spatial structure of Antarctic biodiversity. *Ecol. Monogr.* 84, 203–244. doi: 10.1890/12-2216.1

Cummings, V. J., Hewitt, J. E., Thrush, S. F., Marriott, P. M., Halliday, N. J., and Norkko, A. M. (2018). Linking Ross Sea coastal benthic ecosystems to environmental conditions: documenting baselines in a changing world. *Front. Mar. Sci.* 5:232. doi: 10.3389/fmars.2018.00232

Cummings, V. J., Thrush, S. F., Chiantore, M., Hewitt, J. E., and Cattaneo-Vietti, R. (2010). Macrobenthic communities of the north-western Ross Sea shelf: links to depth, sediment characteristics and latitude. *Antarct. Sci.* 22, 793–804. doi: 10.1017/s0954102010000489

Dayton, P. K., Jarrell, S. C., Kim, S., Parnell, P. E., Thrush, S. F., Hammerstrom, K., et al. (2019). Benthic responses to an Antarctic regime shift: food particle size and recruitment biology. *Ecol. Appl.* 29:e01823.

Dayton, P. K., Kim, S., Jarrell, S. C., Oliver, J. S., Hammerstrom, K., Fisher, J. L., et al. (2013). Recruitment, growth and mortality of an Antarctic hexactinellid sponge, *Anoxycalyx joubini*. *PLoS One* 8:e56939. doi: 10.1371/journal.pone.0056939

Dayton, P. K., Robilliard, G. A., Paine, R. T., and Dayton, L. B. (1974). Biological accommodation in the benthic community at McMurdo Sound, Antarctica. *Ecol. Monogr.* 44, 105–128. doi: 10.2307/1942321

Deppeler, S. L., and Davidson, A. T. (2017). Southern Ocean phytoplankton in a changing climate. *Front. Mar. Sci.* 4:40. doi: 10.3389/fmars.2017.00040

Doney, S. C., Ruckelshaus, M., Duffy, J. E., Barry, J. P., Chan, F., English, C. A., et al. (2012). Climate change impacts on marine ecosystems. *Ann. Rev. Mar. Sci.* 4, 11–37.

Ducklow, H. W., Fraser, W. R., Meredith, M. P., Stammerjohn, S. E., Doney, S. C., Martinson, D. G., et al. (2013). West Antarctic Peninsula: an icedependent coastal marine ecosystem in transition. *Oceanography* 26, 190–203. doi: 10.5670/oceanog.2013.62

Dunn, A., Vacchi, M., and Watters, G. (2017). *The Ross Sea Region Marine Protected Area Research and Monitoring Plan*. CCAMLR document SC-CAMLR-XXXVI/20. Hobart, TAS.

Ellingsen, K. E., Brandt, A., Ebbe, B., and Linse, K. (2007). Diversity and species distribution of polychaetes, isopods and bivalves in the Atlantic sector of the deep Southern Ocean. *Polar Biol.* 30, 1265–1273. doi: 10.1007/s00300-007-0287-x

Frederich, M., Sartoris, F. J., and Pörtner, H. O. (2001). Distribution patterns of decapod crustaceans in polar areas: a result of magnesium regulation? *Polar Biol.* 24, 719–723. doi: 10.1007/s003000100270

Gloersen, P., and Cavalieri, D. J. (1986). Reduction of weather effects in the calculation of sea ice concentrations from microwave radiances. *J. Geophys. Res.* 91, 3913–3919. doi: 10.1029/jc091ic03p03913

Griffiths, H. J., Whittle, R. J., Roberts, S. J., Belchier, M., and Linse, K. (2013). Antarctic crabs: invasion or endurance? *PLoS One* 8:e66981. doi: 10.1371/journal.pone.0066981

Gutt, J. (2006). Coexistence of macro-zoobenthic species on the Antarctic shelf: an attempt to link ecological theory and results. *Deep Sea Res. 2 Top. Stud. Oceanogr.* 53, 1009–1028. doi: 10.1016/j.dsr2.2006.02.012

Gutt, J., Arndt, J., Kraan, C., Dorschel, B., Schröder, M., Bracher, A., et al. (2019). Benthic communities and their drivers: a spatial analysis off the Antarctic Peninsula. *Limnol. Oceanogr.* 62, 2341–2357. doi: 10.1002/lno.11187

Gutt, J., Isla, E., Xavier, J. C., Adams, B. J., Ahn, I. Y., Cheng, C. C., et al. (2020). Antarctic ecosystems in transition – life between stresses and opportunities. *Biol. Rev.* doi: 10.1111/brv.12679

Gutt, J., Zurell, D., Bracegridle, T. J., Cheung, W., Clark, M. S., Convey, P., et al. (2012). Correlative and dynamic species distribution modelling for ecological predictions in the Antarctic: a cross-disciplinary concept. *Polar Res.* 31:11091. doi: 10.3402/polar.v31i0.11091

Halpern, B. S., Walbridge, S., Selkoe, K. A., Kappel, C. V., Micheli, F., D'Agrosa, C., et al. (2008). A global map of human impact on marine ecosystems. *Science* 319, 948–952.

Henley, S. F., Cavan, E. L., Fawcett, S. E., Kerr, R., Monteiro, T., Sherrell, R. M., et al. (2020). Changing biogeochemistry of the Southern Ocean and its ecosystem implications. *Front. Mar. Sci.* 7:581. doi: 10.3389/fmars.2020.00581

Hewitt, J. E., Lundquist, C. J., and Ellis, J. (2018). Assessing sensitivities of marine areas to stressors based on biological traits. *Conserv. Biol.* 33, 142–151. doi: 10.1111/cobi.13181

Hewitt, J. E., Thrush, S. F., and Dayton, P. D. (2008). Habitat variation, species diversity and ecological functioning in a marine system. *J. Exp. Mar. Biol. Ecol.* 366, 116–122. doi: 10.1016/j.jembe.2008.07.016

Hill, P. (2009). Designing a deep-towed camera vehicle using single conductor cable. *Sea Technol.* 50, 49–51.

Huetten, E., and Greinert, J. (2008). *Software Controlled Guidance, Recording and Post-Processing Of Seafloor Observations by ROV And Other Towed Devices: the Software Package OFOP*. Geophysical Research Abstracts 10: EGU2008-A-03088, EGU General Assembly 2008 (poster). Vienna.

Ingels, J., Vanreusel, A., Brandt, A., Catarino, A. I., David, B., De Ridder, C., et al. (2012). Possible effects of global environmental changes on Antarctic benthos: a synthesis across ?ve major taxa. *Ecol. Evol.* 2, 453–485. doi: 10.1002/ece3.96

Isla, E. (2016). "Environmental controls on sediment composition and particle fluxes over the Antarctic continental shelf," in *Source-to Sink Fluxes in Undisturbed Cold Environments*, eds A. Beylich, J. Dixon, and Z. Zwolinski (Cambridge: Cambridge University Press), 199–212. doi: 10.1017/cbo9781107705791.017

Jacobs, S. S., and Giulivi, C. F. (2010). Large multidecadal salinity trends near the Pacific-Antarctic continental margin. *J. Clim.* 23, 4508–4524. doi: 10.1175/2010JCLI3284.1

Jansen, J., Hill, N. A., Dunstan, P. K., Eléaume, M. P., and Johnson, C. R. (2018a). Taxonomic resolution, functional traits, and the influence of species groupings on mapping Antarctic seafloor biodiversity. *Front. Ecol. Evol.* 6:81. doi: 10.3389/fevo.2018.00081

Jansen, J., Hill, N. A., Dunstan, P. K., McKinlay, J., Sumner, M. D., Post, A. L., et al. (2018b). Abundance and richness of key Antarctic seafloor fauna correlates with modelled food availability. *Nat. Ecol. Evol.* 2, 71–80. doi: 10.1038/s41559-017-0392-3

Jones, G. A., and Kaiteris, P. (1983). A vacuum gasometric technique for rapid and precise analysis of calcium carbonate in sediments and soils. *J. Sediment. Res.* 53, 655–660. doi: 10.1306/212f825b-2b24-11d7-8648000102c1865d

Kim, S., Hammerstrom, K., and Dayton, P. K. (2019). Epifaunal community response to iceberg-mediated environmental change in McMurdo Sound, Antarctica. *Mar. Ecol. Prog. Ser.* 613, 1–14. doi: 10.3354/meps12899

Kim, S., Saenz, B., Scanniello, J., Daly, K., and Ainley, D. (2018). Local climatology of fast ice in McMurdo Sound, Antarctica. *Antarct. Sci.* 30, 125–142. doi: 10.1017/s0954102017000578

Kröger, K., and Rowden, A. A. (2008). Polychaete assemblages of the northwestern Ross Sea shelf: worming out the environmental drivers of Antarctic macrobenthic assemblage composition. *Polar Biol.* 31, 971–989. doi: 10.1007/s00300-008-0437-9

Law, C. S., Rickard, G. J., Mikaloff-Fletcher, S. E., Pinkerton, M. H., Behrens, E., Chiswell, S. M., et al. (2017). Climate change projections for the surface ocean around New Zealand. *N. Z. J. Mar. Freshwater Res.* 52, 1–27. doi: 10.1080/00288330.2017.1390772

Legendre, P., and Anderson, M. J. (1999). Distance-based redundancy analysis: testing multispecies responses in multifactorial ecological experiments. *Ecol. Monogr.* 69, 1–24. doi: 10.1890/0012-9615(1999)069[0001:dbratm]2.0.co;2

Levin, L. A., Etter, R. J., Rex, M. A., Gooday, A. J., Smith, C. R., Pineda, J., et al. (2001). Environmental influences on regional deep-sea species diversity. *Ann. Rev. Ecol. Syst.* 32, 51–93. doi: 10.1146/annurev.ecolsys.32.081501.114002

Lutz, M. J., Caldeira, K., Dunbar, R. B., and Behrenfeld, M. J. (2007). Seasonal rhythms of net primary production and particulate organic carbon flux to depth describe the efficiency of biological pump in the global ocean. *J. Geophys. Res.* 112:C10011. doi: 10.1029/2006JC003706

Maksym, T. (2019). Arctic and Antarctic sea ice change: contrasts, commonalities, and causes. *Ann. Rev. Mar. Sci.* 11, 187–213. doi: 10.1146/annurev-marine-010816-060610

McArdle, B. H., and Anderson, M. J. (2001). Fitting multivariate models to community data: a comment on distance-based redundancy analysis. *Ecology* 82, 290–297. doi: 10.1890/0012-9658(2001)082[0290:fmmtcd]2.0.co;2

Moreau, S., Mostajir, B., Belanger, S., Schloss, I. R., Vancoppenolle, M., and Demers, S. (2015). Climate change enhances primary production in the Western Antarctic Peninsula. *Glob. Chang. Biol.* 21, 2191–2205. doi: 10.1111/gcb.12878

NASA Goddard Space Flight Center, Ocean Ecology Laboratory, and Ocean Biology Processing Group. (2018a). *MODIS/Aqua Ocean Color Reprocessing 2018.0*. Available online at: https://oceancolor.gsfc.nasa.gov/reprocessing/r2018/aqua/ (accessed May, 2018).

NASA Goddard Space Flight Center, Ocean Ecology Laboratory, and Ocean Biology Processing Group. (2018b). *SeaWiFS Ocean Color Reprocessing 2018.0*. Available online at: https://oceancolor.gsfc.nasa.gov/reprocessing/r2018/seawifs/ (accessed May, 2018).

Orr, J. C., Fabry, V. J., Aumont, O., Bopp, L., Doney, S. C., Feely, R. A., et al. (2005). Anthropogenic ocean acidification over the twenty-first century and its impact on calcifying organisms. *Nature* 437, 681–686. doi: 10.1038/nature04095

Parker, S. J., and Dunn, A. (2018). *Guidelines for Fisheries-Directed Research Addressing the Ross Sea Region Marine Protected Area Research and Monitoring Plan*. CCAMLR document WG-SAM-18/21. Hobart, TAS: CCAMLR, 10.

Peck, L. S. (2005). Prospects for surviving climate change in Antarctic aquatic species. *Front. Zool.* 2:9. doi: 10.1186/1742-9994-2-9

Peck, L. S., Morley, S. A., and Clark, M. S. (2010). Poor acclimation capacities in Antarctic marine ectotherms. *Mar. Biol.* 157, 2051–2059. doi: 10.1007/s00227-010-1473-x

Pineda-Metz, S. E., and Gerdes, D. (2018). Seabed images versus corer sampling: a comparison of two quantitative approaches for the analysis of marine benthic communities in the southern Weddell Sea (Southern Ocean). *Polar Biol.* 41, 515–526. doi: 10.1007/s00300-017-2211-3

Pineda-Metz, S. E. A., Gerdes, D., and Richter, C. (2020). Benthic fauna declined on a whitening Antarctic continental shelf. *Nat. Commun.* 11:2226. doi: 10.1038/s41467-020-16093-z

Pineda-Metz, S. E. A., Isla, E., and Gerdes, D. (2019). Benthic communities of the Filchner Region (Weddell Sea, Antarctica). *Mar. Ecol. Prog. Ser.* 628, 37–54. doi: 10.3354/meps13093

Pörtner, H. O., Peck, L. S., and Somero, G. N. (2007). Thermal limits and adaptation: an integrative view. *Philos. Trans. R. Soc. Lond. B* 362, 2233–2258. doi: 10.1098/rstb.2006.1947

Reynolds, R. W., Rayner, N. A., Smith, T. M., Stokes, D. C., and Wang, W. (2002). An improved in situ and satellite SST analysis for climate. *J. Clim.* 15, 1609–1625. doi: 10.1175/1520-0442(2002)015<1609:aiisas>2.0.co;2

Rowden, A., Kröger, K., and Clark, M. (2015). Compositional patterns of benthic assemblages on the northwestern Ross Sea shelf, Antarctica: interacting environmental drivers operating at multiple spatial scales. *Hydrobiologia* 761, 1–23.

Sartory, D. P. (1982). *Spectrophotometric Analysis of Chlorophyll a in Freshwater Phytoplankton*. Report No. TR 115. Pretoria: Hydrological Research Institute, Department of Environment Affairs, 163.

Smith, C. R., Mincks, S., and DeMaster, D. J. (2006). A synthesis of bentho-pelagic coupling on the Antarctic shelf: food banks, ecosystem inertia and global climate change. *Deep Sea Res. 2 Top. Stud. Oceanogr.* 53, 875–894. doi: 10.1016/j.dsr2.2006.02.001

Smith, W. O., Ainley, D., Cattaneo-Vietti, R., and Hofmann, E. (2012). "Chap. 7 The Ross Sea continental shelf: regional biogeochemical cycles, trophic interactions, and potential future changes," in *Antarctic Ecosystems: An Extreme Environment in a Changing World*, eds A. D. Rogers, N. M. Johnston, E. J. Murphy, and A. Clarke (New Jersey, NJ: Blackwell Publishing Ltd), 213–235. doi: 10.1002/9781444347241.ch7

Somerfield, P. J., Clarke, K. R., and Olsgard, F. (2002). A comparison of the power of categorical and correlational tests applied to community ecology data from gradient studies. *J. Anim. Ecol.* 71, 581–593. doi: 10.1046/j.1365-2656.2002.00624.x

Stammerjohn, S. E., and Maksym, T. (2017). "Gaining (and losing) Antarctic sea ice: variability, trends and mechanisms," in *Sea Ice*, ed. D. N. Thomas (Chichester: Wiley & Sons), 261–289. doi: 10.1002/9781118778371.ch10

Stammerjohn, S. E., Martinson, D. G., Smith, R. C., Yuan, X., and Rind, D. (2008). Trends in Antarctic annual sea ice retreat and advance and their relation to El Niño–Southern Oscillation and Southern Annular mode variability. *J. Geophys. Res.* 113:C03S90. doi: 10.1029/2007JC004269

Stammerjohn, S. E., Massom, R., Rind, D., and Martinson, D. G. (2012). Regions of rapid sea ice change: an interhemispheric seasonal comparison. *Geophys. Res. Lett.* 39:L06501. doi: 10.1029/2012GL050874

Steinberg, D. K., Ruck, K. E., Gleiber, M. R., Garzio, L. M., Cope, J. S., Bernard, K. S., et al. (2015). Long-term (1993-2013) changes in macrozooplankton off the Western Antarctic Peninsula. *Deep Sea Res. 1* 101, 54–70. doi: 10.1016/j.dsr.2015.02.009

Sumida, P. Y. G., Smith, C. R., Bernardino, A. F., Polito, P. S., and Vieira, D. R. (2014). Seasonal dynamics of megafauna on the deep West Antarctic Peninsula shelf in response to variable phytodetrital influx. *R. Soc. Open Sci.* 1:140294. doi: 10.1098/rsos.140294

Ter Braak, C. J. F., and Smilauer, P. (1998). *CANOCO Release 4 Reference Manual and User's Guide to Canoco for Windows-Software for Canonical Community Ordination*. Ithaca, NY: Microcomputer Power.

Thatje, S. (2012). Effects of capability for dispersal on the evolution of diversity in Antarctic benthos. *Integr. Comp. Biol.* 52, 470–482. doi: 10.1093/icb/ics105

Thrush, S. F., and Cummings, V. J. (2011). Massive icebergs, alteration in primary food resources and change in benthic communities at Cape Evans, Antarctica. *Mar. Ecol.* 32, 289–299. doi: 10.1111/j.1439-0485.2011.00462.x

Thrush, S. F., Dayton, P. K., Cattaneo-Vietti, R., Chiantore, M., Cummings, V., Andrew, N., et al. (2006). Broad-scale factors influencing the biodiversity of coastal benthic communities of the Ross Sea. *Deep Sea Res. 2 Top. Stud. Oceanogr.* 53, 959–971. doi: 10.1016/j.dsr2.2006.02.006

Conflict of Interest: The authors declare that the research was conducted in the absence of any commercial or financial relationships that could be construed as a potential conflict of interest.

frontiers in Marine Science

ORIGINAL RESEARCH
published: 23 July 2021
doi: 10.3389/fmars.2021.629706

Combining Traditional Taxonomy and Metabarcoding: Assemblage Structure of Nematodes in the Shelf Sediments of the Eastern Antarctic Peninsula

Gabriella Pantó, Francesca Pasotti, Lara Macheriotou and Ann Vanreusel*

Biology Department, Marine Biology Research Group, Ghent University, Ghent, Belgium

This study provides a snapshot of the largely understudied meiobenthic and nematode communities in the Prince Gustav Channel (PGC) and Duse Bay (DB). We compared five stations sampled at different water depths along the shelf and investigated their meiobenthic community structure. We approached nematode biodiversity combining traditional taxonomic identification and high throughput sequencing (HTS), with the use of Amplicon Sequence Variants (ASVs). Additionally, we characterized the environment by primary production proxies, grain size and seasonal ice conditions. Our results suggest that the availability of organic matter and its freshness are responsible for the high densities found at all depths. However, potential factors influencing the high local and regional variability of meiofauna density and biodiversity are less clear. A bathymetric transect consisting of three stations in DB (200, 500, and 1,000 m depth) showed increasing pigment concentrations in the first centimeters of the sediment vertical profile with increasing water depth, whereas the meiofauna densities showed the opposite trend. The deepest station of DB seems to function as a sink for fine material as supported by the higher silt fraction and higher organic matter concentrations. When comparing the two basins in the PGC (1,000 and 1,250 m) and the one in DB (1,000 m), differences in terms of environmental variables, meiofaunal densities, and composition were observed. The deepest basin in PGC is located further South (closer to the highly unstable Larsen area), and marked differences with the other basins suggest that it might be experiencing different conditions as a result of its presence near the summer ice margin and its more elongated topography. Both, the shallowest and the deepest stations showed the highest number of unique sequences, suggesting a more biodiverse nematode assemblage. The morphological identification did not show significant differences in the biodiversity of all stations, differently from the ASVs approach. However, the lack of reference sequences in online databases and the thickness of nematode's cuticule are still important issues to consider as they potentially lead to underestimations of biodiversity and functional traits.

Keywords: Eastern Antarctic Peninsula, benthos, nematodes, Prince Gustav Channel, Duse Bay, metabarcoding, ASVs, biodiversity

OPEN ACCESS

Edited by:
Katrin Linse,
British Antarctic Survey,
United Kingdom

Reviewed by:
Gritta Veit-Köhler,
Senckenberg am Meer
Wilhelmshaven, Germany
Federica Semprucci,
University of Urbino Carlo Bo, Italy

****Correspondence:***
Gabriella Pantó
Gabriella.Panto@UGent.be

Specialty section:
This article was submitted to Marine Evolutionary Biology, Biogeography and Species Diversity, a section of the journal Frontiers in Marine Science

Received: *15 November 2020*
Accepted: *18 June 2021*
Published: *23 July 2021*

Citation:
Pantó G, Pasotti F, Macheriotou L and Vanreusel A (2021) Combining Traditional Taxonomy and Metabarcoding: Assemblage Structure of Nematodes in the Shelf Sediments of the Eastern Antarctic Peninsula. Front. Mar. Sci. 8:629706. doi: 10.3389/fmars.2021.629706

INTRODUCTION

Ecosystem dynamics of the sea-bottom are strongly influenced by the density and diversity of organisms inhabiting marine sediments. Macro- and meiofauna organisms have proven to be especially important in investigating biodiversity, as well as characterizing ecosystem dynamics both in shallow and deep waters (Schratzberger and Ingels, 2018). Benthic communities have a positive effect on ecosystem functions by modifying the environment they inhabit, for instance facilitating the biodegradation of organic matter by microbial activity stimulation and influencing the vertical redox potential of sediments by bioturbation (Zeppilli et al., 2018; Hoffmann et al., 2019; Gogina et al., 2020). Even though meiofauna (>32 μm, <1 mm) has been historically understudied because of the tediousness of sampling and identifying such small size organisms (Schratzberger and Ingels, 2018), it plays a key role in aquatic sediments. By feeding on both microalgae and bacteria and being consumed by higher trophic levels, meiofauna taxa can be both, consumers, and producers (Vinagre et al., 2012; Carpentier et al., 2013; Schmid-Araya et al., 2016; Schratzberger and Ingels, 2018). The reduced size of meiofauna makes them extremely sensitive to even the slightest changes in sediment grain size and structure (Taheri et al., 2017; Korbel et al., 2019), but also in oxygen availability and organic load within the sediment (Hoffmann et al., 2018). Because of their short generation time and direct benthic development, free-living nematodes in particular may be able to reveal environmental perturbations on a small spatial and temporal scale, as confirmed in several studies (Kennedy and Jacoby, 1999; Moreno et al., 2011; Semprucci et al., 2015). As they represent >90% of the metazoans inhabiting marine sediments, nematodes are also considered good proxies for assessing benthic biodiversity, especially in relation to meiobenthic influence on ecosystem dynamics. In light of possible climatic changes, the analysis of the biodiversity in extremely sensitive habitats might shed light on potential impacts of ongoing and future climate stressors.

Despite polar regions being particularly sensitive to such climatic alterations, Antarctic marine-shelf habitats are still amongst the least studied on Earth. Their accessibility is limited due to logistic difficulties in light of their remoteness and the regional climatic conditions of the Antarctic (Cook et al., 2005) yet the high diversity and abundance of their biological assemblages and related ecosystem services that they provide are of main interest for a number of scientific questions. The Antarctic Peninsula (AP) is known for being one of the most impacted regions by anthropogenic global warming, which results in catastrophic events such as ice-shelf collapse, glacier thinning (Martín et al., 2009; Kunz et al., 2012), acceleration (Pritchard and Vaughan, 2007) and recession (Cook et al., 2005; Davies et al., 2012). The AP has experienced rates of atmospheric warming greater than the global mean (Vaughan et al., 2003) and a loss of 28 000 km^2 of ice shelves since the 1960s (Cook and Vaughan, 2010). The Eastern Antarctic Peninsula (EAP) is particularly affected by variations in westerly circumpolar winds which are responsible for basal melting leading to the thinning and eventually the collapse of ice shelves (Oppenheimer, 1998; Rignot and Jacobs, 2002; Polvani et al., 2011; Pritchard et al., 2012). From a global warming perspective, it is appropriate to assume that further increase of average global temperatures will lead to dramatic and irreversible changes in the AP (Etourneau et al., 2019; Siegert et al., 2019), especially the already unstable EAP ice shelf.

The ecosystem of the AP is characterized by high primary productivity, with large phytoplanktonic blooms that have a bottom-up effect in sustaining the regional food web, strictly linked to the seasonality of sea-ice dynamics (Prezèlin et al., 2000; Nardelli et al., 2018). When the sea ice has melted and the ocean surface is exposed to solar radiation, conditions are favorable for phytoplankton to grow, and productivity reaches its maximum (Moline and Prezelin, 1996). Previously ice-covered benthic areas seasonally experience a shift to higher phytoplanktonic abundance due to the temporary system transition to more open waters (Montes-Hugo et al., 2009). Because primary productivity is of crucial importance for shaping the communities of benthic organisms living in shallow and deep sediments, ice cover and changes in ice dynamics (determining a shift to open water systems and possibly changing the amount of OM depositing on the seafloor) are essential players when studying the meiofauna community of polar ecosystems.

While morphological identification is still a common practice used in meiofauna diversity assessments, the development of molecular techniques as high throughput sequencing (HTS) has opened the possibility to analyze a larger set of samples in a much shorter timeframe, often resulting in faster and more reliable analysis (Brannock et al., 2018; Steyaert et al., 2020). Molecular approaches can overcome some of the limitations of microscope-based identification: for example, the detection of cryptic species (i.e., individuals with same morphological features but different DNA sequences) is not possible based solely on morphological identification. Traditional meiofauna identification is in fact time-consuming and requires a specific expertise, thus molecular techniques are being increasingly used as alternative diagnostic approach (Dell' Anno et al., 2015; Fonseca et al., 2017; Macheriotou et al., 2019). Disadvantages of the molecular analysis for species identification mainly lie in the incompleteness of online databases used to assign the taxonomical label to a specific DNA sequence and the need to find the right marker for a specific community (Ahmed et al., 2015). Nevertheless, many studies of the last decade have proven this approach to be particularly useful when dealing with such abundant organisms as nematodes, particularly by means of DNA metabarcoding and the use of Amplicon Sequence Variants (ASVs) (Macheriotou et al., 2020; Steyaert et al., 2020).

By analyzing the meiofauna and specifically nematodes along a depth gradient in Duse Bay (DB) and by comparing two adjacent deep basins in the Prince Gustav Channel (PGC), the following hypothesis were tested: (i) the community composition and density of meiofauna and nematodes along a bathymetric transect in DB is dependent on changes with depth and the related environmental variables; (ii) meiobenthic community structure in the three deep basins is dependent on local small-scale variability drivers and seasonal sea-ice cover; (iii) the use of ASVs efficiently provides accurate information on the

connectivity of nematode communities along the shelf and thus possible gene flow between stations.

MATERIALS AND METHODS

Study Sites and Sampling Methodology

The focus of this study are the meiobenthic communities of the PGC and DB, both situated in the EAP. The PGC is a 6–7 km narrow seaway enclosed between the Trinity Peninsula and the James Ross and Vega Islands, northeast of the AP. The bathymetry of the channel is characterized by a "U-shaped" 1,000–1,250 m deep trough with steep walls interrupted by shallow ledges, which separate the deep basins (Camerlenghi et al., 2002). As part of the AP, the PGC has been characterized by the collapse of its ice-shelf since the late 1980s. The glacier dynamics in the region are particularly sensitive to ice-shelf back pressure (which slows down the ice-shelf movement toward the ocean); in fact, the rapid retreat of glaciers after a collapse event seems to be common in the PGC and Larsen A and B districts (Rott et al., 2002). This is confirmed by the disintegration of the PGC ice shelf and Larsen A embayment in 1995 and the northern and central sections of the Larsen B embayment in March 2002, which resulted in considerable ice losses due to intensified ice discharge (Shuman et al., 2011). Mass reduction has been recorded until recent times, and frontal retreat and intensification of calving fluxes is expected to occur in correlation to glaciers which showed significant temporal variations of ice flow during recent years (Rott et al., 2018). DB is a sheltered inlet situated on the south side of the Trinity Peninsula, between Tabarin Peninsula and View Point (**Figure 1**). It is characterized by extremely rapid glacier loss compared to the rest of the region, together with Larsen Inlet, Sjögren Inlet, and Eyrie Bay (Davies et al., 2012). The topography of the area is characterized by a steep slope. Understanding that limited information is available on the benthic ecology of DB, this study represents an initiative for further studies in the area. The designated sites for this study were two deep basins along the PGC at 1,250 and 1,000 m, and a bathymetric transect in DB (200, 500, and 1,000 m depth; **Table 1**). The study area and sampling stations are shown in **Figure 1**.

Sampling was carried out during the RRS James Clark Ross cruise JR17003a in February-March 2018[1]. Sediment samples were collected using a 12-core Multicorer (MUC) type Oktopus, each core having an inner diameter of 10 cm. At each station three to four cores were collected from the same or different MUC deployments, as shown in **Table 1**. Limitations on the amount of deployments were dictated during the cruise by the ice conditions and time constraints. Overlying water from each intact core was filtered over a 32-μm sieve and preserved with the corresponding

[1]https://www.bodc.ac.uk/resources/inventories/cruise_inventory/report/16954/

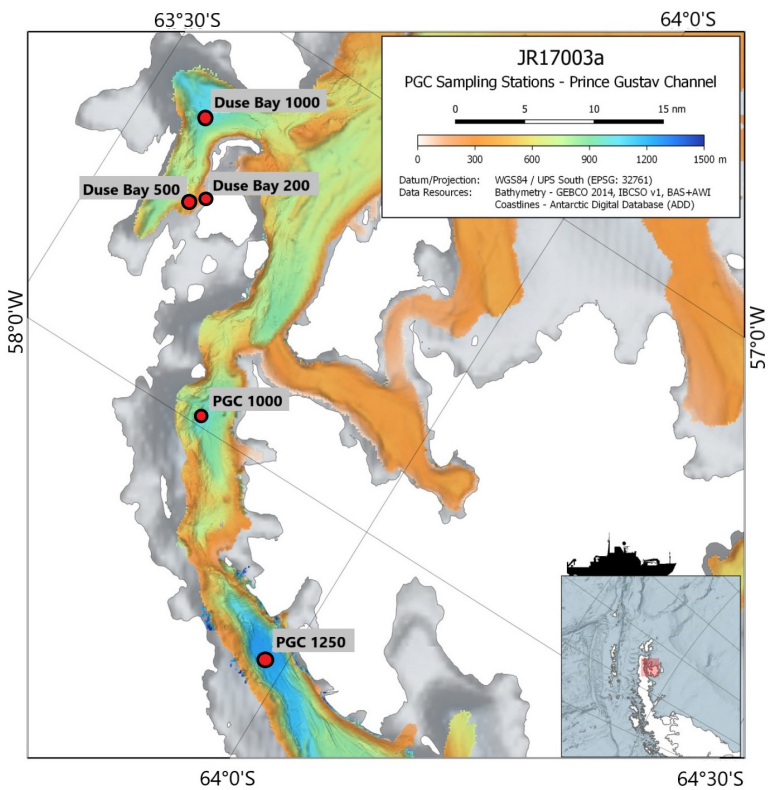

FIGURE 1 | Sampling stations in the Prince Gustav Channel (PGC, 1,000 and 1,250 m) and Duse Bay (DB, 1,000, 500, and 200 m). Bathymetric map courtesy of: "British Antarctic Survey" and "Bathymetry Group of the Alfred-Wegener-Institute."

TABLE 1 | Overview of stations sampled during the RRS James Clark Ross cruise JR17003a (February–March 2018).

Date	Area	Depth (m)	Latitude (S)	Longitude (W)	# cores
2018–03-07	Duse Bay	200	63.62481	57.48192	3
2018–03-07	Duse Bay	500	63.61546	57.49913	4
2018–03-01	Duse Bay	1000	63.57557	57.29855	2
2018–03-01	Duse Bay	1000	63.56889	57.29919	2
2018–03-06	PGC mid	1000	63.76125	57.96736	3
2018–03-05	PGC South	1250	63.97651	58.42942	2
2018–03-05	PGC South	1250	63.397658	58.842954	2

The table shows the date of each sampling event (each row represents a deployment), the depth of the station, coordinated and number of cores deployed.

sediment sample. For each core, the sediment was divided in equal horizontal slices of 2 cm, down to 8 cm depth. In turn, each slice was equally divided in two subsamples and preserved in different conditions according to the prospected analysis. Specifically, the first half was stored in a 250 mL container and fixed with 4% formaldehyde (buffered with pre-filtered seawater) for morphological meiofauna community analysis (density, biodiversity). The second half was placed in plastic bags and frozen at −80°C for molecular analysis of meiofauna (i.e., metabarcoding) and for the examination of environmental variables (pigments, organic matter, sediment grain size).

Environmental Parameters: Pigments and Granulometry Data

From the frozen sliced cores, 250 mg of sediment was subsampled from each layer for phytopigment analysis. Environmental parameters included phaeopigments, organic matter and sediment grain size (**Table 2**). Pigments were extracted with acetone (90%, 8 mL), ultrasonicated for 30 s and further extracted overnight at 4°C. Subsequently, samples were centrifuged for 10 min at 4,000 rpm (4°C) and the supernatant was filtered through 0.2 μm Polytetrafluoroethylene (PTFE) membrane filters (VWR International). As described by Van Heukelem and Thomas (2001), pigments were then separated on a HPLC equipped with a cooled auto-sampler, column heater, a photodiode array detector and a fluorescence detector as described. Authentic pigment standards together with compounds isolated from reference cultures were used to calibrate the system following the Scientific Committee on Oceanic Research (SCOR) protocols (DHI, Denmark). Finally, the concentration of individual pigments was calculated using the response factor of standard pigments (Van Heukelem and Thomas, 2001) and it is reported as μg/g. Sample preparation for total organic carbon (TOC; expressed as% C_{org} w/w – weight of carbon to total weight of sediment) and total nitrogen (TN) (expressed as % N) was performed by first drying and homogenizing the sediment. Subsequently, 37% HCl (purity grade) was added to TOC samples for decalcification. TOC and TN contents were measured using Flash 2000 NC Sediment Analyser from Interscience. Grain size was estimated using the Mastersizer Hydro 2000G (MALVERN) particle size analyser: the measurable particle range size is between 0.01 and 2,000 μm in volume percent. The grain size classes used were the

TABLE 2 | Concentration of all the environmental variables analyzed.

		Chlorophyll C2 (mg/g)		Pheophorbide a (μg/g)		Fucoxanthin (μg/g)		Diadinoxanthin (μg/g)		Diatoxanthin (μg/g)		Chlorophyll a (μg/g)		Pheophytin a (μg/g)		Beta carotene (μg/g)		CPE (μg/g)		TN (%)		TOC (%)		TOM (%)		Clay (%)		Silt (%)		Sand (%)	
Station	**Layer**	**Mean**	**SD**	**Mean**	**SD**	**Mean**	**SD**	**Mean**	**SD**	**Mean**	**SD**	**Mean**	**SD**	**Mean**	**SD**	**Mean**	**SD**	**Mean**	**SD**	**Mean**	**SD**	**Mean**	**SD**	**Mean**	**SD**	**Mean**	**SD**	**Mean**	**SD**	**Mean**	**SD**
Duse Bay 200	0–2	0.98	0.54	9.53	2.22	3.85	1.46	0.28	0.1	1.66	0.57	13.24	5.96	2.36	0.22	0.77	0.24	32.67	9.97	0.2	0.09	0.68	0.25	5.66	0.16	7.71	0.75	49.46	2.05	42.83	2.74
	2–4	1.21	0.3	8.66	0.92	2.66	0.4	0.17	0.04	2.15	0.28	15.93	1.79	1.9	0.58	0.97	0.21	33.65	3.18	0.13	0.02	0.53	0.07	5.6	0.06	7.21	3.05	47.5	8.78	45.29	11.83
	4–6	1.25	0.5	7.39	1.35	2.5	1.13	0.15	0.13	1.99	0.14	10.11	3.35	1.63	0.32	0.99	0.07	26.02	6.7	0.14	0.09	0.52	0.24	5.51	0.16	7.15	1.77	46.83	5.44	46.02	6.46
	6–8	1.28	0.67	6.64	2.64	1.94	0.78	0.1	0.03	1.89	0.8	8.28	3.28	1.38	0.3	0.93	0.23	22.43	8.57	0.12	0.09	0.41	0.27	5.41	0.29	7.13	0.11	43.08	4.1	49.79	4.17
Duse Bay 500	0–2	4.93	2.02	31.02	2.09	16.96	0.51	1.58	0.51	5.47	2.13	52.64	2.29	7.51	0.55	2.33	0.13	122.44	7.59	0.29	0.03	1.32	0.09	6.52	0.27	10.26	0.9	66.71	6.05	23.03	6.92
	2–4	6.33	3.8	21.8	4.14	12.84	7.36	1.26	0.38	6.97	1.03	59.51	18.66	5.62	1.33	2.37	0.51	116.7	36.68	0.29	0.02	1.2	0.05	5.91	0.2	10.58	3.35	62.08	15.49	27.34	18.76
	4–6	3.89	1.51	16.97	0.37	9.09	1.34	0.77	0.12	5.86	0.54	41.43	5.95	5.07	0.9	2.04	0.17	85.12	9.65	0.29	0.02	1.2	0.05	5.66	0.13	10.03	4.03	59.43	16.05	30.54	20.01
	6–8	4	0.85	15.11	1.42	7.11	1.01	0.63	0.12	5.7	0.45	33.54	5.66	4.97	0.09	1.92	0.14	72.97	9.39	0.29	0.05	1.1	0.1	5.6	0.13	11.15	2.61	68.25	7.81	20.6	10.42
Duse Bay 1,000	0–2	6.94	1.99	48.98	7.23	19.61	6.76	2.34	1.09	5.06	1.19	56.57	19.33	6.7	3.64	2.33	0.62	148.53	40.05	0.26	0.03	2.17	0.35	7.99	1.08	10.49	0.58	70.08	2.73	19.43	2.73
	2–4	5.46	1.8	43.56	17.41	17.85	5.01	1.89	0.82	6.39	0.45	66.26	17.69	5.86	3.93	2.5	0.44	149.77	44.45	0.31	0.1	2.15	0.49	6.77	0.36	11.73	0.9	74.35	0.43	13.92	1.12
	4–6	6.67	2.03	26.99	1.62	13.94	2.31	1.35	0.18	6.4	0.64	57.53	5.16	4.91	1.28	2.06	0.3	119.85	10.3	0.23	0.05	1.85	0.34	6.34	0.24	12.55	0.25	74.67	1.84	12.78	1.97
	6–8	5.09	1.67	23.95	2	10.91	1.48	0.91	0.26	5.44	0.37	39.68	8.54	4.46	0.4	1.98	0.07	92.42	11.72	0.25	0.04	1.72	0.11	5.85	0.18	12.68	0.34	73.99	1.71	13.33	1.94
PGC 1,000	0–2	12.4	6.44	116.46	56.85	52.39	29.26	8.07	3.72	15.52	15.06	131.42	48.47	26.71	14.71	4.56	1.78	367.53	172.63	0.33	0.09	1.29	0.26	6.28	0.88	8.22	0.33	60.86	5.24	30.92	5.14
	2–4	5.23	2.94	21.86	3.25	18.66	7.42	1.41	0.76	4.45	1.42	60.76	21.69	5.54	2.45	2.12	0.62	120.02	32.37	0.43	0.36	0.91	0.18	4.47	0.44	6.81	1.56	47.4	6.06	45.79	7.58
	4–6	1.89	1.65	10.01	3.61	5.73	1.86	0.3	0.2	3.07	0.5	20.05	6.67	2.21	0.4	1.19	0.15	44.46	14.39	0.48	0.5	0.69	0.05	3.19	0.25	9.15	0.46	51.24	2.15	39.61	2.61
	6–8	1.01	0.84	5.6	4	2.71	1.12	0.14	0.09	2.01	0.54	9.84	3.71	1.89	0.49	0.92	0.22	24.11	10.57	0.15	0.06	0.53	0.08	3.31	0.23	8.33	0.28	47.26	2.74	44.41	3.01
PGC 1,250	0–2	1.32	0.44	9.76	1.04	3.35	0.61	0.27	0.09	1.36	0.25	9.45	1.45	1.22	0.22	0.6	0.1	27.33	3.8	0.17	0.05	0.83	0.14	3.28	0.44	11.46	0.45	61.06	3.65	27.48	3.46
	2–4	0.98	0.44	5.86	1.88	2.42	0.4	0.1	0.01	1.21	0.08	7.48	0.97	0.72	0.28	0.51	0.07	19.29	3.1	0.16	0.04	0.68	0.08	3.02	0.61	12.82	0.87	60.23	2.19	26.95	3.01
	4–6	0.24	0.22	3.11	1.4	0.66	0.48	0.01	0.02	0.55	0.22	2.24	0.9	0.71	0.18	0.35	0.07	7.88	3.28	0.13	0.05	0.62	0.12	3.14	0.37	9.75	2.95	57.93	4.68	32.32	7.23
	6–8	0.08	0.07	1.78	1.25	0.48	0.34	0	0	0.42	0.19	1.52	0.57	0.76	0.12	0.32	0.05	5.36	2.48	0.13	0.02	0.6	0.07	3.32	0.42	8.63	3.43	53.67	2.95	37.7	5.95
dbRDA ASVs (*p*-value)		0.006**		0.035*		0.017*		0.062		0.085		0.156		0.069		0.178		-		0.707		0.08		0.010**		0.195		0.693		0.162	
dbRDA meiofauna (*p*-value)		0.049*		0.006**		0.131		0.082		0.081		0.031*		0.004**		0.072		-		0.142		0.033		0.007**		0.225		0.06		0.059	

*The table reports the mean and standard deviation (SD) of three to four replicates per layer of each station. At the bottom, significant values for dbRDA analysis are reported for each variable: the first row reports values of the analysis performed on the metabarcoding dataset – dbRDA ASVs (p-value); the second row shows values for the analysis performed on morphological dataset-dbRDA meiofauna (p-value). The number of * indicates the degree of significance.*

following: clay (<4 μm), silt (4–63 μm), and sand (63–500 μm). Grain size distributions were evaluated with the Mastersizer 2000 5.4 program.

Meiofauna Extraction and Characterization

The volume of each sample was recorded after sedimentation in a 250 mL cylinder before extracting the meiofauna fraction. Samples fixed in 4% formaldehyde were then sieved over a 1,000-μm sieve on top of a 32 μm sieve. Organisms larger than 1,000-μm (macrofauna) were dyed with Rose Bengal (0.5 g L^{-1}) and stored in 4% formaldehyde for further analysis. The meiofauna fraction (between 1,000 and 32 μm) was extracted by density-gradient centrifugation (3 × 12 min, at 3,000 rpm) with the colloidal silica polymer LUDOX HS40, with a specific density of 1.18 g/cm^3 (protocol described in Heip et al., 1982; Vanhove et al., 1999). The resulting extracted sample was finally dyed with Rose Bengal (0.5 g L^{-1}) and stored in 4% formaldehyde. The meiofauna was counted at the stereomicroscope. The counting of the most abundant taxon (Nematoda) was performed with the use of an eight-chambered meiofauna sample-splitter (Jensen, 1982). Three out of the eight chambers were randomly chosen as sub-replicates to count nematodes, copepods and copepoda nauplii. Organisms were initially identified to higher taxon level, and results were standardized to individuals per 10 cm^{-2}. We conducted a preliminary inspection on the entire sediment vertical profile at each station to establish which layer hosted the majority of the organisms. The first 2 cm of the sediment are expected to harbor the majority of meiofaunal taxa, which has been reported in previous studies (Ingels et al., 2012) and confirmed by the results of the vertical abundance analysis in this study (**Supplementary Annex A**). Quantification of meiofauna was performed on three replicates (A–C) per station: the abundance analysis of the first replicate (A) was done along the complete depth gradient whereas for the other two replicates only the first 0–2 cm layer was considered. Given the high patchiness and variability of nematode communities within the sediments, it might be necessary to assume a high standard deviation also in the deeper layers of the sediment. For these reasons, the results of the vertical gradient analysis (**Supplementary Annex A**) must be interpreted with care and such considerations taken into account.

Taxonomical Identification of Nematoda

At each station, 80 nematodes specimens from three replicates were picked out from 0 to 2 cm layer, transferred to anhydrous glycerol (Seinhorst, 1959) and mounted on glass slides for identification to genus level. The relatively low number of nematodes identified per replicate (in other studies the number ranges between 100 and 200 specimens), and the choice to analyze only the first 0–2 cm layer is related to the time-consuming identification process and the weight of the morphological analysis in this study. Further, the most abundant genera and their species would be represented in correct proportions in the small subsample used for morphological identification, and their relative importance within the sample would be still the highest. This would constitute meaningful support information to the molecular dataset (ASVs). The molecular analysis allows the identification of a higher number of individuals in a shorter timeframe and (hypothetically) with more accuracy, hence metabarcoding analysis (ASVs) was prioritized for biodiversity assessment over the use of the morphological dataset, which was instead used to integrate any missing information. The Taxonomical classification was carried out following the online key for free living marine nematodes (NeMysKey©, Bezerra et al., 2021) and the pictorial key from Warwick et al. (1998), based on relevant morphological traits (buccal cavity, tail, amphid, and reproductive organs). Nematode were then divided into trophic guilds following the subdivision suggested by Wieser (1953), considering the structure of their buccal cavities. Specifically, the guilds were: selective deposit feeders (1A) with small buccal cavities mainly feeding on bacteria; non-selective-deposit feeders (1B), characterized by a larger unarmed buccal cavity expected to feed on detritus and particulate organic matter; epistrate feeders (2A), with one or more small teeth to perforate the outer shell of unicellular organisms such as microalgae; predators/omnivores (2B), usually larger nematodes with cuticularized teeth (and possibly strong mandible structures) that predate on other meiofauna organisms and/or ingest detritus particles.

Metabarcoding Analysis

DNA Extraction

The molecular analysis of meiofauna was performed on the entire vertical profile (0–8 cm) of all frozen samples (three to four replicates per station). Samples frozen at −80°C were initially defrosted and meiofauna was extracted following the density-gradient centrifugation procedure using LUDOX HS40. The sieved samples were stored in CTAB in 1.5 mL Eppendorf tubes and frozen at −20°C. Genomic DNA extraction was performed by adding 6 μL proteinase-K (10 mg/mL) to the defrosted samples and centrifuging for 5 min at 14,000 rpm at room temperature. The formed pellet was grounded and bead-beaten for 2 min at 30 cycles/s in order to break nematodes' membranes and tubes were then incubated for 1 h at 60°C before adding ammonium acetate (250 μL, 7.5 M). The samples were then centrifuged for 10 min at 14,000 rpm and 750 μL of the supernatant were transferred into a sterile 2.0 mL Eppendorf tube; subsequently 750 μL of cold 80% isopropanol was added. Tubes were incubated for 30 min at room temperature and centrifuged for 10 min at 14,000 rpm at 4°C. After the removal of the supernatant, samples were incubated on ice for 30 min with 1 mL of washing buffer (solution of 10 mM ammonium acetate in 76% ethanol) to remove salts. Tubes were centrifuged for 5 min at 14,000 rpm at 4°C, the supernatant was removed and the pellet was stored in 20 μL of sterile milliQ water. The samples were then stored frozen at −20°C.

Library Preparation and Sequencing

Using the "16S Metagenomic Sequencing Library Preparation" protocol (Amplicon et al., 2013) SSU_F_04-SSU/22_R primers (GCTTGTCTCAAAGATTAAGCC and TCCAAGGAAGGCAGCAGGC, respectively) were assembled with Illumina overhang adapters. The above mentioned primers were used to amplify the 18S (V1–V2 region) ribosomal locus of each sample in triplicate, using the PCR conditions shown in

Annex B (**Supplementary Material**). The PCR mix comprised 8.4 μL of PCR-grade H2O, 4 μL Phusion Buffer, 4 μL Dye, 0.4 μL dNTP (10 mM), 1 μL forward and reverse primer (10 μM), 0.2 μL Phusion Hot Start II High Fidelity Polymerase (New England BioLabs, United States) and 1 μL DNA template, for a total sample volume of 20 μL. All DNA templates were initially diluted 1/10,000: failed amplifications were readjusted with lower ratios (1/1,000, 1/100, and 1/10 dilutions depending on the sample). To confirm amplification of the DNA, PCR products were run on a 1% agarose electrophoresis gel and triplicates pooled. Samples were then purified using Agencourt AMPure XP beads and run on Bioanalyzer 2100 to confirm length and size distribution of the PCR fragments. The FC131-1002 NexteraXT Index Kit (Illumina, United States) and Kapa High Fidelity PCR kit (Kapa Biosystems, United States) were used to implement library indexing. The mix consisted of 11.25 μL PCR-grade water, 5 μL Buffer, 0.75 μL dNTPs (10 mM), 2.5 μL Index1 and Index2, 0.5 μL Kapa Hot Start High Fidelity Polymerase and 2.5 μL PCR product. Index PCR conditions are shown in Annex B (**Supplementary Material**). Indexed PCR products were then purified a second time using Agencourt AMPure XP beads; they were run on a Bioanalyzer 2100 to confirm successful indexing and DNA concentration of each sample was measured using Qubit® dsDNA High Sensitivity Assay Kit. Finally, biological replicates were pooled and sequenced at Edinburgh Genomics on an Illumina MiSeq-v3 2 × 300 bp paired-end read run[2].

Sequence Data Analysis

The removal of gene-specific adapter sequences was performed using Cutadapt (v1.12) where sequences were truncated from the 5′ and 3′ read ends. By truncating the forward and reverse reads (respectively at 225 and 250 bp), ASVs were generated, following the Dada2 tutorial[3]. Subsequently, taxonomic assignment of ASVs was performed in Qiime1 (assign_taxonomy.py) using the Naive Bayesian RDP28 classifier, with an estimate confidence of 0.80 (Macheriotou et al., 2019). The process was completed in two steps: the first step included the employment of a large eukaryotic reference training set (Silva release 123 for Qiime1, 99% OTUs and UGent nematode Sanger sequences; n = 20,201); the second step consisted in the extraction and isolation of all the ASVs which were identified as "Nematoda," in order to have a comprehensive list of nematode sequences separated from the rest of the meiofauna species. The taxonomic assignment (until genus level) was then completed using another, smaller training set (2,178 sequences) containing nematodes exclusively. Finally, the samples were rarefied to the lowest count (n = 25,258) (Qiime1, alpha_rarefaction.py), for further statistical analyses.

Statistical Analysis

Environmental Variables and Morphological Dataset

The meiofauna community dataset and the environmental parameters were initially subjected to univariate data exploration to assess the dispersion of the data. Afterward, a multivariate analysis on the 0–2 cm layer of the meiofauna community data and all environmental variables was performed. This was done with a non-parametric permutational analysis of variance (PERMANOVA) in both cases. Subsequently, a PermDisp analysis (permutational analysis of multivariate dispersion) was used to test for differences in meiofauna densities between groups (Stations). A pairwise comparison was then performed on significant results. For the analysis of morphologically identified meiofauna, a two-factor design was used (the fixed factor "Station" and the factor "Replicate" nested into "Station"), whereas a three-factor design was adopted in the analysis of the environmental variables (the fixed factor "Station," the factor "Replicate" nested into "Station" and the fixed "Layer" factor). For the environmental parameters' analysis, a resemblance matrix was calculated based on Euclidean distances, whereas a Bray–Curtis similarity matrix was used for the meiofauna community. Meiofauna abundance data were fourth root transformed prior to the analysis in order to decrease the influence of most abundant taxa (i.e., Nematoda). Environmental parameters – Chlorophyll C2, Pheophorbide a, Fucoxanthin, Diadinoxanthin, Diatoxanthin, Chlorophyll a, Pheophytin, Beta Carotene, CPE, TN, TOC, total organic matter (TOM) – with different units were analyzed together (**Table 2**) hence normalization was carried out prior to the analyses. Multicollinearity of environmental parameters was tested by means of correlation matrix (Pearson's method). A distance-based redundancy analysis (dbRDA) was used to investigate the relationship between meiofauna and the environmental variables. This was based on Bray–Curtis distance and included automatic data standardization using the "metaMDSdist" argument. Environmental parameters were considered as predictor variables. To graphically visualize the different variation of the environmental variables between stations, a principal component analysis (PCA) was performed both on the complete dataset and subsets considering the significant factors of the dbRDA (**Table 2**). For the analysis of biodiversity, individual numbers of nematode species identified by morphological identification were standardized to ind/10 cm^2 prior to further statistical analysis. Biodiversity indexes were used to test the degree of diversity at each station, particularly the Shannon–Wiener test and the Simpson's test were performed on the dataset. All analysis were performed with the "vegan" and "ggplot2" packages on Rstudio (v 3.6.1) versions 2.5–5 and 3.2.1.

Amplicon Sequence Variants Dataset

A multivariate analysis on the entire depth gradient (0–8 cm) of the ASVs dataset was performed (all replicates). The non-parametric PERMANOVA was used on the nematodes' subset, followed by a PermDisp analysis (permutational analysis of multivariate dispersion). A three-factor design was adopted in the analysis of nematodes' ASVs (the fixed factor "Station," the factor "Replicate" nested into "Station" and the fixed "Layer" factor) using the Bray–Curtis similarity matrix. Data were fourth root transformed prior to the analysis in order to decrease the influence of the most abundant genera. A non-metric Multi-dimensional Scaling (nMDS) was subsequently performed on the relative abundance of nematode genera. The dbRDA was calculated to study the relationship between the nematodes community and the environmental variables at each station. The distance matrix was based on Bray–Curtis dissimilarity matrix and data were standardized using the "metaMDSdist"

[2]https://genomics.ed.ac.uk/

[3]https://benjjneb.github.io/dada2/index.html

argument. An "adonis" analysis confirmed the significance of the model used. Environmental parameters were considered as independent variables while nematode community was the response variable. All above mentioned analysis were performed in Rstudio (version 3.6.1) using the "vegan," and "ggplot2" packages (versions 2.5–5 and 3.2.1, respectively). To graphically visualize the intersection of the five ASVs datasets (where each station is a set), UpSet plots were generated using the "UpsetR" package (version 1.4.0) in Rstudio. The Upset plot shows the commonality between overlapping datasets (intersection between groups): it gives information both on the unique sequences present at a specific site and on the number of sequences shared between selected datasets (i.e., stations). Further biodiversity tests were performed by means of diversity indexes, particularly the Shannon–Wiener (*H*), Simpson (*D*), and inverse Simpson's (*1/D*) indexes. Although both indexes provide similar information on communities' diversity, they are differently influenced by species abundance, particularly the Shannon index is more affected by richness and rare species, while Simpson's index gives more weight to common species. The use of both indexes can provide a more complete set of information on diversity. A PERMANOVA analysis was performed on the biodiversity indexes to test for significant differences between stations.

RESULTS

Grain Size

Clay content of the 0–2 cm layer was rather constant among stations, ranging between 7 and 11%. In contrast, silt percentage was higher in DB 1,000 m (73%) and the two deep basins in PGC where it represented about 73 and 50% of the sediment, respectively. The three stations in DB clearly show a decreasing silt gradient with decreasing depth, from 73% (1,000 m) to 64% (500 m) to 46% (200 m). Interestingly, the two deep basins in PGC had a sand concentration more similar to DB 200 m than DB 1,000 m, although the silt fraction was high at all stations (**Supplementary Annex C**). In general, the grain size composition did not differ much along the sediment depth gradient, with all four layers showing similar concentrations (**Table 2**).

Pigments and Organic Material

The highest values of CPE in the 0–2 cm layer were observed in PGC 1,000 m (367.5 ± 172.63 μg/g), greatly exceeding that of the other stations (values ranging between 32.7 and 148.5 μg/g, see **Supplementary Annex C**). A clear increase along the bathymetric transect in DB was visible: a mean value of 32.7 ± 9.97 μg/g was observed at 200 m depth, 122.4 ± 7.59 μg/g at 500 m and 148.5 ± 40.05 μg/g at 1,000 m. The most southern and deepest station at PGC (1,250 m) showed the lowest concentration of CPE (27.3 ± 3.8 μg/g) and Chlorophyll a (9.45 ± 1.45 μg/g). The results of the Chl-a: CPE ratio were similar across stations, ranging between 0.34 and 0.43 (**Supplementary Annex C**). TOM showed high values in all the stations except PGC 1,250 m, where the lowest value was recorded (3.28 ± 0.44%), and followed no specific vertical gradient distribution within the sediment layers (**Supplementary Annex D**). The Chl-a vertical gradient did not decrease with sediment depth in DB in contrast to the PGC stations (**Figure 2**). In fact, the Chl-a was most abundant in the 2–4 cm layer in all three stations of DB. The vertical gradient of CPE followed the same trend as Chl-a, except for the DB 200 m station, where the amount of Chl-a decreased with depth (**Supplementary Annex E** and **Figure 2**, respectively).

Environmental Characterization

The multivariate PERMANOVA analysis on environmental parameters resulted in a significant *p*-value ($p < 0.05$) for the "Station" factor, indicating statistically significant differences between stations. However, the permutation test for the homogeneity of dispersion (PermDisp) was significant, indicating that the differences in the dispersion of the group variance may influence the main test result and thus require caution in interpreting its significance. The PCA (**Figure 3**) shows separation of the group ellipses (confidence interval 0.95), pointing at differences in environmental variables between the different stations and depths. Some degree of overlap was only observed for the shallowest DB station and the nearest deep PGC station (1,000 m). The sum of the two main principal components (PC1 and PC2) explains together 73.22% of the variance. The main variables contributing along the PC1 axis are the ratio between Chlorophyll-a and CPE (Chloroplastic Pigment Equivalent; Chl-a:CPE), TOC and TN ratio (TOC:TN) and TOM concentration. The dbRDA resulted in a significant value ($p < 0.05$) for some of the pigments, phaeopigments, and TOM (**Table 2**) suggesting a correlation between the amount of fresh and/or degraded organic material and the meiofauna structure at each station.

Meiofauna Densities and Composition

Results for meiofauna densities are displayed in **Table 3**. The highest densities were recorded in DB, with similar values (in the order of 6,000 individuals (ind) 10 cm^{-2}) at 500 and 200 m. Slightly lower values were detected in the two 1,000 m deep basins (one in DB and one in PGC), with abundances ranging in the order of 4,000 ind 10 cm^{-2}). The lowest values were observed in PGC 1,250 m (2,339.524 ± 785.2732 ind 10 cm^{-2} ± SD), but it is noteworthy to mention that the SD value is high. The univariate PERMANOVA analysis on densities showed a significant *p*-value ($p < 0.05$) for the "Station" factor and the PermDisp was non-significant for the same. The vertical distribution of total meiofauna within the sediment followed a depth gradient analogous across all stations, where the 0–2 cm layer showed the highest densities. At each sampling site, nematodes were the major component of the meiofauna, constituting between 69 and 91% of the total abundance (**Supplementary Annex F**). Besides nematodes, the main groups present in the samples were nauplii (3–12%) and Copepoda (4–11%) in the first 0–2 cm layer, with similar relative densities at each of the stations of the bathymetric transect in DB. A different structure could be noticed in PGC, where both groups showed slightly lower densities at 1,000 m and particularly lower at 1,250 m (**Supplementary Annex G**).

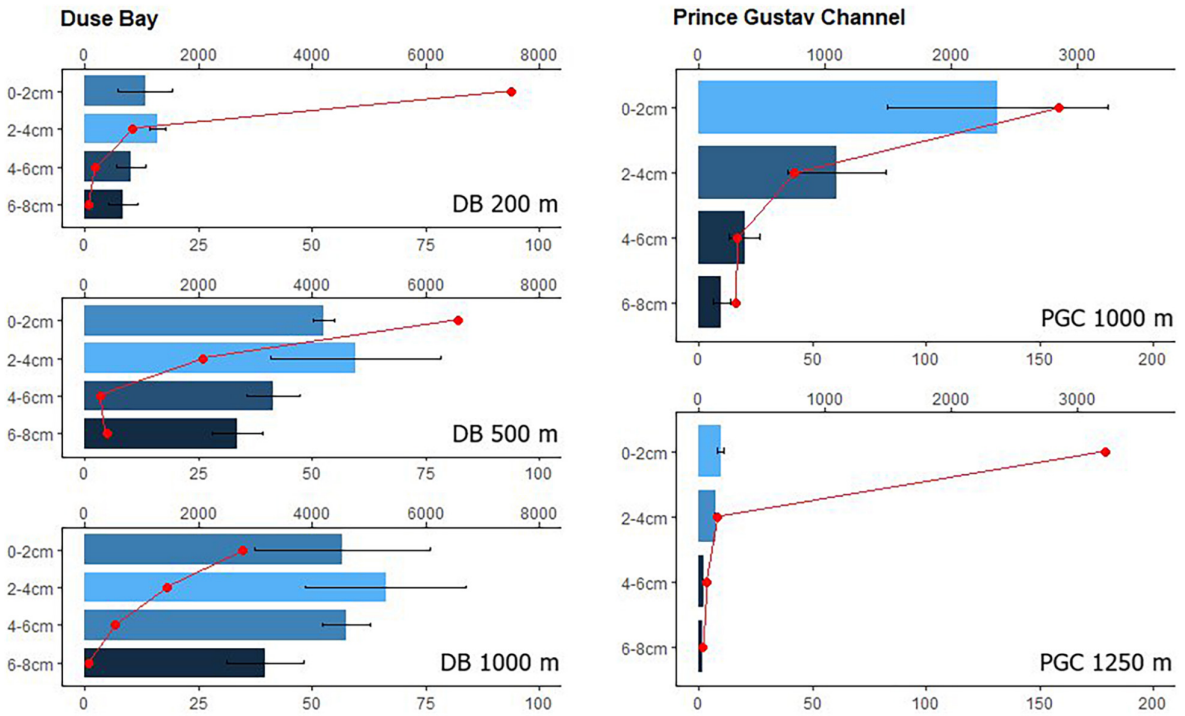

FIGURE 2 | Comparison between Duse Bay stations (from the top 200 m, 500 m and 1,000 m depth) and the Prince Gustav Channel (from the top 1,000 m and 1,250 m depth). The barplot shows Chl-a concentrations (μg/g, bottom axis, plus Sd) within the sediment layers (0–2, 2–4, 4–6, and 6–8 cm). Meiofauna distribution within the same layers expressed in ind 10 cm^{-2} (upper axis) was plotted over the barplot. One replicate per layer was used to calculate meiofauna densities. Note the difference in scale between DB and PGC stations.

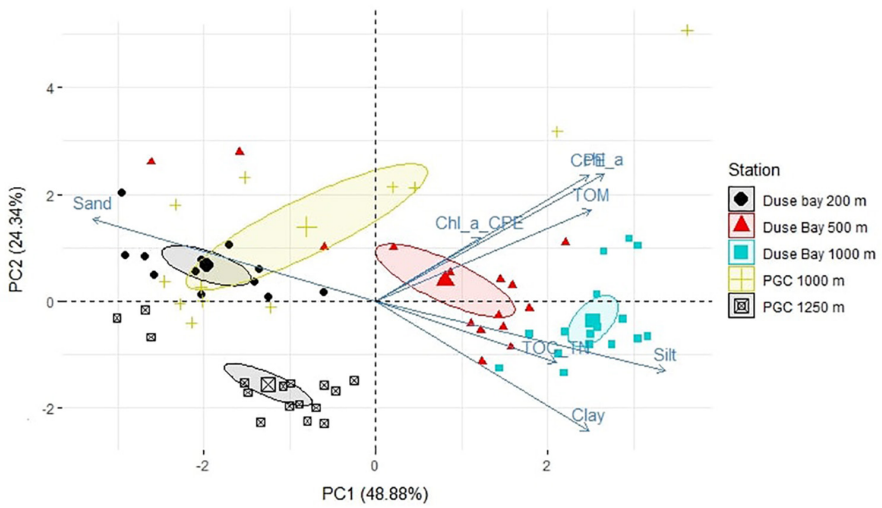

FIGURE 3 | Principal component analysis (PCA) of a subset of environmental characteristics of the sediment of all layers combined (i.e., 0–2, 2–4, 4–6, and 6–8 cm). Particularly, Chlorophyll a, CPE, Chl:CPE ratio, TOM, TOC:TN ratio, Clay, Silt and Sand parameters were considered. Confidence ellipses were plotted around group mean points, represented as larger symbols on the plot.

Nematode Biodiversity

Amplicon Sequence Variants Analysis

The metabarcoding analysis resulted in a total of 7,175 ASVs belonging to the Eukarya domain, of which 2,564 were assigned the label "Nematoda." It was possible to assign a genus to 40.6% of the sequences, whereas the 59.4% of them remained "Unassigned." Nevertheless, all ASVs (including the "Unassigned") were included in the biodiversity analysis (biodiversity tests and UpSet plot), whereas the NMDS and trophic analysis was only based on the genus-assigned ASVs. A total of 49 genera were identified across all stations, of which the most abundant were *Molgolaimus*, *Daptonema*,

TABLE 3 | Number of individuals per 10 cm^{-2} of the 0–2 cm layer showed as mean, followed by standard deviation (SD) values.

Area	Depth	Replicates	Mean	SD
Duse Bay	200 m	3	5,943.33	1,367.21
Duse Bay	500 m	3	6,008.89	814.82
Duse Bay	1,000 m	3	4,551.43	2,577.60
PGC	1,000 m	3	3,993.97	1,045.78
PGC	1,250 m	3	2,339.52	785.27

TABLE 4 | Permutational analysis of variance results for the metabarcoding dataset, considering the three factors "Station," "Layer," and "Replicate" and the interaction between significant values (Station*Layer).

Factors	Df	Sums of sqrs	Mean sqs	F. model	R^2	Pr (>*F*)
Station	4	5.33	1.33	4.94	0.20	**0.001*** **
Layer	3	2.46	0.82	3.04	0.09	**0.001*** **
Replicate	67	20.28	0	0	0.79	1
Station*Layer	12	3.81	0.32	1.17	0.15	**0.023***

*The significant values are indicated in bold. The number of * indicates the degree of significance.*

Halalaimus, *Chromadorita*, *Sabatieria*, and *Bathylaimus* (>11%). The PERMANOVA analysis performed on the ASVs dataset resulted in a significant *p*-value for the fixed factor "Station," as well as the nested factor "Layer" (**Table 4**), suggesting that differences were also present in the vertical profile. The PermDisp test performed after the PERMANOVA analysis was non-significant for both factors. A pairwise comparison was performed subsequently, however, no significant results were detected. Hence, the interpretation of data must consider this issue. The intersection between datasets (all layers pooled together) is visualized in **Figure 4**. Here we observe that the majority of sequences (27.4%) were unique to PGC 1,250 m when all layers were considered followed by the shallowest one in DB 200 m (17.4%). As shown in the NMDS performed on the HTS dataset (**Figure 5**), the PGC 1,250 m and DB 200 m ellipses are markedly separated from each other and from the other stations, suggesting high variation in the assemblages of these two sites compared with the other stations. The DB 200 m ellipse was observed at a similar distance from PGC 1,250 m and DB 1,000 m, although some of DB 200 m sample points are closer to the ones in PGC 1,250 m than DB 1,000 m. This vicinity implies some degree of similarity between the two stations (DB 200 m and PGC 1,250 m) despite being located in different areas. The middle stations, regardless of area, were less isolated and closer to each other in the plot, with PGC 1,000 m and DB 500 m overlapping. This proximity implies a certain amount of similarity between the community composition of the two stations. The dbRDA analysis to investigate relationships between environmental variables and nematode diversity resulted in a significant value ($p < 0.05$) for the main pigments and TOM (**Table 2**), indicating some degree of association between the organic matter in the sediments and nematodes community structure. The results of the Shannon–Wiener (*H*), Simpson (*D*) and inverse Simpson's (*1/D*) tests are shown in **Table 5**. Results show the mean value of each station (all replicates, all layers considered). The Shannon diversity index showed a high degree of biodiversity at all stations, with DB

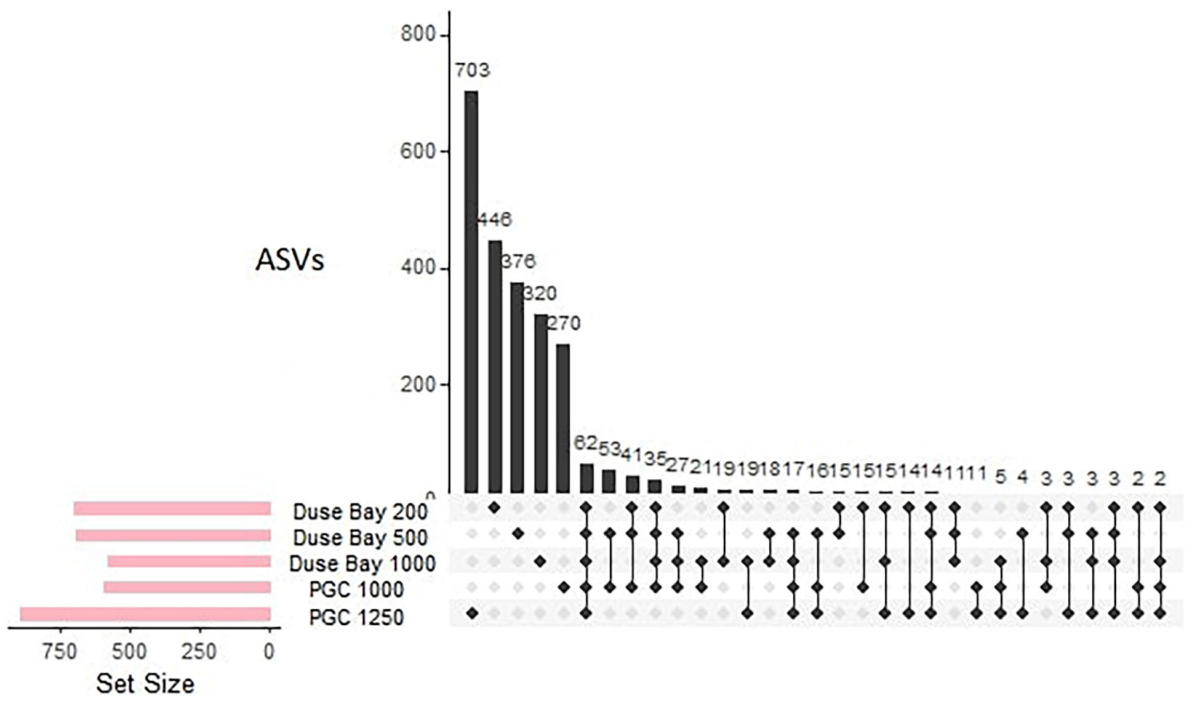

FIGURE 4 | UpSet plot of all ASVs assigned a "Nematoda" label (all layers considered, three to four replicates). The left barplot (Set Size) represents the total number of ASVs per station; the bottom plot shows every possible intersection between sets and the top barplot displays their occurrence.

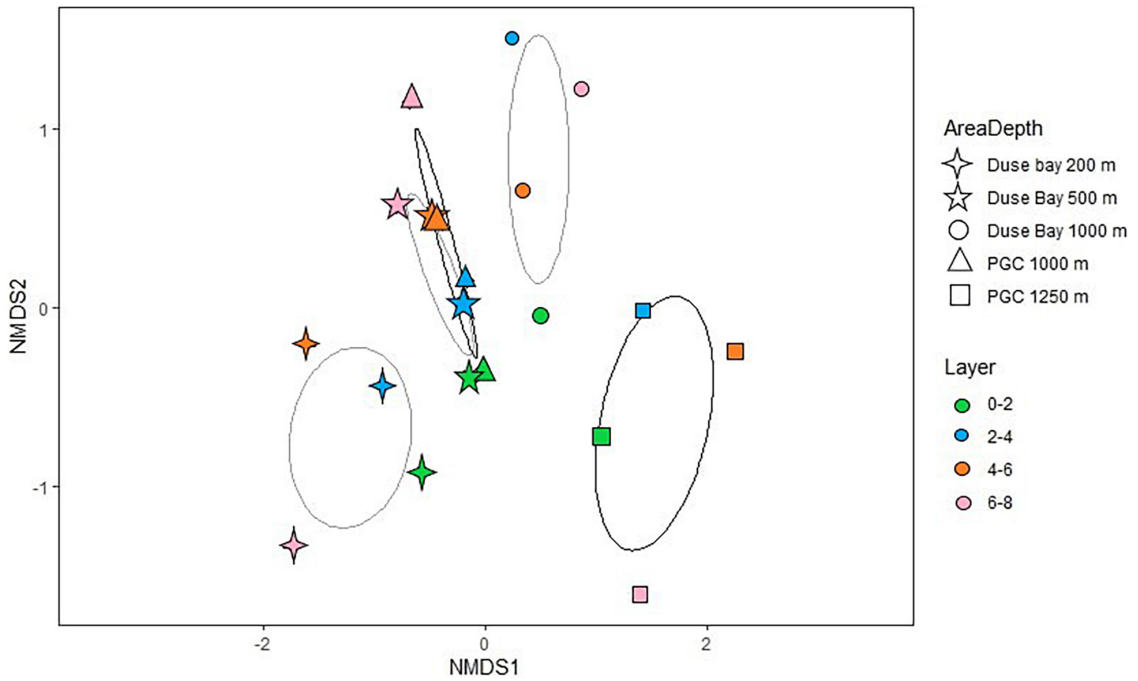

FIGURE 5 | Non-metric Multi-dimensional Scaling analysis performed on the ASVs dataset (three to four replicates per station, all layers considered). The lighter ellipses represent the Duse Bay area, while the darker ones belong to the PGC stations. The further segregated ellipses (lower part of the graph) belong to DB 200 m and PGC 1,250 m, whereas an overlap between DB 500 m and PGC 1,000 m is clearly visible, with DB 1,000 m located closer to the "middle stations."

500 m having the highest values (4.172) and PGC 1,250 the lowest (3.450). These are confirmed by both the Simpson's test and its inverse, which is positively correlated to the Shannon index. Inverse Simpson's values are in fact particularly high at all station, suggesting high biodiversity at all sites, and especially at DB 500 (35.150); the lowest value was recorded at PGC 1,250 (15.188). However, the PERMANOVA analysis performed on biodiversity indexes did not result in significant values for any of the ones considered.

Morphological Identification of Nematodes

A total of 107 nematode genera and 121 morphospecies were identified across the set of subsamples of 80 individuals per sample (0–2 cm, 3 samples per station). The greatest biodiversity was detected at 1,000 PGC and PGC 1,250 m (48 and 47 genera respectively in two replicates per station combined), although a substantial number of genera were observed at each sampling site (43 genera in DB 200 m; 39 in DB 500 m; and 45 in DB 1,000 m). The NMDS performed on this dataset (**Supplementary Annex H**) showed a large distance between the assemblages of the stations in DB (with DB 200 m and DB 500 m particularly isolated), while PGC 1,000 m was located at a similar distance from DB 1,000 m and PGC 1,250 m, when considering all data points. At each station, a few genera (e.g., *Desmodora* in DB 200 and *Chromadorita* in PGC 1,250 m) seem to dominate the assemblage (18.7 and 13.2%, respectively), while the majority of taxa represented less than 2% of the community. **Figure 6** shows the comparison between the most abundant genera detected via morphological identification and ASVs analysis. Although the number of genera detected per station was almost identical, the community composition at each station differed. When ASVs were used, the genus *Daptonema* was dominant, constituting the 32.6% of all nematode genera at DB 500 m, whilst it represented only 11.4% in the morphological dataset at the same station. Similarly, in PGC 1,250 m *Chromadorita* was the most abundant genus using both identification methods: however, it represented 29.3% of all nematode genera when ASVs were used and only the 13.2% in the morphological dataset. It is worth noting that the genus *Desmodora* was absent in the ASVs at DB 200 m, while it represented the most abundant genus (18.7%) when the sample was identified morphologically.

TABLE 5 | Significant values for biodiversity indexes: Shannon–Wiener (H'), Simpson (D), inverse Simpson (1/D) on the metabarcoding dataset (ASVs).

Station	*H'*	*D*	*1/D*
Duse Bay 200 m	3.630	0.933	16.549
Duse Bay 500 m	4.172	0.969	35.150
Duse Bay 1,000 m	3.795	0.943	22.683
PGC 1,000 m	3.845	0.947	20.350
PGC 1,250 m	3.450	0.933	15.188

Trophic Guilds Analysis

The analysis of the trophic structure of nematode communities is shown in **Supplementary Annex J**. The first barplot (**Supplementary Annex JA**) shows the trophic composition of

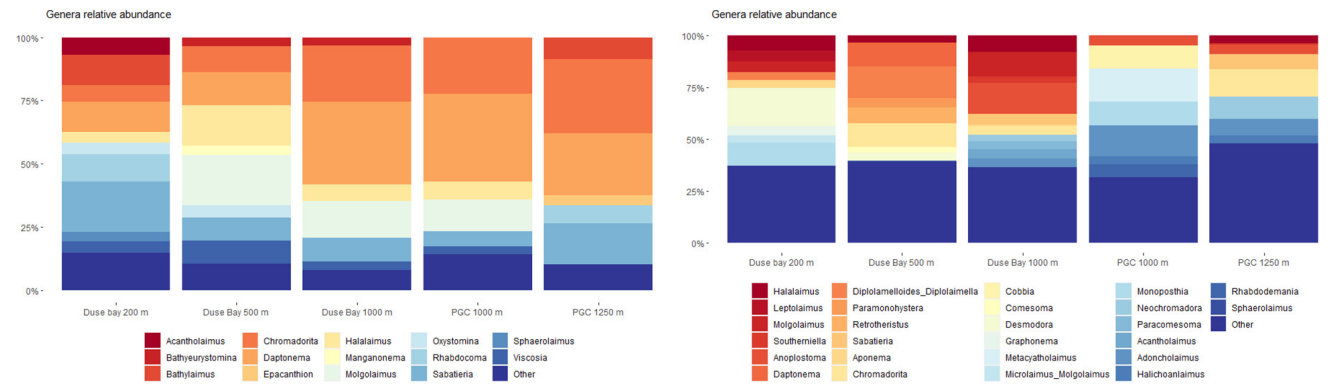

FIGURE 6 | Nematodes community composition for the most abundant genera (>3%). Comparison between ASVs **(A)** and morphologically identified dataset **(B)**; less abundant genera (<3%) were pooled in the "Other" item.From left to right, image sequence of ice melting in the Eastern Antarctic Peninsula during the 4 months preceding the JR17003a research campaign. Satellite images source: https://worldview.earthdata.nasa.gov.

the ASVs dataset based on the assigned genera, where non-selective deposit feeders (**Supplementary Annex JB**) comprised between 46 and 61% of all the trophic groups both in DB and the PGC. Selective deposit feeders were the second most abundant trophic group in DB 200 m and DB 1,000 m (26% in both the stations), while epistrate feeders (2A) had similar percentages in DB 500 m, PGC 1,000 m and PGC 1,250 m (22, 22, and 30%, respectively). On the right (**Supplementary Annex JB**), the trophic analysis performed on the morphological dataset is shown, where epistrate feeders were dominant at all stations (between 31 and 50%).

DISCUSSION

This study investigates the meiobenthos of DB and the PGC for the first time and sets the foundation to understand the benthic ecological dynamics in these areas by applying a unique combination of taxonomical identification and DNA analysis of organisms, with a focus on nematodes. In general, high levels of biodiversity were detected across stations in both areas (**Table 5** and **Figure 4**), which are most likely associated to the abundance and freshness of food.

The DB Bathymetric Transect

Environmental Characterization

The local warming of the AP is responsible for increased algal blooms in the region, related to ice-shelf melting and calving events, which affect the abundance, structure, and dynamics of benthic organisms to a great extent (Veit-Köhler et al., 2018). Because of their tight connection with the sediment organic pool, meiofauna reflects the local dynamics of benthic-pelagic coupling processes. The structure of meiofauna communities in terms of densities and biodiversity are strictly linked to the amount of available organic matter. This is in turn dependent on deposition dynamics occurring in the upper water column. In general, the Chl-a and CPE values in DB were higher than those observed at similar depths in the AP (Vanhove et al., 2004; Hauquier et al., 2015), but relatively low in the DB 200 m station, where they showed an average concentration four times lower than that of the other DB stations (**Table 2**). The lower Chl-a values at the shallowest DB station, coincides with lower TOM concentrations and a higher sand fraction compared to the deeper DB stations. Sediment grain size also plays a crucial role in determining the infaunal assemblage structure and diversity since it relates to the organic matter accumulation/remineralization and oxygen penetration through the sediment. Sediment oxygenation has been observed to have a significant effect on meiofauna abundance and composition considering that different taxa have specific tolerances for oxygen availability (Schratzberger et al., 2006; Vanreusel et al., 2010). The sediment composition is highly affected by the lithology of parent rocks, the local mixing with recycled detritus (Dinis et al., 2017) together with the deposition and stratification of glacial and subglacial meltwater finer particles (Meslard et al., 2018). The latter are regularly resuspended in the water column because of local storms in shallow waters which is less the case in the deeper parts. The finer sediment composition in the deeper DB stations (DB 500 and 1,000 m, **Table 2**) was possibly a consequence of subglacial ablation and the associated disaggregation of the overlying sediment and its mixing with debris. Coupled with local hydrodynamics and geomorphology, this likely determined the transport of finer particles, i.e., silt, to deeper parts of the bay (Lawson, 1982; Nokes et al., 2019; Perolo et al., 2019), hence resulting in a muddier, soft sediment habitat compared to the shallowest station.

Meiofauna Community Structure

Differences in the sediment food availability of the 200 m station were not reflected in the meiofauna densities of the first 0–2 cm of the sediment, since they were equally high in the 500 m station and even higher at 1,000 m despite the lower chlorophyll-a values. In general, the meiofauna densities in the shallower stations (200 and 500 m) in DB were within the range of those found at other Antarctic shelf locations (Vanhove et al., 1995; Ingels et al., 2006; B_West station, Hauquier et al., 2015). High

meiofauna densities are often related to the accumulation of phytoplanktonic organisms in the form of detritus on the surface of shelf sediments. Due to the cold temperatures of Antarctic waters, the process of degradation of the phytodetritus is slower compared to other areas, thus organic matter may accumulate in the form of "foodbanks" (Mincks et al., 2008; Smith et al., 2008). These organically rich sediments which are able to sustain the benthic densities throughout the year, preventing a reduction in biomass during austral winter months. High Chl-a and TOM concentration might be explained by such dynamics. The high densities found at DB 200 m corresponding to lower Chl-a and TOM concentration, might be due to the grazing action of benthic organisms on the food source prior to sampling, which would explain how such high abundances were sustained despite the low values of organic matter recorded. This is confirmed by the dbRDA performed on densities, which highlighted a significant correlation between organic matter and meiofauna abundances (**Table 2**). Copepods were the second most abundant taxon after nematodes (∼9.03% of the total meiofauna density in DB 200 m and ∼6.16% in DB 500 m; **Supplementary Annex G**), which is not surprising, considering that they are able to feed on both microalgae and bacteria (De Troch et al., 2005). The meiofauna densities seemed to decrease with increasing sediment depth, thus hosting the majority of the total meiofauna in the first 0–2 cm layer (**Supplementary Annex A**). The TOM followed the same decreasing vertical gradient, with higher concentrations in the first 0–2 cm layer. However, the Chl-a was distributed in a contrasting pattern in all DB stations, with the second sediment layer (2–4 cm) being the one with higher concentrations (**Figure 3**). The subsurface maximum of Chl-a in the DB stations might be in indication of the presence of larger benthic organisms (macrofauna) which are often responsible for burial of fresh phytodetritus into the deeper sediment layers (Furukawa, 2001; Lohrer et al., 2004; Meysman et al., 2006; Barsanti et al., 2011; van de Velde and Meysman, 2016). Biological interactions, such as the occurrence of macrobenthic organisms, are known to have a strong effect on the small-scale variability of nematodes, due to predator-prey dynamics and competition for food. The diversity of larger consumers has in fact been shown to be a crucial aspect in regulating the access of meiofauna to shared food sources (Nascimento et al., 2011). Although no macrofauna data are available in this study, it is still central to highlight the potential impact of these organisms. The values of CPE and Chl-a were highest at DB 1,000 m and corresponded to lower average meiofauna densities (although with a higher standard deviation). Macroalgal decay and accumulation of organic matter can lead to hypoxic conditions of the sediment surface (Pasotti et al., 2014; Hoffmann et al., 2018), influencing the abundance and composition of meiofauna assemblages. The possible hypoxic conditions of the sediment at this station was also suggested by the presence of the genus *Anoplostoma*, which was recorded in high numbers (15% of all nematode genera at this station) by morphological identification but not in the ASVs dataset (probably linked to the limited sequences deposited in online databases, see section "Morphological Identification Versus Metabarcoding: Drawbacks and Interpretation of Data"). This nematode genus is categorized as a selective deposit feeder often recorded in organically enriched sediments of mangrove ecosystems and muddy estuarine sediment types (Surey-Gent, 1981; Li and Guo, 2016), which are usually associated with hypoxic conditions, hence lower meiofauna abundances (Zeppilli et al., 2018). Moreover, one of the most abundant genera according to the ASVs dataset (**Supplementary Annex H**) was *Sabatieria*, which is also known for being tolerant of hypoxic/anoxic conditions in several environments (Wetzel et al., 2002; Steyaert et al., 2007; Franzo et al., 2019).

Nematode Biodiversity in the DB Area

Based on the molecular analysis of the ASVs, the degree of biodiversity in DB was observed to be very high at all stations, as confirmed by the Shannon (*H*), Simpson (*D*), and inverse Simpson's (*1/D*) indexes (**Table 5**). The most diverse station was found to be DB 500 m in contrast to the highest number of unique ASVs (n = 446) recorded at 200 m when considering all sediment layers. The visual results of the UpSet plot (**Figure 4**) show a decrease of unique sequences in relation to depth, which suggests less biodiversity at the deepest site of the area (DB 1,000 m, 320 ASVs). This is in contrast with the *H* and 1/*D* values, which show little difference between stations, with slightly lower values for DB 200 m. Since the UpSet plot visualization is based on a presence/absence matrix, the reason behind such contrasts is likely due to the influence of richness (for *H*) and samples number (for *D* and *1/D*), which rely on a distance-based similarity matrix. Moreover, the high values of the Shannon and inverse Simpson indexes suggest a uniform distribution of the species at all sites, confirmed by the non-significant PERMANOVA performed to test differences in biodiversity between stations. Previous studies show that nematode diversity is more often dependent on local environmental characteristics and hydrodynamics than bathymetry (Danovaro et al., 2013; Gambi et al., 2014). Also in this study, there was no evidence of increasing biodiversity in relation to depth, whereas differences between stations were more associated to the availability and freshness of food source (**Table 2**). The non-selective deposit feeder *Daptonema* was detected at all stations in DB, with highest concentrations at DB 200 m (**Supplementary Annex J**). This cosmopolitan genus has a long history of records in Antarctic waters, ranging from shallow to deeper sediments (Vanhove et al., 1999; Hauquier et al., 2015; Stark et al., 2020). Surprisingly only 11 ASVs were uniquely shared among all the DB stations (**Figure 4**), whereas the majority were unique to each station, thus it seems likely that the local biodiversity might have been influenced by gene flow external to DB, or by local hydrodynamics and seasonal sea-ice cover. A crucial element in determining the diversity of nematode communities are in fact local currents and the potential colonization from relatively close areas (Boeckner et al., 2009).

The Deep Basins

Ice Cover and Influence on Sediment Characteristics

The changes in sea-ice cover, sea-ice melting, and ice-shelf collapse have a major impact on the intensity and frequency of phytoplankton blooms, and as a consequence, on the primary productivity of the ocean surface in Antarctica (Buffen et al.,

2007; Duprat et al., 2016; Van Leeuwe et al., 2018). Satellite images[4] show that in the period preceding the JR17003a campaign, the sea ice started melting in proximity of the DB area at the end of December 2017, continuing the retreat southwards along the narrow seaway between James Ross Island and the Trinity Peninsula (**Figures 7**, **8**). In fact, this melting allowed DB to be ice-free by the end of January 2018, almost contemporarily in all the stations of the area, together with the 1,000 m station in PGC. However, it looks like the southernmost station (PGC 1,250 m), was free of ice just by mid-February, almost 1 month later. This melting pattern might partly explain the over 10-fold higher Chl-a content in the first 0–2 cm layer in the PGC 1,000 m station, compared to the PGC 1,250 m station which showed the lowest Chl-a. Studies on the Larsen A and B Area, south of the PGC, have shown that newly ice-free regions stimulate phytoplanktonic blooms, affecting the total meiofauna density (Hauquier et al., 2015) and often increasing the abundance and biodiversity of nematodes (Raes et al., 2010). Although the two PGC stations are geographically close and of similar depth, the much lower quantities of Chl-a in PGC 1,250 m resulted in only 1.7 times lower meiofauna densities (**Supplementary Annex G**). Given the longer ice cover at this station it is possible that at the time of sampling a potential phytoplanktonic bloom had not yet taken place, with the meiofauna still thriving on food reserves from the previous year. To confirm these assumptions, a more detailed study on the timing of sea-ice retreat and the related spring phytoplankton bloom would be of significant importance. Other variables to consider are sea-ice thickness, water turbidity and the amount of freshening, which determines the stability of the water column and has a strong influence on phytoplanktonic blooms (Kang et al., 2001; Buffen et al., 2007). The distribution of sea ice depends on a number of factors which fluctuate seasonally and annually, namely wind intensity, wind direction and coastal currents (Scambos et al., 2009; Holland and Kwok, 2012; Stuecker et al., 2017). In light of the large variability of sea-ice extent and duration, dynamics relating to sea-ice cover are indeed particularly difficult to assess.

[4]https://worldview.earthdata.nasa.gov

Meiofauna Densities and Structure in the Deep Basins

The meiofauna abundance in the deepest PGC station (1,250 m) were lower compared to the other two basins (DB 1,000 m and PGC 1,000 m), but still high or similar in comparison to other findings at similar depths (Vanhove et al., 1995; Vermeeren, 2002; Ingels et al., 2011). Even though the lowest values of CPE and Chl-a were recorded at this deep site, the amount of food and its freshness, seemed in fact sufficient to sustain relatively high meiofauna abundances, with pigment concentrations within the range of those found in previous studies from adjacent areas (Hauquier et al., 2015). The two 1,000 m basins in DB and PGC seem to be acting as a sink for organic matter as they display the highest abundance of TOM in the whole region,

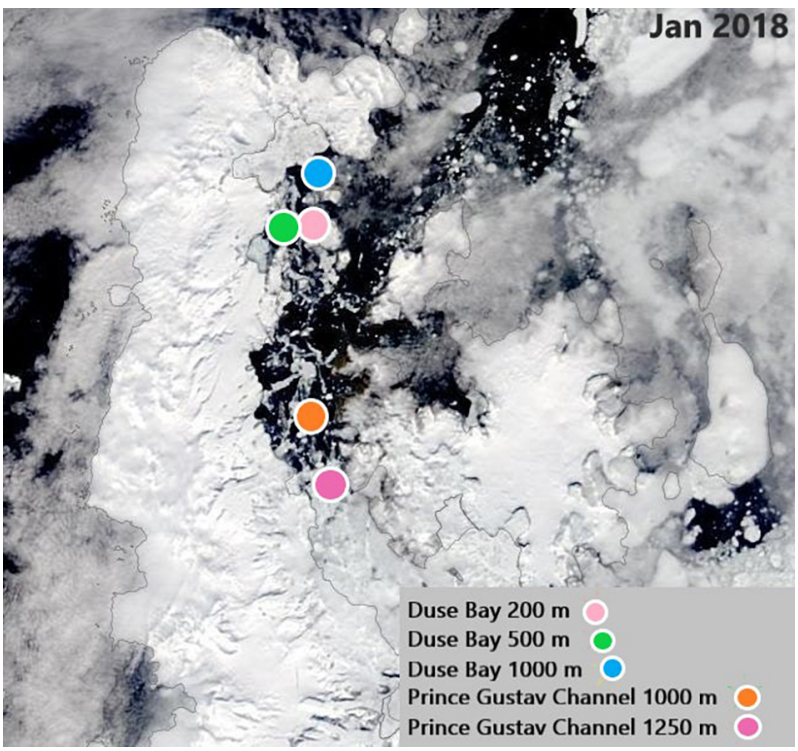

FIGURE 7 | Satellite image of the sampling Area in January 2018, with PGC 1250 still covered by sea-ice while the rest of the stations are ice-free. The different colors indicate each station in the PGC and DB, as shown in the legend. Satellite images source: https://worldview.earthdata.nasa.gov.

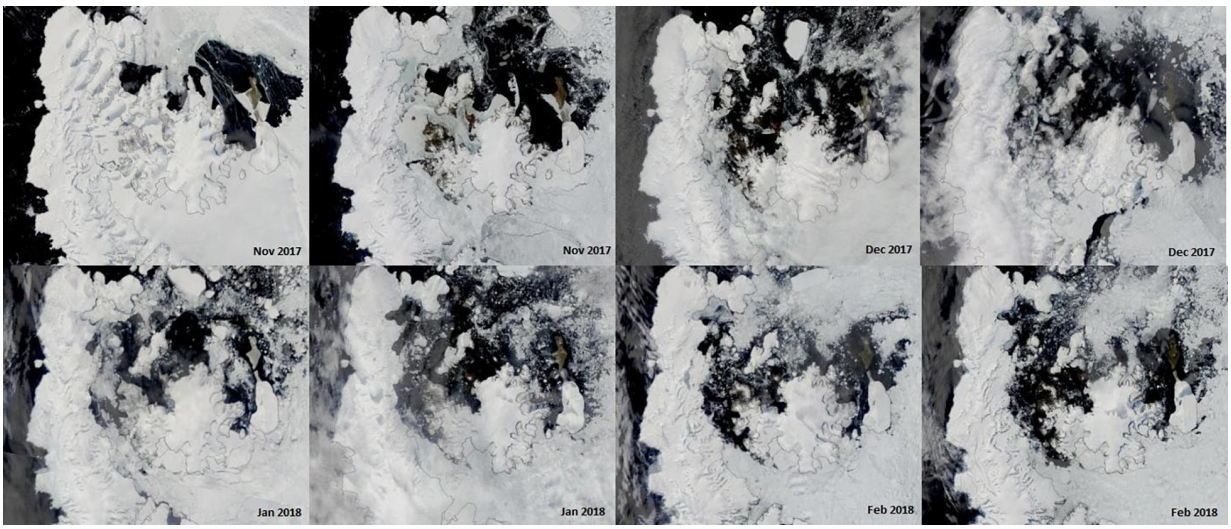

FIGURE 8 | From left to right, image sequence of ice melting in the Eastern Antarctic Peninsula during the four months preceding the JR17003a research campaign. Satellite images source: https://worldview.earthdata.nasa.gov.

and particularly PGC 1,000 m which exhibited almost double the Chl-a concentration compared to DB 1,000 m. The relative abundance of nauplii and copepods was also high in some stations (particularly copepods at DB 1,000 m and PGC 1,000 m, and nauplii at DB 1,000 m, Annex G). Nauplii are early larval stages of mainly copepods, and their assemblage can be a proxy for environmental changes. They are highly sensitive to environmental stressors, and indicate the recruitment of copepods, hence their reproductive success (Bunker and Hirst, 2004; Gonçalves et al., 2010; Darnis et al., 2019). The variability of larval stages is typically linked to the availability and quantity of food, thus potentially representing a proxy of surface primary productivity in DB. The difference in density of nauplii between the three deep basins (DB 1,000 m, PGC 1,000 m, and PGC 1,250 m) with four times lower densities in the PGC compared to DB might be due to a number of variables, such as differences in bottom currents, resuspension potential and vertical mixing of the two areas, since they have been shown to alter oxygen and food availability in the deep sediments (Isla et al., 2006). Based on the UpSetR plot analysis (**Figure 4**) and the NMDS performed on the first 0–2 cm layer of the three basins (DB 1,000 m, PGC 1,000 m, and PGC 1,250 m, **Figure 5**), marked differences in nematode community structure and abundance were visible. The dominant genera were shared among stations (i.e., *Sabatieria*, *Molgolaimus*, and *Daptonema*), albeit in different proportions. When all the sediment layers were considered, the deep PGC 1,250 m showed the highest number of unique ASVs ($n = 703$, **Figure 4**) and only 63 ASVs were shared among all stations. Shannon and Simpson's indexes showed higher values for PGC 1,000 m, suggesting increased biodiversity at this site. However, biodiversity indexes were relatively high at all stations, and showed no significant differences between stations. As frequently reported in other areas worldwide (Raes et al., 2007; Semprucci et al., 2010), also in this study it seems that local small-scale variability has more influence on community structure than depth or even larger spatial distances. The differences in biodiversity through the sediment layers might be of great importance in order to explain the gene flow dynamics in the EAP (Derycke et al., 2013). In fact, endobenthos and especially nematodes mainly depend on passive transportation of individuals (i.e., via bottom currents) for their dispersal, given that they do not have a pelagic larval stage (Hauquier et al., 2017). Hence, their resuspension in the water column is expected to be influenced by their vertical segregation in the sediment (Eskin and Palmer, 1985). This might explain the relatively low abundance of shared ASVs and the distance of ellipses in the NMDS analysis even between geographically close stations (i.e., PGC 1,000 m and PGC 1,250 m), which are expected to be influenced by similar hydrodynamics and sea-ice melting patterns. The deepest basin, more isolated from the rest of the stations but closer to the open waters of the Weddell Sea, shows lower amounts of TOM, CPE and Chl-a and lower densities but the highest number of unique nematode ASVs. As the dbRDA analysis was significant for organic matter and chlorophyll a, suggesting one more time some degree of correlation between food source and nematodes community structure, phytoplanktonic dynamics regulated by local ice-cover are to be considered. It is appropriate to assume that differences between the 1,000 m stations and PGC 1,250 m might be linked to the different ice cover influence on the basins (from sedimentation rates to phytoplanktonic bloom effects), probably together with local physical variables such as bottom currents. Raes et al. (2010) found that higher nematode biodiversity in the B_South station (located south of the Larsen B area) was linked to a longer ice-free period, and open to potential phytoplanktonic blooms. According to their study, quick colonizers might have invaded the relatively new space, free of ice after the retreat of the ice shelf in 1995. The deep basin in PGC 1,250 m might have experienced similar colonization dynamics, also because of its proximity to more open waters of the Weddell Sea, which might have acted as a source for colonizers and food.

Morphological Identification Versus Metabarcoding: Drawbacks and Interpretation of Data

The documentation of nematodes has traditionally been performed via morphological identification (Vanhove et al., 1995; Fabiano and Danovaro, 1999; Lee et al., 2001; Tarjan and Keppner, 2008; Vanreusel et al., 2010). However, such work is known for being particularly time consuming and tedious, and it requires specific skills and deep knowledge of the taxa at hand. With the development of new molecular techniques, it has been proven that DNA metabarcoding is able to increase detection sensitivity, which in turn improves the ability to document dispersion of organisms, their connectivity and biodiversity (Fonseca et al., 2017). However, even new techniques such as metabarcoding are subject to drawbacks, and need to be perfectioned (Deagle et al., 2018). In this study we combined both approaches, using the morphological identification to integrate the data collected from the bio-molecular analysis. In general, a large number of genera per station was observed with both methods: the 0–2 cm layer seemed to host the majority of nematode diversity, with slightly more genera observed in the morphological identification (**Supplementary Annex I**). However, the composition of each station differed notably between the two methods, with many genera undetected in the ASVs dataset. In fact, a total of 107 genera was identified by morphological identification, and only 49 via metabarcoding. It is important to emphasize that differing results of nematode diversity may lead to different interpretation of the data, especially in regard to the assignment of nematode trophic groups and their relative abundance throughout the assemblage (**Figure 6** and **Supplementary Annex J**). For example, the dominance of the morphologically identified genus *Desmodora* in DB 200 m (18.7%), indicated that the main trophic group at this station was represented by epistrate feeders (2A), suggesting that the much lower Chl-a concentration recorded at that station might be the result of grazing pressure by these organisms (probably coupled with macrobenthic grazing). However, the absence of *Desmodora* ASVs, leads to an opposite result where non-selective deposit feeders were the majority, probably influenced by the marked presence of *Molgolaimus* and *Daptonema* (**Figure 6** and Annex J). Macheriotou et al., 2020 (under review) also highlighted a similar problem: although *Desmodora* was identified as dominant by morphological identification in a Mozambique channel site, it was absent from the ASVs analysis. This was most likely explained by failed PCR amplification, which might have been hindered by the thick cuticle typical for this genus. Given the inclusion of eight *Desmodora* sequences in the database, it is likely that these specimens would have been identified in the event of successful PCR amplification. While this explanation is in general satisfactory, it is worth considering also another matter: the possible lack of this particular *Desmodora* sequence in online databases. The majority of known species are indeed based on descriptions from few specimens originating from a small number of localities, which poses the problem of natural variation (Coomans, 2002). Although we would expect *Desmodora* to be identified at least to genus level, it is plausible to assume that one or more *Desmodora* sequences from Antarctica had not been included in ASVs databases yet, thus resulting in a lack of information on this organism. The lack of nematode sequences in online databases results in an incomplete coverage of nematode diversity, which is confirmed in this study also by the amount of non-identified sequences in the dataset (59.4% "Unassigned" ASVs). Finally, the mismatch between morphologically identified organisms and ASVs might also be linked to subjective bias, based on personal skills, eyesight, knowledge of the taxonomist, and the differentiation between related genera is not always easy (Vanreusel et al., 2010).

CONCLUSION

The meiobenthic community of the three stations in DB showed a distinct differentiation following the bathymetric gradient. The meiofauna densities decreased with depth along the transect, in contrast with the concentrations of Chl-a and TOM, which were instead increasing. The lower meiofauna density, despite the high food availability at the deepest DB station, was possibly due to hypoxic conditions of the sediments, as suggested by the presence of the genus *Anoplostoma,* and the higher concentration of TOM. Nematode diversity was higher at the shallowest stations, probably due to heterogeneity of the habitat and food source availability. The three deep basins in DB (1,000 m) and in the PGC (one at 1,000 m and one at 1,250 m depth) were different both in terms of meiofauna densities, pigments, TOM and nematode biodiversity, despite similar depths. Although meiofauna densities in the two 1,000 m basins were similarly high, the deeper PGC 1,250 m showed the lowest densities compared to the other stations. High biodiversity was detected at all stations. The dominant taxa were shared among the stations, however, PGC 1,250 m showed the highest number of unique nematode sequences. The PGC 1,250 m station is indeed located in a more elongated, less isolated basin and likely more impacted by the sea-ice system and the Weddell Sea, hence subject to external colonization. Our data suggest that meiofauna community structure was influenced by the simultaneous action of different variables, including food availability, habitat heterogeneity and seasonal sea-ice dynamics. In general, local physical processes might have had a strong influence both on the densities and on the connectivity of the stations considered. The application of morphological identification to assess nematode biodiversity proved to be a valuable tool, especially to identify less abundant or rare specimens, but nevertheless time consuming and influenced by subjective bias. HTS offers a faster, more sensitive, less laborious option: however, there is a necessity to improve the coverage of reference sequence databases and the potential limitation concerning thicker nematode's cuticules must be taken into consideration. These issues suggest it is premature to completely abandon the traditional taxonomic identification of meiofauna organisms. On the contrary, future studies might benefit from an integrated approach of the two methods. Moreover, given the morphological natural variation of meiofauna in Antarctica and the presence of rare species, it would

be of interest to create a genetic sequence database solely for Antarctic meiobenthos, especially nematodes. The data presented in this study constitute an initial investigation of meiofauna communities in these areas and their link to abiotic variables. In this regard it provides precious baseline information which could feed into future investigations for the creation of time series of temporal variability of the EAP.

DATA AVAILABILITY STATEMENT

The data presented in this study are deposited in the Dryad repository, access number 10.5061, doi: 10.5061/dryad.n8pk0p2tr. The data is publicly available.

AUTHOR CONTRIBUTIONS

AV performed the field-sampling, designed, and coordinated the study. GP processed the samples, performed the statistical analysis, and drafted the manuscript. FP participated in the statistical design and writing. LM participated in the molecular analysis and bioinformatics. All authors contributed to the reviewing process.

FUNDING

This work contributes to project BR/154/A1-Recto of the Belgian Science Policy (BELSPO/BRAIN). The environmental and molecular research was carried out with infrastructure funded by EMBRC Belgium (FWO project GOH3817N).

ACKNOWLEDGMENTS

The authors wish to thank the Principal Scientist Katrin Linse from the British Antarctic Survey for the coordination of the scientific program and the captain and crew of RRS James Clark Ross for the logistic support during the JR17003a expedition. Bruno Vlaeminck, Bart Beuselinck, Annelien Rigaux, Annick Van Kenhove, and Guy De Smet are thanked for their help with analysis of abiotic variables and preparation of biological samples.

SUPPLEMENTARY MATERIAL

The Supplementary Material for this article can be found online at: https://www.frontiersin.org/articles/10.3389/fmars.2021.629706/full#supplementary-material

REFERENCES

Ahmed, M., Sapp, M., Prior, T., Karssen, G., and Back, M. (2015). Nematode taxonomy: from morphology to metabarcoding. *Soil Discuss.* 12, 1175–1220. doi: 10.5194/soild-2-1175-2015

Amplicon, P. C. R., Clean-Up, P. C. R., and Index, P. C. R. (2013). *16s Metagenomic Sequencing Library Preparation*. Available online at: https://support.illumina.com/documents/documentation/chemistry_documentation/16s/16s-metagenomic-library-prep-guide-15044223-b.pdf (accessed March 15, 2019).

Barsanti, M., Delbono, I., Schirone, A., Langone, L., Miserocchi, S., Salvi, S., et al. (2011). Sediment reworking rates in deep sediments of the Mediterranean Sea. *Sci. Total Environ.* 409, 2959–2970. doi: 10.1016/j.scitotenv.2011.04.025

Bezerra, T. N., Eisendle, U., Hodda, M., Holovachov, O., Leduc, D., Mokievsky, V., et al. (2021). *Nemys: World Database of Nematodes*. Available online at: http://www.marinespecies.org/imis.php?module=dataset&dasid=66 (accessed February 10, 2019).

Boeckner, M. J., Sharma, J., and Proctor, H. C. (2009). Revisiting the meiofauna paradox: dispersal and colonization of nematodes and other meiofaunal organisms in low- and high-energy environments. *Hydrobiologia* 624, 91–106. doi: 10.1007/s10750-008-9669-5

Brannock, P. M., Learman, D. R., Mahon, A. R., Santos, S. R., and Halanych, K. M. (2018). Meiobenthic community composition and biodiversity along a 5500 km transect of Western Antarctica: a metabarcoding analysis. *Mar. Ecol. Prog. Ser.* 603, 47–60. doi: 10.3354/meps12717

Buffen, A., Leventer, A., Rubin, A., and Hutchins, T. (2007). Diatom assemblages in surface sediments of the northwestern Weddell Sea, Antarctic Peninsula. *Mar. Micropaleontol.* 62, 7–30. doi: 10.1016/j.marmicro.2006.07.002

Bunker, A. J., and Hirst, A. G. (2004). Fecundity of marine Planktonic copepods: global rates and patterns in relation to chlorophyll a, temperature and body weight. *Mar. Ecol. Prog. Ser.* 279, 161–181. doi: 10.3354/meps279161

Camerlenghi, A., Domack, E., Rebesco, M., Gilbert, R., Ishman, S., Leventer, A., et al. (2002). Glacial morphology and post-glacial contourites in northern Prince Gustav Channel (NW Weddell Sea, Antarctica). *Mar. Geophys. Res.* 22, 417–443. doi: 10.1023/A:1016399616365

Carpentier, A., Como, S., Dupuy, C., Lefrançois, C., and Feunteun, E. (2013). Feeding ecology of Liza spp. in a tidal fl at: evidence of the importance of primary production (bio fi lm) and associated Meiofauna. *J. Sea Res.* 92, 86–91. doi: 10.1016/j.seares.2013.10.007

Cook, A. J., Fox, A. J., Vaughan, D. G., and Ferrigno, J. G. (2005). Retreating glacier fronts on the Antarctic Peninsula over the past half-century. *Science* 308, 541–544. doi: 10.1126/science.1104235

Cook, A. J., and Vaughan, D. G. (2010). Overview of areal changes of the ice shelves on the Antarctic Peninsula over the past 50 years. *Cryosphere* 4, 77–98. doi: 10.5194/tc-4-77-2010

Coomans, A. (2002). Present status and future of nematode systematics. *Nematology* 4, 573–582.

Danovaro, R., Carugati, L., Corinaldesi, C., Gambi, C., Guilini, K., Pusceddu, A., et al. (2013). Multiple spatial scale analyses provide new clues on patterns and drivers of deep-sea nematode diversity. *Deep Sea Res. Part II Top. Stud. Oceanogr.* 92, 97–106.

Darnis, G., Wold, A., Falk-Petersen, S., Graeve, M., and Fortier, L. (2019). Could offspring predation offset the successful reproduction of the arctic copepod *Calanus hyperboreus* under reduced sea-ice cover conditions? *Prog. Oceanogr.* 170, 107–118. doi: 10.1016/j.pocean.2018.11.004

Davies, B. J., Carrivick, J. L., Glasser, N. F., Hambrey, M. J., and Smellie, J. L. (2012). Variable glacier response to atmospheric warming, Northern Antarctic Peninsula, 1988-2009. *Cryosphere* 6, 1031–1048. doi: 10.5194/tc-6-1031-2012

De Troch, M., Steinarsdóttir, M., Chepurnov, V., and Ólafsson, E. (2005). Grazing on diatoms by harpacticoid copepods: species-speciWc density-dependent uptake and microbial gardening. *Aquat. Microb. Ecol.* 39, 135–144.

Deagle, B. E., Clarke, L. J., Kitchener, J. A., Polanowski, A. M., and Davidson, A. T. (2018). Genetic monitoring of open ocean biodiversity: an evaluation of DNA metabarcoding for processing continuous plankton recorder samples. *Mol. Ecol. Resources* 18, 391–406. doi: 10.1111/1755-0998.12740

Dell' Anno, A., Carugati, L., Corinaldesi, C., and Riccioni, G. (2015). Unveiling the biodiversity of deep-sea nematodes through metabarcoding: are we ready to bypass the classical taxonomy? *PLoS One* 10:e0144928. doi: 10.1371/journal.pone.0144928

Derycke, S., Backeljau, T., and Moens, T. (2013). Dispersal and gene flow in free-living marine nematodes. *Front. Zool.* 10:1. doi: 10.1186/1742-9994-10-1

Dinis, P., Garzanti, E., Vermeesch, P., and Huvi, J. (2017). Climatic zonation and weathering control on sediment composition (Angola). *Chem. Geol.* 467, 110–121. doi: 10.1016/j.chemgeo.2017.07.030

Duprat, L. P. A. M., Bigg, G. R., and Wilton, D. J. (2016). Enhanced Southern Ocean marine productivity due to fertilization by giant icebergs. *Nat. Geosci.* 9, 219–221. doi: 10.1038/ngeo2633

Eskin, R. A., and Palmer, M. A. (1985). Suspension of marine nematodes in a turbulent tidal creek: species patterns. *Biol. Bull.* 169, 615–623.

Etourneau, J., Sgubin, G., Crosta, X., Swingedouw, D., Willmott, V., Barbara, L., et al. (2019). Ocean temperature impact on ice shelf extent in the eastern Antarctic Peninsula. *Nat. Commun.* 10, 8–15. doi: 10.1038/s41467-018-08195-6

Fabiano, M., and Danovaro, R. (1999). Meiofauna distribution and mesoscale variability in two sites of the Ross Sea (Antarctica) with contrasting food supply. *Polar Biol.* 22, 115–123. doi: 10.1007/s003000050398

Fonseca, V. G., Sinniger, F., Gaspar, J. M., Quince, C., Creer, S., Power, D. M., et al. (2017). Revealing higher than expected meiofaunal diversity in Antarctic sediments: a metabarcoding approach. *Sci. Rep.* 7, 1–11. doi: 10.1038/s41598-017-06687-x

Franzo, A., Asioli, A., Roscioli, C., Patrolecco, L., Bazzaro, M., Del Negro, P., et al. (2019). Influence of natural and anthropogenic disturbances on foraminifera and free-living nematodes in four lagoons of the Po delta system. *Estuar. Coast. Shelf Sci.* 220, 99–110. doi: 10.1016/j.ecss.2019.02.039

Furukawa, Y. (2001). Biogeochemical consequences of macrofauna burrow ventilation. *Geochem. Trans.* 2:83.

Gambi, C., Pusceddu, A., Benedetti-Cecchi, L., and Danovaro, R. (2014). Species richness, species turnover and functional diversity in nematodes of the deep Mediterranean S ea: searching for drivers at different spatial scales. *Glob. Ecol. Biogeogr.* 23, 24–39.

Gogina, M., Zettler, M. L., Vanaverbeke, J., Dannheim, J., Van Hoey, G., Desroy, N., et al. (2020). Interregional comparison of benthic ecosystem functioning: community bioturbation potential in four regions along the NE Atlantic shelf. *Ecol. Indic.* 110:105945. doi: 10.1016/j.ecolind.2019.105945

Gonçalves, A. M. M., Pardal, M. A., Marques, S. C., De Troch, M., and Azeiteiro, U. M. (2010). Distribution and composition of small-size zooplankton fraction in a temperate shallow estuary (Western Portugal). *Fresenius Environ. Bull.* 19, 3160–3176.

Hauquier, F., Leliaert, F., Rigaux, A., Derycke, S., and Vanreusel, A. (2017). Distinct genetic differentiation and species diversification within two marine nematodes with different habitat preference in Antarctic sediments. *BMC Evol. Biol.* 17:120. doi: 10.1186/s12862-017-0968-1

Hauquier, F., Suja, L. D., Gutt, J., Veit-Köhler, G., and Vanreusel, A. (2015). Different oceanographic regimes in the vicinity of the Antarctic Peninsula reflected in benthic nematode communities. *PLoS One* 10:e0137527. doi: 10.1371/journal.pone.0137527

Heip, C., Vincx, M., Smol, N., and Vranken, G. (1982). The systematics and ecology of marine free-living nematodes. *Helminthological Abstracts Series B, Plant Nematology* 51, 1–31.

Hoffmann, R., Al-Handal, A. Y., Wulff, A., Deregibus, D., Zacher, K., Quartino, M. L., et al. (2019). Implications of glacial melt-related processes on the potential primary production of a microphytobenthic community in potter cove (Antarctica). *Front. Mar. Sci.* 6:655. doi: 10.3389/fmars.2019.00655

Hoffmann, R., Pasotti, F., Vázquez, S., Lefaible, N., Torstensson, A., MacCormack, W., et al. (2018). Spatial variability of biogeochemistry in shallow coastal benthic communities of Potter Cove (Antarctica) and the impact of a melting glacier. *PLoS One* 13:e0207917. doi: 10.1371/journal.pone.0207917

Holland, P. R., and Kwok, R. (2012). Wind-driven trends in Antarctic sea-ice drift. *Nat. Geosci.* 5, 872–875. doi: 10.1038/ngeo1627

Ingels, J., Tchesunov, A. V., and Vanreusel, A. (2011). Meiofauna in the gollum channels and the whittard canyon, celtic margin-how local environmental conditions shape nematode structure and function. *PLoS One* 6:e020094. doi: 10.1371/journal.pone.0020094

Ingels, J., Vanhove, S., De Mesel, I., and Vanreusel, A. (2006). The biodiversity and biogeography of the free-living nematode genera Desmodora and Desmodorella (family Desmodoridae) at both sides of the Scotia Arc. *Polar Biol.* 29, 936–949. doi: 10.1007/s00300-006-0135-4

Ingels, J., Vanreusel, A., Brandt, A., Catarino, A. I., David, B., De Ridder, C., et al. (2012). Possible effects of global environmental changes on Antarctic benthos: a synthesis across five major taxa. *Ecol. Evol.* 2, 453–485. doi: 10.1002/ece3.96

Isla, E., Gerdes, D., Palanques, A., Gili, J. M., and Arntz, W. (2006). Particle fluxes and tides near the continental ice edge on the eastern Weddell Sea shelf. *Deep. Res. II* 53:866.

Jensen, P. (1982). A new meiofauna sample splitter. *Ann. Zool. Fenn.* 9, 233–236.

Kang, S.-H., Kang, J.-S., Lee, S., Chung, K. H., Kim, D., and Park, M. G. (2001). Antarctic phytoplankton assemblages in the marginal ice zone of the northwestern Weddell Sea. *J. Plankton Res.* 23, 333–352.

Kennedy, A. D., and Jacoby, C. A. (1999). Biological indicators of marine environmental health: meiofauna - a neglected benthic component? *Environ. Monit. Assess.* 54, 47–68.

Korbel, K. L., Stephenson, S., and Hose, G. C. (2019). Sediment size influences habitat selection and use by groundwater macrofauna and meiofauna. *Aquat. Sci.* 81, 1–10. doi: 10.1007/s00027-019-0636-1

Kunz, M., King, M. A., Mills, J. P., Miller, P. E., Fox, A. J., Vaughan, D. G., et al. (2012). Multi-decadal glacier surface lowering in the Antarctic Peninsula. *Geophys. Res. Lett.* 39, 1–5. doi: 10.1029/2012GL052823

Lawson, D. (1982). Mobilization, movement and deposition of active subaerial sediment flows, matanuska glacier, Alaska. *J. Geol.* 90, 279–300. doi: 10.1086/628680

Lee, H., Vanhove, S., Peck, L. S., and Vincx, M. (2001). Recolonisation of meiofauna after catastrophic iceberg scouring in shallow Antarctic sediments. *Polar Biol.* 24, 918–925. doi: 10.1007/s003000100300

Li, Y., and Guo, Y. (2016). Two new free-living marine nematode species of the genus *Anoplostoma* (Anoplostomatidae) from the mangrove habitats of Xiamen Bay, East China Sea. *J. Ocean Univ. China* 15, 11–18. doi: 10.1007/s11802-016-2896-x

Lohrer, A. M., Thrush, S. F., and Gibbs, M. M. (2004). Bioturbators enhance ecosystem function through complex biogeochemical interactions. *Nature* 431, 1092–1095. doi: 10.1038/nature03042

Macheriotou, L., Guilini, K., Bezerra, T. N., Tytgat, B., Nguyen, D. T., Phuong Nguyen, T. X., et al. (2019). Metabarcoding free-living marine nematodes using curated 18S and CO1 reference sequence databases for species-level taxonomic assignments. *Ecol. Evol.* 9, 1211–1226. doi: 10.1002/ece3.4814

Macheriotou, L., Rigaux, A., Derycke, S., and Vanreusel, A. (2020). Phylogenetic clustering and rarity imply risk of local species extinction in prospective deep-sea mining areas of the clarion-clipperton fracture zone. *Proc. R. Soc. B* 287:20192666. doi: 10.1098/rspb.2019.2666

Martín, C., Gudmundsson, G. H., Pritchard, H. D., and Gagliardini, O. (2009). On the effects of anisotropic rheology on ice flow, internal structure, and the age-depth relationship at ice divides. *J. Geophys. Res. Earth Surf.* 114, 1–18. doi: 10.1029/2008JF001204

Meslard, F., Bourrin, F., Many, G., and Kerhervé, P. (2018). Suspended particle dynamics and fluxes in an Arctic fjord (Kongsfjorden, Svalbard). *Estuar. Coast. Shelf Sci.* 204, 212–224. doi: 10.1016/j.ecss.2018.02.020

Meysman, F. J. R., Galaktionov, O. S., Gribsholt, B., and Middelburg, J. J. (2006). Bioirrigation in permeable sediments: advective pore-water transport induced by burrow ventilation. *Limnol. Oceanogr.* 51, 142–156. doi: 10.4319/lo.2006.51.1.0142

Mincks, S. L., Smith, C. R., Jeffreys, R. M., and Sumida, P. Y. G. (2008). Trophic structure on the West Antarctic Peninsula shelf, detritivory and benthic inertia revealed by d13C and d15N analysis. *Deep. Res.* 55:2502.

Moline, M. A., and Prezelin, B. B. (1996). Long-term monitoring and analyses of physical factors regulating variability in coastal Antarctic phytoplankton biomass, i n situ productivity and taxonomic composition over subseasonal, seasonal and interannual time scales. *Mar. Ecol. Prog. Ser.* 145, 143–160.

Montes-Hugo, M., Doney, S. C., Ducklow, H. W., Fraser, W., Martinson, D., Stammerjohn, S. E., et al. (2009). Recent Changes in Phytoplankton communities associated with rapid regional climate change along the Western Antarctic Peninsula. *Science* 323, 1470–1473.

Moreno, M., Semprucci, F., Vezzulli, L., Balsamo, M., Fabiano, M., and Albertelli, G. (2011). The use of nematodes in assessing ecological quality status in the Mediterranean coastal ecosystems. *Ecol. Indic.* 11, 328–336. doi: 10.1016/j.ecolind.2010.05.011

Nardelli, S., Kohut, J., Schofield, O., Waite, N., Brown, M., Saba, G., et al. (2018). Changes in the upper ocean mixed layer and phytoplankton productivity along the West Antarctic Peninsula. *Philos. Trans. R. Soc. A Math. Eng. Sci.* 376, 20170173. doi: 10.1098/rsta.2017.0173

Nascimento, F. J. A., Karlson, A. M. L., and Elmgren, R. (2011). Diversity of larger consumers enhances interference competition effects on smaller competitors. *Oecologia* 166, 337–347. doi: 10.1007/s00442-010-1865-0

Nokes, C. R., Bostock, H. C., Strachan, L. J., and Hadfield, M. G. (2019). Hydrodynamics and sediment transport on the North Canterbury Shelf,

New Zealand. *New Zeal. J. Mar. Freshw. Res.* 55, 1–20. doi: 10.1080/00288330.2019.1699584

Oppenheimer, M. (1998). Global warming and the stability of the West Antarctic Ice Sheet. *Nature* 393, 325–332.

Pasotti, F., Convey, P., and Vanreusel, A. (2014). Potter Cove, west Antarctic Peninsula, shallow water meiofauna: a seasonal snapshot. *Antarct. Sci.* 26, 554–562. doi: 10.1017/S0954102014000169

Perolo, P., Bakker, M., Gabbud, C., Moradi, G., Rennie, C., and Lane, S. N. (2019). Subglacial sediment production and snout marginal ice uplift during the late ablation season of a temperate valley glacier. *Earth Surf. Process. Landf.* 44, 1117–1136. doi: 10.1002/esp.4562

Polvani, L. M., Waugh, D. W., Correa, G. J., and Son, S. W. (2011). Stratospheric ozone depletion: the main driver of twentieth-century atmospheric circulation changes in the Southern Hemisphere. *J. Clim.* 24, 795–812. doi: 10.1175/2010JCLI3772.1

Prezèlin, B. B., Hofmann, E. E., Mengelt, C., and Klinck, J. M. (2000). The linkage between Upper Circumpolar Deep Water (UCDW) and phytoplankton assemblages on the west Antarctic Peninsula continental shelf. *J. Mar. Res.* 58, 165–202.

Pritchard, H. D., Ligtenberg, S. R. M., Fricker, H. A., Vaughan, D. G., Van Den Broeke, M. R., and Padman, L. (2012). Antarctic ice-sheet loss driven by basal melting of ice shelves. *Nature* 484, 502–505. doi: 10.1038/nature10968

Pritchard, H. D., and Vaughan, D. G. (2007). Widespread acceleration of tidewater glaciers on the Antarctic Peninsula. *J. Geophys. Res. Earth Surf.* 112, 1–10. doi: 10.1029/2006JF000597

Raes, M., De Troch, M., Ndaro, S. G. M., Muthumbi, A., Guilini, K., and Vanreusel, A. (2007). The structuring role of microhabitat type in coral degradation zones: a case study with marine nematodes from Kenya and Zanzibar. *Coral Reefs* 26, 113–126. doi: 10.1007/s00338-006-0184-8

Raes, M., Rose, A., and Vanreusel, A. (2010). Response of nematode communities after large-scale ice-shelf collapse events in the Antarctic Larsen area. *Glob. Chang. Biol.* 16, 1618–1631. doi: 10.1111/j.1365-2486.2009.02137.x

Rignot, E., and Jacobs, S. S. (2002). Rapid Bottom melting Widespread near Antarctic Ice sheet grounding lines. *Science* 296, 2020–2023. doi: 10.1126/science.1070942

Rott, H., Abdel Jaber, W., Wuite, J., Scheiblauer, S., Floricioiu, D., Van Wessem, J. M., et al. (2018). Changing pattern of ice flow and mass balance for glaciers discharging into the Larsen A and B embayments, Antarctic Peninsula, 2011 to 2016. *Cryosphere* 12, 1273–1291. doi: 10.5194/tc-12-1273-2018

Rott, H., Rack, W., Skvarca, P., and De Angelis, H. (2002). Northern Larsen Ice Shelf, Antarctica: further retreat after collapse. *Ann. Glaciol.* 34, 277–282. doi: 10.3189/172756402781817716

Scambos, T., Fricker, H. A., Liu, C.-C., Bohlander, J., Fastook, J., Sargent, A., et al. (2009). Ice shelf disintegration by plate bending and hydro-fracture: satellite observations and model results of the 2008 Wilkins ice shelf break-ups. *Earth Planet. Sci. Lett.* 280, 51–60. doi: 10.1016/j.epsl.2008.12.027

Schmid-Araya, J. M., Schmid, P. E., Tod, S. P., and Esteban, G. F. (2016). Trophic positioning of meiofauna revealed by stable isotopes and food web analyses. *Ecology* 97, 3099–3109.

Schratzberger, M., and Ingels, J. (2018). Meiofauna matters: the roles of meiofauna in benthic ecosystems. *J. Exp. Mar. Bio. Ecol.* 502, 12–25. doi: 10.1016/j.jembe.2017.01.007

Schratzberger, M., Warr, K., and Rogers, S. I. (2006). Patterns of nematode populations in the southwestern North Sea and their link to other components of the benthic fauna. *J. Sea Res.* 55, 113–127. doi: 10.1016/j.seares.2005.07.002

Seinhorst, J. W. (1959). A rapid method for the transfer of nematodes from fixative to anhydrous glycerin. *Nematologica* 4, 67–69.

Semprucci, F., Colantoni, P., Baldelli, G., Rocchi, M., and Balsamo, M. (2010). The distribution of meiofauna on back-reef sandy platforms in the Maldives (Indian Ocean). *Mar. Ecol.* 31, 592–607. doi: 10.1111/j.1439-0485.2010.00383.x

Semprucci, F., Sbrocca, C., Rocchi, M., and Balsamo, M. (2015). Temporal changes of the meiofaunal assemblage as a tool for the assessment of the ecological quality status. *J. Mar. Biol. Assoc. U.K.* 95, 247–254. doi: 10.1017/S0025315414001271

Shuman, C. A., Berthier, E., and Scambos, T. A. (2011). 2001-2009 elevation and mass losses in the Larsen A and B embayments, Antarctic Peninsula. *J. Glaciol.* 57, 737–754. doi: 10.3189/002214311797409811

Siegert, M., Atkinson, A., Banwell, A., Brandon, M., Convey, P., Davies, B., et al. (2019). The Antarctic Peninsula under a 1.5°C global warming scenario. *Front. Environ. Sci.* 7:102. doi: 10.3389/fenvs.2019.00102

Smith, C. R., Mincks, S., and DeMaster, D. J. (2008). The FOODBANCS project, Introduction and sinking fluxes of organic carbon, chlorophyll-a and phytodetritus on the western Antarctic Peninsula continental shelf. *Deep. Res. II* 55:2404.

Stark, J. S., Mohammad, M., McMinn, A., and Ingels, J. (2020). Diversity, abundance, spatial variation, and human impacts in marine Meiobenthic nematode and copepod communities at casey station, East Antarctica. *Front. Mar. Sci.* 7:480. doi: 10.3389/fmars.2020.00480

Steyaert, M., Moodley, L., Nadong, T., Moens, T., Soetaert, K., and Vincx, M. (2007). Responses of intertidal nematodes to short-term anoxic events. *J. Exp. Mar. Bio. Ecol.* 345, 175–184. doi: 10.1016/j.jembe.2007.03.001

Steyaert, M., Priestley, V., Osborne, O., Herraiz, A., Arnold, R., and Savolainen, V. (2020). Advances in metabarcoding techniques bring us closer to reliable monitoring of the marine benthos. *J. Appl. Ecol.* 57, 2234–2245.

Stuecker, M. F., Bitz, C. M., and Armour, K. C. (2017). Conditions leading to the unprecedented low Antarctic sea ice extent during the 2016 austral spring season. *Geophys. Res. Lett.* 44, 9008–9019. doi: 10.1002/2017GL074691

Surey-Gent, S. C. (1981). Distribution of *Anoplostoma viviparum* (Nematoda) in Southampton Water sediments. *Mar. Biol.* 62, 157–160.

Taheri, M., Bastami, K. D., and Yazdani, M. (2017). "The role of the sediment conditions in shaping meiofauna spatial distribution in the shallow water of the south Caspian Sea," in *Proceedings of the First International Conference on Oceanography for West Asia* (Tehran: Civilica).

Tarjan, A. C., and Keppner, E. J. (2008). *Illustrated Key to the Genera of Free-Living Marine Nematodes in the Superfamily Chromadoroides Exclusive of the Chromadoridae*. Available online at: https://entnemdept.ufl.edu/creatures/nematode/marine_nematodes.htm (accessed December 8, 2019).

van de Velde, S., and Meysman, F. J. R. (2016). The influence of bioturbation on iron and sulphur cycling in marine sediments: a model analysis. *Aquat. Geochem.* 22, 469–504.

Van Heukelem, L., and Thomas, C. S. (2001). Computer-assisted high-performance liquid chromatography method development with applications to the isolation and analysis of phytoplankton pigments. *J. Chromatogr. A* 910, 31–49. doi: 10.1016/S0378-4347(00)00603-4

Van Leeuwe, M. A., Tedesco, L., Arrigo, K. R., Assmy, P., Meiners, K. M., Rintala, J., et al. (2018). Microalgal community structure and primary production in Arctic and Antarctic sea ice: a synthesis. *Elem. Sci. Anthropocene* 6:4.

Vanhove, S., Arntz, W., and Vincx, M. (1999). Comparative study of the nematode communities on the southeastern Weddell Sea shelf and slope (Antarctica). *Mar. Ecol. Prog. Ser.* 181, 237–256. doi: 10.3354/meps181237

Vanhove, S., Vermeeren, H., and Vanreusel, A. (2004). Meiofauna towards the South sandwich trench (750-6300 m), focus on nematodes. *Deep. Res. Part II Top. Stud. Oceanogr.* 51, 1665–1687. doi: 10.1016/j.dsr2.2004.06.029

Vanhove, S., Wittoeck, J., Desmet, G., Van den Berghe, B., Herman, R. L., Bak, R. P. M., et al. (1995). Deep-sea meiofauna communities in Antarctica: structural analysis and relation with the environment. *Mar. Ecol. Prog. Ser.* 127, 65–76.

Vanreusel, A., Fonseca, G., Danovaro, R., Cristina, M., Ferrero, T., Gad, G., et al. (2010). The contribution of deep-sea macrohabitat heterogeneity to global nematode diversity. *Mar. Ecol.* 31, 6–20. doi: 10.1111/j.1439-0485.2009.00352.x

Vaughan, D. G., Marshall, G. J., Connolley, W. M., Parkinson, C., Mulvaney, R., Hodgson, D. A., et al. (2003). Recent rapid regional climate warming on the Antarctic Peninsula. *Clim. Chang.* 60, 243–274.

Veit-Köhler, G., Durst, S., Schuckenbrock, J., Hauquier, F., Durán Suja, L., Dorschel, B., et al. (2018). Oceanographic and topographic conditions structure benthic meiofauna communities in the Weddell Sea, Bransfield Strait and Drake Passage (Antarctic). *Prog. Oceanogr.* 162, 240–256. doi: 10.1016/j.pocean.2018.03.005

Vermeeren, H. (2002). Biogeografie van Antarctische Diepzeenematoden: Species Turn-Over in Dominante Genera van de Familie Chromadoridae. MSc thesis. Gent: Universiteit Gent.

Vinagre, C., Salgado, J. P., Mendonça, V., Cabral, H., and Costa, M. J. (2012). Isotopes reveal fl uctuation in trophic levels of estuarine organisms, in space and time. *J. Sea Res.* 72, 49–54. doi: 10.1016/j.seares.2012.05.010

Warwick, R. M., Platt, H. M., and Somerfield, P. J. (1998). "Freeliving marine nematodes part III Monhysterids: pictorial key to world genera and notes for the identification of British species," in *Synopses of the British Fauna (New Series) 53*, eds R. S. K. Barnes and J. H. Crothers (Shrewsbury: Field Studies Council), 296.

Wetzel, M. A., Weber, A., and Giere, O. (2002). Re-colonization of anoxic/sulfidic sediments by marine nematodes after experimental removal of macroalgal cover. *Mar. Biol.* 141, 679–689. doi: 10.1007/s00227-002-0863-0

Wieser, W. (1953). Die Beziehung zwischen Mundhohlengestalt, ernahrungsweise und vorkommen bei freilebenden marinen Nematoden. *Ark. Zool.* 4, 439–484.

Zeppilli, D., Fuchs, S., Sanchez, N., Sarrazin, J., Leduc, D., Fontanier, C., et al. (2018). Characteristics of meiofauna in extreme marine ecosystems: a review. *Mar. Biodivers.* 48, 35–71. doi: 10.1007/s12526-017-0815-z

Conflict of Interest: The authors declare that the research was conducted in the absence of any commercial or financial relationships that could be construed as a potential conflict of interest.

Publisher's Note: All claims expressed in this article are solely those of the authors and do not necessarily represent those of their affiliated organizations, or those of the publisher, the editors and the reviewers. Any product that may be evaluated in this article, or claim that may be made by its manufacturer, is not guaranteed or endorsed by the publisher.

Advantages of publishing in Frontiers

OPEN ACCESS
Articles are free to read for greatest visibility and readership

FAST PUBLICATION
Around 90 days from submission to decision

HIGH QUALITY PEER-REVIEW
Rigorous, collaborative, and constructive peer-review

TRANSPARENT PEER-REVIEW
Editors and reviewers acknowledged by name on published articles

Frontiers
Avenue du Tribunal-Fédéral 34
1005 Lausanne | Switzerland

Visit us: www.frontiersin.org
Contact us: frontiersin.org/about/contact

REPRODUCIBILITY OF RESEARCH
Support open data and methods to enhance research reproducibility

DIGITAL PUBLISHING
Articles designed for optimal readership across devices

FOLLOW US
@frontiersin

IMPACT METRICS
Advanced article metrics track visibility across digital media

EXTENSIVE PROMOTION
Marketing and promotion of impactful research

LOOP RESEARCH NETWORK
Our network increases your article's readership